VERTICAL FLUX, ECOLOGY AND DISSOLUTION OF RADIOLARIA IN TROPICAL OCEANS: IMPLICATIONS FOR THE SILICA CYCLE

by

KOZO TAKAHASHI

B.A., HOKKAIDO UNIVERSITY
(1972)
B.Sc., UNIVERSITY OF WASHINGTON
(1975)
M.Sc., UNIVERSITY OF WASHINGTON
(1977)

SUBMITTED IN PARTIAL FULFILLMENT OF THE
REQUIREMENTS FOR THE DEGREE OF
DOCTOR OF PHILOSOPHY

at the

MASSACHUSETTS INSTITUTE OF TECHNOLOGY

and the

WOODS HOLE OCEANOGRAPHIC INSTITUTION

NOVEMBER, 1981

Signature of Author . . . .

Joint Program in Oceanography, Massachusetts Institute of Technology - Woods Hole Oceanographic Institution, and Department of Earth & Planetary Sciences, Massachusetts Institute of Technology, November, 1981

Certified by . . . .
Thesis Supervisor

Accepted by . . . .
Chairman, Joint Oceanography Committee in the Earth Sciences, Massachusetts Institute of Technology-Woods Hole Oceanographic Institution

VERTICAL FLUX, ECOLOGY AND DISSOLUTION OF RADIOLARIA IN TROPICAL OCEANS: IMPLICATIONS FOR THE SILICA CYCLE

KOZO TAKAHASHI

Submitted to the Woods Hole Oceanographic Institution-Massachusetts Institute of Technology Joint Program in Oceanography on October 30, 1981, in partial fullfillment of the requirements for the degree of Docotor of Philosophy.

ABSTRACT

Radiolarians which settle through the oceanic water column were recovered from three stations (western Tropical Atlantic-Station E, central Tropical Pacific-P_1 and Panama Basin-PB) using PARFLUX sediment traps in moored arrays at several depths. The taxonomic diversities of the radiolarian assemblages in the sediment traps were very high. A total of 420 taxa, including 23 newly identified taxa, were found at the three stations; of these, 208 taxa were found at station E. The polycystine radiolarians generally reach the sea floor with little change in abundance or species composition, although slight skeletal dissolution occurs throughout their descent. The phaeodarian radiolarians, on the other hand, are largely dissolved within the water column; only a few species reach the sea-floor and these dissolve rapidly at the sediment-water interface. Most radiolarian skeletons sink as individuals through deep water columns without being incorporated into large biogenic aggregates. Because significant numbers of nassellarian and phaeodarian species are deep-water dwelling forms the diversity index of radiolarians increases with increasing depth in the mesopelagic zone.

The vertical flux of the total radiolarians arriving at the trap depths (in x 10^3 individuals/m^2/day) ranged from 16-24 (E), 0.6-17 (P_1), and 29-53 (PB). Of these on the average 25 % and 69 % of the total radiolarian flux is transported by Spumellaria and Nassellaria, respectively, while 5 % is carried by Phaeodaria. The measured SiO_2 content of the skeletons averaged 91, 98 and 71 % of measured weight for Spumellaria, Nassellaria and Phaeodaria, respectively. The supply of radiolarian silica (mg $SiO_2/m^2/day$) to each trap depth ranged from 2.5-4.0 (E), 0.9-3.2 (P_1), and 5.7-10.4 (PB). The Radiolaria appear to be a significantly large portion of the SiO_2 flux in > 63 μm size fraction and thus play an important role in the silica cycle. When the radiolarian fluxes at the three Stations are compared with Holocene radiolarian accumulation rates in the same areas it became apparent that several percent or less of the fluxes are preserved in the sediments in all cases and the rest is dissolved on the sea-floor. Estimated excess Si which is derived from SiO_2 dissolution on the sea-floor is fairly small relative to advective Si in the western North Atlantic and thus it appears to be insignificant to show any deviation in a simple mixing curve of deep water masses.

Weight, length, width, projected area and volume of 58 radiolarian taxa were measured. The density contrast of radiolarians, relative to seawater, generally falls between 0.01 and 0.5 g/cm^3. The sinking speed of 55 radiolarian taxa, measured in the laboratory at 3°C, ranged from 13 to 416 m/day. Despite the wide variety of morphology between the species, sinking speeds were best correlated with weight/shell among all the possible combinations of the examined variables. The estimated residence times of these taxa in the 5 km pelagic water column ranged from 2 weeks to 14 months. Large phaeodarians reached the water-sediment interface relatively quickly and ultimately dissolved on the sea floor. Small-sized taxa dissolved en route during sinking.

The standing stock of 26 examined abundant taxa is on the order of 1 to 100 $shells/m^3$. Total radiolarian standing stock ranges from about 450 $shells/m^3$ at Stations P_1 and E to 1200 $shells/m^3$ at Station PB. The rate of production of total Radiolaria is calculated to be 77 to 225 $shells/m^3/day$. The turnover time for these species ranges from several days to one month depending on the species and the assumption of the depth interval used for the estimation.

Thesis supervisor: Dr. Susumu Honjo
Title: Associate Scientist

This thesis is dedicated to my parents,
Yoshitaka and Mitsuko Takahashi
and to my wife, Kayoko Takahashi

ACKNOWLEDGMENTS

I thank Dr. Susumu Honjo, my thesis advisor, the most for his enthusiastic encouragement and guidance throughout the years. Countless opportunities for discussions with him on oceanography fascinated me and, indeed, sustained my motivation in completing this program. Without the cooperation of the PARFLUX Program supported by the National Science Foundation (Principal Investigators: Drs. S. Honjo, P.G. Brewer, and D.W. Spencer) this study would not have been accomplished. I also thank Dr. John D. Milliman who served as my academic advisor and guided me to the initiation of the silica cycle study. Professor Hsin Yi Ling of the Northern Illinois University initially inspired me on the biogenic-particle transport study and generously aided me in many aspects throughout. Professor Edward A. Boyle of M.I.T. has been helpful in solving problems, especially in geochemical areas, and I appreciate it very much. Dr. David A. Johnson has been generous with his literature including microfiche on radiolarian papers; his critical and constructive reviews and comments on the scientific results were most gratefully received. Drs. Brian E. Tucholke and L. Valentine Worthington gave invaluable tutorial sessions which helped me digest geophysics and physical oceanography.

My thesis advisory committee members include Drs. S. Honjo, J.D. Milliman, H.Y. Ling, E.A. Boyle. Dr. D.A. Johnson is the chairman of the final examination. My academic advisory committee consists of Drs. J.D. Milliman, S. Honjo, E.A. Boyle, V. Worthington and B.E. Tucholke.

I am very appreciative of the help of the members of the W.H.O.I. Education Office, Dr. C. Hollister, Mr. A.L. Peirson, Mrs. Constance Brackett, Abbie Alvin and Dixie Berthel, for their kind cooperation during my tenure as a Joint Program student.

Dr. Catherine Nigrini critically reviewed the systematics portion of the thesis as an outside referee which was extremely valuable. Dr. William R. Riedel of Scripps Institution of Oceanography kindly reviewed a paper on the Atlantic radiolarian flux which was incorporated in the thesis. Dr. Wiley Poag of the U.S. Geological Survey at Woods Hole has been a good teacher of the classics needed for completing the taxonomy for this investigation. Dr. David C. Hurd has collaborated with me in radiolarian dissolution/preservation problems. I have greatly benefited from many discussions with him. Dr. Neil Swanberg of Lamont-Doherty Geological Observatory provided useful comments in the colonial radiolarian study.

Vernon Asper frequently aided in preparing SEM samples and instructed me in SEM operation as well as providing frequent discussions on many aspects of this work. Steve Manganini has always been helpful in the laboratory and at sea. Mrs. Margaret Goreau spent much effort in helping in the laboratory in SEM work and diatom culture. I thank Steve Nolan for his skillful computer work using the SPSS Program which produced most of the figures in this thesis. Steve Swift has been helpful as a consultant in much of the fluid dynamic aspect of this work. Dr. Bruce H. Corliss and Ken Miller have been cooperative in solving problems with taxonomic nomenclature. Drs. June Harrigan and Izja Lederhandler of the Laboratory of Biophysics, the National Institute of Health located at the Marine Biological Laboratory, Woods Hole, kindly provided a photo-optical digitizer for radiolarian dimension measurements. Alan Fleer and Cindy Pilskaln provided aid at sea. I have also benefited from discussions with Drs. K.O. Emery, J. Cole, J. Erez, R. Keir, G.P. Lohmann, W. Curry, C.C. Woo, F. Manheim, R. Guillard, T. Goreau, A. Shor, and those who I have forgotten to specifically mention.

My great appreciation goes to Mrs. Sandra Pelletier who has typed the thesis and many other papers whose conclusions are incorporated in this thesis. Her skillful coordination in organizing all of the complex tables in this thesis is gratefully acknowledged. Mrs. Emily Evans also gave me much secretarial aid. Kayoko Takahashi aided in photographic work for plates as well as much proof reading of the manuscript. Messers. Don Souza, Frank Medeiros, and many others in Graphic Services did an excellent job in producing figures and slides, sometimes in quite a rush. I also thank the members of AII Cruise 108, Leg 2 to the Panama Basin for sediment trap recovery and other field observations for their cooperation.

Finally, I sincerely thank my wife, Kayoko Takahashi, for her endurance of many years and moral support. My children, Alexander and Eileen, always gave me a cheerful time and made easier the completion of the thesis work.

This thesis work has been supported by the National Science Foundation, Submarine Geology and Geophysics Program, Grant OCE80-19386 and the Woods Hole Oceanographic Institution Education Office.

TABLE OF CONTENTS

Page

ABSTRACT 2

ACKNOWLEDGMENTS 5

TABLE OF CONTENTS 7

LIST OF FIGURES 9

LIST OF TABLES 12

CHAPTER I - VERTICAL FLUX, ECOLOGY, RESIDENCE TIME AND DISSOLUTION OF RADIOLARIA: IMPLICATIONS FOR THE SILICA CYCLE 14

1. INTRODUCTION 14
2. SOURCES OF SAMPLES; METHODS OF ANALYSIS 17
3. RESULTS AND DISCUSSION 24
    - Counts of radiolarian taxa 24
    - Diversity index analysis 51
    - Percent similarity analysis 55
    - Vertical fluxes of Radiolaria and suborders at three tropical stations 56
    - Comparison of the radiolarian fluxes with previous work 66
    - Comparison of the radiolarian fluxes with accumulation rates in the Holocene sediments 68
    - Effects of radiolarian dissolution in the water column 69
    - Dimensions of radiolarian skeletons 72
    - Silica content in radiolarian skeletons 91

Page

Laboratory sinking speed of Radiolaria 93
Residence time of Radiolaria in the pelagic water column 103
Radiolarian standing stock, production rate and turnover time 108
Biogenic opal transport to the deep-sea by radiolarian skeletons 111
Estimation of excess Si relative to advective Si in the deep waters of the western North Atlantic 116
4. SUMMARY AND CONCLUSIONS 118
5. REFERENCES 121
6. APPENDIX: Formulae for computed projected area and bulk volume computations 131

CHAPTER II - SYSTEMATICS OF RADIOLARIA 133

1. INTRODUCTION 133
2. OUTLINE CLASSIFICATION 133
3. SYSTEMATICS 149
Suborder Spumellaria 149
Suborder Nassellaria 211
Suborder Phaeodaria 282
4. REFERENCES 319
5. PLATES 332

CURRICULUM VITAE 458
PUBLICATIONS 459

BIOGRAPHY 461

LIST OF FIGURES

Page

Figure 1. Locations of the PARFLUX sediment trap stations. 18

Figure 2. A. Illustration of a system for the sinking speed experiment. B. An enlarged view of the sinking column. a. narrow-neck cylinder, b. temperature bath cylinder, c. thermostat, d. fiberglass optics, e. thermal filters f. disecting microscope. 23

Figure 3. Vertical fluxes (no. of shells/m^2/day) of Radiolaria and their suborders from Stations E, P_1 and PB. Horizontal bars on Station E radiolarian flux show representative standard deviation at 95% confidence level for all the data. 49

Figure 4. Vertical fluxes (no. of shells/m^2/day) of Radiolaria and their suborders from Station E. Horizontal bars represent standard deviation at 95% confidence level. 50

Figure 5. Diversity index (H'), natural bels, of Radiolaria and their suborders from E Station. 54

Figure 6. Percentages of broken shells in radiolarian taxa from Station E. 59

Figure 7. Percentages of shells in biogenic aggregates in radiolarian taxa from Station E. 61

Figure 8. Plots of percentages of shells in biogenic aggregates vs. broken shells in radiolarian taxa from Station E. The shallowest (389 m) samples fall in the lower right side of the figure, whereas the deepest (5,068 m) samples scatter from the lower to upper end of the left side depending on taxon. Samples from 988 to 3,755 m fit in the middle of the curves. 62

Figure 9. Mode of vertical transport and dissolution model for sinking Radiolaria through mesopelagic and bathypelagic zones. Percentage of broken shells of soluble radiolarian species increases exponentially with depth, while resistant species settle without substantial dissolution effect on their shells. 63

Figure 10. The Nassellaria/Spumellaria and Phaedaria/Spumellaria ratios from Stations E, P_1 and PB. 65

LIST OF FIGURES (cont.)

Page

Figure 11. Representative phaeodarian taxa of shallow and deep dwelling species from Station E. The decrease of the shallow dwelling flux with depth is caused by dissolution during sinking. The flux of deep dwelling radiolarians is a mixture of an increase of settling individuals and dissolution of dead shells while sinking. 70

Figure 12. Plot of length vs. weight/shell. Each datum point represents each species. Only representative standard deviations/analytical errors are given to several species for simplicity of the illustration. Symbols used in Figures 12-13, 18-23, and 25 are: ○ : Spumellaria; ■ : Nassellaria; and ☆ : Phaeodaria. 85

Figure 13. Plot of width vs. weight/shell. See Figure 12 for the legend of symbols. 86

Figure 14. Plot of projected area vs. weight/shell. Symbols are the same as in Figure 12 except that all the open symbols are for observed projected areas and black ones are for computed projected areas. 87

Figure 15. Plot of width vs. length for 927 data points of Radiolaria including 58 taxa. Symbols used in Figures 15-17 are: * : One datum point; numerals 2-8 correspond to number of data points superimposed; numeral 9: 9 or more of data points superimposed. 88

Figure 16. Plot of projected area vs. length for 724 data points of Radiolaria including 53 taxa. See Figure 15 for the legend of symbols. 89

Figure 17. Plot of projected area vs. width for 344 data points of Radiolaria including 35 taxa. See Figure 15 for the legend of symbols. 90

Figure 18. Plot of sinking speed in 3°C still water vs. length. See Figure 12 for the legend of symbols. 94

Figure 19. Plot of sinking speed in 3°C still water vs. width. See Figure 12 for the legend of symbols. 95

Figure 20. Plot of sinking speed in 3°C still water vs. projected area. The legend of symbols are basically the same as in Figure 12. Open and solid symbols represent measured and computed projected areas respectively. 96

LIST OF FIGURES (cont.)

Page

Figure 21. Plot of sinking speed in 3°C still water vs. weight/shell. See Figure 12 for the legend of symbols. 97

Figure 22. Plot of sinking speed in 10°C still water vs. weight/shell. See Figure 12 for the legend of symbols. 98

Figure 23. Plot of sinking speed in 20°C still water vs. weight/shell. See Figure 12 for the legend of symbols. 99

Figure 24. Plot of sinking speed in 3°C still water vs. density contrast, $\Delta\rho$. See Figure 12 for the legend of symbols. 102

Figure 25. Plot of the residual factor (W_{obs}/W_{theor}) vs. average diameter using either or both length and width. The horizontal dashed line represents theoretical values using Stokes equation. Only 3 different shapes are separated since further divisions do not improve the understanding of sinking speed governing factors. Symbols: ◉ : spherical group (sphere, ellipsoidal, hemispherical, cylindrical and box in the APPENDIX Table 1); □ : discoidal group (discs and plates); ☆ : Conical group (conical and pyramidal; this group includes only nassellarians). 104

Figure 26. Plot of residence time (τ_1) vs. weight/shell. See Figure 12 for the legend of symbols. 106

Figure 27. Plot of residence time (τ_2) vs. weight/shell. A regression line for τ_3 is almost superimposed upon that of τ_2 and hence not drawn here. See Figure 12 for the legend of symbols. Additional symbols used: ◔ : Spumellarian τ_3; ▣ : Nassellarian τ_3; ☆ : Phaeodarian τ_3. 107

Figure 28. Percent contribution of Phaeodaria to radiolarian SiO_2 flux at Station PB which represents the highest phaeodarian SiO_2 flux among all Stations. Note that phaeodarian SiO_2 flux is ca. 20 % while their counts are only ca. 6 % of Radiolaria (Table 5). 114

Figure 29. Simplified illustration depicting depth of production, sinking, dissolution and preservation of Spumellaria, Nassellaria and Phaeodaria in a pelagic realm. 115

LIST OF TABLES

Page

Table 1. Size of aliquot in each microslide relative to total sediment trap samples. Number of slides used for counts is also presented. 19

Table 2. The radiolarian (species) flux (no. of shells/m^2/day) at three sediment trap stations. Data reported here include all size fractions from <63 µm to 1mm-250 µm. 25

Table 3. The size fractioned radiolarian flux (no. of shells/m^2/day), in each family from Station E. The proportion of counted specimens (%) with respect to the radiolarian flux (shells/m^2/day) is given in the bottom row. 43

Table 4. The size fractioned radiolarian flux (no. of shells/m^2/day) in each family from the sediment trap stations P_1 and PB. The proportion of counted specimens (%) with respect to the radiolarian flux is given in the bottom row of each station. 44

Table 5. Summary of radiolarian (suborders) flux (no. shells/m^3/day) and ratios between suborders at the three sediment trap stations. 48

Table 6. Diversity indices of Radiolaria and their suborders from Station E. 53

Table 7. Percent similarity between depths of Radiolaria and their suborders from Station E. 53

Table 8. Percentages of broken shells and shells in biogenic aggregates in total counts of a given taxon of Radiolaria from Station E. 58

Table 9. Radiolarians from the sediment traps; size, laboratory sinking speed and residence time in the water column. The S.D. is at 95% confidence level (2σ) and n is number of measurements (specimens). See text for explanations for τ_n. 74

Table 10. Logarithmic relationships between variables of Radiolaria. Mean values of the variables are used unless otherwise stated. 82

Table 11. Silica content in selected radiolarian species from the sediment traps. 92

Table 12. Estimation of standing stock, rate of production and turnover time of selected radiolarian species and three suborders. 110

LIST OF TABLES (cont.)

Page

Table 13. An extent of biogenic opal transport to the deep-sea by radiolarians. The values correspond to mid pointsof ranges. 113

Table 14. Estimation of excess Si in the deep waters of the western North Atlantic. 117

CHAPTER 1

VERTICAL FLUX, ECOLOGY, RESIDENCE TIME AND DISSOLUTION OF RADIOLARIA: IMPLICATIONS FOR THE SILICA CYCLE

INTRODUCTION

Biogenic opal is one of the major sedimentary components in the oceans. It is particularly abundant in pelagic realms where little is influenced by land derived minerals. Constituents of biogenic opal are skeletons of radiolarians, diatoms, silicoflagellates, sponge spicules, ebridians, and dinoflagellate endoskeletons. The biomass of the first four groups of particles are more abundant in pelagic oceans than the others.

Silica budget in the ocean with respect to river input, continental weathering, diffusion from the bottom sediments and hydrothermal input has been approximately estimated and the major role of biogenic opal in the oceanic silica budget has become known in recent years (Schutz and Turekian, 1965; McKenzie and Garrels, 1966; Calvert, 1968, 1974; Lisitzin, 1972; Burton and Liss, 1973; Hurd, 1973; Edmond, 1973; Edmond et al., 1979; Heath, 1974; Kharkar et al., 1969; DeMaster, 1979).

It is generally known that biogenic opal remains contribute substantially to the three major latitudinal belts of siliceous sediments in the world oceans. According to Lisitzin (1972), radiolarians account for 62 and 99 weight % of the biogenic opal suspension in the tropical Pacific. Hence they are the major sedimentary components of biogenic opal in such regions. On the other hand, diatoms account for 99.8% in the Antarctic seas.

Since preservation of biogenic opal in the bottom sediments is principally a reflection of the rate of organic production in the overlying waters (Riedel, 1959; Heath, 1969), biogenic opal may retain more oceanic environmental records than other sedimentary counterparts such as carbonate. However, the processes of biogenic opal sedimentation are poorly known. Berger's (1970) basin-basin fractionation model predicts that the Atlantic Ocean, in general, is the least favorable of the three major oceans for preservation of biogenic opal. Indeed, radiolarians in the surface sediments in the Atlantic (Goll and Bjørklund, 1971, 1974) occur generally in smaller numbers per unit weight of sediment than in the Pacific (Lisitzin, 1972). The description of radiolarian remains subsequent to their production and pre-burial is an important approach to understanding the geological and geochemical processes of oceanic opal. Previously, Heath (1974) pointed out that ecological studies of radiolarians bear a key to understanding the silica cycle in the oceans.

Geochemical studies, mainly based on dissolved silicon-alkalinity correlation, indicate that most of the dissolution of biogenic opal occurred on the sea-floor rather than in the water column (Edmond, 1974). Heath (1974) suggested that the major non-oxidative dissolution of biogenic opal occurred on the sea-floor, rather than in the water column. Lisitzin (1972) suggested that the dissolution of radiolarians and silicoflagellates occurred on the sea-floor, whereas most of the diatoms were destroyed in the water column. Previously, Kozlova (1964) studied distribution of diatom frustules throughout the water column and in the sediments of the Antarctic region and showed that only a few diatoms reach the benthic layers. Kanaya and Koizumi (1966) showed that diatom assemblages in the surface sediments in their North Pacific stations reflected the planktonic assemblages in the overlying surface layer. Skeletons of silicoflagellates have been regarded as less important than radiolarians and diatoms in terms of quantitative siliceous sedimentation (Lisitzin, 1972). Silicoflagellates are considered to be more susceptible to dissolution among other opaline particles (Schrader, 1972). Those previous discussions were based on the distribution of suspended biogenic opal particles utilizing an instantaneous standing crop. Those views can be further examined by studying the flux of settling particles which are collected by sediment traps.

Sedimentation of material by large size particles such as fecal pellets has been recently realized (Schrader, 1971; McCave, 1975; Honjo, 1975, 1976, 1978, 1980; Wiebe et al., 1976). Particles larger than 20 μm are rare (e.g. Carder et al., 1971; Sheldon et al., 1967) and they have a statistically low probability of being caught in standard-size water samplers. Even when large particles are caught, they may be extracted due to the design of water samplers and methods of filtration (Gardner, 1977a). This is particularly true for radiolarian shells which are relatively large.

It has been documented that sediment trapping is an efficient method for collecting vertically settling large particles and to approximately determine material fluxes of large particles (e.g. Wiebe et al., 1976; Gardner, 1977b; Soutar et al., 1977; Spencer et al., 1978; Honjo, 1978, 1980; Honjo et al., in press; Brewer et al., 1980; Knauer et al., 1979; Cobler and Dymond, 1980; Sediment Trap Intercomparison Experiment, 1980). The majority of biogenic opal particles, such as radiolarians, diatoms and silicoflagellates, are usually larger than 30-40 μm size; hence they are considered to be large particles or "settling particles" (Honjo, 1980).

Biogenic opal production has been crudely estimated (Lisitzin, 1972; Heath, 1974; Thomas and Dodson, 1974) by a conversion from organic carbon to silica which is based upon an assumption of silica/carbon conversion factor 2.3 (Lisitzin et al., 1967). However, the factor actually varies as large as two to three orders of magnitude depending on the latitude (Lisitzin et al., 1967). An alternative method is a stable isotope tracer method (Nelson and Goering, 1977) but this method has been applied only to primary producers (mainly diatoms) thus far. Vertical flux measurements will furnish important information for production, especially for dissolution resistant taxa. Since radiolarians are, as stated earlier, the most important taxa in biogenic opal production in the tropical oceans (Lisitzin, 1972), radiolarian flux information is most desired for understanding the biogenic opal production for the areas.

Detailed studies on radiolarian population in pelagic environments have been made by many investigators since the classical work by Haeckel

(1887) in the 19th century (e.g. Casey, 1971a, 1971b; Casey et al., 1971, 1979a, 1979b; Petrushevskaya, 1971a, 1971b; Bjørklund, 1974; Kling, 1976, 1979; Renz, 1976; McMillen and Casey, 1978; Leavesley et al., 1978; Boltovskoy and Riedel, 1980; Takahashi and Honjo, 1980, 1981a-c; Takahashi et al., 1981a,b). Renz (1976) compared the living radiolarian community (using plankton pumps and net tow samples) and its counterpart in core tops from the central Tropical Pacific. She reported an elimination of many radiolarian species during their transfer from the living layer to the underlying sediment layer. Petrushevskaya (1971a) did not find that many discrepancies between the two assemblages. However, net towed, cast or pumped samples applied in previous research may involve time and/or space limitations and may not represent realistic biocoenosis.

In this thesis the vertical fluxes of Radiolaria at 4-5 depths from three tropical PARFLUX sediment trap stations (Fig. 1) are quantitatively documented together with a qualitative notion from a temperate station, Sargasso Sea. The flux data are combined with other relevant measurements which are described in detail in the text in order to facilitate pertinent information on the silica cycle.

SOURCE OF SAMPLES; METHOD OF ANALYSIS

The samples used in this study were collected from sediment traps placed at four PARFLUX stations (Fig. 1): Western Tropical Atlantic - Station E, 13°30.2'N, 54°.1'W, corrected water depth: 5,288 m; central Tropical Pacific - P_1: 15°21.1'N, 151°28.5'W, 5792 m; Panama Basin - PB: 5°21'N, 81°53'W, 3856 m; Sargasso Sea - S, 31°32.5'N, 55°55.4'W, 5581 m. These sediment traps were deployed for 98 days (E: 11/1977-2/1978), 61 days (P_1: 7-11/1978), 112 days (PB: 8-12/1979) and 110 days (S: 10/1976-1/1977) (Honjo, 1978, 1980; Honjo et al., 1980). Station E is located about 750 km from the Guyana Coast in a region where there is very little seasonal variation in zooplankton productivity (e.g. Moore and Sander, 1977). The underlying Demerara Abyssal Plain has a gentle topography and is covered with silty clay.

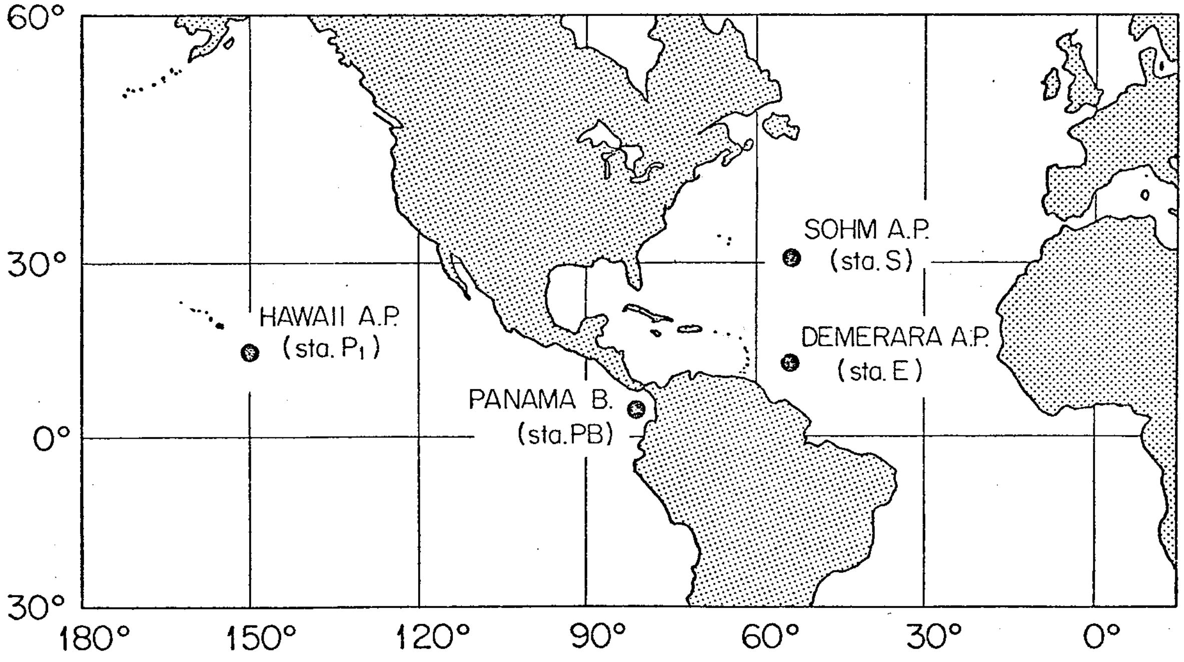

Figure 1. Locations of the PARFLUX sediment trap stations.

Table 1. Size of aliquot in each microslide relative to total sediment trap samples. Number of slides used for counts is also presented.

Station/Depth (m)	Size fraction (μm) 1000-250	250-125	125-63	<63
E389	1/256	1/1024	1/1024	1/8000
988	1/256	1/1024	1/1024	1/8000
3755	1/256	1/1024	1/1024	1/8000
5068	1/256	1/1024	1/1024	1/8000
for statistical assessment at each four depths	1/256	4x1/1024	4x1/1024	2x1/8000
PB667	2x1/4086	1/1024	1/1024	2x1/16384
1268	1/1024	1/1024	1/1024	2x1/4096
2869	2x1/4096	1/1024	1/1024	2x1/16384
3769*	2x1/4096	2x1/4096	2x1/4096	2x1/16384
3791	1/1024	1/1024	1/1024	2x1/16384

Station/Depth (m)	Size fraction (μm) 1000-250	250-63	<63
$P_1$378	1/256	1/256	1/256
978	1/256	1/256	1/256
2778	1/256	1/256	1/1024
4280	1/256	1/256	1/1024
5582	1/256	1/256	1/1024

* Studied only for Phaeodaria

The North Equatorial Current flows in a northwesterly direction, but no deep current measurements have been reported in the study area. Station P_1 is located in the East Hawaii Abyssal Plain which is one of the largest basins in the North Pacific. The bottom sediment is consolidated clay with alternating thin ferro-manganese laminations (Honjo, 1980). Station PB is characterized by high productivity and is relatively close to land (250 km from the nearest shoreline). The Panama Basin has been defined by Heath et al. (1974) as a "mini ocean". Hydrography, geology, biology and physical oceanography are quite well known in this area (e.g. Stevenson, 1970; van Andel, 1973; Kowsman, 1973; Moore et al., 1973; Plank et al., 1973; Heath et al., 1974; Lonsdale, 1975, 1977; Swift, 1977; Swift and Wenkam, 1978).

The sediment trap array deployed at the above stations consisted of four or five traps, PARFLUX Mark II, with 1.5 m^2 opening (Honjo et al., 1980) and they were moored at several depths (Table 1). The receiving cup was sealed by a time-controlled spring shutter prior to recovery.

The samples were wet sieved upon arrival in the laboratory with a 1 mm mesh screen and split into four aliquots by an Erez-Honjo precision rotary liquid splitter (Honjo, 1978). An aliquot of material finer than 1 mm was further split into several aliquots (Table 1). The resulting aliquot of the original sample was wet sieved through 250, 125 and 63 μm screens. When necessary the samples were split further into smaller aliquots prior to filtration (Table 1). Samples of less than 63 μm size fraction from Station E are separately prepared by diluting a 1/64 aliquot to 250 ml in a measuring flask using filtered seawater from the deep Sargasso Sea water, and then 2 ml aliquot was taken by using a pipet.

The above aliquots were filtered through a 47 mm HA Millipore® grid filter with a nominal 0.45 μm pore size using a rectangular filtration funnel with 19 x 42 mm opening. The residue was rinsed with distilled water, then dried at 50°C in an oven. Large foraminiferal specimens in 1,000-250 μm and 250-125 μm size fractions were removed under a dissecting microscope. The dried filter sample was mounted on a standard glass slide after trimming off the excess margins. Drops of Cargile® type B compound was applied to clear the sample filter. It took a few days for the bubbles to escape from all radiolarian shells prior to placing a cover glass over the sample area. No vacuum was applied during the preparation. Aliquot size and number of slides from the three stations which were used in this paper are summarized in Table 1.

The slides were studied to identify radiolarian taxa and to count individuals to the species level, under a transmission light microscope. Two or more of slides shown in Table 1 were used for the species identification (Pls. 1-63). The counts were converted to the flux term; number of individual shells/m^2/day.

An abundant, medium sized radiolarian genus, Pterocorys (P. campanula Haeckel: Plate 42, fig. 5-8; and P. zancleus (Müller): Plate 42, figs. 1-4) was chosen in order to assess the range of errors induced during sample preparation, and the reproducibility of shell counting. The assessment was made by counting Pterocorys shells in a given slide. This taxon occurs mostly in 250-125 μm and 125-63 μm size fractions. The counting reproducibility by duplicate countings of an identical slide proved to be more than 90%. Statistical variablity among four slides prepared from the coarse and medium size fractions is due to errors involving slide preparation including wet sieving and splitting. The standard deviation ranged from 0.14 to 0.26 at 95% confidence interval. The radiolarian species count applied in this dissertation is reproducible to better than 74%.

To prepare enough handpicked specimens for dimension, sinking speed, electron microscopy and SiO_2 content analyses, aliquots of 1/64 or 1/256 of wet samples from the sediment trap are sieved and desalted by the same method as above. Purple grid 47 mm HA millipore® filters with 0.45 μm pore size, are used to retain radiolarian samples. After drying, as many specimens of radiolarian taxa as possible are handpicked using an ultrafine Japanese calligraphy brush.

Reflected light micrographs are taken at x20 and x40 magnification of a dissecting microscope for each taxa. The micrographs are converted to positive slides and projected onto an image digitizer (LW International) for measurements of length, width and maximum projected area. The obtained data are processed by a computer applying the SPSS Program.

After the photography, specimens were dried in high vacuum at 150°C for 2 days, then cooled in a desicator for 10 minutes and quickly weighted. A Cahn 25 Automatic Electrobalance® was used in a room with humidity of less than 40 %. The number of specimens needed for this varies depending on weight/shell of different taxa which is presented in Table 9.

A portion of the picked specimens were mounted on an Aluminum stub with double-sided adhesive tape and coated with carbon and then Pd-Au for scanning electron microscopy (SEM). Samples for transmission electron microscopy were prepared by the method described by Asper (1981).

Silica content of the radiolarian skeletons was measured by Na_2CO_3 fusion method (Kido and Nishimura, 1975) modified by Asper (1981). Several to several tens or more of the radiolarian specimens (see Table 11) were weighed and placed in clean platinum crucibles and excess anhydrous Na_2CO_3 (ca. 15 mg) was added. The crucible was heated over a burner for 15 minutes to fuse the radiolarian silica in the molten Na_2CO_3. After cooling, the pellet of fused Na_2CO_3 sample was dissolved in distilled water in 10 ml volumetric flask. Then the standard silicomolybdate colorimetric method (Strickland and Parsons, 1972) was followed. The experimental errors were less than 8%.

To eliminate entrapped air within the shell structure during sinking speed measurement, the dry specimens are placed in 1 cm diameter with 2.5 cm height plastic vials. Methanol is added and the specimens are kept in a low vacuum for an overnight. About 20% of the methanol is replaced with an equivalent volume of filtered water by using a micropipet. After several hours the same procedure was repeated for a total of ten times; each time there was a gradual increase of the replacement volume of filtered water to completely replace the methanol. Then, Sargasso Sea water is used as a replacement by the same procedure. By the end of this process generally 80% or more of the specimens are maintained in the vial.

As illustrated in Figure 2, the system for the sinking speed experiment consisted of: (a) a narrow-neck graduated cylinder for the sinking column, 2.5 cm diameter, 16 cm high, Pyrex; (b) a temperature

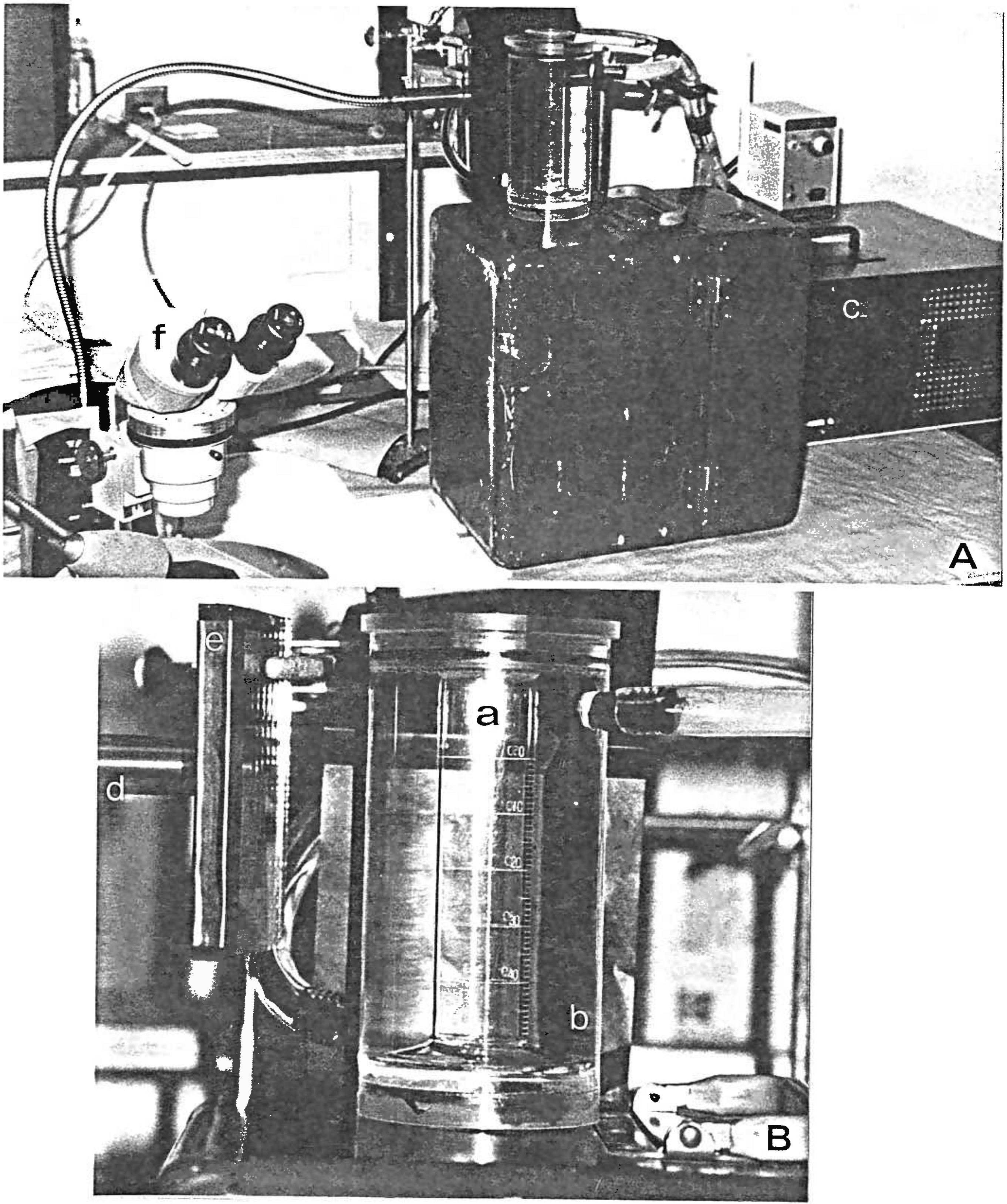

Figure 2. A. Illustration of a system for the sinking speed experiment. B. An enlarged view of the sinking column. a. narrow-neck cylinder, b. temperature bath cylinder, c. thermostat, d. fiberglass optics, e. thermal filters f. disecting microscope.

bath cylinder, 87 mm outer diameter with 6 mm-thick plexiglass (plastic), 18 cm high, closed by a lid with an O-ring and connected to a thermostat with plastic hoses; (c) a thermostat which controls the temperature up to ± 0.5°C; (d) a mobile illumination device of fiberglass optics; (e) thermal filters; (f) a dissecting microscope; and (g) a sheet of black background paper. The experiment was conducted in a dark room with the illumination device in order to enhance visibility with Tindal effect. The sinking column system was designed to become a lens (Figure 2B) so that a sinking specimen can be readily located without using a microscope. Since the plexiglass has poor thermal conductivity the plastic surface did not have water molecule condensation at 3°C under normal laboratory temperature and humidity. Temperature of the inner seawater column equilibrated with the circulating water in the outer column within an hour. The seawater column was examined for stability by using a dye and a satisfactory result for the sinking speed experiment was obtained.

A wet specimen, retained in a water drop, is individually picked using a brush, then placed just below the surface of the still seawater column. The temperature of the specimen generally equilibrates with the surrounding water within a few seconds according to heat flux calculations. The specimen usually reaches a steady settling rate well above a start-line of the measurement. The start-line is located 51 mm below the surface and a finish-line is located 23 mm from the bottom. The measured sinking time for an 83 mm interval is converted to m/day. Generally the particles sink through the center of the column but occasionally their pathways go off the centerline and drag the side wall in which case the data are discarded.

RESULTS AND DISCUSSION

Counts of radiolarian taxa

The majority of radiolarian specimens found in the slide samples were identified to the species level (Table 2, pls. 1-63). A total of 420

(cont. to p. 51)

Table 2. The radiolarian (species) flux (no. of shells/m^2/day) at three sediment trap sations. Data reported here include all size fractions from 63 um to 1mm-250 um.

Sediment Trap Station	E				P_1					PB			
Depth (m)	389	988	3755	5068	378	978	2778	4280	5582	667	1268	2869	3791
Suborder SPUMELLARIA Ehrenberg													
Family COLLOSPHAERIDAE Muller													
Acrosphaera spinosa (Haeckel)	10	58	65	116	0	6	28	31	25	0	49	12	12
Acrosphaera murrayana (Haeckel)	0	0	0	0	0	0	0	6	0	12	43	104	67
Acrosphaera cyrtodon (Haeckel)	0	0	0	0	0	0	0	0	0	0	0	0	0
Clathrosphaera arachnoides Haeckel	0	0	0	0	0	0	0	0	0	0	0	0	0
Collosphaera tuberosa Haeckel	19	9	31	29	0	8	53	34	31	98	37	110	61
Collosphaera confossa n.sp. + *C. armata* Brandt	0	0	0	0	0	0	19	8	31	30	6	24	43
Collosphaera huxleyi Muller	5	46	107	38	3	17	65	53	56	0	0	18	18
Collosphaera macropora Popofsky	0	0	0	0	39	36	81	107	123	55	37	98	73
Collosphaera polygona Haeckel	0	0	0	0	0	0	0	0	0	0	0	0	0
Disolenia collina (Haeckel)	0	0	0	0	6	0	17	0	8	0	0	0	0
Disolenia zanguebarica (Ehrenberg)	0	0	0	0	3	11	14	36	31	0	24	6	0
Disolenia quadrata (Ehrenberg)	0	0	0	0	0	14	34	45	22	0	0	0	0
Disolenia sp. A	0	0	0	0	0	0	0	0	0	0	0	0	0
Disolenia sp. B	0	0	0	0	3	0	0	0	0	0	0	18	0
Otosphaera tenuissima Hilmers	0	0	0	0	0	0	0	0	0	0	0	0	0
Otosphaera polymorpha Haeckel	40	29	40	29	0	14	75	53	95	24	6	18	18
Otosphaera auriculata Haeckel	0	0	0	0	0	0	0	0	0	0	0	0	0
Siphonosphaera magnisphaera n.sp.	0	0	0	0	6	0	8	11	14	18	0	0	6
Siphonosphaera sp. A	0	0	0	0	0	0	0	0	0	0	0	0	0
Siphonosphaera martensi Brandt	0	0	0	0	14	34	95	73	28	6	6	48	18
Siphonosphaera sp. B	0	0	0	0	0	0	0	0	0	0	0	0	0
Siphonosphaera sp. aff. *S. hippotis* (Haeckel)	0	0	0	0	0	0	0	0	0	0	0	0	0
Siphonosphaera socialis Haeckel	19	15	19	26	6	11	34	22	31	0	12	6	6
Total COLLOSPHAERIDAE	88	111	155	200	80	151	523	479	495	243	220	462	322
Family SPHAEROZOIDAE Haeckel													
Rhaphidozoum pandora Haeckel***	86	71	63	12	0	0	0	0	0	12	0	0	0
Total SPHAEROZOIDAE	86	71	63	12	0	0	0	0	0	12	0	0	0

Sediment Trap Station	E				P$_1$					PB			
Depth (m)	389	988	3755	5068	378	978	2778	4280	5582	667	1268	2869	3791
Family ETHMOSPHAERIDAE Haeckel													
Plegmosphaera pachypila Haeckel	74	74	162	143	0	0	0	0	0	0	0	0	0
Plegmosphaera coelopila Haeckel	0	0	0	0	0	0	0	0	0	0	0	0	0
Plegmosphaera sp. aff. P. lepticali Renz	0	0	0	0	0	0	0	0	0	48	49	79	73
Plegmosphaera sp. A	0	0	0	0	0	0	0	0	0	0	0	0	0
Plegmosphaera sp. B	0	0	0	0	0	0	0	0	0	0	0	0	0
Plegmosphaera entodictyon Haeckel	0	0	0	0	0	0	0	0	0	61	110	213	140
Plegmosphaera oblonga n.sp.	0	0	0	0	0	0	0	0	0	0	0	0	0
Plegmosphaera lepticali Renz	21	0	15	18	0	0	20	17	8	0	0	0	0
Plegmosphaera pachyplegma Haeckel	0	0	0	0	0	0	0	0	0	0	18	12	0
Styptosphaera spongiacea Haeckel	0	0	0	0	0	0	3	28	20	24	30	91	134
Styptosphaera sp. A	0	0	0	0	0	0	0	0	0	0	0	0	0
Styptosphaera sp. B	0	0	0	0	0	0	0	0	0	0	0	0	0
Styptosphaera sp. C	0	0	0	0	0	0	0	0	0	0	0	0	0
Thecosphaera capillacea Haeckel	0	0	0	0	0	0	0	0	0	0	0	0	0
Theocosphaera inermis (Haeckel)	251	58	409	194	0	6	6	59	8	0	18	12	6
Carposphaera sp. aff. C. corypha Haeckel	0	0	0	0	0	0	0	0	0	0	0	0	0
Total ETHMOSPHAERIDAE	346	132	586	355	0	6	29	104	36	133	225	407	353
Family ACTINOMMIDAE Haeckel, emend. Riedel													
Subfamily ACTINOMMINAE Haeckel, emend. herein													
Centrocubus cladostylus Haeckel	3	0	3	14	0	0	0	0	0	0	0	0	0
Centrocubus octostylus Haeckel	0	0	0	0	0	0	11	0	3	0	0	0	0
Spongosphaera polycantha Muller	0	0	0	0	0	0	0	0	0	0	0	0	0
Spongosphaera sp. aff. S. helioides Haeckel	0	0	0	0	0	0	0	0	0	0	0	0	0
Spongosphaera streptacantha Haeckel	0	0	0	0	0	0	0	0	0	0	0	0	0
Spongosphaera ? sp. B	0	0	0	0	0	0	0	0	0	0	0	0	0
Lynchnosphaera regina Haeckel	0	0	0	0	0	0	0	0	0	0	6	0	6
Actinomma acadophorum Haeckel	56	40	56	65	0	0	36	22	17	110	116	152	91
Actinomma capillaceum Haeckel	0	0	0	0	0	0	0	0	0	24	6	0	0
Actinomma sp.	0	0	0	0	0	0	0	0	0	0	0	0	0

Sediment Trap Station	E				P_1					PB			
Depth (m)	389	988	3755	5068	378	978	2778	4280	5582	667	1268	2869	3791
Trilobatum ? *acuferum* Popofsky	238	58	673	437	3	112	213	196	171	201	262	256	274
Acanthosphaera actinota (Haeckel)	49	33	81	62	0	28	45	42	62	122	73	140	122
Acanthosphaera tunis Haeckel	0	0	0	0	0	0	0	0	0	12	0	0	0
Acanthosphaera castanea Haeckel	0	0	0	0	0	0	17	22	3	0	0	0	0
Acanthosphaera simplex ? (Haeckel)	0	0	0	0	0	0	0	0	0	0	0	0	0
Heliosphaera radiata Popofsky	10	15	12	9	0	0	3	0	0	0	0	0	0
Cladococcus viminalis Haeckel	0	0	0	0	0	0	0	0	0	0	0	0	0
Cladococcus abietinus Haeckel	0	3	18	2	0	0	3	0	0	12	6	0	0
Cladococcus scoparius Haeckel	5	2	7	14	0	8	14	8	8	49	43	61	61
Cladococcus cervicornis Haeckel	0	0	0	0	0	3	31	22	3	238	238	360	256
Arachnosphaera sp.	0	0	0	0	0	0	0	0	0	0	0	0	0
Arachnosphaera myriacantha Haeckel	21	12	37	23	0	3	3	3	3	49	55	110	104
Leptosphaera minuta ? Popofsky	0	0	0	0	0	0	0	0	0	0	0	0	0
Leptosphaera sp. group	38	45	72	138	0	0	62	42	31	18	6	0	0
Actinosphaera tenella (Haeckel)	0	0	0	0	0	0	0	0	0	0	0	0	0
Actinosphaera acanthophora (Popofsky)	0	0	0	0	0	0	0	0	0	0	0	0	0
Actinosphaera capillacea (Haeckel)	0	0	0	0	0	0	0	0	0	0	0	55	91
Haliomma ? sp.	0	0	0	0	0	0	0	0	0	0	0	0	0
Haliomma castanea Haeckel	0	0	0	0	0	3	8	3	6	0	24	6	43
Heliosoma spp. aff. *radians* Haeckel	0	0	0	0	0	0	0	0	0	0	0	0	0
Elatomma penicillus Haeckel	0	0	0	0	0	0	0	0	0	0	0	0	0
Elatomma pinetum Haeckel	0	0	0	0	0	0	0	0	0	0	0	0	0
Astrosphaera hexagonalis Haeckel	5	5	16	0	0	0	20	14	0	164	152	268	305
Drymosphaera dendrophora Haeckel	0	0	0	0	0	0	0	0	0	0	0	0	0

Sediment Trap Station	E				P_1					PB			
Depth (m)	389	988	3755	5068	378	978	2778	4280	5582	667	1268	2869	3791
Sphaeropyle mespilus Dreyer	0	0	0	0	0	0	0	0	0	0	0	0	0
Cromyomma villosum Haeckel	0	0	0	0	0	0	0	0	0	0	0	0	0
Xiphosphaera gaea Haeckel	0	0	0	0	0	0	0	0	0	0	0	0	0
Xiphosphaera tesseractis Dreyer	2	0	5	2	0	0	11	14	6	0	0	0	0
Staurolonche sp. A group	79	30	33	33	0	11	8	6	8	36	18	6	37
Staurolonche sp. B	2	16	19	14	0	0	0	3	0	12	0	0	6
Stauracontium sp.	9	0	0	0	0	0	0	0	0	0	12	43	12
Hexastylus triaxonius Haeckel	0	0	0	0	0	0	0	0	0	0	0	0	0
Hexastylus sp.	0	0	0	0	0	0	0	0	0	0	0	0	0
Hexalonche sp. A	0	0	0	0	0	0	0	0	0	0	0	0	0
Hexalonche spp. B	47	42	139	80	6	8	14	8	14	18	61	73	91
Centrolonche hexalonche Popofsky	0	3	5	5	0	3	25	8	11	0	0	0	0
Cetracontarium hexacontarium Popofsky	21	23	16	12	0	0	0	0	0	0	0	0	0
Hexacontium sp.	0	0	0	0	0	0	0	0	0	0	0	0	0
Hexacontium amphisiphon Haeckel	0	0	0	0	0	0	0	0	0	0	0	0	0
Hexacontium hostile Cleve	0	0	0	0	0	0	0	0	0	0	0	0	0
Hexacontium arachnoidale Hollande and Enjumet	0	0	0	0	0	0	0	0	0	0	0	0	6
Hexacontium axotrias Haeckel	22	33	71	21	3	67	131	156	112	153	134	134	177
Hexacontium sp. aff. H. hostile Cleve	0	0	0	0	0	0	0	0	0	0	0	0	0
Hexacontium heracliti (Haeckel)	0	0	0	0	0	0	0	3	0	6	6	6	6
Hexacontium hystricina (Haeckel)	0	0	0	0	0	0	0	0	0	0	0	0	0
Hexacromyum elegans Haeckel	0	16	5	7	0	0	3	0	0	0	6	0	30
Heterosphaera sp. A	0	0	0	0	8	17	47	22	36	0	37	55	73
Heterosphaera sp. B	0	0	0	0	0	0	0	0	0	0	0	0	0
Cromyechinus sp. aff. C. borealis (Cleve)	0	3	0	0	0	0	0	0	0	0	0	0	0
Cromyechinus ? sp.	0	0	0	0	0	3	6	3	0	12	6	0	0
Cromyechinus borealis (Cleve)	0	0	0	0	0	3	0	6	3	0	0	0	0
Stomatosphaera sp. A	0	0	0	0	0	0	0	0	0	0	0	0	0
Stomatosphaera sp. B	0	0	0	0	0	0	0	0	0	0	0	0	0
Stomatosphaera sp. C	0	0	0	0	0	0	0	0	0	0	0	0	0

Sediment Trap Station	E				P$_1$					PB			
Depth (m)	389	988	3755	5068	378	978	2778	4280	5582	667	1268	2869	3791
Stylacontarium bispiculum Popofsky	0	0	0	0	6	14	50	48	64	30	49	67	91
Stylosphaera ? sp. A	0	0	0	0	0	0	0	0	0	0	0	0	0
Stylosphaera melpomene Haeckel	132	64	52	110	0	0	3	0	11	0	12	12	12
Stylosphaera ? sp. B	0	0	0	0	0	0	0	0	0	0	0	0	0
Stylosphaera lithatractus Haeckel	0	7	89	166	0	3	28	6	6	0	61	91	79
Druppatractus ostracion Haeckel group	0	0	0	0	0	0	0	0	0	0	0	0	0
Ellipsoxiphium palliatum Haecker	0	0	0	0	0	0	0	0	6	0	0	0	0
Amphisphaera group	0	0	0	0	3	0	0	6	6	0	0	0	0
Axoprunum stauraxonium Haeckel	0	0	0	0	0	0	0	0	0	0	0	0	0
Xiphatractus pluto (Haeckel)	0	2	57	26	0	6	0	0	8	0	0	6	0
Xiphatractus sp. A	0	0	0	0	0	0	0	0	0	0	0	0	0
Xiphatractus spp. B	0	0	0	0	0	0	0	0	0	0	0	0	0
Druppatractus ? sp.	0	0	0	0	0	0	0	0	0	0	0	0	0
Dorydruppa bensoni, new name	0	0	0	0	0	0	0	8	3	0	12	43	18
Total ACTINOMMINAE	739	452	1466	1240	29	292	792	671	601	1266	1401	1944	1991
Subfamily SATURNALINAE Deflandre													
Saturnalis circularis Haeckel	0	0	0	0	0	0	0	0	0	0	0	0	18
Total SATURNALINAE	0	0	0	0	0	0	0	0	0	0	0	0	18
Total ACTINOMMIDAE	739	452	1466	1240	29	292	792	671	601	1266	1401	1944	1911
Family COCCODISCIDAE Haeckel, emend. Sanfilippo and Riedel.													
Subfamily ARTISCINAE Haeckel, emend. Riedel													
Didymocyrtis tetrathalamus tetrathalamus (Haeckel)	125	177	197	176	0	67	201	224	241	54	73	146	104
D. tetrathalamus tetrathalamus (Hkl) juvenile form	-	-	-	-	6	25	107	44	93	0	6	12	6
Didymocyrtis sp.	0	0	0	0	0	0	0	0	0	0	0	0	0
Spongoliva ellipsoides Popofsky	15	18	5	0	3	6	8	8	0	0	0	55	12
Total COCCODISCIDAE	140	185	202	176	9	98	316	276	334	54	79	213	122

Sediment Trap Station	E				P$_1$					PB			
Depth (m)	389	988	3755	5068	378	978	2778	4280	5582	667	1268	2869	3791
Family PORODISCIDAE Haeckel, emend. Petrushevskaya and Kozlova													
Euchitonia elegans (Ehrenberg)	26	39	68	57	3	22	50	48	45	55	55	189	177
Euchitonia cf. furcata Ehrenberg	106	32	128	46	0	0	36	50	48	0	6	0	0
Euchitonia sp.	0	0	0	0	0	8	22	28	45	0	0	0	0
Amphirhopalum ypsilon Haeckel	0	0	7	3	0	0	0	0	0	12	6	18	37
Amphirhopalum straussii (Haeckel)	0	0	0	0	0	0	0	0	3	0	0	0	0
Stylodictya validispina Jorgensen	0	0	0	0	0	0	0	0	0	0	0	0	0
Stylodictya ? sp.	0	0	0	0	3	81	218	293	280	397	433	689	615
Stylodictya multispina Haeckel	0	0	0	0	0	3	3	22	25	0	0	0	18
Circodiscus spp. group	0	0	36	16	0	3	0	0	0	6	24	0	18
Stylochlamydium venustum (Bailey)	0	0	0	0	0	0	0	0	0	0	0	0	0
Stylochlamydium asteriscus Haeckel	121	72	55	91	8	20	109	129	76	153	122	287	219
Porodiscus micromma (Harting)	76	160	257	114	0	0	34	39	64	18	55	103	140
Total PORODISCIDAE	329	303	551	327	14	137	472	609	586	641	701	1286	1224
Family SPONGODISCIDAE Haeckel, emend. Riedel, + Petrushevskaya and Kozlova													
Spongobrachium sp.	0	0	0	0	0	0	0	14	8	0	0	0	0
Dictyocoryne profunda Ehrenberg	81	72	126	102	0	8	31	22	70	6	61	30	79
Dictycoryne truncatum (Ehrenberg)	0	0	0	0	0	3	3	11	6	24	37	0	30
Spongodiscus sp. A	0	0	0	0	0	0	14	17	0	24	43	30	67
Spongodiscus biconcavus Haeckel	0	0	0	0	0	0	0	0	0	0	0	0	0
Spongodiscus resurgens Ehrenberg	*	*	*	*	0	0	3	0	17	49	67	110	98
Spongodiscus spp. B group	808*	929*	1337*	1498*	11	159	590	554	450	2304	1475	2810	2176
Spongotrochus glacialis Popofsky	*	*	*	*	0	25	45	64	48	104	122	135	152
Spongotrochus sp. A	44	45	73	14	0	0	0	0	20	0	0	0	0
Spongotrochus sp. B	0	0	0	0	0	0	11	6	8	0	0	0	0
Stylospongia huxleyi Haeckel	0	0	0	0	0	0	0	0	0	0	0	0	0
Spongocore cylindrica (Haeckel)	23	5	22	7	0	0	17	28	34	61	67	42	85

Sediment Trap Station	E				P_1					PB			
Depth (m)	389	988	3755	5068	378	978	2778	4280	5582	667	1268	2869	3791
Spongopyle setosa Dreyer	0	0	0	0	0	3	8	6	8	61	67	42	24
Spongopyle osculosa Dreyer	0	0	0	0	0	0	0	0	0	0	0	0	0
Spongasater tetras tetras Ehrenberg	42	46	63	99	0	3	0	8	31	43	24	49	73
Spongaster pentas Riedel and Sanfilippo	0	0	0	0	0	0	6	39	36	0	0	6	30
Total SPONGODISCIDAE	998	1097	1621	1720	11	201	728	769	736	2676	1963	3254	2814
Family MYELASTRIDAE Riedel													
Myelastrum quadrifolium n.sp.	0	0	0	0	0	0	0	0	0	0	0	0	6
Myelastrum trinibrachium n.sp.	0	0	0	0	0	0	0	0	0	0	0	24	24
Total MYELASTRIDAE	0	0	0	0	0	0	0	0	0	0	0	24	30
Family LARNACILLIDAE Haeckel, emend. Campbell													
Larnacalpis sp.	0	0	0	0	0	0	0	0	0	0	0	0	0
Family PHACODISCIDAE Haeckel, emend. Campbell													
Heliodiscus ? sp.	0	0	0	0	0	0	0	0	0	0	0	0	0
Heliodiscus asteriscus Haeckel	3	2	2	13	6	3	11	6	14	67	24	79	49
Heliodiscus echiniscus Haeckel	0	0	0	0	0	0	0	0	0	0	0	0	0
Total PHACODISCIDAE	3	2	2	13	6	3	11	6	14	67	24	79	49
Family THOLONIIDAE Haeckel													
Tholoma metallasson Haeckel	0	0	0	0	0	0	0	0	0	6	67	0	0
Total THOLONIIDAE	0	0	0	0	0	0	0	0	0	6	67	0	0
Family PHYLONIIDAE Haeckel, emend. Campbell													
Hexapyle dodecantha Haeckel	32	6	12	33	0	6	0	6	0	0	12	6	12
Hexapyle sp.	163	85	186	111	0	14	22	25	50	244	79	135	0
Octopyle stenozona Haeckel	53	56	72	37	0	6	31	34	73	323	171	91	134
Tetrapyle octacantha Muller	513	444	947	458	11	204	612	805	780	689	652	1280	1085
Total PHYLONIIDAE	761	591	1217	639	11	230	665	870	903	1256	914	1512	1231

Sediment Trap Station	E				P_1					PB			
Depth (m)	389	988	3755	5068	378	978	2778	4280	5582	667	1268	2869	3791
Family LITHELIIDAE Haeckel													
Larcopyle butschlii Dreyer	0	0	0	0	0	0	25	14	8	30	0	37	6
Larcopyle sp. A	0	0	0	0	0	0	0	0	0	0	0	0	0
Larcopyle sp. B	0	0	0	0	0	0	0	0	0	0	0	0	0
Discopyle elliptica Haeckel	0	0	0	0	0	3	78	11	3	24	0	24	37
Tholospira cervicornis Haeckel group	191	365	176	371	25	260	1013	1180	1063	1024	1201	1494	1347
Tholospira dendrophora Haeckel	0	0	0	0	0	0	0	0	0	0	0	0	0
Tholospira ? sp.	0	0	0	0	0	11	31	14	14	0	0	54	98
Lithelius minor ? Jorgensen	0	0	0	0	0	0	0	0	0	0	0	0	0
Larcospira quadrangula Haeckel	2	0	9	3	0	0	8	22	25	12	24	12	37
Total LITHELIIDAE	193	365	185	374	25	274	1155	1241	1113	1090	1225	1621	1525
Spumellaria undet.	-	-	-	-	20	73	98	92	92	377	134	652	543
Total SPUMELLARIA	3688	3355	6155	5094	205	1465	4789	5117	4910	7809	6953	11454	10204
Suborder NASSELARIA Ehrenberg													
Family PLAGIACANTHIDAE Hertwig, emend. Petrushevskaya													
Subfamily PLAGIACANTHINAE Hertwig, emend. Petrushevskaya													
Tetraplecta pinigera Haeckel	0	0	0	0	6	14	48	36	17	91	104	231	226
Tetraplecta plectaniscus Haeckel	0	0	0	0	0	0	3	6	0	12	0	0	12
Tetraplecta corynephorum ? Jorgensen	0	0	0	0	0	0	0	0	0	0	0	0	0
Archiscenium quadrispinum ? Haeckel	17	86	158	152	0	0	0	6	0	37	0	0	6
Plectanium sp.	5	18	0	5	0	0	3	0	6	0	0	0	6
Protoscenium ? sp.	0	0	0	0	0	3	6	0	0	0	0	0	0
Clathromitra pterophormis Haeckel	0	0	0	0	0	0	0	0	0	0	0	0	0
Cladoscenium ancoratum Haeckel	123	320	267	419	22	162	235	330	243	1122	987	1865	1415
Semantis gracilis ? Popofsky	0	0	0	0	0	0	0	0	0	0	0	0	0
Deflandrella cladophora (Jorgensen)	0	0	0	0	0	6	20	25	17	0	0	0	0
Deflandrella sp.	75	239	129	83	0	17	25	28	25	0	0	0	0

Sediment Trap Station	E				P_1					PB			
Depth (m)	389	988	3755	5068	378	978	2778	4280	5582	667	1268	2869	3791
Talariscus pseudocuboides (Popofsky)	83	131	167	113	0	20	20	34	45	311	165	213	140
Gonosphaera primordialis	0	0	0	0	0	0	0	0	0	0	0	0	0
Phormacantha hystrix (Jorgensen)	150	141	330	260	6	73	215	275	280	750	463	1578	701
Neosemantis distephanus Popofsky	39	43	19	98	3	11	34	39	36	79	91	147	110
Total PLAGIACANTHINAE	492	978	1070	1130	37	306	609	779	669	2402	1810	4034	2616
Subfamily LOPHOPHAENINAE Haeckel, emend. Petrushevskaya													
Acanthocorys cf. variabilis Popofsky	594	538	982	146	8	23	134	149	143	988	378	615	658
Lophophaena cf. capito Ehrenberg	21	17	36	28	3	109	632	495	498	1419	768	1292	743
Lophophaena decacantha (Haeckel) group	0	0	0	0	0	0	0	0	0	0	0	0	0
Lophopaena circumtexta (Popofsky)	5	0	37	11	3	53	112	112	76	226	213	445	378
Lophophaena cylindrica (Cleve)	2445*	1283*	1925*	1570*	11	81	280	280	179	2681	1645	2907	2352
Peromelissa phalacra Haeckel	*	*	*	*	28	207	876	762	714	1097	762	1043	1012
Helotholus histricosa Jorgensen	313	251	238	120	0	0	14	0	14	0	0	115	61
Lithomelissa setosa Jorgensen	0	0	0	0	11	17	168	115	104	1907	926	1908	841
Peridium spinipes Haeckel	1251	2184	3114	2173	45	649	2314	2432	2046	7692	4468	7698	5517
Peridium sp.	6	96	41	47	3	14	39	50	72	0	30	116	73
Trisulcus triacanthus Popofsky	0	0	0	0	3	0	0	0	0	36	42	140	0
Total LOPHOPHAENINAE	4635	4369	6373	4095	115	1158	4569	4395	3846	16046	9232	16279	11635
Subfamily SETHOPERINAE Haeckel, emend. Petrushevskaya													
Lithopilium reticulatum Popofsky	0	0	0	0	0	0	0	0	0	0	0	0	0
Clathrocanium insectum (Haeckel)	0	0	0	0	0	0	14	6	25	36	0	92	61
Clathrocanium coarctatum Ehrenberg	0	0	0	0	0	8	42	73	67	0	6	24	0
Clathrocanium diadema Haeckel	0	0	0	0	0	0	0	0	0	0	0	0	0
Callimitra emmae Haeckel	22	27	21	7	0	6	14	11	8	12	6	30	30
Callimitra annae Haeckel	2	3	19	0	0	3	8	0	6	6	0	0	0
Callimitra solocicribrata n.sp.	0	0	0	0	0	0	0	0	3	18	12	0	18
Clathrocorys giltschii Haeckel	0	0	0	0	0	0	0	0	0	0	0	0	0
Clathrocorys murrayi Haeckel	0	0	0	0	0	20	14	20	3	85	43	61	189
Total SETHOPERINAE	24	30	40	7	0	37	92	110	112	157	67	207	298
Total PLAGIACANTHIDAE	5151	5377	7483	5232	152	1501	5270	5284	4627	18605	11109	20520	14549

Sediment Trap Station	E				P$_1$					PB			
Depth (m)	389	988	3755	5068	378	978	2778	4280	5582	667	1268	2869	3791
Family ACANTHODESMIIDAE Haeckel, emend. Riedel													
Zygocircus capulosus Popofsky	248	596	795	285	14	3	444	582	518	635	475	1085	1158
Zygocircus productus (Hertwig) group	453	436	634	431	0	0	260	20	0	146	122	164	207
Zygocircus cf. piscicaudatus Popofsky	0	0	0	0	0	0	0	0	0	0	0	0	0
Acanthodesmia vinculata (Muller)	108	91	69	54	6	45	126	115	148	304	274	829	366
Lophospyris juvenile form group	0	0	0	0	0	0	0	0	0	0	0	0	0
Lophospyris pentagona (Ehrenberg) quadriforis (Haeckel)	0	0	0	0	6	76	168	232	140	597	439	512	427
Lophospyris pentagona pentagona (Ehrenberg)	20	35	60	72	0	22	48	78	42	183	165	134	195
Lophospyris pentagona (Ehrenberg) hyperborea (Jorgensen)	64	44	83	38	0	0	0	0	0	0	0	0	0
Lophospyris cheni Goll	0	0	0	0	0	0	0	0	0	0	0	0	0
Tripodospyris sp.	0	0	0	0	0	22	31	53	11	37	55	85	73
Phormospyris stabilis (Goll) scaphipes (Haeckel)	0	0	0	0	3	17	92	50	106	353	286	871	701
Phormospyris sp. aff. L. pentagona hyperborea (Jorgensen)	0	0	0	0	0	0	0	6	0	103	43	24	37
Phormospyris stabilis (Goll) capoi Goll	0	0	0	0	0	3	3	3	6	55	85	104	91
Phormospyris stabilis stabilis (Goll)	0	0	0	0	0	8	25	14	25	165	122	122	147
Phormospyris ? sp.	0	0	0	0	0	0	0	0	0	12	0	6	0
Dictyospyris sp. group	109	54	36	9	0	0	0	0	0	55	24	18	30
Nephrospyris renilla renilla Haeckel	0	0	0	0	0	0	0	0	0	0	0	12	0
Nephrospyris renilla Haeckel lana Goll	0	0	0	0	0	0	0	0	0	0	0	0	0
Androspyris reticulidisca n.sp.	0	0	0	0	0	0	0	0	0	0	0	0	0
Androspyris huxleyi (Haeckel)	0	0	0	0	0	0	0	0	0	12	12	30	0
Androspyris ramosa (Haeckel)	0	13	0	11	0	3	6	8	6	0	0	0	0
Cephalospyris cancellata Haeckel	0	0	0	0	0	0	0	0	0	0	0	0	0
Cantharospyris platybursa Haeckel	28	83	16	14	0	0	44	14	14	30	12	30	43
Cantharospyris cf. clathrobursa (Haeckel)	0	0	0	0	0	8	0	0	3	18	0	12	12
Tholospyris sp. group	0	0	0	0	0	95	260	342	235	195	201	366	421
Tholospyris baconiana baconiana (Haeckel)	0	0	0	0	0	0	0	0	0	0	0	0	0
Tholospyris baconiana variabilis Goll	0	0	0	0	0	0	3	14	0	49	6	30	43
Tholospyris macropora (Popofsky)	0	0	0	0	0	0	8	6	0	12	6	24	18

Sediment Trap Station	E				P$_1$					PB			
Depth (m)	389	988	3755	5068	378	978	2778	4280	5582	667	1268	2869	3791
Liriospyris sp.	0	0	0	0	0	0	0	0	0	0	0	0	0
Liriospyris thorax (Haeckel) *laticapsa* n.subsp.	0	0	0	0	0	11	34	45	39	55	43	30	73
Liriospyris thorax thorax (Haeckel)	0	0	0	0	0	0	0	0	0	12	0	0	0
Liriospyris reticulata (Ehrenberg)	128	175	56	56	6	31	154	126	95	42	146	311	281
Total ACANTHODESMIIDAE	1158	1527	1749	970	35	344	1706	1708	1388	3070	2516	4799	4232
Family SETHOPHORMIDIDAE Haeckel, emend. Petrushevskaya													
Tetraphormis rotula (Haeckel)	0	6	98	57	0	28	53	78	48	103	37	61	122
Tetraphormis dodecaster (Haeckel)	0	0	0	0	3	17	25	45	28	183	219	304	165
Tetraphormis butschlii (Haeckel)	0	0	0	0	0	0	0	0	0	30	49	116	122
Theophormis callipilium Haeckel	0	0	0	0	0	3	17	20	14	0	30	24	37
Lampromitra schultzei (Haeckel)	0	0	0	18	0	0	0	0	0	12	0	0	0
Lamptomitra cracenta n.sp.	0	0	0	0	0	11	22	36	17	30	18	67	43
Lampromitra cachoni Petrushevskaya	0	0	0	0	0	0	0	0	0	0	0	0	0
Lampromitra spinosiretis n.sp.	0	0	0	0	0	0	0	0	0	0	0	0	0
Eucecryphalus sp.	0	0	0	0	0	0	0	0	0	0	0	0	0
Eucecryphalus gegenbauri Haeckel	46	30	50	43	0	25	67	48	31	183	122	146	49
Eucecryphalus europae (Haeckel)	0	0	0	0	0	0	3	11	0	0	0	24	49
Eucecryphalus clinatus n.sp.	0	0	0	0	0	3	0	11	0	182	146	189	274
Eucecryphalus tricostatus (Haeckel)*	28*	34*	49*	20*	6*	31*	70*	87*	70*	275*	158*	579*	616*
Eucecryphalus sestrodiscos (Haeckel)*	*	*	*	*	*	*	*	*	*	*	*	*	*
Corocalyptra cervus (Ehrenberg)	0	0	0	0	*	*	*	*	*	*	*	*	*
Phrenocodon clathrostomium Haeckel	0	0	0	0	0	0	0	0	0	0	0	0	0
Clathrocyclas sp.	0	0	0	0	0	0	0	0	0	0	0	0	0
Clathrocyclas monumentum (Haeckel)	0	0	0	0	0	0	0	11	11	0	0	0	0
Clathrocyclas cassiopejae Haeckel	0	0	0	0	0	0	0	0	0	0	0	0	0
Total SETHOPHORMIDIDAE	74	70	197	138	9	118	257	347	219	998	779	1510	1477

Sediment Trap Station	E				P_1					PB			
Depth (m)	389	988	3755	5068	378	978	2778	4280	5582	667	1268	2869	3791
Family THEOPERIDAE Haeckel, emend. Riedel													
Subfamily PLECTOPYRAMIDINAE Haecker, emend. Petrushevskaya													
Cornutella profunda Ehrenberg	64	141	367	160	6	73	294	316	359	537	287	543	464
Peripyramis circumtexta Haeckel	0	16	40	39	0	0	0	3	3	0	0	24	0
Litharachnium tentorium Hkl + *L. eupilium* (Hkl)	0	2*	5*	14*	0	6	8	8	6	0	0	24	91
L. tentorium Hkl + *L. eupilium* (Hkl) juvenile form	*	*	*	*	0	8	25	22	47	146	146	269	263
Total PLECTOPYRAMIDINAE	64	159	412	213	6	87	7	349	415	683	433	860	818
Subfamily EUCYRTIDIINAE Ehrenberg, emend. Petrushevskaya													
Archipilium sp. aff. *A. orthopterum* Haeckel	0	0	0	0	0	0	0	0	0	0	0	0	0
Archipilium macropus ? (Haeckel)	0	0	0	0	0	0	0	0	0	0	0	0	0
Pteroscenium pinnatum Haeckel	0	0	0	0	0	17	14	8	8	36	73	55	61
Pterocanium trilobum (Haeckel)	0	0	0	0	0	0	0	0	0	0	0	0	0
Pterocanium grandiporus Nigrini	0	0	0	0	0	6	31	22	14	55	67	54	55
Pterocanium praetextum praetextum (Ehrenberg)	207	158	102	88	3	0	25	145	143	30	49	152	91
Pterocanium praetextum (Ehrenberg) *eucolpum* Haeckel	0	0	0	0	0	0	0	0	0	0	0	0	0
Dictyophimus sp. A	0	0	0	0	0	0	0	0	0	0	0	0	0
Dictyophimus crisiae Ehrenberg	0	2	48	49	0	6	109	118	84	342	165	183	268
Dictyophimus infabricatus Nigrini	0	0	0	0	0	0	0	0	0	0	0	0	0
Dictyophimus macropterus (Ehrenberg)	0	0	0	0	0	8	17	3	3	12	73	67	18
Dictyophimus sp. B	0	0	0	0	3	42	89	90	53	183	207	445	714
Pseudodictyophimus gracilipes (Bailey)	14	163	361	260	3	31	165	143	140	86	238	590	396
Dictyocodon elegans (Haeckel)	0	0	0	0	0	0	0	0	3	0	0	0	0
Dictyocodon palladius Haeckel	0	0	0	0	0	0	0	0	0	0	0	0	0
Conicavus tipiopsis n.sp.	0	0	0	0	0	0	0	0	0	0	0	12	0
Sethoconus myxobrachia Strelkov and Reshetnyak	0	0	0	0	0	0	0	0	0	0	0	0	0
Conarachnium polyacanthum (Popofsky)	0	0	0	0	0	3	6	0	8	18	6	24	12
Conarachnium parabolicum (Popofsky)	0	0	0	0	0	0	3	0	0	12	18	0	49
Conarachnium facetum (Haeckel)	0	0	0	0	0	0	0	0	0	0	0	0	0
Stichopilium bicorne Haeckel	0	0	0	0	0	11	20	14	8	214	85	98	110

Sediment Trap Station	E				P_1					PB			
Depth (m)	389	988	3755	5068	378	978	2778	4280	5582	667	1268	2869	3791
Lithopera bacca Ehrenberg	14	15	27	37	0	6	28	6	0	0	0	0	0
Cyrtopera languncula Haeckel	0	15	46	31	0	0	14	8	17	0	12	61	43
Cyrtopera aglaolampa n.sp.	0	0	0	0	0	0	0	0	0	0	0	0	0
Stichophormis cf. cornutella Haeckel	0	54	7	2	0	0	8	0	3	0	0	24	6
Lophocorys undulata (Popofsky)	0	0	0	0	0	0	0	0	6	0	0	0	24
Theocorys veneris Haeckel	9	24	215	53	0	39	76	98	81	329	171	268	305
Theocorythium trachelium trachelium (Ehrenberg)	0	0	0	0	0	6	0	14	20	0	0	0	0
Lipmanella dictyoceras (Haeckel)	0	0	0	0	0	0	0	0	0	0	0	0	0
Lipmanella pyramidale (Popofsky)	40*	69*	36*	19*	0	0	0	0	0	0	0	0	0
Lipmanella virchowii (Haeckel)	*	*	*	*	0	11	25	39	20	67	79	67	104
Lithostrobus hexagonalis Haeckel	0	0	0	0	0	0	25	3	3	36	30	24	43
Theocalyptra bicornis (Popofsky)	83	122	197	75	6	22	34	64	36	366	207	147	238
Theocalyptra davisiana davisiana (Ehrenberg)	0	0	0	0	0	0	0	6	17	0	0	0	0
Theocalyptra davisiana cornutoides (Petrushevskaya)	82	354	784	207	3	20	67	42	56	98	55	365	250
Total EUCYRTIDIINAE	449	976	1823	821	18	276	756	823	723	1884	1535	2636	2787
Total TEOPERIDAE	513	1135	2235	1034	24	363	1083	1172	1138	2567	1968	3496	3605
Family PTEROCORYTHIDAE Haeckel, emend. Riedel													
Tetracorethra tetracorethra (Haeckel)	0	0	0	0	3	22	481	25	36	12	18	12	18
Pterocorys zancleus (Müller)	2966*	2381*	2698*	1654*	14	243	854	663	563	195	238	165	152
Pterocorys campanula Haeckel	*	*	*	*	15	92	199	274	279	147	61	250	122
Pterocorys sp.	0	0	0	0	0	0	25	8	11	73	49	12	12
Eucyrtidium spp. A group	0	0	0	0	3	6	86	95	65	196	61	37	153
Eucyrtidium acuminatum (Ehrenberg)	0	0	0	0	0	3	11	11	11	55	43	67	73
Eucyrtidium hexagonatum Haeckel	0	0	0	0	0	0	31	17	11	97	104	97	98
Eucyrtidium anomalum (Haeckel)	0	0	0	0	0	0	0	0	0	0	0	0	0
Eucyrtidium sp. aff. E. anomalum (Haeckel)	0	0	0	0	0	0	0	0	0	0	0	0	0
Eucyrtidium dictyopodium (Haeckel)	0	0	0	0	0	0	0	0	0	0	0	0	0
Eucyrtidium hexastichum (Haeckel)	120	45	133	40	0	36	78	100	56	153	183	128	201

Sediment Trap Station	E				P$_1$					PB			
Depth (m)	389	988	3755	5068	378	978	2778	4280	5582	667	1268	2869	3791
Anthocyrtidium zanguebaricum (Ehrenberg)	0	0	0	0	3	20	36	20	25	55	0	67	79
Anthrocyrtidium ophirense (Ehrenberg)	9	37	122	79	0	8	67	36	42	146	61	67	37
Lamprocyclas maritalis Haeckel *polypora* Nigrini	0	0	0	0	0	0	0	0	3	0	0	0	0
Lamprocyclas maritalis maritalis Haeckel	0	0	0	0	0	0	11	0	6	0	0	0	0
Lamprocyclas ? *hannai* (Campbell and Clark)	0	0	0	0	0	0	0	0	0	0	18	6	6
Lamprocyrtis sp.	0	0	0	0	0	0	8	14	14	43	30	122	140
Lamprocyrtis nigriniae (Caulet)	0	0	0	0	0	0	0	0	0	0	6	30	0
Total PTEROCORYTHIDAE	3095	2463	2953	1773	38	430	1454	1263	1122	1172	872	1060	1091
Family ARTOSTROBIIDAE Riedel, emend. Foreman													
Spirocyrtis scalaris Haeckel	91	79	67	101	0	8	36	36	28	280	238	299	341
Spirocyrtis subscalaris Nigrini	0	0	0	0	14	64	280	361	202	1566	1048	1920	1482
Spirocyrtis sp. aff. *S. seriata* + *subscalaris*	1496	629	653	660	0	0	0	0	0	0	0	0	0
Spirocyrtis ? *platycephala* (Ehrenberg) group	0	0	0	0	0	17	25	33	59	0	0	0	0
Artostrobus annulatus (Bailey)	0	0	0	0	3	22	25	30	73	67	67	451	488
Botryostrobus aquilonaris (Bailey)	0	0	0	0	0	3	0	3	6	30	30	12	30
Phormostichoartus corbula (Harting)	0	30	17	17	0	39	51	92	44	146	98	147	208
Siphocampe nodosaria (Haeckel)	0	3	135	26	0	0	0	0	0	0	0	0	0
Siphocampe lineata (Ehrenberg)	0	0	0	0	0	81	185	425	196	878	543	464	658
Siphocampe arachnea (Ehrenberg)	0	0	0	0	0	0	0	0	0	0	0	0	0
Artobotrys borealis (Cleve)	0	0	0	0	8	0	56	22	64	842	329	786	244
Total ARTOSTROBIIDAE	1587	741	872	804	25	234	658	1002	672	3809	2353	4079	3451
Family CARPOCANIIDAE Haeckel, emend. Riedel													
Carpocanistrum	9	69	72	7	0	31	129	121	196	97	49	103	43
Carpocanarium papillosum (Ehrenberg)	0	7	2	56	0	0	3	3	3	30	30	115	67
Total CARPOCANIIDAE	9	76	74	63	0	31	132	124	199	127	79	218	110
Family CANNOBOTRYIDAE Haeckel, emend. Riedel													
Acrobotrys teralans Renz	0	0	0	0	0	0	0	0	0	85	73	232	225
Acrobotrys tessarolobon n.sp.	0	0	0	0	0	0	0	0	0	0	0	0	0

Sediment Trap Station	E				P$_1$					PB			
Depth (m)	389	988	3755	5068	378	978	2778	4280	5582	667	1268	2869	3791
Acrobotrys chelinobotrys n.sp.	0	0	0	0	3	31	131	126	47	353	299	524	390
Acrobotrys spp. A, B and C	123	76	126	68	-	-	-	-	-	-	-	-	-
Acrobotrys sp. C	-	-	-	-	3	3	25	14	11	6	18	6	18
Saccospyris preantarctica Petrushevskaya	0	0	0	0	0	0	0	0	0	0	0	0	0
Centrobotrys thermophila Petrushevskaya	0	0	0	0	6	3	34	39	31	0	0	0	0
Neobotrys quadrituberosa Popofsky	0	0	0	0	0	3	3	8	0	0	0	6	49
Botryocyrtis sp. A	0	0	0	0	0	0	0	0	0	0	0	0	0
Botryocyrtis scutum (Harting)	226	167	212	111	6	78	129	215	238	353	256	365	402
Botryocyrtis elongatum n.sp.	0	0	0	0	14	28	20	42	56	238	177	219	73
Total CANNOBOTRYIDAE	349	243	338	179	32	146	322	444	383	1035	823	1352	1157
Family ARCHIPHORMIDIDAE Haeckel													
Arachnocalpis ? sp. A	0	0	0	0	0	0	0	0	0	0	0	0	0
Arachnocalpis sp. B	0	0	0	0	0	0	0	0	0	0	0	0	0
Arachnocalpis ? *ovatiretalis* n.sp.	0	0	0	0	0	6	0	3	3	0	6	0	37
Arachnocalpis ? sp. C	0	0	0	0	0	0	0	0	0	0	0	0	0
Arachnocalpis ellipsoides Haeckel	0	0	0	0	0	0	3	3	0	0	0	0	0
Total ARCHIPHORMIDIDAE	0	0	0	0	0	6	3	6	3	0	6	0	37
Nassellaria undet.	-	-	-	-	28	143	300	185	212	555	287	1268	835
Total NASSELLARIA	11936	11637	15901	10192	343	3316	11175	11535	9963	31938	20792	38302	30635

Sediment Trap Station	E				P$_1$					PB				
Depth (m)	389	988	3755	5068	378	978	2778	4280	5582	667	1268	2869	3769	3791
Suborder PHAEODARIA Haeckel														
Family CHALLENGERIIDAE Murray, emend. herein														
Challengeron willemoesii Haeckel	128	110	62	36	6	3	0	0	0	122	30	18	24	6
Challengeron lingi n. sp.	0	0	0	0	0	0	3	0	0	0	0	0	0	0
Challengeron radians Borgert	6	0	6	5	0	0	0	0	0	0	0	0	0	0
Challengeron tizardi (Murray)	0	0	0	0	0	0	0	0	0	0	0	0	0	0
Challengerosium balfouri (Murray)	6	2	0	0	0	0	0	0	0	0	6	6	0	0
Challengerosium avicularia Haecker	0	0	0	0	0	0	3	0	0	0	0	0	0	0
Challengeranium diodon (Haeckel)	14	3	19	20	0	0	0	3	0	98	55	12	12	24
Protocystis sp. A	0	0	0	0	0	0	0	0	0	0	0	12	0	24
Protocystis harstoni (Murray)	2	11	0	3	0	0	0	0	0	0	0	0	0	0
Protocystis honjoi n. sp.	0	0	12	0	0	0	0	0	0	12	18	30	0	12
Protocystis tridentata Borgert	0	0	0	0	0	0	0	0	0	0	6	6	0	0
Protocystis auriculata n. sp.	0	0	0	0	0	0	0	0	0	0	0	0	0	0
Protocystis aduncicuspis n. sp.	0	0	0	0	0	0	0	0	0	6	0	18	24	43
Protocystis sp. B	0	0	0	0	0	0	0	0	0	0	0	0	0	0
Protocystis sloggetti (Haeckel)	0	0	0	0	0	0	0	0	0	0	12	0	0	6
Protocystis murrayi (Haeckel)	0	0	0	0	0	0	0	0	0	0	0	6	0	0
Protocystis sp. C	0	0	0	0	0	0	0	0	0	0	0	0	0	0
Protocystis thomsoni (Murray)	0	7	2	2	0	0	0	0	0	0	0	0	0	0
Protocystis xiphodon (Haeckel)	135	64	36	40	0	0	0	3	0	43	24	0	0	0
Protocystis tritonis (Haeckel)	0	2	0	3	0	0	0	0	0	0	0	0	0	0
Protocystis naresi (Murray)	0	0	0	0	0	0	0	0	0	0	0	0	0	0
Pharyngella gastrula Haeckel	0	0	0	0	0	0	0	0	0	0	0	0	0	0
Entocannula infundibulum Haeckel	0	0	0	0	0	0	0	0	0	0	0	0	0	0
Total CHALLENGERIIDAE	291	199	137	109	6	3	6	6	0	281	151	108	60	115
Family MEDUSETTIDAE Haeckel, emend. herein														
Euphysetta elegans Borgert	8	86	96	93	0	0	6	0	0	0	49	116	73	85
Euphysetta staurocodon Haeckel	0	0	0	0	0	0	6	3	0	0	49	177	61	140

Sediment Trap Station	E				P_1					PB				
Depth (m)	389	988	3755	5068	378	978	2778	4280	5582	667	1268	2869	3769	3791
Euphysetta pusilla Cleve	407	229	188	21	0	0	0	0	0	0	0	0	0	0
Euphysetta lucani Borgert	0	0	2	0	0	0	0	0	0	0	0	0	0	0
Medusetta ansata Borgert	73	15	59	33	3	20	3	3	0	6	24	24	49	0
Medusetta inflata Borgert	0	0	0	0	0	0	0	0	0	0	0	6	0	18
Medusetta sp. A	0	0	0	0	0	0	0	0	0	0	0	0	0	0
Total MEDUSETTIDAE	488	330	345	147	3	20	15	6	0	6	122	323	183	243
Family LIRELLIDAE Ehrenberg														
Borgertella caudata (Wallich)	252	62	149	180	3	62	190	120	47	811	524	994	549	658
Lirella baileyi Ehrenberg	0	0	0	0	0	0	0	0	0	0	0	0	0	0
Lirella bullata (Stadum and Ling)	2	384	603	705	6	17	190	142	118	847	335	847	817	1024
Lirella melo (Cleve) + *L. tortuosa* n.sp.	0	7	380	199	0	0	25	59	22	427	85	286	158	165
Total LIRELLIDAE	254	453	1132	1084	9	79	405	321	187	2085	944	2127	1524	1847
Family POROSPATHIDIDAE Borgert, emend. Campbell														
Porospathis holostoma (Cleve)	0	0	8	0	0	0	3	3	0	0	18	12	49	18
Total POROSPATHIDIDAE	0	0	8	0	0	0	3	3	0	0	18	12	49	18
Family CASTANELLIDAE Haeckel														
Castanidium longispinum Haecker	-	-	-	-	0	0	0	0	0	122	98	244	98	128
Castanidium abundiplanatum n. sp.	-	-	-	-	0	0	0	0	0	12	0	37	12	12
Castanella spp.	-	-	-	-	0	3	0	0	0	0	0	0	0	0
Castanidium spp.	-	-	-	-	0	0	0	0	0	12	18	0	37	24
Castanarium spp.	-	-	-	-	0	0	0	0	0	12	12	37	24	18
Castanissa spp.	-	-	-	-	0	0	0	0	0	24	6	0	0	6
Castanellids group	7	3	0	2	-	-	-	-	-	-	-	-	-	-
Total CASTANELLIDAE	7	3	0	2	0	3	0	0	0	182	134	318	171	188
Family CIRCOPORIDAE Haeckel														
Haeckeliana porcellana Haeckel	0	2	0	2	0	3	0	0	0	0	0	0	0	0
Circoporus sexfuscinus Haeckel	0	0	0	0	0	0	0	0	0	0	0	0	0	0
Circoporus oxyacanthus Borgert	5	0	2	3	0	0	0	0	0	0	12	24	12	0
Circogonia sp.	0	0	0	0	0	0	0	0	0	0	0	0	0	0
Total CIRCOPORIDAE	5	2	2	5	0	3	0	0	0	0	12	24	12	0

Sediment Trap Station	E				P$_1$					PB				
Depth (m)	389	988	3755	5068	378	978	2778	4280	5582	667	1268	2869	3769	3791
Family CONCHARIIDAE Haeckel														
Conchellium capsula Borgert+	27	0	10	2	0	0	0	0	3	0	0	0	0	0
Conchellium tridacna Haeckel+	0	1	0	0	0	0	0	0	0	0	0	0	0	0
Conchophacus diatomeus (Haeckel)	0	0	0	0	0	0	0	0	0	0	0	0	0	0
Conchidium argiope Haeckel+	0	0	0	0	3	6	6	6	0	92	128	128	85	79
Conchidium caudatum (Haeckel)+	103	2	25	30	0	0	0	0	0	0	0	0	0	0
Conchopsis compressa Haeckel+	0	3	0	0	0	0	0	0	0	0	0	0	0	0
Total CONCHARIIDAE	130	6	35	32	3	6	6	6	3	92	128	128	85	79
Family AULOSPHAERIDAE Haeckel														
Aulsophaerids group**	2	0	3	2	0	3	8	6	6	85	37	108	98	61
Total AULOSPHAERIDAE	2	0	3	2	0	3	8	6	6	85	37	108	98	61
Family AULACANTHIDAE Haeckel														
Aulographis stellata Hkl + A. tetrancistra Hkl++	-	-	-	-	0	0	0	6	0	0	12	30	49	24
Auloceros spathillaster Haeckel++	-	-	-	-	0	0	0	0	0	0	0	0	0	0
Auloceros arborescens Haeckel birameus (Immermann)++	-	-	-	-	0	0	0	3	0	280	73	177	122	116
Aulographonium bicorne Haecker++	-	-	-	-	0	0	3	20	3	12	0	30	24	6
Aulospaphis taumorpha ? Haeckel++	-	-	-	-	0	3	6	6	12	24	0	6	49	49
Aulospathis variabilis Haeckel bifurca Haecker++	0	0	0	0	0	0	0	0	0	0	0	0	0	0
Total AULACANTHIDAE	0	0	0	0	0	3	9	35	15	316	85	237	244	195
Total PHAEODARIA	1177	993	1662	1381	21	120	452	383	208	3047	1632	3385	2426	2746
Total RADIOLARIA	16801	15985	23718	16667	569	4901	16416	17035	15801	42794	29376	53141	-	43585

* These two or three taxa are counted together

** Incomplete fragments are counted

*** Spicule swarms are counted

\+ Each value is counted as a half (0.5) shell

++ Each tubule is counted

Table 3. The size fractioned radiolarian flux (no. of shells/m^2/day), in each family from Station E. The proportion of counted specimens (%) with respect to the radiolarian flux (shells/m^2/day) is given in the bottom row.

Taxon	Sediment trap depth (m) 389				Sediment trap depth (m) 988				Sediment trap depth (m) 3,755				Sediment trap depth (m) 5,068			
	Size fraction (μm)				Size fraction (μm)				Size fraction (μm)				Size fraction (μm)			
	1000-250 very coarse	250-125 coarse	125-63 medium	< 63 fine	1000-250 very coarse	250-125 coarse	125-63 medium	< 63 fine	1000-250 very coarse	250-125 coarse	125-63 medium	< 63 fine	1000-250 very coarse	250-125 coarse	125-63 medium	< 63 fine
Suborder SPUMELLARIA																
Family SPHAEROZOIDAE	9	12	65	0	5	36	29	0	7	50	6	0	2	0	10	0
COLLOSPHAERIDAE	5	30	51	0	10	12	88	0	42	21	93	0	24	44	77	54
ETHMOSPHAERIDAE	40	36	23	0	59	24	37	0	82	72	75	54	61	77	62	0
ACTINOMMIDAE	176	388	294	272	169	193	279	54	437	401	804	435	293	356	738	218
PHACODISCIDAE	84	285	280	272	94	199	353	381	134	79	631	653	122	192	501	816
PORODISCIDAE	40	255	61	54	84	90	147	54	155	129	231	163	106	186	83	54
LITHELIIDAE	93	486	322	54	56	241	441	218	108	179	625	490	94	159	434	327
Total SPUMELLARIA	447	1492	1096	652	477	795	1374	707	965	931	2465	1795	702	1014	1905	1469
Suborder NASSELLARIA																
Family PLAGONIIDAE	71	583	1138	3320	134	410	1639	3156	367	666	2188	4245	179	520	2422	2014
ACANTHODESMIIDAE	124	322	532	218	61	157	640	707	136	156	822	653	138	164	439	327
SETHOPHORMIDAE	0	0	0	0	0	6	0	0	19	50	29	0	21	27	26	0
THEOPERIDAE	24	225	350	109	59	133	345	707	228	286	972	980	141	268	511	218
PTEROCORYTHIDAE	174	613	1535	653	120	157	1433	707	233	150	1620	816	152	175	1079	327
ARTOSTROBIIDAE	37	158	686	707	24	30	368	327	40	29	370	435	59	49	589	163
CANNOBOTRYIDAE	17	61	107	163	21	18	96	109	10	0	110	218	31	11	83	54
CARPOCANIIDAE	0	0	9	0	7	0	7	54	0	0	17	54	2	0	5	0
Total NASSELLARIA	477	1962	4357	5170	426	911	4528	5767	1033	1337	6128	7401	723	1214	5154	3103
Suborder PHAEODARIA																
Family CHALLENGERIIDAE	14	170	107	0	31	36	22	109	19	36	81	0	30	49	31	0
POROSPATHIDIDAE	0	0	0	0	0	0	0	0	2	0	6	0	0	0	0	0
MEDUSETTIDAE	23	42	42	281	9	12	37	272	31	7	197	109	31	27	88	0
LIRELLIDAE	3	0	33	218	3	0	15	436	10	0	197	925	106	16	36	925
CASTANELLIDAE	7	0	0	0	3	0	0	0	0	0	0	0	2	0	0	0
CIRCOPORIDAE	5	0	0	0	2	0	0	0	2	0	0	0	5	0	0	0
CONCHARIIDAE	11	118	0	0	5	0	0	0	17	18	0	0	10	22	0	0
AULOSPHAERIDAE	2	0	0	0	0	0	0	0	3	0	0	0	2	0	0	0
Total PHAEODARIA	65	330	182	599	53	48	74	817	84	61	481	1034	186	114	155	925
Total RADIOLARIA	959	3784	5635	6421	956	1754	5976	7291	2082	2329	9074	10230	1611	2342	7214	5497
% Counted Specimens	58	16	21	2	58	17	14	2	57	14	17	2	57	18	19	2

Table 4. The size fractioned radiolarian flux (no. of shells/m^2/day) in each family from the sediment trap stations P_1 and PB. The proportion of counted specimens ($^o/o$) with respect to the radiolarian flux is given in the bottom row of each station.

Station/Depth (m)	$P_1$378			$P_1$978			$P_1$2778			$P_1$4280			$P_1$5582		
Size fraction (?m)	1000-250	250-63	63	100-250	250-63	63	1000-250	250-63	63	1000-250	250-63	63	1000-250	250-63	63
Suborder SPUMELLARIA															
Family COLLOSPHAERIDAE	0	36	42	0	120	31	8	369	145	0	386	101	3	411	90
SPHAEROZOIDAE	0	0	0	0	0	0	0	0	0	0	0	0	0	0	0
ETHMOSPHAERIDAE	0	0	0	0	6	0	3	25	0	28	20	56	14	22	0
ACTINOMMIDAE															
ACTINOMMINAE	0	28	0	25	260	6	137	610	45	104	554	11	62	537	0
SATURNALINAE	0	0	0	0	0	0	0	0	0	0	0	0	0	0	0
COCCODISCIDAE	3	6	0	6	90	3	8	263	45	14	241	22	8	280	45
PORODISCIDAE	3	11	0	6	98	34	34	327	112	42	422	145	39	422	123
SPONGODISCIDAE	3	8	0	6	123	73	11	302	414	48	400	325	28	529	179
MYELASTRIDAE	0	0	0	0	0	0	0	0	0	0	0	0	0	0	0
LARNACILLIDAE	0	0	0	0	0	0	0	0	0	0	0	0	0	0	0
PHACODISCIDAE	6	0	0	0	3	0	0	11	0	0	6	0	3	11	0
THOLONIIDAE	0	0	0	0	0	0	0	0	0	0	0	0	0	0	0
PHYLONIIDAE	3	3	6	3	179	48	28	437	201	67	601	201	31	582	291
LITHELIIDAE	3	14	8	6	238	31	39	935	179	62	1035	145	39	878	201
Spumellaria undet.	0	11	8	11	25	36	20	45	34	17	53	22	6	42	45
Total SPUMMELLARIA	21	117	64	63	1142	262	288	3324	1175	382	3718	1028	233	3714	974
Suborder NASSELARIA															
Family PLAGIACANTHIDAE															
PLAGIACANTHINAE	6	28	3	17	271	17	64	532	11	39	660	78	25	568	78
LOPHOPHAENINAE	34	42	39	20	616	523	157	1838	2574	249	2051	2093	118	1914	1813
SETHOPERINAE	0	0	0	6	31	0	11	81	0	8	101	0	0	101	111

Table 4. (cont.)

Station/Depth (m)	P_1378			P_1978			P_12778			P_14280			P_15582		
Size fraction (μm)	1000-250	250-63	<63	100-250	250-63	<63	1000-250	250-63	<63	1000-250	250-63	<63	1000-250	250-63	<63
Family ACANTHODESMIIDAE	6	17	11	14	271	59	48	1021	638	84	185	638	39	946	403
SETHOPHORMIDIDAE	3	6	0	11	106	0	31	227	0	67	280	0	39	179	0
THEOPERIDAE															
PLECTOPYRAMIDINAE	0	0	6	3	28	56	0	92	235	11	104	235	17	118	280
EUCYRTIDIINAE	3	8	6	3	196	76	28	582	145	42	657	123	6	616	101
PTEROCORYIDAE	8	22	8	8	392	34	31	1223	201	45	1097	123	25	1007	90
ARTOSTROBIIDAE	0	6	20	0	56	179	0	187	470	20	213	772	6	218	448
CARPOCANIIDAE	0	0	0	0	8	22	0	42	90	3	31	90	0	87	112
CANNOBOTRYIDAE	14	6	11	3	64	78	3	126	190	20	168	257	3	168	213
ARCHIPHORMIDIDAE	0	0	0	3	3	0	3	0	0	6	0	0	3	0	0
Nassellaria undet.	3	11	14	0	64	78	11	64	224	17	56	112	14	64	134
Total NASSELLARIA	77	146	118	88	2106	1122	387	6015	4778	611	6403	4521	295	5986	3683
Suborder PHAEODARIA															
Family CHALLENGERIIDAE	0	6	0	3	0	0	0	6	0	0	6	0	0	0	0
MEDUSETTIDAE	0	3	0	0	20	0	0	14	0	0	6	0	0	0	0
LIRELLIDAE	0	3	6	0	14	64	8	84	313	6	70	246	8	34	145
POROSPATHIDIDAE	0	0	0	0	0	0	0	3	0	0	3	0	0	0	0
CASTANELLIDAE	0	0	0	0	0	0	0	3	0	0	0	0	0	0	0
CIRCOPORIDAE	0	0	0	3	0	0	0	0	0	0	0	0	0	0	0
CONCHARIIDAE	0	3	0	3	3	0	0	0	0	0	0	0	0	0	0
AULOSPHAERIDAE	0	0	0	3	0	0	0	6	0	0	6	0	0	3	0
AULACANTHIDAE	0	0	0	0	3	0	8	0	0	3	3	0	6	0	0
							3	6	0	28	6	0	6	8	0
Total PHAEODARIA	0	15	6	12	40	64	19	122	313	37	100	246	20	45	145
Total RADIOLARIA	92	278	188	163	3260	1448	694	9461	6266	1030	10221	5795	548	9745	4802
% Counted Specimens	36	36	36	36	36	36	36	36	9	36	36	9	36	36	9

Table 4. (cont.)

Station/Depth (m)	PB667				PB1268				PB2869				PB3791			
Size fraction (?m)	1000-250	250-63	125-63	63	1000-250	250-63	125-63	63	1000-250	250-63	125-63	63	1000-250	250-63	125-63	63
Suborder SPUMELLARIA																
Family COLLOSPHAERIDAE	49	104	91	0	6	140	73	0	98	213	152	0	30	140	152	0
SPHAEROZOIDAE	12	0	0	0	0	0	0	0	0	0	0	0	0	0	0	0
ETHMOSPHAERIDAE	85	30	18	0	146	73	6	0	341	18	49	0	219	85	49	0
ACTINOMMIDAE																
ACTINOMMINAE	780	335	152	0	603	622	165	12	1134	597	213	0	890	786	317	0
SATURNALINAE	0	0	0	0	0	0	0	0	0	0	0	0	0	18	0	0
COCCODISCIDAE	24	30	0	0	37	43	0	0	98	85	30	0	18	79	24	0
PORODISCIDAE	122	201	122	195	91	384	189	37	512	396	280	98	140	396	542	146
SPONGODISCIDAE	475	457	622	1122	219	738	664	341	573	536	1073	1073	183	561	1341	731
MYELASTRIDAE	0	0	0	0	0	0	0	0	24	0	0	0	30	0	0	0
LARNACILLIDAE	0	0	0	0	0	0	0	0	0	0	0	0	0	0	0	0
PHACODISCIDAE	49	18	0	0	6	18	0	0	73	6	0	0	24	24	0	0
THOLONIIDAE	0	0	6	0	12	49	6	0	0	0	0	0	0	0	0	0
PHYLONIIDAE	293	323	347	213	110	496	250	61	427	341	304	439	67	488	481	195
LITHELIIDAE	366	500	226	0	146	853	226	0	646	604	323	49	201	749	573	0
SPUMMELARIA undet.	146	30	55	146	24	43	6	61	158	85	18	390	67	67	165	244
Total SPUMMELARIA	2401	2028	1639	1756	1400	3457	1585	512	4084	2881	2442	2049	1869	3393	3644	1316
Suborder NASSELARIA																
Family PLAGIACANTHIDAE																
PLAGIACANTHINAE	719	512	829	341	268	518	1000	24	1658	707	987	683	244	1042	1036	293
LOPHOPHAENINAE	1914	1975	4846	7314	555	2469	4322	1890	2426	2359	5108	6388	421	1554	5906	3755
SETHOPERINAE	61	79	18	0	6	55	6	0	49	49	61	49	18	91	189	0
ACANTHODESMIIDAE	622	920	798	731	311	1091	969	146	1061	1128	1737	878	280	1073	1896	1073
SETHOPHORMIDIDAE	207	457	189	146	165	408	207	0	549	652	311	0	329	670	475	0
Family THEOPERIDAE																
PLECTOPYRAMIDINAE	73	85	183	341	43	134	134	122	219	158	286	195	79	128	414	195
EUCYRTIDIINAE	451	567	475	390	134	762	603	37	646	786	1012	195	262	750	1627	146

Table 4 . (cont.)

Station/Depth (m)	PB667				PB1268				PB2869				PB3791			
Size fraction (µm)	1000-250	250-63	125-63	<63	1000-250	250-63	125-63	<63	1000-250	250-63	125-63	<63	1000-250	250-63	125-63	<63
PTEROCORYIDAE	195	390	445	146	91	433	347	0	256	366	439	0	91	238	664	98
ARTOSTROBIIDAE	341	518	1048	1902	67	750	939	597	512	549	1164	1853	98	317	1621	1414
CARPOCANIIDAE	24	49	55	0	6	18	43	12	37	177	0	0	0	0	110	0
CANNOBOTRYIDAE	134	122	390	390	30	219	439	134	171	165	524	488	18	55	646	439
ARCHIPHORMIDIDAE	0	0	0	0	0	6	0	0	0	0	0	0	0	18	18	0
NASSELLARIA undet.	110	49	55	341	43	55	67	122	256	165	213	634	67	116	262	390
Total NASSELLARIA	4851	5723	9331	12042	1719	6918	9076	3084	7840	7261	11842	11363	1907	5052	14864	7803

Station/Depth (m)	PB667				PB1286				PB2869				PB3769				PB3791			
Size fraction (µm)	1000 -250	250 -125	125 -63	<63	1000 -250	250 -125	125 -63	<63	1000 -250	250 -125	125 -63	<63	1000 -250	250 -125	125 -63	<63	1000 -250	250 -125	125 -63	<63
Suborder PHAEODARIA																				
Family CHALLENGERIIDAE	85	110	37	49	12	79	49	12	37	49	24	0	0	37	24	0	12	67	37	0
MEDUSETTIDAE	0	0	6	0	6	61	55	0	49	55	219	0	0	49	85	49	18	61	165	0
LIRELLIDAE	73	49	207	1755	61	201	219	463	85	201	573	1268	24	24	256	1219	37	30	561	1219
POROSPATHIDIDAE	0	0	0	0	0	18	0	0	0	12	0	0	0	0	49	0	6	6	6	0
CASTANELLIDAE	183	0	0	0	134	0	0	0	305	12	0	0	158	12	0	0	183	0	6	0
CIRCOPORIDAE	0	0	0	0	12	0	0	0	24	0	0	0	12	0	0	0	0	0	0	0
CONCHARIIDAE	49	43	0	0	30	98	0	0	12	104	12	0	0	85	0	0	12	61	6	0
AULOSPHAERIDAE	73	12	0	0	37	0	0	0	110	0	0	0	49	37	12	0	24	37	0	0
AULACANTHIDAE	122	30	67	98	18	24	30	12	85	30	128	0	85	134	24	0	85	55	55	0
Total PHAEODARIA	585	244	317	1902	310	481	353	487	707	463	956	1268	328	378	450	1268	377	317	836	1219
Total RADIOLARIA	7837	7995	11287	15700	3429	10856	11014	4083	12631	10605	15240	14680	-	-	-	-	4153	8762	19344	10338
% Counted Specimens	8	16	16	2	16	16	16	8	8	16	16	2	8	8	8	2	16	16	16	2

Table 5. Summary of radiolarian (suborders) flux (no. shells/m^2/day) and ratios between suborders at the three sediment trap stations.

Station/ Depth (m)	Flux (no. shells/m^2/day) Spumellaria	(%)	Nassellaria	(%)	Phaeodaria	(%)	Total Radiolaria	Ratio N/S	Ph/S	Ph/P
E389	3688	21	11936	72	1177	7	16801	3.2	0.32	0.075
988	3355	21	11637	73	993	6	15985	3.5	0.30	0.066
3755	6155	26	15901	67	1662	7	23718	2.6	0.27	0.075
5068	5049	31	10192	61	1381	8	16667	2.0	0.27	0.091
$P_1$378	205	36	343	60	21	4	569	1.7	0.10	0.038
978	1465	30	3316	68	120	2	4901	2.3	0.082	0.025
2778	4789	29	11175	68	452	3	16416	2.3	0.094	0.028
4280	5117	30	11535	68	383	2	17035	2.3	0.074	0.023
5582	4910	33	9963	66	208	1	15081	2.0	0.042	0.014
PB667	7809	18	31938	75	3047	7	42794	4.1	0.39	0.077
1268	6953	24	20792	71	1632	6	29376	3.0	0.23	0.059
2869	11454	22	38302	72	3385	6	53141	3.3	0.30	0.068
3769	-	-	-	-	2426	-	-	-	-	-
3791	10204	23	30635	70	2746	6	43585	3.0	0.27	0.067

% = (suborder flux/total radiolarian flux) x 100

N/S ratio = nassellarian flux/spumellarian flux

Ph/s ratio = phaeodarian flux/spumellarian flux

Ph/p ratio = phaeodarian flux/polycystine flux

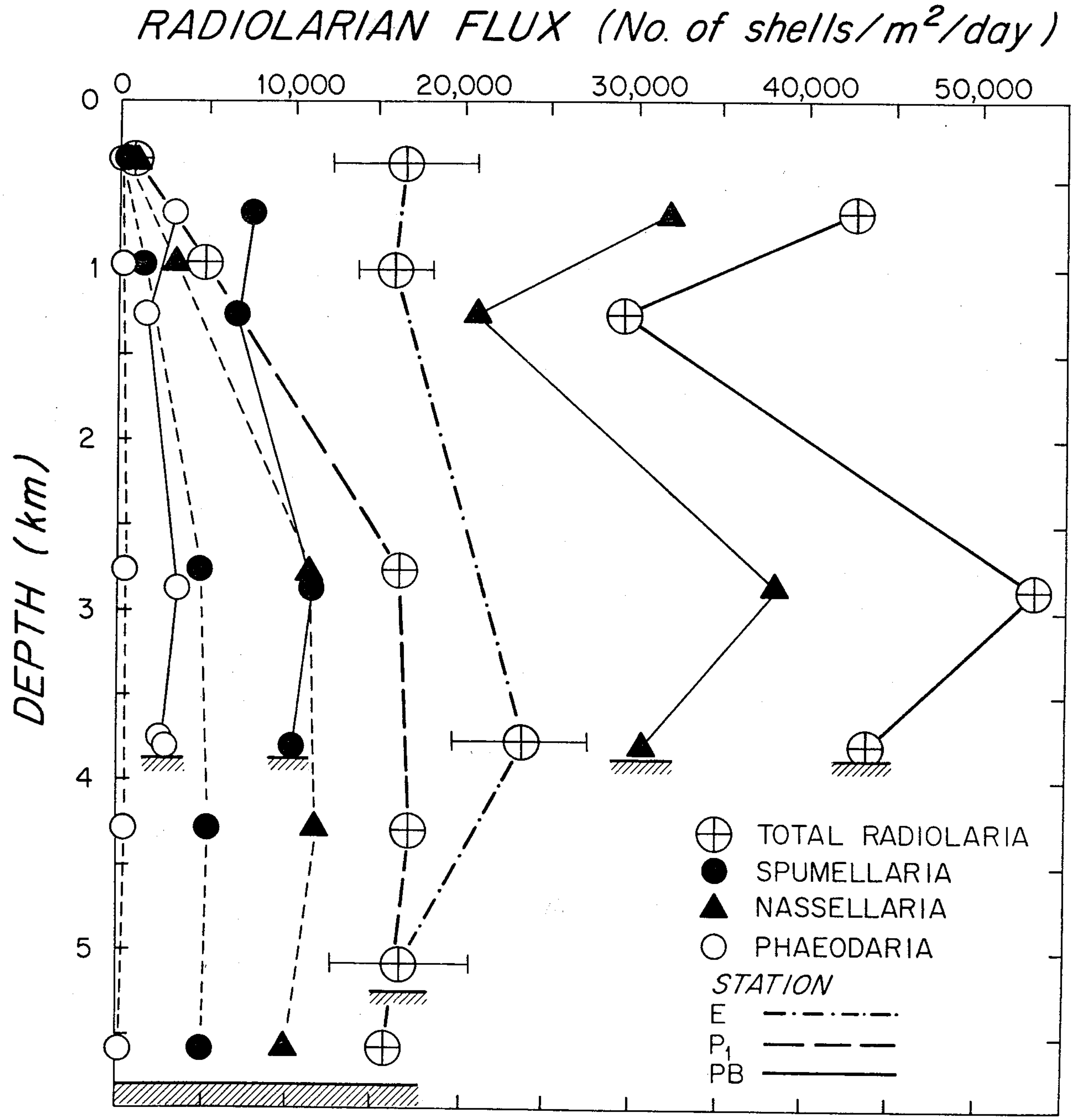

Figure 3. Vertical fluxes (no. of shells/m^2/day) of Radiolaria and their suborders from Stations E, P_1 and PB. Horizontal bars on Station E radiolarian flux show representative standard deviation at 95% confidence level for all the data.

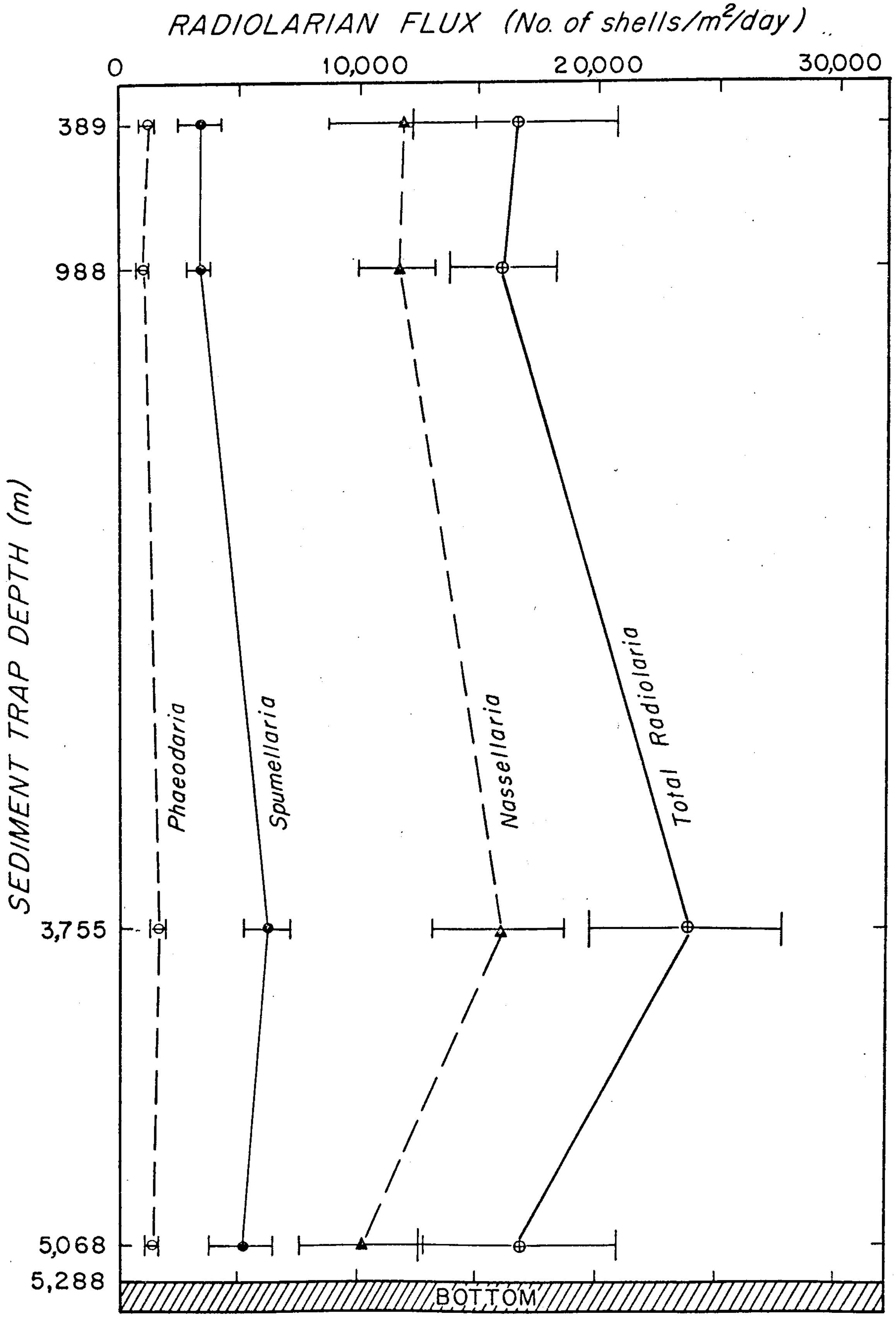

Figure 4. Vertical fluxes (no. of shells/m^2/day) of Radiolaria and their suborders from Station E. Horizontal bars represent standard deviation at 95% confidence level.

taxa, including one new genus, 20 new species, one new subspecies, one new name for a species and 3 new names for subspecies, were recognized from the three stations; of these 208 taxa were found at Station E. According to Casey (1981, pers. comm.), based on all the published literature the best inference on total number of living Radiolaria species in the world ocean is about 600. It seems possible that this report covers majority of tropical species. The 420 taxa are comprized of three suborders: Spumellaria (175 taxa); Nasselaria (182); and Phaeodaria (63). The number of taxa contained in the counting slides (Tables 1,2) appeared to be less than that in slides used for species identification. This is because that I used only one or two slides for counting and one to four slides in each size fraction for species identification. When necessary several species were combined together as one group in counting (Table 2). Radiolarian spicules were not counted.

The radiolarian flux from the three stations is normalized to the number of individual shells/m^2/day for each taxon (Table 2). The size fractioned fluxes of radiolarian families are presented in Tables 3 and 4. Percentages of actual specimens counted in each slide are also given in Tables 3 and 4. The fluxes of suborders are summarized in Table 5 and illustrated in Figs. 3 and 4.

Diversity Index Analysis

The diversity index used in this analysis is that of Pielou (1969), and is computed by the following equation:

$$\underline{H}' \text{ (natural bels)} = - \sum_{\underline{i}=1}^{\underline{n}} \underline{Pi}\ \underline{\ln}\ \underline{Pi}$$

where $\underline{Pi}$ is the proportion of the $\underline{i}$ th species of the total population being dealt with, $\underline{n}$ is the number of species, and $\underline{H}'$ is the diversity in natural bels, i.e., natural logarithms to the base 10. This index is highest with many species, each of which constitutes an equal part of the total population, and lowest when there are few species, or where one species predominates.

Diversity indices were computed for each suborder as well as total Radiolaria at each trap depth from Station E. The results are presented in Table 6 and Fig. 5. The computed diversity indices of total Radiolaria ranged from 3.3 to 3.6 (nat. bel. unit). These values are probably the highest values ever reported in the water column. This is mainly due to the difference in sampling and analytical methods: the present sediment traps collected all size particles as well as rapidly settling particles in the water column, whereas most of the previous works (Casey et al., 1971, 1979a,b; Petrushevskaya, 1971a,b; Kling, 1976; McMillen and Casey, 1978; Boltovskoy and Riedel, 1980) involved plankton tows and/or water bottles which are selective for certain size range. Renz (1976) was able to collect 137 species of Radiolaria in the Central Tropical Pacific by the using a pumping system with a 35 µm mesh as well as plankton nets. McMillen and Casey (1978) reported living polycystine diversity indices of up to 1.2 from the surface to 2,000 m depth in the Gulf of Mexico and Caribbean Sea. Their sampling method involved a use of a Nansen closing net with a 76 µm mesh size. Differences in the degree of taxonomic "splitting" by the various authors are probably responsible for part of the differences in reported diversities.

The diversity indices of Spumellaria and Nassellaria at 988 m and below show (Fig. 5) approximately uniform values with depth, indicating that species diversity of the suborders did not change significantly during their descent from 988 to 5068 m. A relatively low value of nassellarian diversity index at 389 m reflects to the total radiolarian diversity index at that depth. This is because the Nassellaria had a greater flux than the rest of the suborders. One possible explanation of the increase in nassellarian diversity index from 389 to 988 m is the introduction of tropical submergent species proposed by Casey and his associates (Casey, 1971a,b; Casey and McMillen, 1977; Casey et al, 1979a) and introduction of deep water species (Reshetnjak, 1955; Casey et al., 1979a). For example, many species in the families Plagiacanthidae and Theoperidae increased their fluxes between 389 and 988 m trap depth at Station E as shown in Tables 3,4. The representative species that agreed with the scheme of deep water species (Casey et al., 1979a) are:

Table 6. Diversity indices of Radiolaria and their suborders from Station E.

	Sediment trap depth (m) 389	988	3755	5068
Spumellaria	3.0788	2.8410	2.9553	2.8827
Nassellaria	2.4883	2.8223	2.8641	2.8071
Phaeodarina	1.8851	1.8027	1.9189	1.6715
Total Radiolaria	3.3187	3.5609	3.6245	3.6040

Table 7. Percent similarity between depths of Radiolaria and their suborders from Station E.

Sediment trap depth (m)	Sediment trap depth (m) 389	988	3755	5068
	Spumellaria			
389	100.0			
988	73.3	100.0		
3755	79.3	73.8	100.0	
5068	72.9	78.6	76.6	100.0
	Nassellaria			
389	100.0			
988	75.3	100.0		
3755	69.5	86.3	100.0	
5068	70.1	80.8	84.3	100.0
	Phaeodaria			
389	100.0			
988	50.2	100.0		
3755	34.5	59.7	100.0	
5068	27.8	62.2	77.7	100.0
	Total Radiolaria			
389	100.0			
988	73.1	100.0		
3755	68.1	82.8	100.0	
5068	65.4	77.7	81.3	100.0

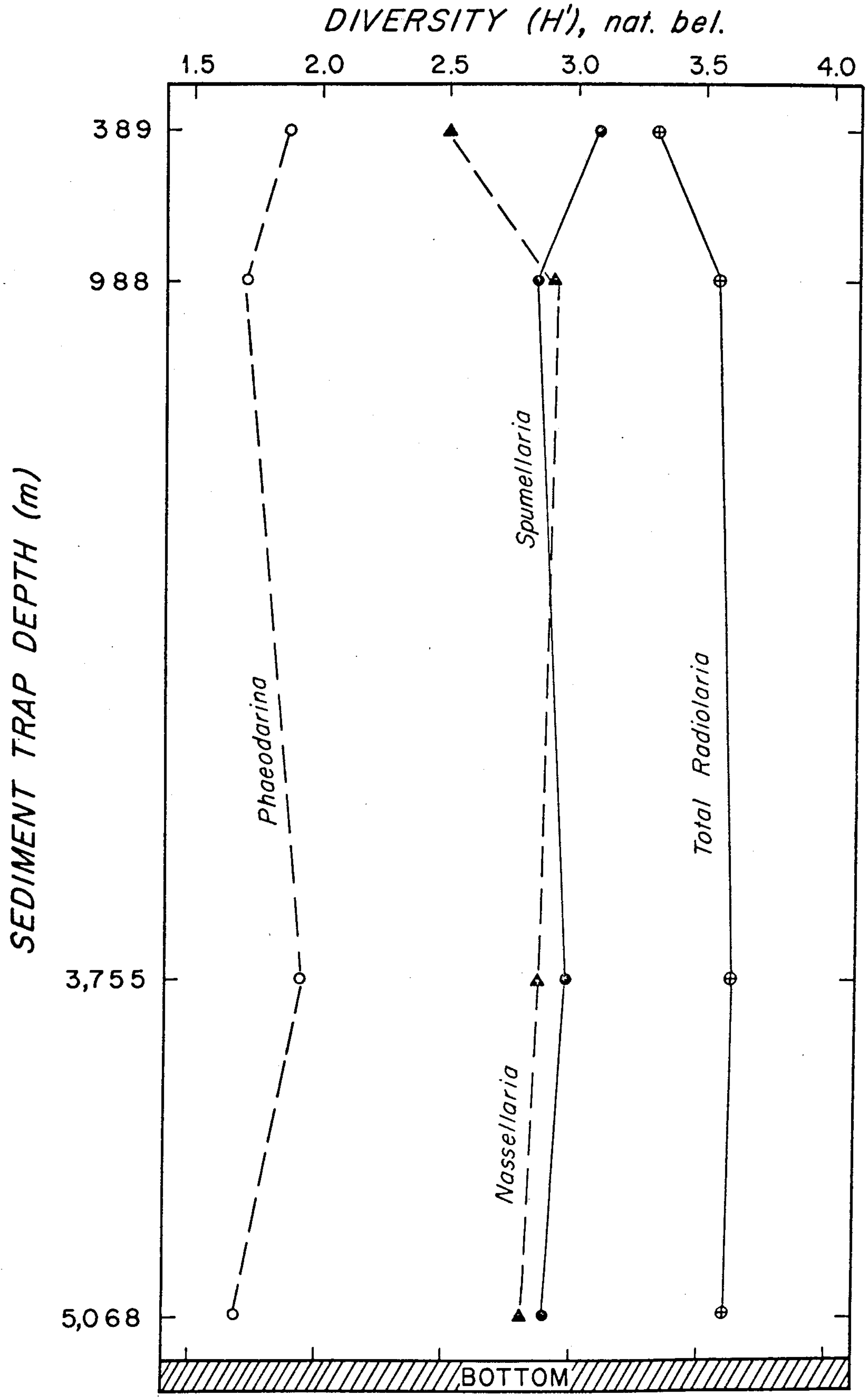

Figure 5. Diversity index (H'), natural bels, of Radiolaria and their suborders from E Station.

Cyrtopera languncula Haeckel; *Peripyramis circumtexta* Haeckel; *Litharachnium tentorium* Haeckel; and *Cornutella profunda* Ehrenberg. An alternative explanation of the increase in nassellarian diversity index is dissolution of some nassellarian shells in the sediment trap receiving cup at 389 m, although I do not believe this is extensive as it will be shown in later sections. The diversity index of Spumellaria decreased slightly from 389 to 988 m.

Phaeodaria presented the lowest indices among the three suborders. They were more variable in the bathypelagic zone. Dissolution of shallow water forms and introduction of deep-water species (Reshetnjak, 1955) result in appearances and disappearance at each trap depth (Table 2, also see Fig. 11). Typical deep-water species are *Euphysetta elegans* Borgert, *Lirella melo* (Cleve), and *L. bullata* (Stadum and Ling) (see Fig. 11). Previously Borgert (1906, p. 174-175) reported occurrence of *E. elegans* between 1,000 and 5,000 m. Haecker (1908b, p. 557) reported *L. melo* from 1,500-5,000 m.

Percent Similarity Analysis

The percent similarity index S (Whittaker and Fairbanks, 1958) has been applied to measure differences in the relative proportion of species in pairs of sediment trap samples at different depths from Station E. Application of this index was analogous to the community comparison reported previously (e.g. Honjo and Okada, 1974). The index is computed by the use of the following equation:

$$S = 100 \times \left(1.0 - 0.5 \sum_{i=1}^{n} \left| P_{ij} - P_{ik} \right| \right)$$

where P_{ij} and P_{ik} are the proportion of the *i*th species in the *j*th and *k*th sample depths, and *n* is the number of species.

As shown in Table 7, the percent similarity indices of Spumellaria from Station E were less variable than other suborders and ranged from 73 to 79. They were within similar values between all the probable pairs of depths. This indicates that composition and population between all possible pairs of depths involving Spumellaria were similar suggesting similar extent of dissolution and population addition effect throughout the depths.

The similarity indices computed for Nassellaria between 389 m and the rest of the depths (70-75%) differs significantly from those of between the rest (81-86%) (Table 7). This is due to an introduction of some deep water species between 389 and 988 m, as discussed earlier. Below 988 m the similarity indices between pairs of depths stayed simiarly high, suggesting little change in nassellarian flux.

Phaeodaria presented a markedly decreasing trend in the similarity indices between 389 m and the progressively greater depths (50 to 28%, Table 7). This was attributed to the additions of deep water species as mentioned in the previous section and to dissolution of specimens probably during their descent. The index between 3,755 and 5,068 m showed about 78%; this was comparable to those of polycystines. Production of deep-dwelling phaeodarians may be accounted for this since the flux includes both effects of dissolution and addition of a population between the depths. Microstructure of phaeodarian shells, which have more porous shells than those of other suborders, contributes to the high rate of dissolution/destruction (Erez et al., in press; Hurd and Takahashi, in press). As stated earlier, since some phaeodarians were already lost in the mesopelagic and upper bathypelagic zones during their descent (Table 2), this is accounted for a continuous addition of the population in the bathypelagic zone which replaces the similar species composition and abundance at 5,068 m.

Vertical flux of Radiolaria and suborders at three tropical stations

Fluxes of three suborders as well as total Radiolaria were more or less uniform throughout the trap depths at the three stations (Table 5, Figs. 3,4), although there are some fluctuations with depth. The fluxes at 3,755 m from Station E were greater than the other depth. This flux maximum at 3,755 m was also true for biogenic opal (Honjo, 1980) and planktonic foraminifera (Thunell and Honjo, 1981) from the same trap samples. The fluxes at 378 and 978 m from Station P_1 were anomalously less than those at deeper depths. This is probably due to exportation of the trapped samples by macro- and megaplankton such as Euphausiids (Honjo, 1980). The fluxes from Station PB appear to fluctuate with depth. Biogenic opal flux from the same samples show a similar trend to this (Honjo et al., in press). Horizontal transport of particles may be responsible for this.

Radiolarian shell flux as a whole showed no decreasing trend throughout the water column at all the three stations (Tables 2,3,4,5; Figs. 3,4). However a significant increase of shell fragmentation with increasing depth was noted; for instance percentage of broken shells to total *Pterocorys* (*P. campanula* Haeckel and *P. zancleus* (Müller)) shells was 12, 10, 20 and 36% at 389, 988, 3,755, and 5,068 m trap depths, respectively, from Station E (Table 8, Fig. 6) (a broken but more than a half preserved shell was counted as one broken shell). The number of shells counted at each depth ranged from 289 to 540. Although less significant than the above, a similar trend in shell fragmentation with depth was observed in Spumellaria, Nassellaria, Phaeodaria, as well as total Radiolaria (Fig. 6). The continuous increase in shell fragmentation with depth suggested that dissolution already initiates during their descent through the water column. Percentages of broken shells at 389 m were slightly higher than at 988 m for all of the taxa shown in Fig. 6 except for Phaeodaria. Field studies (Berger, 1968; Erez et al., in press) and in the laboratory observations (Hurd, 1972, 1973; Hurd and Takahashi, in press) demonstrated much higher dissolution rates of biogenic opal above about 400 m than below in the tropical Pacific. It is possible that some of the trapped radiolarian shells were dissolved within sediment trap receiving cups prior to retrieval. Thus, the higher percentage of broken shells at 389 m than at 988 m could be attributed to trap *in situ* dissolution rather than during their descent in the water column.

Generally the above trend of breakage increase with depth is also true in Phaeodaria. Although there is an opposite trend to this between 389 and 988 m (Fig. 6), this can be explained as follows. Similarity

Table 8. Percentages of broken shells and shells in biogenic aggregates in total counts of a given taxon of Radiolaria from Station E.

	Sediment trap depth (m)			
	389	988	3755	5068
Pterocorys campanula + *P. zancleus*				
(1) Total Counts	540	289	417	317
(2) % broken shells*	12.2	9.7	20.4	36.3
(3) % shells in biogenic aggregates+	13.1	3.7	1.7	0.9
Spirocyrtis sp. aff. *S. seriata*/*S. subscalaris*				
(1) Total counts	187	54	74	123
(2) % broken shells*	4.3	5.6	4.1	5.7
(3) % shells in biogenic aggregates+	7.5	7.4	4.1	0.0
Tetrapyle octacantha				
(1) Total counts	120	68	109	76
(2) % broken shells*	4.2	7.4	9.2	5.3
(3) % shells in biogenic aggregates+	10.0	0.0	1.8	1.0
Spumellaria				
(1) Total counts	749	606	1143	985
(2) % broken shells*	3.9	2.6	4.3	4.6
(3) % shells in biogenic aggregates+	5.3	0.8	2.4	1.8
Nassellaria				
(1) Total counts	1609	1119	1976	1692
(2) % broken shells*	6.3	5.0	7.3	9.0
(3) % shells in biogenic aggregates+	10.4	4.6	2.0	2.1
Phaeodaria				
(1) Total counts	168	67	171	184
(2) % broken shells*	16.7	37.3	29.8	31.0
(3) % shells in biogenic aggregates+	1.8	0.0	1.2	0.5
Total Radiolaria				
(1) Total counts	2526	1792	3290	2861
(2) % broken shells*	6.3	5.4	7.4	8.9
(3) % shells in biogenic aggregates+	8.4	3.1	2.1	1.9

$$\%\ \text{broken shells}^{*} = \frac{\text{broken shells}}{\text{total no. of shells}} \times 100$$

$$\%\ \text{shells in biogenic aggregates}^{+} = \frac{\text{shells in biogenic aggregates}}{\text{total no. of shells}} \times 100$$

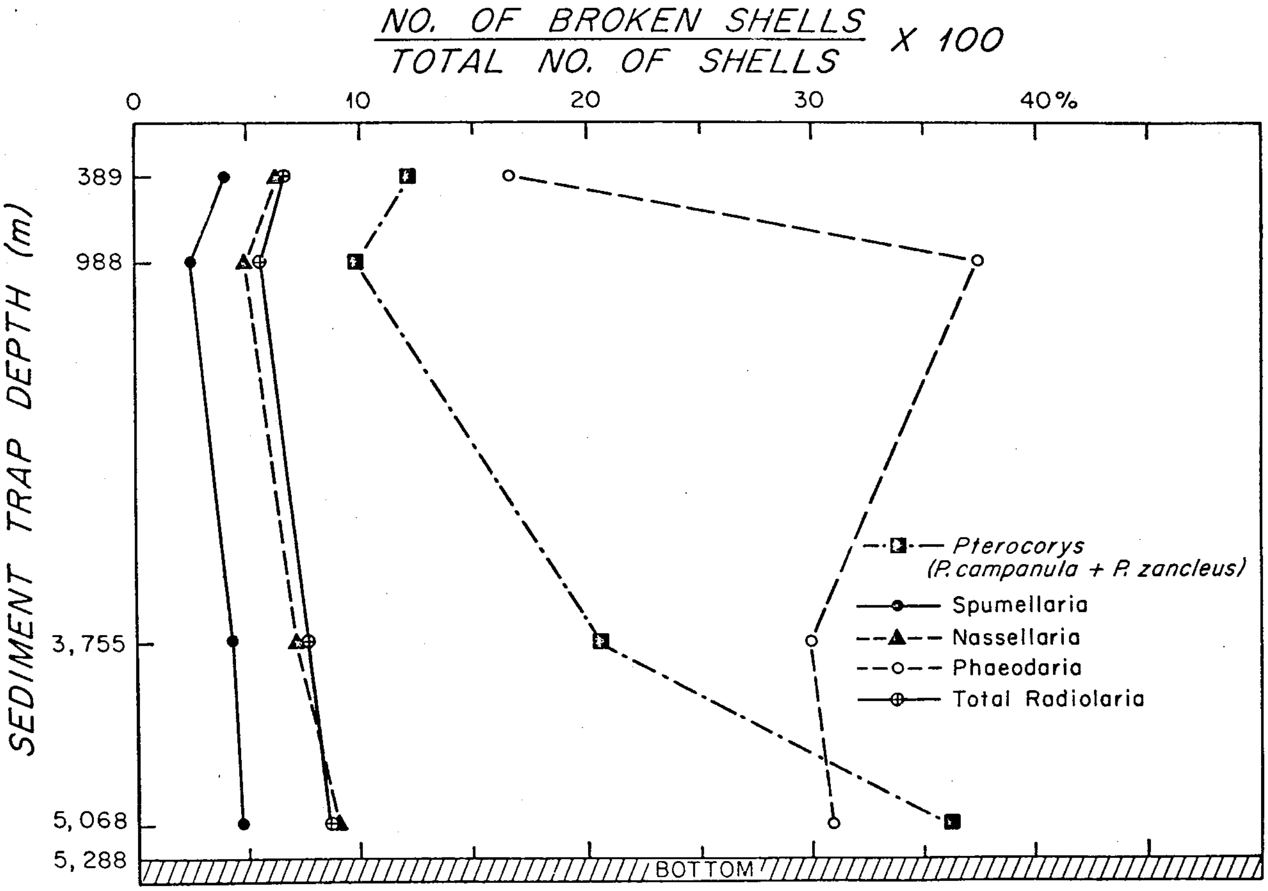

Figure 6. Percentages of broken shells in radiolarian taxa from Station E.

index of Phaeodaria between 988 and 3,755 m was 60 % which is the lowest among all the suborders. An apparent decrease of the percent shell breakage from 988 m to 3,755 m does not necessarily means a true decrease of dissolution effect since species compositions are somewhat different between these two depths shown by the index. Lower values of the percentages of broken shells at 3,755 and 5,068 m than at 988 m were due to introduction of deep water species (Reshetnjak, 1955) which can supply unbroken shells (Table 2). _Challengeron willemoesii_ Haeckel, _Protocystis xiphodon_ (Haeckel), _Euphysetta pusilla_ Cleve, and _Conchidium caudatum_ (Haeckel) appeared to decrease their fluxes significantly as they descend, suggesting their rapid dissolution (see Fig. 11). Phaeodarian dissolution during their descent appeared to be greater than the trap _in situ_ dissolution effect.

Only a few percent of radiolarian shells might be descending more rapidly than the rest of individual shells to the sea-floor. This is substantiated by the following observation where the following types of radiolarian shells were counted in biogenic aggregates: (1) a shell that was incorporated in a biogenically aggregated material (Takahashi and Honjo, 1981; Plate 15, figures 8-11); and (2) an individual shell that was fully or partially wrapped by organic substance which most probably disintegrated from the biogenic aggregates. The examination on _Pterocorys_ (_P. campanula_ Haeckel and _P. zancleus_ (Müller)) showed that the percentages of shells in biogenic aggregates were 13, 4, 2 and 1 % at 389, 988, 3,755, and 5,068 m from Station E respectively (Table 8, Fig. 7). Since the organic components of the samples were preserved _in situ_ in the receiving cups by continuous diffusion of sodium azide (Honjo, 1980) decomposition of the biogenic aggregates was regarded minimal. Total counts used were the same as in the broken shell percentages discussed above. The decrease of the shells in biogenic aggregates with depth is probably due to disintegration/oxidation of the biogenic aggregates during their descent through the water column. The decrease was most significant between 389 and 988 m. Thus, the disintegration of the biogenic aggregates appear to occur more frequently in the mesopelagic than in the bathypelagic zone. A similar trend was observed

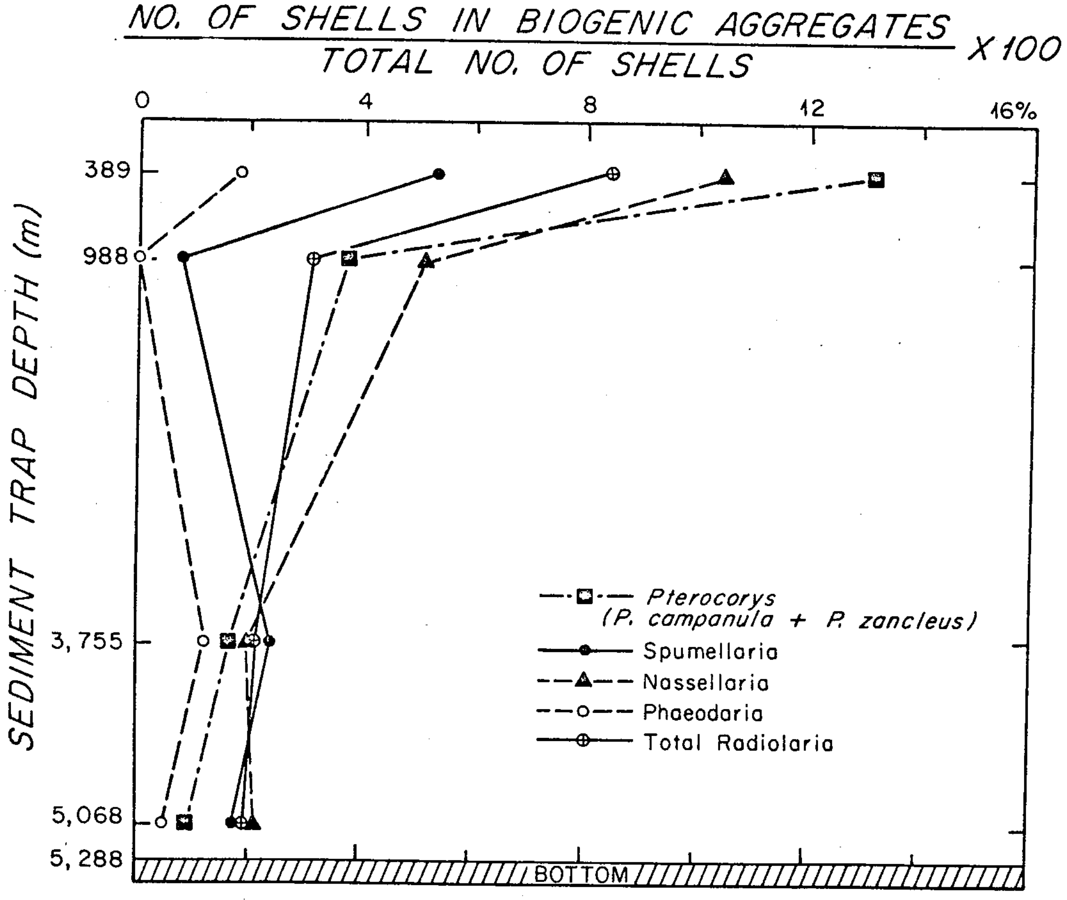

Figure 7. Percentages of shells in biogenic aggregates in radiolarian taxa from Station E.

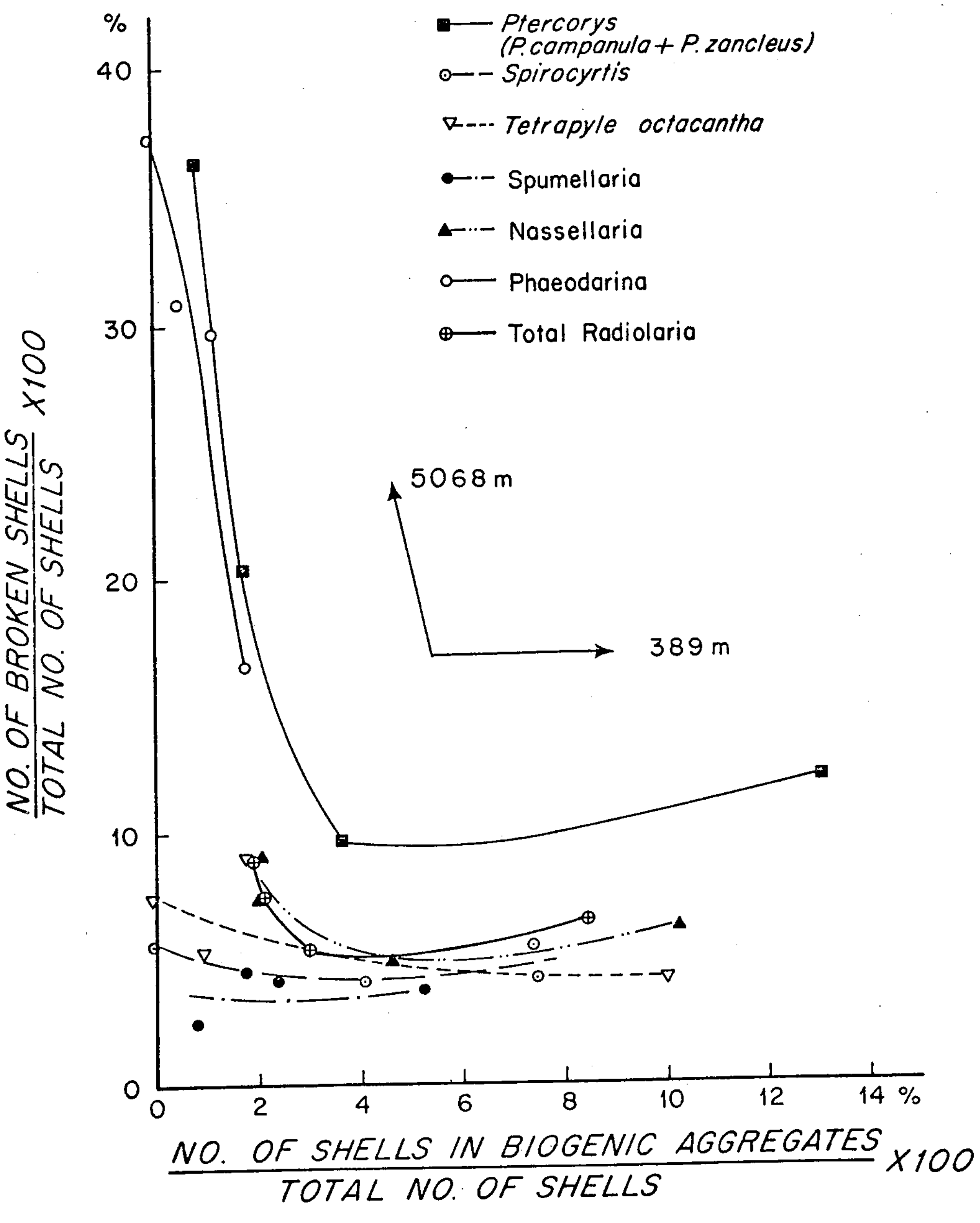

Figure 8. Plots of percentages of shells in biogenic aggregates vs. broken shells in radiolarian taxa from Station E. The shallowest (389 m) samples fall in the lower right side of the figure, whereas the deepest (5,068 m) samples scatter from the lower to upper end of the left side depending on taxon. Samples from 988 to 3,755 m fit in the middle of the curves.

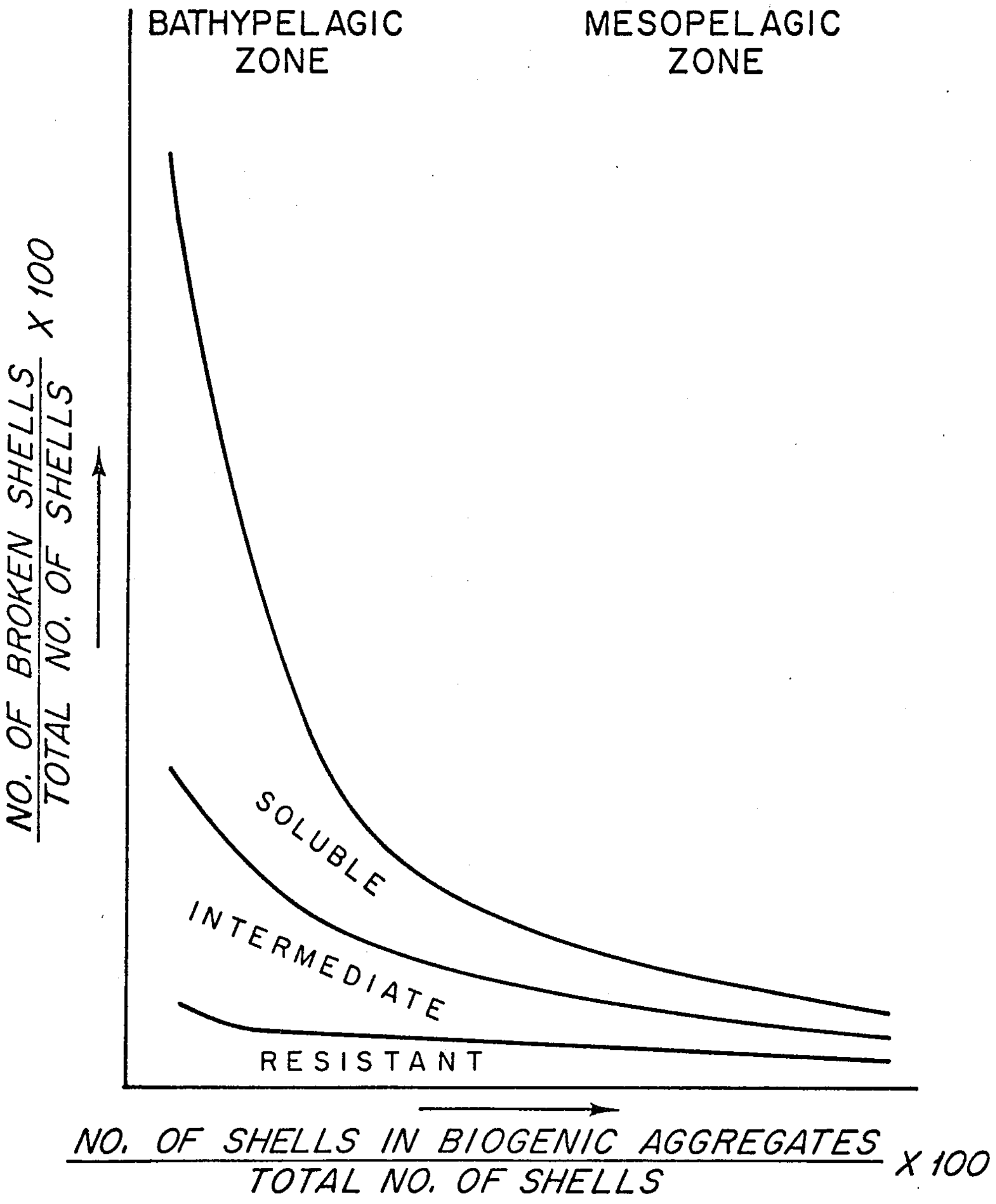

Figure 9. Mode of vertical transport and dissolution model for sinking Radiolaria through mesopelagic and bathypelagic zones. Percentage of broken shells of soluble radiolarian species increases exponentially with depth, while resistant species settle without substantial dissolution effect on their shells.

on all suborders of Radiolaria (Fig. 7). The incrasing values for Spumellaria and Phaeodaria between 988 and 3,755 m were probably due to experimental errors since the biogenic aggregates were rare.

The above shell breakage and the modes of shell transport are combined (Fig. 8) and the following scheme is presented. Generally, the dissolution in the mesopelagic zone is less significant due to their incorporation with the biogenic aggregates. As they descend to the bathypelagic zone, the effect of dissolution sharply increases (Fig. 9). Thus, it appears that the mode of vertical transport plays an important role in not only sinking speed but also skeletal dissolution of Radiolaria.

Percent fluxes of each suborder in total radiolarian shell flux are presented in Table 5. The ratios between two suborders are presented (Fig. 10): Nassellaria and Spumellaria (called N/S ratio in this thesis); Phaeodaria/Spumellaria (Ph/S); and Phaeodaria/Policystina (Ph/P). Nassellaria contributed more than 60% of the total Radiolarian flux counts at all stations and depths and hence this was the predominant suborder. Except between 339 and 988 m at Station E and 378 m and 978 m at Station P_1, the N/S ratio decreased with depth, indicating either an increase in relative Spumellarian flux, or a relative decrease of the Nassellarian flux, or both. The N/S ratios at 389 m at Station E and 378 m at Station P_1 were less than those immediately next depth. This difference is significant and is reasonable considering more input of deep water nassellarians than spumellarians between 389 and 988 m and a possibility of the *in situ* dissolution (Berger, 1968; Erez et al., in press) within the receiving cups.

McMillen and Casey (1978) reported the standing stock of suspended Radiolaria using plankton tows from the surface to a few km depth in the Gulf of Mexico and Caribbean Sea. An analysis by the author based upon their data showed that the N/S ratio decreased three orders of magnitude from the surface to a few km depth. Petrushevskaya (1971a) showed that N/S ratio decreased from her plankton samples to the surface sediments at two stations in the Central Tropical Pacific. The decreasing trend in N/S ratio with depth within the water column appears to be significant.

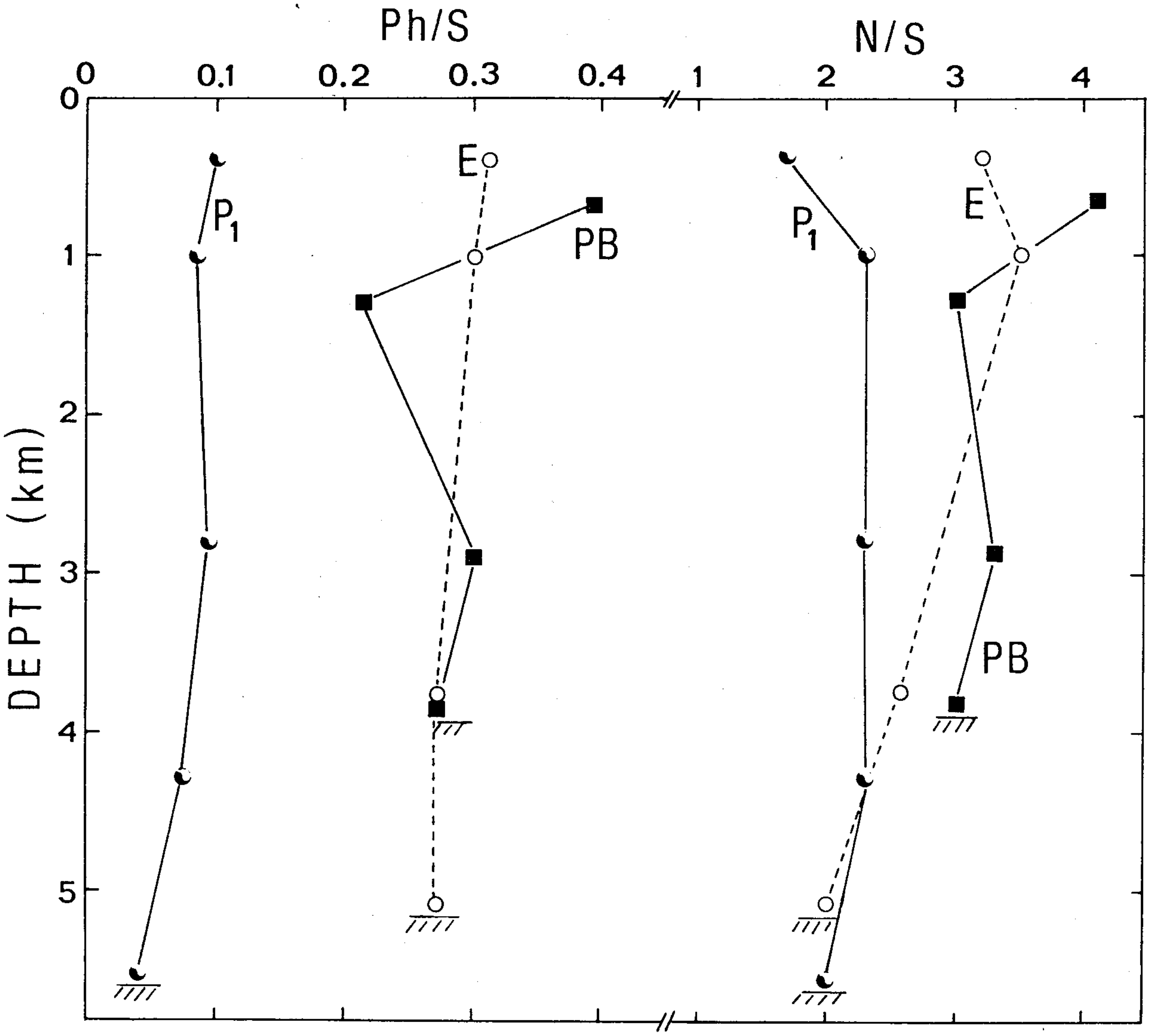

Figure 10. The Nassellaria/Spumellaria and Phaedaria/Spumellaria ratios from Stations E, P_1 and PB.

The reported N/S ratios in the bottom sediments (Berger and Soutar, 1970; Kowsmann, 1973; McMillen, 1979) were generally much lower than my observations in the deepest trap samples from all the three stations suggesting poorer preservation of Nassellaria than Spumellaria in the sediments.

The flux of Phaeodaria was more or less uniform and it was between 6 and 8% in total Radiolaria at all depths at Stations E and PB. Only 1-4% of Phaeodarian flux was observed at Station P_1. As stated previously, species composition of the Phaeodarian flux changed significantly with depth (Table 2). The following species comprised the majority (ca. > 30 shells/m^2/day) of phaeodarian flux in the bathypelagic zone at Stations E and PB: Protocystis xiphodon (Haeckel); Euphysetta elegans Borgert; Euphysetta pusilla Cleve; Medusetta ansata Borgert; Borgertella caudata (Wallich); Lirella melo (Cleve); Lirella bullata (Studam and Ling); Challengeron willemoesii (Haeckel); and Conchidium caudatum (Haeckel). Except for the last two species of medium size, all belonged to the small size category.

Comparison of the radiolarian fluxes with previous work

Range of total radiolarian flux in the unit of x10^3 shells/m^2/day at each Station was: (E) 16.0 - 23.7; (P_1) 0.6 - 17.0; (PB) 29.4 - 53.1 (Table 3). Of these, sum of the flux in 1 mm-250 µm, 250-125 µm, and 125-63 µm size fractions in the unit of x10^3 shells/m^2/day at each Station constituted: (E) 8.7 - 13.4; (P_1) 0.4 - 11.3; and (PB) 25.3 - 38.5 (Tables 3 and 4). These correspond to 56 - 67% (E), 62 - 70 % (P_1) and 63 - 86 % (PB) of the flux in all size fractions; the fine size (<63 µm) fraction contained less than half of the radiolarian flux at all the depths at all the three stations.

Honjo (1978) placed a sediment trap at 5,367 m during winter months in the Sargasso Sea which is known to be one of the least productive areas in the Atlantic (Ryther, 1963). Honjo's total radiolarian shell flux of 14.0x10^3 shells/m^2/day included 10.0x10^3 shells/m^2/day (71%) in the fine size fraction and 4.0x10^3 shells/m^2/day (29%) in

63 μm size fractions. The ratios between >63 μm and the fine size fraction appear to be very different from tropical Stations to the Sargasso Sea. This may also be due to seasonal factors.

Hinga et al. (1979) measured material flux from sediment traps placed at 50 to 100 m above the sea-floor in the slope and rise waters off the Eastern United States. Their data included radiolarian flux of 2.0×10^3 to 6.0×10^3 shells/m^2/day which did not discriminate the fine size fraction. Considering the geographic regions and the deployment depths, it seems possible that their flux measured primary and resuspended radiolarians as assumed by Rowe and Gardner (1979) in the same region. The radiolarian flux values of Hinga et al. (1979) are approximately one order of magnitude smaller than my observations at Station E; however, their total mass and organic carbon fluxes were one order of magnitude greater than those in the same samples from Station E (Honjo, 1980) as to the present study. Judging from their method cited in the text, it appears that their radiolarian flux was severely underestimated. It seems likely that they counted only visible specimens of all size on dry filters under a reflected light microscope.

Berger (1976) calculated supply rates of radiolarians, 0.5×10^3 to 1.1×10^3 shells/m^2/day, to the surface sediments in the Santa Barbara Basin. This was based on Berger and Soutar's (1970) radiolarian counts in the fraction of surface sediments coarser than 62 μm, assuming a sedimentation rate of 1 mm/yr (Emery, 1960). His values are one to two orders of magnitude less than my values of 1 mm-63 μm size fractions from Station E. Considering that carbon flux in the Santa Barbara Basin is two orders of magnitude greater (Soutar et al., 1977) than that of Station E (Honjo, 1980), it seems reasonable to assume that radiolarian production in the former should be greater than at the latter. The radiolarians studied by Berger appear to be already significantly depleted through dissolution process.

Comparison of the radiolarian fluxes with accumulation rates in the Holocene sediments

The total radiolarian flux can be compared with radiolarian accumulation rates in Holocene sediments cited in the literature in order to estimate an extent of preservation. When a unit is converted the flux is: (E) 5.83-8.66x10^5 shells/cm^2/10^3 yrs; (P_1) 0.21-6.22x10^3 shells/cm^2/10^3 yrs; and (PB) 10.72-19.40x10^3 shells/cm^2/10^3 yrs. For instance, the comparison of the flux from Station E with the Holocene sediments involves a sedimentation rate of <0.9 g/cm^2/10^3/yr (Lisitzin, 1972, Fig. 72) and radiolarian abundance of 6000 shells/g of dry surface sediment ($>$ 44 µm: Goll and Bjørklund, 1971: p. 437, 442). These figures combined to yield a radiolarian accumulation rate of $<$5,400 shells/cm^2/10^3 yrs. This rate is equivalent to $<$0.8% of our observed average radiolarian flux. Goll and Bjørklund (1971) stated that their $<$44 µm size fraction contained only small broken fragments of Radiolaria which made the above comparison possible. Furthermore, they noted that the core (raised from 13°29'N, 55°59'W which was located nearest to Station E) contained mostly incomplete radiolarian specimens. The above crude comparison suggests that a high percentage of radiolarians supplied to the bottom sediments has not been preserved due to dissolution process. This is in good agreement with general behavior of biogenic opal discussed by Heath (1974).

Holocene accumalation rates of radiolarian skeletons from the Panama Basin have been estimated by Swift (1976) using counts of whole radiolarians in >63 um size fraction (Kowsmann, 1973): (in the unit of x10^3 shells/cm^2/10^3 yrs) total Radiolaria: 104; Spumellaria: 82; and Nassellaria: 22. In order to compare with the above, average vertical fluxes of Radiolaria (30.8 x 10^3 shells/m^2/day) and the suborders in $>$63 µm size fraction (Table 4) are converted to the unit of x10^3 shells/cm^2/10^3 yrs: total Radiolaria : 1123; Spumellaria: 281; and Nassellaria: 787. The estimated total radiolarian preservation is 9.3 %. This is an order of magnitude higher value than in the equatorial Atlantic Station E where productivity is much less. As it can be predicted on the basis of change in N/S ratio with progress of dissolution, better preservation of Spumellaria is estimated (29.2 % of the flux) than Nassellaria (2.8 %).

Sediment accumulation rate at Station P_1 has been estimated by Honjo (in press). Renz (1976) reported radiolarian counts in >35 µm size fraction per unit dry weight of surface sediments in nearby region: 1400 shells/g. Combining the above data and then comparing with the vertical flux of all size fractions (Table 5), radiolarian preservation of 0.004 % at Station P_1 is obtained.

Although the flux was not quantified, sediment trap samples from Station S were qualitatively studied at 976 m and 3694 m. Analogous to the three other stations, the species composition of flux was similar between the two depths. The surficial bottom sediments obtained by a box core consisted mainly of clay minerals and only a few specimens of robust polycystines such as Tetrapyle octacantha were found in 5 g (wet weight) of samples suggesting a significant dissolution effect to the radiolarian assemblage on the sea-floor.

In conclusion of this section, Radiolaria supplied to the sea-floor are generally largely dissoved there and only a few percent or less is preserved in the underlain Holocene sediments. The extent of preservation may be in part proportional to extent of sedimentation rates.

Effects of radiolarian dissolution in the water column

Since seawater is undersaturated with respect to biogenic silica (e.g. Hurd, 1972), dissolution of the biogenic silica occurs throughout the course of sedimentation. The extent of dissolution varies depending on taxa whose morphology, chemical composition and residence time vary a great deal. An extensive dissolution can dissolve most, if not all, of the descending population of dissolution susceptible taxa such as Challengero willemoesii, a phaeodarian species, within the water column (Table 2; Fig. 11). On the other hand, polycystines are generally not much affected in their species composition and abundance within the water column and only large amounts of statistical data such as N/S ratio can

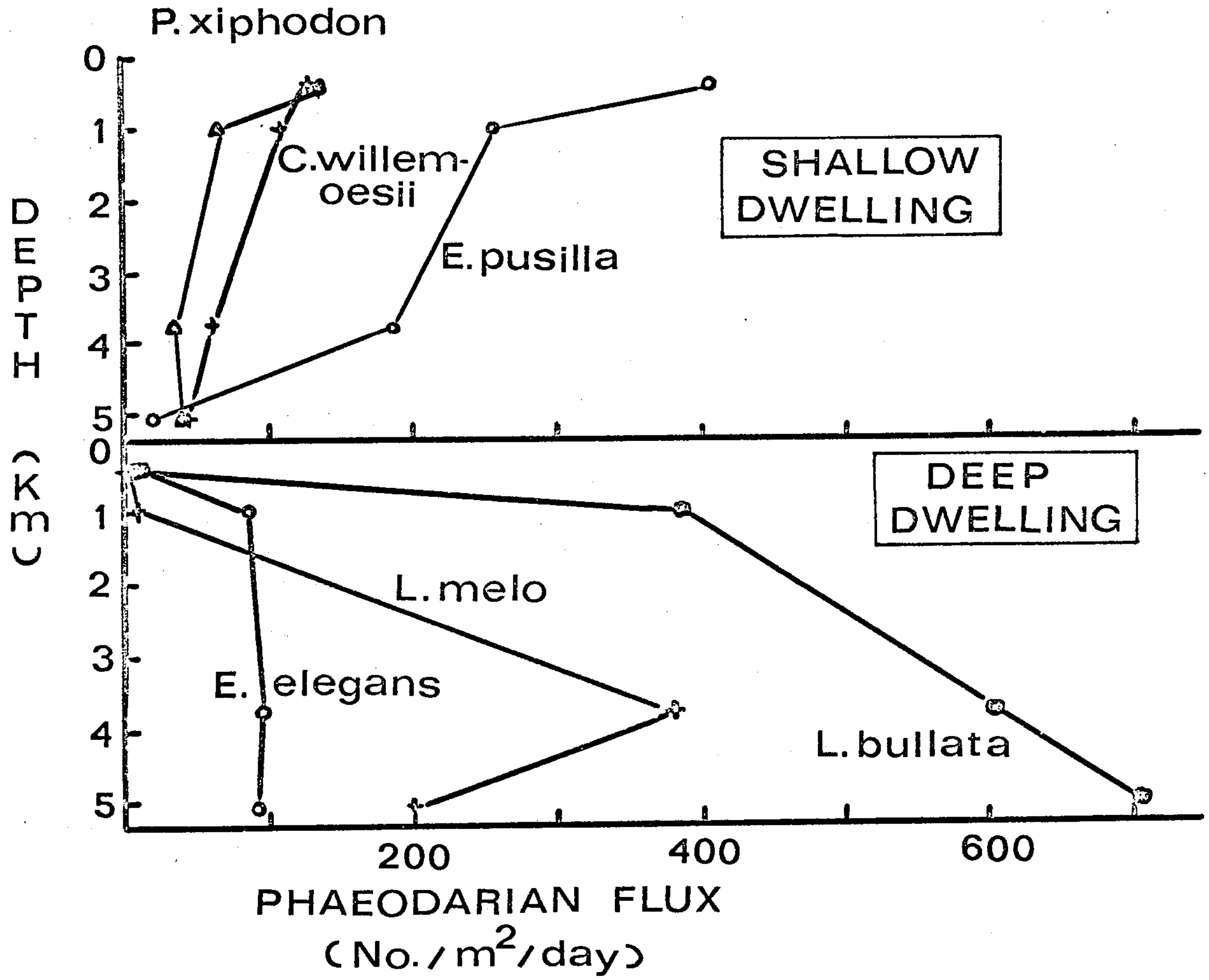

Figure 11. Representative phaeodarian taxa of shallow and deep dwelling species from Station E. The decrease of the shallow dwelling flux with depth is caused by dissolution during sinking. The flux of deep dwelling radiolarians is a mixture of an increase of settling individuals and dissolution of dead shells while sinking.

resolve slight change (Fig. 10). However, when morphology within a shell is examined, an increase of shell breakage with depth has been observed as stated earlier (e.g. Pterocorys).

The above pieces of independent evidence can be further substantiated by ultra- and microstructural evidence of dissolution effects in order to generalize its extent in different taxon groups. Polycystine skeletons from the sediment traps examined by TEM show that generally only approximately 0.1 μm or less of surface layer is porous which is apparently caused by dissolution (e.g. Pl. 43, figs. 10-11). This 0.1 μm or less represents generally very small portion of a cross sectional diameter unless the skeletal elements are extremely thin (e.g. Myelastrum). Therefore, apparent effect of dissolution on bulk morphology is generally insignificant in polycystines and this agrees well with the species counts (Table 2; Figs. 3, 4). Polycystines from the surface sediments are expected to have more porous skeletons than those from the trap samples since they have been exposed to seawater for a long period of time. In fact, they show a trend to be significantly porous (Hurd et al., 1981).

In the case of Phaeodarians, the original skeletal nature of plankton tow samples appears to be very different from the polycystine counterparts. Although they appear somewhat similar to polycystine skeletons at first glance (Pl. 47, fig. 14; Pl. 58, fig. 1), they are different in detail such as having small polygonal pores in the inner part of skeletons except in the surface solid layer of 0.40-0.45 μm thickness. They appear to be dissolved fairly quickly. By the time sediment traps are recovered within a few months, their original structure has drastically changed and become much more porous (e.g. Pl. 47, figs. 11-12; Pl. 53, figs. 9-10; Pl. 58, figs. 3-4). The resulting porous specimens of several taxa have tubular structure (e.g. Pl. 47, fig. 12; Pl. 58, fig. 3; Pl. 59, figs. 12-13). This may be due to a different constitution, e.g., water content, and growth features. The amphora-structure of Challengerids (e.g. Pl. 47, figs. 8-13; Pl. 48, figs. 8-11; Pl. 51, figs. 10-11) appears to be more dissolution-resistant than surrounding cementing parts which are relatively soluble. The amphorae may be made of similar skeletal silica as the polycystine skeletons.

There are several phaeodarian taxa that are generally consistently recovered from bottle casting or plankton net tows but not from the traps. These include Euphysetta sp. (Pl. 63, figs. 12-13), Medusetta robusta Borgert (1902) and Medusetta armata Borgert (1901). It is apparent that such thin shells made of one or two layers of tubuler skeletons, shown in the illustration , are quickly disintegrated and hence never found in the trap samples. The fate of Sticholonche, classified now as Heliozoa (Cachon and Cachon, 1978), is analogous to the above and has never been found as an intact shell but only as dispersed spines in the trap samples (Takahashi and Ling, 1980). Aulosphaerids and Aulacanthids are also readily disintegrated and only partial skeletons of the shells are recovered from the traps (Pl. 63, figs. 1-11).

Dimensions of radiolarian skeletons

Dimensions that are measured here are weight, length, width, maximum projected area (PA) and that computed are computed projected area (CPA), bulk volume (V_b) which includes a parcel of water within a shell, and volume of skeleton (V_{skel}) (Table 9). Since the length and width are normally readily accessible by using a microscope, their correlations with the rest of the dimensional data facilitate fundamental information (Figs. 12-13, 15-17). All the possible combinations of log-log relationships between the above dimension variables are presented (Table 10; Figs. 12-17). As it will be discussed in the following section, laboratory sinking speed of individual radiolarian shells is best correlated with weight values among all the variables of the dimensions. When combined with SiO_2 content data on weight/shell are of interest to geochemistry which will also be discussed in the later section. Previously, Petrushevskaya (1966, cited in Lisitzin, 1972) reported that approximate weight range of radiolarians from plankton samples is 0.33-1.00 μg/shell.

Weight values of fossil radiolarians have been reported from the equatorial Pacific ranging from 0.063 μg/shell of Quaternary to ca. 0.30 μg/shell of Eocene in age (Moore, 1969). The author also independently obtained 0.136 ± 0.009 μg/shell, an average weight of fossil radiolarians from a core V24-58, 777 cm (~1 Ma: Hays et al., 1969) raised in the central Tropical Pacific, by the same method (Moore, 1969) suggesting consistency with Moore's data. It is important to note that values obtained here from the traps are orders of magnitude greater than the above Quaternary samples.

Taxonomic consideration on samples from both sediment traps and bottom sediment preserved radiolarians have a clue to understanding the above difference in the weight between the two different groups. Phaeodarians and large-sized polycystines are generally absent in the sediment samples. The large and heavy polycystines are generally made of thin skeletal elements forming a network of spongy shells (e.g. Conicavus tipiopsis n.sp., Myelastrum trinibrachium n.sp.). Since preservation is a function of skeletal thickness but not the size of a shell (Hurd and Takahashi, in prep.) and hence these species are likely to be dissolved on the sea-floor or soon after burial. Some of the Phaeodaria are also significantly heavier (i.e. most of Castanellids, Haeckeliana porcellana and Conchopsis compressa) than the polycystine counterparts. For instance, a Castanellid weighing 130.0 μg/shell was observed, although this value does not directly appear in Table 9 since only mean values are tabulated. This value is approximately 2000 times heavier than Pterocorys zancleus or Pterocorys campanula which are the most abundant taxa at Station E. Therefore, the heavy weight radiolarians appears to play an important role in transporting and releasing silica and its associated elements in the deep-sea as in the case of Foraminifera (Boyle, 1981). The extent of their vertical silica transport contribution is quantitatively considered in the last section of the discussion.

(cont. to p. 91)

Table 9 . Radiolarians from the sediment traps: size, laboratory sinking speed and residence time in the water column. The S.D. is at 95^{0}/o confidence level (2σ) and n is number of measurements (specimens). See text for explanations for τ_n.

	WEIGHT (μg)				LENGTH (μm)			WIDTH (μm)			PROJECTED AREA ($\times 10^3 \mu m^2$)		
	Mean	Anal. Err.	S.D	n*	Mean	S.D.	n	Mean	S.D.	n	Mean	S.D.	n
SPUMELLARIA													
1. Acrosphaera murrayana (Haeckel)	.46	.01	-	207	176	18	126	-	-	-	-	-	-
2. Actinomma arcadophorum Haeckel	.91	.02	.06	273	269	26	8	-	-	-	-	-	-
3. Amphirhopalum ypsilon Haeckel	.57	.06	-	7	305	42	6	178	34	6	49.0	13.0	5
4. Cladococcus scoparius Haeckel	1.00	1.00	-	1	106	63	2	-	-	-	-	-	-
5. Dictyocoryne profunda Ehrenberg >350 µm	1.69	.05	.55	72	424	33	14	-	-	-	-	-	-
6. Dictyocoryne profunda Ehrenberg <350 µm	.83	.03	.11	241	294	42	50	-	-	-	52.4	10.0	13
7. Dictyocoryne truncatum (Ehrenberg)	2.00	.07	.27	40	308	43	13	-	-	-	-	-	-
8. Euchitonia elegans (Ehrenberg)	.57	.03	.12	226	369	43	43	277	55	43	65.7	15.0	29
9. Heliodiscus asteriscus Haeckel	.36	.04	-	11	176	16	9	-	-	-	-	-	-
10. Myelastrum quadrifolium n.sp.	2.32	.16	-	13	704	49	12	757	51	12	429.1	72.0	12
11. Myelastrum trinibrachium n.sp.	.75	.13	-	16	1027	120	7	-	-	-	283.9	40.0	7
12. Saturnalis circularis Haeckel	.05	.05	-	4	205	6	4	245	27	4	-	-	-
13. Spongaster tetras tetras Ehrenberg	1.23	.15	-	13	258	63	12	-	-	-	-	-	-
14. Spongocore cylindrica (Haeckel)	.36	.09	-	22	280	49	6	99	22	7	21.8	7.0	6
15. Spongodiscus biconcavus (Haeckel) >270 µm	.99	.08	.02	46	313	38	15	-	-	-	-	-	-
16. Spongodiscus biconcavus (Haeckel) <270 µm	.62	.01	-	37	224	35	14	-	-	-	-	-	-
17. Spongosphaera polycantha Muller		-	-	-	298	163	4	-	-	-	-	-	-
18. Spongosphaera sp. aff S. helioides Haeckel	4.10	.20	-	2	878	4	2	-	-	-	-	-	-
19. Spongotrochus glacialis Popofsky	.42	.02	.01	116	236	36	17	-	-	-	-	-	-
NASSELLARIA													
30. Acanthodesmia vinculata (Muller)	.11	.02	-	17	107	12	20	147	22	28	14.0	5.0	6
31. Androspyris reticulidisca n.sp.	.71	.11	.10	18	363	45	20	336	19	20	96.4	10.0	20
32. Anthocyrtidium ophirense (Ehrenberg)	.14	.01	-	77	191	12	6	132	3	6	14.6	2.0	5
33. Anthocyrtidium zanguebaricum (Ehrenberg)	.08	.03	-	14	156	16	11	86	5	11	8.3	1.0	11
34. Callimitra annae Haeckel	.07	.07	.01	29	300	43	13	251	33	13	62.7	18.0	12
35. Callimitra emmae Haeckel	-	-	-	-	322	-	1	342	-	1	93.7	-	1
36. Carpocanistrum spp.	-	-	-	-	109	18	7	77	7	7	-	-	-

TABLE 9 (cont.)

37. Cephalospyris cancellata Haeckel	.11	.02	-	19	301	57	11	206	48	11	50.4	18.0	11
38. Conicavustipiopsis n.sp.	.58	.04	-	25	567	89	31	372	42	36	152.4	28.0	30
39. Cornutella profunda Ehrenberg	.08	.01	-	29	161	18	7	65	9	7	6.9	1.0	7
40. Dictyocodon elegans (Haeckel)	.25	.10	-	4	325	56	4	230	41	4	56.5	16.0	4
41. Eucecryphalus tricostatus (Haeckel)	.10	.03	-	30	206	33	16	-	-	-	41.5	-	1
42. Eucyrtidium acuminatum (Ebg)+hexagonatum Hkl	.29	.02	-	41	248	43	24	105	13	24	20.6	6.0	24
43. Lamprocyclas maritalis maritalis Haeckel	.49	.04	-	23	229	22	23	144	12	24	19.0	4.0	17
44. Liriospyris thorax (Haeckel)	.25	.02	-	24	196	34	6	222	65	5	36.3	15.0	5
45. Lithostrobus hexagonalis Haeckel	.14	.03	-	14	191	32	9	141	18	13	22.0	6.0	9
46. Lophospyris pentagona pentagona (Ehrenberg)	.10	.04	-	9	117	18	7	144	19	7	-	-	-
47. Nephrospyris renilla Haeckel	1.00	.17	-	6	413	71	9	509	71	9	177.3	60.0	7
48. Pterocorys zancleus (Mlr) + campanula Hkl	.07	.03	.01	158	170	28	57	104	15	58	11.9	3.0	30
49. Spirocyrtis scalaris Haeckel	.07	.01	-	69	209	23	20	121	9	20	18.6	3.0	20
<u>PHAEODARIA</u>													
80. Castanellids from E	24.15	.01	30.00	268	473	151	45	-	-	-	-	-	-
81. Castanellids from PB	12.77	.03	-	70	382	91	32	-	-	-	-	-	-
82. Castanellids from PB <300 μm	-	-	-	-	-	-	-	-	-	-	-	-	-
83. Castanellids fragments	-	-	-	-	-	-	-	-	-	-	-	-	-
84. Castanidium abundiplanatum n.sp.	.80	.02	-	22	308	21	18	-	-	-	-	-	-
85. Challengeria tizardi Murray	.54	.03	.16	18	340	25	5	272	30	8	66.7	.6	2
86. Challengeron willemoesii Haeckel	.07	.01	-	15	255	58	2	120	10	2	20.4	6.0	2
87. Challengeron lingi n.sp.	.07	.01	-	15	240	30	6	159	33	7	-	-	-
88. Challengerosium avicularia Haecker	.18	.03	-	8	-	-	-	177	8	11	-	-	-
89. Circoporus oxycanthus Borgert	.10	.01	-	15	231	111	6	-	-	-	-	-	-
90. Conchidium argiope Haeckel	.10	.01	-	126	196	14	19	138	6	4	22.4	3.0	3
91. Conchellium capsula Borgert	.50	.11	-	9	264	11	11	-	-	-	-	-	-
92. Conchopsis compressa Haeckel	3.05	.20	.23	322	587	28	8	329	25	8	147.5	12.0	8
93. Euphysetta elegans Borgert	.05	.01	-	34	258	16	9	112	13	22	12.4	3.0	12
94. Haeckeliana porcellana Haeckel	9.73	.02	-	125	407	54	32	-	-	-	126.8	26.0	22
95. Protocystis sloggetti (Haeckel)	.16	.04	-	5	214	18	5	170	-	2	23.1	3.0	2
96. Protocystis murrayi (Haeckel)	.47	.13	-	3	-	-	-	206	7	3	-	-	-
97. Protocystis curva n.sp.	.16	.01	-	44	180	6	3	145	24	5	17.2	.2	3
98. Protocystis honjoi n.sp.	.10	.05	-	4	-	-	-	148	11	4	-	-	-

n* = total number of specimens used rather than number of measurements

TABLE 9 (cont.)

	COMPUTED PROJECTED AREA ($x10^3 \mu m^2$)			BULK VOLUME V_b ($x10^3 \mu m^3$)	$^o/o$ VOLUME SKELETON IN V_b P_{skel} ($^o/o$)	VOLUME OF SKELETON V_{skel} ($x10^3 \mu m^3$)	BULK DENSITY CONTRAST	
	Mean	S.D.	n				$\Delta\rho$ at 3°C (g/cm^3)	$\Delta\rho$ at 10°C (g/cm^3)
SPUMELLARIA								
1. Acrosphaera murrayana (Haeckel)	24.6	5.0	126	2.85	8.1	230	.07838	.07846
2. Actinomma arcadophorum Haeckel	57.2	11.0	8	10.19	4.5	455	.04337	.04341
3. Amphirhopalum ypsilon Haeckel	-	-	-	1.49	19.1	285	.18578	.18596
4. Cladococcus scoparius Haeckel	10.3	10.0	2	354.39	0.1	500	.00137	.00137
5. Dictyocoryne truncatum (Ehrenberg)	62.9	18.0	13	16.84	5.9	1000	.05768	.05773
6. Euchitonia elegans (Ehrenberg)	-	-	-	5.49	5.2	285	.05042	.05047
7. Heliodiscus asteriscus Haeckel	24.5	4.0	9	2.63	6.8	180	.06647	.06654
8. Dictyocoryne profunda Ehrenberg >350 μm	94.9	15.0	14	1.08	78.2	845	.75995	.76068
9. Dictyocoryne profunda Ehrenberg <350 μm	-	-	-	10.06	4.1	415	.04007	.04011
10. Myelastrum quadrifolium n.sp.	-	-	-	3.85	30.1	1160	.29265	.29294
11. Myelastrum trinibracium n.sp.	-	-	-	30.21	1.2	375	.01205	.01207
12. Saturnalis circularis Haeckel	13.0	2.0	4	29.16	0.1	25	.00083	.00083
13. Spongaster tetras tetras Ehrenberg	70.1	35.0	12	0.44	139.8	615	1.35761	1.35893
14. Spongocore cylindrica (Haeckel)	-	-	-	4.52	4.0	180	.03869	.03872
15. Spongodiscus biconcavus (Haeckel) >270 μm	78.2	19.0	15	2.16	2.9	495	.22259	.22280
16. Spongodiscus biconcavus (Haeckel) <270 μm	40.3	12.0	14	6.12	5.1	310	.04920	.04925
17. Spongosphaera polycantha Muller	85.2	83.0	4	2.26	-	-	-	-
18. Spongosphaera sp. aff S. heloiodes Haeckel	604.8	5.0	2	13.86	14.8	2050	.14366	.14380
19. Spongotrochus glacialis Popofsky	44.8	14.0	17	2.64	8.0	210	.07726	.07734
NASSELLARIA								
30. Acanthodesmia vinculata (Muller)	-	-	-	.88	6.3	55	.06070	.06076
31. Androspyris retidisca n.sp.	-	-	-	8.75	4.1	355	.03941	.03944
32. Anthocyrtidium ophirense (Ehrenberg)	-	-	-	1.05	6.7	70	.06475	.06482
33. Anthocyrtidium zanguebaricum (Ehrenberg)	-	-	-	.37	10.8	40	.10500	.10511
34. Callimitra annae Haeckel	-	-	-	3.15	1.1	35	.01079	.01080
35. Callimitra emmae Haeckel	-	-	-	6.28	-	-	-	-
36. Carpocanistrum spp.	6.9	2.0	7	.42	-	-	-	-

TABLE 9 (cont.)

37. Cephalospyris cancellata Haeckel	-	-	-	3.34	1.7	55	.01599	.01601
38. Conicavus tipiopsis n.sp..	-	-	-	20.54	1.4	290	.01371	.01373
39. Cornutella profunda Ehrenberg	-	-	-	.18	2.2	40	.21584	.21605
40. Dictyocodon elegans (Haeckel)	-	-	-	5.45	2.3	125	.02227	.02229
41. Eucecryphalus tricostatus (Haeckel)	34.1	11.0	16	1.83	2.7	50	.02654	.02656
42. Eucyrtidium acuminatum (Ebg) + hexagonatum Hkl	-	-	-	.87	16.7	145	.16188	.16204
43. Lamprocyclas maritalis maritalis Haeckel	-	-	-	1.50	16.3	245	.15864	.15580
44. Liriospyris thorax (Haeckel)	-	-	-	4.98	2.5	125	.02438	.02440
45. Lithostrobus hexagonalis Haeckel	-	-	-	1.20	5.8	70	.05666	.05671
46. Lophospyris pentagona pentagona (Ehrenberg)	13.7	4.0	7	1.28	3.9	50	.03794	.03798
47. Nephrospyris renilla Haeckel	-	-	-	12.20	4.1	500	.03981	.03984
48. Pterocorys zancleus (Mlr) + campanula Hkl	-	-	-	.58	6.0	355	.05861	.05867
49. Spirocyrtis scalaris Haeckel	-	-	-	.97	3.6	35	.03504	.03508
PHAEODARIA								
80. Castanellids from E	193.0	131.0	45	55.41	21.8	12075	.21166	.21187
81. Castanellids from PB	120.7	68.0	32	29.19	21.9	6385	.21246	.21267
82. Castanellids from PB <300 µm	-	-	-	-	-	-	-	-
83. Castanellids fragments	-	-	-	-	-	-	-	-
84. Castanidium abundiplanatum n.sp.	74.1	9.0	13	15.15	2.6	400	.02564	.02567
85. Challengeria tizardi Murray	-	-	-	8.23	3.3	270	.03186	.03189
86. Challengeron willemoesii Haeckel	-	-	-	1.54	2.3	35	.02207	.02209
87. Challengeron lingi n.sp.	24.8	9.0	7	1.59	2.2	35	.02138	.02140
88. Challengerosium avicularia Haecker	24.8	2.0	11	1.92	4.7	90	.04553	.04557
89. Circoporus oxycanthus Borgert	60.0	48.0	6	6.45	0.8	50	.00753	.00753
90. Conchidium argiope Haeckel	-	-	-	0.98	5.1	50	.04955	.04960
91. Conchellium capsula Borgert	56.3	5.0	4	5.04	5.0	250	.04818	.04823
92. Conchopsis compressa Haeckel	-	-	-	52.95	2.9	1525	.02800	.02800
93. Euphysetta elegans Borgert	-	-	-	0.74	3.4	25	.03281	.03284
94. Haeckeliana porcellana Haeckel	-	-	-	35.30	13.8	4865	.13386	.13400
95. Protocystis sloggetti (Haeckel)	-	-	-	1.95	4.1	80	.03985	.03988
96. Protocystis murrayi (Haeckel)	40.0	3.0	3	4.58	5.1	235	.04984	.04988
97. Protocystis curva n.sp.	-	-	-	1.19	6.7	80	.06529	.06536
98. Protocystis honjoi n.sp.	20.0	3.0	4	1.02	4.9	50	.04761	.04766

TABLE 9 (cont.)

	SINKING SPEED, $W_{observed}$											
	T=3^{o}C, S=36.1^{o}/oo (m/day)			T=10^{o}C, S=36.1^{o}/oo (m/day)			T=20^{o}C, S=36.1^{o}/oo (m/day)			T=20°C, S=30.5^{o}/oo (m/day)		
	Mean	S.D.	n	Mean	S.D.	n	Mean	S.D.	n	Mean	S.D	n
SPUMELLARIA												
1. Acrosphaera murrayana (Haeckel)	64.1	11.0	14	131.3	49.1	11	-	-	-	-	-	-
2. Actinomma arcadophorum Haeckel	71.8	21.9	12	91.5	11.1	9	-	-	-	-	-	-
3. Amphirhopalum ypsilon Haeckel	68.2	25.2	5	-	-	-	-	-	-	-	-	-
4. Cladococcus scoparius Haeckel	19.0	-	1	-	-	-	-	-	-	-	-	-
5. Dictyocoryne profunda Ehrenberg >350 µm	163.9	42.5	14	183.8	24.7	13	218.8	30.0	13	-	-	-
6. Dictyocoryne profunda Ehrenberg <350 µm	100.8	21.4	10	114.4	16.5	10	-	-	-	-	-	-
7. Dictyocoryne truncatum (Ehrenberg)	177.3	29.6	12	-	-	-	-	-	-	-	-	-
8. Euchitonia elegans (Ehrenberg)	69.3	22.9	27	115.1	58.6	16	93.5	33.0	12	166.0	34.8	20
9. Heliodiscus asteriscus Haeckel	65.2	24.9	8	-	-	-	-	-	-	-	-	-
10. Myelastrum quadrifolium n.sp.	40.1	11.7	11	-	-	-	-	-	-	-	-	-
11. Myelastrum trinibrachium n.sp.	27.8	4.7	8	-	-	-	-	-	-	-	-	-
12. Saturnalis circularis Haeckel	24.6	5.9	3	-	-	-	-	-	-	-	-	-
13. Spongaster tetras tetras Ehrenberg	152.9	55.4	12	-	-	-	-	-	-	-	-	-
14. Spongocore cylindrica (Haeckel)	61.7	28.5	20	-	-	-	-	-	-	-	-	-
15. Spongodiscus biconcavus (Haeckel) >270 µm	108.9	15.0	13	152.5	36.5	13	-	-	-	-	-	-
16. Spongodiscus biconcavus (Haeckel) <270 µm	85.7	21.0	12	-	-	-	-	-	-	-	-	-
17. Spongosphaera polycantha Muller	77.6	56.9	7	-	-	-	-	-	-	-	-	-
18. Spongosphaera sp. aff S. heliodes Haeckel	146.2	68.9	2	-	-	-	-	-	-	-	-	-
19. Spongotrochus glacialis Popofsky	76.1	18.5	10	97.5	26.6	6	-	-	-	-	-	-
NASSELLARIA												
30. Acanthodesmia vinculata (Muller)	31.0	5.4	12	-	-	-	-	-	-	-	-	-
31. Androspyris retidisca n.sp.	70.0	22.4	9	-	-	-	-	-	-	-	-	-
32. Anthocyrtidium ophirense (Ehrenberg)	27.2	5.3	12	58.8	9.3	5	-	-	-	-	-	-
33. Anthocyrtidium zanguebaricum (Ehrenberg)	28.0	9.1	4	-	-	-	-	-	-	-	-	-
34. Callimitra annae Haeckel	15.9	7.2	7	-	-	-	-	-	-	-	-	-
35. Callimitra emmae Haeckel	23.5	14.1	2	-	-	-	-	-	-	-	-	-
36. Carpocanistrum spp.	-	-	-	-	-	-	-	-	-	-	-	-

TABLE 9 (cont.)

37. Cephalospyris cancellata Haeckel	15.1	8.6	9	-	-	-	-	-	-	-	-	-
38. Conicavus tipiopsis n.sp.	38.6	8.6	14	-	-	-	-	-	-	-	-	-
39. Cornutella profunda Ehrenberg	21.5	12.1	16	-	-	-	-	-	-	68.0	12.2	11
40. Dicyocodon elegans (Haeckel)	22.0	2.0	4	-	-	-	-	-	-	-	-	-
41. Eucecryphalus tricostatus (Haeckel)	14.3	6.0	15	18.7	6.8	2	-	-	-	61.3	15.8	11
42. Eucyrtidium acuminatum (Ebg)+hexagonatum Hkl	61.0	13.4	13	-	-	-	-	-	-	-	-	-
43. Lamprocyclas maritalis maritalis Haeckel	105.1	32.4	12	-	-	-	134.8	-	1	-	-	-
44. Liriospyris thorax (Haeckel)	35.1	7.0	15	59.2	7.6	8	-	-	-	83.2	7.6	5
45. Lithostrobus hexagonalis Haeckel	43.3	27.9	10	-	-	-	-	-	-	-	-	-
46. Lophospyris pentagona pentagona (Ehrenberg)	-	-	-	-	-	-	-	-	-	-	-	-
47. Nephrospyris renilla Haeckel	62.9	27.3	6	-	-	-	-	-	-	-	-	-
48. Pterocorys zancleus (Mlr) + campanula Hkl	24.9	5.7	24	27.0	9.3	6	-	-	-	-	-	-
49. Spirocyrtis scalaris Haeckel	21.5	7.8	9	-	-	-	-	-	-	-	-	-
PHAEODARIA												
80. Castanellids from E	384.3	334.8	21	-	-	-	-	-	-	-	-	-
81. Castanellids from PB	126.1	119.4	32	-	-	-	-	-	-	208.6	81.9	15
82. Castanellids from PB <300 µm	53.4	21.5	15	89.3	41.1	13	97.9	48.3	15	-	-	-
83. Castanellids fragments	43.5	23.2	8	-	-	-	-	-	-	-	-	-
84. Castanidium abundiplanum n.sp.	58.8	25.6	12	-	-	-	-	-	-	-	-	-
85. Challengeria tizardi Murray	43.3	9.3	5	-	-	-	-	-	-	-	-	-
86. Challengeron willemoesii Haeckel	20.2	3.9	4	-	-	-	-	-	-	-	-	-
87. Challengeron lingi n.sp.	21.8	3.6	2	-	-	-	-	-	-	-	-	-
88. Challengerosium avicularia Haecker	20.5	.3	3	-	-	-	-	-	-	-	-	-
89. Circoporus oxycanthus Borgert	14.5	4.6	4	-	-	-	-	-	-	-	-	-
90. Conchidium argiope Haeckel	17.0	5.3	14	-	-	-	-	-	-	-	-	-
91. Conchellium capsula Borgert	-	-	-	-		-	-	-	-	-	-	-
92. Conchopsis compressa Haeckel	176.0	25.6	11	-	-	-	-	-	-	-	-	-
93. Euphysetta elegans Borgert	12.9	2.6	14	-	-	-	-	-	-	-	-	-
94. Haeckeliana porcellana Haeckel	416.4	202.8	18	443.6	142.4	11	674.2	212.4	11	-	-	-
95. Protocystis sloggetti (Haeckel)	39.1	1.1	2	-	-	-	-	-	-	-	-	-
96. Protocystis murrayi (Haeckel)	46.2	23.5	3	-	-	-	-	-	-	-	-	-
97. Protocystis curva n.sp.	35.6	26.4	11	-	-	-	-	-	-	-	-	-
98. Protocystis honjoi n.sp.	22.6	1.6	2	-	-	-	-	-	-	-	-	-

TABLE 9 (cont.)

	RESIDENCE TIME				STOKES LAW $W_{theoretical}$		RESIDUAL FACTOR $\frac{W_{observed}}{W_{theoretical}}$		SAMPLE SOURCE Station/depth (m)
	τ_1 Mean	τ_1 S.D.	τ_2 Mean	τ_3 Mean	at 3°C (m/day)	at 10°C (m/day)	at 3°C	at 10°C	
SPUMELLARIA									
1. Acrosphaera murrayana (Haeckel)	80.0	13.3	71.6	-	67.2	81.7	.954	1.608	PB3769/3791
2. Actinomma arcadophorum Haeckel	75.4	21.3	67.2	-	86.8	105.5	.827	.867	E^+;PB3769/3791;E389
3. Amphirhopalum ypsilon Haeckel	80.5	25.2	-	-	299.8	364.4	.227	-	PB3769/3791
4. Cladococcus scoparius Haeckel	263.3	-	-	-	.4	.5	44.717	-	PB3769/3791
5. Dictyocoryne profunda Ehrenberg >350 µm	32.4	7.9	30.0	29.8	3780.4	4594.9	.043	.040	PB3769/3791
6. Dictyocoryne profunda Ehrenberg <350 µm	51.9	12.0	48.7	-	95.8	116.5	1.052	.982	P_1 4280/5582;E^+
7. Dictyocoryne truncatum (Ehrenberg)	29.0	5.3	-	-	151.4	184.0	1.171	-	PB3769/3791
8. Euchitonia elegans (Ehrenberg)	80.2	26.6	67.6	67.0	145.6	176.9	.476	.651	PB3769/3791;P_1 4280/5582;E^+
9. Heliodiscus asteriscus Haeckel	88.0	35.3	-	-	57.0	69.3	1.144	-	PB3769/3791
10. Myelastrum quadrifolium n.sp.	137.5	49.9	-	-	4321.2	5252.3	.009	-	PB3769/3791
11. Myelastrum trinibrachium n.sp.	184.6	33.5	-	-	351.8	427.6	.079	-	PB3769/3791
12. Saturnalis circularis Haeckel	211.0	50.7	-	-	1.2	1.4	21.141	-	PB3769/3791
13. Spongaster tetras tetras Ehrenberg	37.1	14.0	-	-	2500.5	3039.3	.061	-	PB3769/3791
14. Spongocore cylindrica (Haeckel)	95.2	34.8	-	-	38.4	46.7	1.605	-	PB3769/3791
15. Spongodiscus biconcavus (Haeckel) >270 µm	46.8	6.8	43.8	-	603.4	733.4	.180	.208	E^+;PB3769/3791
16. Spongodiscus biconcavus (Haeckel) <270	61.9	16.2	-	-	68.3	83.0	1.255	-	PB3769/3791
17. Spongosphaera polycantha Muller	88.5	45.7	-	-	-	-	-	-	PB3769/3791
18. Spongosphaera sp. aff S. helioides Haeckel	38.5	18.1	-	-	3064.4	3724.7	.048	-	PB3769/3791
19. Spongotrochus glacialis Popofsky	68.9	15.3	63.4		119.1	144.7	.639	.674	PB3769/3791
NASSELLARIA									
30. Acanthodesmia vinculata (Muller)	165.8	29.6	-	-	27.1	32.9	1.144	-	PB3769/3791
31. Androspyris retidisca n.sp.	78.0	23.4	-	-	133.2	161.9	.526	-	PB3769/3791
32. Anthocyrtidium ophirense (Ehrenberg)	190.6	38.0	168.0	-	46.7	56.8	.582	1.035	PB3769/3791
33. Anthocyrtidium zanguebaricum (Ehrenberg)	198.9	84.9	-	-	42.5	51.7	.658	-	PB3769/3791
34. Callimitra annae Haeckel	375.6	172.4	-	-	22.7	27.5	.702	-	P_1 4280/5582;E^+;P_1^+
35. Callimitra emmae Haeckel	259.3	155.5	-	-	-	-	-	-	P_1 4280/5582
36. Carpocanistrum spp.	-	-	-	-	-	-	-	-	PB3769/3791

TABLE 9 (cont.)

37. Cephalospyris cancellata Haeckel	436.0	242.4	-	-	28.4	34.6	.531	-	PB3769/3791
38. Conicavus tipiopsis n.sp.	136.7	35.8	-	-	83.6	101.7	.462	-	PB3769/3791
39. Cornutella profunda Ehrenberg	295.3	140.3	-	-	76.3	92.7	.282	-	PB3769/3791
40. Dictyocodon elegans (Haeckel)	228.3	21.6	-	-	47.5	57.7	.463	-	PB3769/3791
41. Eucecryphalus tricostatus (Haeckel)	404.3	150.2	336.5	329.1	31.2	37.9	.459	.494	PB3769/3791
42. Eucyrtidium acuminatum (Ebg)+hexagonatum Hkl	86.0	20.1	-	-	139.5	169.6	.437	-	PB3769/3791
43. Lamprocyclas maritalis maritalis Haeckel	52.2	18.0	-	-	152.7	185.6	.688	-	PB3769/3791
44. Liriospyris thorax (Haeckel)	147.7	29.6	133.2	132.2	29.5	35.8	1.191	1.653	PB3769/3791
45. Lithostrobus hexagonalis Haeckel	144.6	62.9	-	-	43.2	52.5	1.002	-	PB3769/3791
46. Lophospyris pentagona pentagona (Ehrenberg)	-	-	-	-	17.9	21.7	-	-	PB3769/3791
47. Nephrospyris renilla Haeckel	95.9	47.8	-	-	234.1	284.5	.269	-	PB3769/3791
48. Pterocorys zancleus (Mlr) + campanula Hkl	212.4	57.2	198.3	-	30.4	37.0	.818	.730	PB3769/3791
49. Spirocyrtis scalaris Haeckel	258.0	84.2	-	-	26.4	32.1	.814	-	PB3769/3791
PHAEODARIA									
80. Castanellids from E	22.1	19.4	-	-	1310.4	1592.7	.293	-	E^+
81. Castanellids from PB	56.5	28.7	-	-	857.9	1042.7	.147	-	PB3769/3791
82. Castanellids from PB <300 µm	104.5	32.6	87.6	87.4	-	-	-	-	PB3769/3791
83. Castanellids fragments	140.5	58.0	-	-	-	-	-	-	PB3769/3791
84. Castanidium abundiplanum n.sp.	101.0	41.9	-	-	66.9	81.3	.879	-	PB3769/3791
85. Challengeria tizardi Murray	119.0	21.3	-	-	82.6	100.3	.524	-	PB3769/3791
86. Challengeron willemoesii Haeckel	253.9	41.6	-	-	21.5	26.1	.941	-	PB3769/3791
87. Challengeron lingi n.sp.	232.3	38.6	-	-	23.5	28.6	.926	-	PB3769/3791
88. Challengerosium avicularia Haecker	243.9	3.8	-	-	39.5	48.0	.519	-	PB3769/3791
89. Circoporus oxycanthus Borgert	374.5	130.9	-	-	11.1	13.5	1.304	-	PB3769/3791
90. Conchidium argiope Haeckel	319.7	94.4	-	-	38.2	46.5	.445	-	PB3769/3791
91. Conchellium capsula Borgert	-	-	-	-	95.7	116.4	-	-	E^+
92. Conchopsis compressa Haeckel	29.0	4.7	-	-	162.4	197.3	1.084	-	E^+
93. Euphysetta elegans Borgert	401.6	85.1	-	-	31.1	37.8	.415	-	PB3769/3791
94. Haeckeliana porcellana Haeckel	15.2	7.7	11.9	11.7	613.6	745.8	.679	.595	P_1 978;E^+:P_1^+
95. Protocystis sloggetti (Haeckel)	127.9	3.6	-	-	40.6	49.4	.962	-	PB3769/3791
96. Protocystis murrayi (Haeckel)	125.3	51.2	-	-	58.5	71.1	.790	-	PB3769/3791
97. Protocystis curva n.sp.	185.8	72.7	-	-	47.7	58.0	.746	-	PB3769/3791
98. Protocystis honjoi n.sp.	222.1	15.6	-	-	28.9	35.1	.783	-	PB3769/3791

$^+$ all depths

Table 10. Logarithmic relationships between variables of Radiolaria. Mean values of the variables are used unless otherwise stated.

$$Y = 10^a X^b$$

Y	X	a	b	r***	Number of taxa used
Radiolaria:					
W**	L**	0.08	0.94	0.83	927*(58)
PA**	W**	0.78	1.66	0.93	344*(35)
PA**	L**	-0.00043	0.92	0.93	724*(53)
W	WT	2.48	0.33	0.69	33
L	WT	2.51	0.20	0.62	53
PA	WT	1.83	0.51	0.74	53
SS(3)	WT	1.88	0.50	0.86	51
SS(10)	WT	2.13	0.59	0.94	12
SS(20)	WT	2.20	0.37	0.88	8
SS(3)	W	0.75	0.34	0.31	33
SS(10)	W	-0.83	1.16	0.88	4
SS(20)	W	1.05	0.44	0.68	4
SS(3)	L	-0.19	0.77	0.41	50
SS(10)	L	-2.63	1.90	0.74	12
SS(20)	L	-1.99	1.70	0.84	8
SS(3)	PA	0.96	0.44	0.51	53
SS(10)	PA	0.52	0.88	0.75	12
SS(20)	PA	1.21	0.58	0.75	8
SS(3)	$\alpha(3)$	1.76	-0.11	-0.11	49
SS(10)	$\alpha(10)$	2.06	-0.13	-0.17	12
SS(3)	$\Delta\rho(3)$	2.16	0.38	0.56	51
SS(10)	$\Delta\rho(10)$	2.56	0.53	0.60	12
$\alpha(3)$	WT	0.58	-0.19	-0.32	49

Table 10 (cont.)

Y	X	a	b	r***	Number of taxa used
$\alpha(10)$	WT	0.72	-0.25	-0.30	12
$\alpha(3)$	D^+	-0.69	0.42	-0.47	49
$\alpha(10)$	D^+	-2.00	-0.87	-0.56	12
$\alpha(3)$	$\Delta\rho(3)$	0.14	-0.42	-0.49	49
$\alpha(10)$	$\Delta\rho(10)$	-0.03	-0.73	-0.63	12
τ_1	WT	1.87	-0.47	-0.84	51
τ_2	WT	1.68	-0.65	-0.97	12
τ_3	WT	1.71	-0.72	-0.99	5
Spumellaria:					
PA	W	1.08	1.53	0.89	55*(5)
PA	L	0.58	1.69	0.94	311*(19)
W	L	0.17	0.92	0.90	364*(19)
Nassellaria:					
PA	W	0.61	1.74	0.97	229*(19)
PA	L	-0.23	1.97	0.93	246*(20)
W	L	0.13	0.88	0.79	328*(20)
Phaeodaria:					
PA	W	1.00	1.50	0.61	53*(11)
PA	L	0.11	1.91	0.96	160*(14)
W	L	0.43	0.82	0.88	228*(17)

Legend: W: Width

L: Length

D^+ Average diameter (L+W)/2 where both L and W are available. If only one of them is available, D^+ = L or W.

continued next page

Table 10 (cont.)

PA: Maximum projected area

WT: Weight

SS(3,10,20): Sinking speed in still water at 3, 10, 20^{o}C respectively.

α(3,10): Residual factor (= W_{obs}/W_{theor}) at 3, 10^{o}C respectively.

$\Delta\rho$(3,10) Bulk density contrast at 3, 10^{o}C respectively.

τ_1: Residence time computed assuming 3^{o}C - 5 Km water column.

τ_2: Residence time computed assuming 10^{o}C - 800 m, underlain by 3^{o}C - 4200 m still water column.

τ_3: Residence time computed assuming 20^{o}C - 200 m, 10^{o}C - 600 m, and 3^{o}C - 4200 m water column.

** : All of the available raw values rather than mean values are used.

*** : Computed for the data fit with log Y = b log X + a.

* : Number of specimens used for the relationships between PA and W (35 taxa involved) and PA and L (53 taxa).

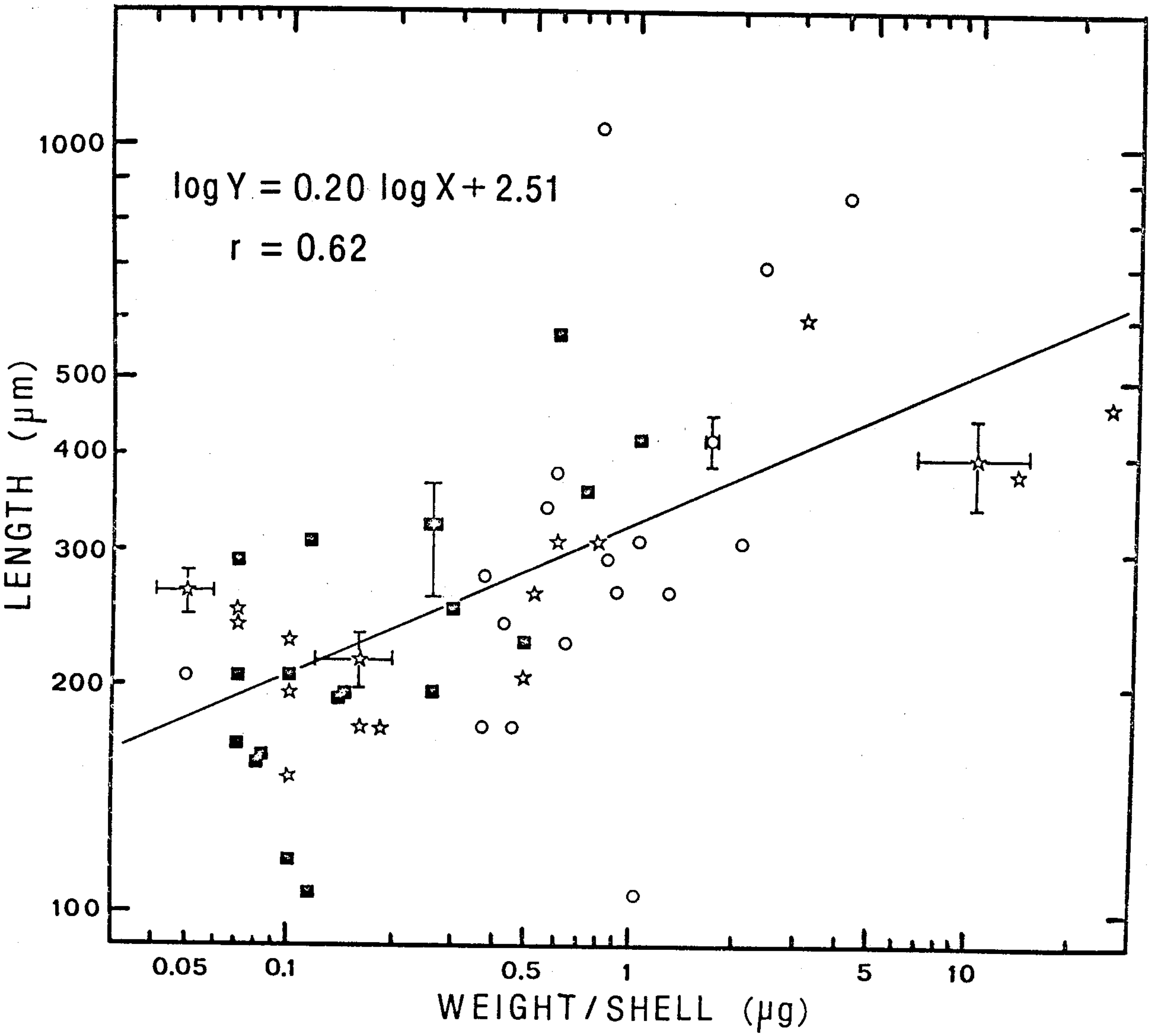

Figure 12. Plot of length vs. weight/shell. Each datum point represents each species. Only representative standard deviations/analytical errors are given to several species for simplicity of the illustration. Symbols used in Figures 12-13, 18-23, and 25 are: ○: Spumellaria; ▣: Nassellaria; and ☆: Phaeodaria.

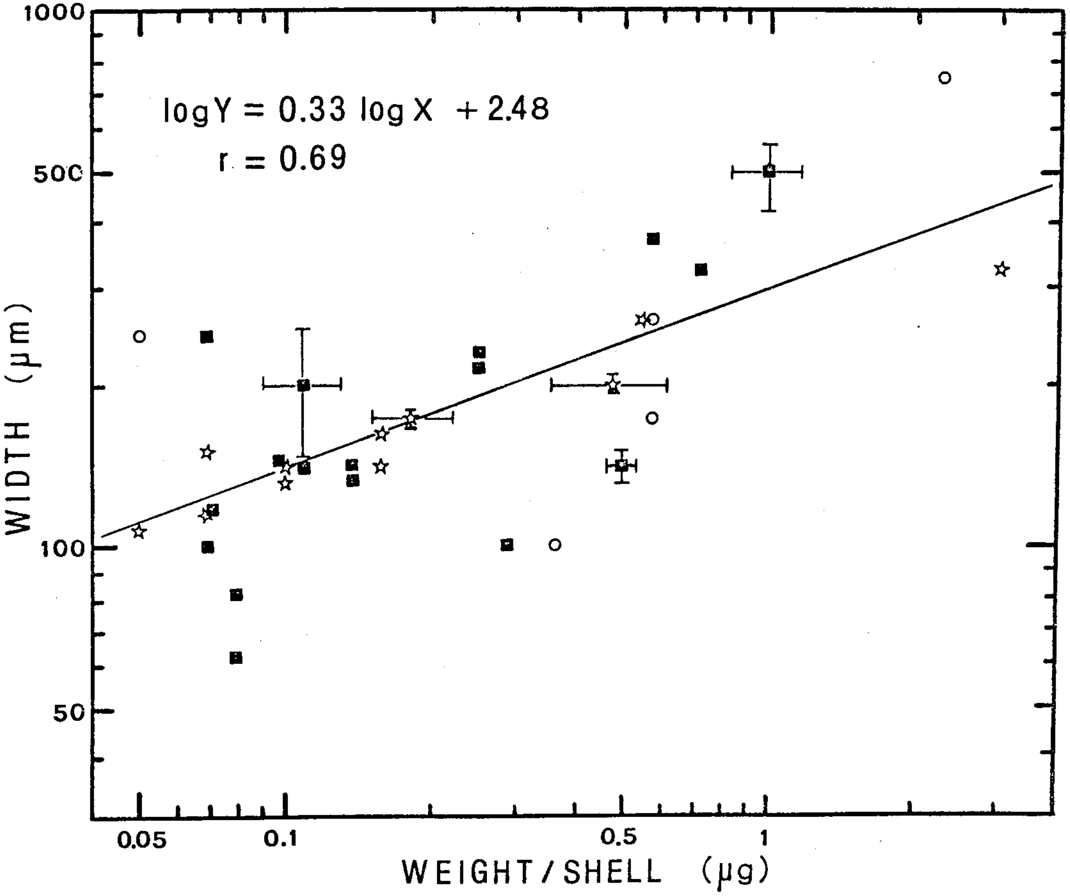

Figure 13. Plot of width vs. weight/shell. See Figure 12 for the legend of symbols.

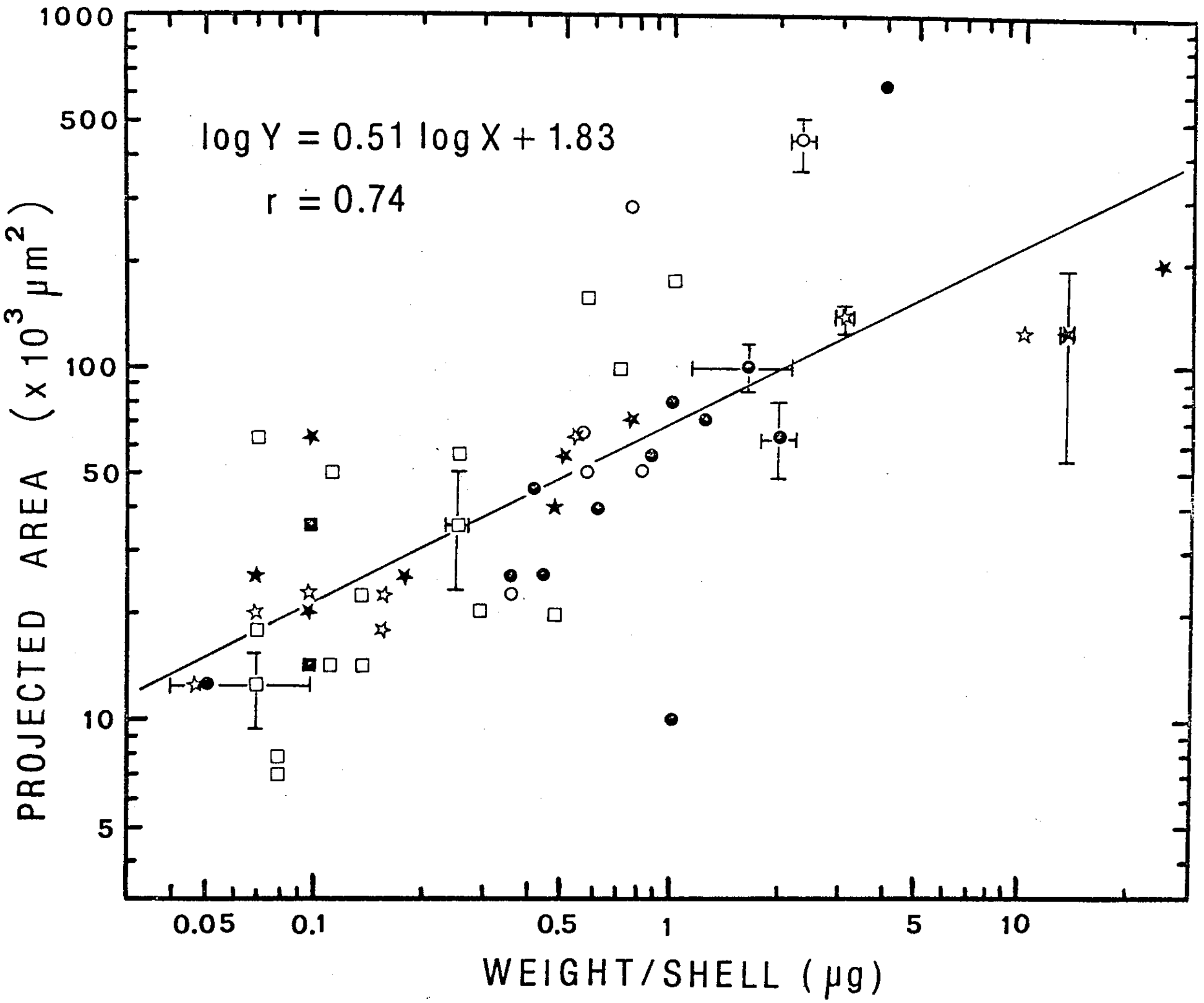

Figure 14. Plot of projected area vs. weight/shell. Symbols are basically same as in Figure 12 but all the open symbols are for observed projected areas and black ones are for computed projected areas.

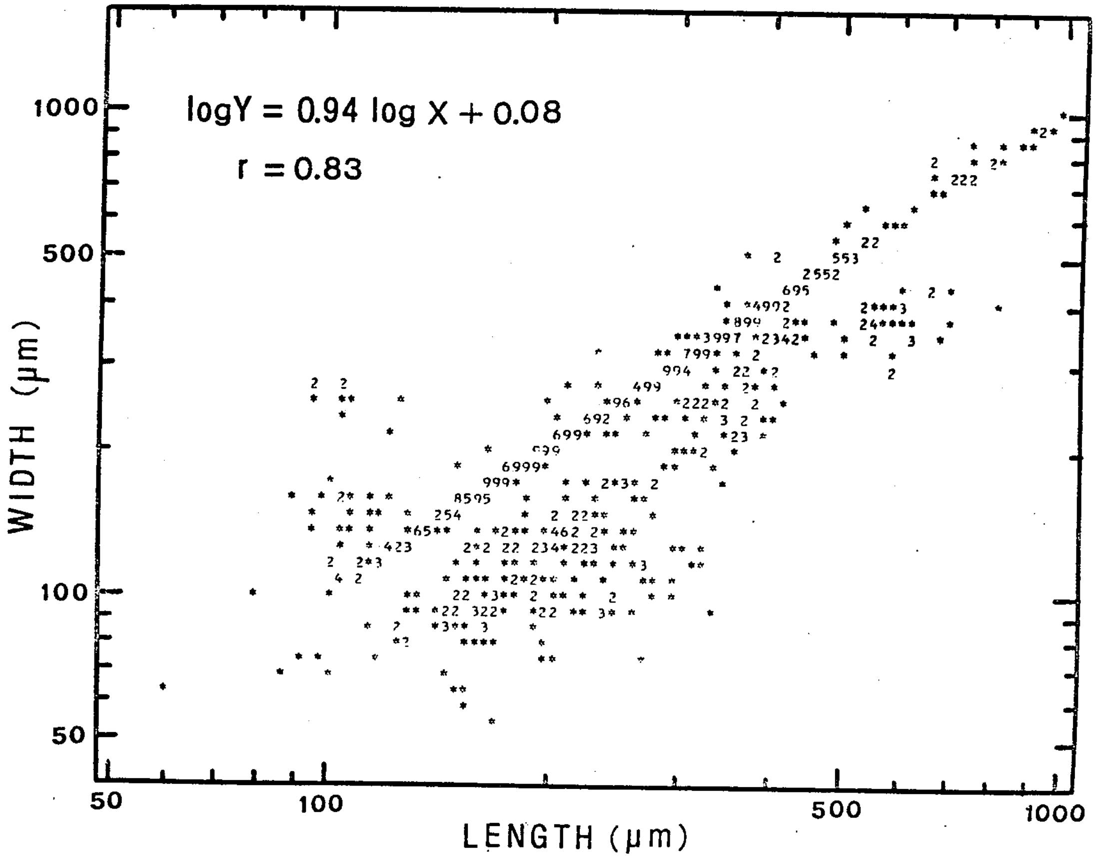

Figure 15. Plot of width vs. length for 927 data points of Radiolaria including 58 taxa. Symbols used in Figures 15-17 are: * : One datum point; numerals 2-8 correspond to number of data points superimposed upon; numeral 9: 9 or more of data points superimposed upon.

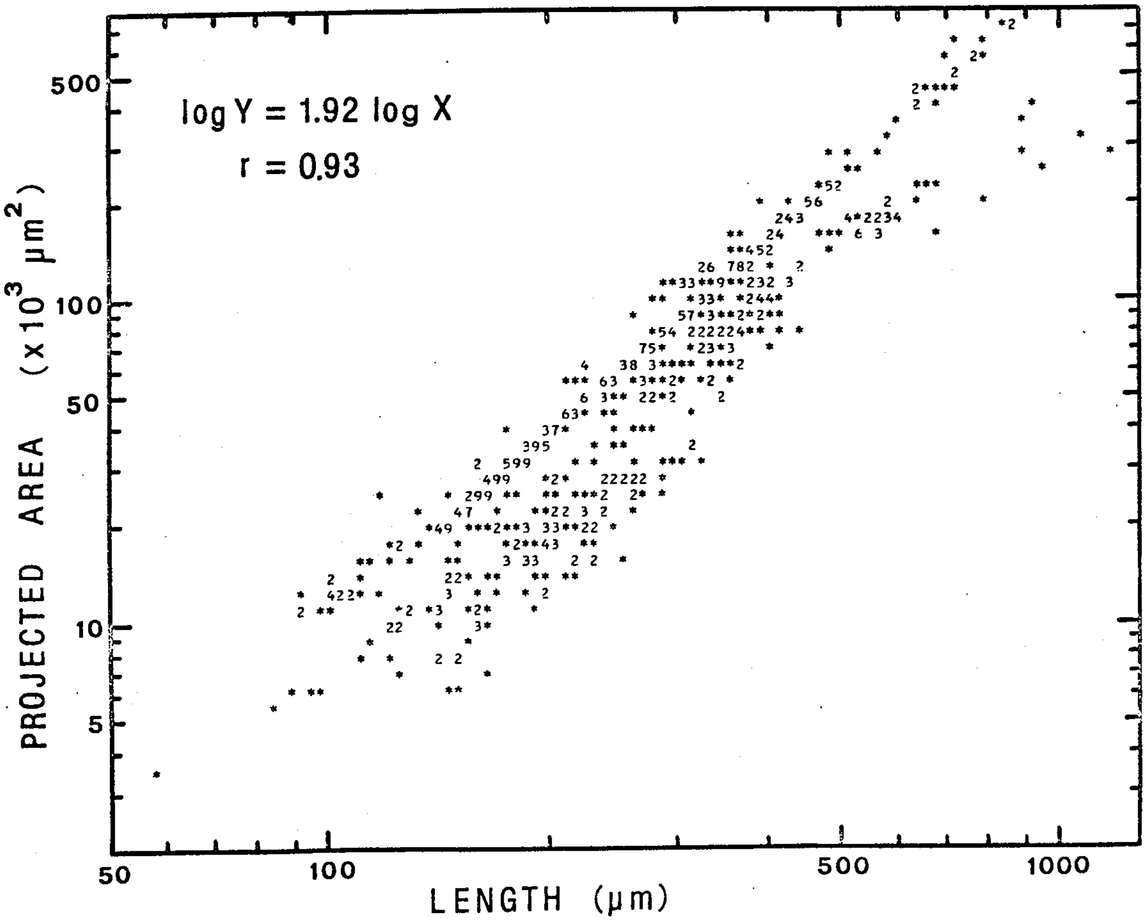

Figure 16. Plot of projected area vs. length for 724 data points of Radiolaria including 53 taxa. See Figure 15 for the legend of symbols.

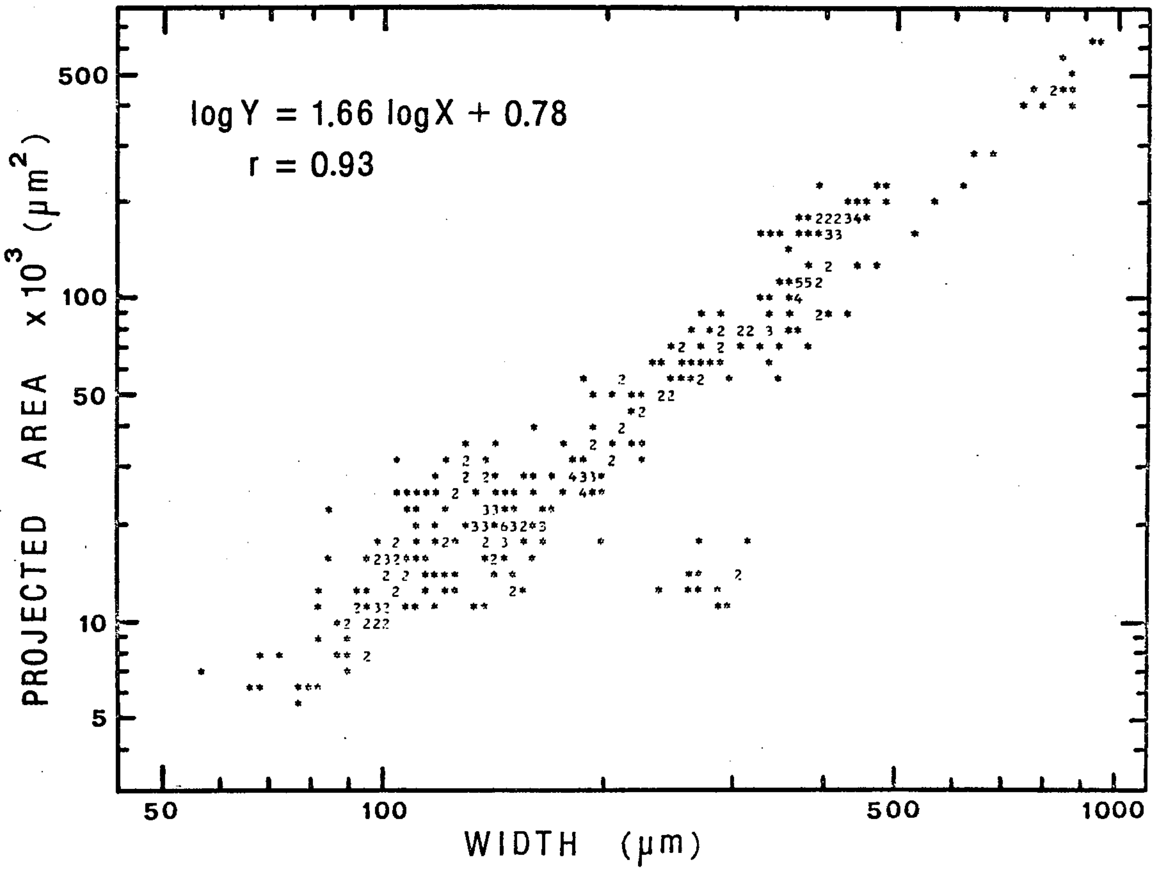

Figure 17. Plot of projected area vs. width for 344 data points of Radiolaria including 35 taxa. See Figure 15 for the legend of symbols.

Silica content in radiolarian skeletons

Silica content with respect to weight value in 26 radiolarian taxa is reported in Table 11. The value tends to be consistent within a suborder. Nassellaria show the highest SiO_2 values among the three suborders. Conicavus tipiopsis has thin meshwork while the rest of the taxa in this group have thick and solid skeletons. It is possible that some skeletons have greater than 100% SiO_2 considering large analytical errors (<8%) as well as introduction of contaminants such as water molecules and salts despite of a thorough cleaning procedure prior to the analysis. Spumellaria give relatively uniform values ca. 90% among all. Acrosphaera murrayana has solid latticed simple one layer shell wheras the rest of the species have spongy framework with the exception of Actinimma arcadophorum. Phaeodaria are the lowest in silica content. The value of Challengeron tizardi is anomalously high and hence it is eliminated in discussion. A comparison was made between the values of clean shells and shells with a tan color tint in the skeleton or with organic aggregates inside of the sphere. The results show no significant difference between the two suggesting that the values are not governed by the amount of organic matter.

High values of silica appear to be associated with thick and simple structured skeletons and, in contrast, low values are associated with spongy or porous skeletons. Since thick nassellarian shells such as Lamprocyclas maritalis maritalis are rarely dissolved in the water column (pl. 43, figs. 10-11), there is little room where contaminants can remain. The skeletons with the high values appear to contain no water in $SiO_2.nH_2O$. This is very different from fossil radiolarian water content of 7-17% based on refractive index analysis (Hurd and Theyer, 1977). On the contrary, spumellarians have generally thin and numerous skeletal members than nassellarians. Thus, despite their similar solid microstructures to the nassellarians, their surface areas are larger and have more capacity to retain contaminants which may slightly lower the values.

Table 11. Silica content in selected radiolarian species from the sediment traps.

Species	Total No. specimens	No. of analysis	SiO_2/shell (μg)±2 S.D.	% SiO_2 ±2 S.D.
SPUMELLARIA				
Acrosphaera murrayana (Haeckel)	120	3	.470±.031	97.9±3.6
Actinomma arcadophorum Haeckel	60	3	.703±.081	85.7±5.7
Dictyocoryne profunda Eherenbeg >350 μm	30	2	1.561±.029	90.6±0.4
Dictyocoryne profunda Eherenbeg <350 μm	64	3	.766±.057	93.8±3.5
Dictyocoryne truncatum (Ehrenberg)	13	2	1.846±.018	87.5±10.3
Euchitonia elegans (Ehrenberg)	105	6	.451±.157	91.9±5.0
Myelastrum trinibrachium	6	1	.658	89.8
Spongodiscus biconcavus (Haeckel) >270 μm	42	2	.766±.187	94.4±2.6
Spongotrochus glacialis Popofsky	75	2	.343±.040	82.9±8.4
Mean				90.5±4.7
NASSALLARIA				
Androspyris reticulidisca n. sp.	9	1	.671	100.0
Anthocyrtidium ophirense (Ehrenberg)	60	1	.147	100.0
Conicavus tipiopsis n. sp.	22	1	.524	90.3
Eucyrtidium acuminatum + hexagonatum Hkl	22	1	.336	100.0
Lamprocyclas maritalis maritalis Haeckel	7	1	.497	100.0
Nephrospyris renilla Haeckel	4	1	1.048	100.0
Spirocyrtis scalaris Haeckel	60	1	.044	-
Mean				98.4±4.0
PHAEODARIA				
Castanella sp.	2	2	73.125±1.803	66.2±12.9
Castanidium abundiplanutum n. sp.	10	1	.540	67.5
Castanidium longispinum Haecker*	98	6	2.132±.346	65.6±6.4
Castanidium sp.	21	2	2.780±.905	80.8
Castanellids	23	12	12.000±5.512	76.7±13.7
Challengeria tizardi Murray	6	1	.482	100.0
Conchidium argiope Haeckel	68	1	.058	56.4
Conchopsis compressa Haeckel	9	2	2.353±.244	73.7±3.0
Haeckeliana porecellana Haeckel	33	6	5.842±2.104	59.9±7.8
Protocystis curva n. sp.	22	1	.107	59.0
Mean				70.6±13.0

*Samples used in Erez et al.(in prep.): recovered from 3978 m; 36% weight loss.

It is not clear if the difference between the spumellarians and nassellarian values are related to different water contents or morphology-governed contaminants. A similar contrast to the above between values of polycystines and phaeodarians is observed: the high values with solid polycystines and low values with porous phaeodarians skeletons (pls. 47-63).

As a summary of this section, silica content observed here varies significantly from one suborder to the other, but is rather consistent within a suborder since the values are at least partially related to their morphology. For a later discussion of silica transport from the production depth to the dissolution depth, the SiO_2/shell (μg) values given in Table 11 facilitate essential information.

Laboratory sinking speed of Radiolaria

Sinking speed measurements were conducted in the laboratory in the Sargasso Sea water (salinity 36.1^{o}/oo) at 3°C for 55 taxa, at 10°C for 13 taxa and 20°C for 10 taxa (5 taxa each in Salinity 36.1^{o}/oo and 30.5^{o}oo) (Table 9, Figs. 18-23). The results at 3°C are the most essential among all three temperatures since 3°C water temperature is distributed extensively in the bathypelagic layer of the world's oceans (e.g. Reid, 1965; Worthington, 1976).

With the method used here specimens greater than ca. 200 μm (e.g. *Anthocyrtidium ophirense*) are readily recognized and traceable in the experimental column without using a microscope but those of ca. 100 μm (e.g. *C. profunda*) or smaller size required an effort to positively identify before they reach the start-line of the measurements. The majority of nassellarians were observed to sink upside down with respect to the orientation of ordinary illustrations widely appear in the literature. For instance, 10 specimens of *Anthocyrtidium ophirense*, a typical nassellarian, sinks with the apical horn downward and only one specimen obliquely and one specimen horizontally sunk out of 12 measurements. Cephalis and the apical horn are heavy and hence they are supposed to be playing a role in orienting a shell even for live

(cont. to p. 100)

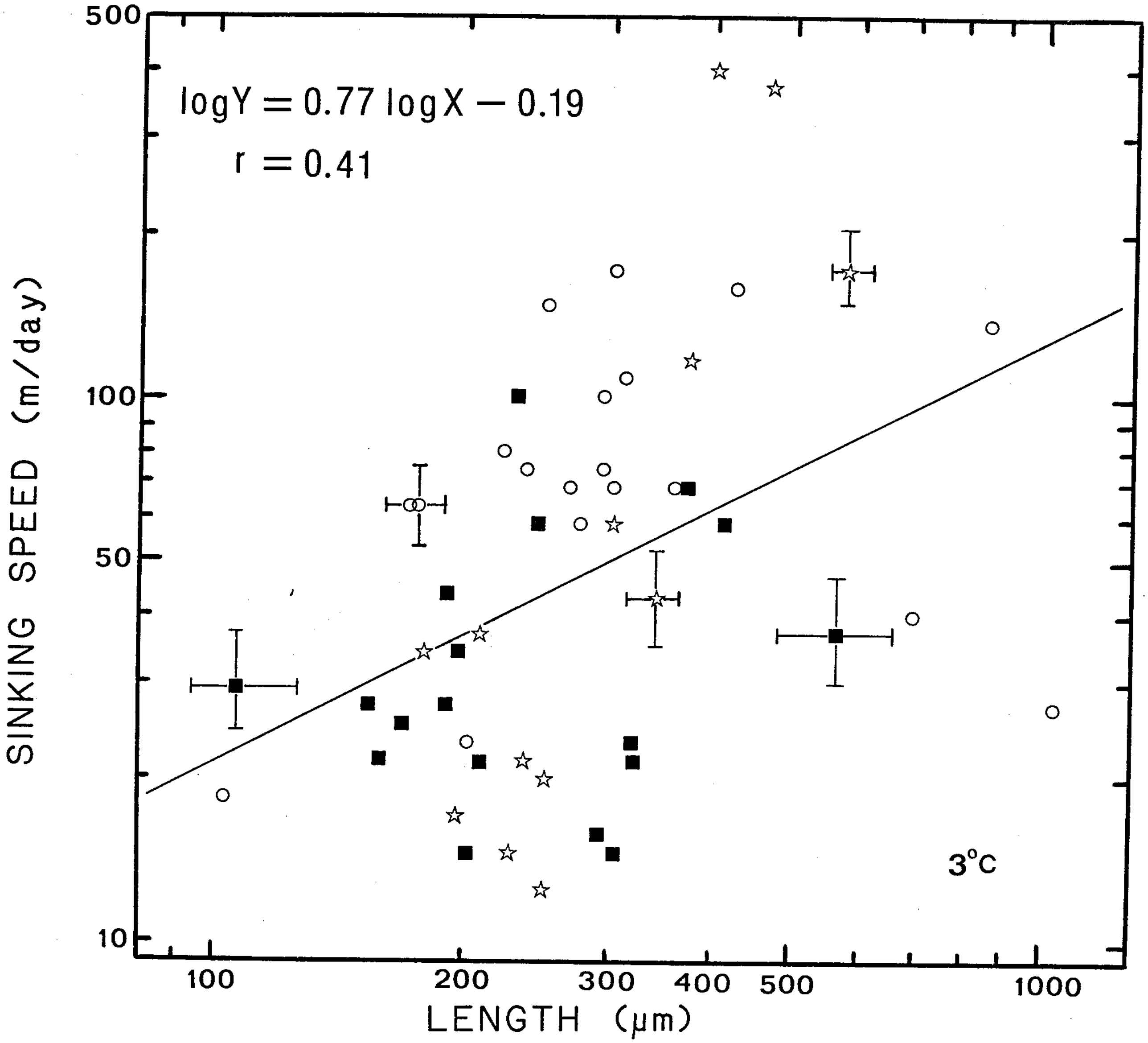

Figure 18. Plot of sinking speed in 3°C still water vs. length. See Figure 12 for the legend of symbols.

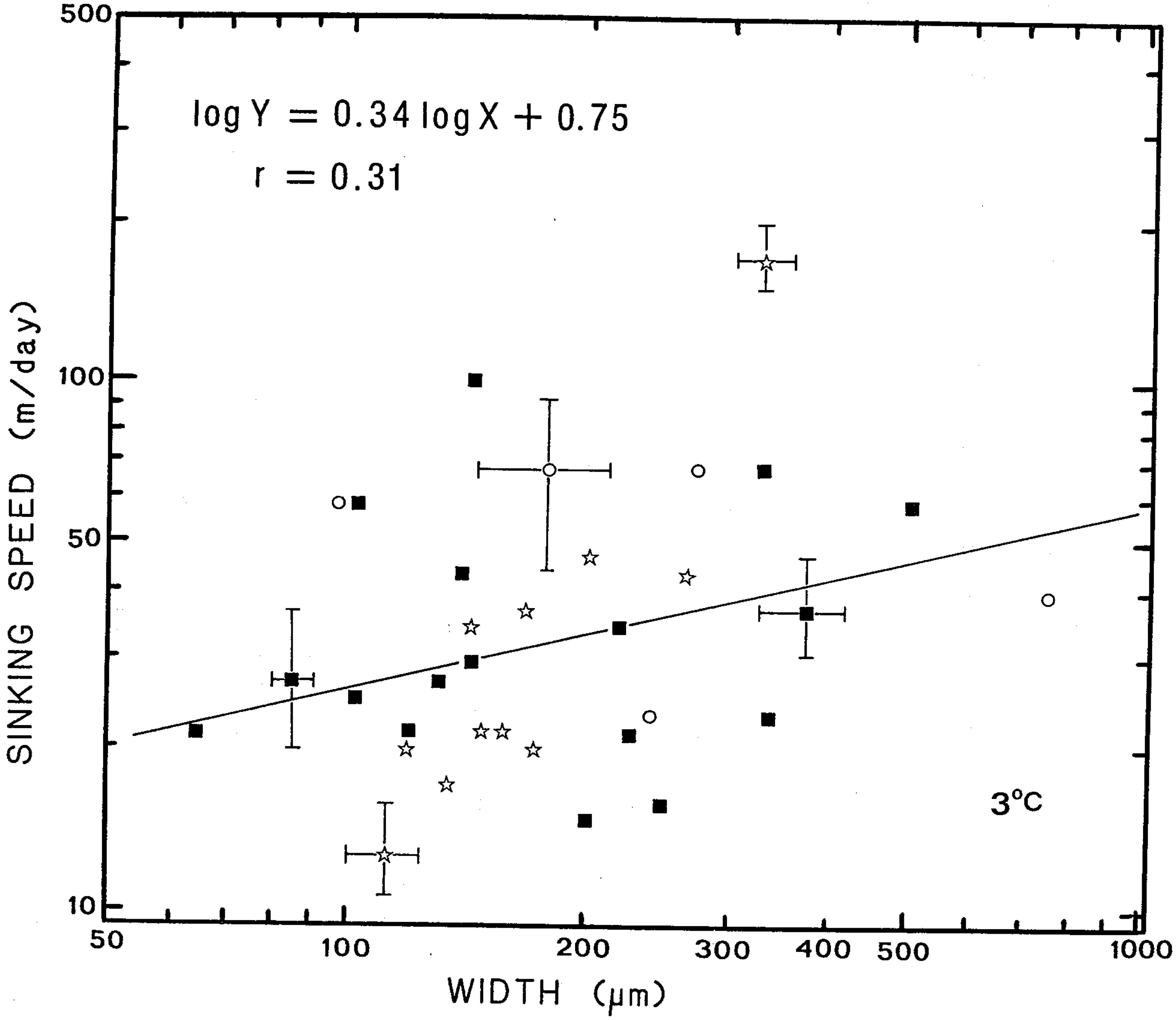

Figure 19. Plot of sinking speed in 3°C still water vs. width. See Figure 12 for the legend of symbols.

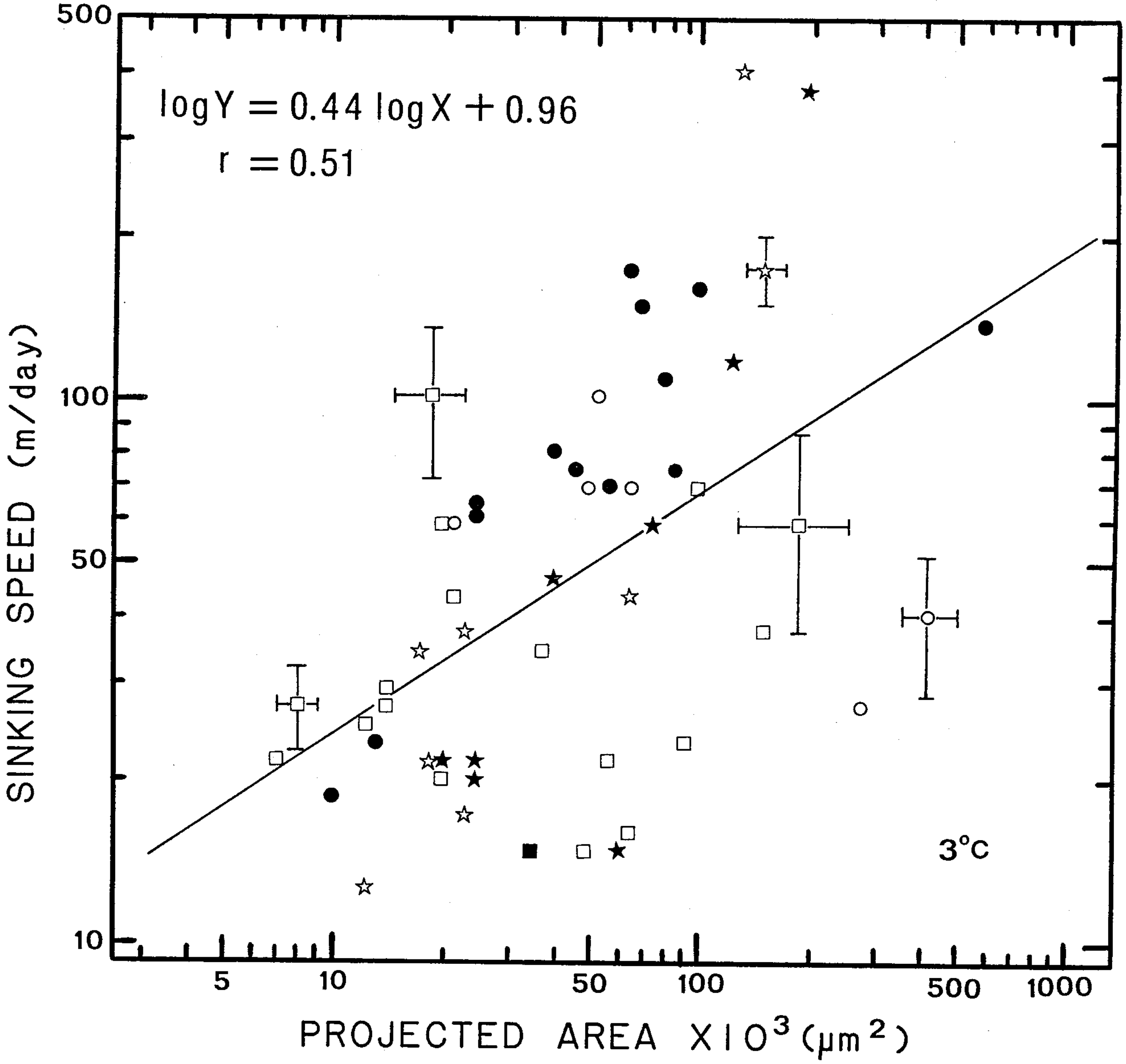

Figure 20. Plot of sinking speed in 3°C still water vs. projected area. The legend of symbols are basically the same as in Figure 12. Open and solid symbols represent measured and computed projected areas respectively.

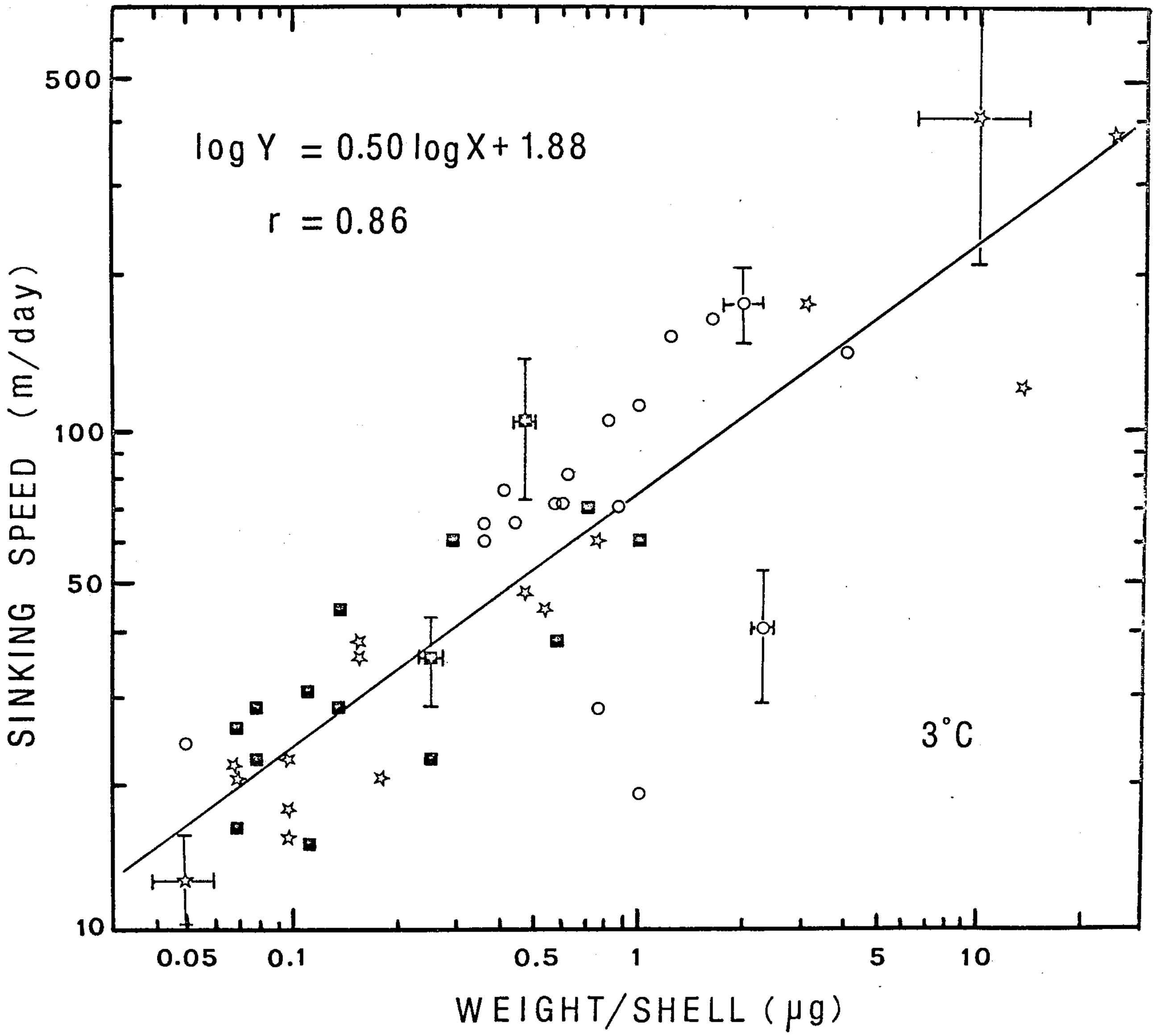

Figure 21. Plot of sinking speed in 3°C still water vs. weight/shell. See Figure 12 for the legend of symbols.

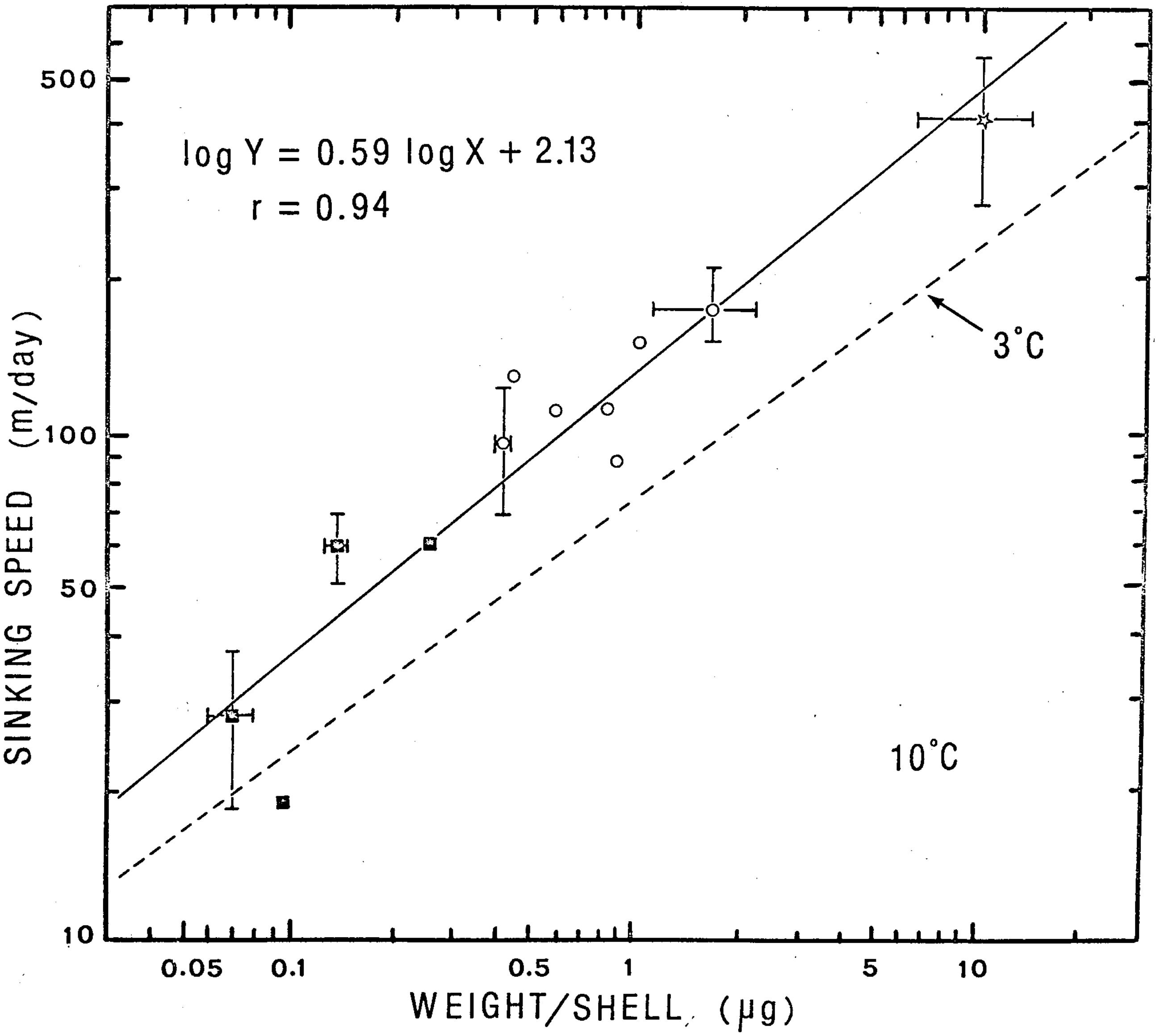

Figure 22. Plot of sinking speed in 10°C still water vs. weight/shell. See Figure 12 for the legend of symbols.

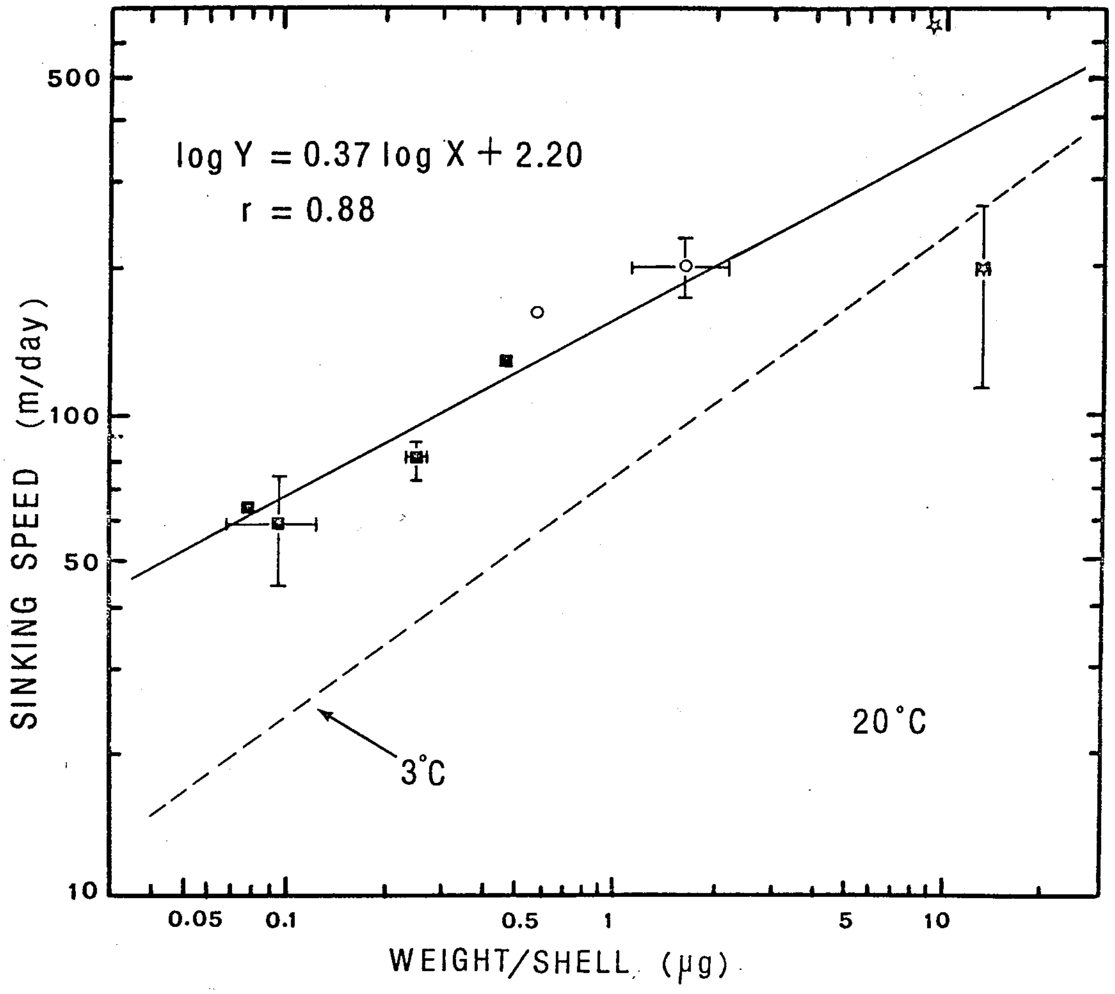

Figure 23. Plot of sinking speed in 20°C still water vs. weight/shell. See Figure 12 for the legend of symbols.

specimens (R. Goll, 1980, pers. comm.). Among many literature, Haecker (1908a) is one of the few that illustrated the nassellarians with the apical horn downward. Although the orientation widely used in the literature including this paper is misleading with respect to how radiolarians are oriented in the water, it may be better to keep the current usage with an awareness of the above notion considering vast amounts of literature already published. It is also of interest to note that sinking orientation of discoidal radiolarians is nearly always steadily vertical through the experimental water column but never will be as the way a sheet of paper falls through the air.

The obtained sinking speed ranged from 13 m/day of Euphysetta elegans to 416 m/day of Haeckeliana porcellana (Table 9; Figs. 18-21). Each datum point in Figs. 18-23 represent each species and standard deviations are only given to a few taxa in order to maintan simple illustrations, but the rest can be referred in Table 9. As is can be readily seen in Figs. 18 and 19, the correlations between sinking speed at 3°C and length or width are poor (r=0.4 and 0.3 respectively). When projected area which is analogous to squar of diameter is used the correlation becomes better (Fig. 20; r=0.5), but still not satisfactory in order to furnish a predictive regression line. When weight/shell, which is equivalent to mass, is used the correlation becomes much better (Fig. 21). Despite of the fact that variety of taxa have wide range of morphology, the correlation between sinking speed and weight (r=0.86 at 3°C) is remarkably good suggesting a treatment as a whole Radiolaria is reasonable without dividing them into morphologically dependent groups. Nassellarians observed here sink somewhat slower (14-105 m/day) compared to spumellarians (25-177 m/day) mainly due to lesser weight. These two groups tend to separately cluster respectively in areas along the regression line (Fig. 21). Phaeodarians, on the other hand, spread out their values from 13 to 416 m/day mainly due to wide range of weight.

Existing data on radiolarian sinking speed in the literature include only one measurement on the 500 μm size specimen (350 m/day) by Kuenen (1950, p. 253) and unpublished data cited by Casey et al. (1979b, p. 232) (35.6 m/day for tropical species, and "three to ten times faster rates for larger and heavier polar species"). Both of these data fall in the range of the present observations which include all the possible size of taxa except the smallest sized taxa such as Peridium spinipes. From a theoretical point of view, Lerman (1979) proposed a hypothetical sinking speed of Radiolaria based on laboratory sinking speeds on planktonic foraminiferal tests (Berger and Piper, 1972) and diatom frustule (Smayda, 1969, 1970, 1971). However, my observations do not agree with Lerman's model (Lerman, 1979, p. 268, fig. 6.3). Also, a classical and theoretical consideration of particle sinking by Munk and Riley (1952) is available.

Combining information on weight, V_b, and an assumed density of biogenic silica (2.0 g/cm^3), one can estimate bulk density contrast ($\Delta\rho$) which is the density difference between a parcel of water including the skeleton and adjacent seawater. The resulting values are shown in Table 9. When they are plotted against sinking speed, a positive correlation is found (Fig. 24). The majority of $\Delta\rho$ values fall between 0.01 and 0.5 g/cm^3 whose range is much narrower than other available biogenically originated particles such as fecal pellets (e.g. Komar et al., 1981; Honjo, pers. comm.). Previously, Bishop et al. (1977) used an assumption of $\Delta\rho$ = 0.1 g/cm^3 for radiolarian silica flux which was reasonable.

In order to determine whether a Stokes Law is applicable to the settling scheme of radiolarian skeletons Re, Reynold's number, of the sinking particle has to be examined:

$$\underline{Re} = \frac{\rho \cdot W_{obs} \cdot D}{\mu} \qquad (1)$$

where ρ and μ are the water density and viscosity, W_{obs}, is the sinking speed of a particle, and D is the nominal diameter of the particle. The Reynolds number computed ranges from 0.02 to 1.4 at 3°C, and only the two species showed relatively high Re and the rest are less than 0.6. Thus the following Stokes equation is applicable (Raudkivi, 1976) to the sinking speed of radiolarian skeletons:

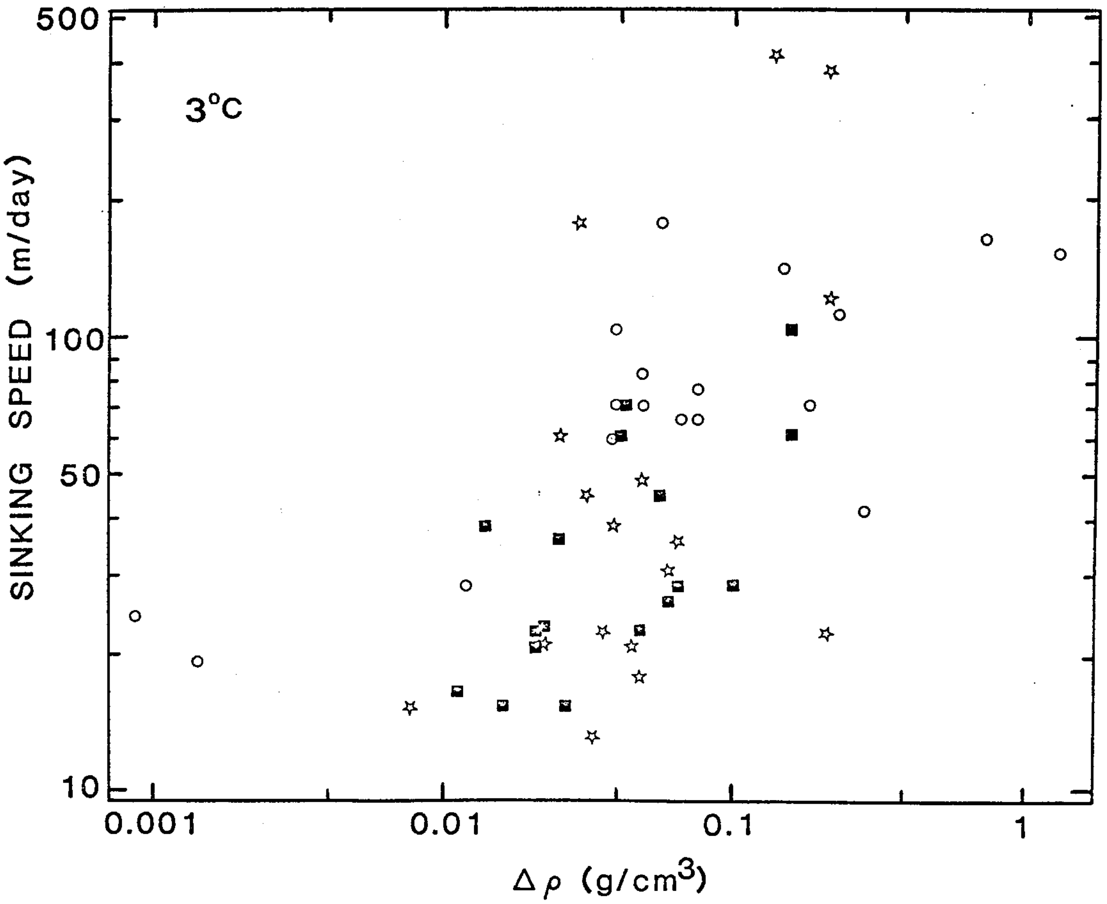

Figure 24. Plot of sinking speed in 3°C still water vs. density contrast, Δρ. See Figure 12 for the legend of symbols.

$$W_{theor} = \frac{1}{18} \cdot \frac{1}{\mu} \cdot \Delta\rho \cdot g \cdot D^2 \qquad (2)$$

where W_{theor} is the Stokes settling rate, $\Delta\rho$ is the bulk density contrast between the water and the sinking particle, g is the acceleration of gravity (981 cm/sec^2), and D is the nominal diameter of the particle.

The computed theoretical values by Stokes equation are compared with the observed values and presented in Table 9 and Fig. 25. Cladococcus scoparius and Saturnalis circularis showed abnormally high values of W_{theor}; this can be readily explained by their characteristic morphology (Pl. 10, figs. 1-4; Pl. 15, figs. 15-18). For instance, in the case of Cladococcus scoparius, if full length of the spines were taken as the shell diameter instead of taking cortical shell diameter which is extraordinarily small compared with the spine length, the value would have been much smaller. The values for these two taxa (Table 9) are eliminated in the plot of Fig. 25.

A correlation between Stokes law and the measured sinking speed, residual factor α (W_{obs}/W_{theor} ratio), are plotted against average diameter (Fig. 25). Up to ca. 250 μm in diameter the ratio follows the Stokes law (ca. $\alpha = 0.9 \pm 0.5$) where Re is fairly small and above it the ratio deviates (ca. $\alpha = 0.4 \pm 0.4$) where Re is relatively larger. As a whole, there is a negative correlation between the ratio and the diameter which is partially governed by Re.

Residence time of Radiolaria in the pelagic water column

The above sinking speed is used to estimate amount of time that individual radiolarians are expected to stay in a water column (residence time) assuming that steady state settling occurs without dissolution. In the case of dissolution susceptible taxa this is only hypothetical measure but it still supplies usefull information especially when

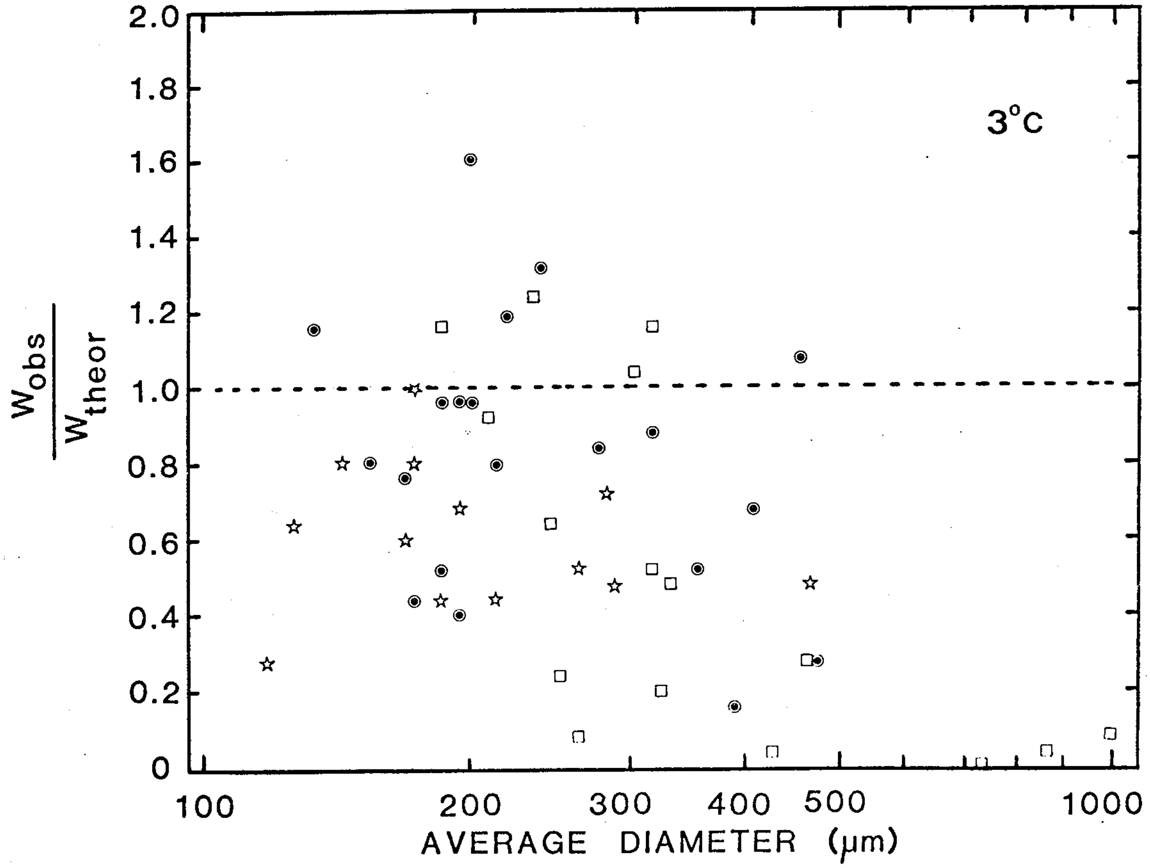

Figure 25. Plot of the residual factor (W_{obs}/W_{theor}) vs. average diameter using length and/or width. The horizontal dashed line represents theoretical values using Stokes equation. Only 3 different shapes are separated since further divisions do not improve the understanding of sinking speed governing factors. Symbols: ◉ : spherical group (sphere, ellipsoidal, hemispherical, cylindrical and box in the APPENDIX Table 1); ☐ : discoidal group (discs and plates); ☆ : Conical group (conical and pyramidal: this group includes only nassellarians).

combined with dissolution rate data. Applying the speed obtained in the laboratory water column with limited height at three temperatures the residence times is: (1) τ_1: residence time computed assuming 3°C and 5 km still water column; (2) τ_2: residence time computed assuming 10°C and 800 m, underlain by 3°C and 4200 m still water column; and (3) τ_3: residence time computed assuming 20°C and 200 m, 10°C and 600 m, and 3°C and 4200 m still water column.

According to the correlations between τ_n and weight as shown in Table 9 and Figs. 26-27, and within the limits of present observations, the residence time range of τ_1 is from 2 weeks to over a year. A regression line of τ_2 is below that of τ_1 which is expected but it has higher slope than that of τ_1 (Fig. 26) which might be due to small number of taxa used since each species has different morphological characteristics which may influence sinking speed. A regression line of τ_3 is nearly identical to that of τ_2 and superimposed upon it and hence it is not illustrated in Fig. 27.

Nassellarian τ_1 ranges from ca. 2 months to slightly over a year. Taking 0.12 µg/shell, an average nassellarian stays 6 and 7 months during settling in the water column using τ_2 and τ_1 respectively. Taking 0.6 µg/shell, an average spumellarian stays 2 and 3 months using τ_2 and τ_1, respectively. This suggests that spumellarian skeletons are least subjected to dissolution during their descent in the water column among all the suborders. Castanellids, and Circoporids which are large-sized phaeodarians, spend less than two months (majority of them stay less than a month) and the rest of the phaeodarian taxa spend three months to a year in a 5 km water column.

Based on TEM-SEM morphological observations (Pl. 43, figs. 10-11; pls. 47-63) sediment trap radiolarian counts (Tables 2-5) most of the polycystine assemblages eventually reach the bottom with different extents of dissolution effects depending on the residence time of the taxa. On the other hand, Phaeodarians behave differently: that is, species with heavy weight/shell sink quickly to the bottom without being dissolved and there they are dissolved within a few months based on an in situ dissolution experiment (Erez et al., in press; Hurd and Takahashi,

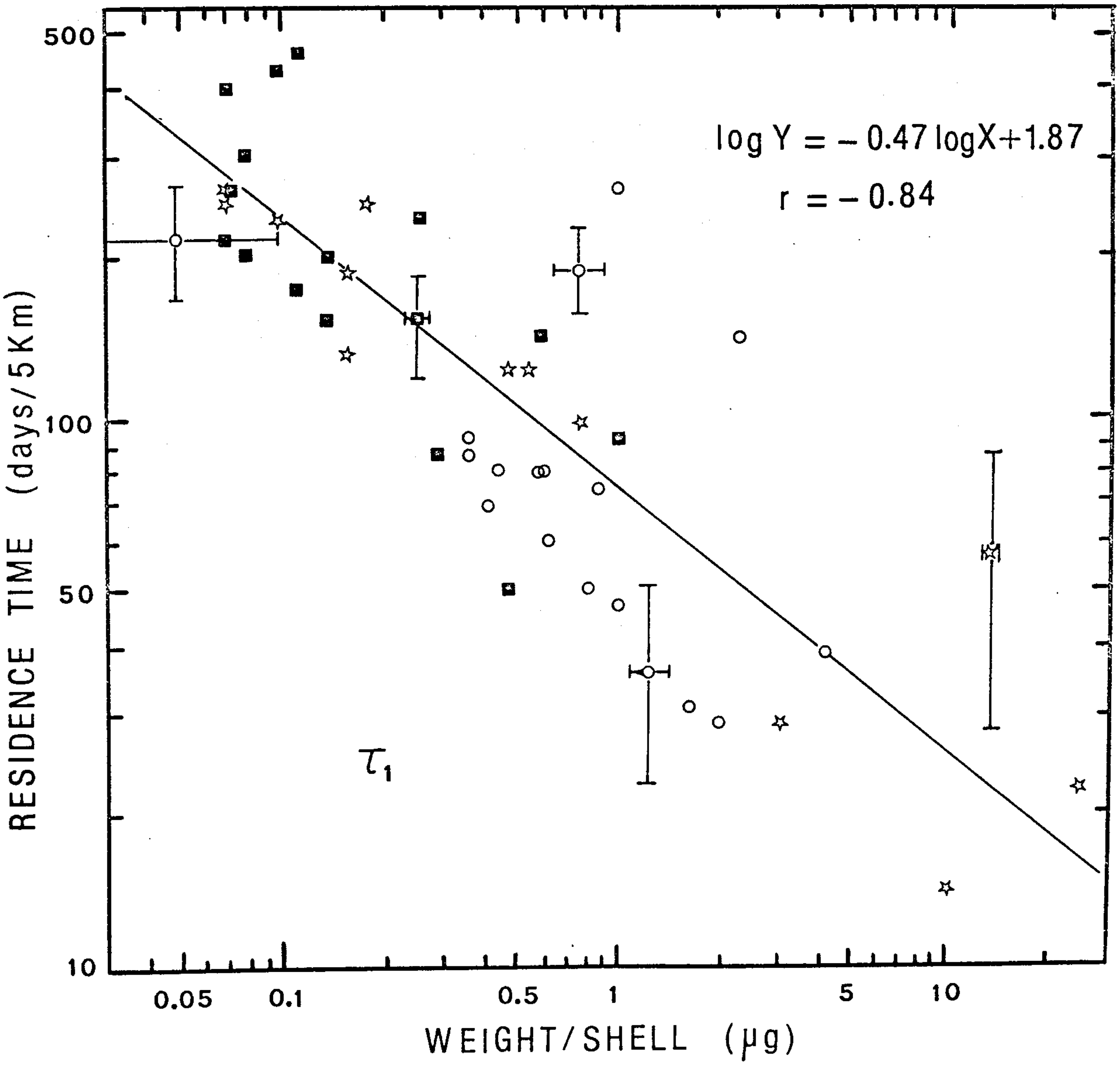

Figure 26. Plot of residence time (τ_1) vs. weight/shell. See Figure 12 for the legend of symbols.

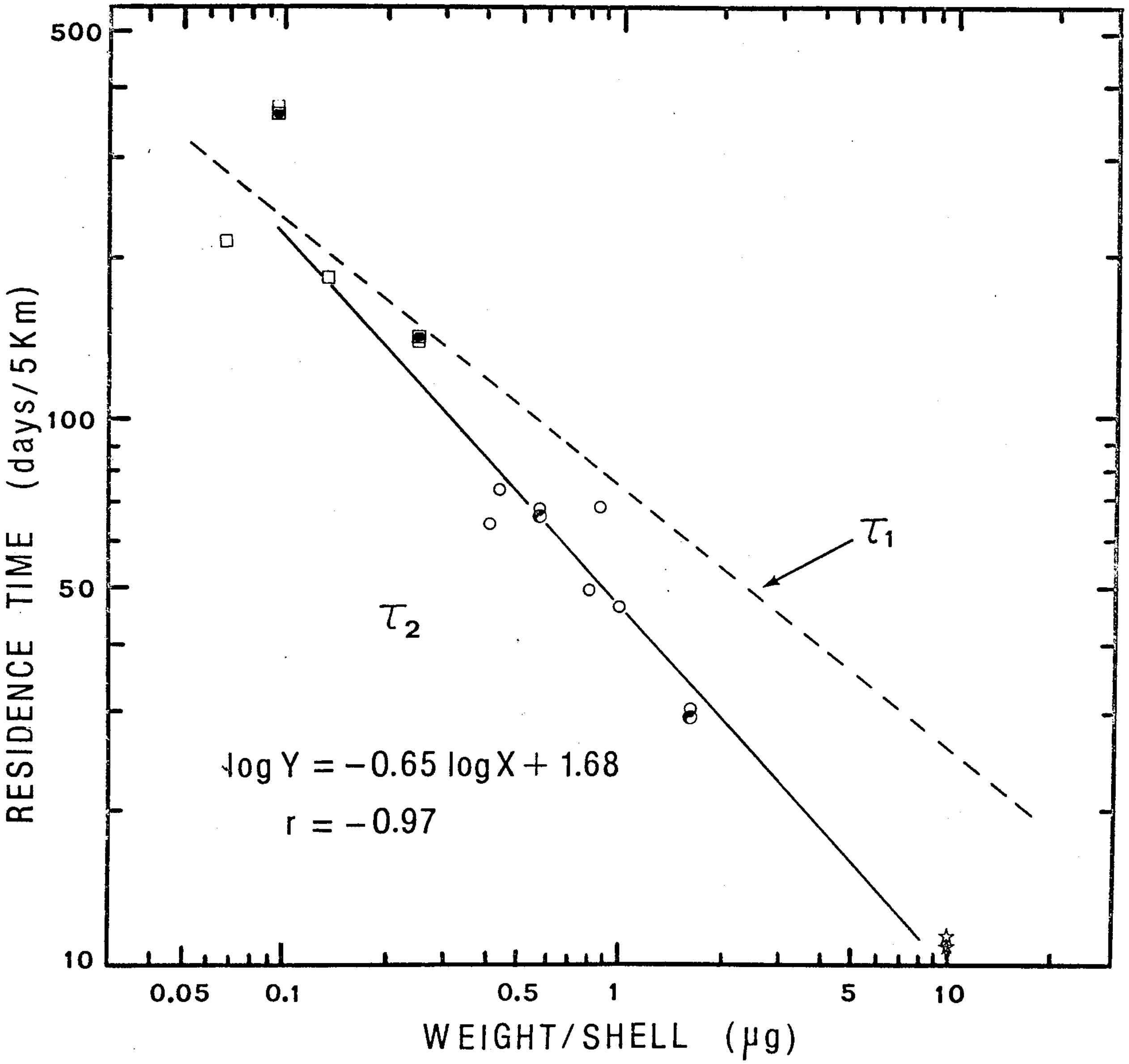

Figure 27. Plot of residence time (τ_2) vs. weight/shell. A regression line for τ_3 is almost superimposed upon that of τ_2 and hence not drawn here. See Figure 12 for the legend of symbols. Additional symbols used:
◔ : Spumellarian τ_3; ▣ : Nassellarian τ_3;
★ : Phaeodarian τ_3.

in press). These are represented by Castanellids, Haeckeliana porcellana and Conchopsis compressa. Smaller and lighter phaeodarians represented by Challengeron willemoesii have little chance to reach the bottom due to their long residence time with dissolution susceptible nature. The phaeodarian species (Castanidium longispinum Haecker) used by Erez et al. (in press) is considered to be an end member of the phaeodarians in terms of dissolution susceptibility because its large size (i.e. 470±34 μm). Since specimens of this species are mostly dissolved within 3-4 months period in the deep sea environment it is evident that small-sized phaeodarians will be dissolved within shorter period of time than them.

Radiolarian standing stock, production rate and turnover time

Not much is known about rate of production and turnover time for radiolarians and most of the published information on these are indirectly obtained. Radiolarian standing stock is moderately known especially in tropical regions (Renz, 1976; Bishop et al., 1977, 1978, 1980; Kling, 1976, 1979; Takahashi and Ling, 1980; Boltovskoy and Riedel, 1980).

Casey et al. (1971) have estimated turnover time of 11 polycystine species in the Santa Barbara Basin, off the coast of California, based on their abundance in plankton tow samples and in the underlying varved sediment layers of the past 10 years. The turnover time is the amount of time necessary to replace a whole population of a taxon. The turnover time ranges from less than a day to 43 days depending on the species. They further suggested that life span of two species (Teoconus zancleus and Eucytidium hexagonatum) are about one month judging from the turnover times. This indirect method involves many unestablished assumptions, e.g., no dissolution loss in the sediments. Anderson (1978) directly observed at least 3 weeks of life span for the skeletonless spcies (Thalassiccolla nucleata) in the laboratory culture.

Berger (1976) estimated that residence time of radiolarians (>61 μm) in the upper 100 to 200 m of the Santa Barbara Basin is between 3 weeks and 3 months. This was based on radiolarian counts in bottom sediments

(Berger and Soutar, 1970) and a sedimentation rate (Emery, 1960) which give supply rates (0.5×10^3 to 1.1×10^3 shells/m^2/day) to the sediment-water interface.

The standing stock, rate of production, and turnover time can be delineated as follows:

(1) Flux of radiolarian species, F(no. of shells/m^2/day), is obtained from species counts of sediment trap samples.

(2) Descending speed of radiolarian species, D_s(m/day), is obtained by laboratory sinking speed experiment on the samples collected by the sediment traps.

(3) Standing stock of radiolarian species, S(no. of shells/m^3), is computed as follows:

$$F / D_s = S \quad \text{(no. of shells/m}^3\text{)}$$

(4) Rate of production is computed as:

$$F / h_{prod} = R_{prod} \quad \text{(no. of shells/m}^3\cdot\text{day)}$$

(5) Turnover rate is estimated as follows:

$$S \,.\, h / F = T \quad \text{(days)}$$

where h_{prod} is the height of water column where production occurs and assuming steady state condition of S and F during the sediment trap experiment. Although these assumptions are yet partially improved, they will sufice first order approximation.

The estimated standing stock shows abundant species being on the order of 10 individuals/m^3 or more and ca. 0.1 or less for the minor species (Table 12). The standing stock for total Radiolaria ranges from ca. 430 shells/m^3 at Station P_1 to 1230 shells/m^3 of Station PB. This is in a good agreement with direct observations made by Bishop et al. (1977, 1978, 1980). For example, Bishop et al. (1980) reported that total radiolarian counts of 1220 shells/m^3 in >53 µm size fraction from 1500 m depth of the Panama Basin in June-July. Considering different methods, seasons and that their exclusion of <53 µm size fraction and inclusion of Sticholonche which is absent in my data, it is at least reasonable to state that the above values are similar each other. The standing stock can be used to compute for amount of radiolarian biogenic silica in unit amount of water. For instance,

Table 12. Estimation of standing stock, rate of production and turnover time of selected abundant radiolarian species and three suborders.

Station	Standing Stock $S(\text{no./m}^3)$ E	P_1	PB	Range of production rate (no./m^3/day) where h_{prod}=200m	Turnover time (days) where h_{prod}= 200m	where h_{prod}= 500m
SPUMELLARIA						
Actinomma arcadophorum	0.8	0.4	1.6	0.2-0.6	3	7
Amphirhopalum ypsilon	0.1	0	0.4	0-0.1	3	8
Cladococcus scoparius	0.4	0.4	2.6	0.04-0.03	10	26
Dictyocorne profunda	0.8	0.4	0.5	0.3-0.5	2	4
Euchitonia elegans	0.8	0.7	1.4	0.2-0.5	3	7
Heliodiscus asteriscus	0.1	0.2	1.0	0.04-0.3	3	7
Spongaster tetras tetras	0.4	0.1	0.3	0.04-0.3	1	3
Spongocore cylindrica	0.3	0.5	1.1	0.1-0.3	3	8
Spongotrochus glacialis	-	0.7	1.8	0.3-0.7	3	7
Total SPUMELLARIA	63	61	125	25-50	1	2
NASSELLARIA						
Acanthodesmia vinculata	3.2	4.1	11.8	0.5-1.8	6	16
Anthocyrtidium ophirense	3.7	1.8	3.7	0.3-0.5	7	19
Callimitra annae	0.6	0.4	0.4	0.03-0.05	13	33
Callimitra emmae	0.9	0.5	1.3	0.06-0.2	9	22
Cornutella profunda	9.3	14.0	23.3	1.0-2.5	9	23
Eucecryphalus tricostatus + C. sestrodiscus	2.4	5.2	38.5	0.2-2.8	14	35
Liriospyris thorax	0	1.2	1.6	0-0.3	6	15
Pterocorys campanula	108.4*	10.0	8.0	1.0-1.3	8	20
Pterocorys zancleus	*	28.1	8.0	1.0-3.5	8	20
Spirocyrtis scalaris	4.2	1.6	14.0	0.2-1.5	9	23
Total NASSELLARIA	400	367	1067	50-160	0.4	1
PHAEODARIA						
Castanellids	0.04	0.02	1.0	0.02-1.0	-	-
Challengeron willemoesii	6.3	0.3	6.0	0.03-0.6	10	25
Circoporus oxycanthus	0.3	0	1.7	0-0.1	14	35
Conchopsis compressa	0.02	0	0	0-0.02	-	-
Euphysetta elegans	7.0	0.5	7.8	0.03-0.5	16	39
Haeckeliana porecellana	0.01	0.01	0	0-0.02	-	-
Protocystis honjoi	0.5	0	1.3	0.1-0.2	9	22
Total PHAEODARIA	18	5	38	2-15	0.4	1
Total RADIOLARIA	481	433	1230	77-225	-	-

*: two species combined

h_{prod}: height of water column where production occurs

sinking speed used for each suborder's: S: Spumellaria - 80; Nassellaria -30; and Phaeodaria - 80 m/day taking the radiolarian suborder fluxes from Staton PB (Table 5), weight and mean SiO_2 content (Tables 11,13), 225 μg SiO_2/m^3 is estimated in the average water column between the trap depths at Station PB. This agrees well with particulate silica obtained from 1500 m of the Panama Basin by Bishop et al. (1980): 124 μg SiO_2/m^3 in > 53 μm.

Values of production rate and turnover time are dependent on assumptions on h_{prod}, height of water column where production occurs. With the assumption of h_{prod} being 200 m the estimated R_{prod}, rate of production, is on the order of 0.01 shells/m^3.day for minor species and 1-4 shells/m^3.day for abundant species. The turnover time obtained appears to be on the order of a few days to several weeks depending on the species and assumptions. This generally agree with the previous reports of more indirect methods (Casey et al., 1971; Berger 1976). However, some values are one to two orders of magnitude differnt from Casey et al.(1971)(e.g. Cornutella profunda).

Biogenic opal transport to the deep-sea by radiolarian skeletons

Based on microscopic analysis combined with an inferred weight value Takahashi and Honjo (1981) quantitatively demonstrated an importance of radiolarian SiO_2 transport to the deep-sea at least in the equatorial Atlantic during a season. To further quantify the radiolarian SiO_2 flux it is necessary to combine radiolarian counts (Table 2), weight values and mean SiO_2 content in each suborder (Table 11). Choosing the weight values is the most critical for the estimation. Utilizing the data on 55 taxa (Table 2-4; Pls. 1-63) and taxon-morphological background, the most logically representative average values are subjectively chosen (Table 13).

Computation results show that spumellarian SiO_2 transport is generally 50% or more of the total radiolarian SiO_2 flux and nassellarians and phaeodarians follow them respectively at all the stations. Although phaeodarian SiO_2 transport appears to be up to a few percent at Stations E and P_1 and ca. 20 % at Station PB (Fig. 28), as it has been discussed earlier they play an important role in quick silica release in the water column and on the seafloor (Fig. 29) due to their dissolution susceptible nature and high dissolution rate. Some of Castanellids are extremely large but rare and hence an introduction of a few such large specimens results in a significant contribution to the SiO_2 flux. Since the results in Table 13 are based on observations of microslides which may not always contain such a rare taxa due to small aliquots, an inclination toward higher phaeodarian flux should also be considered. A finding of a dense, large patch of monospecific Castanidium longispinum (whose size is 470±34 μm and wieght is ca. 5 μg/shell) in the Gulf of Oman suggests its predominance in certain time and space (Erez et al., in press) .

Radiolarian SiO_2 flux ranges from ca. 3 mg/m^2/day at Stations E and P_1 and 6-10 mg/m^2/day at Station PB. When these values, especially the values from Station E, are compared with the existing data, it seems that Bishop et al. (1977) underestimated the radiolarian SiO_2 flux by several factors to an order of magnitude due to many assumptions involved.

The radiolarian SiO_2 flux is compared to biogenic opal flux values (Honjo et al., in press) and expressed as percentage in total biogenic SiO_2 (Table 13). That the percentages generally increases with depth suggests more dissolution of other components than intact radiolarian skeletons such as radilarian and diatom fragments in the water column. When the radiolarian flux data from Station PB (the Panama Basin) are compared with size fractioned biogenic SiO_2 values, they appear to agree well: the radiolarian SiO_2 flux ranges from 22 to 30% which suggests that the rest of the SiO_2 is transported by silicoflagellates, small diatoms (< 63 μm) and fragmented SiO_2 particles including radiolarian frangments which are < 63 μm. The values of 20 - 30 % is approximately equivalent to biogenic SiO_2 flux of > 63 μm size fraction. Radiolarians appear to be only the major biogenic silica carrier that can be microscopically identifiable. Contributions of diatoms to biogenic SiO_2 flux at Stations PB and P_1 are

Table 13. An extent of biogenic opal transport to the deep-sea by radiolarians. The values correspond to mid points of ranges.

Station/ Depth (m)	SiO_2 flux ($mg/m^2/day$) Spumellaria	Nassellaria	Phaeodaria Castanellids + *H. porcellana*	Others	Radiolaria	$\frac{\text{Phaeodaria}}{\text{Radiolaria}} \times 100$ (%)	$\frac{\text{Rad. } SiO_2}{\text{Total } SiO_2} \times 100$ (%)
Weight /shell (μg)	0.36-0.60	0.07-0.09	8-10	0.07-0.11	-	-	-
Mean SiO_2 Content (%)	90.5	98.4	70.6		-	-	-
E389	1.60±0.40	0.94±0.12	0.08±0.005	0.07-0.02	2.69±0.54	6	38±8
988	1.46±0.35	0.92±0.11	0.03±0.005	0.06±0.02	2.47±0.48	4	44±18
3755	2.67±0.66	1.25±0.16	0.01±0.004	0.11±0.02	4.04±0.84	3	99±21
5068	2.19±0.55	0.80±0.10	0.04±0.01	0.09±0.002	3.12±0.68	4	75±16
P1378	0.09±0.02	0.03±0.0004	0	0.001±0.001	1.21±0.02	0.1	318±5
978	0.64±0.16	0.26±0.03	0.02±0.001	0.01±0.009	0.93±0.20	3.2	145±31
2778	2.08±0.52	0.88±0.11	0	0.03±0.005	2.99±0.64	1.0	113±24
4280	2.22±0.55	0.91±0.11	0	0.02±0.009	3.15±0.67	0.6	127±27
5582	2.31±0.53	0.78±0.10	0	0.01±0.006	2.92±0.64	0.3	126±28
PB667	3.39±0.85	2.51±0.32	1.16±0.13	0.18±0.04	7.24±1.34	19	24±4
1268	3.02±0.75	1.64±0.20	0.93±0.10	0.09±0.03	5.68±1.08	18	22±4
2869	4.98±1.23	3.02±0.37	2.17±0.25	0.19±0.05	10.36±1.90	23	30±5
3769	-	-	1.16±0.13	0.14±0.03	-	-	-
3791	4.43±1.11	2.41±0.30	1.20±0.13	0.16±0.04	8.20±1.58	17	27±5

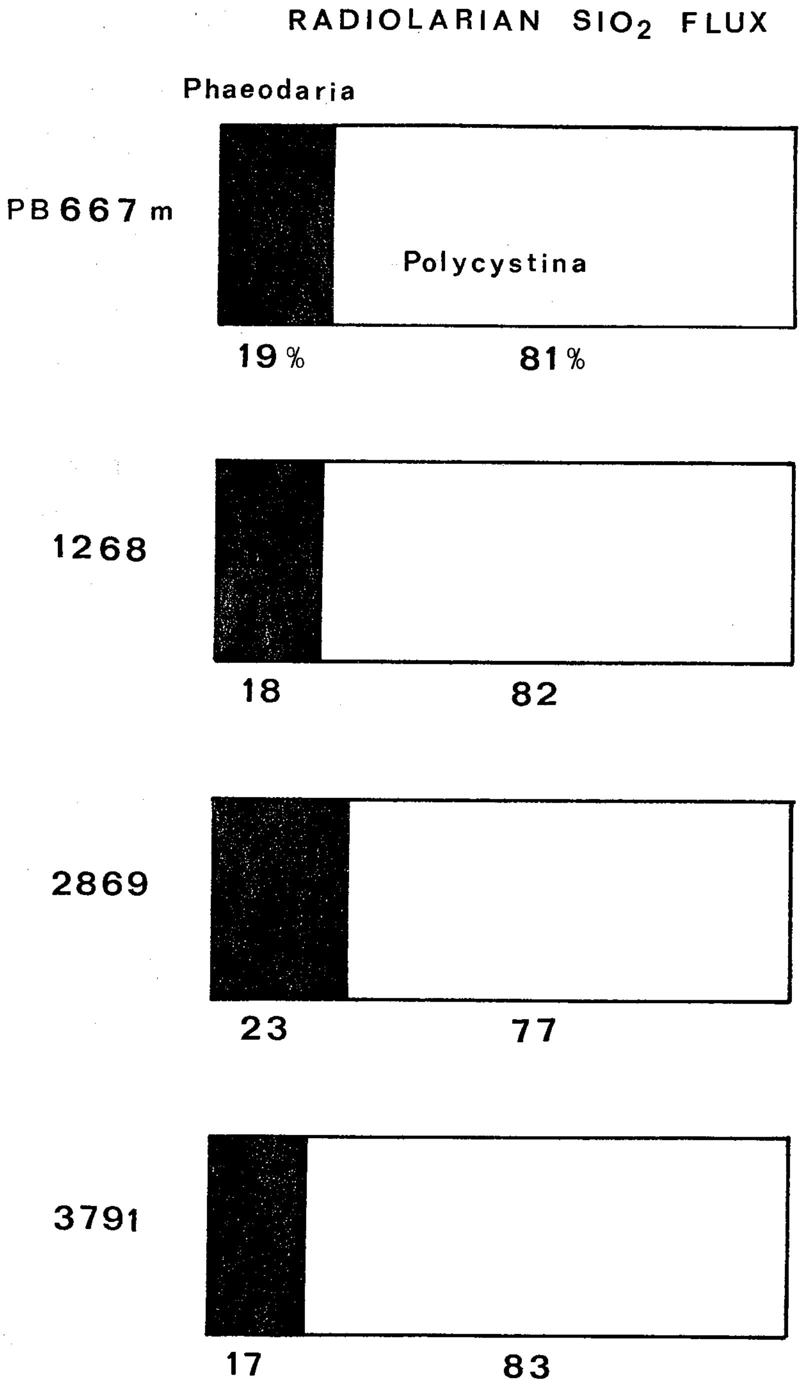

Figure 28. Percent contribution of Phaeodaria to radiolarian SiO_2 flux at Station PB which represents the highest phaeodarian SiO_2 flux among all Stations. Note that phæodarian SiO_2 flux is ca. 20 % while their counts are only ca. 6 % of Radiolaria (Table 5).

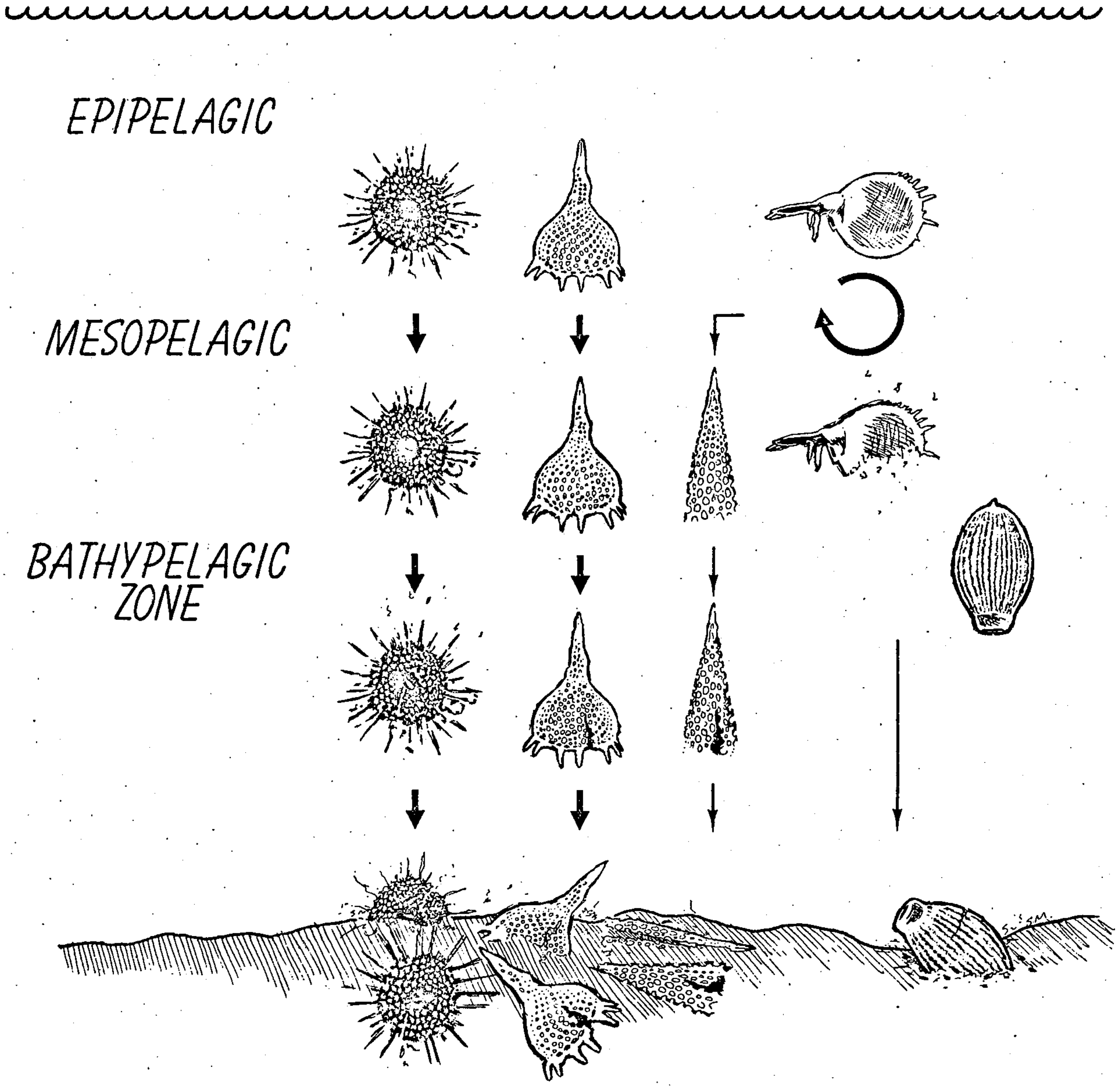

Figure 29. Simplified illustration depicting production depth, sinking, dissolution and preservation of Spumellaria, Nassellaria and Phaeodaria in a pelagic realm.

insignificant. Large diatoms (>63 μm) are minor components except at E station; at Station E (Equatorial Atlantic) Rhizosolenia styliformis, a centric diatom, contributes approximately one quater of total SiO_2 flux. The percentages of the radiolarian SiO_2 flux obtained for Stations E and P_1 appear to be too large because most of the weight data were obtained from 3769 and 3791 m samples at the Panama Basin which seems to be responsible for an overestimation. The datum at P_1 378 m anomalously deviates from the rest, but as stated earlier the recovery of this depth and 978 m samples was much less than the rest of the depths causing less reliability on the statistics. Microscopic examinations indicate that some taxa of the Panama Basin specimens are more robust and/or developed than the same taxa in other stations. For instance, patagium of Euchitonia elegans is generally present in samples from Station PB but absent in samples from Station P_1. Such a morphological difference as well as composition difference in assemblages are accounted for the exceeding values at E and P_1.

Estimation of excess Si relative to advective Si in the deep waters of the western North Atlantic

In the two studied areas of the western North Atlantic a major portion of the biogenic opal supply to the sediments appears to dissolve on the sea-floor. Consequently, an upward flux of dissolved silicon should be nearly equal to the supply rate assuming a steady state flux with time. This can be compared and further used to assess mixing regime of the deep waters in the North Atlantic. A linear relationship between Si and salinity below potential temperature 2° has been observed in the western North Atlntic, suggesting a simple mixing of North Atlantic Deep Water (NADW) and Antarctic Bottom Water(AABW) (Spencer, 1972: Broecker et al., 1980). A vetilation time of the deep western Atlantic is about 100 years (Broecker. 1979). If an upward flux of Si is significantly large relative to advective Si in the water column, a deviation from the above linear relationship should be detected.

Results of computations estimating upper and lower limits of excess Si (Δ Si) in the lowermost 1500 m of the water column are presented in

Table 14. Estimation of excess Si relative to advective Si in the deep waters of the western North Atlantic.

	Sargasso Sea Station S	Demerara A. P. Station E
Upward flux* (Si mg/m^2.yr)	51.1	712.0
ΔSi accumulation during a year below 3.5 km depth (Si μ mol/kg)	1.22×10^{-3}	1.695×10^{-2}
ΔSi accumulation during 100 years below below 3.5 km depth (Si μ mol/kg)	>0.12	<1.70

*Upward flux is assumed to be equivalent of 99 % of the biogenic opal flux to the sea-floor. Biogenic opal flux data are from Honjo (1980) and Honjo et al. (in press).

Table 14. This depth interval is chosen because Si concentration appears to be uniform below 3.5 km. It is possible to further mix Δ Si with overlain water masses during the ventilation time, then the resulting ΔSi values would be even smaller. The Sargasso Sea (Station S) and Demerara Abyssal Plain (E) perhaps represent close to lower and upper limits of the biogenic opal flux in the North Atlantic respectively. Over 100 years of the ventilation time 0.12-1.69 Δ Si μ mol/kg is added to the advective Si. Obviously, the range of the values is insignificantly small and thus cannot be detected as a deviation in the mixing curve. This is consistent with the previous reports of a simple mixing of NADW and AABW in the western North Atlantic (Spencer, 1972; Broecker et al., 1980).

SUMMARY AND CONCLUSIONS

(1) Total number of radiolarian taxa encountered combining all three stations is 420: 175 Spumellaria; 182 Nassellaria; 63 Phaeodaria. They include 1 new genus, 20 new species, 1 new subspecies, 1 new name for a species and 3 new names for subspecies. From E Station alone 208 taxa were found. To my knowledge, such a diversified marine community from the water column has never been reported in science.

(2) The observed vertical flux of individual radiolarian shells in the unit of $\times 10^3$ shells/m^2.day at each Station was: (E) 16 - 24; (P_1) 0.6 - 17; and (PB) 29 - 44. The radiolarian SiO_2 flux is converted from the radiolarian counts, weight and SiO_2 content data resulting in a range of 22 to 30% of total biogenic SiO_2 flux at Station PB. The values for Stations P_1 and E are higher than realistic because weight values from Station PB were used. These percentages tend to slightly increase with depth indicating that radiolarians are less affected by dissolution in the water column than other components such as diatom fragments.

(3) A total radiolarian diversity index of 3.6 is obtained from Station E. Diversity indices of Spumellaria and Nassellaria from Station

E were uniform below 988 m, suggesting their sinking without much loss due to dissolution (Fig. 29). The diversity index of Nassellaria increased significantly from 389 to 988 m. This is mainly attributed to an introduction of deep water species.

(4) Most of the radiolarian shells recovered from below 1 km were observed to be single rather than being incorporated with biogenic aggregates. Only a few percent of radiolarian shells is in the form of biogenic aggregates and that appeared to be descending more rapidly than the rest of individual shells to the sea floor.

(5) Fragmentation of radiolarian shells are interpreted as an effect of dissolution. Percent broken shell counts of Pterocorys as well as three suborders of Radiolaria suggest that slow dissolution of radiolarian shells takes place through the water column.

(6) Nassellaria and Phaeodaria are decreasing with depth relative to Spumellaria shown by change in N/S and Ph/S ratios.

(7) Phaeodarians and dissolution susceptible polycystines (e.g. Myleastrum and Conicavus) whose sizes are often large, transport a significant amount of SiO_2 to the deep-sea. They quickly release Si either in the water column or on the seafloor depending on their residence time in the water column. Thus, they are playing an important role in quick silica transport and recycling in the ocean.

(8) Estimated excess Si which is derived from SiO_2 dissolution on the sea-floor is farily small relative to advective Si in the western North Atlantic and thus it appears to be insignificant to show a deviation in a simple mixing curve of deep water masses. This is consistent with previous reports.

(9) When the radiolarian fluxes at the three Stations are compared with Holocene radiolarian accumulation rates in the same areas it became apparent that several percent or less of the fluxes are preserved in the sediments in all cases.

(10) Fundamental dimensions of 58 radiolarian taxa are presented. These include: weight, length, width, projected area, which were measured and computed projected area, bulk volume, skeletal volume and bulk density contrast which were computed.

(11) Mean values of silica content in the skeletons in each suborder show: Spumellaria: 91%; Nassellaria: 98%; and Phaeodaria: 71%.

(12) Observed laboratory sinking speed of 55 radiolarian taxa ranges from 13 to 416 m/day in 3°C still water. The values are best correlated with weight/shell among all the possible combinations of examined variables. The regression line is $\log Y = 0.50 \log X + 1.88$ ($r = 0.86$). By allowing a factor of two the Stokes equation is generally applicable to the sinking speed of less than 250 μm size radiolarians.

(13) Residence time of radiolarian skeletons estimated from the sinking speed ranges from 2 weeks to 14 months in 5 km sea water column; large phaeodarians spend only a few weeks in a water column and hence they reach the abyssal floor essentially intact despite of their soluble skeletons while small-sized species do not reach the bottom but dissolved during descent because of their longer residence times.

(14) Standing stock for abundant species is on the order of 1 to 100 individuals/m^3 depending on the species and stations. Total radiolarian standing stock ranges from ca. 450 shells/m^3 at Stations P_1 and E to 1200 shells/m^3 at Station PB.

(15) Rate of production of total Radiolaria ranges from 77 to 225 shells/m^3/day assuming that their production occurs in 200 m of water column.

(16) Turnover time for the studied radiolarian species ranges from several days to a month.

CHAPTER I REFERENCES

ASPER, V., 1981. Ultrastructural changes in diatom frustules associated with dissolution, and a review of methods for preparing frustules for surface area measurements. M.Sc. Thesis, Univ. Hawaii, 79 pp.

BERGER, W.H., 1968. Radiolarian skeletons: solution at depths. Science, 159: 1237-1238.

----, 1970. Biogenous deep-sea sediments: Fractionation by deep-sea circulation. Geol. Soc. Amer., Bull., 81(5): 1385-1402.

----, 1976. Biogenous deep sea sediments: production, preservation and interpretation. In Reley, J.P., and Chester, R., Eds., Chemical Oceanography, volume 5: 265-388, Academic Press.

----, and SOUTAR, A., 1970. Preservation of plankton shells in an anaerobic basin off California. Geol. Soc. Amer., Bull., 81: 275-282.

----, and PIPER, D.J.W., 1972. Planktonic foraminifera: differential settling, dissolution and redeposition. Limnol. Oceanogr., 17: 275-286.

BISHOP, J.K.B., EDMOND, J.M., KETTEN, D.R., BACON, M.P. and SILKER, W.B., 1977. The chemistry, biology and vertical flux of particulate matter from the upper 400 m of the equatorial Atlantic Ocean. Deep-Sea Res., 24: 511-548.

----, KETTEN, D.R., and EDMOND, J.M., 1978. The chemistry, biology and vertical flux of particulate matter from the upper 400 m of the Cape Basin in the southeast Atlantic Ocean. Deep-Sea Res., 25: 1121-1161.

----, COLLIER, R.W., KETTEN, D.R., and EDMOND, J.M., 1980. The chemistry, biology and vertical flux of particulate matter from the upper 1500 m of the Panama Basin. Deep-Sea Res., 27A: 615-640.

BJØRKLUND, K.R., 1974. The seasonal occurrence and depth zonation of radiolarians in SKorsfjorden, Western Norway. Sarsia, 56: 13-42.

BOLTOVSKOY, D., and RIEDEL, W.R., 1980. Polycystine radiolaria from the Southwestern Atlantic Ocean plankton. Revista Espanola de Micropaleontologia, 12(1): 99-146.

BOYLE, E.A., 1981. Cadimium, zinc, copper, and barium in Foraminifera tests. Earth Planet. Sci. Lett., 53: 11-35.

BREWER, P.G., NOZAKI, Y., SPENCER, D.W., and FLEER, A.P., 1980. A sediment trap experiment in the deep sub-tropical Atlantic: isotopic and elemental fluxes. Jour. Mar. Res., 38(4): 703-728.

BROECKER, W.S. 1979. A revised estimate for the radiocarbon age of North Atlantic deep water. Jour. Geophy. Res., 84(C6): 3218-3226.

----., TAKAHASHI, T., and STUIVER, M., 1980. Hydrography of the central Atlantic-II. Waters beneath the two-degree discontinuity. Deep-Sea Res., 27A: 397-419.

BURTON, J.D., and LISS, P.S., 1973. Processes of supply and removal of dissolved silica in the oceans. Geochim. Cosmochim. Acta, 37: 1761-1773.

CACHON, J., and CACHON, M., 1978. A reinterpretation of its phylogenetic position based upon new observations on its ultrastructure. Arch. f. Protistenk. 120: 148-168.

CALVERT, S.E., 1968. Silica balance in the ocean and diagenesis. Nature, 219: 919-920.

----, 1974. Deposition and diagenesis of silica in marine sediments. In: Hsu, K.J., and Jenkyns, H.C., Eds., Pelagic Sediments: On Land and Under the Sea, Spec. Publs. Int. Ass. Sediment., 1: 273-299.

CARDER, K.L., BEARDSLEY, G., and PAK, H., 1971. Particle size distributions in the Eastern Equatorial Pacific. Jour. Geophys. Res., 24: 5070-5077.

CASEY, R., PARTRIDGE, T.M., and SLOAN, J.R., 1971. Radiolarian life spans, mortality rates, and seasonality gained from recent sediment and plankton samples. In: Farinacci, A., Ed., Proceedings of the II Planktonic Conference, Roma, 1970, 1: 159-165.

----, and MCMILLEN, K.J., 1977. Cenozoic radiolarians of the Atlantic Basin and margins. In: Swain, F.M., Eds., Stratigraphic Micropaleontology of Atlantic Basin and Borderlands: Amsterdam, Elsevier: 226-238.

----, GUST, L., LEAVESLEY, A., WILLIAMS, D., REYNOLDS, R., DUIS, T., and SPAW, J.M., 1979a. Ecological niches of radiolarians, planktonic foraminiferans and pteropods inferred from studies on living forms in the Gulf of Mexico and adjacent waters. Gulf Coast Assoc. Geol. Socs. Trans., 29: 216-223.

----, SPAW, J.M., KUNZE, F., REYNOLDS, R., DUIS, T., MCMILLEN, K., PRATT, D., and ANDERSON, V., 1979b. Radiolarian ecology and the development of the radiolarian component in Holocene sediments, Gulf of Mexico and adjacent seas with potential paleontological applications. Gulf Coast Assoc. Geol. Socs. Trans., 29: 228-237.

COBLER, R., and DYMOND, J., 1980. Sediment trap experiment on the Galapagos Spreading Center, equatorial Pacific. Science, 209: 801-803.

DEMASTER, D.J., 1979. The marine budgets of silica and ^{32}Si. Ph.D. Thesis, Yale Univ., 308 pp.

EDMOND, J.M., 1973. The silica budget of the Antarctic Circumpolar Current. Nature, 241(5389): 391-393.

----, 1974. On the dissolution of carbonate and silicate in the deep ocean. Deep-Sea Res., 21: 455-480.

----, MEASURES, C., MCDOFF, R.E., CHAN, L.H., COLLIER, R., GRANT, B., GORDON, L.I., and CORLISS, J.B., 1979. Ridge crest hydrothermal activity and the balances of the major and minor elements in the ocean: The Galapagos data. Earth Planet. Scsi. Lett., 46: 1-18.

EMERY, K.O., 1960. The sea off southern California. John Wiley and Sons, Inc. 366 pp.

EREZ, J., TAKAHASHI, K., and HONJO, S., in press. In situ dissolution of Radiolaria in the Central North Pacific Ocean. Earth Planet. Sci. Lett.

GARDNER, W.D., 1977a. Fluxes, dynamics and chemistry of particles in the ocean. Ph.D. Thesis, Massachusetts Institute of Technology/Woods Hole Oceanographic Institution Joint Program in Oceanography.

GARDNER, W.D., 1977b. Incomplete extraction of rapidly settling particles from water samplers. Limnol. Oceanogr., 22: 764-768.

GOLL, R.M. and BJORKLUND, K.R., 1971. Radiolaria in surface sediments of the north Atlantic Ocean. Micropaleontology, 17(4): 434-454.

----, and BJORKLUND, K.R., 1974. Radiolaria in surface sediments of the South Atlantic. Micropaleontology, 20(1): 38-75.

HAECKEL, E., 1887. Reports on the Radiolaria collected by H.M.S. "Challenger" during the years 1873-1876. Repts., Voy. Challenger, Zool., 18(1-2): i-clxxxviii + 1-1803, pls. 1-140.

HAECKER, V., 1908., Tiefsee Radiolarien Speziel Teil. L1, Aulacanthidae-Concharidae. Deutsch. Tiefsee-Exped., Wiss. Ergeben., 14: 1-336.

HAYS, J.D., SAITO, T., OPDYKE, N.D., and BURCKLE, L.H., 1969. Pliocene-Pleistocene sediments of the equatorial Pacific: Their paleomagnetic, biostratigraphic and climatic record. Geol. Soc. Amer., Bull., 80: 1481-1514.

HEATH, G.R., 1969. Mineralogy of Cenozoic deep-sea sediments from the equatorial Pacific Ocean. Geol. Soc. Amer., Bull., 80: 1997-2018.

HEATH, G.R., 1974. Dissolved silica and deep-sea sediments. In: Hay, W.W., Ed., Studies in Paleo-Oceanography. Soc. Econ. Paleont. Mineral., Spec. Publ. No. 20: 77-93.

----, MOORE, T.C., JR., and ROBERTS, G.L., 1974. Mineralogy of surface sediments from the Panama Basin, eastern equatorial Pacific. Jour. Geology, 82: 145-160.

HINGA, K.R., SIEBURTH, J.M., and HEATH, G.R., 1979. The supply and use of organic material at the deep-sea floor. Jour. Mar. Res., 37(3): 557-579.

HONJO, S., 1975. Dissolution of suspended coccoliths in the deep-sea water column and sedimentation of coccolith ooze. In: Silter, W., A.W.H. Be, and W.H. Berger, Eds., Cushman Found. Foram. Res., Spec. Publ. No. 13, p. 115-128.

----, 1976. Coccoliths: production, transportation and sedimentation. Mar. Micropaleo., 1: 65-79.

----, 1977. Biogenic carbonate particles in the ocean; do they dissolve in the water column? In: Andersen, N.R., and Malahoff, A., Eds., The Fate of Fossil Fuel CO_2 in the Oceans. Plenum Publ. Corp., p. 269-294.

----, 1978. Sedimentation of materials in the Sargasso Sea at a 5,367 m deep station. Jour. Mar. Res., 36: 469-492.

----, 1980. Material fluxes and modes of sedimentation in the mesopelagic and bathypelagic zones. Jour. Mar. Res., 38: 53-97.

----, in press. Remineralization and accumalation of materials in the deep sea sediments.

----, and OKADA, H., 1974. Community structure of coccolithophores in the photic layer of the mid-Pacific. Micropaleontology, 20(2): 209-230.

----, and ROMAN, M.R., 1978. Marine copepod fecal pellets: production, preservation and sedimentation. Jour. Mar. Res., 36(1): 45-57.

----, CONNELL, J.F., and SACHS, P.L., 1980. Deep ocean sediment trap: design and function of PARFLUX Mark II. Deep Sea Res., 27: 745-753.

----, MANGANINI, S., and COLE, J.J., in press. Sedimentation of biogenic matter in the deep ocean. Deep-Sea Res.

HURD, D.C., 1972. Factors affecting solution rate of biogenic opal in seawater. Earth Planet. Sci. Lett., 15: 411-417.

HURD, D.C., 1973. Interactions of biogenic opal, sediment and seawater in the central Equatorial Pacific. Geochim. Cosmochim. Acta, 37: 2257-2287.

----, and THEYER, F., 1977. Changes in the physical and chemical properties of biogenic silica from the central equatorial Pacific: Part II. Refractive index, density and water content of acid-cleaned samples. Amer. Jour. Sci., 277: 1168-1202.

----, PANKRATZ, H.S., ASPER, V., FUGATE, T., and MORROW, H., 1981. Changes in the physical and chemical properties of biogenic silica from the central equatorial Pacific: Part III, specific pore volume, mean pore size, and skeletal ultrastructure of acid-cleaned samples. Amer. Jour. Science, 281: 833-895.

----, and TAKAHASHI, K., in press. On the estimation of minimum mechanical loss during an in situ biogenic silica dissolution experiment. Mar. Micropaleont.

JOHNSON, T.C., 1974. The dissolution of siliceous microfossils in surface sediments of the western tropical Pacific. Deep-Sea Res., 21: 851-864.

JOUSE, A.P., MUKHINA, V.V., and KOZLOVA, O.G., 1969. Diatoms and silicoflagellates in the surface layer sediments of the Pacific Ocean. In: Bezrukov, P.L., Ed., The Pacific Ocean. Volume 8: Microflora and microfauna in the Recent sediments of the Pacific Ocean. Miscow: Izd. "Nauka", pp. 7-47 (in Russian).

KANAYA, T., and KOIZUMI, I., 1966. Interpretation of diatom thanatocoenoses from the North Pacific applied to a study of core V20-130. Sci. Repts. Tohoku Univ., 2nd Ser. (Geol.), 37: 89-130.

KHARKAR, D.P., TUREKIAN, K.K., and SCOTT, M.R., 1969. Comparison of sedimentation rates obtained by ^{32}Si and uranium decay series determinations in some siliceous Antarctic cores. Earth Planet. Sci. Lett., 6: 61-68.

KIDO, K., and NISHIMURA, M., 1975. Silica in the sea - its forms and dissolution rate. Deep-Sea Res., 22: 323-338.

KLING, S.A., 1976. Relation of radiolarian distributions to subsurface hydrography in the North Pacific. Deep-Sea Res., 23: 1043-1058.

----, 1979. Vertical distribution of polycystine radiolarians in the central North Pacific. Marine Micropaleontology, 4(4): in press.

KNAUER, G.A., MARTIN, J.H., and BRULAND, K.W., 1979. Fluxes of particulate carbon, nitrogen and phosphorous in the upper water column of the Northeast Pacific. Deep-Sea Res., 26: 97-108.

KOMAR, P.D., MORSE, A.P., SMALL, L.F., and FOWLER, S.W., 1981. An analysis of sinking rates of natural copepod and euphausiid fecal pellets. Limnol. Oceanogr., 26(1): 172-180.

KOWSMANN, R.O., 1973. Surface sediments of the Panama Basin: Coarse components. M.Sc. Thesis, Oregon State Univ.: 73 pp.

KOZLOVA, O.G., 1964. Diatoms of the Indian and Pacific sectors of the Antarctic. In: Lisitzin, A.P., Ed., Izdatel'stvo "Nauka". Translated into English by Hoffman, S., Israel Prog. Scientific Translations, Jerusalem, 1966, 191 pp.

KUENEN, P.H., 1950. Marine Geology. John Wiley and Sons, Inc., 568 pp.

LEAVESLEY, A., BAUER, M., MCMILLEN, K., and CASEY, R., 1978. Living shelled microzooplankton (radiolarians, foraminiferens, and pteropods) as indicators of oceanographic processes in water over the outer continental shelf of south Texas. Gulf Coast Assoc. Geol. Socs. Trans., 28: 229-238.

LERMAN, A., 1979. Geochemical Processes Water and Sediment Environments. John Wiley & Sons, N.Y., 481 pp.

LISITZIN, A.P., 1971. Distribution of siliceous microfossils in suspension and in bottom sediments. In: Funnell, B.M., and Riedel, W.R., Eds., The Micropaleontology of Oceans, p. 173-195, Cambridge University Press.

----, 1972. Sedimentation in the world ocean. Soc. Econ. Paleont. Mineral., Spec. Publ. No. 17: 218 pp.

----, BELAYAYEV, Y.I., BODANOV, Y.A., and BOGORJAVLENSKIY, A.N., 1967. Distribution relationships and forms of silicon suspended in waters of the world ocean. Internat. Geol. Rev., 9: 253-274.

LONSDALE, P., 1975., Detailed abyssal sedimentation studies in the Panama Basin: cruise report of expedition Cocotow legs 2b and 3. S.I.O. Ref. 75-4, 17pp.

----., 1977. Inflow of bottom water to the Panama Basin. Deep-Sea Res., 24: 1065-1101.

MACKENZIE, F.T., and GARRELS, R.M., 1966. Silica bicarbonate balance in the ocean and early diagenesis. Jour. Sed. Petrol., 36: 1075-1084.

MCCAVE, I.N., 1975. Vertical flux of particles in the ocean. Deep-Sea Res., 22: 491-502.

MCMILLEN, K.J., 1979. Radiolarian ratios and the Pleistocene-Holocene boundary. Gulf Coast Assoc. Geol. Socs. Trans., 29: 298-301.

----, and CASEY, R.E., 1978. Distribution of living polycystine radiolarians in the Gulf of Mexico and Caribbean Sea, and composition with sedimentary record. Mar. Micropal. 3: 121-145.

MOORE, T.C., Jr., 1969. Radiolaria: change in skeletal weight and resistance to solution. Geol. Soc. Amer., Bull., 80: 2103-2108.

----, HEATH, G.R., and KOWSMANN, R.O., 1973. Biogenic sediments of the Panama Basin. Jour. Geology, 81: 458-472.

MOORE, E., and SANDER, F., 1977. A study of the offshore zooplankton of the tropical western Atlantic near Barbados. Ophelia, 16: 77-96.

MUNK, W.H., and RILEY, G.A., 1952. Absorption of nutrients by aquatic plants. Jour. Mar. Res., 11(2): 215-240.

NELSON, D.M., AND GOERING, J.J., 1977. A stable isotope tracer method to measure silicic acid uptake by marine phytoplankton. Anal. Biochem., 78: 139-147.

PAASCHE, E., 1973. The influence of cell size on growth rate, silica content, and some other properties of four marine diatom species. Norw. Jour. Bot., 20: 197-204.

PETRUSHEVSKAYA, M., 1971a. Spumellarian and Nasselarian Radiolaria in the plankton and bottom sediments of the Central Pacific. In: Funnell, B.M., and Riedel, W.R., Eds., The Micropaleontology of Oceans, pp. 309-317, Cambridge Univ. Press.

----, 1971b. Radiolaria in the plankton and recent sediments from the Indian Ocean and Antarctic. In: Funnell, B.M., and Riedel, W.R., Eds., The Micropaleontology of Oceans, pp. 319-329, Cambridge Univ. Press.

PIELOU, E.C., 1969. An Introduction to Mathematical Ecology. Wiley-Interscience, 286 pp.

PLANK, W.S., ZANEVELD, J.R., and PAK, H., 1973. Distribution of suspended matter in the Panama Basin. Jour. Geophys. Res., 78: 7113-7121.

RAUDKIVI, A.J., 1976. Loose boundary hydraulics. Pergamon Press, N.Y. 397 pp.

REID, J.L., 1965. Intermediate waters of the Pacific Ocean. The Johns Hopkins Oceanographic Studies No. 2, The Johns Hopkins Univ. Press, Baltimore.

RENZ, G.W., 1976. The distribution and ecology of Radiolaria in the Central Pacific plankton and surface sediments. Bull. Scripps Inst. of Oceanogr., 22: 1-267.

RIEDEL, W.R., 1959. Siliceous organic remains in pelagic sediments. In: Ireland, H.A., Ed., Silica in Sediments. Soc. Econ. Paleontologists and Mineralogists, Spec. Publ., 7: 80-91.

ROWE, G.T., and GARDNER, W.D., 1979. Sedimentation rates in the slope water of the northwest Atlantic Ocean measured directly with sediment traps. Jour. Mar. Res., 37(3): 581-600.

RYTHER, J.H., 1963. Geographic variations in productivity. In: Hill, M.H., Ed., The Sea, 2: 347-380.

SCHRADER, H.J., 1971. Fecal pellets: role in sedimentation of pelagic diatoms. Science, 1974: 55-57.

----, 1972. Kieselsaure-Skelette in Sedimenten des ibero-marokkanischen Kontinentalrandes und angrenzender Tiefsee-Ebenen "Meteor"-Forsch.-Ergebnisse, C(8): 10-36. (in German)

SCHULTZ, D.F., and TUREKIAN, K.K., 1965. The investigation of the geographical and vertical distribution of several trace elements in sea water using neutron activation analysis. Geochim. Cosmochim. Acta, 29: 259-313.

SHELDON, R.W., EVELYN, T.P.T., and PARSONS, R.R., 1967. On the occurrence and formation of small particles in seawater. Limnol. Oceanogr., 12: 367-375.

SMAYDA, T.J., 1969. Some measurements of the sinking rate of fecal pellets. Limnol. Oceanogr., 14: 621-625.

----, 1970. The suspension and sinking of phytoplankton in the sea. Oceanogr. Mar. Biol. Ann. Rev., 8: 353-414.

----, 1971. Normal and accelerated sinking of phytoplankton in the sea. Mar. Geol., 11: 105-122.

SOUTAR, A., KLING, S.A., CRILL, P.A., and DUFFRIN, E., 1977. Monitoring the marine environment through sedimentation. Nature, 266(5598): 136-139.

SPENCER, D.W., 1972. GEOSECS II, the 1970 North Atlantic Station: Hydrgraphic features, oxygen, and nutrients. Earth Planet. Sci. Lett., 16: 91-102.

----, BREWER, P.G., FLEER, A., HONJO, S., KRISHNASWAMI, S., and NOZAKI, Y., 1978. Chemical fluxes from a sediment trap experiment in the deep Sargasso Sea. Jour. Mar. Res., 36(3): 493-523.

STEVENSON, M., 1970. Circulation in the Panama Bight. Jour. Geophys. Res., 75(3): 659-672.

STRICKLAND, J.D.H., and PARSONS, T.R., 1972. A practical handbook of sea water analysis. Fish. Res. Bd. Can. Bull., 167: 311 pp.

SWIFT, S. A., 1976. Holocene accumulation rates of Pelagic sediment components in the Panama Basin, eastern equatorial Pacific. M. Sc. Thesis, Oregon State University, 91 pp.

----, 1977. Holocene rates of sediment accumulation in the Panama Basin, eastern equatorial Pacific, Pelagic sedimentation and lateral transport. Jour. Geology, 85: 301-319.

----, and WENKAM, C., 1978. Holocene accumulation rates of calcite in the Panama Basin: lateral and vertical variation in calcite dissolution. Mar. Geology, 27: 67-77.

TAKAHASHI, K., and LING, H.Y., 1980. Distribution of Sticholonche (Radiolaria) in the upper 800 m of the waters in the Equatorial Pacific. Mar. Micropaleotol., 5: 311-319.

----, and HONJO, S., 1980. Radiolarian flux to the deep-sea and depth of production and dissolutionin the tropical Atlantic and Pacific. Geol. Soc. Amer. Proc., 12(7): 533 (abstract).

----, and HONJO, S., 1981a. Vertical flux of Radiolaria: A taxon-quantitative sediment trap study from the western Tropical Atlantic. Micropaleontology, 27(2): 140-190.

----, and HONJO, S., 1981b. Radiolaria: Standing stock, residence time and turnover time in the equatorial Atlantic Ocean. Geol. Soc. Amer. Proc., 13(17): 564 (abstract).

----, and HONJO, S., 1981c. Sinking speed, residence time and dissolution of Radiolaria. Geol. Soc. Amer. Proc., 13(7): 564 (abstract).

----, HURD, D.C., ASPER, V., and HONJO, S., 1981a. Sequential dissolution of Radiolaria in the tropical water column and sediments. Geol. Soc. Amer. Proc., 13(7): 564 (abstract).

----, HURD, D.C., and HONJO, S., 1981b. Dissolution of Radiolaria during settling in the water column and preservation in the sediments. EOS, Trans. Amer. Geophy. Union., 62(45): 938 (abstract).

THOMAS, W.H., and DODSON, A.N., 1974. Inhibition of diatom phytosynthesis by Germanic acid: separation of diatom productivity from total primary productivity. Mar. Biol., 217: 11-19.

THUNELL, R.C., and HONJO, S., 1980. Planktonic foraminiferal flux to the deep ocean: Sediment trap results from the Equatorial Atlantic and the Central Pacific. Mar. Geol., 40: 237-253.

TURNER, J.T., and FERRANTE, J.G., 1979. Zooplankton Fecal pellets in aquatic ecosystem. BioScience, 27(11): 670-676.

van Andel, Tj.H., 1973. Texture and dispersal of sediments in the Panama Basin. Jour. Geol., 81: 434-457.

WHITTAKER, R.H., and FAIRBANKS, C.W., 1958. Study of planktonic copepod communities in the Columbia Basin, southwestern Washington. Ecology, 39: 46-65.

WIEBE, P.H., BOYD, S.T., and WINGET, C., 1976. Particlate matter sinking to the deep-sea floor at 2000 m in the Tongue of the Ocean, Bahamas, with a description of a new sedimentation trap. Jour. Mar. Res., 34: 341-354.

WORTHINGTON, L.V., 1976. On the North Atlantic circulation. The Johns Hopkins Oceanographic Studies No. 6, The Johns Hopkins Univ. Press, Baltimore, 110 pp.

APPENDIX

Table 1. Formulae for computed projected area and bulk volume computations.

	Shape	Computed maximum projected area, CPA	Bulk volume, V_b	Thickness h (μm)	Assumed thickness, h
SPUMELLARIA					
1. Acrosphaera murrayana (Haeckel)	Sphere	$\pi (L/2)^2$	$(4/3)\ \pi\ (L/2)^3$		
2. Actinomma arcadophorum Haeckel	Sphere	$\pi (L/2)^2$	$(4/3)\ \pi\ (L/2)^3$		
3. Amphirhopalum ypsilon Haeckel	Rectangular plate		PA.h		L/10
4. Cladococcus scoparius Haeckel	Sphere (thorny)	$\pi (L/2)^2$	$(4/3)\pi(L/2x3)^3$		
5. Dictyocoryne profunda Ehrenberg >350 μm	Triangular plate	$(L^2/2)\ 1.05$	CPA.h		L/4
6. Dictyocoryne profunda Ehrenberg <350 μm	Triangular plate		CPA.h		L/4
7. Dictyocoryne truncatum (Ehrenberg)	Triangular plate	$(L^2/2)\ 1.3$	CPA (2/3) h	130	
8. Euchitonia elegans (Ehrenberg)	Triangular plate		PA.h	40	
9. Heliodiscus asteriscus Haeckel	Discoidal plate		CPA.h		L/4
10. Myelastrum quadrifolium n.sp.	Discoidal plate		PA.h		L/10
11. Myelastrum trinibrachium n.sp.	Discoidal plate		PA.h		L/10
12. Saturnalis circularis Haeckel	Saturn-like	$((L+W)/4)^2\pi\ 0.324$	CPA.h		L/6
13. Spongaster tetras tetras Ehrenberg	Quadrate plate	L^2	CPA.h		L/4
14. Spongocore cylindrica (Haeckel)	Cylinder		$\pi\ (W/2)^2L$		
15. Spongodiscus biconcavus (Haeckel) >270 μm	Discoidal plate	$\pi (L/2)^2$	CPA.h		L/4
16. Spongodiscus biconcavus (Haeckel) <270 μm	Discoidal plate	$\pi (L/2)^2$	CPA.h		L/4
17. Spongosphaera polycantha Muller	Sphere	$\pi (L/2)^2$	$(4/3)\pi(L/2)^3$		
18. Spongosphaera sp. aff S. helioides Haeckel	Sphere	$\pi (L/2)^2$	$(4/3)\pi(L/2)^3$		
19. Spongotrochus glacialis Popofsky	Discoidal plate		CPA.h		L/4
NASSELLARIA					
30. Acanthodesmia vinculata (Muller)	Ellipsoid	$(4/3)\pi(L/2)^2W/2$			
31. Androspyris reticulidisca n.sp.	Discoidal plate		PA.h		L/4
32. Anthocyrtidium ophirense (Ehrenberg)	Pseudo-cone		$(1/3)\pi(1.1W/2)^2L$		
33. Anthocyrtidium zanguebaricum (Ehrenberg)	Pseudo-cone		$(1/3)\pi(1.1W/2)^2L$		
34. Callimitra annae Haeckel	Pyramid		$(1/3)(W2/2)L$		
35. Callimitra emmae Haeckel	Pyramid		$(1/3)(W2/2)L$		
36. Carpocanistrum spp.	Pseudo-sphere	$\pi((L+W)/4)^2$	$(4/3)\pi((L+W)/4)^3$		
37. Cephalospyris cancellata Haeckel	Cone		$(1/3)\pi(W/2)^2L$		
38. Conicavus tipiopsis n.sp.	Cone		$(1/3)\pi(W/2)^2L$		

APPENDIX Table 1. (Cont.)

	Shape	Computed maximum projected area, CPA	Bulk volume, V_b	Thickness h (μm)	Assumed thickness, h
39. Cornutella profunda Ehrenberg	Cone		$(1/3)\pi(W/2)^2L$		
40. Dictyocodon elegans (Haeckel)	Pseudo-cone		$(1/3)\pi(1.1W/2)^2h$		
41. Eucecryphalus tricostatus (Haeckel)	Cone	$\pi\ (L/2)^2$	$(1/3)\pi(L/2)^2h$		8L/10
42. Eucyrtidium acuminatum (Ebg)+hexagonatum Hkl	Pseudo-cone		$(1/3)\pi(1.1W/2)^2L$		
43. Lamprocyclas maritalis maritalis Haeckel	Pseudo-cone		$(1/3)\pi(1.1W/2)^2L$		
44. Liriospyris thorax (Haeckel)	Rectangular box		PA.h		7L/10
45. Lithostrobus hexagonalis Haeckel	Pseudo-cone		$(1/3)\pi(1.1W/2)^2L$		
46. Lophospyris pentagona pentagona (Ehrenberg)	Rectangular box	$\pi((L+W)/4)^2$	CPA.h		8L/10
47. Nephrospyris renilla Haeckel	Discoidal plate		PA.h		L/6
48. Pterocorys zancleus (Mlr) + campanula Hkl	Pseudo-cone		$(1/3)\pi(1.1W/2)^2L$		
49. Spirocyrtis scalaris Haeckel	Pseudo-cone		$(1/3)\pi(1.1W/2)^2L$		
<u>PHAEODARIA</u>					
80. Castanellids from E	Sphere	$\pi\ (L/2)^2$	$(4/3)\pi(L/2)^3$		
81. Castanellids from PB	Sphere	$\pi\ (L/2)^2$	$(4/3)\pi(L/2)^3$		
82. Castanellids from PB <300 μm					
83. Castanellids fragments					
84. Castanidium abundiplanatum n.sp.	Sphere	$\pi\ (L/2)^2$	$(4/3)\pi(L/2)^3$		
85. Challengeria tizardi Murray	Ellipsoid		$(4/3\pi(L/2)(W/2)(L/4)$	L/2	
86. Challengeron willemoesii Haeckel	Ellipsoid		$(4/3)\pi(L/2)(W/2)^2 8/10$		
87. Challengeron lingi n.sp.	Ellipsoid	$\pi\ (W/2)^2\ 1.2$	$(4/3)\pi(L/2)(W/2)^2\ 5/10$		
88. Challengerosium avicularia Haecker	Ellipsoid	$\pi\ (W/2)^2$	$(4/3)\pi(W/2)(6W/20)(11W/20)$	6W/10	
89. Circoporus oxycanthus Borgert	Sphere	$\pi\ (L/2)^2\ 1.2$	$(4/3)\pi(L/2)^3$		
90. Conchidium argiope Haeckel	Hemi-ellipsoid		$(4/3)\pi(L/2)(W/2)^2\ 1/2$		
91. Conchellium capsula Borgert	Hemisphere	$\pi\ (L/2)^2$	$4/3)\pi(L/2)^3\ 1/2$		
92. Conchopsis compressa Haeckel	Ellipsoid		$(4/3)\pi(L/2)^2(1/4)$		
93. Euphysetta elegans Borgert	Sphere		$(4/3)\pi(W/2)^3$		
94. Haeckeliana porcellana Haeckel	Sphere		$(4/3)\pi(L/2)^3$		
95. Protocystis sloggetti (Haeckel)	Triangular plate/ellipsoid		PA.h or $(4/3)\pi(L/2)(W/2)^2\ 6/10$		W/2
96. Protocystis murrayi (Haeckel)	Sphere	$\pi\ (W/2)^2\ 1.2$	$(4/3)\pi(W.2)^3$		
97. Protocystis curva n.sp.	Ellipsoid		$(4/3)\pi(L/2)(W/2)^2\ 6/10$		6W/10
98. Protocystis honjoi n.sp.	Ellipsoid	$\pi(W/2)^2\ 1.15$	$(4/3)\pi(W/2)^2(W/2)(6/10)$		

CHAPTER II

SYSTEMATICS OF RADIOLARIA

INTRODUCTION

The high-level classification followed herein is based mainly on that proposed by Riedel (1967a, 1967b, 1971) for polycystines and by Haeckel (1887), Haecker (1908b) and Borgert (1901a, 1906, 1907, 1910, 1911) for phaeodarians with some emendations. A classification given by Takahashi and Honjo (1981) is slightly modified here. Synonymies of taxa include the original descriptions, those which reflect the current usage for polycystines, and relevant ones mainly from plankton and surface sediments. In the case of phaeodarians relatively little documentation has been accomplished thus far and available literature is much less than that for polycystines. Therefore, the author has attempted to list all references for phaeodarians where possible together with giving definitions of families and genera.

OUTLINE CLASSIFICATION

	Plate	Figure
Subclass RADIOLARIA Müller, 1858a		
Order POLYCYSTINA Ehrenberg, 1838, emend. Riedel, 1967a		
Suborder SPUMELLARIA Ehrenberg, 1875		
Family COLLOSPHAERIDAE Müller, 1858a		
Acrosphaera spinosa (Haeckel) *longispina*, new name	1	1,4
Acrosphaera spinosa (Haeckel) *coniculispina*, new name	1	2
Acrosphaera spinosa (Haeckel) *coronula*, new name	1	5

Acrosphaera murrayana (Haeckel)	1	3,6-11
Acrosphaera cyrtodon (Haeckel)	1	1,13
Acrosphaera spinosa (Haeckel) *lappacea* (Haeckel)	1	14,16
Clathrosphaera arachnoides Haeckel	1	15
Collosphaera tuberosa Haeckel	2	1-3
Collosphaera confossa n.sp.	2	4-5
Collosphaera armata Brandt	2	6-7,12
Collosphaera huxleyi Müller	2	8-11
Collosphaera macropora Popofsky	2	13-18
Collosphaera polygona Haeckel		
Disolenia collina (Haeckel)	3	1,5-7
Disolenia zanguebarica (Ehrenberg)	3	2-4,8-9
Disolenia quadrata (Ehrenberg)	5	1-5
Disolenia sp. A	5	6
Disolenia sp. B		
Otosphaera tenuissima (Hilmers)	3	11
Otosphaera polymorpha Haeckel	3	12,14-15
Otosphaera auriculata Haeckel	3	10,13
Siphonosphaera magnisphaera n.sp.	4	1,3
Siphonosphaera sp. A	4	2
Siphonosphaera martensi Brandt	4	4-5,7-8
Siphonosphaera sp. B	4	6
Siphonosphaera socialis Haeckel	4	9-12,15-16
Siphonosphaera sp. aff. *S. hippotis* (Haeckel)	4	13,14
Siphonosphaera polysiphonia Haeckel		
Family SPHAEROZOIDAE Haeckel, 1862, emend. Campbell, 1954		
Rhaphidozoum pandora Haeckel		
Family ETHMOSPHARIDAE Haeckel, 1862		
Plegmosphaera pachypila Haeckel	5	7-9
Plegmosphaera coelopila Haeckel	5	10
Plegmosphaera sp. aff. *P. lepticali* Renz	5	11
Plegmosphaera sp. A	5	14

	Plate	Figure
Plegmosphaera sp. B	6	1
Plegmosphaera entodictyon Haeckel	6	8,10-11
Plegmosphaera oblonga n.sp.	6	3
Plegmosphaera lepticali Renz		
Plegmosphaera pachyplegma Haeckel		
Styptosphaera spongiacea Haeckel	6	6-7,9
Styptosphaera sp. A	6	12-14
Styptosphaera sp. B	5	12
Styptosphaera sp. C	5	13
Thecosphaera capillacea Haeckel	6	2
Thecosphaera inermis (Haeckel)	11	9
Carposphaera sp. aff. *C. corypha* Haeckel	9	12
Family ACTINOMMIDAE Haeckel, 1862, emend. Riedel, 1971		
Subfamily ACTINOMMINAE Haeckel, 1862, emend. herein		
Centrocubus cladostylus Haeckel		
Centrocubus octostylus Haeckel	7	1
Spongosphaera polycantha Muller	7	2-3,5
Spongosphaera sp. aff. *S. helioides* Haeckel	7	4,7-8
Spongosphaera streptacantha Haeckel	7	6
Spongosphaera ? sp. B	7	9
Lynchnosphaera regina Haeckel	7	10
Actinomma acadophorum Haeckel	8	8-9,11
Actinomma capillaceum Haeckel	8	10
Actinomma sp.	13	11
Trilobatum ? *acuferum* Popofsky		
Acanthosphaera actinota (Haeckel)	8	1
Acanthosphaera tunis Haeckel	8	2,3
Acanthosphaera castanea Haeckel	8	4,5
Acanthosphaera simplex ? (Haeckel)	12	15
Heliosphaera radiata Popofsky		
Cladococcus viminalis Haeckel	8	6

	Plate	Figure
Cladococcus viminalis Haeckel	8	7
Cladococcus abietinus Haeckel	10	5
Cladococcus scoparius Haeckel	10	6-7
Cladococcus cervicornis Haeckel	10	8-10
Arachnosphaera sp.	7	12
Arachnosphaera myriacantha Haeckel	10	11-12
Leptosphaera minuta ? Popofsky	7	11
Leptosphaera sp. group		
Actinosphaera tenella (Haeckel)	9	1
Actinosphaera acanthophora (Popofsky)	9	2,3
Actinosphaera capillacea (Haeckel)	9	4,5
Haliomma ? sp.	8	12
Haliomma castanea Haeckel	9	7,11
Heliosoma spp. aff. radians Haeckel	9	6,8
Elatomma penicillus Haeckel	9	9-10
Elatomma pinetum Haeckel	10	1-4
Astrosphaera hexagonalis Haeckel	11	1-3
Drymosphaera dendrophora Haeckel	11	4
Sphaeropyle mespilus Dreyer	11	7-8
Cromyomma villosum Haeckel	11	10-11
Xiphosphaera gaea Haeckel	12	1,2
Xiphosphaera tesseractis Dreyer	12	3-5
Staurolonche sp. A group		
Staurolonche sp. B		
Stauracontium sp.	12	6
Hexastylus triaxonius Haeckel	12	7,8
Hexastylus sp.	12	9
Hexalonche sp. A	11	14,15
Hexalonche spp. B	12	10-11
Centrolonche hexalonche Popofsky		
Cetracontarium hexacontarium Popofsky		

	Plate	Figure
Hexacontium sp.	12	12
Hexacontium amphisiphon Haeckel	12	13-14
Hexacontium hostile Cleve	13	1-2
Hexacontium arachnoidale Hollande and Enjumet		
Hexacontium axotrias Haeckel	13	3
Hexacontium sp. aff. H. hostile Cleve	13	6
Hexacontium heracliti (Haeckel)	15	8-9
Hexacontium hystricina (Haeckel)	15	10
Hexacromyum elegans Haeckel	13	4-5,7
Heterosphaera sp. A	13	9-10
Heterosphaera sp. B	13	8
Cromyechinus sp. aff. C. borealis (Cleve)	13	13
Cromyechinus ? sp.	13	12
Cromyechinus borealis (Cleve)		
Stomatosphaera sp. A	13	14
Stomatosphaera sp. B	13	15
Stomatosphaera sp. C	13	16
Stylacontarium bispiculum Popofsky		
Stylosphaera ? sp. A	11	5-6
Stylosphaera melpomene Haeckel	14	1,2
Stylosphaera ? sp. B	14	5
Stylosphaera lithatractus Haeckel		
Druppatractus ostracion Haeckel group	14	3-4
Ellipsoxiphium palliatum Haecker	14	11-17
Amphisphaera group	14	6-7
Axoprunum stauraxonium Haeckel	14	8-10
Xiphatractus pluto (Haeckel)	15	1-3
Xiphatractus sp. A	15	4
Xiphatractus spp. B	15	6-7
Druppatractus ? sp.	15	5
Dorydruppa bensoni, new name	15	11-14

	Plate	Figure
Subfamily SATURNALINAE Deflandre, 1953		
Saturnalis circularis Haeckel	15	15-18
Family COCCODISCIDAE Haeckel, 1862, emend. Sanfilippo and Riedel, 1980		
Subfamily ARTISCINAE Haeckel, 1881, emend. Riedel, 1967		
Didymocyrtis tetrathalamus tetrathalamus (Haeckel)	21	2-14
Didymocyrtis tetrathalamus tetrathalamus (Haeckel) juvenile form	21	1
Didymocyrtis sp.	21	15
Spongoliva ellipsoides Popofsky	22	15-16
Family PORODISCIDAE Haeckel, 1881, emend. Petrushevskaya and Kozlova, 1972		
Euchitonia elegans (Ehrenberg)	16	1-6
Euchitonia cf. *furcata* Ehrenberg	16	8
Euchitonia sp.	16	9,11
Amphirhopalum ypsilon Haeckel	17	1-3
Amphirhopalum straussii Haeckel	17	4
Stylodictya validispina Jorgensen	19	11
Stylodictya ? sp.	19	12-13
Stylodictya multispina Haeckel	20	10,12
circodiscus spp. group	20	5-9
Stylochlamydium venustum (Bailey)	20	11
Stylochlamydium asteriscus Haeckel		
Porodiscus micromma (Harting)	20	13-14
Family SPONGODISCIDAE Haeckel, 1862, emend. Riedel, 1967a and Petrushevskaya and Kozlova, 1972		
Spongobrachium sp.		
Dictyocoryne profunda Ehrenberg	16	10,12-13,15
Dictycoryne truncatum (Ehrenberg)	16	14
Spongodiscus sp. A	16	7
Spongodiscus resurgens Ehrenberg	19	1
Spongodiscus spp. B group	19	2-3
Spongodiscus biconcavus Haeckel	19	4-6

	Plate	Figure
Spongotrochus sp. A	19	7
Spongotrochus sp. B		
Spongotrochus glacialis Popofsky	19	10
Stylospongia huxleyi Haeckel	19	8
Spongocore cylindrica (Haeckel)	17	6-9
Spongopyle setosa Dreyer	19	9
Spongopyle osculosa Dreyer	20	1-4
Spongasater tetras tetras Ehrenberg	17	10-11
Spongaster pentas Riedel and Sanfilippo	17	12-16
Family MYELASTRIDAE Riedel, 1971		
Myelastrum quadrifolium n.sp.	18	1-6
Myelastrum trinibrachium n.sp.	18	7-12
Family LARNACILLIDAE Haeckel, 1887, emend. Campbell, 1954		
Larnacalpis sp.	21	16-18
Family PHACODISCIDAE Haeckel, 1881, emend. Campbell, 1954		
Heliodiscus ? sp.	22	14
Heliodiscus asteriscus Haeckel	23	1-3
Heliodiscus echiniscus Haeckel	23	4-6
Family THOLONIIDAE Haeckel, 1887		
Tholoma metallasson Haeckel	11	12-13
Family PHYLONIIDAE Haeckel, 1881, emend. Campbell, 1954		
Hexapyle dodecantha Haeckel		
Hexapyle sp.	23	7
Octopyle stenozona Haeckel	23	8
Tetrapyle octacantha Muller	23	9-10
Family LITHELIIDAE Haeckel, 1862		
Larcopyle butschlii Dreyer	22	1-4
Larcopyle sp. A	22	5
Larcopyle sp. B	22	6
Discopyle elliptica Haeckel		
Tholospira cervicornis Haeckel group	22	7-9,12

	Plate	Figures
Tholospira dendrophora Haeckel	22	11
Tholospira ? sp.		
Lithelius minor ? Jorgensen	22	10
Larcospira quadrangula Haeckel	23	11-12
Suborder NASSELARIA Ehrenberg, 1875		
Family PLAGIACANTHIDAE Hertwig, 1879, emend. Petrushevskaya, 1971d		
Subfamily PLAGIACANTHINAE Hertwig, 1879, emend. Petrushevskaya, 1971d		
Tetraplecta pinigera Haeckel	24	1-5
Tetraplecta plectaniscus Haeckel	24	7
Tetraplecta corynephorum ? Jorgensen	24	6
Archiscenium quadrispinum ? Haeckel		
Plectanium sp.		
Protoscenium ? sp.		
Clathromitra pterophormis Haeckel	24	8
Cladoscenium ancoratum Haeckel	24	9-14
Semantis gracilis ? Popofsky	24	15-16
Deflandrella cladophora Jorgensen	24	17
Deflandrella sp.		
Talariscus pseudocuboides Popofsky	26	1
Gonosphaera primordialis	26	2
Phormacantha hystrix (Jorgensen)	26	3
Neosemantis distephanus Popofsky	27	12
Subfamily LOPHOPHAENINAE Haeckel, 1881, emend. Petrushevskaya, 1971d		
Acanthocorys cf. *variabilis* Popofsky	25	1
Lophophaena cylindrica (Cleve)	25	3-5
Lophophaena cf. *capito* Ehrenberg	25	6-9
Lophophaena decacantha (Haeckel) group	25	2,8,10
Lophopaena circumtexta (Popofsky)		
Helotholus histricosa Jorgensen		
Peromelissa phalacra Haeckel	25	11-15
Lithomelissa setosa Jorgensen	25	16-22

	Plate	Figures
Peridium spinipes Haeckel	26	4-6
Peridium sp.		
Trisulcus triacanthus Popofsky		
Subfamily SETHOPERINAE Haeckel, 1881, emend. Petrushevskaya, 1971d		
Lithopilium reticulatum Popofsky	26	10
Clathrocanium insectum (Haeckel)	26	7-9
Clathrocanium coarctatum Ehrenberg	26	11-13
Clathrocanium diadema Haeckel		
Callimitra emmae Haeckel	26	14
Callimitra annae Haeckel	26	15
Clathrocorys giltschii Haeckel	26	16
	27	1-3,9
Clathrocorys murrayi Haeckel	27	4-8
Callimitra solocicribrata n.sp.	27	10-11
Family ACANTHODESMIIDAE Haeckel, 1862, emend. Riedel, 1971		
Zygocircus capulosus Popofsky		
Zygocircus productus (Hertwig) group	27	13-14
Zygocircus cf. *piscicaudatus* Popofsky	27	18
Acanthodesmia vinculata (Muller)	28	6-8
Lophospyris juvenile form group	28	1-4
Lophospyris pentagona quadriforis (Haeckel), emend. Goll	28	5
Lophospyris pentagona pentagona (Ehrenberg) emend Goll		28
9-14		
Lophospyris pentagona hyperborea (Jorgensen), emend. Goll	29	1-3,5-10
Lophospyris cheni Goll	29	4
Tripodospyris sp.		
Phormospyris stabilis scaphipes (Haeckel)	29	11-12,14
Phormospyris sp. aff. *L. pentagona hyperborea* (Jorgensen)	29	13

	Plate	Figures
Phormospyris stabilis capoi Goll	29	15-18
Phormospyris stabilis stabilis (Goll)	30	2-5
Phormospyris ? sp.	30	6
Dictyospyris sp. group	30	1
Nephrospyris renilla renilla Haeckel	30	7-9
Nephrospyris renilla lana Goll	30	10
Androspyris reticulidisca n.sp.	30	12-14
Androspyris huxleyi (Haeckel)	30	15-16
Androspyris ramosa (Haeckel)	31	1-2
Cephalospyris cancellata Haeckel	31	3-4
Cantharospyris platybursa Haeckel	31	5
Cantharospyris cf. *clathrobursa* (Haeckel)		
Tholospyris sp. group	27	15-17
Tholospyris baconiana baconiana (Haeckel)	31	6-7
Tholospyris baconiana variabilis Goll	31	8
Tholospyris macropora (Popofsky)	31	9
Liriospyris sp.	30	11
Liriospyris thorax (Haeckel) *laticapsa*, n.subsp.	31	10-11,13
Liriospyris thorax thorax (Haeckel)	31	12
Liriospyris reticulata (Ehrenberg)	31	14-16
Family SETHOPHORMIDIDAE Haeckel, 1881, emend. Petrushevskaya, 1971d		
Tetraphormis rotula (Haeckel)	32	1-3
Tetraphormis dodecaster (Haeckel)	32	7
Tetraphormis butschlii (Haeckel)	32	6
Theophormis callipilium Haeckel	32	9-12
Lampromitra schultzei (Haeckel)	32	4-5
Lamptomitra cracenta n.sp.	32	8
Lampromitra cachoni Petrushevskaya	33	2-3
Lampromitra spinosiretis n.sp.	34	1-2,7
Eucecryphalus sp.	33	1
Eucecryphalus tricostatus (Haeckel)	33	4,6

	Plate	Figures
Eucecryphalus sestrodiscos (Haeckel)	33	5,7-8
Eucecryphalus gegenbauri Haeckel	33	13-15
Eucecryphalus europae (Haeckel)	34	5-6
Eucecryphalus clinatus n.sp.	35	1-2
Corocalyptra cervus (Ehrenberg)	33	9-12
Phrenocodon clathrostomium Haeckel	34	3-4
Clathrocyclas sp.	34	8
Clathrocyclas monumentum (Haeckel)	34	9-11
Clathrocyclas cassiopejae Haeckel	34	12-14
Family THEOPERIDAE Haeckel, 1881, emend. Riedel, 1967a		
Subfamily PLECTOPYRAMIDINAE Haecker, 1908a, emend. Petrushevskaya, 1971d		
Cornutella profunda Ehrenberg	35	3-9
Peripyramis circumtexta Haeckel	35	10-13
Litharachnium tentorium Haeckel	35	14-18
Litharachnium eupilium (Haeckel)	36	1-4
Subfamily EUCYRTIDIINAE Ehrenberg, 1847b, emend. Petrushevskaya, 1971d		
Archipilium sp. aff. *A. orthopterum* Haeckel	36	5,7
Archipilium macropus ? (Haeckel)	36	6
Pteroscenium pinnatum Haeckel	36	8-9
Pterocanium trilobum (Haeckel)	36	10-11
Pterocanium grandiporus Nigrini	36	12-13
Pterocanium praetextum praetextum (Ehrenberg)	36	15-18
Pterocanium praetextum (Ehrenberg)aff.*eucolpum* Haeckel	36	14
Dictyophimus sp. A	37	1
Dictyophimus crisiae Ehrenberg	37	2
Dictyophimus infabricatus Nigrini	37	3-5
Dictyophimus macropterus (Ehrenberg)	39	8-11
Dictyophimus sp. B	39	12
Pseudodictyophimus gracilipes (Bailey)	37	12-14
Dictyocodon elegans (Haeckel)	37	6-7,9
Dictyocodon palladius Haeckel	37	8,10-11

	Plate	Figures
Conicavus tipiopsis n.sp.	38	1-6
Sethoconus myxobrachia Strelkov and Reshetnyak	38	7-8
Conarachnium polaycanthum (Popofsky)	39	1-4
Conarachnium parabolicum (Popofsky)	39	5-6
Conarachnium facetum (Haeckel)	39	7
Stichopilium bicorne Haeckel	39	13-19
Lithopera bacca Ehrenberg	40	1-2
Cyrtopera languncula Haeckel	40	3-6
Cyrtopera aglaolampa n.sp.	40	7-8
Stichophormis cf. *cornutella* Haeckel		
Lophocorys undulata (Popofsky)	40	9-10
Theocorys veneris Haeckel	40	11-14
Theocorythium trachelium trachelium (Ehrenberg)	40	15-16
Lipmanella dictyoceras (Haeckel)	40	17
Lipmanella pyramidale (Popofsky)	40	18
Lipmanella virchowii (Haeckel)	40	19-21
Lithostrobus hexagonalis Haeckel	41	1-3
Theocalyptra bicornis (Popofsky)	41	4-6,8-11
Theocalyptra davisiana davisiana (Ehrenberg)	41	7
Theocalyptra davisiana cornutoides (Petrushevskaya)	41	12-16
Family PTEROCORYTHIDAE Haeckel, 1881, emend. Riedel, 1967a		
Tetracorethra tetracorethra (Haeckel)	41	17-18
Pterocorys zancleus (Müller)	42	1-4
Pterocorys campanula Haeckel	42	5-8
Pterocorys sp.		
Eucyrtidium spp. A group	38	11-13
Eucyrtidium acuminatum (Ehrenberg)	42	9-10,16-17,20
Eucyrtidium hexagonatum Haeckel	42	18-19
Eucyrtidium anomalum Haeckel	42	11-14
Eucyrtidium sp. aff. *E. anomalum* (Haeckel)	42	15
Eucyrtidium dictyopodium (Haeckel)	42	21

	Plate	Figures
Eucyrtidium hexastichum (Haeckel)	42	22
Anthocyrtidium zanguebaricum (Ehrenberg)	41	19-22
Anthrocyrtidium ophirense (Ehrenberg)	43	1-7
Lamprocyclas maritalis polypora Nigrini	43	12, 15
Lamprocyclas maritalis maritalis Haeckel	43	8-11,13-14
Lamprocyclas ? *hannai* (Campbell and Clark)		
Lamprocyrtis sp.	43	16
Lamprocyrtis nigriniae (Caulet)	43	17-19
Family ARTOSTROBIIDAE Riedel, 1967b, emend. Foreman, 1973		
Spirocyrtis scalaris Haeckel	44	1-2
Spirocyrtis subscalaris Nigrini	44	3-6
Spirocyrtis sp. aff. *S. seriata* Jørgensen and *S. subscalaris* Nigrini		
Spirocyrtis ? *platycephala* (Ehrenberg) group	44	7-8
Artostrobus annulatus (Bailey)	38	9-10
Botryostrobus aquilonaris (Bailey)	44	9-13
Phormostichoartus corbula (Harting)	44	14-16
Siphocampe nodosaria (Haeckel)		
Siphocampe lineata (Ehrenberg)	44	17-20
Siphocampe arachnea (Ehrenberg)	44	21-23
Artobotrys borealis (Cleve)	44	24
	45	1-3
Family CARPOCANIIDAE Haeckel, 1881, emend. Riedel, 1967b		
Carpocanistrum flosculum Haeckel	45	4,6-7
Carpocanistrum cephalum Haeckel	46	5,12
Carpocanistrum favosum (Haeckel)	45	8
Carpocanistrum coronatum (Ehrenberg)	45	10
Carpocanistrum sp.	45	11
Carpocanistrum acutidentatum n.sp.	45	9,13-15
Carpocanarium papillosum (Ehrenberg)	45	16-17

	Plate	Figures
Family CANNOBOTRYIDAE Haeckel, 1881, emend. Riedel, 1967a		
Acrobotrys teralans Renz	45	18-19
Acrobotrys tessarolobon n.sp.	45	20
Acrobotrys chelinobotrys n.sp.	45	22-24
Acrobotrys sp. C		
Saccospyris preantarctica Petrushevskaya	45	21
Centrobotrys thermophila Petrushevskaya	46	1-2
Neobotrys quadrituberosa Popofsky	46	3
Botryocyrtis sp. A	46	4-6
Botryocyrtis scutum (Harting)	46	6-7
Botryocyrtis elongatum n.sp.	46	8-9
Family ARCHIPHORMIDIDAE Haeckel, 1881		
Arachnocalpis ? sp. A	46	10
Arachnocalpis sp. B	46	11
Arachnocalpis?*ovatiretalis* n.sp.	46	12-14
Arachnocalpis ? sp. C	46	16
Arachnocalpis ellipsoides Haeckel	46	17
Order TRIPYLEA Hertwig, 1879		
Suborder PHAEODARIA Haeckel, 1879		
Family CHALLENGERIIDAE Murray, 1876, emend. herein		
Challengeron willemoesii Haeckel	47	1-14
Challengeron lingi n. sp.	48	1-5
Challengeron radians Borgert	48	6
Challengeron tizardi (Murray)	48	13-16
Challengerosium balfouri (Murray)	48	7-10
Challengerosium avicularia Haecker	49	1-13
Challengeranium diodon (Haeckel)	52	11-16
Protocystis sp. A	49	14-15
Protocystis harstoni (Murray)		
Protocystis honjoi n. sp.	50	1-2

	Plate	Figure
Protocystis tridentata Borgert	50	3
Protocystis auriculata n. sp.	50	4-7
Protocystis aduncicuspis n. sp.	50	8-10
Protocystis sp. B	50	11
Protocystis sloggetti (Haeckel)	50	12-15
Protocystis murrayi (Haeckel)	50	16-18
	51	1-3
Protocystis sp. C	51	4
Protocystis thomsoni (Murray)	51	5
Protocystis xiphodon (Haeckel)	52	1-3
Protocystis tritonis (Haeckel)	52	4-5
Protocystis naresi (Murray)	52	6-8
Pharyngella gastrula Haeckel	51	6-14
Entocannula infundibulum Haeckel	52	9,10
Family MEDUSETTIDAE Haeckel, 1887, emend. herein		
Euphysetta elegans Borgert	53	1-10
Euphysetta staurocodon Haeckel	53	11-14
Euphysetta pusilla Cleve	53	15
Euphysetta lucani Borgert	54	10-12
Medusetta ansata Borgert	54	1-7
Medusetta inflata Borgert		
Medusetta sp. A	54	8-9
Medusetta sp. B	63	12-13
Family LIRELLIDAE Ehrenberg, 1872c		
Borgertella caudata (Wallich)	54	13-17
	55	1-6
Lirella baileyi Ehrenberg	55	7
Lirella bullata (Stadum and Ling)	55	8-11
Lirella melo (Cleve)	55	12-18
	56	1-8

	Plate	Figure
Lirella tortuosa n.sp.	55	19-20
	56	9-11
Family POROSPATHIDIDAE Borgert, 1901a, emend. Campbell, 1954		
Porospathis holostoma (Cleve)	57	1-8
Family CASTANELLIDAE Haeckel, 1879		
Castanidium longispinum Haecker	57	9-13
	58	1-4
Castanidium abundiplanatum n. sp.	58	5-8
Castanidium sp.	58	10
Castanissa circumvallata Schmidt	58	9
Castanella aculeata Schmidt	58	11,13
	59	1
Castanella macropora (Borgert)	58	12
Castanella sloggetti Haeckel	59	2
Castanella balfouri Haeckel	58	3
Family CIRCOPORIDAE Haeckel, 1879		
Haeckeliana porcellana Haeckel	59	4-13
Circoporus sexfuscinus Haeckel	60	1,3,5
Circoporus oxyacanthus Borgert	60	2,4,6-13
Circogonia sp.	20	9-10
Family CONCHARIIDAE Haeckel, 1879		
Conchellium capsula Borgert	61	1-5,7-8,10
Conchellium tridacna Haeckel	61	6,9,11
Conchophacus diatomeus (Haeckel)	61	12
Conchidium argiope Haeckel	62	1-2
Conchidium caudatum (Haeckel)	62	3-8
Conchopsis compressa Haeckel	62	9-16
Family AULOSPHAERIDAE Haeckel, 1862		
Aularia ternaria Haeckel	63	1-2

Family AULACANTHIDAE Haeckel, 1862

Aulographis stellata Haeckel	63	3
Aulographis tetrancistra Haeckel	63	10
Auloceros spathillaster Haeckel	63	4
Auloceros arborescens Haeckel *birameus* (Immermann)	63	9
Aulographonium bicorne Haecker	63	5-6
Aulospaphis taumorpha ? Haeckel	63	7-8
Aulospathis variabilis Haeckel *bifurca* Haecker	63	11

SYSTEMATICS

Kingdom PROTISTA Haeckel, 1866
Phylum SARCODINA Hertwig and Lesser, 1874
Class ACTINOPODA Calkins, 1909
Subclass RADIOLARIA Müller, 1858a
Order POLYCYSTINA Ehrenberg, 1838, emend. Riedel, 1967a
Suborder SPUMELLARIA Ehrenberg, 1875
Family COLLOSPHAERIDAE Müller, 1858a

Definition: Colonial spumellarians with lattice-shells (and one genus with no skeletal elements) (Riedel, 1971).

Genus ACROSPHAERA Haeckel, 1881

Acrosphaera spinosa (Haeckel) *longispina*, new name
Plate 1, figures 1,4

Acrosphaera spinosa (Haeckel). - POPOFSKY, 1917, p. 253, text-fig. 16 (partim). - STRELKOV and RESHETNYAK, 1971, p. 340, pl. 6, figs. 39, 41 (partim)

Polysolenia flammabunda (Haeckel). - NIGRINI, 1967, p. 15, pl. 1, fig. 2; NIGRINI and MOORE, 1979, p. S13, pl. 2, fig. 2

Acrosphaera flammabunda (Haeckel). - JOHNSON and NIGRINI, 1980, p. 116, pl. 1, fig. 1, text-fig. 3a

Description: Shell smooth, polyhedron shape, with long radiated spines of up to 1/3 of shell diameter whose bases are elevated, with numerous circular to subcircular small pores of slightly variable size, with fewer number of large pores of about 3-5 times of the small pore diameter. Number of spines is one on the small pore margin and up to several (and occasionally forming coronas) on the large pore margin.

Remarks: Main differences of the present taxon from A. spinosa coniculispira and A. spinosa coronula are length and shape of spines and number of spines on the large pore margin. The author's concept of this subspecies is similar to that of Nigrini (1967) except elimination of forms close to Choenicosphaera flammabunda Haeckel. A view of Popofsky (1917) and Strelkov and Reshetnyak (1971) is lumping all of these three taxa together. On the contrary, Nigrini (e.g. 1967) and her co-workers' view is that they split A. spinosa longispina from A. spinosa coniculispina but lump A. spinosa longispina and A. spinosa coronula together. It is important to note that both Popofsky (1917) and Strelkov and Reshetnyak (1971) describe different forms from one colony (not necessarily in all of the present groups in question though). Such a kind of observation of the colony is the key to improving the taxonomy of colonial Radiolaria. Thus, the four forms presented here may well be the identical taxon in the true biological sense in which case splitting into several subspecies is invalid. However, until further satisfactory information on the colonies of these groups is obtained, the author proposes to classify them into four different subspecies.

Derivation of name: The latin meaning long thorn.

Acrosphaera spinosa (Haeckel) coniculispina, new name
Plate 1, figure 2

Collosphaera spinosa HAECKEL, 1860b, p. 845; 1862, p. 536, pl. 34, figs. 12,13

Acrosphaera spinosa (Haeckel). - BRANDT, 1885, p. 263, pl. 2, fig. 4. - HAECKEL, 1887, p. 100. - STRELKOV and RESHETNYAK, 1971, p. 340, pl. 5, figs. 33-38, pl. 6, figs. 40,43 (partim). - JOHNSON and NIGRINI, 1980, p. 119, pl. 1, fig. 3. - BOLTOVSKOY and RIEDEL, 1980, p. 144, pl. 1, fig. 6. - TAKAHASHI and HONJO, 1981, p. 144, pl. 1, fig. 6

Polysolenia spinosa (Haeckel). - NIGRINI, 1967, p. 14, pl. 1, fig. 1. - NIGRINI and MOORE, 1979, p. S19, pl. 2, fig. 5

Remarks: This form is the major component of the present species counts at all the three Stations.

Derivation of name: The name of this species is the Latin meaning conical thorn.

Acrosphaera spinosa (Haeckel) coronula, new name
Plate 1, figure 5

Choenicosphaera flammabunda HAECKEL, 1887, p. 103, pl. 8, fig. 5

Acrosphaera spinosa (Haeckel). - POPOFSKY, 1917, p. 254, text-figs. 14, 15 (partim). - STRELKOV and RESHETNYAK, 1971, p. 340, pl. 8, fig. 59 (partim)

Remarks: Although this taxon is morphologically very different from A. spinosa longispina and A. spinosa coronula, all of these taxa may well be identical taxon which depends on further investigations. This taxon is rare at all the three Stations.

Derivation of name: This subspecies name is a diminutive of the Latin corona meaning crown.

Acrosphaera spinosa (Haeckel) lappacea (Haeckel)
Plate 1, figures 14, 16

Xanthiosphaera lappacea HAECKEL, 1887, p. 120, pl. 8, figs. 10,11

Polysolenia lappacea (Haeckel). - NIGRINI, 1967, p. 16, pl. 1, figs. 3a,b. - NIGRINI and MOORE, 1979, p. S15, pl. 2, figs. 3a,b

Acrosphaera lappacea (Haeckel). - JOHNSON and NIGRINI, 1980, p. 119, pl. 1, fig. 2

Remarks: This taxon is very rare at all three Stations and it did not appear in any of the counting slides.

Acrosphaera murrayana (Haeckel)
Plate 1, figures 3, 6-11

Choenicosphaera murrayana HAECKEL, 1887, p. 102, pl. 8, fig. 4. - BENSON, 1966, p. 120, pl. 2, fig. 3

Trypanosphaera brachysiphon CLEVE, 1900b, p. 13, pl. 6, fig. 3

Polysolenia murrayana (Haeckel). - NIGRINI, 1968, p. 52, pl. 1, fig. 1a-b

Acrosphaera murrayana (Haeckel). - POPOFSKY, 1917, p. 259, text-figs. 22,23. - STRELKOV and RESHETNYAK, 1971, p. 347, text-fig. 25

Remarks: This species is very abundant at the Panama Basin station. Shell diameter is 176 ± 18 µm (2 S.D.) (126 specimens), and its weight is 0.46 ± 0.01 µg (207 specimens). Specimens of two shells splitting apart have been occasionally observed (Pl. 1, figs. 3, 9-10). An SEM view of this species' skeletal cross section (Pl. 1, fig. 11), typical of polycystine skeletons, shows solid silica in contrast to those of porous Phaeodaria (Pls. 47-63).

Acrosphaera cyrtodon (Haeckel)
Plate 1, figures 12-13

Odontosphaera cyrtodon HAECKEL, 1887, p. 102, pl. 5, fig. 6

Acrosphaera cyrtodon (Haeckel). - STRELKOV and RESHETNYAK, 1971, p. 344, pl. 7, fig. 51, pl. 8, fig. 54, text-fig. 24

See Strelkov and Reshetnyak (1971) for a more complete synonymy.

Genus CLATHROSPHAERA Haeckel, 1881

Clathrosphaera arachnoides Haeckel
Plate 1, figure 15

Clathrosphaera arachnoides HAECKEL, 1887, p. 119, pl. 8, fig. 7

Description: Shell elliptical with many elevated cones, numerous straight strands connecting among the cones forming triangular to polygonal geometric network of outer sphere, pores of numerous small subcircular and a few large quadrilateral shape.

Genus COLLOSPHAERA Muller, 1855

Collosphaera tuberosa Haeckel
Plate 2, figures 1-3

Collosphaera tuberosa HAECKEL, 1887, p. 97. - STRELKOV and RESHETNYAK, 1971, p. 336, pl. 4, figs. 24, 25, text-fig. 22. - NIGRINI, 1970, p. 166, pl. 1, fig. 1, text-fig. 2; 1971, p. 445, pl. 34.1, fig. 1. - NIGRINI and MOORE, 1979, p. S1, pl. 1, fig. 1. - JOHNSON and NIGRINI, 1980, p. 119, pl. 1, fig. 8. - BOLTOVSKOY and RIEDEL, 1980, p. 104, pl. 1, fig. 7. - TAKAHASHI and HONJO, 1981, p. 144, pl. 1, fig. 2. See Strelkov and Reshetnyak (1971) and Nigrini (1971) for more complete synonymies.

Collosphaera confossa n.sp.
Plate 2, figures 4-5

Description: Shell single lattice, thin-walled, smooth, spherical to slightly crumpled, with numerous circular to subcircular pores of variable size. Width of the interporous septa is about same as average pore diameter. Number of pores is about 23 on the half perimeter of the shell and twice as many as that of *C. huxleyi*.

Dimension: Shell diameter: 125-225 µm

Type locality: 15°21.1'N, 151°28.5'W, sediment trap 5582 m. Collected during July-November 1978.

Remarks: This taxon is different from *C. huxleyi* in shell diameter variability, number and size of pores.

Derivation of name: The name of this species is the Latin meaning full of holes.

Collosphaera armata Brandt
Plate 2, figures 6-7, 12

Collosphaera armata BRANDT, 1905, p. 331, pl. 10, figs. 17,18. - POPOFSKY, 1917, p. 246, pl. 14, fig. 1. - STRELKOV and RESHETNYAK, 1971, p. 337, text-fig. 23

Collosphaeraera huxleyi Müller
Plate 2, figures 8-11

Thalassicola punctata HUXLEY, 1851, p. 434, pl. 14, fig. 6 (partim)

Collosphaera huxleyi MÜLLER, 1855, p. 238; 1858a, p. 55, pl. 8, figs. 6-9. - POPOFSKY, 1917, p. 241, text-figs. 2,3, pl. 13, figs. 1-9. - STRELKOV and RESHETNYAK, 1971, p. 332, pl. 4, figs. 21,23, text-figs. 19-21. - BOLTOVOSKOY and RIEDEL, 1980, p. 103, pl. 1, fig. 5. See Strelkov and Reshetnyak (1971) and Boltovskoy and Riedel (1980) for more synonymies.

Collosphaera macropora Popofsky
Plate 2, figures 13-18

Without a name. - HILMERS, 1906, pl., fig. 3

Collosphaera macropora POPOFSKY, 1917, p. 247, text-figs. 5,6, pl. 14, fig. 2a-c. - STRELKOV and RESHETNYAK, 1971, p. 337, pl. 4, figs. 30, 31. - BOLTOVSKOY and RIEDEL, 1980, p. 103, pl. 1, fig. 6

Collosphaera polygona Haeckel

? *Collosphaera huxleyi* Müller. - HAECKEL, 1862, pl. 34, fig. 5

Collosphaera polygona HAECKEL, 1887, p. 96, pl. 5, fig. 13. - STRELKOV and RESHETNYAK, 1971, p. 338, pl. 4, figs. 26,27. - TAKAHASHI and HONJO, 1981, p. 144, pl. 1, fig. 3

Genus DISOLENIA Ehrenberg, 1860a

Disolenia collina (Haeckel)
Plate 3, figures 1, 5-7

Acrosphaera collina HAECKEL, 1887, p. 101, pl. 8, fig. 2. - BRANDT, 1905, p. 334-335, pl. 9, figs. 14-15, pl. 10, figs. 32,33.

Solenosphaera collina (Haeckel) - HILMERS, 1906, p. 41-44. - POPOFSKY, 1917, p. 250, pl. 14, fig. 3, text-fig. 10. - STRELKOV and RESHETNYAK, 1971, p. 362, pl. 8, fig. 52

Disolenia zanguebarica (Ehrenberg)
Plate 3, figures 2-4, 8-9

Trisolenia zanguebarica EHRENBERG, 1872a, p. 321; 1872b, p. 149, pl. 10, fig. 11

Solenosphaera zanguebarica (Ehrenberg). - BRANDT, 1905, p. 330, pl. 10, figs. 28-31. - POPOFSKY, 1917, p. 249, text-fig. 9. - STRELKOV and RESHETNYAK, 1971, p. 360, pl. 10, figs. 74-76

Disolenia zanguebarica (Ehrenberg). - NIGRINI, 1967, p. 20, pl. 1, fig. 6. - RENZ, 1976, p. 87, pl. 1, fig. 2. - NIGRINI and MOORE, 1979, p. S5, pl. 1, fig. 3. - JOHNSON and NIGRINI, 1980, p. 119, pl. 1, fig. 10. - BOLTOVSKOY and RIEDEL, 1980, p. 105, pl. 1, fig. 11. - TAKAHASHI and HONJO, 1981, p. 145, pl. 1, fig. 11

Disolenia quadrata (Ehrenberg)
Plate 5, figures 1-5

Tetrasolenia quadrata EHRENBERG, 1972a, p. 320; 1872b, p. 301, pl. 10, fig. 20

Solenosphaera variabilis HAECKEL, 1887, p. 113. - ? RIEDEL, 1953, p. 808, pl. 84, fig. 8

Solenosphaera pandora HAECKEL, 1887, p. 113, pl. 7, figs. 10,11. - STRELKOV and RESHETNYAK, 1971, pl. 362, pl. 10, figs. 77,78

Disolenia quadrata (Ehrenberg). - NIGRINI, 1967, p. 19, pl. 1, fig. 5. - NIGRINI and MOORE, 1979, p. S3, pl. 1, fig. 2. - JOHNSON and NIGRINI, 1980, p. 119, pl. 1, fig. 9

Disolenia cf. *variabilis* (Haeckel). - BENSON, 1966, p. 123, pl. 2, fig. 5

Remarks: Bjørklund and Goll (1979, p. 1321, pl. 5, figs. 1-21) described a similar taxon to this species, *Trisolenia megalactis megalactis* Ehrenberg. The author regards it as a different taxon from the present species because of distinct morphological differences of tubules and pore size of the shells. See the synonymy of *O. polymorpha* below.

Disolenia sp. A
Plate 5, figure 6

Description: Shell small with three large tubules of cylindrical shape and obliquely truncated. The shell is part of the three connecting tubules and has subcircular pores of finer than interporous septa. Pore size significantly increases (up to more than five times of the width of interporous septa) and become polygonal toward the terminal end of the tubules.

Dimentions of the illustrated specimen: length of long axis: 150 μm; diameter of tubules: 30 μm.

Remarks: This species occurs rarely at the three Stations.

Disolenia sp. B

Disolenia sp. - TAKAHASHI and HONJO, 1981, p. 145, pl. 1, fig. 10

Genus OTOSPHAERA Haeckel, 1887, emend. Nigrini, 1967

Otosphaera tenuissima (Hilmers)
Plate 3, figure 11

Solenosphaera tenuissima HILMERS, 1906, p. 48, pl., fig. 2. - POPOFSKY, 1917, p. 252, text-fig. 13

Otosphaera polymorpha Haeckel
Plate 3, figures 12, 14-15

Otosphaera polymorpha HAECKEL, 1887, p. 116, pl. 7, fig. 6. - NIGRINI, 1967, p. 23, pl. 1, fig. 8. - NIGRINI and MOORE, 1979, p. 59, pl. 1, fig. 5. - TAKAHASHI and HONJO, 1981, p. 146, pl. 1, fig. 12

? *Trisolenia megalactis megalactis* Eherenberg. - BJØRKLUND and GOLL, 1979, p. 1321, pl. 5, figs. 1-21.

Otosphaera auriculata Haeckel
Plate 3, figures 10, 13

Otosphaera auriculata HAECKEL, 1887, p. 116, pl. 7, fig. 5. - NIGRINI, 1967, p. 22, pl. 1, fig. 7. - NIGRINI and MOORE, 1979, p. S7, pl. 1, fig. 4. - JOHNSON and NIGRINI, 1980, p. 119, pl. 1, fig. 11

Solenosphaera chierchiae BRANDT, 1905, p. 346, pl. 10, fig. 27. - STRELKOV and RESHETNYAK, 1971, p. 363, pl. 8, figs. 55,56

Genus SIPHONOSPHAERA Muller, 1858a

Siphonosphaera magnisphaera n. sp.
Plate 4, figures 1,3

Description: Shell large, spherical, with numerous subcircular to polygonal small pores and 10-17 large polygonal pores of 1/4-1/2 length of the shell diameter. Number of the small and large pores are ca. 30-40 and 2-4 respectively on the half meridian. The large pores form very short tubules.

Dimensions: Shell diameter: 175-220 μm (6 specimens); large pore diameter: 12-65 μm (6 specimens)

Type locality: 15°21.1'N, 151°28.5'W. Sediment trap 378 m. Collected during July-November 1978.

Remarks: This species has relatively large shell among *Collosphaeridae* and is different from *Siphonosphaera* sp. A (Pl. 4, fig. 2) in shell size and number and shape of small and large pores.

Derivation of name: The name of this species is the Latin meaning having the nature of a large sphere.

Siphonosphaera sp. A
Plate 4, figure 2

Description: Shell small and smooth, spherical, with small and large circular to subcircular pores. Interporous septa is wider than large pore diameter. The small pores are much less abundant than those of *S. brachyporosa* and regularly distributed over the shell wall. The large pores form very short tubules of ca. 1/7 of the pore diameter.

Siphonosphaera martensi Brandt
Plate 4, figures 4-5, 7-8

Siphonosphaera martensi BRANDT, 1905, p. 339, pl. 9, figs. 9-12. - HILMERS, 1906, p. 80. - STRELKOV and RESHETNYAK, 1971, p. 356, fig. 28. - BOLTOVSKOY and RIEDEL, 1980, p. 104, pl. 1, fig. 8. - TAKAHASHI and HONJO, 1981, p. 145, pl. 1, fig. 9

Siphonosphaera tenera ? Brandt. - POPOFSKY, 1917, p. 262, text-fig. 27 (partim)

Remarks: The present taxon has pores of variable size which tend to protrude outward and some of the large ones form short straight or conical tubules. Many of the pores are much smaller than width of the interporous septa. Thus, the present taxon is different from *S. macropora* Strelkov and Reshetnyak (1971, p. 357, text-fig. 29).

Siphonosphaera sp. B
Plate 4, figure 6

Description: Shell spherical, with many large pores of about equal width as interporous septa and fewer small pores of ca. 1/3 of the large pore diameter. There are usually 4-6 large and 1-3 small pores in half meridian. The rims of the large pores are elevated and forming short tubules of ca. 1/4 length of the pore diameter.

Remarks: This species is different from *S. partinaria* and *S. cyathina* both described by Haeckel (1887) in height and shape (and size and number for the latter) of the tubules.

Siphonosphaera socialis Haeckel
Plate 4, figures 9-12, 15-16

Siphonosphaera socialis HAECKEL, 1887, p. 106, pl. 6, figs. 1-2. - HILMERS, 1906, p. 74. - POPOFSKY, 1917, p. 264, pl. 16, figs. 1-11, pl. 17, figs. 1-6, text-fig. 29. - STRELKOV and RESHETNYAK, 1971, p. 353, pl. 8, fig. 60, pl. 9, fig. 72, text-fig. 27

Remarks: Specimens shown by Popofsky (1917) and Strelkov and Reshetnyak (1971) are the closest to the ones presented here. Haeckel's specimens of original *S. socialis* have larger pores than those shown by other workers. *S.* cf. *socialis* shown by Benson (1966: p. 121, pl. 2, fig. 4) is similar to the present taxon. *S. socialis* is prefered to *S. polysiphonia* because (1) specimens observed here do not have as many prolonged tubules of original *S. polysiphonia* Haeckel (as pointed also illustrated by Boltovskoy and Riedel, 1980); and (2) There are well illustrated descriptions of this taxon under *S. socialis* in the above synonymy. All of the specimens of this species observed under SEM have small numerous rectangular prisms or cubic crystals on the shell surface (e.g. pl. 4, fig. 16). This is common to many collosphaerids but never been observed on any other families under the identical desalting procedure. Thus this may be due to the difference in skeletal nature from other groups.

Siphonosphaera polysiphonia HAECKEL, 1887, p. 106. - NIGRINI, 1967, p. 18, pl. 1, figs. 4a, 4b. - RENZ, 1976, p. 89, pl. 1, fig. 7. - NIGRINI and MOORE, 1979, p. S21, pl. 1, figs. 6a,b. - JOHNSON and

NIGRINI, 1980, p. 119. - BOLTOVSKOY and RIEDEL, 1980, p. 104, pl. 1, fig. 9. - TAKAHASHI and HONJO, 1981, p. 145, pl. 1, fig. 8. See Boltovskoy and Riedel (1980) for an additional synonymy.

Siphonosphaera sp. aff. *S. hippotis* (Haeckel)
Plate 4, figures 13-14

Siphonosphaera sp. aff. *S. hippotis* (Haeckel). - RENZ, 1976, p. 89, pl. 1, fig. 1

Description: Shell smooth and thick, spherical, with 5-10 tubules of 1/6 to 1/4 length of shell diameter, pores of much smaller and more abundant than those of *S. socialis*.

Remarks: The present taxon is identical to that shown by Renz (1976).

Family SPHAEROZOIDAE Haeckel, 1862, emend. Campbell, 1954

Definition: Growth exclusively colonial (Campbell, 1954).

Genus RHAPHIDOZOUM Haeckel, 1862

Rhaphidozoum pandora Haeckel

Rhaphidozoum pandora HAECKEL, 1887, p. 49, pl. 4, fig. 6. - TAKAHASHI and HONJO, 1981, p. 144, pl. 1, fig. 1

Family ETHMOSPHAERIDAE Haeckel, 1862

Definition: Without spines on shell surface (Campbell, 1954).

Remarks: Widely used name Liosphaeridae for this family is invalid. See Loeblick and Tappan (1961).

Genus PLEGMOSPHAERA Haeckel, 1881

Plegmosphaera pachypila Haeckel
Plate 5, figures 7-9

Plegmosphaera pachypila HAECKEL, 1887, p. 88

Styptosphaera sp. - TAKAHASHI and HONJO, 1981, p. 146, pl. 1, fig. 13

Plegmosphaera coelopila Haeckel
Plate 5, figure 10

Plegmosphaera coelopila HAECKEL, 1887, p. 88

Plegmosphaera sp. aff. P. lepticali Renz
Plate 5, figure 11

Plegmosphaera lepticali RENZ, 1976, p. 115, pl. 1, fig. 14.

Description: Shell ovate, smooth, with single layer of spongy meshwork.

Plegmosphaera sp. A
Plate 5, figure 14

Description: Shell ovate, surface smooth and hollow with irregular spongy meshwork. Thickness of the spongy layer is ca. half radius of the cavity. Radii of axes ratio 1:2.2.

Plegmosphaera sp. B
Plate 6, figure 1

Description: Shell, large, smooth and spherical with single layer of fine spongy meshwork.

Plegmosphaera entodictyon Haeckel
Plate 6, figures 8, 10-11

Plegmosphaera entodictyon HAECKEL, 1887, p. 88. - HOLLANDE and ENJUMET, 1960, p. 103, pl. 48, fig. 1. - BOLTOVSKOY and RIEDEL, 1980, p. 106, pl. 1, fig. 16

? Styptosphaera spongiacea Haeckel. - RENZ, 1976, p. 116, pl. 1, fig. 13

Remarks: A specimen shown in Pl. 6, fig. 8 has inside shell wall closed by a less dense lattice than those of figs. 10-11.

Plegmosphaera oblonga n.sp.
Plate 6, figure 3

Description: Elongate hollow shell made of irregular polygonal spongy meshwork, without spines and with two large circular openings of different sizes on two opposite lateral sides. Either anterior or posterior half is slightly thicker in diameter than the other.

Dimensions: (3 specimens) Shell length: 220-580 μm; width: 70-220 μm; radii of axes ratio: 1:2.6-3.0; diameter of lateral openings: 10-60 μm.

Type locality: 5°21'N, 81°53'W, sediment trap depth 667 m. Collected during August-December 1979.

Remarks: This species is rare in the Panama Basin. Wide size variation is observed.

Derivation of name: The name of this species is the Latin meaning having the nature of longer than broad.

Plegmosphaera lepticali Renz

Plegmosphaera lepticali RENZ, 1976, p. 115, pl. 1, fig. 14. - TAKAHASHI and HONJO, 1981, p. 146, pl. 1, figs. 15,16

Plegmosphaera pachyplegma Haeckel

Plegmosphaera pachyplegma HAECKEL, 1887, p. 89.-BOLTOVSKOY and RIEDEL, 1980, p. 106, pl. 1. fig. 17

Genus STYPTOSPHAERA Haeckel, 1881

Styptosphaera spongiacea Haeckel
Plate 6, figures 6-7, 9

Styptosphaera spongiacea HAECKEL, 1887, p. 87

Octodendron nidum TAN and TCHANG, 1976, p. 233, text-fig. 10

Remarks: S. spongiacea shown by Renz (1976) has an inside cavity bounded by latticed wall and hence it should be placed in the genus plegmosphaera.

Styptosphaera sp. A
Plate 6, figues 12-14

Dimensions: Shell diameter (long axis) of the illustrated specimens: fig. 12: 107 μm; fig. 13: 190 μm; and fig. 14: 34 μm.

Remarks: This could be the juvenile form of S. spongicea.

Styptosphaera sp. B
Plate 5, figure 12

Description: Shell smooth and ovate with irregular polygonal meshwork on the surface which is connected to the central part with fine radial strands.

Dimensions of the illustrated specimen: Diameter of long axis: 240 µm; short axis: 183 µm.

Styptosphaera sp. C
Plate 5, figure 13

Description: Shell large and ovate with smooth surface. Very fine spongy meshwork, rather dense in the central part and loose in the subsurface layer.

Dimension of the illistrated specimen: Diameter of long axis: 800 µm; short axis: 710 µm.

Genus THECOSPHAERA Haeckel, 1881

Thecosphaera capillacea Haeckel
Plate 6, figure 2

Theocosphaera capillacea HAECKEL, 1887, p. 81

Thecosphaera inermis (Haeckel)
Plate 11, figure 9

Haliomma inerme HAECKEL, 1860a, p. 815

Actinomma inerme HAECKEL, 1862, p. 440, pl. 24, fig. 5

Theocosphaera inermis HAECKEL, 1887, p. 80

Theocosphaera inermis (Haeckel). - BOLTOVSKOY and RIEDEL, 1980, p. 114, pl. 3, fig. 6

Genus CARPOSPHAERA Haeckel, 1881

Carposphaera sp. aff. *C. corypha* Haeckel
Plate 9, figure 12

Spongoplegma antarcticum Haeckel. - KEANY, 1979, p. 53, pl. 2, fig. 1

? *Carposphaera corypha* HAECKEL, 1887, p. 75

Remarks: Since specimens observed here as well as the one shown by Keany (1979) do not have spongy cortical shell the generic name of this species is not *Spongoplegma*. This species is close to Haeckel's illustrated description of *Carposphaera corypha*, but its cortical shell thickness seems to be much thicker than the latter.

Family ACTINOMMIDAE Haeckel, 1862, emend. Sanfilippo and Riedel, 1980

Definition: Solitary spumellarians with shells spherical or ellipsoidal or modifications of those shapes, but not discoidal, nor equatorially constricted ellipsoids, usually without internal spicules, generally much smaller than orosphaerids (Sanfilippo and Riedel, 1980).

Subfamily ACTINOMMINAE Haeckel, 1862, emend. herein

Definition: Actinommidae excluding Saturnalinae.

Genus CENTROCUBUS Haeckel, 1887

Centrocubus cladostylus Haeckel

Centrocubus cladostylus HAECKEL, 1887, p. 278, pl. 18, fig. 1. - TAKAHASHI and HONJO, 1981, p. 148, pl. 4, fig. 1

Centrocubus octostylus Haeckel
Plate 7, figure 1

Centrocubus octostylus HAECKEL, 1887, p. 278

Genus SPONGOSPHAERA Ehrenberg, 1847b

Spongosphaera polycantha Müller
Plate 7, figures 2-3, 5

Spongosphaera polycantha MÜLLER, 1858a, p. 32, pl. 4, figs. 1-4. - HAECKEL, 1887, p. 282. - HOLLANDE and ENJUMET, 1960, pl. 46, fig. 1

? Spongosphaera streptacantha ? Haeckel. - POPOFSKY, 1912, pl. 8, fig. 4

Spongosphaera sp. aff. S. helioides Haeckel
Plate 7, figures 4, 7-8

Spongosphaera helioides HAECKEL, 1862, p. 456, pl. 12, figs. 11-13; 1887, p. 283

Remarks: This taxon is similar to S. helioides, but not the same because radial bi-spines are branching.

Spongosphaera streptacantha Haeckel
Plate 7, figure 6

Spongosphaera streptacantha Haeckel, 1862, p. 455, pl. 26, figs. 1-3; 1887, p. 282. - MAST, 1910, p. 187. - POPOFSKY, 1912, p. 109, text-fig. 22. - HOLLANDE and ENJUMET, 1960 ?, pl. 20, figs. 5-7, pl. 45, fig. 4, pl. 58, fig. 5. - TAN and TCHANG, 1976, p. 234, text-fig. 11

Spongosphaera ? sp. B
Plate 7, figure 9

Description: Shell large polyhedral and made of dense spongy meshwork with 20 thick branched radial spines. Bases of the spines are elevated and hence each shell surface plane becomes convex. Shell surface of pylome end is rather flat.

Genus LYNCHNOSPHAERA Haeckel, 1881

Lynchnosphaera regina Haeckel
Plate 7, figure 10

Lynchnosphaera regina HAECKEL, 1887, p. 277, pl. 11, figs. 1-4

Genus ACTINOMMA Haeckel, 1860a, emend. Nigrini, 1967; Bjørklund, 1977

Actinomma acadophorum Haeckel
Plate 8, figures 8-9, 11

Actinomma arcadophorum HAECKEL, 1887, p. 255, pl. 29, figs. 7,8. - NIGRINI, 1967, p. 29, pl. 2, fig. 3. - NIGRINI and MOORE, 1979, p. S29, pl. 3, fig. 4

Actinomma capillaceum Haeckel
Plate 8, figure 10

Actinomma capillaceum HAECKEL, 1887, p. 255, pl. 29, fig. 6

Actinomma sp. aff. A. arcadophorum Haeckel and A. medianum Nigrini. - TAKAHASHI and HONJO, 1981, p. 147, pl. 2, fig. 4

non Actinimma capillaceum NAKASEKO, 1959, p. 11, pl. 3, fig. 2a, 2b.

Remarks: Heliomma capillaceum Haeckel (1862, p. 426, pl. 23, fig. 2; 1887, p. 236) is very similar to this taxon except for the absence of outer medullary shell.

Actinomma sp.
Plate 13, figure 11

Actinomma sp. B. - TAKAHASHI and HONJO, 1981, p. 147, pl. 2, fig. 6

Description: Similar to Heterosphaera sp. A (Pl. 13, figs. 9, 10), but this species lacks bi-spines and it has more and shorter main-spines than the former.

Genus TRILOBATUM Popofsky, 1912

Trilobatum ? acuferum Popofsky

Trilobatum acuferum POPOFSKY, 1912, p. 132, text-fig. 48. - TAKAHASHI and HONJO, 1981, p. 147, pl. 2, fig. 7

Genus ACANTHOSPHAERA Ehrenberg, 1858

Acanthosphaera actinota (Haeckel)
Plate 8, figure 1

Heliosphaera actinota HAECKEL, 1860a, p. 803; 1862, p. 352, pl. 9, fig. 3; 1887, p. 218. - SCHRÖDER, 1909, p. 20, text-fig. 10

Acanthosphaera tenuissima (Haeckel). - RENZ, 1976, p. 99, pl. 2, fig. 11

Acanthosphaera sp. - HOLLANDE and ENJUMET, 1960, p. 113, pl. 55, fig. 5 (only)

Acanthosphaera actinota (Haeckel). - BOLTOVSKOY and RIEDEL, 1980, p. 107, pl. 1, fig. 19. - TAKAHASHI and HONJO, 1981, p. 146, pl. 1, figs. 18,19

See Boltovskoy and Riedel (1980) for a more complete synonymy.

Acanthosphaera tunis Haeckel
Plate 8, figures 2-3

Acanthosphaera tunis HAECKEL, 1887, p. 210

Acanthosphaera castanea Haeckel
Plate 8, figures 4-5

Acanthosphaera castanea HAECKEL, 1887, p. 211, pl. 26, fig. 3

Acanthosphaera simplex ? (Haeckel)
Plate 12, figure 15

Cladococcus simplex HAECKEL, 1860a, p. 800

Rhaphidococcus simplex (Haeckel), 1862, p. 336, pl. 13, figures 5,6

Acanthosphaera simplex (Haeckel). - 1887, p. 216

Remarks: Shell size about one half of Haeckel's descriptions and spines are straight.

Genus HELIOSPHAERA Haeckel, 1862

Heliosphaera radiata Popofsky

Heliosphaera radiata POPOFSKY, 1912, p. 98, text-fig. 10. - BENSON, 1966, p. 160, pl. 5, figs. 1,2. - TAKAHASHI and HONJO, 1981, p. 146, pl. 1, fig. 22

Genus CLADOCOCCUS Muller, 1857

Cladococcus viminalis Haeckel
Plate 8, figures 6-7

Cladococcus viminalis HAECKEL, 1862, pl. 14, figs. 2,3. - BJØRKLUND, 1976a, pl. 1, figs. 10-12

Cladococcus abietinus Haeckel
Plate 10, figure 5

Cladococcus abietinus HAECKEL, 1887, p. 226, pl. 27, fig. 3. - TAKAHASHI and HONJO, 1981, p. 148, pl. 2, fig. 10

Cladococcus scoparius Haeckel
Plate 10, figures 6-7

Cladococcus scoparius HAECKEL, 1887, p. 225, pl. 27, fig. 2. - TAKAHASHI and HONJO, 1981, p. 148, pl. 2, fig. 11

Cladococcus cervicornis Haeckel
Plate 10, figures 8-10

Cladococcus cervicornis HAECKEL, 1860a, p. 801; 1862, p. 370, pl. 14, figs. 4-6. - DREYER, 1913 (partim), p. 30, pl. 1, figs. 1,5 (only). - BOLTOVSKOY and RIEDEL, 1980, p. 110, pl. 2, fig. 5

Elaphococcus cervicornis (Haeckel). - HAECKEL, 1887, p. 228. - BENSON, 1966, p. 172, pl. 6, fig. 1

Elaphococcus gaussi POPOFSKY, 1912, p. 100, pl. 6, fig. 1

Genus ARACHNOSPHAERA Haeckel, 1862

Arachnosphaera sp.
Plate 7, figure 12

Description: Shells 7-8 concentric latticed sphere with branched spines of 1/2 of outermost shell diameter.

Arachnosphaera myriacantha Haeckel
Plate 10, figures 11-12

Arachnosphaera myriacantha HAECKEL, 1862, p. 357, pl. 10, fig. 3, pl. 11, fig. 4; 1887, p. 268. - TAN and TCHANG, 1976, p. 232, text-fig. 8

Arachnosphaera hexasphaera POPOFSKY, 1912, p. 108, text-figs. 19-21. - TAKAHASHI and HONJO, 1981, p. 147, pl. 2, fig. 13

Genus LEPTOSPHAERA Haeckel, 1887

Leptosphaera minuta ? Popofsky
Plate 7, figure 11

Leptosphaera minuta POPOFSKY, 1912, p. 104, text-fig. 14

Remarks: This species has two layers of fragile cortical shell whereas Popofsky described only one layer.

Leptosphaera sp. group

Leptosphaera sp.- TAKAHASI and HONJO, 1981, p. 148, pl. 3, figs. 19, 20

Genus ACTINOSPHAERA Hollande and Enjumet, 1960

Actinosphaera tenella (Haeckel)
Plate 9, figure 1

Haliomma tenellum HAECKEL, 1862, p. 428; 1887, p. 236

Haliomma spinulosa aff. MÜLLER, 1858a, p. 40, pl. 4, fig. 7

Actinosphaera capillaceum (Haeckel). - HOLLANDE and ENJUMET (partim), pl. 52, fig. 3 (only)

Actinosphaera acanthophora (Popofsky)
Plate 9, figures 2-3

Haliomma acanthophora POPOFSKY, 1912, p. 101, text-fig. 13. - DUMITRICA, 1972, p. 832, pl. 20, figs. 1,2

Actinosphaera capillacea (Haeckel)
Plate 9, figures 4-5

Haliomma capillaceum HAECKEL, 1862, p. 426, pl. 23, fig. 2; 1887, p. 236

Haliomma erinaceum HAECKEL, 1862, p. 427, pl. 23, figs. 3,4; 1887, p. 236

Actinosphaera capillaceum (Haeckel). - HOLLANDE and ENJUMET (partim), 1960, pl. 52, figs. 1,2 (only)

Genus HALIOMMA Ehrenberg, 1838

Haliomma ? sp.
Plate 8, figure 12

Description: Cortical shell thin usually hexagonally meshed with spines of one kind which extend from thick and thorny medullary shell surface to outside of the cortical shell up to 1/3 of shell radius.

Remarks: Medullary shell is tentatively considered to be one sphere under SEM observations.

Haliomma castanea Haeckel
Plate 9, figures 7,11

Haliomma castanea HAECKEL, 1862, p. 428, pl. 24, fig. 4; 1887, p. 232

Genus HELIOSOMA Haeckel, 1881

Heliosoma spp. aff. radians Haeckel
Plate 9, figures 6,8

Heliosoma radians HAECKEL, 1887, p. 240, pl. 28, fig. 3

Genus ELATOMMA Haeckel, 1887

Elatomma penicillus Haeckel
Plate 9, figures 9-10

Elatomma penicillus HAECKEL, 1887, p. 243

Elatomma pinetum Haeckel
Plate 10, figures 1-4

Elatomma pinetum HAECKEL, 1887, p. 242

Cladococcus stalactites HAECKEL ?, 1887, p. 227, pl. 27, fig. 4. - BENSON, 1966, p. 173, pl. 6, figs. 2,3

? Haeckeliella macrodoras (Haeckel). - HOLLANDE and ENJUMET, 1960, pl. 56, figs. 2-6

Genus ASTROSPHAERA Haeckel, 1887

Astrosphaera hexagonalis Haeckel
Plate 11, figures 1-3

Astrosphaera hexagonalis HAECKEL, 1887, p. 250, pl. 19, fig. 4. - MAST, 1910, p. 174. - POPOFSKY, 1912, p. 105, text-fig. 16, pl. 8, fig. 2. - RENZ, 1976, p. 100, pl. 2, fig. 12. - TAN and TCHANG, 1976, p. 228-229, text-figs. 4a,b. - TAKAHASHI and HONJO, 1981, p. 147, pl. 2, fig. 12

Remarks: Generally bi-spines are very short but some specimens (e.g. pl. 11, fig. 3) have long wavy bi-spines.

Genus DRYMOSPHAERA Haeckel, 1881

Drymosphaera dendrophora Haeckel
Plate 11, figure 4

Drymosphaera dendrophora HAECKEL, 1887, p. 249-250, pl. 20, figs. 1, 1a,1b. - TAN and TCHANG, 1976, p. 229-230, text-figs. 5a,b

Genus SPHAEROPYLE Dreyer, 1889

Sphaeropyle mespilus Dreyer
Plate 11, figures 7-8

Sphaeropyle mespilus DREYER, 1889, p. 207, pl. 8, fig. 39

Genus CROMYOMMA Haeckel, 1881

Cromyomma villosum Haeckel
Plate 11, figures 10-11

Cromyomma villosum HAECKEL, 1887, p. 261, pl. 30, fig. 2

Genus XIPHOSPHAERA Haeckel, 1881

Xiphosphaera gaea Haeckel
Plate 12, figures 1-2

Xiphosphaera gaea HAECKEL, 1887, p. 123, pl. 14, fig. 5. - DREYER, 1913, p. 15, pl. 2, fig. 5

Xiphosphaera tesseractis Dreyer
Plate 12, figures 3-5

Xiphosphaera tesseractis DREYER, 1913, p. 10, pl. 2, figs. 3,3a,4. - RENZ, 1976, p. 106, pl. 2, fig. 2. - MCMILLEN and CASEY, 1978, pl. 1, fig. 18. - TAKAHASHI and HONJO, 1981, p. 148, pl. 3, fig. 9

Genus STAUROLONCHE Haeckel, 1881

Stauralonche sp A group

Staurolonche group.-TAKAHASHI and HONJO, 1981, p. 147, pl. 3, fig. 7

Staurolonche ? sp B.

Staurolonche ? sp.-TAKAHASHI and HONJO, 1981, p. 147, pl. 3, fig. 8

Genus STAURACONTIUM Haeckel, 1881

Staurocontium sp.
Plate 12, figure 6

Genus HEXASTYLUS Haeckel, 1881

Hexastylus triaxonius Haeckel
Plate 12, figures 7-8

Hexastylus triaxonius HAECKEL, 1887, p. 175, pl. 21, fig. 2. - BENSON, 1966, p. 140, pl. 3, figs. 6,7

Hexastylus dictyotus HAECKEL, 1887, p. 176, pl. 21, figs. 8,9

Hexastylus sp.
Plate 12, figure 9

Description: Cortical shell spherical with mesh size of 3-4 times as wide as interporous bars. Six three-bladed spines of as long as shell diameter radiating from the cortical shell lye on two perpendicular planes.

Genus HEXALONCHE Haeckel, 1881

Hexalonche sp. A
Plate 11, figures 14-15

Description: Two small concentric latticed with six equal sized long main-spines (3-3.5 times of shell diameter) of straight or slightly curved and many bi-spines of 1.5 length of shell diameter.

Hexalonche spp. B
Plate 12, figures 10-11

Hexancistra sp. - TAKAHASHI and HONJO, 1981, p. 148, pl. 3, fig. 10

Genus CENTROLONCHE Popofsky, 1912

Centrolonche hexalonche Popofsky

Centrolonche hexalonche POPOFSKY, 1912, pl. 1, fig. 1. - TAKAHASHI and HONJO, 1981, p. 148, pl. 3, fig. 18

Genus CETRACONTARIUM Popofsky, 1912

Centracontarium hexacontarium POPOFSKY, 1912, p. 90, textfig. 4. - TAKAHASHI and HONJO, 1981, p. 148, pl. 3, fig. 17

Genus HEXACONTIUM Haeckel, 1881

Hexacontium sp.
Plate 12, figure 12

Hexacontium amphisiphon Haeckel
Plate 12, figures 13-14

Hexacontium amphisiphon HAECKEL, 1887, p. 182, pl. 25, fig. 2

Remarks: Specimens with more than 6 main-spines have been observed.

Hexacontium hostile Cleve
Plate 13, figures 1-2

Hexacontium hostile CLEVE, 1900a, p. 9, pl. 6, fig. 4. - SCHRODER, 1909, p. 14, text-fig. 6. - GOLL and BJORKLUND, 1971, p. 449, text-fig. 6. - BOLTOVOSKOY and RIEDEL, 1980, p. 112, pl. 2, fig. 13

Hexacontium pachydermum JØRGENSEN, 1905, p.115, pl. 8, figs. 31a,b. - BJORKLUND, 1976, pl. 1, figs. 4-9. - KLING, 1977, pl. 1, fig. 18

? *Hexacontium setosum* HAECKEL, 1887, p. 198. - CLEVE, 1900a, p. 9, pl. 5, fig. 6. - SCHRÖDER, 1909, p. 13, text-fig. 5

Hexacontium sp. aff. *H. hostile* Cleve
Plate 13, figure 6

Remarks: This species is simlar to *H. hostile* but has finer mesh.

Hexacontium arachnoidale Hollande and Enjumet

Hexacontium arachnoidale HOLLANDE and ENJUMET, 1960, p. 96, pl. 53, fig. 1. - BJØRKLUND, 1976b, p. 118, pl. 1, figs. D-F. - TAKAHASHI and HONJO, 1981, p. 148, pl. 3, fig. 13

Hexacontium axotrias Haeckel
Plate 13, figure 3

Hexacontium axotrias HAECKEL, 1887, p. 192, pl. 24, fig. 3. - BOLTOVSKOY and RIEDEL, 1980, p. 112, pl. 2, fig. 11. - TAKAHASHI and HONJO, 1981, p. 148, pl. 3, fig. 14

Remarks: Size of the shell corresponds to Boltovskoy and Riedel (1980) but much smaller than that illustrated by Haeckel (1887).

Hexacontium heracliti (Haeckel)
Plate 15, figures 8-9

Hexalonche heracliti HAECKEL, 1887, p. 187, pl. 22, fig. 7

Hexacontium cf. *heracliti* (Haeckel). - BENSON, 1966, p. 158, pl. 4, figs. 8-10

Hexacontium hystricina (Haeckel)
Plate 15, figure 10

Hexalonche hystricina Haeckel, 1887, p. 187, pl. 25, fig. 6. - TAKAHASHI and HONJO, 1981, p. 148, pl. 3, fig. 16

Remarks: Generic name is changed here because two medullary shells were commonly observed in the Pacific Stations.

Genus HEXACROMYUM Haeckel, 1881

Hexacromyum elegans Haeckel
Plate 13, figures 4-5, 7

Hexacromyum elegans HAECKEL 1887, p. 201, pl. 24, fig. 9. - TAKAHASHI and HONJO, 1981, p. 148, pl. 3, fig. 15

Remarks: Specimens with seven spines are rarely observed.

Genus HETEROSPHAERA MAST, 1910

Heterosphaera sp. A
Plate 13, figures 9-10

Description: Cortical shell very thick and rough surface with regular and circular pores of equal size as large as thickness of the interporous bars and with 7-9 three bladed radial main-spines of shell diameter long and numerous bi-spines as long as 1/3 shell diameter.

Heterosphaera sp. B
Plate 13, figure 8

Remarks: Similar to Heterosphaera sp. A but it has four denticles in the pores.

Genus CROMYECHINUS Haeckel, 1881

Cromyechinus ? sp.
Plate 13, figure 12

Cromyechinus sp. aff. C. borealis (Cleve)
Plate 13, figure 13

See the synonymy below under C. borealis.

Cromyechinus borealis (Cleve)

Actinomma boreale CLEVE, 1899, p. 26, pl. 1, fig. 5c

Chromyomma boreale (Cleve). - JØRGENSEN, 1900, p. 59

Cromyechinus borealis (Cleve). - JØRGENSEN, 1905, p. 117, pl. 8, fig. 35, pl. 9, figs. 36-37. - BJØRKLUND, 1974, p. 20, figs. 5-7; 1976a, pl. 2, figs. 7-15. - TAKAHASHI and HONJO, 1981, p. 147, pl. 2, fig. 8

Genus STOMATOSPHAERA Dreyer, 1889

Stomatosphaera sp. A
Plate 13, figure 14

Remarks: Cortical shell ellipsoidal and smooth with circular pores of unequal size. The type species of this genus is S. dinoceras Dreyer (1889, p. 211, pl. 10, fig. 76)

Stomatosphaera sp. B
Plate 13, figure 15

Remarks: This and the following sp. B resemble S. dinoceras Dreyer (1889, p. 211, pl. 10, fig. 76) but differ in size of shell and pores and cortical shell surface texture.

Stomatosphaera sp. C
Plate 13, figure 16

Remarks: About twice as large as the above sp. B otherwise similar to that.

Genus STYLACONTARIUM Popofsky 1912

Stylacontarium bispiculum Popofsky

Stylacontarium bispiculum POPOFSKY, 1912, pl. 2, fig. 2. - BENSON, 1966, p. 141, pl. 3, figs. 8-11. - TAKAHASHI and HONJO, 1981, p. 148, pl. 3, fig. 11

Genus STYLOSPHAERA Ehrenberg, 1847a

Stylosphaera ? sp. A
Plate 11, figures 5-6

Remarks: Lacking in polar spines and thus the generic name is tentative.

Stylosphaera melpomene Haeckel
Plate 14, figures 1-2

Stylosphaera melpomene HAECKEL, 1887, p. 135, pl. 16, fig. 1. - TAKAHASHI and HONJO, 1981, p. 147, pl. 2, fig. 14

Stylosphaera ? sp. B
Plate 14, figure 5

Stylosphaera lithatractus Haeckel

Stylosphaera lithatractus HAECKEL, 1887, pl. 16, figs. 4,5. - TAKAHASHI and HONJO, 1981, p. 147, pl. 3, fig. 1

Genus DRUPPATRACTUS Haeckel, 1887

Druppatractus ostracion Haeckel group
Plate 14, figures 3-4

? Druppatractus ostracion HAECKEL, 1887, p. 326, pl. 16, figs. 9,10

Genus ELLIPSOXIPHIUM Haeckel, 1887

Ellipsoxiphium palliatum Haecker
Plate 14, figures 11-17

Ellipsoxiphium palliatum HAECKER, 1908a, p. 441, pl. 84, fig. 587

Druppatractus acquilonius Hays. - TAKAHASHI and HONJO, 1981, p. 147, pl. 3, fig. 5

non Ellipsoxiphus elegens var. palliatus Haeckel, 1887, p.296, pl. 14, fig. 7

non Druppatractus acquilonius HAYS, 1970, p. 214, pl. 1, figs. 4, 5

Description: Two medullary shells spherical to ellipsoidal. Inner cortical shell ellipsoidal and thick with circular pores of relatively uniform size which is about 2-2.5 times as large as the thickness of interporous bars. There are about ten pores on a half equator. Outer cortical shell extremely thin and delicate, consisting of a polygonal meshwork; close to the inner cortical shell. The meshwork is connected everywhere with inner cortical shell's interporous bars and hence it resembles a form of bi-spines in poorly developed or extensively dissolved specimens. Polar spines dissimilar in length, having ratio of 1:2. The spines are cylindrical up to halfway and become conical distally. The bases of the spines are simply jointed with the inner cortical shell and almost not bladed.

Dimensions: (12 specimens) Length of inner cortical shell major axis: 146 ± 22 µm (2 S.D.); range 148-207 µm. Length of inner cortical shell minor axis: 154 ± 17 µm (2 S.D.); range 136-179 µm. Length of major polar spine: 103 ± 12 µm (2 S.D.); range: 91-119 µm. Length of minor polar spine: 51 ± 7 µm (2 S.D.); range: 38-80 µm. Length of outer medullary shell major axis: 45-60 µm.

Remarks: This species resembles D. acquilonius Hays (HAYS, 1970, p. 214, pl. 1, figs. 4,5. - KLING, 1971, p. 1086, pl. 1, figs. 5,6. - LING, 1975, p. 717, pl. 1, figs. 17, 18; 1980, p. 367, pl. 1, fig. 1; Stylocantarium acquilonium (Hays). - KLING, 1973, p. 634, pl. 1, figs. 17-20, pl. 14, figs. 1-4. - LING, 1973, p. 777, pl. 1, figs. 6,7) but length of the dissimilar polar spines are generally longer and ratio between the spines differs. Delicate meshwork of the outer cortical shell similar to this species has been recorded on some specimens of D. acquilonius (see Ling, 1975, pl. 1, figs. 17,18; Kling, 1973, pl. 14, fig. 2). It is possible that D. acquilonius gave rise to the present species. The polar spines are always cylindro-conical, and not three bladed, and thus the present species differs from Ellipsoxiphus elegans var. palliatus Haeckel (1887, p. 296, pl. 14, fig. 7).

Genus AMPHISPHAERA Haeckel, 1881

Amphisphaera group
Plate 14, figures 6-7

Amphisphaera group. - TAKAHASHI and HONJO, 1981, p. 147, pl. 3, fig. 3

Genus AXOPRUNUM Haeckel, 1887

Axoprunum stauraxonium Haeckel
Plate 14, figures 8-10

Axoprunum stauraxonium HAECKEL, 1887, p. 298, pl. 48, fig. 4. - HAYS, 1965, p. 170, pl. 1, fig. 3. - PETRUSHEVSKAYA and KOZLOVA, 1972, p. 521, pl. 10, fig. 10. - NIGRINI and MOORE, 1979, p. S57, pl. 7, figs. 2,3

? Cromyatractus elegans Dogel. - DUMITRICA, 1972, p. 834, pl. 20, fig. 8

? Amphisphaera cristata Carnevale. - DUMITRICA, 1972, p. 833-834, pl. 20, fig. 10

Remarks: Specimens observed here have thinner shell and smoother surface than those described by Hays (1965) and Nigrini and Moore (1979). Interconnecting rods between medullary and cortical shells lie in the equatorial plane as Petrushevskaya and Kozlova (1972) noted.

Genus XIPHATRACTUS Haeckel, 1887

Xiphatractus pluto (Haeckel)
Plate 15, figures 1-3

Amphisphaera pluto HAECKEL, 1887, p. 144, pl. 17, figs. 7,8

? Stylatractus neptunus Haeckel, 1887, p. 328, pl. 17, fig. 6. - RIEDEL, 1958, p. 226, pl. 1, fig. 9

Xiphatractus pluto (Haeckel). - BENSON, 1966, p. 184, pl. 7, figs. 14-17

? Xiphatractus cronos (Haeckel). - BENSON, 1966, p. 182, pl. 7, figs. 12,13

? Stylactractus spp. - NIGRINI and MOORE, 1979, p. S55, pl. 7, figs. 1a,b

Xiphatractus sp. A
Plate 15, figure 4

? Xiphatractus stahli DREYER, 1889, p. 129, pl. 6, fig. 17

Xiphatractus pluto ? (Haeckel). - TAKAHASHI and HONJO, 1981, p. 147, pl. 3, fig. 4

Description: Two medullary shells are slightly ellipsoidal. Cortical shell thick and thorny with dissimilar thick and short polar spines.

Xiphatractus spp. B
Plate 15, figures 6-7

Description: Cortical shell single and medullary shell double. The cortical and outer medullary shells are ellipsoidal and made of hexagonal framework. The cortical shell has short bi-spines or conical projections at every intersection of interporous bars and has circular or hexagonal pores of 2-4 times as large as the thickness of the interporous bars. The outer medullary shell has circular pores bounded by interporous bars of the same width as the pore diameter. Cortical-medullary interconnecting rods, which are arising from every intersection of the medullary framework, lie in many planes. Two polar spines are short, smooth conical shape and dissimilar in length.

Remarks: There are variations among specimens in pore size and shape as well as length of the spines and thus these characteristics may correspond to more than one species.

Genus DRUPPATRACTUS Haeckel, 1887

Druppatractus ? sp.
Plate 15, figure 5

Remarks: This species is similar to *Druppatractus* ? sp. (Dumitrica, 1972, p. 833, pl. 20, fig. 5).

Genus DORYDRUPPA Vinassa, 1898

Dorydruppa bensoni, new name
Plate 15, figures 11-14

? *Haliomma pyriformis* BAILEY, 1856, p. 2, pl. 1, fig. 29

Druppatractus cf. *pyriformis* (Bailey). - BENSON, 1966, p. 177-180, pl. 7, figs. 2-6

Description: Medullary shell single and pear-shaped with circular pores of equal size and spines which become interconnecting rods when cortical shell is present. Cortical shell absent or single, usually thick but variable and rarely thick and hexagonally framed with single three bladed polar spine of as long as length of the medullary shell main axis.

Dimensions (8 specimens): Length of cortical shell major axis: 74-91 μm; Length of medullary shell major axis: 47-58 μm; Length of medullary shell minor axis: 36-45 μm.

Type locality: 15°21.1'W, 151°28.5'W sediment trap depth 4280 m. Collected during July-November 1978.

Remarks: Bailey (1856) illustrated a pear-shaped (*pyriformis*) shell which may or may not correspond to medullary shell of the present species. However, he did not illustrate nor describe for the cortical shell and hence Benson (1966) was the first one to describe the species. *Druppatractus irregularis* Popofsky (1913, p. 114-115, text-figs. 24-26. - BENSON, 1966, p. 180, pl. 7, figs. 7-11) also has similar pear-shaped medullary shell to the present species but differs primarily in cortical mesh size.

Derivation of name: This species is named after Dr. Richard N. Benson.

Subfamily SATURNALINAE Deflandre, 1953

Definition: Spherical latticed or spongy shell, with two opposite spines jointed by a ring. In some species, there are no spines and the ring (or two incomplete half-rings) joins the shell directly (Riedel, 1971).

Genus SATURNALIS Haeckel, 1881, emend. Nigrini, 1967

Saturnalis circularis Haeckel
Plate 15, figures 15-18

Saturnalis circularis HAECKEL, p. 131. - NIGRINI, 1967, p. 25, pl. 1, fig. 9. - RENZ, 1976, p. 107, pl. 1, fig. 15. See Nigrini (1967) for a more complete synonymy.

Family COCCODISCIDAE Haeckel, 1862, emend. Sanfilippo and Riedel, 1980

Definition by Sanfilippo and Riedel (1980): Discoidal forms consisting of a lenticular cortical shell enclosing a small single or double medullary shell, and surrounded by an equatorial zone of spongy or concentrically-chammbered structure, or forms with ellipsoidal cortical shell, usually equatorially constricted and enclosing a single or double medullary shell, the opposite poles of the shell generally bearing spongy columns and/or single or multiple latticed caps.

Subfamily ARTISCINAE Haeckel, 1881, emend. Riedel, 1967

Definition: Ellipsoidal coccodiscids (Sanfilippo and Riedel, 1980).

Genus DIDYMOCYRTIS Haeckel, 1881, emend. Riedel, 1971

Didymocyrtis tetrathalamus tetrathalamus (Haeckel)
Plate 21, figures 1-14

Panartus tetrathalamus HAECKEL, 1887, p. 378, pl. 40, fig. 3. - NIGRINI, 1967, p. 30, pl. 2, figs. 4a-4d

Ommatartus tetrathalamus (Haeckel). - RENZ, 1976, p. 107, pl. 1, fig. 6. - MCMILLEN and CASEY, 1978, pl. 2, figs. 13a,13b. - BOLTOVOSKOY and RIEDEL, 1980, p. 114, pl. 3, fig. 3. - TAKAHASHI and HONJO, 1981, p. 148, pl. 4, figs. 2-6 (including both subspp. A and B)

Ommatartus tetrathalamus tetrathalamus (Haeckel). - NIGRINI and MOORE, 1979, p. S49, pl. 6, 1a-d. - JOHNSON and NIGRINI, 1980, p. 121, pl. 1, fig. 17

Remarks: Major thick cortical-medullary interconnecting rods lie in the vicinity of equatorial plane and additional minor (thin) rods lie randomly. Development of delicate cortical lateral meshwork as well as polar caps varies significantly. Distinction of two separate forms (subspp. A and B) was possible only at Station E. Juvenile form (pl. 21, fig. 1) of this species is counted separatly and reported in the flux table. See Sanfilippo and Riedel (1980, p. 1010) for assignment of the generic name for this species.

Didymocyrtis sp.
Plate 21, figure 15

Description: Cortical shell ellipsoidal and not constricted in the equatorial plane, with coarser meshwork than that of D. tedrathalamus and a few short spines. Double medullary shells same as those of D. tetrathalamus.

Genus SPONGOLIVA Haeckel, 1887

Spongoliva ellipsoides Popofsky
Plate 22, figures 15-16

Spongoliva ellipsoides POPOFSKY, 1912, p. 117, text-fig. 28. - RENZ, 1976, p. 108, pl. 1, fig. 5

Spongoliva cf. ellipsoides Popofsky. - TAKAHASHI and HONJO, 1981, p. 148, pl. 1, fig. 17

? Spongoliva cf. ellipsoides Popofsky. - BENSON, 1966, p. 190, pl. 8, fig. 6

Family PORODISCIDAE Haeckel, 1881, emend. Petrushevskaya and Kozlova, 1972

For a definition see Petrushevskaya and Kozlova (1972, p. 524).

Genus EUCHITONIA Ehrenberg, 1860b, emend. Haeckel, 1887

Euchitonia elegans (Ehrenberg)
Plate 16, figures 1-6

Pteractis elegans EHRENBERG, 1872a, p. 319; 1872b, p. 299, pl. 8, fig. 3

Euchitonia elegans (Ehrenberg). - HAECKEL, 1887, p. 535. - NIGRINI, 1967, p. 39, pl. 4, figs. 2a,2b. - NIGRINI and MOORE, 1979, p. S83, pl. 11, figs. 1a,b. - JOHNSON and NIGRINI, 1980, p. 127, pl. 2, fig. 7. - TAKAHASHI and HONJO, 1981, p. 149, pl. 5, fig. 2

Euchitonia sp. - RENZ, 1976, (partim) p. 93, pl. 3, fig. 2

Remarks: Morphology of the patagium varies considerably but that of main spongy arms is fairly consistent.

Euchitonia cf. furcata Ehrenberg
Plate 16, fig. 8

Euchitonia furcata EHRENBERG, 1860a, p. 767; 1860b, p. 832; 1872a, p. 308; 1872b, p. 289, pl. 6 (III), fig. 6. - HAECKEL, 1887, p. 532. - LING and ANIKOUCHINE, 1967, p. 1484, pls. 189, 190, figs. 1-2, 5-7. - NIGRINI and MOORE, 1979, p. S85, pl. 11, figs. 2a,b. - TAKAHASHI and HONJO, 1981, p. 149, pl. 3, fig. 6

Remarks: This taxon is usually much smaller than *E. elegans* and its spongy arms are truncated at the terminal ends. A patagium is rarely seen. Thus, the present taxon may be a juvenile form of *E. furcata*. Completely developed *E. furcata* was not observed in my samples.

Euchitonia sp.
Plate 16, figures 9,11

Description: Shell spongy triangular and plate shaped with three short arms of tapering toward terminal ends. The plate surface is slightly convex on both sides. Shell size much smaller than that of *E. elegans*. A contral chamber surrounded by centric rings is about equal size as that of *D. profunda*.

Remarks: This taxon may well be a juvenile or poorly developed form of other species (e.g. *D. profunda*).

Genus AMPHIRHOPALUM Haeckel, 1881

Amphirhopalum ypsilon Haeckel
Plate 17, figures 1-3

Amphicraspedum wyvilleanum HAECKEL, 1887, p. 523, pl. 45, fig. 12

Amphirhopalum ypsilon HAECKEL, 1887, p. 522. - NIGRINI, 1967, p. 35, pl. 3, figs. 3a-3d. - LING, 1975, p. 725, pl. 14, fig. 2. - NIGRINI and MOORE, 1979, p. S75-S77, pl. 10, figs. 1a-e. - BOLTOVSKOY and RIEDEL, 1980, p. 117, pl. 3, fig. 16. - JOHNSON and NIGRINI, 1980, p. 121, pl. 2, fig. 5. - TAKAHASHI and HONJO, 1981, p. 149, pl. 5, fig. 1

Amphirhopalum straussii (Haeckel)
Plate 17, figure 4

Tessarastrum straussii HAECKEL, 1887, p. 547, pl. 45, fig. 8. - RENZ, 1976, p. 112, pl. 3, fig. 7

Amphirhopalum cf. Tessarastrum straussii Haeckel. - JOHNSON and NIGRINI, 1980, p. 121, pl. 2, fig. 4, pl. 5, figs. 1,2

Genus STYLODICTYA Ehrenberg, 1847a

Stylodictya validispina Jorgensen
Plate 19, figure 11

Stylodictya validispina JØRGENSEN, 1905, p. 119, pl. 10, figs. 40a,b. - NIGRINI and MOORE, 1979, p. S103, pl. 13, figs. 5a,b

Stylodictya ? sp.
Plate 19, figures 12-13

Stylodictya multispina Haeckel
Plate 20, figures 10,12

Stylodictya multispina HAECKEL, 1860b, p. 842; 1862, p. 496, pl. 29, fig. 5. - RENZ, 1976, p. 111, pl. 3, fig. 13. - MCMILLEN and CASEY, 1978, pl. 2, fig. 17. - BOLTOVSKOY and RIEDEL, 1980, p. 118, pl. 4, figs. 4a-4b. - TAKAHASHI and HONJO, 1981, p. 149, pl. 5, fig. 10

Genus CIRCODISCUS Kozlova, 1972

Circodiscus spp. group
Plate 20, figures 5-9

Ommatodiscus murrayi Dreyer. - TAKAHASHI and HONJO, 1981, p. 150, pl. 5, fig. 11

Description: Shell circular to elliptical and biconvex lenticular disc with a pylome, numerous very small pores, 2 to 4 central rings, and with or without spines.

Remarks: Observed major differences among specimens are number of the central rings and presence/absence of marginal or lateral spines. Porodiscus microporus (Stöhr) illustrated by Renz (1976, p. 109, pl. 3, fig. 15) is very similar to this group. Ommatodiscus murrayi Dreyer (1889, pl. 9, fig. 56) is included in this group. The generic name assigned here is that of Kozlova in Petrushevskaya and Kozlova (1972, p. 526).

Genus STYLOCHLAMYDIUM Haeckel, 1881

Stylochlamydium venustum (Bailey)
Plate 20, figure 11

Perichlamidium venustum BAILEY, 1856, p. 5, pl. 1, figs. 16,17

Stylochlamydium venustum (Bailey). - HAECKEL, 1887, p. 515. - LING et al., 1971, p. 711, pl. 1, figs. 7, 8, textfig. 5. - RENZ, 1976, p. 110, pl. 3, fig. 11. - BOLTOVSKOY and RIEDEL, 1980, p. 118, pl. 4, fig. 3

Spongotrochus ? venustum (Bailey). - NIGRINI and MOORE, 1979, p. S119, pl. 15, figs. 3a,b

Stylochlamydium asteriscus Haeckel

Stylochlamydium asteriscus HAECKEL, 1887, p. 514, pl. 41, fig. 10. - RENZ, 1976, p. 109, pl. 3, fig. 12. - MCMILLEN and CASEY, 1978, pl. 2, fig. 20. - BOLTOVSKOY and RIEDEL, 1980, p. 118, pl. 4, fig. 2

Genus PORODISCUS Haeckel, 1881

Porodiscus micromma (Harting)
Plate 20, figures 13-14

Flustrella micromma HARTING, 1863, p. 16, pl. 3, fig. 47

Porodiscus micromma (Harting). - BOLTOVSKOY and RIEDEL, 1980, p. 117, pl. 3, fig. 17. - TAKAHASHI and HONJO, 1981, p. 149, pl. 5, figs. 7,8

Family SPONGODISCIDAE Haeckel, 1862, emend. Riedel, 1967a and Petrushevskaya and Kozlova, 1972

Definition: Discoidal, spongy or finely-chambered skeleton which is disposed irregularly or in a dense spiral, or in closely disposed spheres, with or without surficial pore-plate, often with radiating arms or marginal spines, and without a large central phacoid shell. The central chamber is usually not visible (Riedel, 1971; Petrushevskaya and Kozlova, 1972).

Genus SPONGOBRACHIUM Haeckel, 1881

Spongobrachium sp.

Spongobrachium sp.-JONHSON and NIGRINI, 1980, p. 127, textfig. 8f, pl. 2, fig. 13, pl. 5, fig.3

Genus DICTYOCORYNE Ehrenberg, 1860b

Dictyocoryne profunda Ehrenberg
Plate 16, figures 10, 12-13, 15

Dictyocoryne profunda EHRENBERG, 1860a, p. 767; 1872a, p. 307; 1872b, p. 288, pl. 7, fig. 23. - HAECKEL, 1887, p. 592. - NIGRINI and MOORE, 1979, p. S87, pl. 12, fig. 1. - BOLTOVSKOY and RIEDEL, 1980, p. 115, pl. 3, fig. 10. - JOHNSON and NIGRINI, 1980, p. 127, pl. 2, fig. 9

Hymeniastrum euclidis HAECKEL, 1887, p. 531, pl. 43, fig. 13. - BENSON, 1966, p. 222, pl. 12, figs. 1-3. - LING and ANIKOUCHINE, 1967, p. 1488, pl. 191, fig. 3, pl. 192, fig. 3. - NIGRINI, 1970, p. 168, pl. 2, fig. 4, text-fig. 16. - NIGRINI and MOORE, 1979, p. S91, pl. 12, fig. 3. - JOHNSON and NIGRINI, 1980, p. 127, pl. 2, fig. 11. - TAKAHASHI and HONJO, 1981, p. 149, pl. 5, figs. 3-5

Dictycoryne truncatum (Ehrenberg)
Plate 16, figure 14

Rhopalodictyum truncatum EHRENBERG, 1861b, p. 301. - HAECKEL, 1887, p. 589

Dictyocoryne cf. truncatum (Ehrenberg). - BENSON, 1966, p. 235, pl. 15, fig. 1

Dictyocoryne truncatum (Ehrenberg). - NIGRINI and MOORE, 1979, p. S89, pl. 12, figs. 2a,b. - JOHNSON and NIGRINI, 1980, p. 127, pl. 2, fig. 10

Remarks: The specimen illustrated (Pl. 16, fig. 14) is an end member of the present population close to D. profunda. This species usually has much wider arms which are truncated and the corners are rounded than the illustrated specimen.

Genus SPONGODISCUS Ehrenberg, 1854

Spongodiscus sp. A
Plate 16, figure 7

Spongodiscus sp. aff. *S.* *resurgens* Ehrenberg. - RENZ, 1976, p. 96, pl. 3, fig. 10

Spongodiscus sp. A. - TAHAHASHI and HONJO, 1981, p. 149, pl. 4, fig. 13

Spongodiscus *resurgens* Ehrenberg
Plate 19, figure 1

Spongodiscus *resurgens* EHRENBERG, 1854, p. 21, pl. 35B, fig. 16. - HAECKEL, 1887, p. 577. - PETRUSHEVSKAYA and KOZLOVA, 1972, p. 5528, pl. 21, fig. 5. - TAKAHASHI and HONJO, 1981, p. 149, pl. 4, fig. 11

Spongodiscus *resurgens* *resurgens* Ehrenberg. - PETRUSHEVSKAYA and BJORKLUND, 1974, p. 40, text-fig. 6

Spongodiscus spp. B group
Plate 19, figures 2-3

Spongodiscus *biconcavus* Haeckel
Plate 19, figures 4-6

Spongodiscus *biconcavus* HAECKEL, 1887, p. 577. - POPOFSKY, 1912, p. 143, pl. 6, fig. 2. - TAN and TCHANG, 1976, p. 255, text-fig. 25

Spongaster *disymmetricus* (Dogel). - PETRUSHEVSKAYA and KOZLOVA, 1972, p. 528, pl. 21, fig. 14

Elliptical" spongodiscid. - MCMILLEN and CASEY, 1978, pl. 3, fig. 13

See Boltovskoy and Riedel (1980) for a more complete synonomy.

Genus SPONGOTROCHUS Haeckel, 1860b

Spongotrochus sp. A
Plate 19, figure 7

Description: Shell circular flat disc, with numerous fine spines arising from surface as well as edge of the disc, pores small and irregular, and without a pylome.

Spongotrochus sp. B

Spongotrochus sp B.-TAKAHASHI and HONJO, 1981, p. 149, pl. 4, fig. 19

Spongotrochus glacialis Popofsky
Plate 19, figure 10

Spongotrochus glacialis POPOFSKY, 1908, p. 228, pl. 26, fig. 8, pl. 27, fig. 1, pl. 28, fig. 2. - RIEDEL, 1958, p. 227, text-fig. 1, pl. 2, figs. 1,2. - CASEY, 1971b, p. 337, pl. 23.1, figs. 4,5. - KEANY, 1979, p. 54, pl. 2, fig. 7; pl. 5, fig. 7. - BOLTOVSKOY and RIEDEL, 1980, p. 117, pl. 3, fig. 15. - TAKAHASHI and HONJO, 1981, p. 149, pl. 4, fig. 17

Spongotrochus arachnius Haeckel. - POPOFSKY, 1908, p. 227, pl. 26, figs. 5,6,6a,7, pl. 28, fig. 1

Spongotrochus multispinus Haeckel. - RENZ, 1976, p. 97, pl. 3, fig. 9

Genus STYLOSPONGIA Haeckel, 1862

Stylospongia huxleyi Haeckel
Plate 19, figure 8

Stylospongia huxleyi HAECKEL, 1862, p. 473, pl. 28, fig. 7

Stylotrochus huxleyi (Haeckel). - HAECKEL, 1887, p. 586

Genus SPONGOCORE Haeckel, 1887

Spongocore cylindrica (Haeckel)
Plate 17, figures 6-9

Spongurus cylindricus HAECKEL, 1860b, p. 845; 1862, p. 465, pl. 27, fig. 1; 1887, p. 334

Spongocore diplocylindrica HAECKEL, 1887, p. 346. - RENZ, 1976, p. 95, pl. 3, fig. 8

Spongocore puella HAECKEL, 1887, p. 347, pl. 48, fig. 6. - BENSON, 1966, p. 187, pl. 8, figs. 1-3. - NIGRINI, 1970, p. 168, pl. 2, fig. 3. - CASEY, 1971b, p. 341, pl. 23.3, fig. 20. - NIGRINI and MOORE, 1979, p. S69, pl. 8, figs. 5a-c. - TAKAHASHI and HONJO, 1981, p. 149, pl. 4, fig. 20

Spongocore cylindrica (Haeckel). - BOLTOVSKOY and RIEDEL, 1980, p. 116, pl. 3, fig. 12

Remarks: The predated species name cylindrica should replace widely used puella because long spines of cylindrica are dissolved and consequently broken off and become like puella.

Genus SPONGOPYLE Dreyer, 1889

Spongopyle setosa Dreyer
Plate 19, figure 9

Spongopyle setosa DREYER, 1889, p. 119, pl. 11, figs. 97,98. - ? BOLTOVSKOY and RIEDEL (partim), p. 116, pl. 3, fig. 14

Spongopyle osculosa Dreyer
Plate 20, figures 1-4

Spongopyle osculosa DREYER, 1889, p. 42, pl. 11, figs. 99,100. - RIEDEL, 1958, p. 226, pl. 1, fig. 12. - NIGRINI and MOORE, 1979, p. S115, pl. 15, fig. 1

Genus SPONGASTER Ehrenberg, 1860b

Spongasater tetras tetras Ehrenberg
Plate 17, figures 10-11

Spongaster tetras EHRENBERG, 1860b, p. 833; 1872b, p. 299, pl. 6, fig. 8. - HAECKEL, 1887, p. 597. - CASEY, 1971b, p. 341, pl. 23.3, figs. 18,19. - GOLL and BJØRKLUND, 1974, p. 64, text-fig. 14. - BOLTOVSKOY and RIEDEL, 1980, p. 116, pl. 3, fig. 11

Spongaster tetras tetras Ehrenberg. - NIGRINI, 1967, p. 41, pl. 5, figs. 1a,1b; 1970, p. 169, pl. 2, fig. 7. - RENZ, 1976, p. 94, pl. 3, fig. 4. - NIGRINI and MOORE, 1979, p. S93, pl. 13, fig. 1. - JOHNSON and NIGRINI, 1980, p. 127, pl. 2, fig. 13. - TAKAHASHI and HONJO, 1981, 148, pl. 4, fig. 9. For a more complete synonymy see Nigrini (1967).

Spongaster pentas Riedel and Sanfilippo
Plate 17, figures 12-16

Spongaster pentas RIEDEL and SANFILIPPO, 1970, p. 523, pl. 15, fig. 3; 1971, p. 1589, pl. 1D, figs. 5-7; 1978, p. 74, pl. 2, figs. 5-8. - MCMILLEN and CASEY, 1978, pl. 3, fig. 14

Spongaster cf. pentas Riedel and Sanfilippo. - TAKAHASHI and HONJO, 1981, p. 148, pl. 4, fig. 10

Description: Spongy disc typically pentagonal to hexagonal and often up to decagonal. Central area of the disc is elevated and forms a convex mound on one side and a concave depression on the other. The convex mound has much coarser spongy mesh than the rest of the area. The concave area has fine short spines perpendicular to disc plane.

Family MYELASTRIDAE Riedel, 1971

Original Definition: Spogodiscidae with arms much more delicately constructed than the small central area, which is the only part of the skeleton sufficiently robust to be preserved in sediments.

Remarks: Subfamily Myelastrinae of Riedel (1971) is elevated to family level here.

Genus MYELASATRUM Haeckel, 1881, emend. herein

Definition: Porodiscidae with three or four forked, spongy or chambered arms, without a patagium; shell bilaterally symmetric. In the case of three armed species, at least two arms of equal shape and length. In the case of four armed species, two equal anterior arms of different shape from the two equal posterior arms.

Remarks: Haeckel's (1887) definition includes only four forked forms. An appearance of three forked species which is closely related to the four forked group necessitates either establishment of a new genus or emendation of the existing genus. I hereby propose to emend Haeckel's definition.

Myelastrum quadrifolium n.sp.
Plate 18, figures 1-6

Description: Shell large, spongy disc, uniformly very thin and delicate, with four major arms. Central rings similar to those of *Euchitonia*. All of the four arms are about equal in length and width. Anterior arms are bifurcated and form lobes with slight incisions. Posterior arms are trifurcated and form lobes with more conspicuous incisions than those of the anterior. Sagital incisions at the posterior end is deep and varying in width from one specimen to another, but the anterior one is shallow. Transverse incisions are shallow.

Dimensions: Length: 704 ± 49 µm (2 S.D.) (n = 12 specimens); width: 757 ± 51 µm (2 S.D.) (n = 12); weight: 2.32 ± 0.16 µg (n = 13).

Type locality: 5°21'N, 81°53'W, sediment trap depth 3791 m. Collected during August-December 1979.

Remarks: The present species differs from *Myelastrum decaceros* Haeckel (1887, p. 554, pl. 47, fig. 7) in sagital and transverse incisions, width ratio between anterior and posterior arms and number of branched subarms. The delicate arms are often almost invisible in Cargile® type B mounting medium, but the central rings are clearly visible.

Derivation of name: The name of this species is the Latin meaning having the nature of four leaves.

Myelastrum trinibrachium n.sp.
Plate 18, figures 7-12

Description: Shell large, uniformly very thin, delicate spongy disc with three tapering arms. Central rings similar to those of Euchitonia. At least a pair of arms equal shape and length and the remaining one equal or slightly different length (longer or shoter). Length of arms 2-6 times diameter of the outermost ring.

Dimensions: Length between terminal ends of the two longest arms: 1027 ± 120 μm (2 S.D.) (n = 7 specimens); weight: 0.75 ± 0.13 μg (n = 16).

Type locality: 5°21'N, 81°53'W, sediment trap depth 1268 m. Collected during August-December 1979.

Remarks: The concentric central rings as well as three arms are generally slightly more conspicuous than those of M. quadrifolium in Cargile® type B mounting medium. This species as well as M. quadrifolium are so thin and delicate that specimens are easily broken with a touch of brush. Observations of skeletal cross sections under TEM show solid nature. However, the skeletons of the arms are so thin that only the central rings may be preserved in the bottom sediments.

Derivation of name: The name of this species is the Latin meaning having the nature of three arms.

Family LARNACILLIDAE Haeckel, 1887, emend. Campbell, 1954

Definition: Shell with open gates or annular constrictions; medullary shell trizonal (Campbell, 1854).

Genus LARNACALPIS Haeckel, 1887

Larnacalpis sp.
Plate 21, figures 16-18

Larnacalpis sp. - TAKAHASHI and HONJO, 1981, p. 150, pl. 6, fig. 1

Description: Single ellipsoidal cortical shell connecting with outer medullary shell in similar manner to *Octopyle*, thus it looks as if constricted in equatorial plane in lateral view. Cortical shell pores of 3-6 times as wide as interporous bars. Some specimens have two additional connecting bars to the medullary shell and/or a pylome with surrounding spines at one polar end. Medullary shell double.

Family PHACODISCIDAE Haeckel, 1881, emend. Campbell, 1954

Definition: Single lenticular latticed cortical shell and single or double medullary shell; without chambered equatorial girdles (Campbell, 1954).

Genus HELIODISCUS Haeckel, 1862

Heliodiscus ? sp.
Plate 22, figure 14

Description: Cortical shell bilaterally convex with numerous conical bispines and circular to subcircular unequal sized pores of as wide as interporous bars. Major spines conical and thicker but not much longer than the bi-spines, lie on the marginal edge. Shell size is about same as *H. asteriscus* and *H. echiniscus*.

Heliodiscus asteriscus Haeckel
Plate 23, figures 1-3

Heliodiscus asteriscus HAECKEL, 1887, p. 445, pl. 33, fig. 8. - NIGRINI, 1967, p. 32, pl. 3, figs. 1a,1b; 1970, pl. 2, fig. 1. - RENZ, 1976, p. 92, pl. 2, fig. 1. - NIGRINI and MOORE, 1979, p. 573, pl. 9, figs. 1,2. .- BOLTOVSKOY and RIEDEL, 1980, p. 115, pl. 3, fig. 8. - JOHNSON and NIGRINI, 1980, p. 121, pl. 2, fig. 2. - TAKAHASHI and HONJO, 1981, p. 148, pl. 4, figs. 7,8

Heliodiscus echiniscus Haeckel
Plate 23, figures 4-6

Heliodiscus echiniscus HAECKEL, 1887, p. 448, pl. 34, fig. 5. - NIGRINI, 1967, p. 34, pl. 3, figs. 2a,2b. - JOHNSON and NIGRINI, 1980, p. 121, pl. 2, fig. 3

Heliodiscus asteriscoides HAECKER, 1907a, p. 22, fig. 7; 1908a, p. 444, pl. 83, figs. 578-580

Family THOLONIIDAE Haeckel, 1887, emend. Campbell, 1954

Definition: Cortical shell with 2 to 4 or more annular constrictions separated by 3 to 6 or more cupolas; constrictions in diagonal planes, cupolas in dimensive axes (Campbell, 1954).

Genus THOLOMA Haeckel, 1887

Tholoma metallasson Haeckel
Plate 11, figures 12-13

Tholoma metallasson HAECKEL, 1887, p. 672, pl. 10, fig. 13

Cubotholus regularis Haeckel. - RENZ, 1976, p. 113, pl. 1, fig. 18

Family PHYLONIIDAE Haeckel, 1881, emend. Campbell, 1954

Definition: Cortical shell latticed; with 2 to 4 or more symmetrically disposed gates (Campbell, 1954).

Genus HEXAPYLE Haeckel, 1881

Hexapyle dodecantha Haeckel

Hexapyle dodecantha HAECKEL, 1887, p. 569, pl. 48, fig. 16. - RENZ, 1976, p. 113, pl. 1, fig. 11. - TAKAHASHI and HONJO, 1981, p. 150, pl. 6, fig. 3

Hexapyle sp.
Plate 23, figure 7

Remarks: This species is about 1/4 size of H. dodecantha.

Genus OCTOPYLE Haeckel, 1881

Octopyle stenozona Haeckel
Plate 23, figure 8

Octopyle stenozona HAECKEL, 1887, p. 652, pl. 9, fig. 11. - BENSON, 1966, p. 251, pl. 16, figs. 3,4. - NIGRINI and MOORE, 1979, p. S123, pl. 16, figs. 2a,b. - TAKAHASHI and HONJO, 1981, p. 150, pl. 6, fig. 7

Genus TETRAPYLE Müller, 1858b

Tetrapyle octacantha Müller
Plate 23, figures 9-10

Tetrapyle octacantha MÜLLER, 1858b, p. 154; 1858a, p. 33, figs. 1-6. - BENSON, 1966, p. 245, pl. 15, figs. 3-10. - MCMILLEN and CASEY, 1978, pl. 3, figs. 2a,2b. - NIGRINI and MOORE, 1979, p. S125, pl. 16, figs. 3a,b. - TAKAHASHI and HONJO, 1981, p. 150, pl. 6, figs. 5,6

Family LITHELIIDAE Haeckel, 1862

Definition: Planispiral cortical shell (Campbell, 1954).

Genus LARCOPYLE Dreyer, 1889

Larcopyle butschlii Dreyer
Plate 22, figures 1-4

Larcopyle butschlii DREYER, 1889, pl. 10, fig. 10. - BENSON, 1966, p. 280, pl. 19, figs. 3-5. - NIGRINI and MOORE, 1979, p. S131, pl. 17, figs. 1a,b. - TAKAHASHI and HONJO, 1981, p. 150, pl. 5, fig. 15

Larcopyle sp. A
Plate 22, figure 5

Description: Cortical shell ovate and about 1/2 size of L. butschlii with irregular circular to subcircular pores of as wide as interporous bars, numerous short spines lie every 2-3 interporous bars on the cortical shell, and a pylome surrounded by divergent long spines.

Larcopyle sp. B
Plate 22, figure 6

Description: Cortical shell smooth, ovate and same size as the above Larcopyle sp. A with irregular subcircular pores of smaller than interporous wall, conical spines much less than the species A, and a pylome surrounded by divergent spines.

Genus DISCOPYLE Haeckel, 1887

Discopyle elliptica HAECKEL, 1887, p. 573, pl. 48, fig. 20. - TAKAHASHI and HONJO, 1981, p. 150, pl. 5, fig. 14

Genus THOLOSPIRA Haeckel, 1887

Tholospira cervicornis Haeckel group
Plate 22, figures 7-9, 12

Tholospira cervicornis HAECKEL, 1887, p. 700, pl. 49, fig. 5

Tholospira cervicornis Haeckel group. - TAKAHASHI and HONJO, 1981, p. 150, pl. 5, figs. 16-18

Remarks: The present species group is fairly abundant throughout depths in our sediment trap stations.

Tholospira dendrophora Haeckel
Plate 22, figure 11

Tholospira dendrophora HAECKEL, 1887, p. 700, pl. 49, fig. 6

Genus LITHELIUS Haeckel, 1862

Lithelius minor ? Jørgensen
Plate 22, figure 10

Lithelius minor JØRGENSEN, 1899, p. 65-66, pl. 5, fig. 24. - BENSON, 1966, p. 262, pl. 17, figs. 9,10, pl. 18, figs. 1-4

Larcospira minor (Jørgensen). - 1905, p. 121

Genus LARCOSPIRA Haeckel, 1887

Larcospira quadrangula Haeckel
Plate 23, figures 11-12

Larcospira quadrangula Haeckel, 1887, p. 696, pl. 49, fig. 3. - BENSON, 1966, p. 266, pl. 18, figs. 7,8. - NIGRINI, 1970, p. 169, pl. 2, fig. 9, text-fig. 21. - NIGRINI and MOORE, 1979, p. S133, pl. 17, fig. 2. - TAKAHASHI and HONJO, 1981, p. 150, pl. 6, fig. 2

Suborder NASSELARIA Ehrenberg, 1875

Family PLAGIACANTHIDAE Hertwig, 1879, emend. Petrushevskaya, 1971d

Definition: Plagiacanthidea with conical or ovate skeleton. Thorax nearly reduced. The apical spine may form a columella or may approach the front wall of the cephalis. The vertical spine is nearly always present. In the cephalis are developed eucephalic and antecephalic lobes. They are separated by means of the apical arches which extend in the walls of the cephalis and makes deep furrows (Petrushevskaya, 1971d).

Subfamily PLAGIACANTHINAE Hertwig, 1879, emend. Petrushevskaya, 1971d

Definition: Plagiacanthidae with thorax reduced. The walls of the cephalis also may be reduced. In such cases the skeleton consists only of the spines and arches. The disposition of these elements, unlike all other nasselarian families, may vary within the limits of one species. The central capsule of the appoaxoplastique type (Petrushevskaya, 1971d).

Genus TETRAPLECTA Haeckel, 1881, emend. herein

Definition: Plagiacanthidae with 4 equal radial spines, arising from either one of closely located 2 central points. The skeletons form a tetrahedron.

Tetraplecta pinigera Haeckel
Plate 24, figures 1-5

Tetraplecta pinigera HAECKEL, 1887, p. 924, pl. 91, fig. 8

Plectaniscus cortiniscus HAECKEL, 1887, p. 925, pl. 91, fig. 9

Remarks: A priority on genus *Tetraplecta* is given over *Plectaniscus* (Haeckel, 1887) since specimen observed here have 4 equal spines. Haeckel's *P. cortiniscus* has three equal and one short spine but the short one may have been broken since I observed many specimens like *P. cortiniscus* with four equal spines. Haeckel's two taxa, cited above, are apparently end members of the same species. The four main spines are cylindrical rods in the central area and become three bladed toward terminmal ends in contrast to Haeckel's description of all three bladed spines.

Tetraplecta *plectaniscus* Haeckel
Plate 24, figure 7

Euscenium *plectaniscus* HAECKEL, 1887, p. 1146, pl. 98, fig. 1

Cladoscenium sp. - TAKAHASHI and HONJO, 1981, p. 150, pl. 6, fig. 13

Tetraplecta *corynephorum* ? Jørgensen
Plate 24, fig. 6

? *Plectanium* *trigeminium* HAECKEL, 1887, pl. 91, fig. 11

Eucenium *corynephorum* JØRGENSEN, 1900, p. 77; 1905, p. 133, pl. 15, fig. 70. - BJØRKLUND, 1976a, pl. 7, figs. 1-4

Genus ARCHISCENIUM Haeckel, 1881

Archiscenium *quadrispinum* ? Haeckel

Archiscenium *quadrispinum* ? HAECKEL, 1887, p. 1150, pl. 53, fig. 11. - TAKAHASHI AND HONJO, 1981, p. 150, pl. 6, figs. 10, 11

Genus PLECTANIUM Haeckel, 1881

Plectanium sp.

Plectanium sp.- TAKAHASHI and HONJO, 1981, p. 150, pl. 6, fig. 8

Genus PROTOSCENIUM Jørgensen, 1905

Protoscenium ? sp. - TAKAHASHI and HONJO, 1981, p. 150, pl. 6, fig. 9

Genus CLATHROMITRA Haeckel, 1881, emend. herein

Definition: Plagoniidae with nearly a tetrahedron-shaped latticed shell; five prismatic, three-sided spines.

Remarks: This genus is already classified under the present family by Riedel (1971).

Clathromitra pterophormis Haeckel
Plate 24, figure 8

Clathromitra pterophormis HAECKEL, 1887, p. 1219, pl. 57, fig. 8. - TAKAHASHI and HONJO, 1981, p. 150, pl. 6, fig. 16

Remarks: Observed specimens here are about twice as lagre as Haeckel's.

Genus CLADOSCENIUM Haeckel, 1881

Cladoscenium ancoratum Haeckel
Plate 24, figures 9-14

Cladoscenium ancoratum Haeckel, 1887, p. 1149, pl. 53, fig. 13. - GOLL, 1976, pl. 1, figs. 1-3, 6-8. - TAKAHASHI and HONJO, 1981, p. 150, pl. 6, fig. 14. - PETRUSHEVSKAYA and KOZLOVA, 1979, p. 118, figs. 304, 476, 477.

Remarks: Mesh size of the cephalis significantly varies among specimens. Some fully grown specimens have bi-spines nearly at terminal end of main spines completely connected to other bi-spines on other main spines (e.g. pl. 24, fig. 10).

Genus SEMANTIS Haeckel, 1887

Semantis gracilis ? Popofsky
Plate 24, figures 15-16

Semantis gracilis POPOFSKY, 1908, p. 268, pl. 30, fig. 5; 1913, p. 298, pl. 28, figs. 7,8

Definition: It lacks a cephalis but has two characteristic glasses-shaped openings formed by connecting skeleton between spines.

Genus DEFLANDRELLA Loeblich and Tappan, 1961

Deflandrella cladophora (Jørgensen)
Plate 24, figure 17

Campylacantha cladophora JØRGENSEN, 1905, p. 129, pl. 12, fig. 47. - Bjørklund, 1976a, pl. 6, figs. 1-6

Deflandrella sp.

Campylacantha sp. - TAKAHASHI and HONJO, 1981, p. 150, pl. 6, fig. 12

Remarks: The generic name used here is that proposed by Loeblich and Tappan (1961, p. 227) which replaces *Campylacantha* Jorgensen, 1905.

Genus TALARISCUS Loeblich and Tappan, 1961

Talariscus pseudocuboides (Popofsky)
Plate 26, figure 1

Obeliscus pseudocuboides POPOFSKY, 1913, pl. 29, figs. 4,5. - TAKAHASHI and HONJO, 1981, p. 150, pl. 6, fig. 15

Remarks: The generic name used here is that proposed by Loeblich and Tappan (1961, p. 227) which replaces Obeliscus Popofsky, 1913.

Genus GONOSPHAERA Jørgensen, 1905

Gonosphaera primordialis ? Jørgensen
Plate 26, figure 2

Gonosphaera primordialis JØRGENSEN, 1905, p. 133, pl. 14, figs. 64-68. - BJØRKLUND, 1976a, pl. 9, figs. 7-10

Genus PHORMACANTHA Jorgensen, 1905

Phormacantha hystrix (Jorgensen)
Plate 26, figure 3

Peridium hystrix JØRGENSEN, 1900, p. 76

Phormacantha hystrix (JØRGENSEN), 1905, p. 132, pl. 14, figs. 59-63. - TAKAHASHI and HONJO, 1981, p. 150, pl. 6, figs. 17-19

Genus NEOSEMANTIS Popofsky, 1913

Neosemantis distephanus Popofsky
Plate 27, figure 12

Neosemantis distephanus POPOFSKY, 1913, p. 299, pl. 29, fig. 2. - PETRUSHEVSKAYA, 1971c, p. 152, figs. 77: I-III. - KLING, 1979, p. 309, pl. 1, figs. 15,16. - BOLTOVSKOY and RIEDEL, 1980, pl. 4, fig. 14. - TAKAHASHI and HONJO, 1981, p. 151, pl. 7, fig. 17

Subfamily LOPHOPHAENINAE Haeckel, 1881, emend. Petrushevskaya, 1971d

Definition: Plagiacanthidae with the skeleton consisting of two equal segments: cephalis and thorax. Cephalis with a large eucephalic lobe and a small antecephalic lobe which is not separated from the thorax (Petrushevskaya, 1971d).

Genus ACANTHOCORYS Haeckel, 1881

Acanthocorys cf. *variabilis* Popofsky
Plate 25, figure 1

Acanthocorys variabilis POPOFSKY, 1913, p. 360, text-figs. 71,72(Only)

Acanthocorys sp. aff. *A. variabilis* Popofsky. - RENZ, 1976, p. 155, pl. 6, fig. 20

Acanthocorys cf. *variabilis* POPOFSKY. - TAKAHASHI and HONJO, 1981, p. 151, pl. 7, fig. 1

Genus LOPHOPHAENA Ehrenberg, 1847b

Lophophaena cylindrica (Cleve)
Plate 25, figures 3-5

Acanthocorys variabilis POPOFSKY, 1913, p. 360, text-figs. 74-77 (only). - BENSON, 1966, p. 373, pl. 24, fig. 19

Lophophaena cylindrica (Cleve). - PETRUSHEVSKAYA, 1971c, p. 117, fig. 61, IV-VI. - RENZ, 1976, p. 159, pl. 6, fig. 21. - TAKAHASHI and HONJO, 1981, p. 151, pl. 7, fig. 2

Lophophaena cf. capito Ehrenberg

Plate 25, figures 6-9

? Lophophaena capito EHRENBERG, 1873, p. 242; 1875, pl. 8, fig. 6

Lophophaena cf. capito Ehrenberg. - BENSON, 1966, p. 378, pl. 24, figs. 22,23; pl. 25, fig. 1. - TAKAHASHI and HONJO, 1981, p. 151, pl. 6, fig. 22

Lophophaena decacantha (Haeckel) group

Plate 25, figures 2,8,10

Lithomelissa decacantha HAECKEL, 1887, p. 1208, pl. 56, fig. 2

Lophophaena circumtexta (Popofsky)

Lampromitra circumtexa POPOFSKY, 1913, p. 346, pl. 32, fig. 1, text-fig. 53. - TAKAHASHI and HONJO, 1981, p. 151, pl. 6, fig. 23

Remarks: The author proposes to place the present species under this genus.

Genus HELOTHOLUS Jørgensen, 1905

Helotholus histricosa Jørgensen

Helotholus histricosa Jørgensen, 1905, p. 137, pl. 16, figs. 86-88. - BENSON, 1966, p. 459, pl. 31, figs. 4-8. - TAKAHASHI and HONJO, 1981, p. 151, pl. 7, figs. 6,7

Remarks: Artostrobus joergenseni Petrushevskaya illustrated by Bjørklund (1976a, pl. 11, figs. 12,13) is similar to this species but different because its pores are in transverse raws.

Genus PEROMELISSA Haeckel, 1881

Peromelissa phalacra Haeckel
Plate 25, figures 11-15

Peromelissa phalacra HAECKEL, 1887, p. 1236, pl. 57, fig. 11. - MCMILLEN and CASEY, 1978, pl. 4, fig. 20. - BOLTOVSKOY and RIEDEL, 1980, p. 122, pl. 5, fig. 3. - TAKAHASHI and HONJO, 1981, p. 151, pl. 7, figs. 3-5

Psilomelissa longispina CLEVE, 1900a, p. 10, pl. 4, fig. 4

Psilomelissa phalacra (Haeckel). - POPOFSKY, p. 283, 1908, pl. 32, fig. 4

Psilomelissa tricuspidata POPOFSKY, 1908, pl. 32, fig. 9

Psilomelissa tricuspidata abdominalis POPOFSKY, 1908, pl. 33, fig. 4

Lithomelissa monoceras POPOFSKY, 1913, p. 335, text-fig. 43, pl. 32, fig. 7. - RENZ, 1976, p. 158, pl. 6, fig. 12

Lithomelissa setosa Jorgensen
Plate 25, figures 16-22

Lithomelissa setosa JØRGENSEN, 1900, p. 81, pl. 4, fig. 21; 1905, p. 135, pl. 16, figs. 81-83, pl. 18, figs. 108a,b. - BJØRKLUND, 1976a, pl. 8, figs. 1-13, pl. 11, figs. 19-23. - KLING, 1977, p. 217, pl. 1, fig. 2. - BOLTOVSKOY and RIEDEL, 1980, p. 121, pl. 5, fig. 1.

For a more complete synonymy see Boltovskoy and Riedel (1980).

Genus PERIDIUM Haeckel, 1887

Peridium spinipes Haeckel
Plate 26, figures 4-6

Peridium spinipes HAECKEL, 1887, p. 1154, pl. 53, fig. 9. - TAKAHASHI and HONJO, 1981, p. 151, pl. 6, fig. 20

Peridium longispinum JØRGENSEN, 1905, p. 135, pl. 15, figs. 75-79, pl. 16, fig. 80. - BENSON, 1966, p. 359, pl. 23, fig. 27, pl. 24, figs. 1-2 (only) (partim).

Psilomelissa calvata HAECKEL, 1887, p. 1209, pl. 56, fig. 3. - RENZ, 1976, p. 160, pl. 6, fig. 15

Peridium sp.

Peridium sp. - TAKAHASHI and HONJO, 1981, p. 151, pl. 6, fig. 21

Remarks: One spine very long up to five times of shell length and otherwise similar to *P. spinipes*.

Genus TRISULCUS Popfsky, 1913

Trisulcus triacanthus POPFSKY

Trisulcus triacanthus POPFSKY, 1913, p.354, textfig. 59, 60. - RENZ, 1976, p. 161, pl. 6, fig. 10

Subfamily SETHOPERINIDAE Haeckel, 1881, emend. Petrushevskaya, 1971d

Definition: Plagicanthidae with skeleton consisting of the cephalis surrounded by latticed plates built with branches of the spines.

Three plates attached to a vertical spine and the cephalis and the remaining three plates which may be regarded as a thorax attached to divergent spines and the cephalis. Cephalis pyramidal.

Genus LITHOPILIUM Popofsky, 1913

Lithopilium reticulatum Popofsky
Plate 26, figure 10

Lithopilium reticulatum POPOFSKY, 1913, p. 379, pl. 35, figs. 4,5. - RENZ, 1976, p. 164, pl. 7, fig. 2

Genus CLATHROCANIUM Ehrenberg, 1860a

Clathrocanium insectum (Haeckel)
Plate 26, figures 7-9

Dictyoceras insectum HAECKEL, 1887, p. 1324, pl. 71, figs. 6,7

Corocalyptra columba (Haeckel). - TAKAHASHI and HONJO, 1981, p. 153, pl. 9, fig. 16

Description: Abdomen divided from the thorax by a constriction. The cephalis and spines similar to those of _C. coarctatum_. Abdominal mesh is very delicate and made of irregular polygons.

Clathrocanium coarctatum Ehrenberg
Plate 26, figures 11-13

Lychnocanium fenestratum EHRENBERG, 1860a, p. 767

Clathrocanium coarctatum EHRENBERG, 1872a, p. 303; 1872b, p. 287, pl. 7, fig. 6

Clathrocanium coarctatum HAECKEL, 1887, p. 1211. - POPOFSKY, 1913, p. 341, text-fig. 50

Clathrocanium triomma HAECKEL, 1887, p. 1211, pl. 64, fig. 3

Clathrocanium coronatum POPOFSKY, 1913, p. 342, pl. 33, fig. 1

Clathrocanium cf. coronatum Popofsky. - BENSON, p. 394, pl. 26, figs. 1,2

Clathrocanium ornatum POPOFSKY, 1913, p. 343, pl. 33, fig. 2

Remarks: Apical horn straight, three bladed and its branches are connected with fine strands extending from cephalis and thorax. The apical horn differs from a fenestrated and denticulate horn of C. diadema which is present at E station.

Clathrocanium diadema Haeckel

Clathrocorona diadema HAECKEL, 1881, p. 431

Clathrocanium diadema HAECKEL, 1887, p. 1212, pl. 64, fig. 2. - POPOFSKY, 1913, pl. 32, fig. 4. - MCMILLEN and CASEY, 1978, pl. 5, fig. 5. - TAKAHASHI and HONJO, 1981, p. 151, pl. 7, fig. 8

Genus CALLIMITRA Haeckel, 1881

Callimitra emmae Haeckel
Plate 26, figure 14

Callimitra emmae HAECKEL, 1887, p. 1218, pl. 63, figs. 3,4. - BENSON, 1966, p. 390, pl. 25, fig. 12. - TAKAHASHI and HONJO, 1981, p. 151, pl. 7, fig. 11

Remarks: This species differs from *C. annae* in absence of the marginal frame of dense geometric meshwork. Beams extending from cephalis toward margins commonly cross each other near the end.

Callimitra annae Haeckel
Plate 26, figure 15

Callimitra annae HAECKEL, 1887, p. 1217, pl. 63, fig. 2

Callimitra agnesae HAECKEL, 1887, p. 1217, pl. 63, fig. 5

Callimitra elisabethae HAECKEL, 1887, p. 1218, pl. 63, fig. 6. - TAKAHASHI and HONJO, 1981, p. 151, pl. 7, figs. 9-10

Callimitra sp. - RENZ, 1976, p. 162, pl. 7, fig. 1

Remarks: Note presence of a laterally extending tubule from a middle part of the cephalis. The cephalis is made of this solid sheet rather than meshwork. Transverse beams of this species rarely cross each other whereas they commonly cross in *C. emmae*. The present species resembles the type species of this genus, *C. carolotae* Haeckel (1887, p. 1217, pl. 63, figs. 1,7,8) but differs in presence of basal marginal dense meshwork. Specimens like *C. carolotae* have not been observed here and hence it is not included in the synonymy. However, it is quite possible that it may become the name of this species depending on future studies. Sinking experiments show that specimens of this species typically settle in the water column upside down with respect to the orientation of the micrograph in the plate. This is common to most nassellarian species.

Callimitra solocicribrata n.sp.
Plate 27, figures 10-11

Description: Cephalis hemispherical made of thin wall combined with meshwork similar to that of *C. annae*; a tubule on the cephalis similar to *C. giltschii*. Three vertical wings are made of much coarser irregular polygonal meshwork than those of *C. annae* and without conspicuous transverse beams. Thorax pyramidal in the upper half (cephalis side) and become cylindrical near the basal opening; mesh size finer than that of the vertical wings. Terminal ends of spines dented from the vertical wings.

Dimensions: (6 specimens) Cephalis width: 40-80 μm; Length between two terminal ends of divergent spines: 180-215 μm; Height (top of apical horn to thorax opening): 235-380 μm; Apical spine length: 132-182 um.

Type locality: 5°21'N, 81°53'W Sediment trap depth 3791 m. Collected during August-December 1979.

Remarks: Considerable difference in size has been observed.

Derivation of name: The name of this species is the Latin meaning having the nature of a coarse sieve.

Genus CLATHROCORYS Haeckel, 1881

Clathrocorys giltschii Haeckel
Plate 26, figure 16, Plate 27, figures 1-3,9

Clathrocorys giltschii HAECKEL, 1887, p. 1220, pl. 64, fig. 9

Clathrocorys teuscheri HAECKEL, 1887, p. 1220, pl. 64, fig. 10

Clathrocorys sp. - RENZ, 1976, p. 163, pl. 7, fig. 4a (partim)

Remarks: This species is present at P_1 and PB stations (Pacific) but not at E station (Atlantic).

Clathrocorys murrayi Haeckel
Plate 27, figures 4-8

Clathrocorys murrayi HAECKEL, 1887, p. 1219, pl. 64, fig. 8. - POPOFSKY, 1913, p. 352, text-fig. 57, pl. 32, figs. 2,3. - BENSON, 1966, p. 391, pl. 25, figs. 13-15

Clathrocorys sp. - RENZ, 1976, p. 163, pl. 7, fig. 4b (partim)

Family ACANTHODESMIIDAE Haeckel, 1862, emend. Riedel, 1971

Definition: Nassellaria possessing a sagital ring.

Genus ZYGOCIRCUS Butschli, 1882

Zygocircus capulosus Popofsky

Zygocircus capulosus POPOFSKY, 1913, p. 287, pl. 28, fig. 4. - RENZ, 1976, p. 169, pl. 8, fig. 6. - TAKAHASHI and HONJO, 1981, p. 151, pl. 7, fig. 12

Zygocircus productus (Hertwig) group
Plage 27, figures 13-14

Lithocircus productus HERTWIG, 1879, p. 197, pl. 12(7), fig. 4

Zygocircus productus (Hertwig). - PETRUSHEVSKAYA, 1971c, p. 281, fig. 16: II, 145: 10,11. - BOLTOVSKOY and RIEDEL, 1980, p. 121, pl. 4, fig. 17. - TAKAHASHI and HONJO, 1981, p. 151, pl. 7, figs. 13-14

Zygocircus cf. *piscicaudatus* Popofsky
Plate 27, figure 18

Zygocircus piscicaudatus POPOFSKY, 1913, p. 287, pl. 28, fig. 3

Zygocircus sp. cf. *Z. piscicaudatus* Popofsky. - RENZ, 1976, p. 171, pl. 8, fig. 3. - TAKAHASHI and HONJO, 1981, p. 151, pl. 7, fig. 15

Genus ACANTHODESMIA Müller, 1857

Acanthodesmia vinculatus (Müller)
Plate 28, figures 6-8

Lithocircus vinculata MÜLLER, 1857, p. 484

Acanthodesmia vinculata MÜLLER, 1858a, p. 30, pl. 1, figs. 4-7. - PETRUSHEVSKAYA, 1971c, p. 278, figs. 143, I-VII; 144, I-VI. - LING, 1972, p. 169, pl. 1, fig. 6. - BOLTOVSKOY and RIEDEL, 1980, p. 120, pl. 4, fig. 12. - TAKAHASHI and HONJO, 1981, p. 151, pl. 7, figs. 18,19

Eucoronis nephrospyris HAECKEL, 1887, p. 977, pl. 82, fig. 5. - BENSON, 1966, p. 304, pl. 21, figs. 6-8

Eucoronis angulata HAECKEL, 1887, p. 978, pl. 82, fig. 3

Eucoronis challengeri HAECKEL, 1887, p. 978, pl. 82, fig. 4

Giraffospyris angulata (Haeckel). - GOLL, 1969, p. 331, pl. 59, figs. 4,6,7,9, text-fig. 2. - RENZ, 1976, p. 167, pl. 8, fig. 5. - NIGRINI and MOORE, 1979, p. N11, pl. 19, figs. 2a-d, 3a,b

Genus LOPHOSPYRIS Haeckel, 1881, emend. Goll, 1977

Lophospyris juvenile form group
Plate 28, figures 1-4

Remarks: This juvenile group includes at least L. pentagona pentagona, L. pentagona hyperborea but not L. pentagona quadriforis.

Lophospyris pentagona (Ehrenberg) quadriforis (Haeckel), emend. Goll, 1977
Plate 28, figure 5

Semantrum quadrifore HAECKEL, 1887, p. 958, pl. 92, fig. 5

Lophospyris pentagona quadriforis (Haeckel). - GOLL, 1977, p. 398-400, pl. 13, figs. 1-13, pl. 14, figs. 1-3,7,10,13

For a more complete synonymy see Goll (1977).

Lophospyris pentagona pentagona (Ehrenberg) emend. Goll, 1977
Plate 28, figures 9-14

Ceratospyris pentagona EHRENBERG, 1872a, p. 303; 1872b, p. 302, pl. 15, fig. 15

Ceratospyris allmersii HAECKEL, 1887, p. 1067, pl. 86, fig. 3

Ceratospyris strasburgeri HAECKEL, 1887, p. 1067, pl. 86, fig. 2

Ceratospyris polygona Haeckel. - BENSON, 1966, p. 321-324, pl. 22, figs. 15-16 (partim)

Ceratospyris sp. - NIGRINI, 1967, p. 48-49, pl. 5, fig. 6. - RENZ, p. 172, pl. 8, fig. 8

Dorcadospyris pentagona (Ehrenberg). - Goll, 1969, p. 338-339, pl. 59, figs. 1-3,5. - LING, 1972, p. 168, pl. 2, fig. 5

Lophospyris pentagona pentagona (Ehrenberg). - GOLL, 1977, p. 384,398, pl. 10, figs. 1-7; pl. 11, figs. 1-3,5. - NIGRINI and MOORE, 1979, p. N15, pl. 19, fig. 5. - TAKAHASHI and HONJO, 1981, p. 151, pl. 7, figs. 20,21

Lophospyris pentagona (Ehrenberg) *hyperborea* (Jørgensen), emend. Goll,1977
Plate 29, figures 1-3, 5-10

Ceratospyris hyperborea JORGENSEN, 1905, p. 130-131, pl. 13, fig. 49. - GOLL and BJØRKLUND, 1971, p. 449, text-fig. 7

Ceratospyris polygona Haeckel. - POPOFSKY, 1913, p. 305-308, pl. 30, fig. 1 (partim). - BENSON, 1966, p. 321-324, pl. 22, figs. 17-18 (partim)

Ceratospyris sp. A. - RENZ, 1976, p. 173, pl. 8, fig. 9

Lophospyris pentagona hyperborea (Jørgensen), emend. GOLL, 1977, p. 400, pl. 14, figs.4-6, 8-9, 11-12; pl. 15, figs. 1-12. - TAKAHASHI and HONJO, 1981, p. 152, pl. 7, figs. 22-26

Lophospyris cheni Goll
Plate 29, figure 4

Lophospyris cheni GOLL, 1977, p. 402, pl. 11, fig. 4, pl. 12, figs. 1-7

Genus TRIPODOSPYRIS Haeckel, 1881

Tripodospyris sp.

Tripodospyris sp.-TAKAHASHI and HONJO, 1981, p. 152, pl. 7, fig. 27

Genus PHORMOSPYRIS Haeckel, 1881, emend. Goll, 1977

Phormospyris stabilis (Goll) scaphipes (Haeckel)
Plate 29, figures 11-12,14

Tholospyris scaphipes (Haeckel). - GOLL, 1969, p. 328-329, pl. 58, figs. 1-6 (partim)

Tristylospyris scaphipes Haeckel. - BENSON, 1966, p. 316-321, pl. 22, figs. 7,9-10

Phormospyris stabilis scaphipes (Haeckel). - GOLL, 1977, p. 394, pl. 8, figs. 1-15, pl. 9, figs. 1-5

Fora a more complete synonymy see Goll (1977).

Phormospyris sp. aff. L. pentagona hyperborea (Jorgensen)
Plate 29, figure 13

Remarks: Characteristic spines on basal ring are conical and connected at the bases to adjacent other spines so that they become flare-shaped. Usually specimens are robust.

Phormospyris stabilis (Goll) capoi Goll
Plate 29, figures 15-18

Rhodospyris sp. - BENSON, 1966, p. 329-331, pl. 23, figs. 3-5

Phormospyris stabilis capoi GOLL, 1977, p. 392, pl. 5, figs. 1-2, pl. 6, figs. 1-13, pl. 7, figs. 1-9

Phormospyris stabilis stabilis (Goll)
Plate 30, figures 2-5

Desmospyris anthocyrtoides (Butschli). - BENSON, 1966, p. 324-334, pl. 23, figs. 6-8

Dendrospyris stabilis GOLL, 1968, p. 1422-1423, pl. 173, figs. 16-18,20

Phormospyris stabilis (Goll) stabilis GOLL, 1977, p. 390, pl. 1, figs. 1-13, pl. 2, figs. 7-14. - KLING, 1979, p. 309, pl. 1, fig. 18.

For a more complete synonymy see Goll (1977).

Phormospyris ? sp.
Plate 30, figure 6

Genus DICTYOSPYRIS Ehrenberg, 1847b

Dictyospyris sp. group
Plate 30, figure 1

Dictyospyris sp. B. - TAKAHASHI and HONJO, 1981, p. 152, pl. 7, fig. 29

Genus NEPHROSPYRIS Haeckel, 1881

Nephrospyris renilla renilla Haeckel
Plate 30, figures 7-9

Nephrospyris renilla HAECKEL, 1887, p. 1101, pl. 90, figs. 9,10. - RENZ, 1976, p. 176, pl. 8, fig. 18

Nephrodictyum renilla (Haeckel). - BENSON, 1966, p. 302-304, pl. 21, fig. 5

Nephrospyris renilla renilla Haeckel. - GOLL, 1980, p. 437, pl. 5, fig. 2

Nephrospyris renilla Haeckel *lana* Goll
Plate 30, figure 10

Nephrospyris renilla lana GOLL, 1980, p. 438, pl. 5, fig. 1

Genus ANDROSPYRIS Haeckel, 1887

Androspyris reticulidisca n.sp.
Plate 30, figures 12-14

Description: Shell flat disc with two branching feet and a sagital ring of ca. 1/5 - 1/4 as long as longitudinal shell length; meshwork with pores of irregular and polygonal shape and increasing in size toward margin where a thick skeletal frame is present. An apical spine small when present.

Dimensions: (20 specimens) Longitudinal length (excluding an apical spine and feet): 363 ± 45 µm (2 S.D.); Width: 336 ± 19 µm (2 S.D.).

Type locality: 5°21'N, 81°53'W Sediment trap depth 3791 m. Collected during August-December 1979.

Remarks: This species has finer mesh size and a proportionally smaller sagital ring than A. huxleyi does. The former is discoidal and has a thick marginal frame whereas the latter is renticular and does not have such a thick frame.

Derivation of name: The name of this species is the Latin meaning a net-like disc.

Androspyris huxleyi (Haeckel)
Plate 30, figures 15-16

Lamprospyris huxleyi HAECKEL, 1887, p. 1094, pl. 89, fig. 14

Androspyris huxleyi (Haeckel). - GOLL, 1980, p. 436, pl. 4, figs. 4,5

Androspyris ramosa (Haeckel)
Plate 31, figures 1-2

Tholospyris ramosa HAECKEL, 1887, p. 1079, pl. 89, fig. 3

? Tholospyris cupola HAECKEL, 1887, p. 1080, pl. 89, fig. 4

Tholospyris fornicata POPOFSKY, 1913, p. 309, pl. 30, fig. 2. - RENZ, 1976, p. 177, pl. 8, fig. 15. - TAKAHASHI and HONJO, 1981, p. 152, pl. 7, fig. 30

? Tripospyris semantis HAECKEL, 1887, p. 1026, pl. 84, fig. 2

? Tripospyris diomma HAECKEL, 1887, p. 1026, pl. 84, fig. 5

Remarks: Under the present observation A. ramosa and T. fornicata are indistinguishable.

Genus CEPHALOSPYRIS Haeckel, 1881

Cephalospyris cancellata Haeckel
Plate 31, figures 3-4

Cepholospyris cancellata HAECKEL, 1887, p. 1035, pl. 83, fig. 10

Genus CANTHAROSPYRIS Haeckel, 1887

Cantharospyris platybursa Haeckel
Plate 31, figure 5

Cantharospyris platybursa HAECKEL, 1887, p. 1051, pl. 53, fig. 7. - RENZ, 1976, p. 171, pl. 8, fig. 10. - TAKAHASHI and HONJO, 1981, p. 152, pl. 7, fig. 32

Cantharospyris cf. clathrobursa (Haeckel)

Tessarospyris clathrobursa HAECKEL, 1887, p. 1045, pl. 53, fig. 8

Cantharospyris cf. clathrobursa (Haeckel). - TAKAHASHI and HONJO, 1981, p. 152, pl. 7, fig. 32

Genus THOLOSPYRIS Haeckel, 1881, emend. Goll, 1969

Tholospyris sp. group
Plate 27, figures 15-17

Remarks: The following taxa are included in this group: Unnamed transition specimens between Tholospyris baconiana spinula and Tholospyris rhombus (Goll, 1972a, pl. 15, figs. 1-11); Tholospyris rhombus (Haeckel)(Goll, 1972a, p. 455, pl. 16, figs. 1-11); Tholospyris sp. (TAKAHASHI and HONJO, 1981, p. 152, pl. 7, fig. 16).

Tholospyris baconiana baconiana (Haeckel)
Plate 31, figures 6-7

Tricolospyris baconiana HAECKEL, 1887, p. 1098, pl. 88, fig. 8

Tholospyris baconiana baconiana (Haeckel). - GOLL, 1972a, p. 451, pl. 1, figs. 7-9; pl. 2, figs. 1-8; pl. 4, figs. 1-4; pl. 5, figs. 1-3

Tholospyris baconiana (Haeckel) variabilis Goll
Plate 31, figure 8

Tholospyris baconiana variabilis GOLL, 1972a, p. 452, pl. 8, figs. 1-8; pl. 9, figs. 1-12

Tholospyris baconiana baconiana (Haeckel). - TAKAHASHI and HONJO, 1981, p. 151, pl. 8, fig. 3

Tholospyris macropora (Popofsky)
Plate 31, figure 9

Phormospyris macropora POPOFSKY, 1913, p. 310, pl. 30, fig. 3

Tholospyris baconiana cf. variabilis Goll. - TAKAHASHI and HONJO, 1981, p. 151, pl. 8, fig. 4

Genus LIRIOSPYRIS Haeckel, 1881, emend. Goll, 1968

Liriospyris sp.
Plate 30, figure 11

Description: Similar to L. thorax laticapsa including shape, size and position of sagital ring and its branches, but differs in mesh size and robust outer framework which is the extension of the sagital branches which encloses the mesh.

Liriospyris thorax (Haeckel) laticapsa n. subsp.
Plate 31, figures 10-11,13

Amphispyris toxarium Haeckel. - BENSON, 1966, p. 293-297, pl. 20, figs. 3,5-6 (partim)

Description: Sagital ring thick and similar shape to that of L. thorax (Haeckel) whose cross section look like a clover leaf; the ring is proportionally smaller compared to L. reticulata and as along as 1/3 of shell height. Major branches from the sagital ring thick and branch further and spread out fine surface meshwork made of irregular polygons with pores of equal to 3 times as broad as sagital ring thickness. The meshwork forms crests between the branches on lateral side. The meshwork wraps the sagital ring and branch system. Shape of the shell is more or less rectangular prism and length/width ratio is similar to reciprocal of that of L. reticulata.

Dimensions: (8 specimens) length: 160-280 µm; width: 195-360 µm; width/length ratio: 1.15-1.35.

Type locality: 5°21'N, 81°53'W Sediment trap depth 3791 m. Collected during August-December 1979.

Remarks: The name of this subspecies is the Latin meaning a wide box.

Liriospyris thorax thorax (Haeckel)
Plate 31, figure 12

Amphispyris thorax HAECKEL, 1887, p. 1096, pl. 88, fig. 4

Liriospyris reticulata (Ehrenberg)
Plate 31, figures 14-16

Dictyospyris reticulata EHRENBERG, 1872a, p. 307, 1872b, p. 289, pl. 10, fig. 19

Amphispyris costata HAECKEL, 1887, p. 1097, pl. 88, fig. 3. - NIGRINI, 1967, p. 45, pl. 5, fig. 4. - MCMILLEN and CASEY, 1978, pl. 5, fig. 9. - TAKAHASHI and HONJO, 1981, p. 152, pl. 8, figs. 1-2

Amphispyris reticulata (Ehrenberg). - NIGRINI, 1967, p. 44, pl. 5, fig. 3

Liriospyris reticulata (Ehrenberg). - GOLL, 1968, p. 1429, pl. 176, figs. 9,11,13; 1972b, p. 967, pl. 71, fig. 1. - NIGRINI and MOORE, 1979, p. N13, pl. 19, figs. 4a-b. - JOHNSON and NIGRINI, 1980, p. 127, pl. 3, fig. 2

For a complete synonymy see Goll (1968).

Family SETHOPHORMIDIDAE Haeckel, 1881, emend. Petrushevskaya, 1971d

Definition: Plagiacanthoidea with flat cephalic skeleton. Thorax, if present, in the shape of an umbrella. Cephalis large, in the form of a tent; with thin walls. The walls of the cephalis are separated from those of the thorax by arches. Pores on the cephalis and on the thorax are different in size and shape (Petrushevskaya, 1971d).

Genus TETRAPHORMIS Haeckel, 1881

Tetraphormis rotula (Haeckel)
Plate 32, figures 1-3

Sethophormis rotula HAECKEL, 1887, p. 1246, pl. 57, fig. 9. - RENZ, 1976, p. 166, pl. 7, fig. 14. - TAKAHASHI and HONJO, 1981, p. 152, pl. 8, fig. 6 (non. fig. 7)

Tetraphormis dodecaster (Haeckel)
Plate 32, figure 7

Sethophormis dodecaster HAECKEL, 1887, p. 1248, pl. 56, fig. 12

Sethophormis cf. dodecaster Haeckel. - TAKAHASHI and HONJO, 1981, p. 152, pl. 8, fig. 8

Tetraphormis butschlii (Haeckel)
Plate 32, figure 6

Dictyophimus butschlii HAECKEL, 1887, p. 1201, pl. 60, fig. 2. - TAKAHASHI and HONJO, 1981, pl. 8, fig. 14

Remarks: The three divergent spines are usually long as Haeckel illustrated. The author proposes to place this species in the genus Tetraphormis.

Genus THEOPHORMIS Haeckel, 1881

Theophormis callipilium Haeckel
Plate 32, figures 9-12

Theophormis callipilium HAECKEL, 1887, p. 1367, pl. 70, figs. 1-3

Sethophormis umbrella HAECKEL, 1887, p. 1248, pl. 70, figs. 4,5

Sethophormis aurelia HAECKEL, 1887, p. 1248, pl. 55, fig. 3. - RENZ, 1976, p. 165, pl. 7, fig. 16

Remarks: Some specimens show faint radial ribs especially in basal view. The number and curvature of the ribs vary among the specimens. Illustrations of T. callipilium by Haeckel represent the best for this taxon and hence the name is selected here.

Genus LAMPROMITRA Haeckel, 1881

Lampromitra schultzei (Haeckel)
Plate 32, figures 4-5

Eucecryphalus schultzei HAECKEL, 1862, p. 309, pl. 5, figs. 16-19; 1887, p. 1216

Lampromitra coronata HAECKEL, 1887, p. 1214, pl. 60, fig. 7

? Sethophormis pentalactis HAECKEL, 1887, p. 1244, pl. 56, fig. 5. - RENZ, 1976, p. 165, pl. 7, fig. 7. - TAKAHASHI and HONJO, 1981, p. 152, pl. 8, fig. 5

(non) Lampromitra coronata Haeckel. - KEANY, 1979, p. 56, pl. 4, fig. 10, pl. 5, fig. 14

Lampromitra cracenta n. sp.
Plate 32, figure 8

Lampromitra cf. coronata Haeckel. - BENSON, 1966, p. 452, pl. 30, figs. 9,10 (only) (partim)

Description: Cephalis cap-shaped with small pores. Thorax with three ribs which penetrate the perimeter and form spines and with coarse irregular polygonal mesh; marginal mesh forms a zone of fine mesh with small circular to subcircular pores. Number of short spines on the perimeter is about 30 and they are conical. The perimeter of the thorax is an irregularly curved circle.

Dimension: (5 specimens) Thorax diameter: 153-164 µm

Type locality: 5°21'N, 81°53'W, Sediment trap depth 3791 m. Collected during August-December 1979.

Remarks: This species is rare at PB station.

Derivation of name: The name of this species is the Latin meaning graceful.

Lampromitra *cachoni* Petrushevskaya
Plate 33, figures 2-3

Lampromitra ? sp. - DZINORIDZE et al., 1976, pl. 33, fig. 10

Lampromitra *cachoni* PETRUSHEVSKAYA and KOZLOVA, 1979, p. 128, text-figs. 362, 363, 497

? *Lampromitra* *erosa* CLEVE, 1900, p. 10, pl. 4, figs. 2,3. - DUMITRICA, 1972, p. 838, pl. 24, figs. 8,9

Lampromitra *spinosiretis* n. sp.
Plate 34, figures 1-2,7

Helotholus *histricosa* Jorgensen. - BENSON, 1966, p. 459, pl. 31, figs. 6,7 (only) (partim)

Description: Cephalis hemispherical with several short and long spines of up to thorax length and with circular pores. Thorax conical net-shaped and similar to *L. cachoni* but has coarser circular to hexagonal meshwork. Radial ribs absent in most specimens. The margin of the thorax thorny.

Dimensions: (8 specimens) Thorax diameter: 175-280 µm; Diameter of pores next to marginal thorns: 20-35 µm

Type locality: 5°21'N, 81°53'W, Sediment trap depth 3791 m. Collected during August-December 1979

Remarks: This species has slightly convex cone, coarse mesh and many spines on the cephalis whereas *L. cachoni* has flatter and slightly concave cone, fine mesh and a few short spines on the cephalis.

Derivation of name: The name of this species is the Latin meaning a thorny net.

Genus EUCECRYPHALUS Haeckel, 1860

Eucecryphalus sp.
Plate 33, figure 1

Remarks: This species resembles *T. gegenbauri* but differs in detail of marginal meshwork.

Eucecryphalus tricostatus (Haeckel)
Plate 33, figures 4,6

Theopilium tricostatum HAECKEL, 1887, p. 1322, pl. 70, fig. 6. - POPOFSKY, 1913, p. 375, pl. 37, fig. 6. - BENSON, 1966, p. 444, pl. 30,figs. 1,2. - TAKAHASHI and HONJO, 1981, p. 152, pl. 8, fig. 12

? *Corocalyptra elisabethae* HAECKEL, 1887, p. 1323, pl. 59, fig. 10

? *Corocalyptra agnesae* HAECKEL, 1887, p. 1323, pl. 59, fig. 3

Remarks: The author proposes to put this taxon into the present genus.

Eucecryphalus sestrodiscus (Haeckel)
Plate 33, figures 5,7-8

Cecryphalium sestrodiscus HAECKEL, 1887, p. 1399, pl. 58, fig. 1

Theocalyptra sp. - RENZ, 1976, p. 137, pl. 5, fig. 13

Eucecryphalus gegenbauri Haeckel
Plate 33, figures 13-15

Eucecryphalus gegenbauri HAECKEL, 1860b, p. 836; 1862, p. 308, pl. 5, figs. 12-15; 1887, p. 1222. - HERTWIG, 1879, p. 76, pl. 8, figs. 5,5a,b.

Clathrocyclas danaes HAECKEL, 1887, p. 1388, pl. 59, figs. 13,14. - TAKAHASHI and HONJO, 1981, p. 152, pl. 8, fig. 13

Clathrocyclas alcmenae HAECKEL, 1887, p. 1388, pl. 59, fig. 6

? Clathrocyclas latonae HAECKEL, 1887, p. 1389, pl. 59, fig. 7

Clathrocyclas ionis HAECKEL, 1887, p. 1389, pl. 59, fig. 9

Corocalyptra gegenbauri (Haeckel). - POPOFSKY, 1913, p. 384, pl. 34, figs. 1,2

Theocalyptra gegenbauri - BOLTOVSKOY and RIEDEL, 1980, p. 126, pl. 5, fig. 18 (partim)

Remarks: Mesh size and morphology of the outermost circle varies significantly.

Eucecryphalus europae (Haeckel)
Plate 34, figures 5-6

Clathrocyclas europae HAECKEL, 1887, p. 1388, pl. 59, figs. 11, 12

Eucecryphalus clinatus n.sp.
Plate 35, figures 1-2

Eucecryphalus sp. - BENSON, 1966, p. 450, pl. 30, figs. 6,7. - RENZ, 1976, p. 130, pl. 5, fig. 3

Description: Cephalis hemispherical with small pores and spines. Thethorax smooth and characteristically beret-shaped with regular hexagonal meshwork whose pores are 2-5 times as wide as interporous bars. There are 11-14 rows of pores in thorax in the longest meridian.

Dimensions: (11 specimens) Minimum diameter: 120-145 um; maximum diameter: 150-175 um.

Type locality: $5^{o}21'$N, $81^{o}53'$W, Sediment trap depth 2869 m. Collected during August-December 1979.

Remarks: This species is abundant at PB Station.

Derivation of name: The name of this species is the Latin meaning slanted.

Genus COROCALYPTRA Haeckel, 1887

Corocalyptra cervus (Ehrenberg)
Plate 33, figures 9-12

Eucyrtidium cervus EHRENBERG, 1872b, p. 291, pl. 9, fig. 21

Corocalyptra cervus (Ehrenberg). - POPOFSKY, 1913, p. 383, pl. 34, fig. 3. - BENSON, 1966, p. 447, pl. 30, figs. 3-5. - RENZ, 1976, p. 129, pl. 5, fig. 2

For a more complete synonymy see BENSON (1966).

Genus PHRENOCODON Haeckel, 1887

Phrenocodon clathrostomium Haeckel
Plate 34, figures 3-4

Phrenocodon clathrostomium HAECKEL, 1887, p. 1434, pl. 70, figs. 7, 8

Genus CLATHROCYCLAS Haeckel, 1881

Clathrocyclas sp.
Plate 34, figure 8

Description: Cephalis cap-shaped with small apical spine and fine pores. Thorax conical, dilated and made of very thick skeleton. Pores on the thorax circular and smaller than interporous bars adjacent to cephalis and increasing their size and become elliptical toward the dilated opening.

Clathrocyclas monumentum (Haeckel)
Plate 34, figures 9-11

Calocyclas monumentum HAECKEL, 1887, p. 1385, pl. 73, fig. 9. - RENZ, 1976, p. 128, pl. 5, fig. 1

Clathrocyclas ? sp. - BENSON, 1966, p. 457, pl. 31, figs. 2,3

Remarks: The apical spine is a conical rod but not three bladed. The author proposes to put this species in the present genus because that it resembles to many species of Clathrocyclas (e.g. C. caassiopejae listed below), although it does not very much like the type species of the genus, C. principessa Haeckel (1887, p. 1386, pl. 74, fig. 7).

Clathrocyclas cassiopejae Haeckel
Plate 34, figures 12-14

Clathrocyclas cassiopejae HAECKEL, 1887, p. 1390, pl. 59, fig. 5

Family THEOPERIDAE Haeckel, 1881, emend. Riedel, 1967a

Definition by Riedel (1967a): Cephalis relatively small, approximately spherical, often poreless or sparsely perforate, the internal spicule, homologous with that of plagoniids, reduced to a less conspicuous structural element than in the latter group.

Subfamily PLECTOPYRAMIDINAE Haecker, 1908a, emend. Petrushevskaya, 1971d

Definition by Petrushevskaya (1971d): Encyrtidiidae with a small dome-shaped cephalis and a vast thorax. Cephalis consists of the encephalic part only, poreless. Thorax sometimes with the upper part poreless. The pores on its middle and lower part quadrangular, disposed in longitudinal rows. Internal spines nearly reduced.

Genus CORNUTELLA Ehrenberg, 1838

Cornutella profunda Ehrenberg
Plate 35, figures 3-9

Cornutella profunda EHRENBERG, 1858, p. 31. - NIGRINI, 1967, p. 60, pl. 6, figs. 5a-5c. - RENZ, 1976, p. 149, pl. 7, fig. 11. - KLING, 1979, p. 309, pl. 1, fig. 21. - BOLTOVSKOY and RIEDEL, 1980, p. 123, pl. 5, fig, 6. - TAKAHASHI and HONJO, 1981, p. 152, pl. 8, fig. 9

Remarks: Significant variations in skeletal thickness and apical spine length have been observed.

Genus PERIPYRAMIS Haeckel, emend. Riedel, 1958

Peripyramis circumtexta Haeckel
Plate 35, figures 10-13

Peripyramis circumtexta HAECKEL, 1887, p. 1162, pl. 54, fig. 5. - RIEDEL, 1958, p. 231, pl. 2, figs. 8,9. - BENSON, 1966, p. 426, pl. 29, fig. 4. - NIGRINI and MOORE, 1979, p. N29, pl. 21, figs. 4a,b. - TAKAHASHI and HONJO, 1981, p. 152, pl. 8, figs. 10-11

Genus LITHARACHNIUM Haeckel, 1860b

Litharachnium tentorium Haeckel
Plate 35, figures 14-18

Litharachnium tentorium HAECKEL, 1860b, p. 836; 1862, p. 281, pl. 4, figs. 7-10; CASEY, 1971, p. 341, pl. 23.3, fig. 11. - RENZ, 1976, p. 150, pl. 7, fig. 6. - BOLTOVSKOY and RIEDEL, 1980, p. 125, pl. 5, fig. 14

Litharachnium eupilium (Haeckel)
Plate 36, figures 1-4

Sethophormis eupilium Haeckel, 1887, p. 1247, pl. 56, fig. 9

Remarks: This species is placed in Litharachnium because of its affinity to L. tentorium.

Subfamily EUCYRTIDIINAE Ehrenberg, 1847b, emend. Petrushevskaya, 1971d

Definition by Petrushevskaya (1971d): Eucyrtidiidae with a cephalis in which only the encephalic part is well developed. Very often it looks like a ball with thick, rough walls. The apical spine forms an apical horn, and the vertical spine may form a small occipital horn. Sometimes they are followed by tubes. The dorsal and lateral spines form the so-called feet. The postthoracic segments may be reduced or consist only of the abdomen. The pores are numerous, disposed in a checkerboard order.

Genus ARCHIPILIUM Haeckel, 1881

Archipilium sp. aff. A. orthopterum Haeckel
Plate 36, figures 5,7

See Archipilium orthopetrum HAECKEL, 1887, p. 1139, pl. 98, fig. 7

Archipilium macropus ? (Haeckel)
Plate 36, figure 6

Sethopilium macropus HAECKEL, 1887, p. 1203, pl. 97, fig. 9

Archipilium spp. aff. A. macropus. - PETRUSHEVSKAYA and KOZLOVA, 1972, p. 553 (partim), pl. 29, figs. 13,14

Genus PTEROSCENIUM Haeckel, 1881

Pteroscenium pinnatum Haeckel
Plate 36, figures 8-9

Pteroscenium pinnatum HAECKEL, 1887, p. 1152, pl. 53, figs. 14-16

Verticillata hexacantha POPOFSKY, 1913, p. 282, text-fig. 11. - BENSON, 1966, p. 397, pl. 26, fig. 3. - RENZ, 1976, p. 161, pl. 6, fig. 5

Genus PTEROCANIUM Ehrenberg, 1847a

Pterocanium trilobum (Haeckel)
Plate 36, figures 10-11

Dictyopodium trilobum HAECKEL, 1860b, p. 839

Pterocanium trilobum (Haeckel). - NIGRINI, 1967, p. 71, pl. 7, figs. 3a,b. - KLING, 1979, p. 311, pl. 2, fig. 13. - NIGRINI and MOORE, 1979, p. N45, pl. 23, figs. 4a-c. - BOLTOVSKOY and RIEDEL, 1980, p. 126, pl. 5, fig. 15. - JOHNSON and NIGRINI, 1980, p. 129, pl. 3, fig. 12.- (non RENZ, 1976, p. 135, pl. 5, fig. 17)

Pterocanium grandiporus Nigrini
Plate 36, figures 12-13

Pterocanium grandiporus NIGRINI, 1968, p. 57, pl. 1, fig. 7. - NIGRINI and MOORE, 1979, p. N47, pl. 23, fig. 5

Pterocanium praetextum praetextum (Ehrenberg)
Plate 36, figures 15-18

Lychnocanium praetextum EHRENBERG, 1872a, p. 316; 1872b, p. 297, pl. X, fig. 2

Pterocanium praetextum (Ehrenberg). - HAECKEL, 1887, p. 1330, . TAKAHASHI and HONJO, 1981, p. 153, pl. 9, figs. 5,6

Pterocanium praetextum praetextum (Ehrenberg). - NIGRINI, 1967, p. 68, pl. 7, fig. 1. - NIGRINI and MOORE, 1979, p. N41, pl. 23, fig. 2. - JOHNSON and NIGRINI, 1980, p. 127, pl. 3, fig. 10

Pterocanium praetextum (Ehrenberg) aff. eucolpum Haeckel
Plate 36, figure 14

Pterocanium eucolpum HAECKEL, 1887, p. 1322, pl. 73, fig. 4

Pterocanium praetextum (Ehrenberg) eucolpum Haeckel. - NIGRINI, 1967, p. 70, pl. 7, fig. 2. - KLING, 1979, p. 311, pl. 2, figs. 14-16. - NIGRINI and MOORE, 1979, p. N43, pl. 23, fig. 3. - JOHNSON and NIGRINI, 1980, p.127, pl. 3, fig. 11

Genus DICTYOPHIMUS Ehrenberg, 1847a

Dictyophimus sp. A
Plate 37, figure 1

Description: Cephalis nearly spherical with very fine pores and a stout conical apical horn of 2-3 times its length. Three divergent wing-like spines three sided (but not bladed) with grooves. Stout, slightly curved downward and slightly longer than thorax's transverse diameter. Thorax conical with small regular circular pores of narrower than its interporous bars and with numerous accessory spines. Abdomen stout and nearly cylindrical with large circular to hexagonal pores of 4-6 times its interporous bar thickness.

Dictyophimus crisiae Ehrenberg
Plate 37, figure 2

Dictyophimus crisiae EHRENBERG, 1854a, p. 241. - NIGRINI, 1967, p. 66, pl. 6, figs. 7a,b. - NIGRINI and MOORE, 1979, p. N33, pl. 22, figs. 1a,b. - JOHNSON and NIGRINI, 1980, p. 127, pl. 3, fig. 9

Pterocorys hirundo HAECKEL, 1887, p. 1318, pl. 71, fig. 4. - LING et al., 1971, p. 715, pl. 2, figs. 8,9

? Pterocorys sp. - BENSON, 1966, p. 412, pl. 28, fig. 4 (partim)

Dictyophimus infabricatus Nigrini
Plate 37, figures 3-5

Dictyophimus infabricatus NIGRINI, 1968, p. 56, pl. 1, fig. 6. - NIGRINI and MOORE, 1979, p. N37, pl. 22, fig. 5

Dictyophimus macropterus (Ehrenberg)
Plate 39, figures 8-11

Lithomelissa macroptera EHRENBERG, 1875, p. 78 (partim), pl. 3, figs. 9-10 (only)

Carpocanarium sp. - RIEDEL and SANFILIPPO, 1971, p. 1599, pl. 1I, fig. 21. - RENZ, 1976, p. 117, pl. 4, fig. 4

Remarks: Some specimens show characteristic shell surface ornamentation like ripple marks (e.g. pl. 39, fig. 9).

Dictyophimus sp. B
Plate 39, figure 12

Pterocorys cf. columba Haeckel. - BENSON, 1966, p. 414, pl. 28, fig. 7

Remarks: Three divergent spines extending obliquely downward from the thorax are as long as the length from tip of apical spine to end of abdomen. This species resembles illustrations of *P. hirundo* and *D. insectum* by Haeckel (1887, pl. 71, figs. 4,5).

Genus PSEUDODICTYOPHIMUS Petrushevskaya, 1971c

Pseudodictyophimus gracilipes (Bailey)
Plate 37, figures 12-14

Dictyophimus gracilipes BAILEY, 1856, p. 4, pl. 1, fig. 8. - HAECKEL, 1887, p. 1197. - CLEVE, 1899, p. 29, pl. 2, fig. 2. - POPOFSKY, 1908, p. 274, pl. 30, figs. 12,13, pl. 31, fig. 15, pl. 34, fig. 6. - RIEDEL, 1958, p. 233, text-fig. 5, pl. 3, fig. 5. - BOLTOVSKOY and RIEDEL, 1980, p. 124, pl. 5, fig. 8

Pseudodictyophimus gracilipes (Bailey). - PETRUSHEVSKAYA, 1971c, p. 93, fig. 48: I,IV,V. - BJØRKLUND, 1976a, pl. 9, figs. 1-5, pl. 11, figs. 6,7. - KLING, 1979, p. 309, pl. 1, figs. 23,24. - TAKAHASHI and HONJO, 1981, p. 153, pl. 9, figs. 3,4

Genus DICTYOCODON Haeckel, 1881

Dictyocodon elegans (Haeckel)
Plate 37, figures 6-7,9

Artopilium elegans HAECKEL, 1887, p. 1440, pl. 75, fig. 1

Pterocanium cf. *elegans* (Haeckel). - BENSON, 1966, p. 403, pl. 27, figs. 1,2

Remarks: The author proposes to place this species in the present genus because of the observed morphology shown in the plate including many terminal feet.

Dictyocodon palladius Haeckel
Plate 37, figures 8,10-11

Dictyocodon palladius HAECKEL, 1887, p. 1335, pl. 71, figs. 12,13. - RENZ, 1976, p. 121, pl. 4, fig. 16

Remarks: Observed specimens have always two large, cephalic spines similar to those of D. elegans. The thorax is not constricted as that of D. elegans and always smooth without any accessory spines. The terminal feet are very delicate and usually poorly preserved. The present species and the above D. elegans are members of the most fragile nassellarians.

Genus CONICAVUS n. gen.

Definition: Conical shell semi-enclosed with very fine irregular, polygonal and non-segmented meshwork, one or two apical horns, three or more basal feet made of the meshwork, one or two apical openings. Basal end of the shell is enclosed by the mesh but has a few large basal pores. Sagital ring absent.

Remarks: The present genus differs from Cephalospyris Haeckel 1881 in the absence of a sagital ring and many other features. The type species: C. tipiopsis n.sp. Position of this genus is uncertain and hence it is tentatively assigned to the present family.

Derivation of name: The name of this genus is the Latin meaning a conical cage.

Conicavus tipiopsis n.sp.
Plate 38, figures 1-6

Description: Shell conical with semi-enclosed irregular and very fine meshwork; numerous triangular to polygonal irregular pores. Sagital ring and constriction absent. A characteristic apical opening is located on a right or left side of the apical part next to one or two conical apical horns and forms a triangular cavity which has occasionally a frame extending from one of the apical horns. A few circular to oval basal pores vary considerably in size from 1/10 to 1/3 of the shell width. Three to four feet are made of the meshwork, ca. 1/8 of the shell length and extending parallel to a plane of the cone.

Dimensions: Length (31 specimens): 567 ± 89 μm (2 S.D.); Width (36 specimens): 372 ± 42 μm.

Type locality: 5°21'N, 81°53'W, Sediment trap depth 3791 m. Collected during August-December 1979.

Remarks: This species is large in size and commonly observed at PB station but poor preservation in the sediments is expected due to its fragile skeleton.

Derivation of name: The name of this species is from a diminutive of tepee and meaning having the appearance of a tipi.

Genus SETHOCONUS Haeckel, 1881

Sethoconus myxobrachina Strelkov and Reshetnyak
Plate 38, figures 7-8

Sethoconus myxobrachia Strelkov and Reshetnyak. - RENZ, 1976, p. 136, pl. 5, fig. 4

Genus CONARACHNIUM Haeckel, 1881

Conarachnium polyacanthum (Popofsky)
Plate 39, figures 1-4

Lophocorys polyacantha POPOFSKY, 1913, p. 400, text-fig. 122. - BENSON, 1966, p. 494 (partim), pl. 34, fig. 3 (only). - KLING, 1979, p. 309, pl. 1, fig. 27

Remarks: Thorax length and extent of constriction varies significantly. This and the following two species are apparently closely related and thus the same generic name Conarachnium is assigned for these.

Conarachnium parabolicum (Popofsky)
Plate 39, figures 5-6

? Sethoconus anthocyrtis HAECKEL, 1887, p. 1296, pl. 62, fig. 21

? Periarachnium periplectum HAECKEL, 1887, p. 1297, pl. 55, fig. 11

Lampromitra parabolica POPOFSKY, 1913, p. 348, text-fig. 54. - RENZ, 1966, p. 122, pl. 4, fig. 14

Conarachnium facetum (Haeckel)
Plate 39, figure 7

Sethoconus facetus HAECKEL, 1887, p. 1296, pl. 55, fig. 1

Genus STICHOPILIUM Haeckel, 1881

Stichopilium bicorne Haeckel
Plate 39, figures 13-19

Stichopilium bicorne HAECKEL, 1887, p. 1437, pl. 77, fig. 9. - BENSON, 1966, p. 422, pl. 29, figs. 1,2. - RENZ, 1976, p. 125, pl. 4, fig. 9. - KLING, 1979, p. 311, pl. 2, figs. 11,12. - NIGRINI and MOORE, 1979, p. N91, pl. 26, figs. 1a,b. - TAKAHASHI and HONJO, 1981, p. 153, pl. 9, fig. 11

Genus LITHOPERA Ehrenberg, 1847a

Lithopera bacca Ehrenberg
Plate 40, figures 1-2

Lithopera bacca EHRENBERG, 1872a, p. 314. - NIGRINI, 1967, p. 54, pl. 6, fig. 2. - RENZ, 1976, p. 133, pl. 5, fig. 12. - KLING, 1979, p. 309, pl. 2, figs. 4-7. - JOHNSON and NIGRINI, 1980, p. 127, pl. 3, fig. 8. - TAKAHASHI and HONJO, 1981, p. 153, pl. 9, fig. 13

Lithopera ananassa HAECKEL, 1887, p. 1234, pl. 57, fig. 3

Genus CYRTOPERA Haeckel, 1881

Cyrtopera languncula Haeckel
Plate 40, figures 3-6

Cyrtopera languncula HAECKEL, 1887, p. 1451, pl. 75, fig. 10. - BENSON, 1966, p. 510, pl. 35, figs. 3,4. - CASEY, 1971b, pl. 23.1, fig. 10. - RENZ, 1976, p. 120, pl. 4, fig. 7. - TAKAHASHI and HONJO, 1981, p. 153, pl. 9, fig. 14

Cyrtopera aglaolampa n.sp.
Plate 40, figures 7-8

Description: Cephalis spherical with a conical stout apical horn 2-3 time of its length and with very small pores. There are 6-8 equal length abdominal segments which gradually increase their width toward the last abdominal chamber. The chamber is ca. 4-6 times as wide as cephalic diameter. Constrictions between the segments are equal or less than those in *C. laguncula*. There are a few short spines on the thorax as well as on the basal side of the last chamber. Four to five abdominal ribs attached on the wall and extending out of the last chamber and become feet which are as long as the chamber's length and slightly curved inward. Pores circular and small in the thorax and gradually increase their size and become hexagonal toward the last chamber. The last chamber's pores are as wide as 2-3 times thickness of interporous bars.

Dimensions: (5 specimens) Length (cephalis to last chamber): 220-270 µm; Width (last chamber): 120-195 µm.

Type locality: 15°21.1'N, 151°28.5'W, Sediment trap depth 2778 m. Collected during July-November 1978.

Remarks: The apical spines are usually straight and not curved as that of *C. laguncula*.

Derivation of name: The name of this species is from Greek meaning a beautiful lamp.

Genus STICHOPHORMIS Haeckel, 1881

Stichophormis cf. *cornutella* Haeckel

? Stichophormis cornutella HAECKEL, 1887, p. 1455, pl. 75, fig. 9

? Stichophormis novena HAECKEL, 1887, p. 1455, pl. 79, fig. 9

Stichophormis cf. cornutella Haeckel. - TAKAHASHI and HONJO, 1981, p. 153, pl. 9, fig. 15

Genus LOPHOCORYS Haeckel, 1881

Lophocorys undulata (Popofsky)
Plate 40, figures 9-10

Artopilium undulatum POPOFSKY, 1913, p. 405, pl. 36, figs. 4,5

Lophocorys polyacantha Popofsky. - BENSON, 1966, p. 494 (partim), pl. 34, figs. 1,2 (only)

? Stichopilium anocor RENZ, 1976, p. 124, pl. 5, fig. 10

Remarks: Artopilium is a junior objective synonym of Triacartus whose type species, A. elegans, does not resemble this species. The type species of Stichopilium, S. bicorne, does not resemble this species either. Lophocorys is tentatively used here, although the generic assignment is uncertain.

Genus THEOCORYS Haeckel, 1881

Theocorys veneris Haeckel
Plate 40, figures 11-14

Theocorys veneris HAECKEL, 1887, p. 1415, pl. 69, fig. 5. - BENSON, 1966, p. 492, pl. 33, figs. 12,13. - RENZ, 1976, p. 137, pl. 5, fig. 11. - TAKAHASHI and HONJO, 1981, p. 153, pl. 9, fig. 17

Genus THEOCORYTHIUM Haeckel, 1887

Theocorythium trachelium trachelium (Ehrenberg)
Plate 40, figures 15-16

Eucyrtidium trachelius EHRENBERG, 1872a, p. 312; 1872b, p. 293, pl. 7, fig. 8

Calocyclas amicae HAECKEL, p. 1382, pl. 74, fig. 2

Calocyclas vestalis HAECKEL, p. 1382, pl. 74, fig. 3

Theocyrtis trachelius (Ehrenberg). - HAECKEL, p. 1405

Theocorythium trachelium trachelium (Ehrenberg). - NIGRINI, 1967, p. 79, pl. 8, fig. 2. pl. 9, fig. 2. - JOHNSON and NIGRINI, 1980, p. 135, text-fig. 13e, pl. 4, fig. 3

Theocorythium trachelium (Ehrenberg). - RENZ, 1976, p. 147, pl. 6, fig. 13. - RIEDEL and SANFILIPPO, 1978, p. 76, pl. 9, fig. 17

Genus LIPMANELLA Loeblich and Tappan, 1961

Lipmanella dictyoceras (Haeckel)
Plate 40, figure 17

Lithornithium dictyoceras HAECKEL, 1860b, p. 840

Dictyoceras acanthicum JØRGENSEN, 1900, p. 84; 1905, p. 140, pl. 17, fig. 101a, pl. 18, fig. 101b. - BENSON, 1966, p. 417, pl. 28, figs. 8-10

Dictyoceras xiphephorum JØRGENSEN, 1900, p. 84, pl. 5, fig. 25; 1905, p. 140

Lithopilium sphaerocephalum POPOFSKY, 1913, p. 380, pl. 35, fig. 2,3. - RENZ, 1976, p. 123, pl. 4, fig. 8

Lipmanella dictyoceras (Haeckel). - KLING, 1973, p. 636, pl. 4, figs. 24-26; 1977, p. 217, pl. 2, fig. 2; 1979, p. 309, pl. 2, fig. 8. - PETRUSHEVSKAYA and KOZLOVA, 1979, p. 137

Lipmanella pyramidale (Popofsky)
Plate 40, figure 18

Theopilium pyramidale POPOFSKY, 1913, p. 376, pl. 37, fig. 1. - RENZ, 1976, p. 126, pl. 4, fig. 13

Dictyoceras pyramidale (Popofsky). - TAKAHASHI and HONJO, 1981, p. 153, pl. 9, fig. 9

Lipmanella virchowii (Haeckel)
Plate 40, figures 19-21

Dictyoceras virchowii HAECKEL, 1862, p. 333, pl. 8, figs. 1-5. - TAN and CHANG, 1976, p. 285, text-fig. 63. TAKAHASHI and HONJO, 1981, p. 153, pl. 9, figs. 7,8

Dictyoceras neglectum CLEVE, 1900a, p. 7, pl. 4, fig. 5. - POPOFSKY, 1913, pl. 34, fig. 4. - RENZ, 1976, p. 121, pl. 4, fig. 10

Dictyoceras prismaticum TAN and CHANG, 1976, p. 285 (partim), text-figs. 64,65a,c (only)

Genus LITHOSTROBUS Butschli, 1882

Lithostrobus hexagonalis Haeckel
Plate 41, figures 1-3

Lithostrobus hexagonlis HAECKEL, 1887, p. 1475, pl. 79, fig. 20. - RENZ, 1976, p. 123, pl. 5, fig. 15. - TAKAHASHI and HONJO, 1981, p. 153, pl. 9, fig. 10

Lithostrobus cf. hexagónalis Haeckel. - BENSON, 1966, p. 508, pl. 35, figs. 1,2

Genus THEOCALYPTRA Haeckel, 1881

Theocalyptra bicornis (Popofsky)
Plate 41, figures 4-6,8-11

Pterocorys bicornis POPOFSKY, 1908, p. 208, pl. 34, figs. 7,8

Clathrocyclas alcmanae Haeckel. - POPOFSKY, 1913, pl. 37, fig. 4

Theocalyptra bicornis (Popofsky). - RIEDEL, 1958, p. 240, pl. 4, fig. 4. - NIGRINI and MOORE, 1979, p. N53, pl. 24, fig. 1. - LING, 1980, p. 369, pl. 2, fig. 3

Theocalyptra davisiana davisiana (Ehrenberg). - TAKAHASHI and HONJO, 1981, p. 153, pl. 9, figs. 19,20

Theocalyptra davisiana davisiana (Ehrenberg)
Plate 41, figure 7

Cycladophora ? davisiana EHRENBERG, 1861, p. 297; 1872b, pl. 2, fig. 11

Theocalyptra davisiana (Ehrenberg). - RIEDEL, 1958, p. 239, pl. 4, figs. 2,3, text-fig. 10. - BENSON, 1966, p. 441 (partim), pl. 29, figs. 14,15 (only). - NIGRINI and MOORE, 1979, p. N59, pl. 24, figs. 2a,b

Cycladophora davisiana davisiana Ehrenberg. - MORLEY, 1980, p. 206, pl. 1, figs. 1-5

Theocalyptra davisiana cornutoides (Petrushevskaya)
Plate 41, figures 12-16

Halicaliptra ? cornuta BAILEY, 1856, p. 5, pl. 1, figs. 13,14 (*nomen oblitum*)

Theocalyptra davisiana (Ehrenberg). - BENSON, 1966, p. 441 (partim), pl. 29, fig. 16 (only)

Cycladophora davisiana Ehrenberg *cornutoides* PETRUSHEVSKAYA, 1967, pl. 70, figs. 1-3. - LING et al., 1971, p. 714, pl. 2, figs. 6,7. - MORLEY, 1980, p. 206, pl. 1, figs. 7-10

? *Cycladophora davisiana semeloides* Petrushevskaya. - MORLEY, 1980, p. 206, pl. 1, figs. 11-14

Theocalyptra davisiana cornutoides (Petrushevskaya). - TAKAHASHI and HONJO, 1981, p. 153, pl. 9, fig. 18

Family PTEROCORYTHIDAE Haeckel, 1881, emend. Riedel, 1967a

Definition by Riedel (1967a): Cephalis subdivided into three lobes by two obliquely downwardly directed lateral furrows arising from the apical spine, in the manner described for *Anthocytidium cineraria* Haeckel and *Calocyclas virginis* Haeckel by Riedel (1959).

Genus TETACORETHRA Haeckel, 1881, emend. Petrushevskaya, 1971c

Tetracorethra tetracorethra (Haeckel)
Plate 41, figures 17-18

Tetraspyris tetracorethra HAECKEL, 1887, p. 1044, pl. 53, fig. 19

Tetracorethra tetracorethra (Haeckel). - RENZ, 1976, p. 145, pl. 6, fig. 23

Genus PTEROCORYS Haeckel, 1881

Pterocorys zancleus (Müller)
Plate 42, figures 1-4

Eucyrtidium zanclaeum MÜLLER, 1858a, p. 41, pl. 6, figs. 1-3

Theoconus zancleus (Müller). - BENSON, 1966, p. 482, pl. 33, fig. 4 (not fig. 5)

Pterocorys zancleus (Müller). - NIGRINI and MOORE, 1979, p. N89, pl. 25, figs. 11a,11b. - TAKAHASHI and HONJO, 1981, p. 154, pl. 10, figs. 1-3

Remarks: The present species is distinguished from P. campanula by its short conical apical spine, rounded thorax and abdomen and absent or very small wings.

Pterocorys campanula Haeckel
Plate 42, figures 5-8

Pterocorys campanula HAECKEL, 1887, p. 1316, pl. 71, fig. 3. - TAKAHASHI and HONJO, 1981, p. 154, pl. 10, figs. 4,5

Genus EUCYRTIDIUM Ehrenberg, 1847a

Eucyrtidium spp. A group
Plate 38, figures 11-13

Eucyrtidium sp. - JOHNSON, 1974, pl. 10, figs. 17,18

Eucyrtidium acuminatum (Ehrenberg)
Plate 42, figures 9-10,16-17,20

Lithocampe acuminatum EHRENBERG, 1844, p. 84

Eucyrtidium acuminatum (Ehrenberg). - EHRENBERG, 1854, p. 43, pl. 22, fig. 27. - POPOFSKY, 1913, p. 406, text-fig. 127. - NIGRINI, 1967, p. 81, pl. 8, figs. 3a,b. - RENZ, 1976, p. 130, pl. 5, fig. 5. - NIGRINI and MOORE, 1979, p. N61, pl. 24, figs. 3a,b. - JOHNSON and NIGRINI, 1980, p. 129, text-fig. 11d, pl. 3, fig. 15

Eusyringium siphonostoma HAECKEL, 1887, p. 1499, pl. 80, fig. 14. - BENSON, 1966, p. 498, pl. 34, figs. 6-9

? Eusyringium cannostoma HAECKEL, 1887, p. 1499, pl. 80, fig. 13

Stichopilium rapaeformis POPOFSKY, 1913, p. 404, text-fig. 126

Remarks: Specimens shown by Benson (1966) are very close to the specimens observed under the transmission light microscope in this study. Thoracic ribs form small wings extended from cephalis, attached on the thorax and terminate in the first abdominal segment. A significant variation in skeletal thickness has been observed.

Eucyrtidium hexagonatum Haeckel
Plate 42, figures 18-19

Eucyrtidium hexagonatum HAECKEL, 1887, p. 1489, pl. 80, fig. 11. - NIGRINI, 1967, p. 83, pl. 8, figs. 4a,b. - RENZ, 1976, p. 132, pl. 5, fig. 6. - NIGRINI and MOORE, 1979, p. N63, pl. 24, figs. 4a,b. - JOHNSON and NIGRINI, 1980, p. 129, text-fig. 11e, pl. 3, fig. 16

Eusyringium siphonostoma Haeckel. - TAKAHASHI and HONJO, 1981, p. 154, pl. 10, fig. 7

Eucyrtidium cienkowskii HAECKEL, 1887, p. 1493, pl. 80, fig. 9

Remarks: A specimen illustrated by Boltovskoy and Riedel (1980, p. 124, pl. 5, fig. 9) has much wider thorax than those observed here and thus excluded from the above synonymy.

Eucyrtidium anomalum (Haeckel)
Plate 42, figures 11-14

Lithocampe anomala HAECKEL, 1860, p. 839

Eucyrtidium anomalum HAECKEL, 1862, p. 323, pl. 7, figs. 11-13. - BENSON, 1966, p. 496, pl. 34, figs. 4,5. - DUMITRICA, 1972, pl. 7, fig. 11. - RENZ, 1976, p. 131, pl. 5, fig. 8. - MCMILLEN and CASEY, 1978, pl. 4, fig. 5

Eucyrtidium sp. aff. E. anamalum (Haeckel)
Plate 42, figure 15

Remarks: Thorax much smaller than that of E. anomalum.

Eucyrtidium dictyopodium (Haeckel)
Plate 42, figure 21

Stichopodium dictyopodium HAECKEL, 1887, p. 1447, pl. 75, fig. 6

Eucyrtidium hexastichum (Haeckel)
Plate 42, figure 22

Lithostrobus hexastichus HAECKEL, 1887, p. 1470, pl. 80, fig. 15. - BENSON, 1966, p. 506 (partim), pl. 34, figs. 15,16 (only)

Stichopilium annulatum POPOFSKY, 1913, p. 403, pl. 37, figs. 2,3

Eucyrtidium hexastichum (Haeckel). - PETRUSHEVSKAYA, 1971c, p. 221, fig. 99. - RENZ, 1976, p. 132, pl. 5, fig. 9. - BOLTOVSKOY and RIEDEL, 1980, p. 124, pl. 5, fig. 10. - TAKAHASHI and HONJO, 1981, p. 153, pl. 9, fig. 12

Genus ANTHOCYRTIDIUM Haeckel, 1881

Anthocyrtidium zanguebaricum (Ehrenberg)
Plate 41, figures 19-22

Anthocyrtis zanguebarica EHRENBERG, 1872a, p. 301; 1872b, p. 285, pl. 9, fig. 12

Anthocyrtium zanguebaricum (Ehrenberg). - HAECKEL, 1887, p. 1277

Anthocyrtis ovata HAECKEL, 1887, p. 1272, pl. 62, fig. 13

Sethocyrtis oxycephalis HAECKEL, 1887, p. 1299, pl. 62, fig. 9

Anthocyrtium oxycephalis (Haeckel). - BENSON, 1966, p. 468, pl. 32, figs. 3-5

Anthocyrtidium zanguebaricum (Ehrenberg). - NIGRINI, 1967, p. 58, pl. 6, fig. 4. - RENZ, 1976, p. 143, pl. 6, fig. 18. - NIGRINI and MOORE, 1979, p. N69, pl. 25, fig. 2. - JOHNSON and NIGRINI, 1980, p. 129, text-fig. 12b, pl. 3, fig. 19. - TAKAHASHI and HONJO, 1981, p. 153, pl. 9, figure 21

Anthocyrtidium ophirense (Ehrenberg)
Plate 43, figures 1-7

Anthocyrtis ophirense EHRENBERG, 1872a, p. 301; 1872b, p. 285, pl. 9, fig. 13

Anthocyrtidium cineraria HAECKEL, 1887, p. 1278, pl. 62, fig. 16

Anthocyrtidium ophirense (Ehrenberg). - NIGRINI, 1967, p. 56, pl. 6, fig. 3. - RENZ, 1976, p. 143, pl. 6, fig. 25. - NIGRINI and MOORE, 1979, p. N67, pl. 25, fig. 1. - KLING, 1979, p. 309, pl. 2, fig. 21. - JOHNSON and NIGRINI, 1980, p. 129, text-fig. 12a, pl. 3, fig. 18. - TAKAHASHI and HONJO, 1981, p. 154, pl. 9, fig. 22

Remarks: It appears that skeletons of this species are very little dissolved in the water column (Pl. 43, figs. 10-11) as are many other polycystines.

Genus LAMPROCYCLAS Haeckel, 1881

Lamprocyclas maritalis Haeckel *polypora* Nigrini
Plate 43, figures 12, 15

Lamprocyclas maritalis Haeckel polypora NIGRINI, 1967, p. 76, pl. 7, fig. 6. - KLING, 1979, p. 309, pl. 2, fig. 25. - NIGRINI and MOORE, 1979, p. N77, pl. 25, fig. 5. - JOHNSON and NIGRINI, 1980, p. 129, text-fig. 12e, pl. 3, fig. 22

Lamprocyclas maritalis maritalis Haeckel
Plate 43, figures 8-11, 13-14

Lamprocyclas maritalis maritalis Haeckel. - NIGRINI, 1967, p. 74, pl. 7, fig. 5. - NIGRINI and MOORE, 1979, p. N75, pl. 25, fig. 4. - JOHNSON and NIGRINI, 1980, p. 129, text-fig. 12d, pl. 3, fig. 21. - TAKAHASHI and HONJO, 1981, p. 154, pl. 9, fig. 26

Lamprocyclas maritalis HAECKEL, 1887, p. 1390, pl. 79, figs. 13,14

Genus LAMPROCYRTIS Kling, 1973

Lamprocyrtis ? hannai (Campbell and Clark)

Theoconus junonis HAECKEL, 1887, p. 1401, pl. 69, fig. 7

? Lamprocyclas junonis (Haeckel) group. - PETRUSHEVSKAYA and KOZLOVA, 1972, p. 545, pl. 36, fig. 8

Calocyclas hannai CAMPBELL and CLARK, 1944, p. 48, pl. 6, figs. 21,22

Lamprocyrtis ? hannai (Campbell and Clark). - KLING, 1973, p. 638, pl. 5, figs. 12-14, pl. 12, figs. 10-14. - NIGRINI and MOORE, 1979, p. N83, pl. 25, fig. 8. - JOHNSON and NIGRINI, 1979, p. N83, pl. 25, fig. 8.

Lamprocyclas ? hannai (Campbell and Clark).- TAKAHASHI and HONJO, 1981, p. 154, pl. 9, fig. 25

Lamprocyrtis sp.
Plate 43, figure 16

Conarachnium ? sp. - NIGRINI, 1968, p. 56 (partim), pl. 1, fig. 5b (only)

Remarks: This taxon differs from L. nigriniae in its larger conical thorax and more hexagonal pores than the latter. However, it may be combined with the latter pending future studies.

Lamprocyrtis nigriniae (Caulet)
Plate 43, figures 17-19

Conarachnium ? sp. - NIGRINI, 1968, p. 56 (partim), pl. 1, fig. 5a (only)

Conarachnium nigriniae CAULET, 1971, p. 3, pl. 3, figs. 1-4, pl. 4, figs. 1-4

Lamprocyrtis haysi KLING, 1973, p. 639, pl. 5, figs. 15,16, pl. 15, figs. 1-3. - SANFILIPPO and RIEDEL, 1974, p. 1022, pl. 3, figs. 9,10. - RIEDEL and SANFILIPPO, 1978, p. 69, pl. 5, fig. 9

Lamprocyrtis nigriniae Caulet. - NIGRINI and MOORE, 1979, p. N81, pl. 25, fig. 7. - KLING, 1979, p. 309, pl. 2, fig. 26. - JOHNSON and NIGRINI, 1980, p. 129, text-fig. 13a, pl. 3, fig. 24

Family ARTOSTROBIIDAE Riedel, 1967b, emend. Foreman, 1973

Definition: Radiolarians with six collar pores, a well-developed vertical tube, no appendages, and the pores of at least one major segment arranged in transverse rows. They may have a smooth or ridged surface, and the last segment is not flared (Forman, 1973).

Genus SPIROCYRTIS Haeckel, 1881

Spirocyrtis scalaris Haeckel
Plate 44, figure 1-2

Spirocyrtis scalaris HAECKEL, 1887, p. 1509, pl. 76, fig. 14. - RENZ, 1976, p. 142, pl. 6, fig. 1. - NIGRINI, 1977, pl. 2, fig. 12. - JOHNSON and NIGRINI, 1980, p. 135, text-fig. 14e, pl. 4, fig. 9. - TAKAHASHI and HONJO, 1981, p. 154, pl. 10, fig. 15

Spirocyrtis subscalaris Nigrini
Plate 44, figures 3-6

Spirocyrtis subscalaris NIGRINI, 1977, p. 259, pl. 3, figs. 1,2. - LING, 1980, p. 368, pl. 2, fig. 21

Spirocyrtis sp. aff. *S. seriata* Jørgensen and *S. subscalaris* Nigrini

Spirocyrtis seriata JØRGENSEN, 1905, p. 140, pl. 18, figs. 102-104. - BJORKLULND, 1976a, pl. 10, figs. 7-12

Spirocyrtis subscalaris NIGRINI, 1977, p. 259, pl. 3, figs. 1,2

Spirocyrtis sp. aff. *S. seriata* Jørgensen and *S. subscalaris* Nigrini. - TAKAHASHI and HONJO, 1981, p. 154, pl. 10, fig. 16

Spirocyrtis ? *platycephala* (Ehrenberg) group
Plate 44, figures 7-8

Lithomitra platycephala ? (Ehrenberg). - BJØRKLUND, 1976a, p. 1124, pl. 11, figs. 17,18

Remarks: Pores are much larger and the angle of the siphon is larger than those of *S. subscalaris*.

Genus ARTOSTROBUS Haeckel, 1887

Artostrobus annulatus (Bailey)
Plate 38, figures 9-10

Cornutella ? *annulata* BAILEY, 1856, p. 3, pl. 1, figs. 5a,5b

Artostrobus annulatus (Bailey). - HAECKEL, 1887, p. 1481. - RENZ, 1976, p. 117, pl. 4, fig. 5. - LING, 1975, p. 731, pl. 13, fig. 10. - TAKAHASHI and HONJO, 1981, p. 154, pl. 10, fig. 8

Genus BOTRYOSTROBUS Haeckel, 1887

Botryostrobus aquilonaris (Bailey)
Plate 44, figures 9-13

Eucyrtidium aquilonaris BAILEY, 1856, p. 4, pl. 1, fig. 9

Eucytidium tumidium BAILEY, 1856, p. 5, pl. 1, fig. 11

Botryostrobus aquilonaris (Bailey). - NIGRINI, 1977, p. 246, pl. 1, fig. 1. - NIGRINI and MOORE, 1979, p. N99, pl. 27, fig. 1. - KLING, 1979, p. 309, pl. 2, fig. 18. - JOHNSON and NIGRINI, 1980, p. 135, text-fig. 14a, pl. 4, fig. 5. - TAKAHASHI and HONJO, 1981, p. 154, pl. 10, figs. 9,10

For a synonymy prior to 1977 see Nigrini (1977).

Remarks: Variations in pore size, shell surface texture and position of the largest post-cephalic segment have been observed.

Genus PHORMOSTICHOARTUS Campbell, 1951, emend. Nigrini, 1977

Phormostichoartus corbula (Harting)
Plate 44, figures 14-16

Lithocampe corbula HARTING, 1863, p. 12, pl. 1, fig. 21

Siphocampe corbula (Harting). - NIGRINI, 1967, p. 85, pl. 8, fig. 5. - RIEDEL and SANFILIPPO, 1971, p. 1601, pl. 1H, figs. 18-25. - RIEDEL and SANFILIPPO, 1978, p. 73, pl. 9, fig. 7. - RENZ, 1976, p. 141, pl. 6, fig. 8

Phormostichoartus corbula (Harting). - NIGRINI, 1977, p. 252, pl. 1, fig. 10. - JOHNSON and NIGRINI, 1980, p. 135, text-fig. 14c, pl. 4, fig. 7. - TAKAHASHI and HONJO, 1981, p. 154, pl. 10, figs. 13,14

Genus SIPHOCAMPE Haeckel, 1887

Siphocampe nodosaria (Haeckel)

Lithomitra nodosaria HAECKEL, 1887, p. 1484, pl. 79, fig. 1. - PETRUSHEVSKAYA and KOZLOVA, 1972, pl. 24, figs. 29,30

Lithomitra eruca HAECKEL, 1887, p. 1485, pl. 79, fig. 3. - PETRUSHEVSKAYA and KOZLOVA, 1972, p. 539, pl. 24, figs. 32,33

Siphocampe nodosaria (Haeckel). - NIGRINI, 1977, p. 256, pl. 3, fig. 11. - TAKAHASHI and HONJO, 1981, p. 154, pl. 10, figs. 11,12

Siphocampe lineata (Ehrenberg)
Plate 44, figures 17-20

Lithocampe lineata EHRENBERG, 1838, p. 130 (partim)

Eucyrtidium lineatum (Ehrenberg). - EHRENBERG, 1847, p. 43 (partim): 1854, pl. 22, fig. 26

Tricolocampe cylindrica HAECKEL, 1887, p. 1412, pl. 66, fig. 21

Siphocampe lineata (Ehrenberg) group. - NIGRINI, 1977, p. 256, pl. 3, figs. 9,10. - JOHNSON and NIGRINI, 1980, p. 135, text-fig. 14d, pl. 4, fig. 8

For a more complete synonymy see Nigrini (1977).

Siphocampe arachnea (Ehrenberg)
Plate 44, figures 21-23

Eucyrtidium lineatum arachneum Ehrenberg, 1861b, p. 299

Lithomitra vanhoffeni POPOFSKY, 1908a, p. 296, pl. 36,fig. 9

Lithomitra arachnea (Ehrenberg). - RIEDEL, 1958, p. 242, pl. 4, figs. 7,8. - PETRUSHEVSKAYA, 1966, p. 232, text-fig. 7(4). - 1971b, text-fig. 22.4b; 1975, p. 586, pl. 10, figs. 13-17

Remarks: Genus Siphocampe is assigned here in order to conform with the generic name of other species in this group.

Genus ARTOBOTRYS

Artobotrys borealis (Cleve)
Plate 44, figure 24, Plate 45, figures 1-3

Theocorys borealis CLEVE, 1899, p. 33, pl. 3, fig. 5.

Artobotrys borealis (Cleve). - BJØRKLUND, 1976, p. 1124, pl. 11, figs. 24-27

Family CARPOCANIIDAE Haeckel, 1881, emend. Riedel, 1967b

Definition: Cephalis small, not sharply distinguished in contour from thorax, and tending to be reduced to a few bars within top of thorax (Riedel, 1971).

Genus CARPOCANISTRUM Haeckel, 1887

Carpocanistrum flosculum Haeckel
Plate 45, figures 4,6-7

Carpocanistrum flosculum HAECKEL, 1887 p. 1171, pl. 52, fig. 9

Carpocanium verecundum HAECKEL, 1887, p. 1284, pl. 52, fig. 12, 13

Carpocanium petalospyris Haeckel. - BENSON, 1966, p. 434 (partim), text-fig. 25, pl. 29, fig. 10 (only)

Carpocanium spp. - NIGRINI, 1970, p. 171 (partim), pl. 4, figs. 5,6

Carpocanistrum spp. - DUMITRICA, 1972, p. 838, pl. 14, fig. 4, pl. 15, figs. 11,12, pl. 24, fig. 1,3,6. - RENZ, 1976, p. 151, pl. 6, fig. 4. - NIGRINI and MOORE, 1979, p. N23 (partim), pl. 21, figs. 1b,c. - JOHNSON and NIGRINI, 1980, p.127 (partim), text-fig. 9f, pl. 3, fig. 5. - TAKAHASHI and HONJO, 1981, p. 155, pl. 10, figs. 21,22

Remarks: Pore size varies. Terminal teeth present on the peristome in well developed specimens.

Carpocanistrum cephalum Haeckel
Plate 45, figures 5,12

Carpocanistrum cephalum HAECKEL, 1887, p.1171, pl. 52, fig. 10

Carpocanistrum evacuatum HAECKEL, 1887, p. 1172, pl. 52, fig. 11

Carpocanium petalospyris Haeckel. - BENSON, 1966, p. 434 (partim), pl. 29, fig. 9 (only)

Carpocanium sp. - BENSON, 1966, p. 438, pl. 29, figs. 11,12

Carpocanium sp. A. - NIGRINI, 1968, p. 55, pl. 1, fig. 4. - NIGRINI and MOORE, 1979, p. N25, pl. 21, fig. 2

Remarks: This species is distinguished by its cylindrical shape rather than amphora-shaped counterparts in the present genus. Present species differs from Cryptoprora ornata Ehrenberg (see Sanfilippo and Riedel, 1973, p. 530, pl. 35, figs. 3,4).

Carpocanistrum favosum (Haeckel)
Plate 45, figure 8

Sethamphora favosa HAECKEL, 1887, p. 1252, pl. 57, fig. 4

Carpocanistrum ? odysseus Haeckel. - DUMITRICA, 1972, p. 838, pl. 15, fig. 10, pl. 24, fig. 2

Remarks: Basal opening rather small surrounded by terminal teeth whose surface is smooth. Shell surface rough caused by numerous rounded denticles. This species should not be confused with Carpocanopsis favosa (Haeckel) (Sanfilippo et al., 1973, p. 224, pl. 6, figs. 7,8).

Carpocanistrum coronatum (Ehrenberg)
Plate 45, figure 10

Carpocanium coronatum EHRENBERG, 1875, p. 66, pl. 5, fig. 7

Carpocanistrum sp. D. - LING, 1975, p. 730, pl. 12, fig. 6

Carpocanistrum spp. - NIGRINI, 1970, p. 171 (partim), pl. 4, fig. 4 (only). - NIGRINI and MOORE, 1979, p. N23 (partim), pl. 21, fig. 1a (only)

Remarks: Pores smaller and more in number than in the relative species shown in Pl. 45. The number is ca. 16-18 in an equatorial half meridian.

Carpocanistrum sp.
Plate 45, figure 11

Remarks: This taxon resembles some of specimens shown by Riedel and Sanfilippo (1971, see Pl. 2F).

Carpocanistrum acutidentatum n.sp.
Plate 45, figures 9,13-15

Description: Shell thick and ovate with cephalis completely hidden, pores elongate but occasionally subcircular and smaller than longitudinal crests. There are ca. 14-18 such crests in a half meridian. Peristome surrounded by ca. 12-16 sharp conical teeth of 1/4 to 3/4 shell length which are straight or inwardly curved near the terminal end. One tooth is connected with 1-3 crests.

Dimensions: (11 specimens) Shell length (exclusive of teeth): 87-110 µm; tooth length: 24-71 µm; transverse width: 80-96 µm.

Type locality: 15°21.1'N, 151°28.5'W, Sediment trap depth 4280 m. Collected during July-November 1978.

Remarks: The present species differs from *C. flosculum* Haeckel primarily pore shape and presence of the strong crests.

Derivation of name: The name of this species is the Latin meaning sharp tooth.

Genus CARPOCANARIUM Haeckel, 1887, emend. Nigrini and Moore, 1979

Carpocanarium papillosum (Ehrenberg)
Plate 45, figures 16-17

Eucyrtidium papillosum EHRENBERG, 1872a, p. 310; 1872b, p. 293, pl. 7, fig. 10

Dictyocryphalus papillosus (Ehrenberg). - HAECKEL, 1887, p.1307. - RIEDEL, 1958, p. 236, pl. 3, fig. 10, text-fig. 8. - NIGRINI, 1967, p. 63, pl. 16, fig. 6. - LING, 1975, p. 731, pl 13, fig. 10. - RENZ, 1976, p. 139, pl. 6, fig. 9

Carpocanarium papillosum (Ehrenberg) group. - NIGRINI and MOORE, 1979, p. N27, pl. 21, fig. 3. - JOHNSON and NIGRINI, 1980, p. 127, text-fig. 10a, pl. 3, fig. 6

Carpocanarium papillosum (Ehrenberg). - TAKAHASHI and HONJO, 1981, p. 155, pl. 10, fig. 17

Family CANNOBOTRYIDAE Haeckel, 1881, emend. Riedel, 1967a

Definition by Riedel (1967a): Cephalis consisting of two or more unpaired lobes, only one of which is homologous with the cephalis of theoperids.

Genus ACROBOTRYS Haeckel, 1881

Acrobotrys teralans Renz
Plate 45, figures 18-19

Acrobotrys cf. disolenia Haeckel. - BENSON, 1966, p. 339, text-fig. 21, pl. 23, figs. 13,14

Gen. et sp. indet. - RIEDEL and SANFILIPPO, 1971, pl. 1J, figs. 17,18

Acrobotrys teralans RENZ, 1976, p. 152, pl. 7, fig. 8

? Neobotrys sp. - TAN and CHANG, 1976, p. 273, text-fig. 46

Acrobotrys tessarolobon n.sp.
Plate 45, figure 20

Description: Cephalis quadrilobate with a single tubule projecting laterally. The cephalic lobes of unequal size and shape. Main cephalic lobe spherical and exposing nearly half of its surface area and with fine circular pores and thick skeleton. A polar lobe of the cephalis is conical shape and characteristically projecting straight poleward. It has fine circular pores of much smaller than the interporous septae. The largest lobe lies between the conical polar lobe and post-cephalic lobe. A collar constriction forms an upside down wide angle "V" and has a few fine spines. Postcephalic lobe cylindrical and with circular pores which are at least latitudinally regularly arranged and with a large basal opening. There is no wing.

Dimensions: (3 specimens) Length: 95-110 µm; Breadth (including the tubule): 85-98 µm.

Type locality: 15°21.1'N, 151°28.5'W, Sediment trap depth 978 m. Collected during July-November 1978.

Remarks: This species differs from *A. teralans* in number and shape of the cephalic lobes and its absence of wings.

Derivation of name: The name of this species is Greek meaning four lobes.

Acrobotrys chelinobotrys n.sp.
Plate 45, figures 22-24

Botryopyle dictyocephalus Haeckel group. - RENZ, 1976, p. 154, pl. 7, fig. 10

Acrobotrys sp. A. - TAKAHASHI and HONJO, 1981, p. 155, pl. 10, fig. 18

Description: Cephalis trilobate with a single tapering tubule which is laterally or obliquely (toward postcephalic side) projecting. The three cephalic lobes unequal in size and shape. The central lobe of the cephalis is spherical, exposing 1/4 of its surface ot outside and having the thickest skeleton and the smallest pore size among all of the lobes. A collar stricture between the cephalic lobes and a postcephalic lobe makes an arch. The postcephalic lobe nearly cylindrical but tapering toward basal opening. Both cephalis and thorax are made of meshwork with subcircular irregular pores whose diameter varies from 1-4 times the interporous bars. There is no wing.

Dimension: (11 specimens) Length: 80-105 μm; Breadth (excluding the tubule): 40-60 μm

Type locality: 15°21.1'N, 151°28.5'W, Sediment trap depth 978 m. Collected during July-November 1978.

Remarks: This species apparently differs from *Botryopyle dictyocephalus* group illustrated by Riedel and Sanfilippo (1971, p. 1602, pl. 1J, fig. 21-26) typically in presence of a tubule.

Derivation of name: The name of this species is from Greek meaning netted cluster of grapes.

Acrobotrys sp. C

Acrobotrys sp. C - TAKAHASHI and HONJO, 1981, p. 155, pl. 10, fog. 20

Genus SACCOSPYRIS Haecker, 1908b

Saccospyris preantarctica Petrushevskaya
Plate 45, figure 21

Saccospyris preantarctica PETRUSHEVSKAYA, 1975, p. 589, pl. 13, figs. 19,20

Remarks: The present finding of this species indicates that it has long range at least back to Miocene. This species resembles *Bisphaerocephalus minutus* Popofsky (1908a, pl. 33, fig. 9).

Genus CENTROBOTRYS Petrushevskaya, 1965

Centrobotrys thermophila Petrushevskaya
Plate 46, figures 1-2

Androspyris aptenodytes Haeckel. - POPOFSKY, 1913, p. 294, text-figs. 17,18

Centrobotrys thermophila PETRUSHEVSKAYA, 1965, p. 115. - NIGRINI, 1967, p. 49, text-fig. 26, pl. 5, fig. 7. - RIEDEL and SANFILIPPO, 1971, p. 1602, pl. 1J, figs. 27-31, pl. 2J, fig. 19, pl. 3F, fig. 14. - RENZ, 1976, p. 155, pl. 7, fig. 15

Genus NEOBOTRYS Popofsky, 1913

Neobotrys quadrituberosa Popofsky
Plate 46, figure 3

Neobotrys quadrituberosa POPOFSKY, 1913, p. 320-321, pl. 30, fig. 4

Botryocyrtis sp. A
Plate 46, figures 4-5

Description: Cephalis trilobate with very fine pores, spines and rough surface. Thorax cylindrical and short with irregular circular pores.

Remarks: This could be a juvenile form of *B. scutum*.

Genus BOTRYOCYRTIS Ehrenberg, 1860b

Botryocyrtis scutum (Harting)
Plate 46, figures 6-7

Haliomma scutum HARTING, 1863, p. 11, pl. 1, fig. 18

Botryocyrtis caput serpentis EHRENBERG, 1872a, p. 301; 1872b, p. 287, pl. 10, fig. 21

? *Lithobotrys homunculus* POPOFSKY, 1913, p. 317, pl. 31, figs. 5,6

Botryopyle erinaceus POPOFSKY, 1913, p. 319, text-figs. 28,28a

Botryocyrtis scutum (Harting). - NIGRINI, 1967, p. 52, pl. 6, figs. 1a-1c. - NIGRINI and MOORE, 1979, p. N105, pl. 28, figs. 1a,b. - TAKAHASHI and HONJO, 1981, p. 155, pl. 10, figs. 23,24

Botryocyrtis elongatum n.sp.
Plate 46, figures 8-9

Description: Cephalis trilobate with spherical lobes of increasing size from one side to another, a few spines longer than lobes, rough surface and very small pores. Thorax elongate and cylindrical and 2-3 times of cephalic length with fine spines and pores, rough surface in the anterior half and become porous and smooth in the posterior half which looks hyaline under the transmission light microscope. There is no segmentation in the thorax.

Dimensions: (8 specimens) Length: 65-160 µm; Width: 35-64 µm

Type locality: $5^{o}21'$N, $81^{o}53'$W, Sediment trap depth 3769 m. Collected during August-December 1979.

Remarks: This species is common at P_1 and PB stations.

Derivation of name: The name of this species the Latin meaning prolonged.

Family ARCHIPHORMIDIDAE Haeckel, 1881

Definition: Phaenocalpida with the basal mouth of the shell open (Haeckel, 1887).

Arachnocalpis ? sp. A
Plate 46, figure 10

Description: Large ellipsoidal shell with fine spongy and fragile network composed of irregular size polygons and without an apical horn, spines, and sagital ring.

Remarks: This species is very rare. The systematic position of this taxon position is uncertain.

Arachnocalpis sp. B
Plate 46, figure 11

Arachnocalpis?*ovatiretalis* n.sp.
Plate 46, figures 12-14

Description: Shell ovate with a fragile thin mesh composed of polygons and a basal opening at one pole, without an apical horn, spines, ribs and a sagital ring. Usually one pole is slightly protruded from the ellipsoidal perimeter but some specimens have smooth poles. The polygons of the metwork are mostly triangular. There are two kinds of interconnecting networks: thin and thick ones. Size of the polygons is ca. 1-4 times thickness of the thicker mesh.

Dimensions: (8 specimens) Length: 175-290 μm; Width: 105-205 μm; Mean Length/Width Ratio: 1.62 ± 0.16

Type locality: $5^{o}21'$N, $81^{o}53'$W, Sediment trap depth 667 m. Collected during August-December 1979

Remarks: Position of this species is uncertain because there is no closely related species to this has been reported and thus the present assignment is tentative.

Derivation of name: The name of this species is the Latin meaning having the nature of an egg-shaped net.

Arachnocalpis ? sp. C
Plate 46, figure 16

Description: Shell elongate fragile spongy network with tubules associated with 7-10 large pores.

Remarks: Very rare and systematic position is uncertain.

Genus ARACHNOCALPIS Haeckel, 1881

Arachnocalpis ellipsoides Haeckel
Plate 46, figure 17

Arachnocalpis ellipsoides HAECKEL, 1887, p.1172, pl. 98, fig. 13

Order TRIPYLEA Hertwig, 1879
Suborder PHAEODARIA Haeckel, 1879
Family CHALLENGERIIDAE Murray, 1876, emend. herein

Definition: Shell ovate or lens-shaped with a mouth and peristome and is usually provided with oral teeth, but without articulated feet. Surface of the shell usually smooth with numerous regularly arranged pores and some species bear a zone of dimples causing alveolate surface. Skeletal unit of shell made of amphora structure cemented with soluble silica.

Remarks: The above emendation bases on the following reasons: 1) finding of a form without oral teeth (i.e. *C. lingi* n. sp.); 2) information on surface morphology (i.e. smooth and alveolate surfaces); and 3) SEM-TEM information on micro- and ultra skeletal structures.

Genus CHALLENGERON Haeckel, 1887, emend. herein

Definition: *Challengerida* without pharynx. Shell smooth without dimples. Marginal spines present in well developed individuals. Oral teeth may be present or absent.

Remarks: The emendation is made for the same reasons as 1) and 2) in the above Challengeriidae.

Challengeron willemoesii Haeckel
Plate 47, figures 1-14

Challengeron willemoesii HAECKEL, 1887, p. 1659, pl. 99, fig. 13 - BORGERT, 1911, p. 456, pl. 34, figs. 4-6 - TAKAHASHI and HONJO, 1981, p. 155, pl. 10, figs. 25,29

Challengeron rottenburgi BORGERT, 1892, p. 182, pl. 6, fig. 1; 1911, p. 458, pl. 35, figs. 1,2 - HAECKER, 1906a, p. 301, pl. 6, fig. 1, text-figs. f,k

Challengeron armatum BORGERT, 1901a, p. XV33, fig. 39; 1911, p. 454, pl. 34, figs. 7-9

Challengeron gracile BORGERT, 1911, p. 458, pl. 35, figs. 6,7

Challengeron gracilimum BORGERT, 1911, p. 459, pl. 35, figs. 3-5

Challengeron walwini WOLFENDEN, 1902, p. 359, pl. 2, figs. 1, 1a

? *Challengeron wyvillei* HAECKEL, 1887, p. 1660, pl. 99, fig. 15

Challengeron sp. LING and TAKAHASHI, 1977, p. 208, pl. 1, figs. 1-5

Remarks: The concept of this species herein is somewhat broader than Borgert's. Based on examinations of several tens of specimens the author believes that intra-species morphological variations of the present species occur to such an extent that previous authors separated this group into several species. The variations observed include size and shape of the shell, length, number and arrangement (i.e. alternation of longer and shorter ones) of spines. However, the angle between 2 pairs of divergent teeth is consistent. Splitting of ovate form from compressed ellipsoidal form was possible, but this may or may not be natural. A form with sabre-shaped terminal teeth such as those of *Challengeron wyvillei* Haeckel (1887, p. 1660, pl. 99, fig. 15) has not been recognized from the present study areas (Haeckel's specimens were from the eastern tropical Atlantic).

Micro- and ultra-structural studies shown in Plate 47 reveal that basic unit of skeleton is regularly arranged amphora-shaped structure cemented by relatively soluble silica. This structure is common to all of 17 species studied in the present family except *Challengeranium diodon* (Haeckel) as shown in Plates 47-52.

Challengeron lingi n. sp.
Plate 48, figures 1-5

Description: Shell ovate to compressed ellipsoid, usually with spines along longitudinal rim. Shell wall smooth with regularly arranged numerous pores which are one open end of amphora structure common to all of the species in the present family. Peristome smooth without teeth and the mouth opens obliquely.

Dimensions: Length 240 ± 30 (2 S.D.) μm (6 specimens); width: 159 ± 33 μm (7 specimens); weight: 0.07 ± 0.01 μg (15 specimens)

Type locality: 5°21'N, 81°53'W, sediment traps, 3769/3791 m. Collected during August-December 1979

Remarks: The present species is closely related to *C. willemoesii*. Absent of oral teeth is the major difference from the latter. More than 30 specimens observed showed smooth peristome as shown in Plate 48 without any exceptions.

Derivation of name: This species is dedicated to Professor Hsin Yi Ling who inspired the present study.

Challengeron radians Borgert
Plate 48, figure 6

Challengeron radians BORGERT, 1803, p. 743, text-fig. J. - BORGERT, 1911, p. 453, pl. 34, fig. 3 - TAKAHASHI and HONJO, 1981, p. 155, pl. 11, figs. 1,2

Challengeron tizardi (Murray)
Plate 48, figures 13-16

Challengeria tizardi MURRAY, 1885, p. 226, pl. A, figs. 7-7b

Challengeron tizardi (Murray). - HAECKEL, 1887, p. 1656

Protocystis tizardi (Murray). - HAECKER, 1908b, p. 266, pl. 50, figs. 405-406

Remarks: Size of this species is fairly uniform based on 20 specimens and close to Murray's and larger than Haeckel's specimens. Dimensions obtained from Takahashi and Honjo (in prep.): length 340 ± 25μ(2 S.D.) (5 specimens); width: 272 ± 30 μm (8 specimens); weight: 0.54 ± 0.16 (2 S.D.) μg (18 specimens).

Genus CHALLENGEROSIUM Haeckel, 1887, emend. herein

Definition: Challengeridae with marginal spines, oral teeth and two different kinds (smooth and dimpled) of surfaces on a lens-shaped shell.

Type species: Challengerosium avicularia Haecker, 1906a

Remarks: Subgenus Challengerosium of Haeckel (1887) is herein elevated and separated from Challengeron in analogous manner with what Haecker (1906a) proposed for Heliochallengeron for presence of alveolate girdle zone in H. channeri (Murray).

Challengerosium balfouri (Murray)
Plate 48, figures 7-10

Challengeria balfouri MURRAY, 1885, p. 226, pl. A, fig. 10

Challengeron balfouri (Murray). - HAECKEL, 1887, p. 1655. - BORGERT, 1901a, p. XV31, fig. 37; 1911, p. 449, pl. 33, figs. 5-9. - WOLFENDEN, 1902, p. 360, pl. 2, figs. 2, 2a, 3, 3a. - TAKAHASHI and HONJO, 1981, p. 155, pl. 11, figs. 5,6. See Borgert (1911) for additional references.

Protocystis balfouri (Murray). - 1908b, p. 268, pl. 50, fig. 395

Remarks: Surface texture of the shell of two kinds: smooth on lateral sides; alveolate on sagital plane. Microstructure study by use of SEM show no signficant difference in internal amphora structure in both smooth and rough surface areas of the shell wall. These two kinds of surface morphology also exist also in C. avicularia.

Challengerosium avicularia Haecker
Plate 49, figures 1-13

Challengerosium avicularia HAECKER, 1906a, p. 300, plate 11, figure 8

Challengeron avicularia (Haecker). - BORGERT, 1911, p. 466

? Challengeria bethelli MURRAY, 1885, plate A, figure 6

? Challengerosium bethelli (Murray). - HAECKER, 1906a, p. 299, text-fig. F, h.

Remarks: Contrast between smooth and dimpled rough surfaces is clear in most specimens observed under SEM except some determined to be dissolution effect. Number of marginal spines are generally close to 10 and occasionally 2 or 3 spines. None of the specimens here has as many spines as of C. bethelli (Murray) shown by Murray (1885) and Haecker (1906a).

Genus CHALLENGERANIUM Haecker, 1908b

Original Definition: Shell ovate. Peristome with two fenestrated perforations. Two oral spines. An apical spine often surrounded by secondary spines (Haecker, 1908b, translated by the author).

Challengeranium diodon (Haeckel)
Plate 52, figures 11-16

Challengeron diodon HAECKEL, 1887, p. 1654, pl. 99, fig. 6..- BORGERT, 1901a, p. 30, fig. 34; 1911, p. 448, pl. 33, figs. 10,11. - JØRGENSEN, 1905, p. 141. - BJØRKLUND, 1974, p. 28, fig. 10; 1976a, pl. 12, figs. 8-11. - TAKAHASHI and HONJO, 1981, p. 155, pl. 12, figs. 1-3. See Borgert (1911) for additional references.

Challengeron narthorsti CLEVE, 1899, pl. 1, figs. 9a,9b

Challengeron heteracanthum JØRGENSEN, 1900, pl. 3, figs. 16-17

Remarks: Microstructure of this species appears to be very different from other Challengerida in presence of: (1) alveolate surface; 2) clusters of small pores associated with individual amphora; and 3) thin and delicate amphorae which are different shape from other species of the family. Thus, the author prefers to choose Haecker's separate classification of the present genus from Challengeron.

Genus PROTOCYSTIS Wallich, 1869, emend. herein

Definition: Challengeridae without pharynx, with none or up to several oral teeth and without marginal spines.

Remarks: Wallich (1869), Borgert (1901a, 1911) and Haecker (1906a) defined the present genus having one or several oral teeth. However, appearance of specimens with peristome without oral teeth necessitated this emendation. Generic classification of the present genus as well as Challengeron and Challengerosium may be artificial and hence it may require further emendations in the future work.

Protocystis sp. A
Plate 49, figures 14-15

Description: Shell lens-shaped, without marginal spines. Compressed sides of shell relatively smooth and girdle zone of alveolate surface. Peristome smooth without teeth.

Protocystis harstoni (Murray)

Challengeria harstoni MURRAY, 1885, p. 226, pl. A, fig. 14a (not fig. 14). - HAECKEL, 1887, p. 1650

Protocystis harstoni (Murray). - BORGERT, 1901a, p. XV28, fig. 30. - BJ0RKLUND, 1976a, pl. 12, fig. 5. - DUMITRICA, 1973, p. 755, pl. 8, fig. 5. - TAKAHASHI and HONJO, 1981, p. 156, pl. 11, fig. 11

? Protocystis harstoni (Murray). - HAECKER, 1908b, p. 49, text-fig. 150. - BORGERT, 1911, p. 436, text-fig. 4a. - STADUM and LING, 1969, p. 483, pl. 1, figs. 1-3. - BJ0RKLUND, 1976a, pl. 12, figs. 6,7

Protocystis natuiloides BORGERT, 1903, p. 738, text-figs. Da, Db

Protocystis antarctica SCHRODER, 1913, pl. 21, fig. 1

? Challengeria zetlandica WOLFENDEN, 1902, p. 361, pl. 2, fig. 5. See Borgert (1911) for additional references.

Remarks: Specimens shown by Haecker (1908), Borgert (1911), Stadum and Ling (1969) and Bjørklund (1976a, p. 12, figs. 6,7 of the Cleve collection) are different in angle, length and shape of peristome from the rest in the references listed above and the examined specimens. The former can be classified as a subspecies of the present species.

Protocystis honjoi n. sp.
Plate 50, figures 1-2

Protocystis sp. TAKAHASHI and HONJO, 1981, p. 156, pl. 11, figs. 8-9

Description: Shell lens-shaped and circular, with two characteristic wing-like oral teeth on the peristome. Shell surface texture of two kinds: rough girdle zone and smooth compressed sides. Contrast between the two surface texture is not as marked as in Challengerosium.

Dimensions: (12 specimens) Shell diameter: 147 ± 13 (2 S.D.) μm; weight: 0.10 ± 0.05 μg (4 specimens).

Type locality: $5^{o}21'$N, $81^{o}53'$W, sediment trap 2869 m. Collected during August-December 1979.

Remarks: This species is closely related to P. gravida Borgert (1903, p. 741, figs. Ga, Gb) and P. macleari (Murray) (1885, p. 226, pl. A, fig. 3; Haeckel, 1887, p. 1651). Specimens from the Pacific are slightly larger than those of the Atlantic (Takahashi and Honjo, 1981).

Derivation of name: This species is dedicated to Dr. Susumu Honjo for his contribution to this work in recovery of the samples.

Protocystis tridentata Borgert
Plate 50, figure 3

Protocystis tridentata BORGERT, 1903, p. 743, text-fig. H; 1911, p. 444, pl. 32, fig. 7. - HAECKER, 1906, p. 294, 295; 1908b, p. 266, pl. 50, fig. 404

Protocystis auriculata n. sp.
Plate 50, figures 4-7

Description: Shell lens-shaped and extending toward posterior end where peristome exists, with two ear-shaped winged teeth. The wings extend perpendicular to sagital plane. The teeth as long as 1/2 to 2/3 of transverse shell diameter.

Dimensions: (8 specimens) transverse shell diameter: 98 ± 9 (2 S.D.) µm.

Type locality: 5°21'N, 81°53'W, sediment trap 2869 m. Collected during August-December 1979.

Derivation of name: Name of this species is the Latin meaning having the nature of ear.

Protocystis aduncicuspis n. sp.
Plate 50, figures 8-10

Description: Shell compressed and semi-triangular, with two divergent oral teeth on peristome causing a sharp bend on girdle circumference. Girdle zone is covered by dimples causing rough surface.

Dimensions: Transverse shell diameter; 139 ± 21 (2 S.D.) µm (13 specimens); longitudinal length including teeth: 174 ± 12 µm (6 specimens).

Type locality: 5°21'N, 81°53'W, sediment trap 3791 m. Collected during August-December 1979.

Remarks: Shape of the peristome and teeth thickness vary.

Derivation of name: The name of this species is the Latin meaning having the nature of bent and pointed ends.

Protocystis sp. B
Plate 50, figure 11

Description: Shell spherical, with two divergent teeth having similar angle to those of *P. aduncicuspis*. Specimen shown in the plate is 205 µm in shell diameter.

Protocystis sloggetti (Haeckel)
Plate 50, figures 12-15

Challengeron harstoni MURRAY, 1885, p. 226, pl. A, fig. 14 (*nomen oblitum*)

Challengeria sloggetii HAECKEL, 1887, p. 1649, 1650, pl. 99, fig. 4

Protocystis sloggetii (Haeckel). - HAECKER, 1906, p. 297, 298; 1908b, p. 271, pl. 50, figs. 401, 402. - BORGERT, 1911, p. 435, text-fig. 3.

Remarks: Bifurcated oral teeth varies in thickness and length. Shape of compressed triangular lenticular shell is consistent and less round than the previous workers report.

Protocystis murrayi (Haeckel)
Plate 50, figures 16-18, Plate 51, figures 1-3

Challengeria aldrichi MURRAY, 1885, pl. A, fig. 4 (*nomen oblitum*)

Challengeria murrayi HAECKEL, 1887, p. 1653, pl. 99, fig. 1

Protocystis murrayi (Haeckel). - HAECKER, 1906, p. 299, text-fig. F, g; 1908b, p. 272, 273, pl. 50, fig. 409, 411, text-fig. 29, g. - BORGERT, 1911, p. 445, text-figs. 11a,b

? Protocystis thyroma HAECKER, 1906, p. 299, pl. 6, fig. 6

Protocystis sp. C
Plate 51, figure 4

Description: Shell strongly compressed, with winged teeth similar to those of P. murrayi (Haeckel), but extending beyond shell thickness.

Protocystis thomsoni (Murray)
Plate 51, figure 5

Challengeria thomsoni MURRAY, 1885, pl. A, figs. 2, 2a. - HAECKEL, 1887, p. 1650

Protocystis thomsoni (Murray). - HAECKER, 1906a, p. 291, text-fig. Fb; 1908b, p. 261, pl. 49, figs. 388-389, text-fig. 29b. - BORGERT, 1911, p. 440, text-figs. 7a,b. - RESHETNYAK, 1955, p. 98; 1 pl., figs. 1,2. - LING, 1966, p. 206, pl. 1, figs. 1-11; pl. 2, figs. 1-7. - LING and TAKAHASHI, 1977, p. 209, pl. 2, figs. 1-6. - TAKAHASHI and HONJO, 1981, p. 155, pl. 11, fig. 4

Protocystis bicornis BORGERT, 1901a, p. XV29, text-fig. 32, pl. 33, figs. 3,4

Protocystis xiphodon (Haeckel)
Plate 52, figures 1-3

Challengeria naresii MURRAY dwarf variety, pl. A, fig. 1b (nomen ablitum)

Challengeria xiphodon HAECKEL, 1887, p. 1648. - HAECKER, 1908b, p. 260, pl. 49, figs. 378-381

Protocystis xiphodon (Haeckel). - BORGERT, 1901a, p. XV27, fig. 28; 1903, p. 738; 1911, p. 433, pl. 31, figs. 5-7. - JØRGENSEN, 1905, p. 141. - STADUM and LING, 1969, p. 483, pl. 1, figs. 4, 5. - BJØRKLUND, 1976, pl. 12, fig. 4. - TAN and TCHANG, 1916, p. 297, text-fig. 78. - TAKAHASHI and HONJO, 1981, p. 156, pl. 11, fig. 14. See Borgert (1911) for additional references.

Remarks: This is the smallest species among one-toothed trio of Protocystis (including P. tritonis and P. naresi) whose shell is compressed ovate tapering toward oral tooth. Ratio of mouth/shell diameter is the largest among the trio.

Protocystis tritonis (Haeckel)
Plate 52, figures 4-5

Challengeria tritonis HAECKEL, 1887, p. 1649, pl. 99, fig. 5. - WOLFENDEN, 1902, p. 360, pl. 2, fig. 4

Protocystis tritonis (Haeckel). - BORGERT, 1901a, p. XV28, fig. 29; 1911, p. 434, pl. 31, figs. 8,9. - TAKAHASHI and HONJO, 1981, p. 156, pl. 11, fig. 13.

Protocystis naresi (Murray)
Plate 52, figures 6-8

Challengeria naresii MURRAY, 1885, p. 226, pl. A, figs. 1, 1a-1e. - HAECKEL, 1887, p. 1648

Challengeria naresi Murray. - HAECKER, 1906a, p. 290, text-figs. A, Fa; 1908b, p. 258, pl. 48, fig. 370; pl. 49, fig. 377; pl. 52, figs. 429, 430, text-figs. 27, 28. - RESHETNYAK, 1955, p. 95, pl. fig. 62

Protocystis naresi (Murray). - BORGERT, 1911, p. 432, text-rfig. 2. - TAKAHASHI and HONJO, 1981, p. 156, pl. 52, fig. 12

Remarks: This is the largest of the *Protocystis* one-toothed trio whose longer axis of compressed oval shell diameter range 480 to 680 um. Mouth is relatively small compared to the former two species of the trio. Examination of microstructure shows this species has elongated amphorae (pl. 52, fig. 9), but otherwise very similar to all other species of family *Challengeridae* studied.

Genus PHARYNGELLA Haeckel, 1887

Original definition: *Challengerida* with a pharynx, and with one or more teeth on the mouth, but without marginal spines (Haeckel, 1887)..

Pharyngella gastrula Haeckel
Plate 51, figures 6-14

Pharyngella gastrula HAECKEL, 1887, p. 1662, pl. 99, fig. 18. - BORGERT, 1901, p. 34, text-fig. 41; 1903, p. 746, text-fig. N; 1911, p. 461, pl. 31, fig. 3,4. - HAECKER, 1906, p. 303

Protocystis thomsoni (Murray). - TAKAHASHI and HONJO, 1981, p. 155, pl. 11, fig. 3

Remarks: Presence of characteristic pharynx separate the present species from *Protocystis thomosoni* (Murray).

Genus ENTOCANNULA Haeckel, 1879

Definition by Haeckel (1887): *Challengerida* with a pharynx, without teeth on the mouth, and without marginal spines.

Entocannula infundibulum Haeckel
Plate 52, figs. 9,10

Challengeria bromleyi MURRAY, 1885, pl. A, fig. 5 (*nomen oblitum*)

Entocannula infundibulum HAECKEL, 1887, p. 1661, pl. 99, fig. 19. - BORGERT, 1903, p. 745-746, text-fig. M; 1911, p. 460, pl. 31, fig. 1 - HAECKER, 1906a, p. 303-304; 1908b, p. 279, pl. 51, fig. 425

Family MEDUSETTIDAE Haeckel, 1887, emend. herein

Definition: Phaeodaria with an ovate, hemispherical or cap-shaped shell of alveolate, smooth or smooth with raised-striae texture, and with articulate hollow feet on the peristome.

Remarks: Shell surface texture has been observed to be variable depending on species. Observations of microstructures show significant variations between species of the present family and they are very different from amphorae of family *Challengeridae*. As Phaeodaria, shells of this family are small next to those of families *Porospathidae* and *Lirellidae*.

Genus EUPHYSETTA Haeckel, 1887

Original description by Haeckel (1887): *Medusettida* with four articulate feet on the peristome, one odd very large, and three small or rudimentary feet.

Euphysetta elegans Borgert
Plate 53, figures 1-10

Euphysetta elegans BORGERT, 1902, p. 569, text-fig. F; 1906, p. 154, pl. 11, figs. 7-9. - HAECKER, 1904a, p. 138; 1906a, p. 273; 1908b, p. 307, pl. 53, figs. 435, 438. - DUMITRICA, 1973, p. 756, pl. 5, fig. 8; pl. 6, figs. 1-3, pl. 12, fig. 8. - TAKAHASHI and HONJO, 1981, p. 156, pl. 12, figs. 4-5

? *Euphysetta amphicodon* HAECKEL, 1887, p.1670, pl. 118, fig. 3

Remarks: Length of an apical spine and odd large foot appear to vary such that *E. amphicodon* cannot be separated from the present species. The specimens observed here have always three small feet in contrast to Haeckel's nine small thorns of one specimen. Microstructure shown in Plate 53 demonstrates layers of circular pores.

Euphysetta staurocodon Haeckel

Plate 53, figures 11-14

Euphysetta staurocodon HAECKEL, 1887, p. 1670, pl. 118, figure 2

Remarks: Shell is usually much smaller and shell surface is much finely alveolated than that of *E. elegans*. The form studied here has always large foot extending toward terminal end but not bent like Haeckel (1887) described.

Euphysetta pusilla Cleve

Plate 53, figure 15

Euphysetta pusilla CLEVE, 1900a, p. 7, pl. 3, fig. 16; 1900b, p. 160. - BORGERT, 1902, p. 567, fig. D; 1906, p. 152, pl. 11, figs. 1-3. - DUMITRICA, 1973, p. 756, pl. 9, fig. 6; pl. 12, fig. 5. - TAKAHASHI and HONJO, 1981, p. 156, pl. 12, fig. 8

Remarks: The author also observed a few specimens with an apical spine, as noted by Borgert (1906).

Euphysetta lucani Borgert
Plate 54, figures 10-12

Euphysetta lucani BORGERT, 1892, p. 181, pl. 6, fig. 8; 1901a, p. 37, fig. 45; 1901b, p. 242, pl. 11, fig. 4; 1906, p. 151, pl. 6, figs. 4-6. - HAECKER, 1908b, p. 306, pl. 53, figs. 436, 439, 442. - DUMITRICA, 1973, p. 756, pl. 9, fig. 1; pl. 12, fig. 6. - TAKAHASHI and HONJO, 1981, p. 156, pl. 11, fig. 7

Remarks: Microstructure shows regularly arranged one lyaer of ovate shape amphorae cemented with silica. The amphorae are different shaped from those of Challengeridae.

Genus MEDUSETTA Haeckel, 1887

Original definition by Haeckel (1887): Medusettida with four equidistant articulate feet of equal size on the peristome.

Medusetta ansata Borgert
Plate 54, figures 1-7

Medusetta ansata BORGERT, 1902, p. 564, fig. B; 1906, p. 146, pl. 12, figs. 1,2. .- TAKAHASHI and HONJO, 1981, p. 156, pl. 12, figs. 6-7

Remarks: Two different forms exist: One has an ovate shell with feet obliquely extending and abruptly bent at the branching joints (Pl. 54, figs. 1-5) whereas the other has elongated shell with foot gently curved toward the terminal end (Pl. 54, figs. 6-7). At Atlantic E site, only the former form was found while both forms were found at Pacific P_1 and PB sediment trap sites. Cross sectional microstructure shows one layer of square to rectangular shaped pores bounded by outer and inner shell walls.

Medusetta inflata Borgert

Medusetta inflata BORGERT, 1902, p. 563, fig. A; 1906, p. 146, pl. 11, figs. 10,11. - CLEVE, 1903, p. 354. - HAECKER, 1908b, p. 305, pl. 53, fig. 437. - DUMITRICA, 1973, p. 756, pl. 13, fig. 1. - TAN and TCHANG, 1976, p. 297, text-fig. 79. - TAKAHASHI and HONJO, 1981, p. 157, pl. 12, fig. 11

Medusetta sp. A
Plate 54, figures 8-9

Description: Shell longitudinally compressed spherical with four bifurcated feet on the peristome of large mouth. Alveolate shell surface similar to that of *E. elegans*. Other than shown in Plate 54, figs. 8-9 presence/absence of apical spines remains to be further examined upon collection of more specimens.

Medusetta sp. B
Plate 63, figures 12-13

Description: Shell smooth hemispherical cap with four equal articulate feet which have many spines. No apical spine has been observed.

Remarks: The above figures are TEM partial cross-sections. Note that skeletons shown here collected from plankton tows are made of one layer of very thin tubes. This species has never been found in the sediment trap samples.

Family LIRELLIDAE Ehrenberg, 1872c

Remarks: Present family represents the most abundant Phaeoadaria in the deep sea water column, although diversity is low. Only two genera and three species were encountered.

Genus BORGERTELLA Dumitrica, 1973

See Dumitrica (1973) for diagnosis of this genus.

Borgertella caudata (Wallich)
Plate 54, figures 13-17, plate 55, figures 1-6

Cadium caudatum WALLICH, 1869, pl. 3, figs. 7-10. - BUTSCHLI, 1882, pl. 32, fig. 15a

Cadium inauris BORGERT, 1903, p. 747, fig. 0; 1910, p. 402, pl. 30, figs. 4-10

Borgertella caudata (Wallich). - DUMITRICA, 1973, p. 755, pl. 8, figs. 6-8; pl. 12, figs. 13-17. - LING, 1975, p. 732, pl. 13, fig. 24. - TAKAHASHI and HONJO, 1981, p. 157, pl. 12, fig. 12

Genus LIRELLA Ehrenberg, 1872c

Remarks: Species of the present genus are characterized by a small ovate or ellipsoidal shell with straight or curved wavy lines of furrows and crests.

Lirella baileyi Ehrenberg
Plate 55, figure 7

Cadium marinum BAILEY, 1856, p. 3, pl. 1, fig. 2.

Lirella baileyi EHRENBERG, 1872c, p. 248, pl. 3, fig. 29a,b. - LOEBLICH and TAPPAN, 1961, p. 231, 232. - LING, 1973, p. 781, 782; 1975, p. 732, pl. 13, fig. 28. - LING and TAKAHASHI, 1977, p. 209, pl. 3, figs. 1-3

Lirella marina (Bailey). - DUMITRICA, 1973, p. 755, pl. 6, fig. 8, pl. 8, fig. 8, pl. 12, figs. 10-12

Remarks: About 60-70 longitudinal striae terminate without reaching the tapered ends and form smooth surfaces.

Lirella bullata (Stadum and Ling)
Plate 55, figures 8-11

Cadium bullatum STADUM and LING, 1969, p. 484, pl. 1, figs. 9-14

Lirella bullata (Stadum and Ling). - LING, 1975, p. 732, pl. 13, fig. 29. - TAKAHASHI and HONJO, 1981, p. 157, pl. 13, figs. 1-2

Lirella melo (Cleve)
Plate 55, figures 12-18, plate 56, figures 1-8

Beroetta melo CLEVE, 1899, p. 27, pl. 1, fig. 8

Cadium melo (Cleve). - BORGERT, 1901a, p. XV50, fig. 58; 1910, p. 401, pl. 30, figs. 3-5. - JØRGENSEN, 1905, p. 142, pl. 18, fig. 13. - HAECKER, 1908b, p. 282, pl. 51, fig. 415. - SCHRÖDER, 1913, p. 168, text-fig. 10. - STADUM and LING, 1969, p. 484, pl. 1, figs. 6-8. - DUMITRICA, 1973, p. 755, pl. 7, figs. 3,4; pl. 12, fig. 9. - TAKAHASHI and HONJO, 1981, p. 157, pl. 12, figs. 13,14,16

Remarks: Several forms of peristome have been observed: 1) Smooth and significantly protruded; 2) Smooth, short and non-protruded; and

3) slightly obliquely open. Also two differnt kinds of microstructures have been recognized (Plate 56, figs. 2-4, 6-8). Even within a specimen the two kinds of microstructures have been observed. These are perhaps secondary features due to dissolution judging from observation of other species from plankton tows.

Lirella tortuosa n. sp.
Plate 55, figures 19-20, Plate 56, figures 9-11

Description: Shell ovate, with 25-35 coiled longitudinal striae and crests, with a short apical spine, and with peristome open straight.

Dimensions: (12 specimens), length: 105 ± 5 μm; width: 67 ± 3 μm.

Type locality: 15°21.1'N, 151°28.5'W, sediment trap depth 4280 m. Collected during July-November 1978.

Remarks: Both right and left coiled specimens have been observed.

Derivation of name: The name of this species is the Latin meaning twisted.

Family POROSPATHIDIDAE Borgert, 1901a, emend. Campbell, 1954

Definition: Shell covered by paneled or tubulated surface or covered by trizonal meshwork; radial spines on all sides.

Genus POROSPATHIS Haeckel, 1879

Remarks: This is the type genus of the family.

Porospathis holostoma (Cleve)
Plate 57, figures 1-8

Polypetta holostoma CLEVE, 1899, p. 32, pl. 3, figs. 4a,4b; 1900b, p. 180

Porospathis holostoma (Cleve). - BORGERT, 1901a, p. 48, figs. 56, 56a; 1903, p. 752; 1910, p. 387, pl. 29, figs. 1-8; pl. 30, figs. 1,2. - HAECKER, 1908b, p. 240, pl. 48, figs. 371-376; pl. 49, figs. 392, 393. - SCHRÖDER, 1913, p. 166, text-fig. 9. - RESHETNYAK, 1955, p. 95, fig. 66 (in plate); 1966, p. 166, fig. 52. - STADUM and LING, 1969, p. 485, pl. 1, figs. 16-18. - DUMITRICA, 1973, p. 754, pl. 5, figs. 1,2,6. - TAKAHASHI and HONJO, 1981, p. 156, pl. 11, fig. 15

Porospathis sp. aff. P. holostoma - DUMITRICA, 1972, p. 842, pl. 15, fig. 14

Family CASTANELLIDAE Haeckel, 1879

Definition by Haeckel (1887): Phaeodaria with a spherical or subspherical shell, exhibiting ordinary lattice-work, with circular or roundish pores. Radial spines without circles of basal pores. Mouth of the shell large, usually circular and armed with teeth. Central capsule excentric, placed in the aboral half of the shell-cavity.

The following systematics originally given by Haeckel (1887) and Haecker (1908b) and emended by Kling (1966) represents generic classification criteria for the present family.

A. Shells with pores distributed over the entire shell wall

Main spines absent	-Mouth without teeth or other ornamentation		*Castanarium*
	-Mouth with teeth		*Castanella*
Main spines present	-Mouth without teeth or other ornamentation.	-Main spines unbranched.	*Castanidium*
		-Main spines branched.	*Castanopsis*
	-Mouth with teeth	-Main spines unbranched.	*Castanissa*
		-Main spines branched.	*Castanea*

Main spines usually present, absent in some specimens. Mouth with thickened rim, blunt protuberances, or raised collar-shaped rim. *Castanura*

B. Shell with some pore positions occupied by enclosed, hollow spaces. *Circocastanea*

Remarks: Biogeography of the present family in the eastern North Pacific has been given by Kling (1966).

Genus CASTANIDIUM Haeckel, 1879

Castanidium longispinum Haecker
Plate 57, figures 9-13, plate 58, figures 1-4

Castanidium longispinum HAECKER, 1908, pp. 163-164, pl. 37, figs. 285-286, pl. 38, figs. 290-291, pl. 40, fig. 296; SCHRÖDER, 1913, p. 151; KLING, 1966, p. 115, pl. 5, figs. m-r; KLING, 1971, p. 664, pl. 2, figs. 5-7.

Description: Shell spherical, with unbranched main-spines and numerous short bi-spines of uniform length, with small pores circular to polygonal shape, with usually one main-spine on the rim of a small mouth. Main-spines slightly wavy and as long as shell diameter. Shell diameter of the specimens observed here range 310-450 μm and surface plankton tow samples from the Gulf of Oman (collected by J. Erez) range 390-510 um (470 ± 34 μm; n = 40 specimens).

Remarks: The above ranges of shell diameter are much smaller than that observed by Kling (1966: 240-630 μm). Mouth size is similar to Kling (1966) but smaller than that of Haecker (1908b). Cross sections of intervening bars show rectangular shape as Kling (1966) noted.

Castanidium abundiplanatum n. sp.
Plate 58, figures 5-8

Description: Shell relatively small as a Castanellid, without bi-spines, with slightly wavy main-spines, mouth usually with one main-spine on the rim, pores circular to polygonal. Bases of the main-spines fenestrated, shell wall often elevated there and forming polyhedral shell. Length of the main-spines 1/2 up to as long as shell diameter.

Dimensions: Shell diameter 308 ± 21 μm (2 S.D.) (18 specimens); weight: 0.80 ± 0.02 μg (22 specimens)

Type locality: $5^{o}21'N$, $81^{o}53'W$, sediment trap 1268 m. Collected during August-December 1979.

Remarks: The present species has narrow size range and is distinctly smaller than *C. longispinum*. Specimens of two shells dividing are occasionally observed.

Derivation of name: The name of this species is the Latin meaning having the nature of copious planes.

Castanidium sp.
Plate 58, figure 10

Description: Shell polyhedral, with very large pores of 1/4 to 1/5 of shell diameter combined with a few small pores of skeleton thickness, main-spines as long as 1/2 of shell diameter whose bases are elevated causing the shell shape, bi-spines of equal or shorter length than pore diameter.

Genus CASTANISSA Haeckel, 1879

Castanissa circumvallata Schmidt
Plate 58, figure 9

Castanissa circumvallata SCHMIDT, 1907, p. 301, fig. 6. - SCHMIDT, 1908, p. 257, pl. 20, fig. 6. - KLING, 1966, p. 123, pl. 3, figs. a-h; 1971 p. 665, pl. 4, figs. 1-4. - TAKAHASHI and HONJO, 1981, p. 157, pl. 13, fig. 4

Castanissa similis SCHMIDT, 1908, p. 257, pl. 20, fig. 5

Remarks: Specimen illustrated here has more developed teeth than those shown by the previous workers, although bi-spines are broken off thus not showing well in the illustration.

Genus CASTANELLA Haeckel, 1879

Castanella aculeata Schmidt
Plate 58, figure 11,13, Plate 59, figure 1

Castanella aculeata SCHMIDT, 1907, p. 299, fig. 4; 1908, p. 250, pl. 18, fig. 6. - KLING, 1966, p. 110, pl. 2, figs. j-o

Castanella macropora (Borgert)
Plate 58, figure 12

Castanidium macroporum Schmidt, 1908, p. 252, pl. 19, fig. 2

Description: Shell small as a Castanellid, pores circular and unequal size, bi-spines 1/10 length of shell diameter and variable in thickness, mouth circular and 1/5 to 1/4 length of shell diameter with divergently curved conical teeth.

Remarks: According to Schmidt (1908), main spines of his *Castanidium macroporum* were broken off, but his illustration suggests that the main spines could well be thicker bi-spines. The author proposes to make emendation in generic name of the present species and accordingly change the gender to the species name on the basis of absence of main spines observed here.

Castanella sloggetti Haeckel
Plate 59, figure 2

Castanella sloggetti HAECKEL, 1887, p. 1683. - BORGERT, 1903, p. 750. - HAECKER, 1908b, p. 157, pl. 34, figs. 260-261

Remarks: Teeth observed here are four compared to more than five shown by the previous workers. The present species resembles Castanella maxima SCHMIDT (1907, p. 297, fig. 1; 1908, p. 251, pl. 18, fig. 8. - SCHRÖDER, 1913, p. 148), although the size of the latter is ca. 1 mm.

Castanella balfouri Haeckel
Plate 58, figure 3

Castanella balfouri HAECKEL, 1887, p. 1683. - SCHMIDT, 1908, p. 249, pl. 18, fig. 3

Family CIRCOPORIDAE Haeckel, 1879

Definition: Phaeodaria with a spherical or polyhedral shell, exhibiting peculiar solid procellanous structure, with a stellate circle of radial pores around the base of the hollow radial spines. Mouth usually with teeth. Surface of the shell tabulate, paneled or dimpled. Central capsule excentric, placed in the aboral half of the shell cavity (Haeckel, 1887).

Genus HAECKELIANA Haeckel, 1887

Original definition: Circoporida with spherical shell of a peculiar dimpled, porcellaneous structure, and with a variable number of simple radial main spines which are usually not regularly arranged.

Haeckeliana porcellana Haeckel
Plate 59, figures 4-13

Haeckeliana porcellana Murray. - HAECKEL, 1887, p. 1701, pl. 114, fig. 6. - HAECKER, 1908b, p. 182, text-fig. 20, pl. 20, fig. 177. - SCHRÖDER, 1913, p. 155-156. - KLING, 1966, p. 137, pl. 8, figs. i-n

Haeckeliana maxima HAECKEL, 1887, p. 1701, pl. 114, fig. 5

Haeckeliana murrayi HAECKEL, 1887, p. 1702

Haeckeliana geotheana HAECKEL, 1887, p. 1702, pl. 114, fig. 3

Haeckeliana darwiniana HAECKEL, 1887, p. 1702, pl. 114, figs. 1-2. - TAKAHASHI and HONJO, 1981, p. 157, pl. 13, figs. 7-8

Haeckeliana laboradoriana BORGERT, 1901, p. 43, fig. 51; 1909, p. 330-331, pl. 24, figs. 1-3

Remarks: Some specimens entirely lack in bi-spines and thus shell surface appears very smooth in contrast to other thorny specimens. The author accepts classification by Kling (1966) which involves combining Haeckel's six species of Haeckeliana shown in the above synonomy. Cross-sectional microstructures show several different layers including the innermost part of polygons made of tubes (Plate 59, figs. 10-12).

Genus CIRCOPORUS Haeckel, 1879

Definition by Haeckel (1887): Circoporida with a spherical or regularly octahedral shell, composed of eight congruent, triangular plates, with six corners from which arise six radial spines, opposite in pairs in three diameters, perpendicular one to another.

Circoporus sexfuscinus Haeckel
Plate 60, figures 1,3,5

Circoporus sexfuscinus HAECKEL, 1887, p. 1695, pl. 115, fig. 1. - BORGERT, 1901b, p. 243-244, pl. 11, fig. 7; 1909, p. 336-337, pl. 24, figs. 4-5, pl. 25, figs. 5-7. - HAECKER, 1908b, p. 186, pl. 20, figs. 174-175.

Remarks: This species has six major radial spines which are divergently three-forked at the terminal ends in contrast to straight terminal ends of C. oxyacanthus.

Circoporus oxyacanthus Borgert
Plate 60, figures 2, 4, 6-13

Circoporus oxyacanthus BORGERT, 1902, p. 571-572, fig. Hb; 1903, p. 753; 1909, p. 335-336, pl. 25, figs. 1-4. - HAECKER, 1908b, p. 185, pl. 20, fig. 173. - TAKAHASHI and HONJO, 1981, p. 157, pl. 15, figs. 6-7.

Genus CIRCOGONIA Haeckel, 1887

Original definition: Circoporida with a regular icosahedral shell, composed of twenty congruent, triangular plates, with twelve corners, from which arise twelve radial spines.

Circogonia sp.
Plate 20, figures 9-10

Description: Shell icosahedral, smooth and delicate, with twelve equal hollow major spines whose bases are fenestrated with 4-6 oval pores and well elevated so that each plate of shell become convex, mouth circular with several small spines.

Family CONCHARIIDAE Haeckel, 1879

Definition: Phaeodaria with a bivalved lattice-shell, which is spherical or lenticular, and composed of two equal or unequal boat-shaped valves, a dorsal and a ventral. The valves bear neither an apical latticed cupola or glea, nor hollow radial tubes. The central capsule is placed in the aboral half of the shell-cavity, and so enclosed between both valves, that its three openings lie in the open frontal fissure between them (the astropyle on the oral pole of the main axis, the two parapylae on both sides of its aboral pole, at right and left) (Haeckel, 1887).

The following is the synopsis of the genera of *Concharidae* originally presented by Haeckel (1887) and emended by Haecker (1908b) and Campbell (1954) and further emended herein:

I. Subfamily *Conchariinae* Lateral edges of the two valves smooth, without teeth	- Valves without sagittal keel, nearly hemispherical or slightly compressed	- Aboral hinge without horns,	*Concharium*
		- Aboral hinge with two horns (one on each valve)	*Conchasma*
II. Subfamily *Conchidiinae* Lateral edges of the two valves dentate, with a series of prominent teeth on both sides.	- Valves without sagittal keel, nearly hemispherical or slightly compressed.	- Aboral hinge without horns,	*Conchellium*
		- Aboral hinge with two horns. No apical horn.	*Conchidium*
		- Aboral hinge with two horns. Apex also with a horn.	*Conchonia*

		- No horn. Diatom like texture	*Conchocystis*
		- Like *Conchocystis*, but slitlike pores.	*Conchophacus*
III. Subfamily *Conchopsidinae* Lateral edges of the two valves dentate, with a series of prominent teeth on both sides.	Valves with a sharp sagittal keel, strongly compressed on both sides, boat-shaped	- Aboral hinge without horns.	*Conchopsis*
		- Aboral hinge with two horns (one on each valve).	*Conchoceras*

Remarks: Skeletal cross-sections for this family represent similar morphology in all of the species examined here (e.g. pls. 61-62).

Genus CONCHELLIUM Haeckel, 1887

Conchellium capsula Borgert
Plate 61, figures 1-5, 7-8, 10

Conchellium capsula BORGERT, 1907, p. 208, pl. 17, figs. 1-4. - TAKAHASHI and HONJO, 1981, p. 157, pl. 14, figs. 1-4

Remarks: This species has smoother shell surface, thinner skeleton and smaller shell size than those of *Conchellium tridacna* Haeckel. Measurements on longer axis of shell diameter represent 264 ± 11 μm based on 11 specimens.

Conchellium tridacna Haeckel
Plate 61, figures 6, 9, 11

Conchellium tridacna HAECKEL, 1887, p. 1720, pl. 123, figs. 7, 7a

Remarks: This species is different from C. capsula in shell size, skeletal thickness and shell surface texture. The shell size ranges 350-500 µm in longer axis and the surface texture is rough (pl. 61, fig. 9) as described in Haeckel (1887).

Genus CONCHOPHACUS Haecker, 1906b

Conchophacus diatomeus (Haeckel)
Plate 61, figure 12

Concharium diatomeum HAECKEL, 1887, p. 1717, pl. 123, fig. 1. - BORGERT, 1901b, p. 244

Conchidium diatomeum (Haeckel). - HAECKER, 1906b, p. 34

Conchophacus diatomeus (Haeckel). - BORGERT, 1907, p. 212, pl. 15, figs. 5-8. - TAKAHASHI and HONJO, 1981, p. 158, pl. 15, fig. 2

Genus CONCHIDIUM Haeckel, 1887

Conchidium argiope Haeckel
Plate 62, figures 1-2

Conchidium argiope HAECKEL, 1887, p. 1722, pl. 124, figs. 7-9. - BORGERT, 1903, p. 755-756, text-fig. R; 1907, p. 209, pl. 16, figs. 1-4

Remarks: Shell smaller than C. caudatum and it lacks in window at the base of a short horn. Dimensions from the Panama Basin samples: shell length: 196 ± 14 µm (n = 19); width: 138 ± 6 µm (n = 4).

Conchidium caudatum (Haeckel)
Plate 62, figures 3-8

Conchoceras caudatum HAECKEL, 1887, p. 1727, pl. 24, fig. 15. - HAECKER, 1905, p. 351; 1906b, p. 34, figl 1; 1908b, p. 331-332, pl. 58, fig. 457, pl. 60, figs. 467-468

Conchidium caudatum (Haeckel). - BORGERT, 1903, p. 756, fig. 5; 1907, p. 210, pl. 16, figs. 5-7. - TAKAHASHI and HONJO, 1981, p. 158, pl. 14, figs. 5-7

Remarks: Formation of the keel is considered to be incomplete here since it does not reach aboral end and also it's thickness is comparable to many other longitudinal lines (although it is elevated and form a conspicuous crest in the posterior part). Thus, the present species should be placed in Conchidium rather than Concoceras.

Genus CONCHOPSIS Haeckel, 1887

Conchopsis compressa Haeckel
Plate 62, figures 9-16

Conchopsis compressa HAECKEL, 1887, p. 1725, pl. 125, figs. 7,8. - TAKAHASHI and HONJO, 1981, p. 158, pl. 14, figs. 8-10, pl. 15, fig. 1

Conchopsis aspidium HAECKEL, 1887, p. 1726, pl. 125, figs. 1-2

Conchopsis barca BORGERT, 1907, p. 215-216, pl. 17, figs. 5-7

Description: Lenticular shell composed of strongly compressed bivalves, with narrow smooth keels, about 32-42 teeth on one side of each valve, pores circular near the hinge and slitlike shape in the rest of the shell, shell surface rough at highly magnified view. Length and thickness of teeth are variable even in the same specimen.

Remarks: The following closely related species were excluded in the above synonomy since specimens like them were not found: *C. orbicularis* (type species of the genus), *C. carinata*, *C. lenticula*, *C. navicula*, and *C. pilidium* all described by Haeckel (1887). The criteria used in the above classification by the author are: (1) number and location of teeth; (2) width of keels; (3) shape of valves in lateral view; and (4) whether pores are surrounded by hexagonal framework.

Family AULOSPHAERIDAE Haeckel, 1862

Definition by Haeckel (1887): Phaeodaria with a large spherical or subspherical (rarely spindle-shaped) articulated shell, which is composed of hollow tangential tubes. Nodal points of the loose network stellate, with a nodal cavity and astral septa. Meshes either triangular or polygonal. Hollow radial spines arise usually at the nodal points of the surface. No peculiar mouth in the shell. Central capsule tripylean, placed in the centre of the shell.

Genus AULARIA Haeckel, 1887

Original description: *Aulosphaerida* with triangular meshes in the network, the tangential tubes of which form a simple smooth lattice-sphere. No radial tubes at the nodal points.

Aularia ternaria Haeckel

Plate 63, figures 1-2

Aularia ternaria HAECKEL, 1887, p. 1621, pl. 111, fig. 2

Family AULACANTHIDAE Haeckel, 1862

Definition by Haeckel (1887): Phaeodaria with an incomplete skeleton, composed of numerous hollow radial tubes, which pierce the spherical calymma and touch with their proximal ends the surface of the tripylean central capsule.

Genus AULOGRAPHIS Haeckel, 1879

Definition by Haeckel (1887): Aulacanthida with a veil of tangential needles, and with radial tubes, which bear no lateral branches, but at the distal end a vertical of simple terminal branches.

Aulographis stellata Haeckel
Plate 63, figure 3

Aulographis stellata HAECKEL, 1887, p. 1578, pl. 103, figs. 23a-c. - HAECKER, 1908b, p. 41-42, pl. 1, figs. 4-7, pl. 2, fig. 19, pl. 42, figs. 313-314. - TIBBS, 1976, p. 31

Aulographis tetrancistra Haeckel
Plate 63, figure 10

Aulographis tetrancistra HAECKEL, 1887, p. 1581, pl. 103, fig. 22. - TIBBS, 1976, p. 32, text-figs. 6,7

Genus AULOCEROS Haeckel, 1887

Original defintion: Aulacanthidae with a veil of tangential needles, and with radial tubes, which bear no lateral branches, but at the distal end a verticil of ramified or forked terminal branches.

Auloceros spathillaster Haeckel
Plate 63, figure 4

Auloceros spathillaster HAECKEL, 1887, p. 1585, pl. 102, fig. 12

Auloceros arborescens Haeckel birameus (Immermann)
Plate 63, figure 9

Auloceros arborescens HAECKEL, 1887, p. 1584, pl. 102, figs. 11,13

Auloceros spathillaster (Haeckel) var. birameus IMMERMANN, 1904, p. 51, pl. 5, fig. 10

Auloceros arborescens birameus (Immermann). - HAECKER, 1908b, p. 53, pl. 3, figs. 21-25, 34-35, pl. 10, fig. 102

Genus AULOGRAPHONIUM Haeckel, 1887

Original definition: Terminal branche of the radial tubes armed with numerous lateral denticles, and with terminal spathillae (or whorls of small radial teeth).

Remarks: This genus was elevated from the original subgenus to the present level by Haecker (1908b)

Aulographonium bicorne Haecker
Plate 63, figures 5-6

Aulocoryne candelabrum IMMERMAN, 1904, p. 59, pl. 6, figs. 5-7

Aulographonium bicorne HAECKER, 1908b, p. 69-70, pl. 1, fig. 1, pl. 6, fig. 57. - TIBBS, 1976, p. 42

Genus AULOSPATHIS Haeckel, 1887

Original definition: *Aulacanthidae* with a veil of tangential needles, and with radial tubes, which bear two verticils of branches, a distal verticil of terminal branches, and a proximal verticil of lateral branches.

Aulospaphis taumorpha ? Haeckel
Plate 63, figures 7-8

Aulospaphis taumorpha HAECKEL, 1887, p. 1577, pl. 103, fig. 16

Aulospathis variabilis Haeckel *bifurca* Haecker
Plate 63, figure 11

Aulospathis bifurca HAECKEL, 1887, p. 1586, pl. 104, figs. 1-5. - BORGERT, 1901a, p. XV8, text-fig. 6

Aulospathis variabilis bifurca HAECKER, 1904a, p. 125-127, text-figs. 2; 1908b, p. 86-87, pl. 6, figs. 63-67, pl. 7, figs. 72-75. - TIBBS, 1976, p. 49, text-fig. 20

Aulospathis variabilis grandis TIBBS, 1976, p. 50, text-figs. 21,22

CHAPTER II REFERENCES

BAILEY, J.W. 1856. Notice of microscopic forms found in the soundings of the Sea of Kamtschatka - with a plate. Amer. Jour. Sci. Arts, ser. 2, 22: 1-6.

BENSON, R.N., 1966. Recent Radiolaria from the Gulf of California. Ph.D. Thesis, Univ. of Minnesota, 578 pp.

BJØRKLUND, K.R., 1974. The seasonal occurrence and depth zonation of radiolarians in Korsfjorden, Western Norway. Sarsia, 56: 13-42.

----, 1976a. Radiolaria from the Norwegian Sea, Leg 38 of the Deep Sea Drilling Project. In: Talwani, M., Udintsev, G., et al., Initial Reports of the Deep Sea Drilling Project, Volume 38: 1101-1168. U.S. Government Printing Office (Washington, D.C.).

----, 1976b. Actinoma haysi, n.sp., its Holocene distribution and size variation in Atlantic Ocean sediments. Micropaleontology, 23(1): 114-126.

----, and GOLL, R. M., 1979. Internal Skeletal structure of Collosphaera and Trisolenia: A case of repetitive evolution in the collosphaeridae (Radiolaria). Jour. Paleontology, 53(6): 1293-1326.

BOLTOVSKOY, D., and RIEDEL, W.R., 1980. Polycystine radiolaria from the Southwestern Atlantic Ocean plankton. Revista Espanola de Micropaleontologia, 12(1): 99-146.

BORGERT, A., 1892. Vorbericht uber einige Phaeodarien-(Triplyeen-) Familien der Plankton-Expedition. In: Ergebn. der Plankton-Expedition, 1A(cruise description): 176-184.

----, 1901a. Die nordischen Tripyleen-Arten. In: Brandt, K., and Apstein, C., Eds., Nordisches Plankton, (15): 1-52.

----, 1901b. Die tripyleen Radiolarien des Mittelmeeres. In: Mitteilungen aus der Zoolog. Station zu Neapel, 14: 239-246.

----, 1902. Mittheilungen uber die Tripyleen-Ausbeute der Plankton-Expedition, I. Neue Medusettidae, Circoporidae und Tuscaroridae. Zoologischen Jahrbuchem, 2: 566-577.

--- , 1903. Mitteilungen uber die Tripyleen-Ausbeute der Plankton-Expedition, II. Die Tripyleenarten aus den Schliessnetzfangen. Zoolog. Jahrb., Abt. f. Systematik, 19: 733-740.

----, 1906. Die tripleen Radiolarien der Plankton-Expedition. Medusettidae. In: Ergebnisse der Plankton-Expedition, 3 l.h.: 133-192.

BORGERT, A., 1907. Die tripyleen Radiolarien der Plankton-Expedition. Concharidae. In: Ergebnisse der Plankton-Expedition, 3 l.h. (5): 195-232.

----, 1908. Die Tripyleen Radiolarien der Plankton- Expedition, Castanellidae. Plankton-Exped. Humboldt-Stiftung, Ergebn., 3 L.h.(6): 235-279.

-- -, 1909. Die tripyleen Radiolarien der Plankton-Expedition. Circoporidae. In: Ergebnisse der Plankton-Expedition, 3 L.h. (8): 319-352.

----, 1910. Die tripyleen Radiolarien der Plankton-Expedition. Porospathidae und Cadiidae. In: Ergebnisse der Plankton-Expedition, 3 L.h. (10): 383-415.

--- , 1911. Die Tripyleen Radiolarien der Plankton-Expedition. Challengeridae. In: Ergebnisse der Plankton-Expedition der Humboldt-Stiftung, 3 L.h. (11): 419-536.

BRANDT, K., 1885. Die koloniebildenden Radiolarien (Sphaerozoeen) des Golfes von Neapel und der angrenzenden Meers-Abschnitte. Berlin, 276 pp., pls. 1-8.

----, 1905. Zur systematik der kolonienbildenden Radiolarien. In: Festschrift zum 80. Geburstag des Herrn Geh. Regierungstats Prof. Dr. Karl Mobius in Berlin. Jena, Suppl., 8: 311-352.

BUTSCHLI, O., 1882. Klassen und Ordnungen des Thier-Reichs, wissenschaftlich dargestellt in Wort und Bild. Paleontologische Entwicklung der Rhizopoda von C. Schwager. I. Abtheilung: Sarkodia und Sporozoa, volume 1: 321-616.

CALKINS, G.N., 1909. Protozoology. Lea and Febiger Co., 349 pp.

CAMPBELL, A.S.,, 1951. New genera and subgenera of Radiolaria. Jour. Paleontol., 25(47): 527-530.

----, 1954. Radiolaria. In: Moore, R.C., Ed., Treatise on Invertebrate Paleontology, New York: Geol. Soc. Amer., pt. D, Protista 3: 11-163.

----, and CLARK, B.L., 1944. Miocene radiolarian faunas from Southern California. Geol. Soc. Am. Spec. Paper 51: 1-76.

CASEY, R.E., 1971a. Distribution of polycystine radiolaria in the oceans in relation to physical and chemical conditions. In: Funnell, B.M., and Riedel, W.R., Eds., The Micropaleontology of Oceans, Cambridge University Press: 151-159.

CASEY, R.E., 1971b. Radiolarians as indicators of past and present water-masses. In: Funnell, B.M., and Riedel, W.R., Eds., The Micropaleontology of Oceans, Cambridge University Press: 331-341.

CAULET, J., 1971. Contribution a l'etude de quelques Radiolaires Nassellaires des boues de la Mediterranee et du Pacifique. Arch. orig. Centre de Documentation C.N.R.S., Cah. Micropaleontol., Ser. 2, vol. 10, No. 498: 10 pp.

CLEVE, P.T., 1899. Plankton collected by the Swedish Expedition to Spitzbergen in 1898. K. Svenska Vetensk.-Akad., Handl., 32(3): 1-51.

----, 1900a. Notes on some Atlantic-plankton organisms. Goteborgs Kgl. Vetensk.-Noch. Vetterh.-Samh., Handl., 34(1): 1-22.

----, 1900b. The seasonal distribution of Atlantic planktonic organisms. Goteborgs K. Vetensk.-O. Vitterhsamh. Handl., 4(3): 1-396.

----, 1903. Report on plankton collected by Mr. Thorid Wulff during a voyage to and from Bombay. Arkiv for Zoologi., K. Svenska Vetenskaps Akademien, 1: 329-380.

DEFLANDRE, G., 1953. Radiolaires fossiles. In: Traite de Zoologie, Grasse, P.P., Ed., Paris: Masson, 1(2): 389-436.

DREYER, F., 1889. Morphologische Radiolarienstudien. I. Die Pylombildungen in vergleitschend-anatomischer und entwicklungsgschichlicher Bezeihung bei Radiolarien und bei Protisten Uberhaupt, nebst system und Beschreibung neuer und des bis jetzt bekannten pylomatischen Spumellarien. Jen. Zeitschr. Naturw., 23(n. ser., vol. 16): 1-138.

DREYER, F., 1913. Die Polycystinen der Plankton-Expedition. Ergebn. Plankton-Exped. Humboldt-Stiftung, 3 (L.d.e.): 1-104.

DUMITRICA, P., 1973. Phaeodarian Radiolaria in southwest Pacific sediments cored during Leg 21 of the Deep Sea Drilling Project. In: Burns, R.E., Andrews, J.E., et al., Initial Reports of the Deep Sea Drilling Project, 21: 751-785, U.S. Government Printing Office.

----, 1972. Cretaceous and Quaternary Radiolaria in deep sea sediments from the northwest Atlantic Ocean and Mediterranean Sea. In: Ryan, W.B.F., Hsu, K.J., et al., Initial Reports of the Deep Sea Drilling Project, Volume 13: 829-901. U.S. Government Printing Office (Washington, D.C.).

DZINORIDZE, R.N., JOUSE, A.P., KOROLEVA-GOLIKOVA, G.S., KOZLOVA, G.E., NAGAEVA, G.S., PETRUSHEVSKAYA, M.G., and STROLNIKOVA, N.I., 1976. Diatom and radiolarian Cenozoic stratigraphy, Norwegian Basin; DSDP Leg 38. In: Talwani, N., Udintsev, G., et al., Eds., Initial Reports of the Deep Sea Drilling Project, Volume 38 (supplement): 289-427. Washington, D.C. (U.S. Government Printing Office).

EHRENBERG, C.G., 1838. Ueber die Bildung der Kreidefelsen und des Kreidemergels durch unsichtbare Organismen. K. Akad. Wiss. Berlin, Abh., for 1838: 59-147.

----, 1844. Ueber 2 neue Lager von Gebirgsmassen aus Infusorien als Meeres-Absatz in Nord-Amerika und eine Vergleichung derselben mit den organischen Kreide-Gebilden in Europa und Afrika: Montsber. Kgl. Preuss Akad. Wiss. Berlin, Jahrg., p. 57-97.

----, 1847a. Ueber eine halibiontische, von Herrn R. Schomburgk entdeckte, vorherrschend aus mikroscopischen Polycystinen gebildete, Gebirgsmasse von Barbados. K. Akad. Wiss. Berlin, Ber., Jahrg. for 1846: 382-385.

----, 1847b. Ueber die mikroskopischen kieselschaligen Polycystinen als machtige Gebirgsmasse von Barbados. K. preuss. Akad. Wiss., Monatsber., for 1847: 40-60.

----, 1854a. Die systematische Characteristik der neuen mikroskopischen Organismen des tiefen Atlantischen Oceans. K. preuss. Akad. Wiss., Monatsber., for 1854: 236-250.

----, 1854b. Mikrogeologie. Leopold Voss, Leipzig, 374 pp.

----, 1858. Kurze Characteristik der 9 neuen GEnera und der 105 neuen Species des agaischen Meeres und des Tiefgrundes des Mittel-Meeres. K. preuss. Akad. Wiss., Monatsber., for 1858: 10-41.

----, 1860a. Ueber die organischen und unorganischen Mischungsverhaltnisse des Meeresgrundes in 1800 Fuss Tiefe. K. preuss. Akad. Wiss., Monatsber., for 1860: 765-744.

----, 1860b. Ueber den Tiefgrund des stillen Oceans zwischen Californien und des Sandwich-Inseln. K. preuss. Akad. Wiss., Monatsber., for 1860: 819-833.

----, 1861b. Ueber die Tiefgrund-Verhaltnisse des Oceans am Eingange der Davisstrasse und bei Island. K. preuss. Akad. Wiss., Monatsber., for 1861: 275-315.

----, 1872a. Mikrogeologische Studien als Zusammenfassung seiner Beobachtungen des kleinsten Lebens der Meeres-Tiefgrunde aller Zonen und dessen geologischen Einfluss. K. preuss. Akad. Wiss., Monatsber., for 1872: 265-322.

EHRENBERG, C.G., 1872b. Mikrogeologische Studien ueber das kleinste Leben der Meeres-Tiefgrunde aller Zonen und dessen geologischen Einfluss. K. Akad. Wiss. Berlin, Abh., for 1872: 131-399.

----, 1872c. Nachtrag zur ubersicht der organischen Atmospharilen. Kgh. Akad. Wiss. Berlin, Jahrg. 1871, p. 233.

----, 1873. Grossere Felsproben des Polycystinen-Mergels von Barbados. K. preuss. Akad. Wiss., Monatsber., for 1873: 213-263.

----, 1875. Forsetzung der mikrogeologischen Studien als Gesammt-Uebersicht der mikroskopischen Palaeontologio. K. Akad. Wiss., Berlin, Abh., for 1875: 226 p.

FOREMAN, H.P., 1973. Radiolaria of Leg 10 with systematics and ranges for the families Amphipynadacidae, Artostrobiidae, and Theoperidae. In: Worzel, J.L., Bryant, W., et al., Initial Reports of the Deep Sea Drilling Project, 10: 407-474, U.S. Government Printing Office.

GOLL, R.M., 1969. Classification and phylogeny of Cenozoic Trissocyclidae (Radiolaria) in the Pacific and Caribbean Basins. Part II. Jour. Paleontology, 43(2): 322-339.

----, 1972a. Systematics of eight Tholospyris taxa (Trissocyclidae, Radiolaria). Micropaleontology, 18(4): 443-475.

----, 1972b. Leg 9 Synthsis, Radiolaria. In: Hays, J.D., et al., Initial Reports of the Deep Sea Drilling Project, Volume 9, 947-1058. Washington, D.C. (U.S. Government Printing Office).

----, 1976. Five Trissocyclid Radiolaria from Site 338. In: Talwani, M., Udintzev, G., et al., Eds., Initial Reports of the Deep Sea Drilling Project, Volume 38 (supplement): 177-180. Washington, D.C. (U.S. Government Printing Office).

----, 1977. Morphological integradation between modern populations of Lophospyris and Phormospyris (Trissocyclidae, Radiolaria). Micropaleontology: 22(4): 379-418.

----, 1980. Pliocene-Pleistocene Radiolarians from the East Pacific Rise and the Galapagos spreading center, Deep Sea Drilling Project Leg 54. In: Rosendahl, B.R., Hekinian, R., et al., Eds., Initial Reports of the Deep Sea Drilling Project, Volume 54: 425-453 Washington, D.C. (U.S. Government Printing Office).

----, and BJØRKLUND, K.R., 1971. Radiolaria in surface sediments of the north Atlantic Ocean. Micropaleontology, 17(4): 434-454.

----, and BJØRKLUND, K.R., 1974. Radiolaria in surface sediments of the South Atlantic. Micropaleontology, 20(1): 38-75.

HAECKEL, E., 1860a. Uber neue, lenende Radiolarien des Mittelmeeres und... due dazu gehoringen Abbildungen. K. Akad. Wiss. Berlin, Montatsber., Janrg. 1860: 794-817.

----, 1860b. Fernere Abbildungen und Diagnosen neuer Gattungen und Arten von lebenden Radiolarien des Mittelmeeres. K. Akad. Wiss. Berlin, Monatsber., Jahrg. 1860: 835-845.

----, 1862. Die Radiolarien (Rhizopoda Radiaria). Eine Monographie. Berlin, Reimer: i-xiv, 1-572.

----, 1866. Generelle Morphologie der Organismen, 2.

----, 1879. Uber die Phaeodarien, eine neue Gruppe kieselschaliger mariner Rhizopoden. Med. Naturw. Ges. Jena. Sitzber., Suppl., 13 (n. ser. volume 6): 151-157.

----, 1881. Entwurf eines Radiolarien-Systems auf Grund von Studien der Challenger-Radiolarien. Jen. Zeitschr. Naturw., 15 (n. ser., vol. 8; 1882)(3): 418-472.

----, 1887. Report on the Radiolaria collected by H.M.S. "Challenger" during the years 1873-1876. Repts., Voy. Challenger, Zool., 18: i-clxxxiii, 1-1803.

HAECKER, V., 1904a. Bericht uber die Tripyleen-Ausbeute der Deutschen Tiefsee-Expedition. Deutsch. Zool. Ges., Verh., 14: 122-157.

----, 1905. Finales und Causales uber das Tripyleenskelett. Critte Mitteilung uber die Tripyleen der "Valdivia"-Ausbeute. In: Zeitschr. f. wiss. Zool., volume 83.

----, 1906a. Zur Kenntnis der Challengeriden; Vierte Mitteilung uber die Tripyleen-Ausbeute der deutschen Tiefsee-Expedition. Archiv Protistenk., 7(2): 259-306.

----, 1906b. Uber die Mittel der Formbildung in Radiobrien Rorper. Sechste Mittelung uber die Tripyleen den "Valdiria"-Ausbeute. Verhandl. d. Deutsch. Zool. Gesellsch., p. 31-50.

----. 1907a. Altertumliche Spharellarien und Cyrtellarien aus grossen Meerestiefen, Archiv. f. Protistenkunde, 10: 114-126.

----, 1907b. Zur Kenntnis der Castanelliden und Porospathiden. Arch. Protistenk, 8: 52-65.

----, 1908a. Tiefsee-Radiolarien. Spezieller Teil. Die Tripyleen, Collodarien und mikroradiolarien der Tiefsee. Deutsch Tiefsee Exped. auf dem Dampfer "Valdivia" 1898-1899, Wiss. Ergebn., 14: 1-476. Allgemeiner Teil. Form. und Formbuldung bei den Radiolarien. Ibib.: 477-706.

HAECKER, V., 1908b. Tiefsee Radiolarien Speziel Teil, L1, Aulacanthidae-concharidae. Deutsch. Tiefsee-Exped., Wiss. Engebn. 14: 1-336.

HARTING, P., 1863. Bijdrage tot de Kennis Mikroskopische Fauna en Flora van de Banda-Zee. K. Akad. v. Wetensch., Amsterdam, Verhand, 10: 1-34.

HAYS, J.D., 1970. Stratigraphy and evolutionary trends of radiolaria in North Pacific deep-sea sediments. In: Hays, J.D., Ed., Geological Investigations of the North Pacific. Geol. Soc. Amer., Memoir 126: 185-218.

HEATH, G.R., 1974. Dissolved silica and deep-sea sediments. In: Hay, W.W., Ed., Studies in Paleo-Oceanography. Soc. Econ. Paleont. Mineral., Spec. Publ. No. 20: 77-93.

HERTWIG, R., 1877. Studien uber Rhizopoden. Jen. Zeitschr. f. Naturw. 11: 324-348.

----, 1879. Der Organismus der Radiolarien. Jena. G. Fischer: i-iv, 1-149.

----, and LESSER, E., 1874. Ueber rhizopoden und denselben nahestehende organismen. Arch. Mikr. Anat. 10, Suppl.: 35-243.

HOLLANDE, A. and ENJUMET, M., 1960. Cytologie, evolution et systematique des Sphaeroides (Radiolaires). Mus. Nation. Hist. Natur., Paris, Arch., ser. 7, 7: 1-134.

HUXLEY, Th., 1851. Zoological notes and observations made on board H.M.S. Rattlesnake. III. Upon Thalassicolla a new Zoophyte. Ann. and Mag. Nat. Hist., London, Ser. 2, vol. 8: 433-442.

IMMERMAN, F., 1804. Die Triplyeen-Familie der Aulacanthiden der Plankton Expedition. Erg. d. Plankt.-Exp. Bd. 3, L.h.

JOHNSON, D.A., 1974. Radiolaria from the Eastern Indian Ocean, DSDP Leg 22. In: von der Borch, C.C., Sclater, J.G., Eds., Initial Reports of the Deep Sea Drilling Project, Volume 22, Washington, D.C. (U.S. Government Printing Office), pp. 521-575.

----, and NIGRINI, C., 1980. Radiolarian biogeography in surface sediments of the western Indian Ocean. Mar. Micropaleontology, 5: 111-152.

JØRGENSEN, E., 1900. Protophyten und Protozoen im Plankton aus der norwegischen Westkuste. Bergens Museums Aarbog. 1899, no. 6: 51-95.

----, 1905. The protist plankton and the diatoms in bottom samples. Bergens Museums Skrifter Ser. 1, 7: 49-151, 195-225.

KEANY, J., 1979. Early Pliocene radiolarian taxonomy and biostratigraphy in the Antarctic Region. Micropaleontology, 25(1): 50-74.

KLING, S.A., 1966. Castanellid and Circoporid radiolarians: systematics and zoogeography in the eastern North Pacific. Ph.D. dissertation, Univ. Calif., San Diego, 175 p.

----, 1971. Dimorphism in radiolaria. In: Farinacci, A., Ed., Proceedings of the II Planktonic Conference, Roma 1970, 1: 663-672.

----, 1973. Radiolaria from the eastern North Pacific, Deep Sea Drilling Project, Leg 18. In: Kulm, L.D., von Huene, R., et al., Initial Reports of the Deep Sea Drilling Project, 18: 617 (U.S. Government Printing Office).

----, 1976. Relation of radiolarian distributions to subsurface hydrography in the North Pacific. Deep-Sea Res., 23: 1043-1058.

----, 1977. Local and regional imprints on radiolarian assemblages from California Coastal Basin sediments. Mar. Micropaleontol., 2: 207-221.

----, 1979. Vertical distribution of polycystine radiolarians in the central North Pacific. Marine Micropaleontology, 4(4): 295-318.

LING, H.Y., 1966. The radiolarian Protocystis thomsoni (Murray) in the northeast Pacific Ocean. Micropaleontology, 12(2): 203-214.

----, 1972. Polycystine Radiolaria from surface sediments of the South China Sea and the adjacent seas of Taiwan. Acta Oceanogrpahica taiwanica, (2): 159-178.

----, 1973. Radiolaria: Leg 19 of the Deep Sea Drilling Project. In: Scholl, D.W., et al., Initial Reports of the Deep sea drilling Project, 19: 777-797 (U.S. Government Printing Office).

----, 1975. Radiolaria: Leg 31 of the Deep Sea Drilling Project. In: Karig, D.E., Ingle, J.C., Jr., et al., Initial Reports of the Deep Sea Drilling Project, 31: 703-761 (U.S. Government Printing Office).

----, 1980. In: Jackson, E.D., Koizumi, I., et al., Eds., Initial Reports of the Deep Sea Drilling Project, Volume 55: 365-373. Washington, D.C. (U.S. Government Printing Office).

----, and ANIKOUCHINE, W.A., 1967. Some Spumellarian Radiolaria from the Java, Philippine and Mariana Trenches. J. Paleontol., 41(6): 1481-1491.

----, STADUM, C.J., and WELCH, M.L., 1971. Polycystine Radiolaria from Bering Sea surface sediments. In: Farinacci, A., Ed., Proc. II Planktonic Conference, Roma, 1970, p. 705-729.

LING, H.Y., and TAKAHASHI, K., 1977. Observation on microstructure of selected phaeodarian radiolaria. Memoir Geol. Soc. of China, (2): 207-212.

LISITZIN, A.P., 1972. Sedimentation in the world ocean. Soc. Econ. Paleont. Mineral., Spec. Publ. No. 17: 218 pp.

LOEBLICH, A.R., Jr. and TAPPAN, H., 1961. Remarks on the systematics of the Sarkodina (Protozoa), renamed homonyms and new and validated genera. Biol. Soc. Washington, Proc., v. 74: 213-234.

MAST, H., 1910. Die Astrosphaeriden. Deutsch. Tiefsee-Exped., Dampfer "Valdivia" 1898-1899, Wiss. Ergebn., 19)pt. 4): 123-190.

MCMILLEN, K.J., and CASEY, R.E., 1978. Distribution of living polycystine radiolarians in the Gulf of Mexico and Caribbean Sea, and composition with sedimentary record. Mar. Micropal., 3: 121-145.

MORLEY, J.J., 1980. Analysis of the abundance variations of the subspecies of Cycladophora davisiana. Mar. Micropaleontol., 5: 205-214.

MÜLLER, J., 1855. Uber Sphaerozoum und Thalassicolla, K. Acad. Wiss. Berlin, Monatsber., Jahrg. for 1855: 229-253.

----, 1857. Uber die Thalassicollen, Polycystinen und Acanthometren des Mittelmeeres. Akad. Wiss. Berlin, Monatsber., Jahrg. for 1856: 474-503.

----, 1858a. Uber due Thalassicollen, Polycystinen und Acanthometren des Mittelmeeres. Wiss. Berlin, Abh., Jahrg. for 1858: 1-62 (plates 1-11).

----, 1858b. Einige neue bei St. Tropez am Mittelmeer beobachtete Polycystinen und Acanthometren aus den Abbildungen. Akad. Wiss. Berlin, Monatsber., Jahrg. for 1858: 154-155.

MURRAY, J., 1876. Preliminary reports to Professor Wyville Thompson, F.R.S., director of the civilian scientific staff, on work don on board the "Challenger". Roy. Soc. London, Proc., 24(170): 471-544.

----, 1885. The Radiolaria. In: Tizard, T.H., Moseley, H.N., Buchanan, J.Y., and Murray, J., Eds., Narrative of the cruise of the H.M.S. Challenger with a general account of the scientific results of the expedition. Rept. Voy. Challenger, Narrative, 1(pt. 1): 219-227.

NAKASEKO, K., 1959. On suprafamily Liosphaericae (Radiolaria) from sediments in the sea near Antarctica. Biol. Results of the Japanese Antarctic Research Exped. 2: Sp. Publ., Seto Marine Biological Lab., 13 pp.

NIGRINI, C.A., 1967. Radiolarian in pelagic sediments from the Indian and Atlantic Oceans. Scripps Inst. of Oceanography, Bull., 11: 1-125.

----, 1968. Radiolaria from eastern tropical Pacific sediments. Micropaleontology, 14(1): 51-63.

----, 1970. Radiolarian assemblages in the North Padific and their application to a study of Quaternary sediments in Core V20-130. Geol. Soc. Amer., Mem., no. 126: 139-175.

----, 1971. Radiolarian zones in the Quaternary of the equatorial Pacific Ocean. In: Funnell, B.M., and Riedel, W.R., Eds., The Micropaleontology of Oceans, pp. 443-461. Cambridge Univ. Press.

----, 1977. Tropical Cenozoic Artostrobiidae (Radiolaria). Micropaleontology, 23(3): 241-269.

----, and MOORE, T.C., 1979. A guide to modern Radiolaria. Cushman Found. Foram. Res., Spec. Publ. No. 16: S1-N105, 28 plates.

PETRUSHEVSKAYA, M., 1965. Peculiarities of the construction of the skeleton of Botryoid Radiolarians (order Nassellaria). Trudy Zoologicheskogo Inst. (Akad. Nauk SSSR), vol. 35, pp. 79-118.

----, 1966. Radiolarians in plankton and in bottom sediments. In: Strackhov, N.M., Ed., Geochemistry of Silica, p. 219-245, Publishing Office "Science" Nauka Moscow. (In Russian).

----, 1967. Radiolarian of orders Spumellaria and Nassellaria of the Antarctic region. In: Andriyashev, A.P., and Ushakov, P.V., Eds., Biological Reports of the Soviet Antarctic Expedition (1955-1958), 3: 2-186 (in Russian).

----, 1971a. Spumellarian and Nessellarian Radiolaria in the plankton and bottom sediments of the Central Pacific. In: Funnell, B.M., and Riedel, W.R., Eds., The Micropaleontology of Oceans, p. 309-317, Cambridge University Press.

----, 1971b. Radiolaria in the plankton and recent sediments from the Indian Ocean and Antarctic. In: Funnell, B.M., and Riedel, W.R., Eds., The Micropaleotology of Oceans, pp. 319-329, Cambridge Univ. Press.

----, 1971c. Radiolarii Nassellaria v planktons mirovago okeana. In: Radiolarii mirovogo okeana po materialam sovetskikh ekspeditsii, Issled. Fauni Morei. Leningrad, Nauka, 9(17): 5-294. (in Russian)

PETRUSHEVSKAYA, M., 1971d. On the natural system of polycystine Radiolaria. In: Farinacci, A., Ed., Proc. II Planktonic Conf. Rome 1970, vol. 2: 981-992.

----, 1975. Cenozoic radiolarians of the Antarctic, Leg 29, DSDP. In: Kennett, J.P., Houtz, R.E., et al., Initial Reports of the Deep Sea Drilling Project, Volume 29: 541-675. Washington, D.C. (U.S. Government Printing Office).

----, and BJORKLUND, K.R., 1974. Radiolarians in Holocene sediments of the Norwegian-Greenland Seas. Sarsia, (57): 33-46.

----, and KOZLOVA, G.E., 1972. Radiolaria. In: Hayes, D.E., Ed., Initial Reports of the Deep Sea Drilling Project, 14: 495-648 (U.S. Government Printing Office).

----, and KOZLOVA, G.E., 1979. Description of the radiolarian genera and species. In: Explorations of the Fauna of the Seas, Volume 23(31): The history of the microplankton of the Norwegian Sea (on the Deep Sea Drilling materials). IZD. Nauka, pp. 86-157.

POCHE, F., 1913. Das System der Protozoen. Arch. f. Protistenk., 30: 125-321.

POPOFSKY, A., 1908. Die Radiolarien des Antarktis (mit Ausnahme der Tripyleen). Deutsche Sudpolar-Exped., 1901-1903, Rept., 10 (Zool., vol. 2)(3): 183-305.

----, 1912. Die Sphaerellarien des Warmwassergebietes. Deutsche Sudpolar-Exped., 13 (Zool., vol. 5, pt. 2): 73-159.

----, 1913. Die Nassellarien des Warmwassergebietes. Deutsche Sudpolar-Exped., 14 (Zool., vol. 6): 217-416.

----, 1917. Die Collosphaeriden der Deutschen Sudpolar-Expedition 1901-1903. Mit. Nachtrag zu den Spumellarien und der Nassellarien. Deutsche Sudpolar-Exped., 16 (Zool., vol. 8): 235-278.

RENZ, G.W., 1976. The distribution and ecology of Radiolaria in the Central Pacific plankton and surface sediments. Bull. Scripps Inst. of Oceanogr., 22: 1-267.

RESHETNYAK, V., 1955. Vertical distribution of the Radiolaria of the Kurilo-Kamchatka deep. Akad. Nauk SSSR, Zool. Inst., Trudy, 21: 94-101. (in Russian)

----, 1966. The deep-water radiolarian Phaeodaria in the northwestern part of the Pacific Ocean. In: Fauna of the USSR, Radiolaria. Akad. Nauk SSSR, Zool. Inst., n. ser., (94): 1-208.

RIEDEL, W.R., 1953. Mesozoic and late Tertiary Radiolaria of Rotti. Jour. Paleont., 27(6): 805-813

----, 1957. Radiolaria: a preliminary stratigraphy. Rep. Swed. Deep Sea Exped., Series B, 6(B): 61-96.

----, 1958. Radiolaria in Antarctic Sediments. Repts. B.A.N.Z. Antarct. Res. Exped., ser. B, 6 (pt. 10): 217-255.

----, 1959. Siliceous organic remains in pelagic sediments. In: Ireland, H.A., Ed., Silica in Sediments. Soc. Econ Paleontologists and Mineralogists, Spec. Publ., volume 7: 80-91.

----, 1967a. Subclass Radiolaria. In: Harland, W.B., et al., Eds., The Fossil Record. London, Geol. Soc. London: 291-298.

----, 1967b. Some new families of Radiolaria. Proc. Geol. Soc. London, (1640): 148-149.

----, 1971. Systematic classifications of Polycystine Radiolaria. In: Funnell, B.M., and Riedel, W.R., Eds., the Micropaleontology of Oceans: 649-661, Cambridge Univ. Press.

----, and SANFILIPPO, A., 1970. Radiolaria, Leg 4, Deep Sea Drilling Project. In: Bader, R.G., Gerard, R.D., et al., Initial Reports of the Deep Sea Drilling Project, 4: 503-575 (U.S. Government Printing Office).

----, 1971. Cenozoic Radiolaria from the western tropical Pacific, Leg 7, Deep Sea Drilling Project. In: Winterer, E.L., Riedel, W.R., et al., Initial Reports of the Deep Sea Drilling Project, 7: 1529-1672 (U.S. Government Printing Office).

----, 1978. Stratigraphy and evolution of tropical Cenozoic radiolarians. Micropaleontology, 23(1): 61-96.

SANFILIPPO, A., and RIEDEL, W.R., 1973. Cenozoic Radiolaria (exclusive of Theoperids, Artostrobiids and Amphipyndacids) from the Gulf of Mexico, DSDP Leg 10. In: Worzel, J.L., Bryant, W., et al., Initial LReports of the Deep Sea Drilling Project, Volume 10: 475-611. Washington, D.C. (U.S. Government Printing Office).

----, and RIEDEL, W.R., 1974. Radiolaria from the west central Indian Ocean and Gulf of Aden, DSDP Leg 24. In: Fisher, R.L., Bunce, E.T., et al., Eds., Initial Reports of the Deep Sea Drilling Project, Volume 24: 997-1035. Washington, D.C. (U.S. Government Printing Office).

----, and RIEDEL, W.R., 1974. A revised generic and suprageneric classification of the Artiscins (Radiolaria). Jour. Paleontology, 54(5); 1008-1011.

SANFILIPPO, A., BURCKLE, L.H., MARTINI, E., and RIEDEL, W.R., 1973. Radiolarians, diatoms, silicoflagellates and calcareous nannofossils in the Mediterranean Neogene.

SCHMIDT, W.J., 1907. Einige neue Castanelliden-Arten. Zool. Anzeiger, XXXII: 297-302.

SCHRÖDER, O., 1909. Die Nordischen Spumellarien. In: Brandt, K., and Apstein, C., Eds., Nordisches Plankton Zoology, Kiel, Lipsius and Tischer, pt. 17, pp. 1-66.

----, 1913. Die tripyleen Radiolarien (Phaeodarien). Deutsche Sudpolar-Exped., 1901-1903, 14 (Zool., vol. 6, pt. 2): 113-215.

STADUM, C.J., and LING, H.Y., 1969. Tripylean Radioalria in deep sea sediments of the Norwegian Sea. Micropaleontolgoy, 15(4): 481-489.

STÖHR, E., 1880. Die Radiolarien fauna der Tripoli von grotte, Provinz Girenti in Sicilien. Paleontographica, 26 (ser. 3, vol. 2): 69-124.

STRELKOV, A.A., and RESHETNYAK, V.V., 1971. Colonial spumellarian radiolarians of the world ocean. In: Radiolarians of the Ocean - Reports on the Soviet Expeditions, Explorations of the Fauna of the Seas Leningrad, Nauka. Volume 9(7): 295-369. (In Russian - translated into English by W.R. Riedel).

TAKAHASHI, K., and HONJO, S., 1981. Vertical flux of Radiolaria: A taxon-quantitative sediment trap study from the western Tropical Atlantic. Micropaleontology, 27(2): 140-190.

TAN, Z. and TCHANG, T.R., 1976. Studies on the Radiolaria of the East China Sea. Studia Marina Sinica, 11: 217-313 (in Chinese with English abstract).

TIBBS, J.F., 1976. The Aulacanthidae (Radiolaria: Phaeodaria) of the Antarctic Seas. Antarctic Res. Ser., 23: 21-65.

VINASSA DE REGNY, P.E., 1898. Nuovi generi di Radiolari del Miocene di Arcevia. Boll. Soc. Geol. Italiana, vol. 17, fasc. H, pp. 197-198.

----, 1900. Radiolari Miocenici Italiani. R. Accad. Sci. Ist. Bologna, Mem., ser. 5, 8: 227-257 (565-595).

WALLICH, G.C., 1869. On some undescribed testaceous rhizopods from the North Atlantic deposits. Monthly Microsc. Jour., 1(2): 104-110.

WOLFENDEN, R.N., 1902. The plankton of the Faroe Channel and Shetlands. Preliminary notes on some Radiolaria and Copepoda. Journal Mar. Biol. Assoc., 6(3): 344-374.

PLATE 1

Suborder: Spumellaria
Family: Collosphaeridae

Figure		Station Depth	Type of Micrograph	Magnification
1	*Acrosphaera spinosa* (Haeckel) *longispina*, new name	$P_1$4280m	SEM	x260
2	*Acrosphaera spinosa* (Haeckel) *coniculispina*, new name	$P_1$5582m	SEM	x300
3	*Acrosphaera murrayana* (Haeckel) Two shells linked together	PB3791m	LM	x210
4	*Acrosphaera spinosa* (Haeckel) *longispina*, new name	$P_1$5582m	LM	x210
5	*Acrosphaera spinosa* (Haeckel) *coronula*, new name	$P_1$2778m	LM	x210
6	*Acrosphaera murrayana* (Haeckel)	PB1268m	LM	x210
7	*Acrosphaera murrayana* (Haeckel)	$P_1$4280m	SEM	x230
8	*Acrosphaera murrayana* (Haeckel)	PB3791m	SEM	x220
9	*Acrosphaera murrayana* (Haeckel) Two shells linked together	PB3769m	SEM	x120
10	*Acrosphaera murrayana* (Haeckel) Same specimen. Some of spines are still linked.	PB3769m	SEM	x880
11	*Acrosphaera murrayana* (Haeckel) A typical skeletal cross section which is common to most of polycystines, if not all.	PB3769m	SEM	x4700
12	*Acrosphaera cyrtodon* (Haeckel)	$P_1$978m	SEM	x440
13	*Acrosphaera cyrtodon* (Haeckel)	PB3769m	LM	x210
14	*Acrosphaera spinosa* (Haeckel) *lappacea* (Haeckel)	PB3769m	LM	x210
15	*Clathrosphaera arachnoides* Haeckel	$P_1$4280m	SEM	x370
16	*Acrosphaera lappacea* (Haeckel)	$P_1$4280m	SEM	x340

SEM: scanning electron micrograph
TEM: transmission electron micrograph
LM: transmission light micrograph
RLM: reflection light micrograph

PLATE 1 Spumellaria

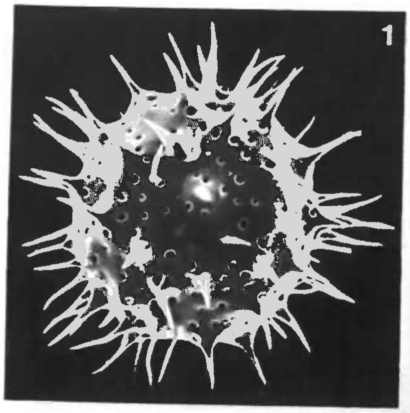

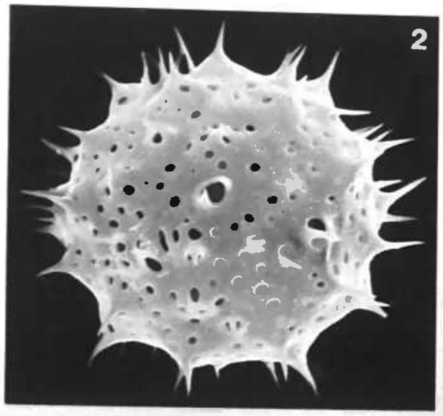

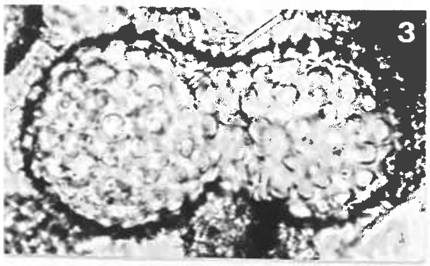

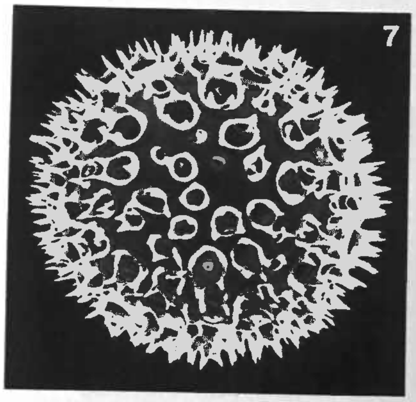

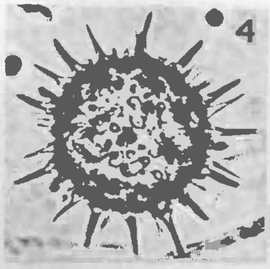

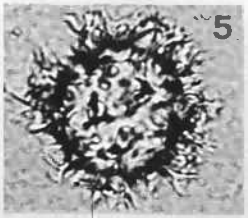

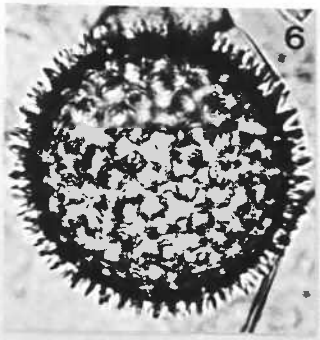

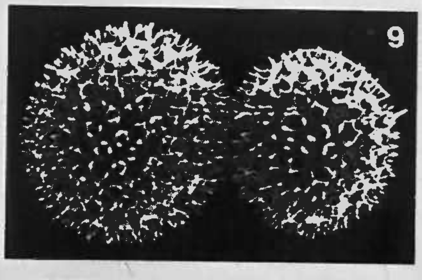

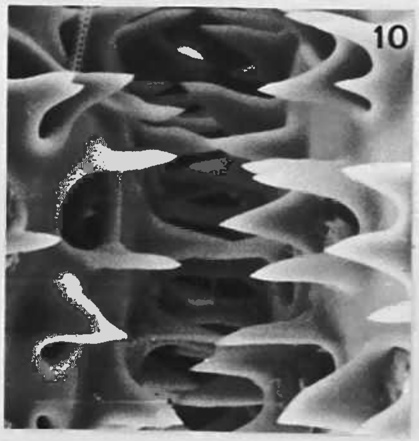

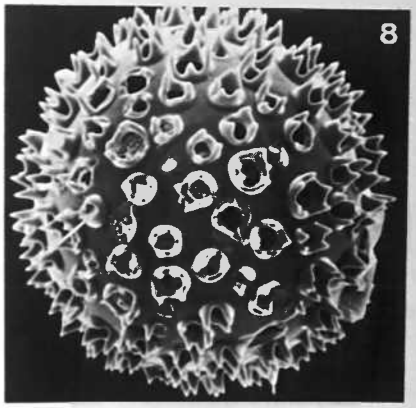

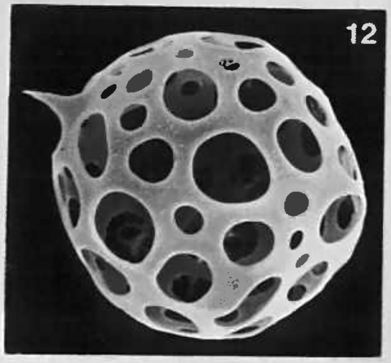

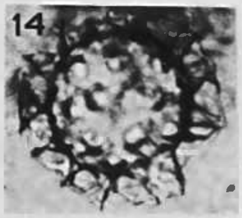

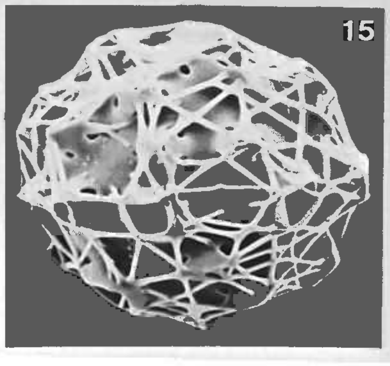

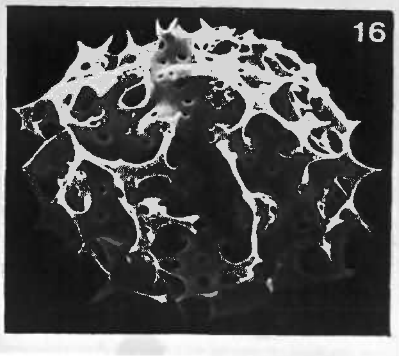

PLATE 2

Suborder: Spumellaria
Family: Collosphaeridae

Figure		Station Depth	Type of Micrograph	Magnification
1	*Collosphaera tuberosa* Haeckel	$P_1$5582m	SEM	x280
2	*Collosphaera tuberosa* Haeckel	PB2869m	LM	x210
3	*Collosphaera tuberosa* Haeckel	$P_1$5582m	LM	x210
4	*Collosphaera confossa* n.sp. Holotype	$P_1$5582m	SEM	x215
5	*Collosphaera confossa* n.sp. Paratype	$P_1$2778m	LM	x210
6	*Collosphaera armata* Brandt	PB2869m	LM	x210
7	*Collosphaera armata* Brandt	$P_1$5582m	LM	x210
8	*Collosphaera huxleyi* Müller	$P_1$4280m	SEM	x210
9	*Collosphaera huxleyi* Müller	PB2869m	LM	x210
10	*Collosphaera huxleyi* Müller	$P_1$978m	LM	x210
11	*Collosphaera huxleyi* Müller	$P_1$2778m	LM	x210
12	*Collosphaera armata* Brandt	PB3769m	SEM	x350
13	*Collosphaera macropora* Popofsky	$P_1$4280m	LM	x210
14	*Collosphaera macropora* Popofsky Two shells linked together	$P_1$978m	SEM	x520
15	*Collosphaera macropora* Popofsky	$P_1$4280m	SEM	x370
16	*Collosphaera macropora* Popofsky Same specimen as fig. 14	$P_1$978m	SEM	x2200
17	*Collosphaera macropora* Popofsky	$P_1$978m	SEM	x940
18	*Collosphaera macropora* Popofsky A group of shells probably derived from a colony.	$P_1$2778m	LM	x240

PLATE 2 Spumellaria

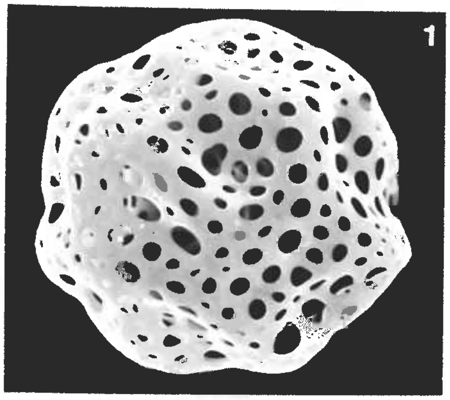

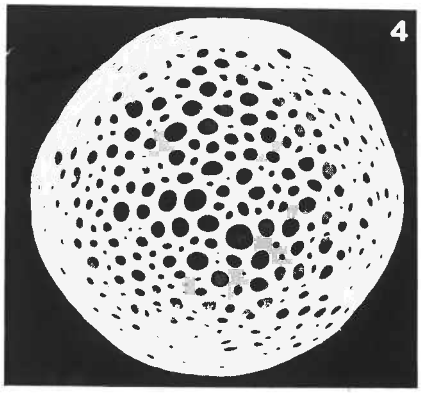

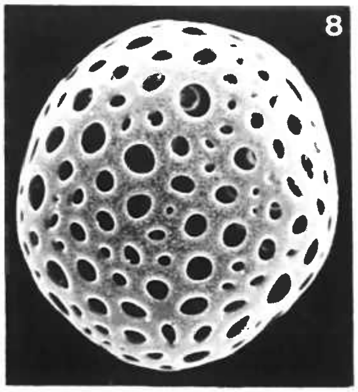

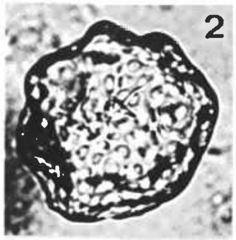

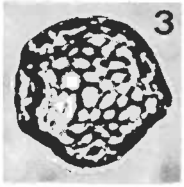

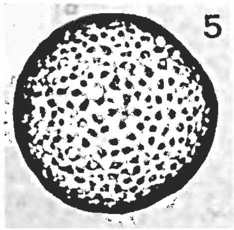

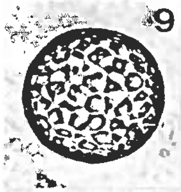

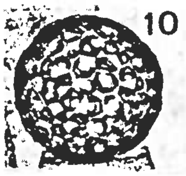

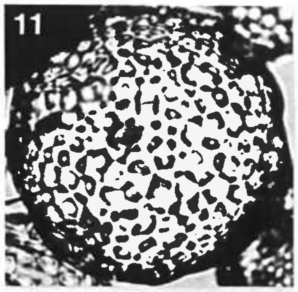

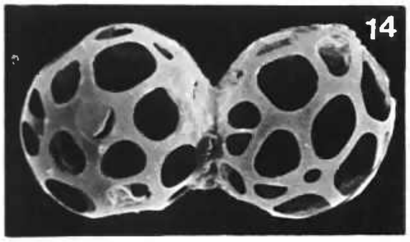

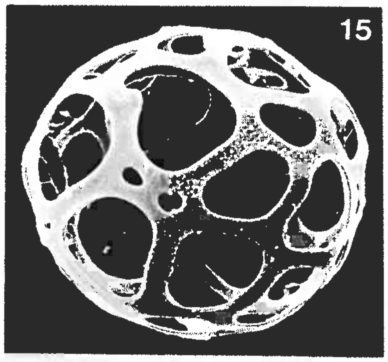

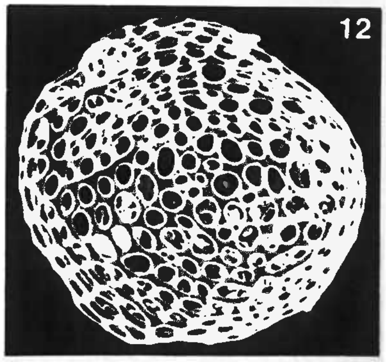

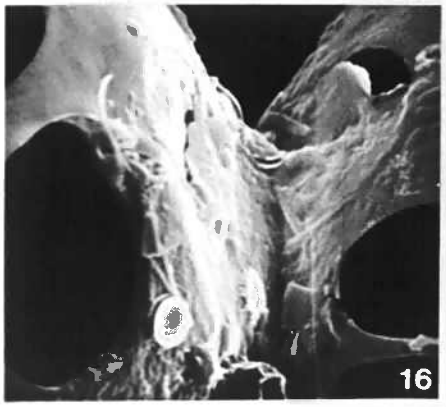

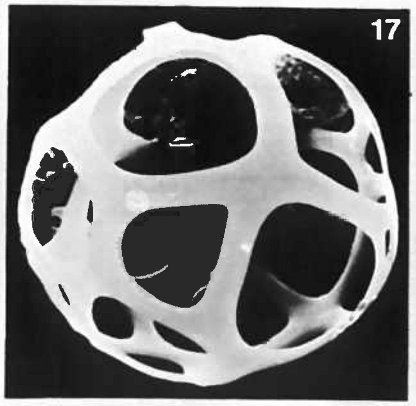

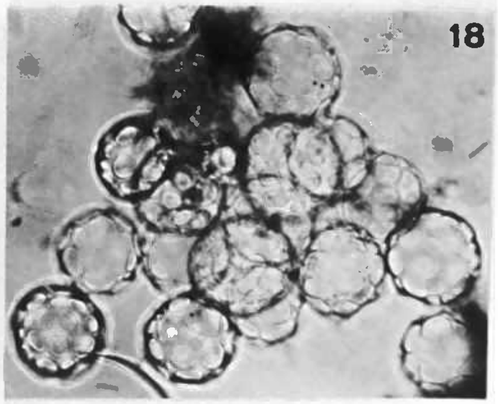

PLATE 3

Suborder: Spumellaria
Family: Collosphaeridae

Figure		Station Depth	Type of Micrograph	Magnification
1	<u>Disolenia</u> <u>collina</u> (Haeckel) Two shells linked together	$P_1$378m	LM	x210
2	<u>Disolenia</u> <u>zanguebarica</u> (Ehrenberg) Two shells linked together	$P_1$978m	LM	x210
3	<u>Disolenia</u> <u>zanguebarica</u> (Ehrenberg) Two shells linked together	PB3769m	SEM	x230
4	<u>Disolenia</u> <u>zanguebarica</u> (Ehrenberg) Same specimen	PB3769m	SEM	x1650
5	<u>Disolenia</u> <u>collina</u> (Haeckel)	$P_1$5582m	SEM	x226
6	<u>Disolenia</u> <u>collina</u> (Haeckel)	$P_1$5582m	SEM	x230
7	<u>Disolenia</u> <u>collina</u> (Haeckel)	$P_1$5582m	SEM	x226
8	<u>Disolenia</u> <u>zanguebarica</u> (Ehrenberg)	$P_1$4280m	SEM	x450
9	<u>Disolenia</u> <u>zanguebarica</u> (Ehrenberg)	$P_1$4280m	LM	x210
10	<u>Otosphaera</u> <u>auriculata</u> Haeckel A specimen without spines	$P_1$5582m	SEM	x340
11	<u>Otosphaera</u> <u>tenuissima</u> (Hilmers)	$p_1$978m	SEM	x520
12	<u>Otosphaera</u> <u>polymorpha</u> Haeckel	PB2869m	LM	x210
13	<u>Otosphaera</u> <u>auriculata</u> Haeckel	$P_1$4280m	SEM	x350
14	<u>Otosphaera</u> <u>polymorpha</u> Haeckel	$P_1$5582m	LM	x210
15	<u>Otosphaera</u> <u>polymorpha</u> Haeckel	$P_1$2778m	LM	x210

PLATE 3 Spumellaria

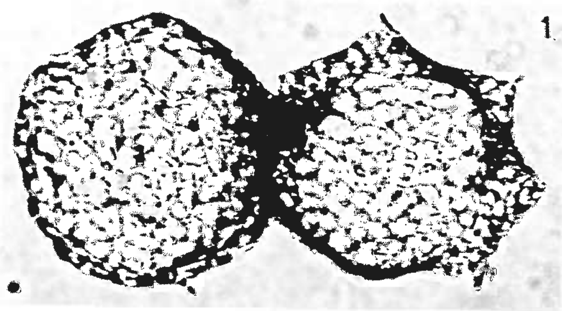

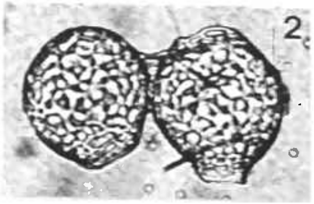

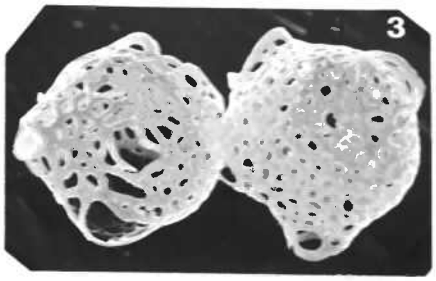

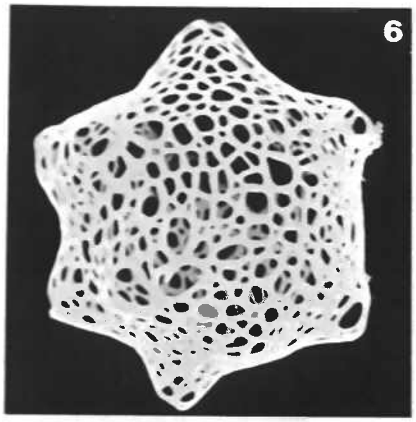

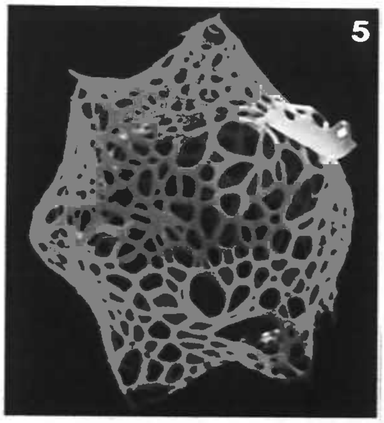

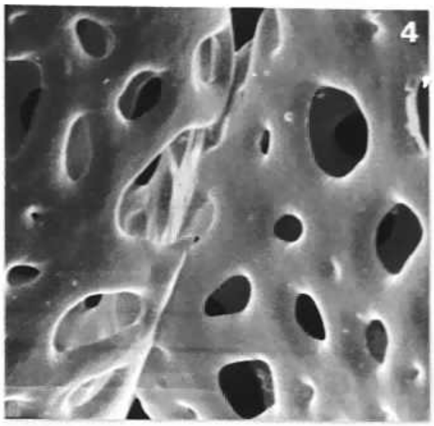

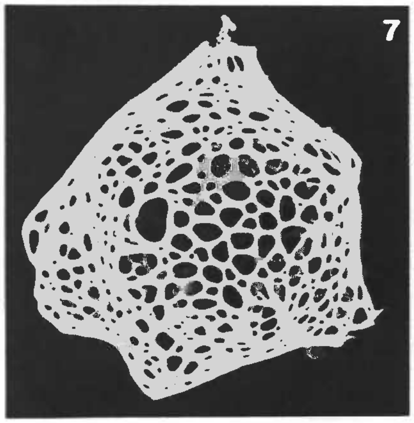

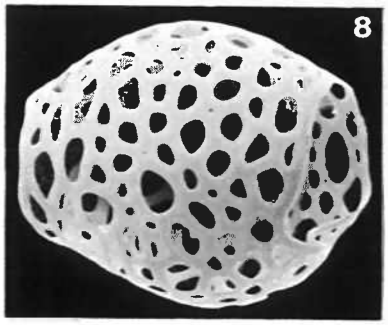

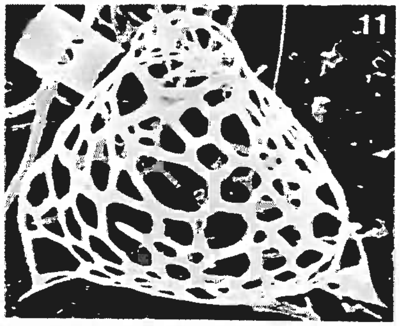

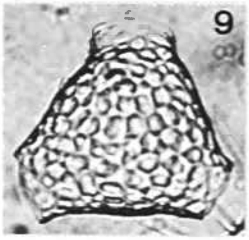

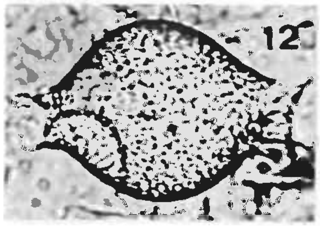

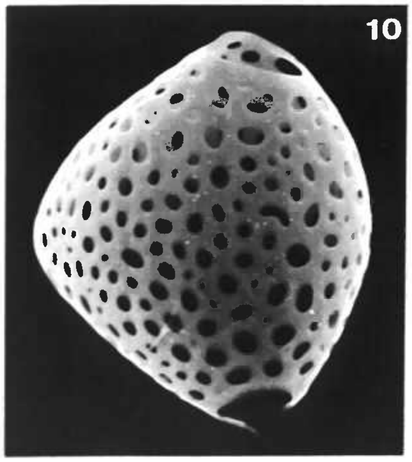

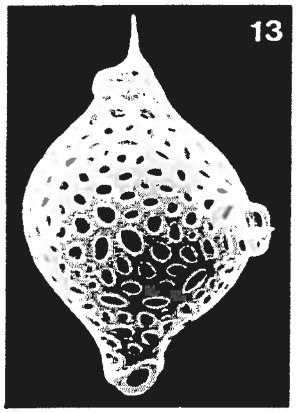

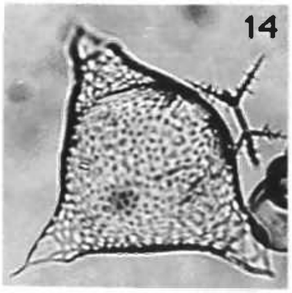

PLATE 4

Suborder: Spumellaria
Family: Collosphaera

Figure		Station Depth	Type of Micrograph	Magnification
1	*Siphonosphaera magnisphaera* n.sp. Paratype	PB2869m	LM	x210
2	*Siphonosphaera* sp. A	$P_1$4280m	SEM	x550
3	*Siphonosphaera magnisphaera* n.sp. Holotype	$P_1$378m	LM	x210
4	*Siphonosphaera martensi* Brandt	$P_1$2778m	LM	x210
5	*Siphonosphaera martensi* Brandt	$P_1$2778m	LM	x210
6	*Siphonosphaera* sp. B	$P_1$978m	SEM	x550
7	*Siphonosphaera martensi* Brandt	$P_1$4280m	SEM	x560
8	*Siphonosphaera martensi* Brandt	$P_1$4280m	SEM	x480
9	*Siphonosphaera socialis* Haeckel	$P_1$4280m	SEM	x390
10	*Siphonosphaera socialis* Haeckel	$P_1$4280m	SEM	x280
11	*Siphonosphaera socialis* Haeckel	$P_1$978m	SEM	x250
12	*Siphonosphaera socialis* Haeckel Two shells linked together	$P_1$978m	LM	x210
13	*Siphonosphaera* sp. aff. *S. hippotis* (Haeckel)	$P_1$2778m	LM	x210
14	*Siphonosphaera* sp. aff. *S. hippotis* (Haeckel)	$P_1$2778m	LM	x210
15	*Siphonosphaera socialis* Haeckel	$P_1$4280m	SEM	x370
16	*Siphonosphaera socialis* Haeckel Same specimen. Note presence of many rectangular prisms to cubic crystals on the surface which are absent in those of other families with identical desalting preparation.	$P_1$4280m	SEM	x2760

PLATE 4 Spumellaria

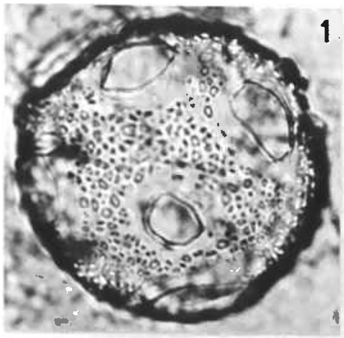

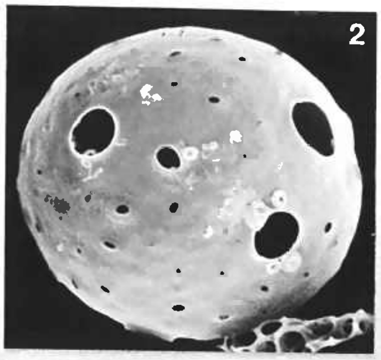

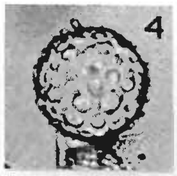

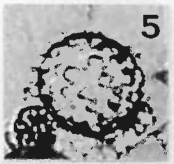

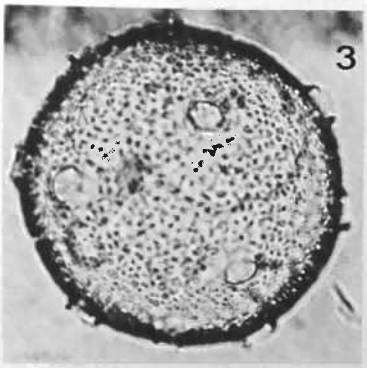

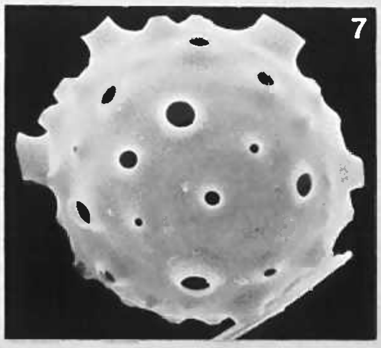

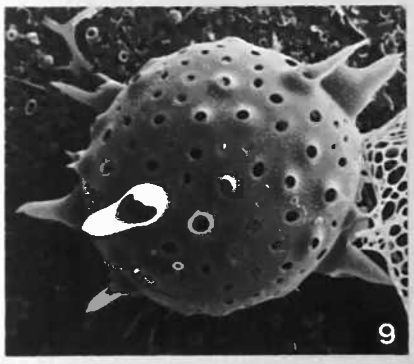

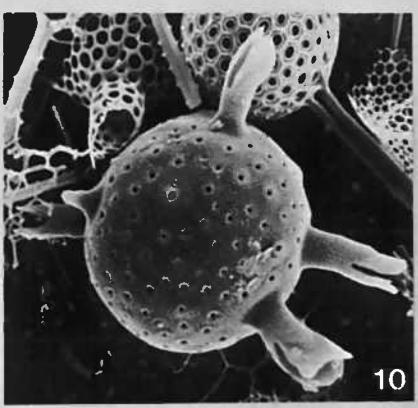

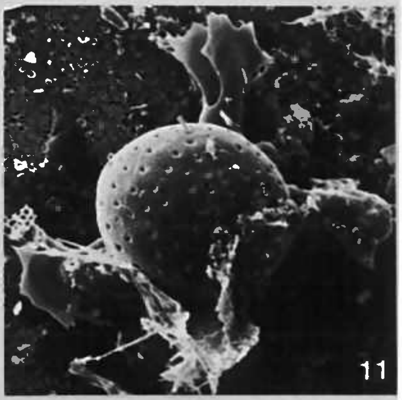

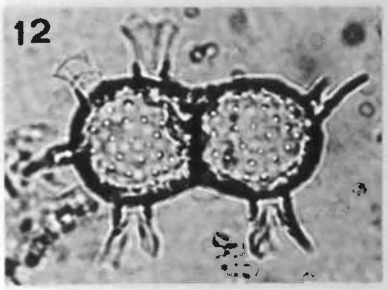

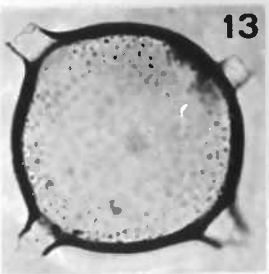

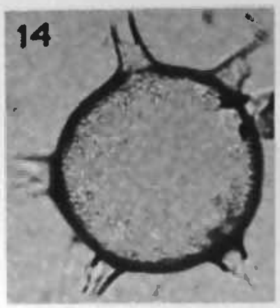

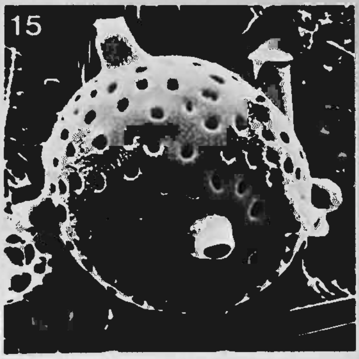

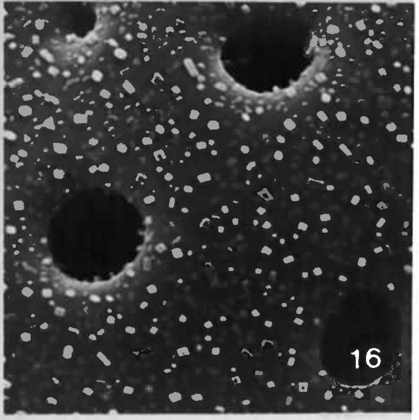

PLATE 5

Suborder: Spumellaria
Families: Collosphaeridae, Ethmosphaeridae

Figure		Station Depth	Type of Micrograph	Magnification
1	<u>Disolenia</u> <u>quadrata</u> (Ehrenberg)	$P_1$4280m	SEM	x340
2	<u>Disolenia</u> <u>quadrata</u> (Ehrenberg)	$P_1$4280m	SEM	x340
3	<u>Disolenia</u> <u>quadrata</u> (Ehrenberg)	$P_1$5582m	SEM	x280
4	<u>Disolenia</u> <u>quadrata</u> (Ehrenberg)	$P_1$2778m	LM	x210
5	<u>Disolenia</u> <u>quadrata</u> (Ehrenberg)	$P_1$4280m	SEM	x340
6	<u>Disolenia</u> sp. A	$P_1$4280m	SEM	x340
7	<u>Plegmosphaera</u> <u>pachypila</u> Haeckel	E389m	LM	x150
8	<u>Plegmosphaera</u> <u>pachypila</u> Haeckel	PB3791m	LM	x154
9	<u>Plegmosphaera</u> <u>pachypila</u> Haeckel	PB1268m	LM	x162
10	<u>Plegmosphaera</u> <u>coelopila</u> Haeckel	$P_1$5582m	SEM	x154
11	<u>Plegmosphaera</u> sp. aff. <u>P.</u> <u>lepticali</u> Renz	$P_1$2778m	SEM	x260
12	<u>Styptosphaera</u> sp. B	PB667m	SEM	x210
13	<u>Styptosphaera</u> sp. C	PB3769m	SEM	x55
14	<u>Plegmosphaera</u> sp. B	PB3769m	LM	x160

PLATE 5 Spumellaria

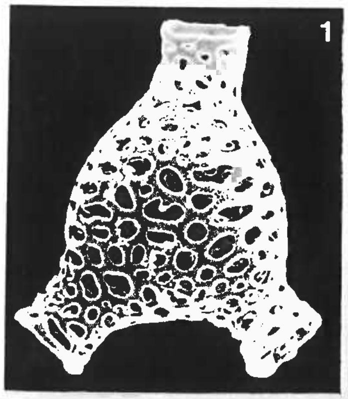

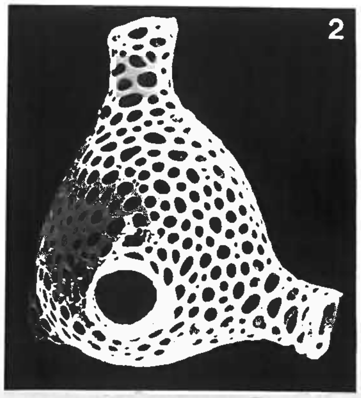

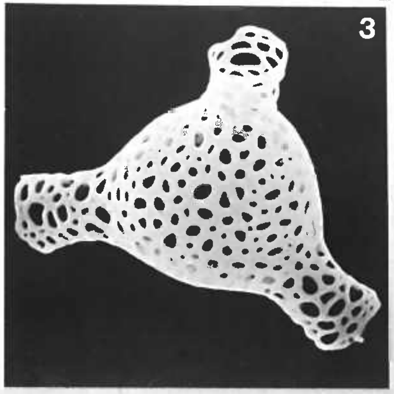

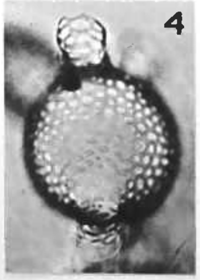

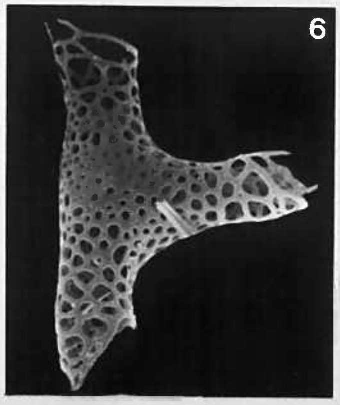

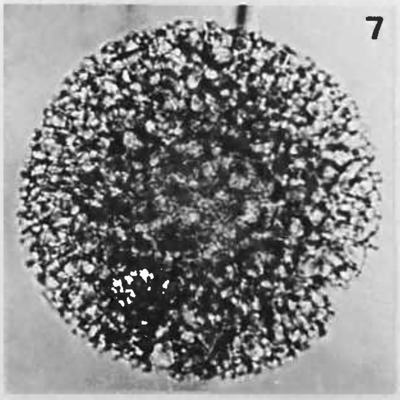

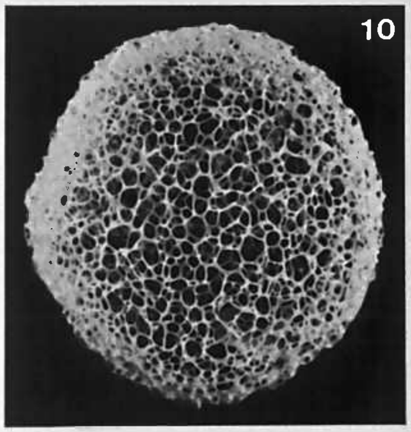

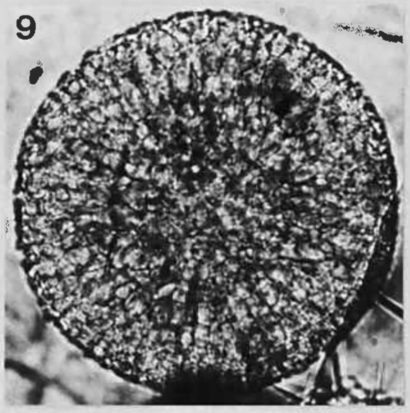

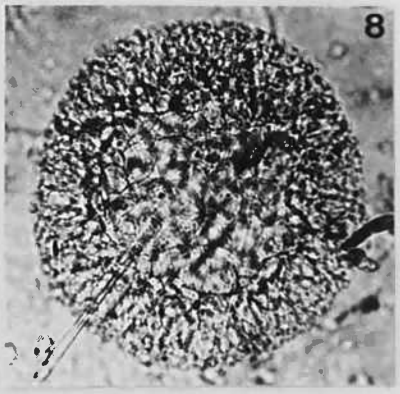

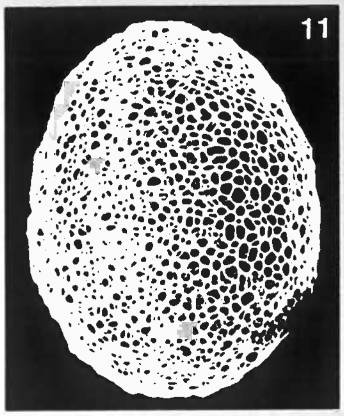

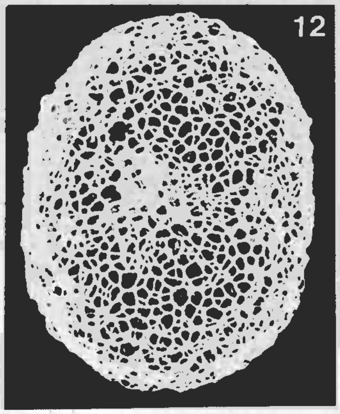

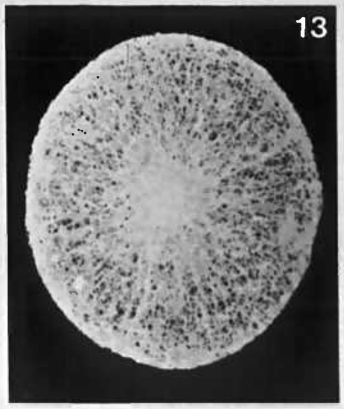

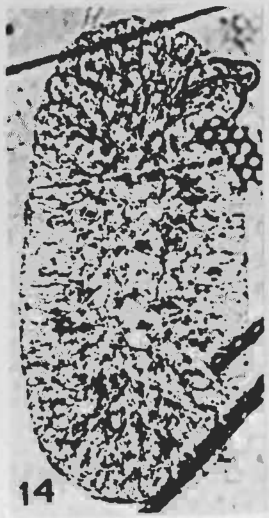

PLATE 6

Suborder: Spumellaria

Family: Ethmosphaeridae

Figure		Station Depth	Type of Micrograph	Magnifcation
1	*Plegmosphaera* sp. B	PB3769m	SEM	x55
2	*Theocosphaera capillacea* Haeckel	$P_1$5582m	SEM	x110
3	*Plegmosphaera oblonga* n.sp. Paratype	PB3791m	SEM	x220
4	*Plegmosphaera oblonga* n.sp. Holotype	PB667m	SEM	x105
5	*Plegmosphaera oblonga* n.sp. Same specimen, an enlarged view of the opening.	PB667m	SEM	x280
6	*Styptosphaera spongiacea* Haeckel	PB3769m	LM	x210
7	*Styptosphaera spongiacea* Haeckel	PB2869m	LM	x210
8	*Plegmosphaera entodictyohn* Haeckel	PB3791m	SEM	x290
9	*Styptosphaera spongiacea* Haeckel	$P_1$4280m	LM	x105
10	*Plegmosphaera entodictyon* Haeckel	$P_1$2778m	LM	x210
11	*Plegmosphaera entodictyon* Haeckel	$P_1$5582m	SEM	x190
12	*Styptosphaera* sp. A	$P_1$978m	SEM	x440
13	*Styptosphaera* sp. A	$P_1$5582m	SEM	x250
14	*Styptosphaera* sp. A	PB3769m	SEM	x1270

PLATE 6 Spumellaria

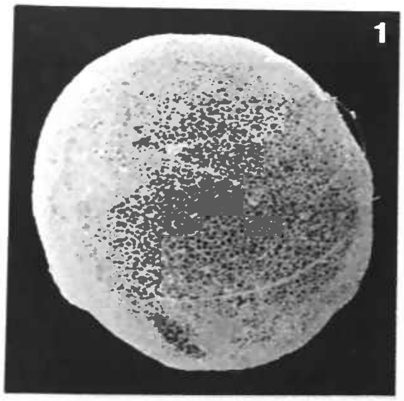

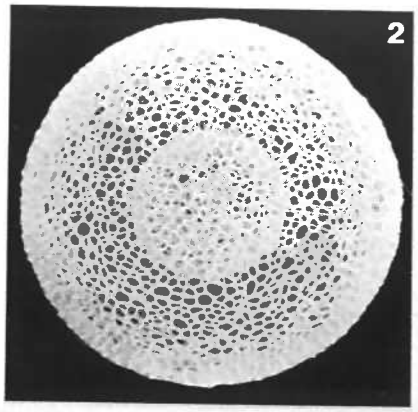

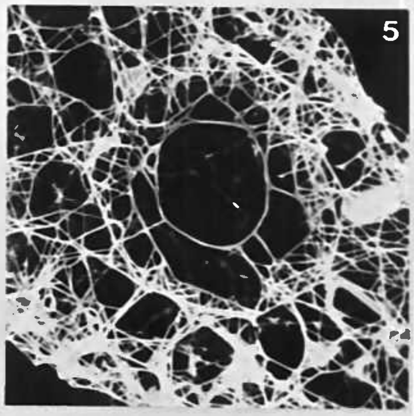

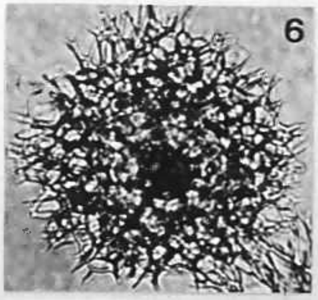

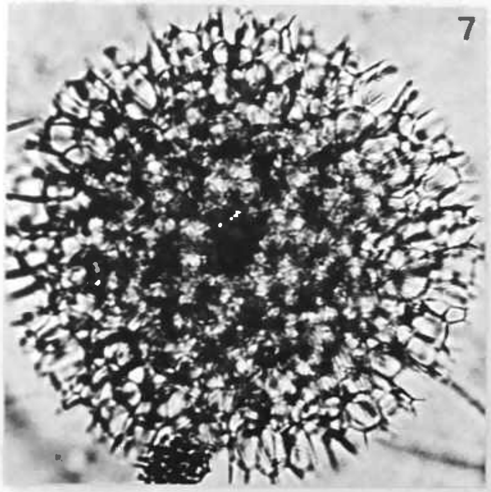

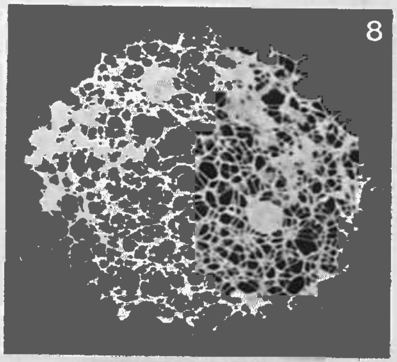

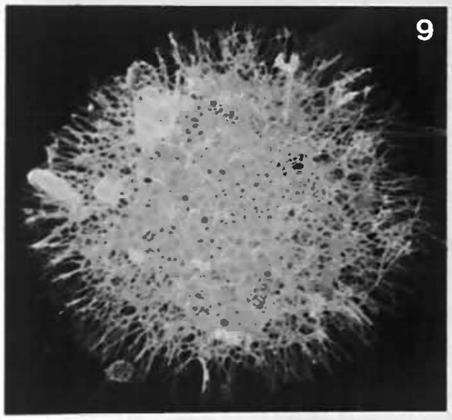

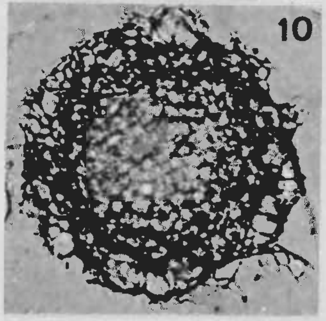

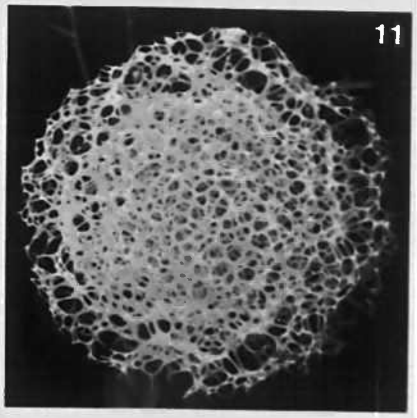

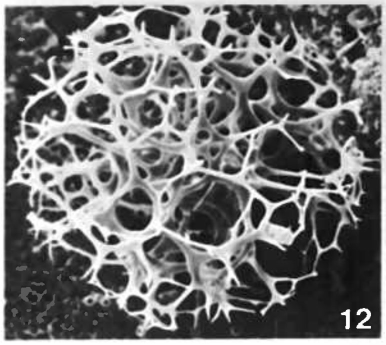

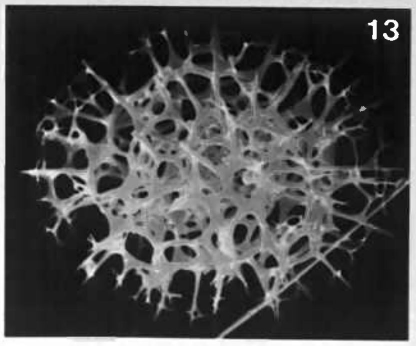

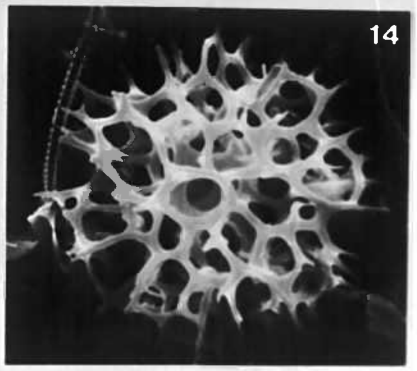

PLATE 7

Suborder: Spumellaria
Family: Actinommidae; Subfamily: Actinomminae

Figure		Station Depth	Type of Micrograph	Magnification
1	Centrocubus octostylus Haeckel	PB1268m	LM	x104
2	Spongosphaera polycantha Müller	PB3769m	LM	x106
3	Spongosphaera polycantha Müller	$P_1$5582m	SEM	x165
4	Spongosphaera sp. aff. S. helioides Haeckel	PB3791m	LM	x130
5	Spongosphaera polycantha Müller	PB667m	SEM	x66
6	Spongosphaera sp. A	PB2778m	SEM	x28
7	Spongosphaera sp. aff. S. helioides Haeckel	$P_1$2778m	SEM	x36
8	Spongosphaera sp. aff. S. helioides Haeckel	$P_1$2778m	SEM	x40
9	Spongosphaera ? sp. B	$P_1$2778m	SEM	x40
10	Lynchnosphaera regina Haeckel	PB667m	LM	x66
11	Leptosphaera minuta Popofsky	$P_1$2778m	SEM	x280
12	Arachnosphaera sp.	$P_1$2778m	LM	x158

PLATE 7 Spumellaria

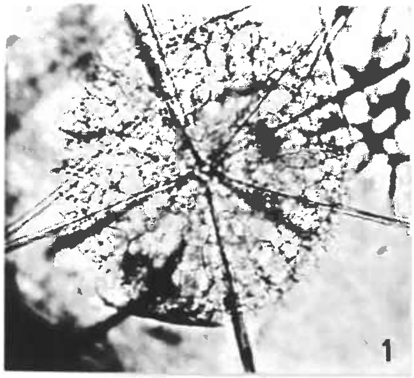
1

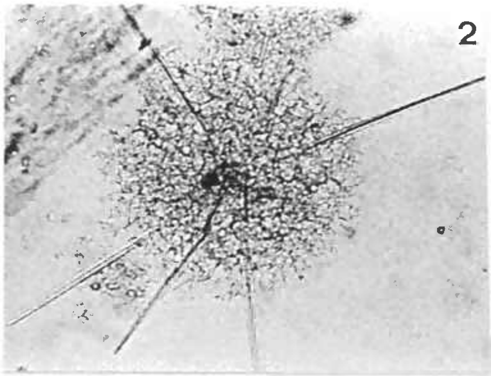
2

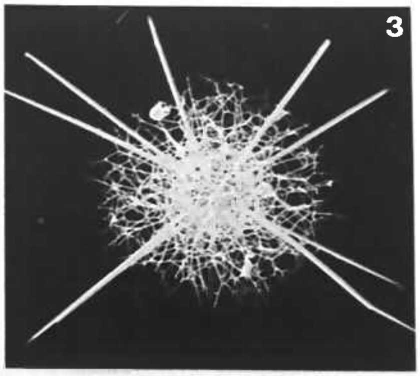
3

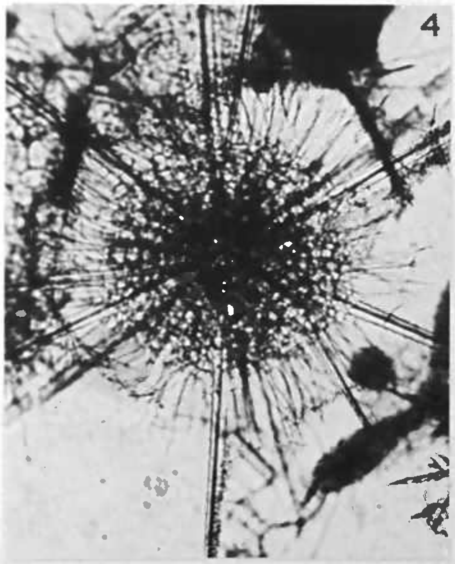
4

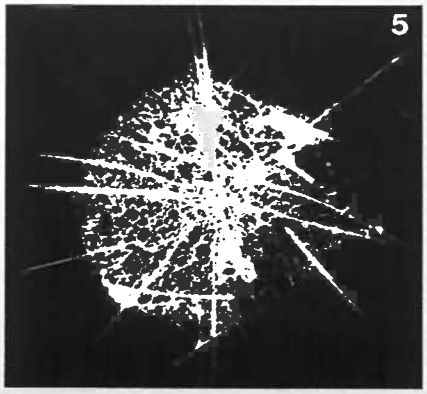
5

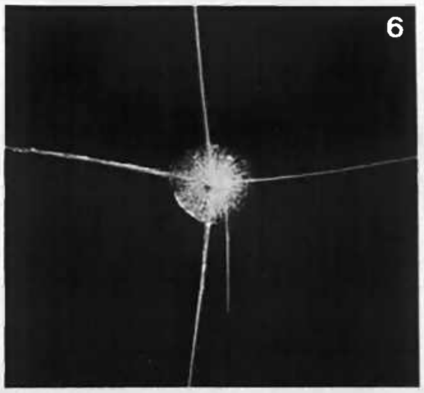
6

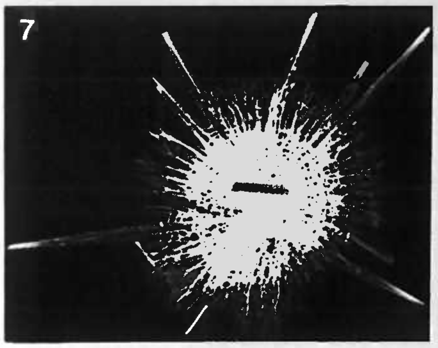
7

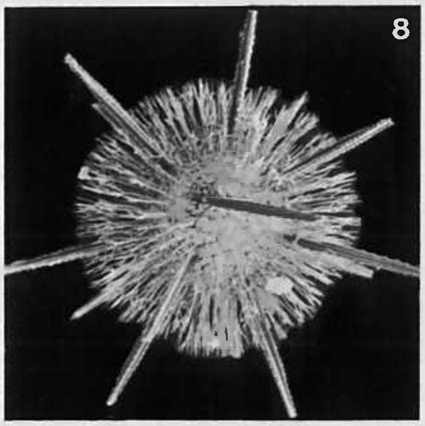
8

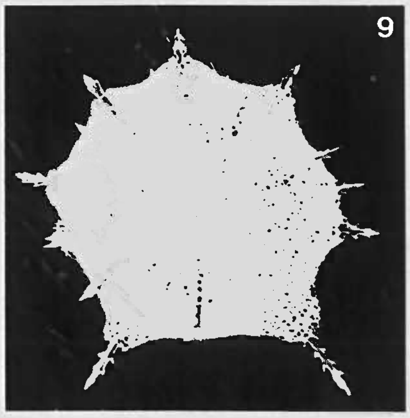
9

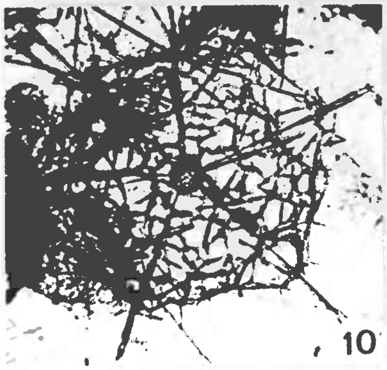
10

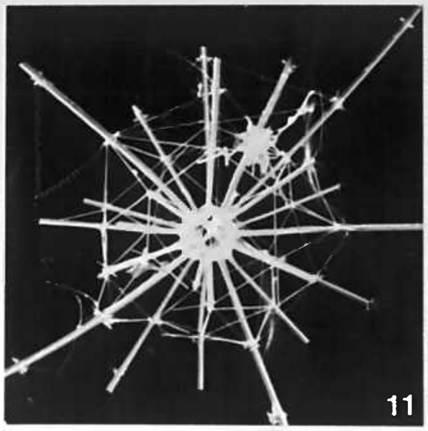
11

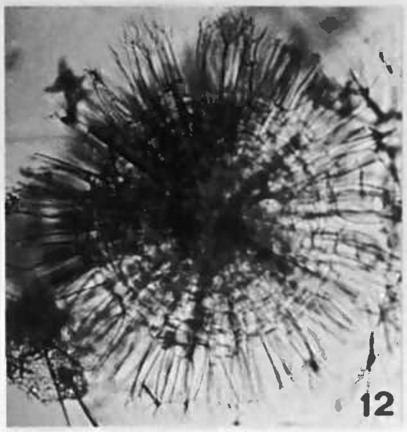
12

PLATE 8

Suborder: Spumellaria
Family: Actinommidae; Subfamily: Actinomminae

Figure		Station Depth	Type of Micrograph	Magnification
1	*Acanthosphaera actinota* (Haeckel)	$P_1$5582m	LM	x210
2	*Acanthosphaera tunis* Haeckel	PB667m	LM	x210
3	*Acanthosphaera tunis* Haeckel	PB667m	LM	x210
4	*Acanthosphaera castanea* Haeckel	$P_1$5582m	SEM	x165
5	*Acanthosphaera castanea* Haeckel	$P_1$2778m	LM	x210
6	*Cladococcus viminalis* Haeckel	$P_1$2778m	LM	x210
7	*Cladococcus viminalis* Haeckel	$P_1$978m	SEM	x200
8	*Actinomma arcadophorum* Haeckel	PB1268m	LM	x210
9	*Actinomma arcadophorum* Haeckel	$P_1$5582m	SEM	x165
10	*Actinomma capillaceum* Haeckel	$P_1$4280m	SEM	x150
11	*Actinomma arcadophorum* Haeckel	$P_1$4280m	SEM	x140
12	*Haliomma* ? sp.	$P_1$4280m	SEM	x440

PLATE 8 Spumellaria

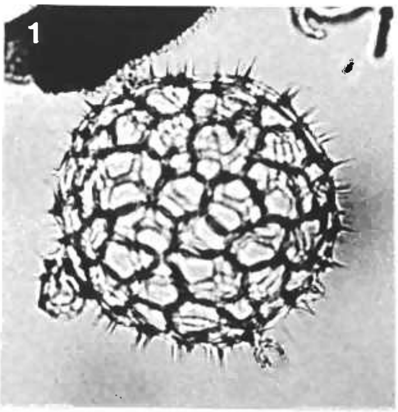

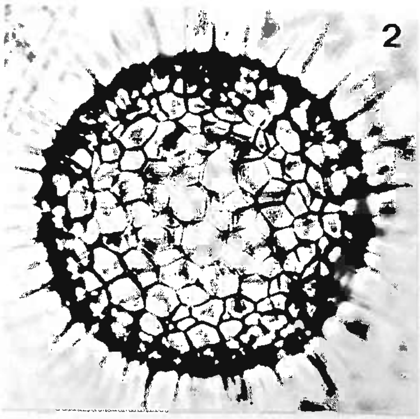

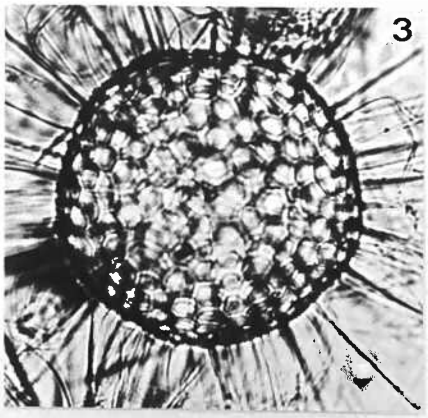

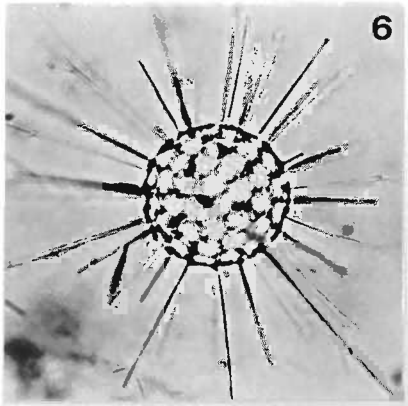

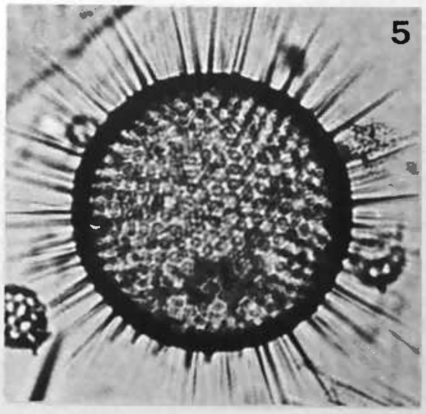

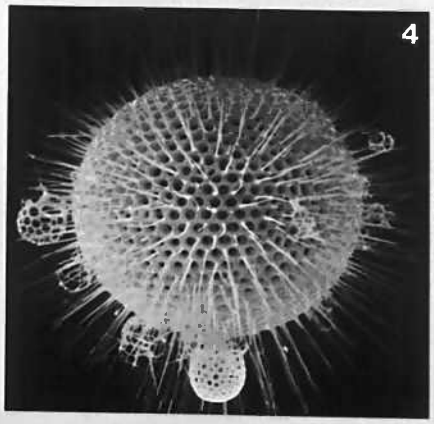

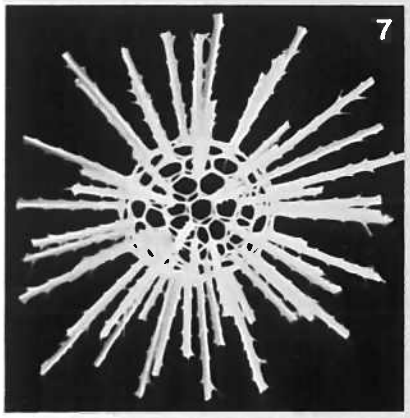

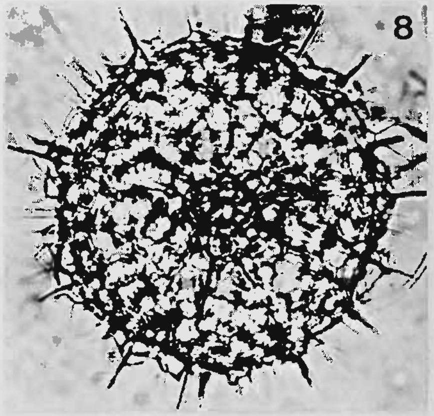

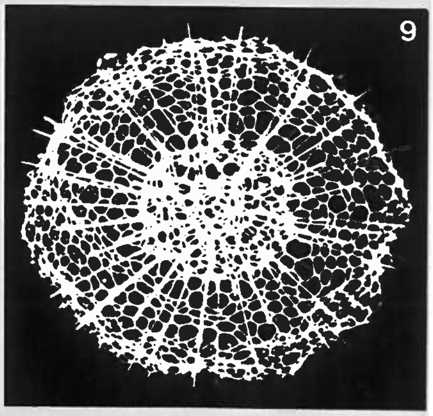

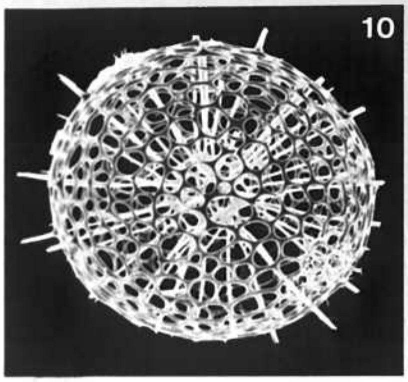

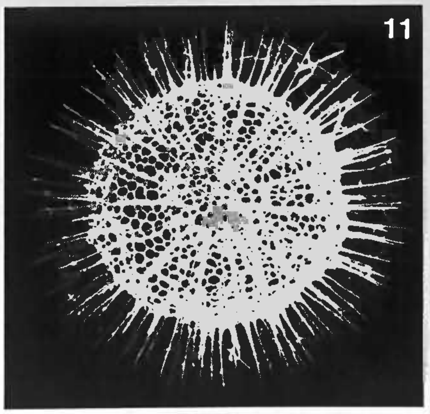

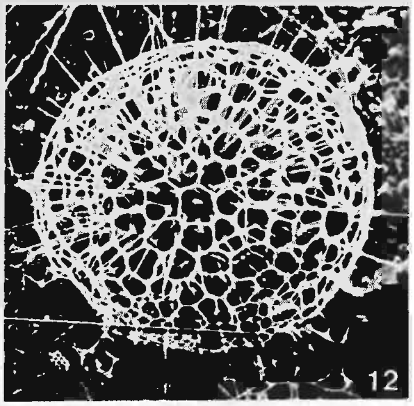

PLATE 9

Suborder: Spumellaria
Family: Actinommidae, Subfamily: Actinomminae
Family: Ethmosphaeridae

Figure		Station Depth	Type of Micrograph	Magnification
1	*Actinosphaera tenella* (Haeckel)	$P_1$4280m	SEM	x165
2	*Actinosphaera acanthophora* (Popofsky) Specimen broken to show the medullary shell	PB1268m	SEM	x180
3	*Actinosphaera acanthophora* (Popofsky)	PB3791m	SEM	x160
4	*Actinosphaera capillaca* (Haeckel)	$P_1$4280m	SEM	x180
5	*Actinosphaera capillaca* (Haeckel)	PB3791m	LM	x210
6	*Heliosoma* sp.	$P_1$4280m	SEM	x440
7	*Haliomma castanea* Haeckel	$P_1$4280m	SEM	x440
8	*Heliosoma* sp.	$P_1$378m	LM	x210
9	*Elatomma penicillus* Haeckel	$P_1$5582m	SEM	x150
10	*Elatomma penicillus* Haeckel	PB1268m	LM	x210
11	*Haliomma castanea* Haeckel	E988m	LM	x210
12	*Carposphaera* sp. aff. *C. corypha* Haeckel	$P_1$5582m	LM	x210

PLATE 9 Spumellaria

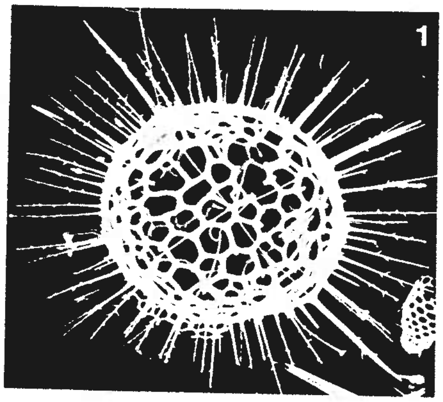
1

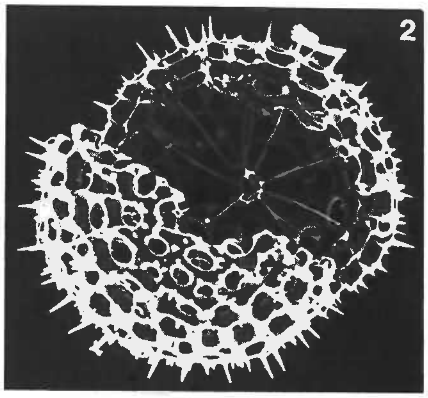
2

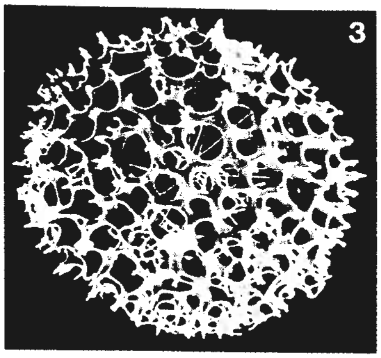
3

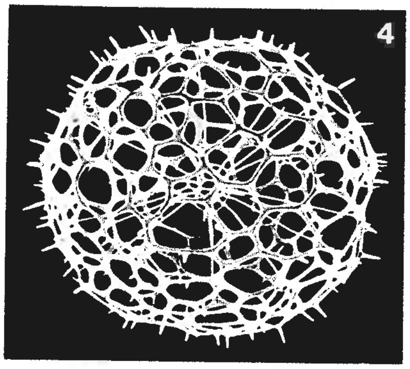
4

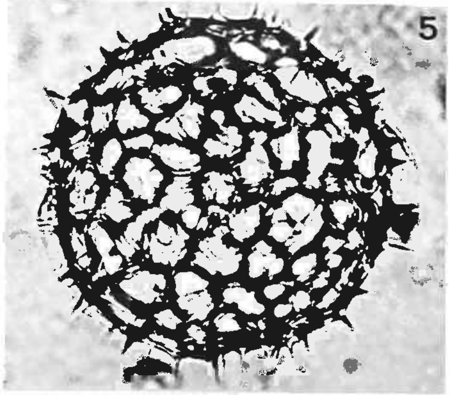
5

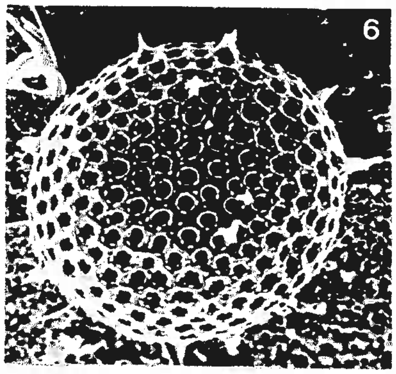
6

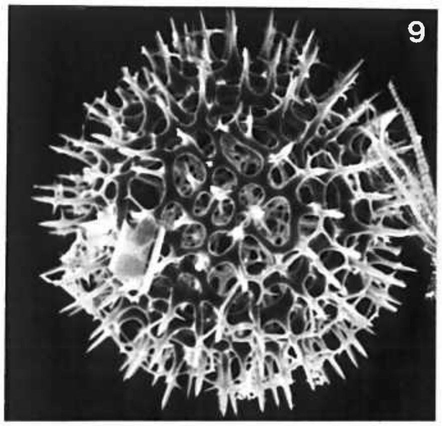
9

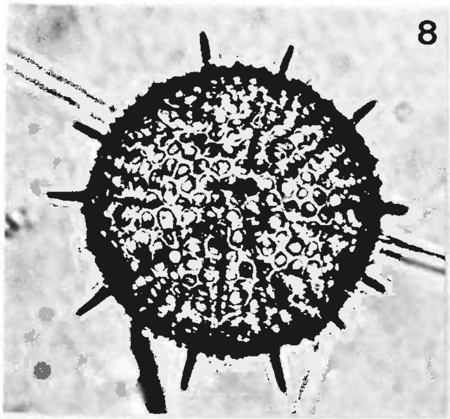
8

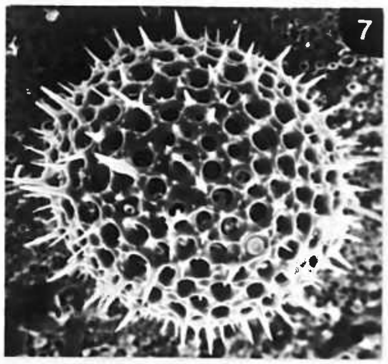
7

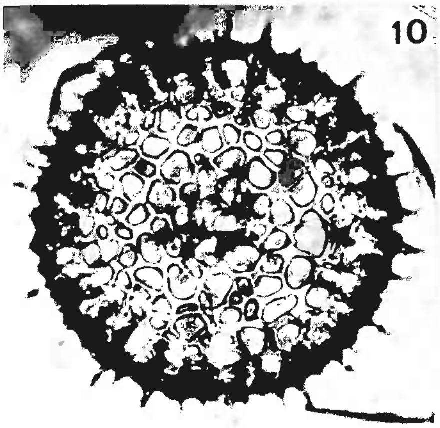
10

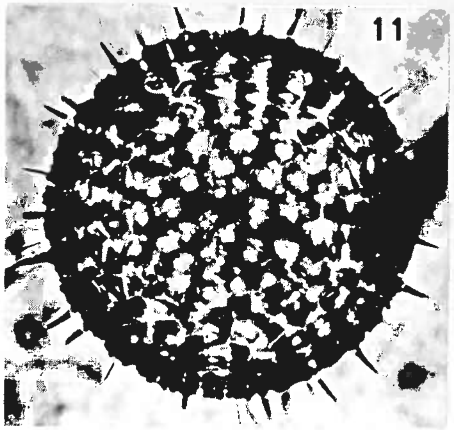
11

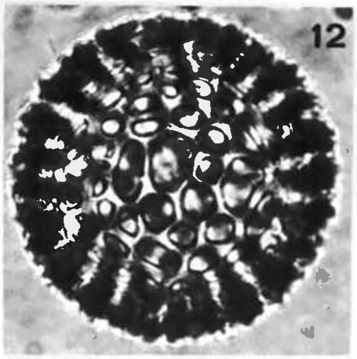
12

PLATE 10

Suborder: Spumellaria
Family: Actinommidae; Subfamily: Actinomminae

Figure		Station Depth	Type of Micrograph	Magnification
1	*Elatomma pinetum* Haeckel	$P_1$978m	SEM	x110
2	*Elatomma pinetum* Haeckel Detail of inner medullary shell	$P_1$978m	SEM	x350
3	*Elatomma pinetum* Haeckel	$P_1$378m	LM	x210
4	*Elatomma pinetum* Haeckel	$P_1$978m	SEM	x110
5	*Cladococcus abietinus* Haeckel	PB667m	LM	x152
6	*Cladococcus scoparius* Haeckel	PB3769m	LM	x160
7	*Cladococcus scoparius* Haeckel	$P_1$978m	SEM	x140
8	*Cladococcus cervicornis* Haeckel	$P_1$4280m	SEM	x190
9	*Cladococcus cervicornis* Haeckel	PB3769m	LM	x210
10	*Cladococcus cervicornis* Haeckel	PB2869m	LM	x210
11	*Arachnosphaera myriacantha* Haeckel	PB3791m	LM	x132
12	*Arachnosphaera myriacantha* Haeckel	$P_1$5582m	SEM	x105

PLATE 10 Spumellaria


1

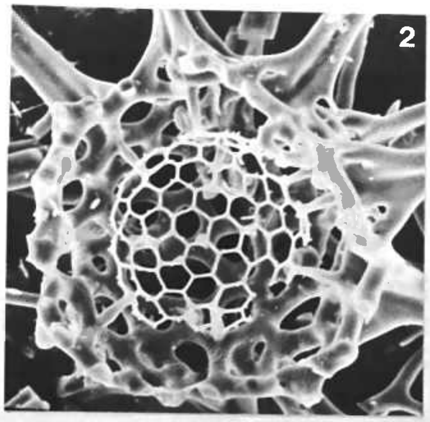
2

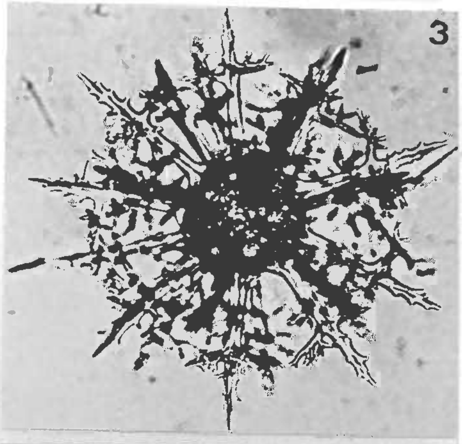
3

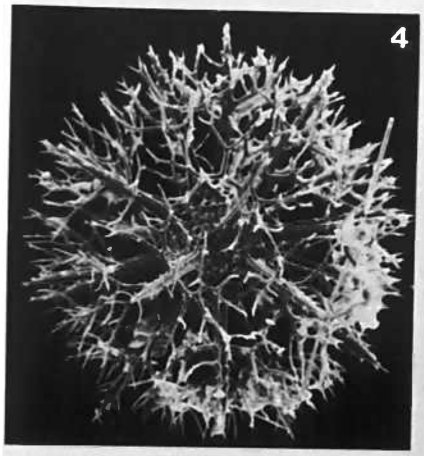
4

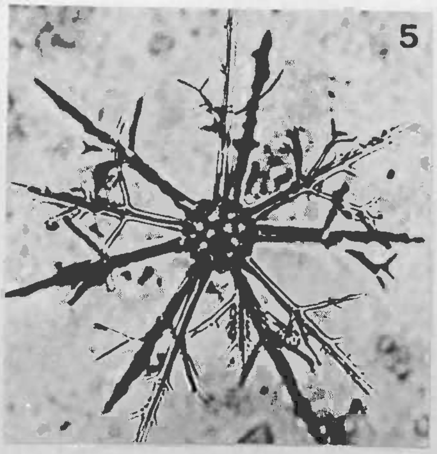
5

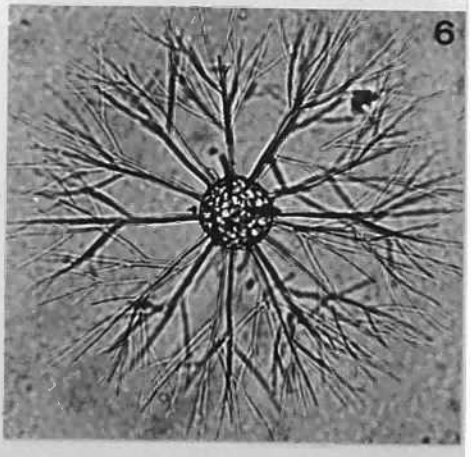
6

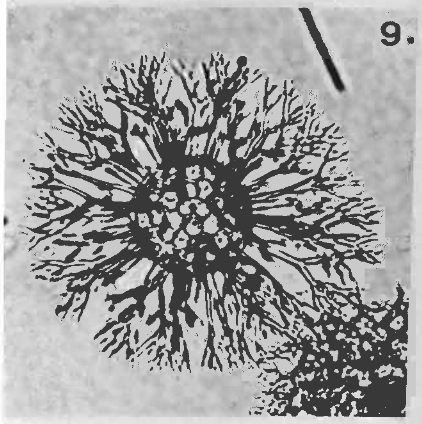
9.

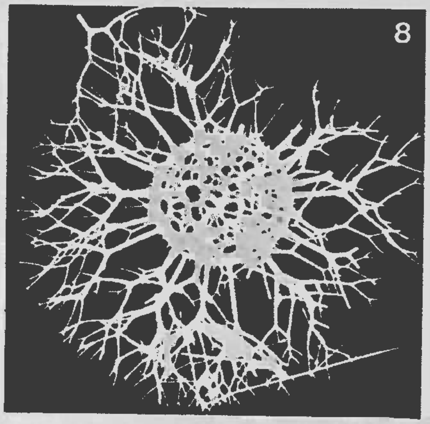
8

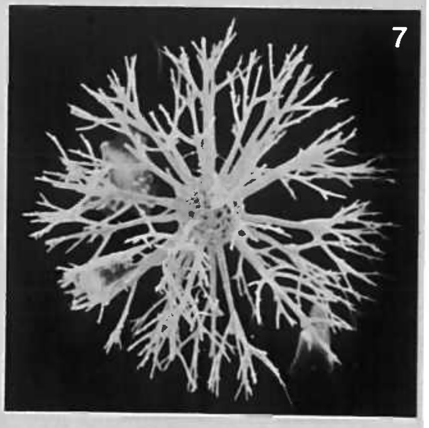
7

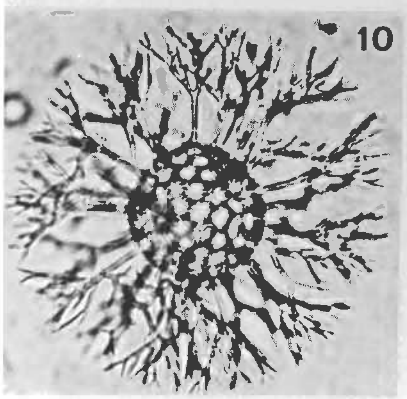
10

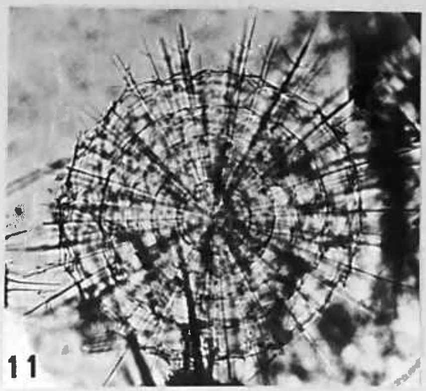
11

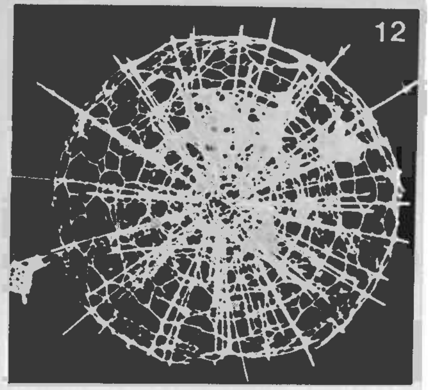
12

PLATE 11

Suborder: Spumellaria
Family: Actinommidae, Subfamily: Actinimminae
Families: Tholoniidae, Ethmosphaeridae

Figure		Station Depth	Type of Micrograph	Magnification
1	Astrosphaera hexagonalis Haeckel	PB667m	SEM	x120
2	Astrosphaera hexagonalis Haeckel	PB3791m	LM	x158
3	Astrosphaera hexagonalis Haeckel A form with long wavy bi-spines	PB1268m	LM	x133
4	Drymosphaera dendrophora Haeckel	PB3769m	LM	x120
5	Stylosphaera ? sp. A	$P_1$978m	SEM	x500
6	Stylosphaera ? sp. A	$P_1$2778m	SEM	x440
7	Sphaeropyle mespilus Dreyer	PB2869m	LM	x210
8	Sphaeropyle mespilus Dreyer	$P_1$378m	LM	x210
9	Theocosphaera inermis (Haeckel)	$P_1$4280m	SEM	x440
10	Cromyomma villosum Haeckel	PB2869m	LM	x210
11	Cromyomma villosum Haeckel	PB3769m	LM	x210
12	Tholoma metallasson Haeckel	$P_1$2778m	LM	x210
13	Tholoma metallasson Haeckel	PB3791m	LM	x210
14	Hexalonche sp. A	$P_1$2778m	LM	x210
15	Hexalonche sp. A	PB3769m	LM	x210

PLATE 11 Spumellaria

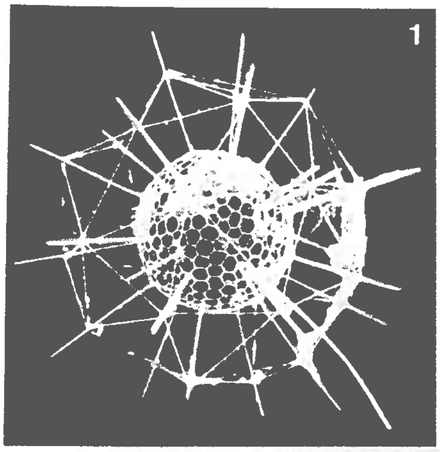
1

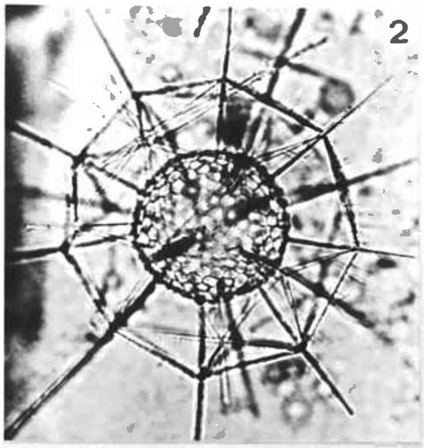
2


3

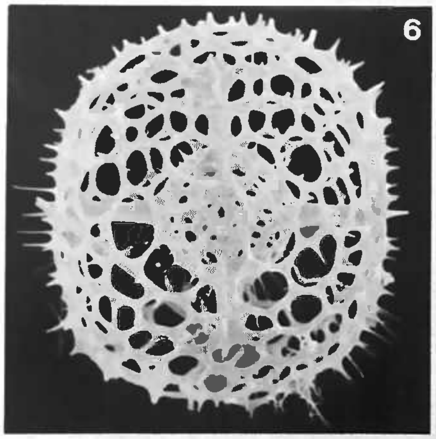
6

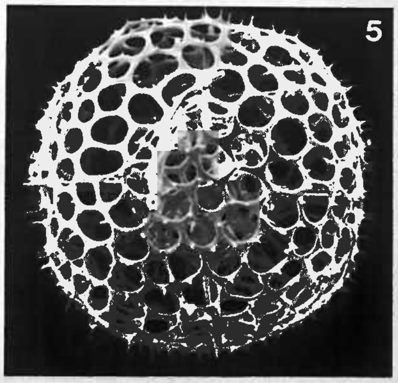
5

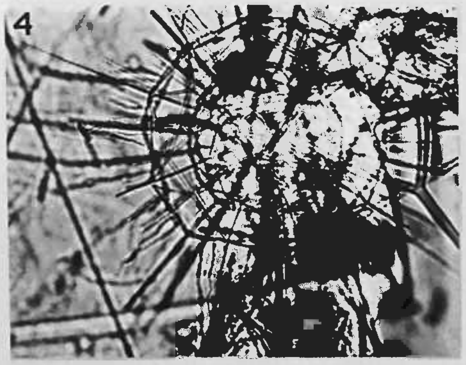
4

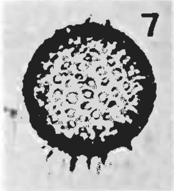
7

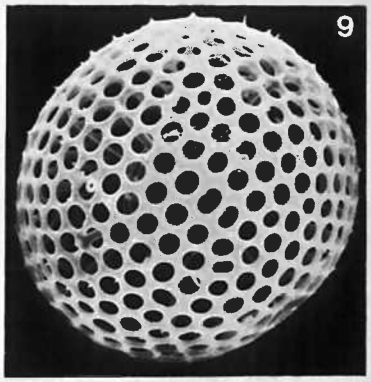
9

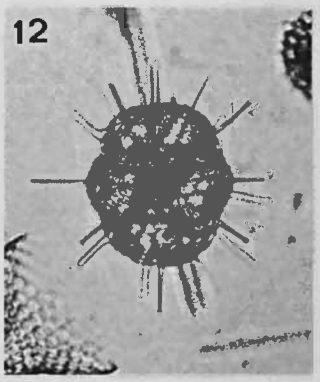
12

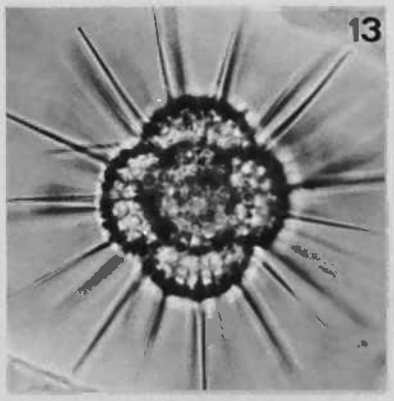
13

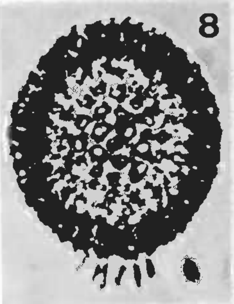
8

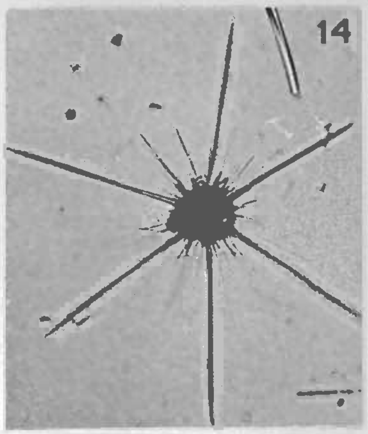
14

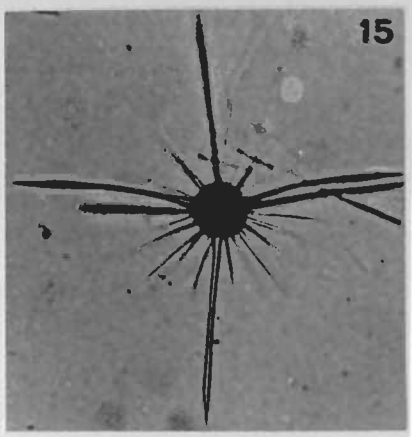
15

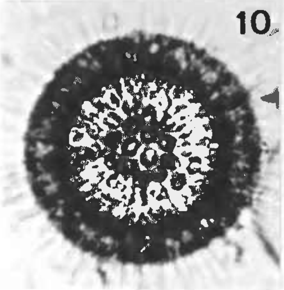
10

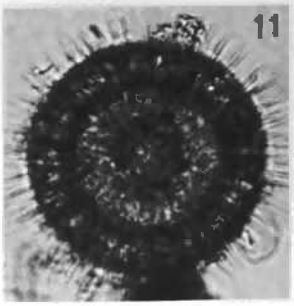
11

PLATE 12

Suborder: Spumellaria
Family: Actinommidae; Subfamily: Actinimminae

Figure		Station Depth	Type of Micrograph	Magnification
1	*Xiphosphaera gaea* Haeckel	$P_1$4280m	SEM	x330
2	*Xiphosphaera gaea* Haeckel	$P_1$2778m	LM	x130
3	*Xiphosphaera tesseractis* Dreyer	$P_1$5582m	SEM	x140
4	*Xiphosphaera tesseractis* Dreyer	PB3769m	LM	x150
5	*Xiphosphaera tesseractis* Dreyer	$P_1$4280m	SEM	x280
6	*Stauracontium* sp.	$P_1$2778m	LM	x126
7	*Hexastylus triaxonius*	PB3791m	LM	x210
8	*Hexastylus triaxonius*	PB3791m	SEM	x165
9	*Hexastylus* sp.	$P_1$4280m	SEM	x440
10	*Hexalonche* sp. B	$P_1$4280m	SEM	x550
11	*Hexalonche* sp. B	$P_1$978m	SEM	x660
12	*Hexacontium* sp.	$P_1$5582m	SEM	x360
13	*Hexacontium amphisiphon* Haeckel	$P_1$4280m	SEM	x130
14	*Hexacontium amphisiphon* Haeckel	$P_1$4280m	SEM	x180
15	*Acanthosphaera simplex* ? (Haeckel)	$P_1$978m	SEM	x440

PLATE 12 Spumellaria

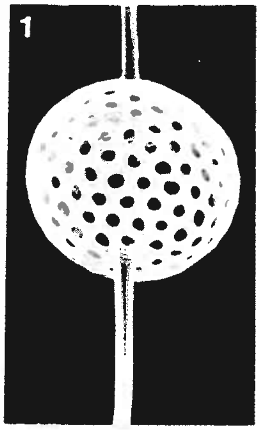
1


2

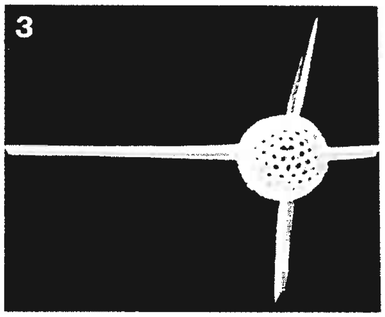
3

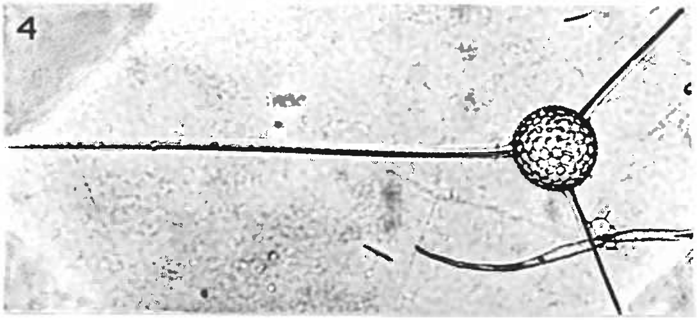
4


8

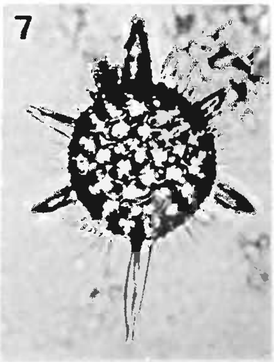
7


6

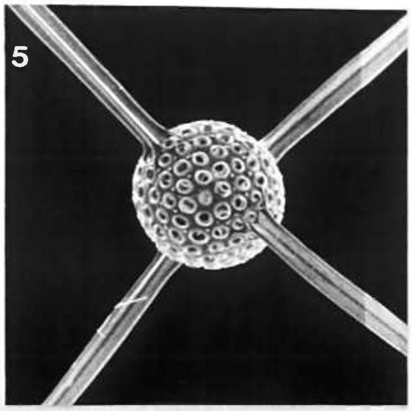
5

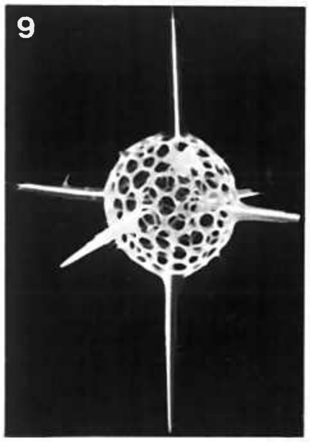
9

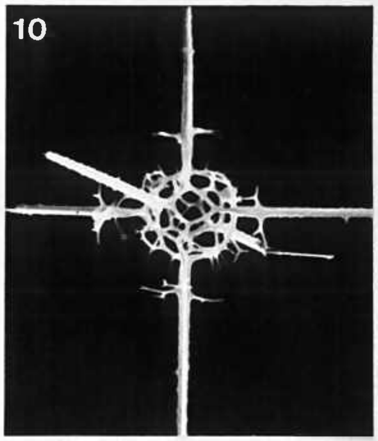
10

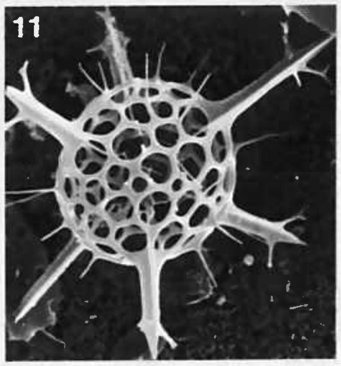
11

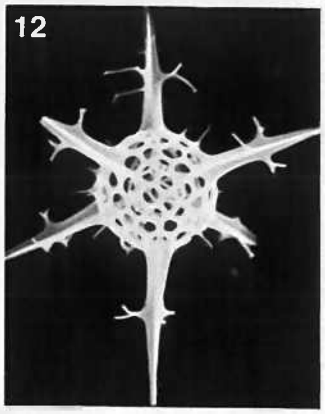
12

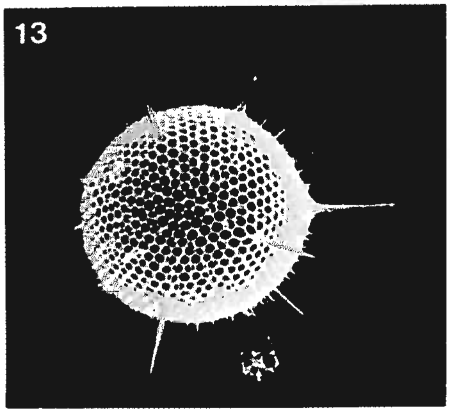
13

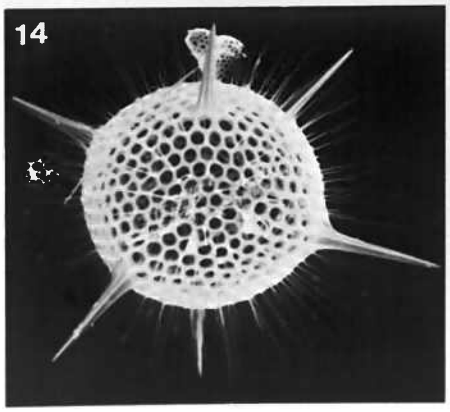
14

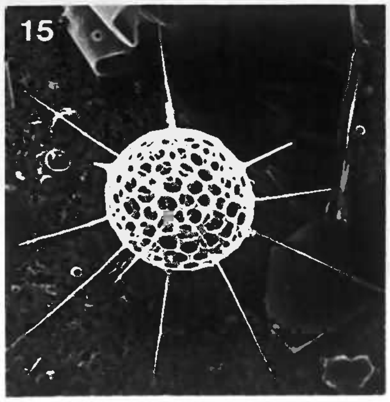
15

PLATE 13

Suborder: Spumellaria
Family: Actinommidae; Subfamily: Actinomminae

Figure		Station Depth	Type of Micrograph	Magnification
1	*Hexacontium hostile* Cleve	$P_1$4280m	SEM	x220
2	*Hexacontium hostile* Cleve	PB2869m	LM	x210
3	*Hexacontium axotrias* Haeckel	$P_1$5582m	LM	x210
4	*Hexacromyum elegans* Haeckel	E389m	LM	x210
5	*Hexacromyum elegans* Haeckel A specimen with 7 radial spines	E389m	LM	x210
6	*Hexacontium* sp. aff. *H. hostile* Cleve	$P_1$4280m	SEM	x180
7	*Hexacromyum elegans* Haeckel	$P_1$4280m	SEM	x230
8	*Heterosphaera* sp. B	$P_1$4280m	SEM	x250
9	*Heterosphaera* sp. A	PB3791m	LM	x210
10	*Heterosphaera* sp. A	$P_1$2778m	LM	x210
11	*Actinomma* sp.	$P_1$5582m	LM	x210
12	*Cromyechinus* ? sp.	$P_1$4280m	SEM	x130
13	*Cromechinus* sp. aff. *C. borealis* (Cleve)	$P_1$978m	LM	x210
14	*Stomatosphaera* sp. A	$P_1$978m	SEM	x340
15	*Stomatosphaera* sp. B	$P_1$4280m	SEM	x210
16	*Stomatosphaera* sp. C	PB3769m	SEM	x170

PLATE 13 Spumellaria

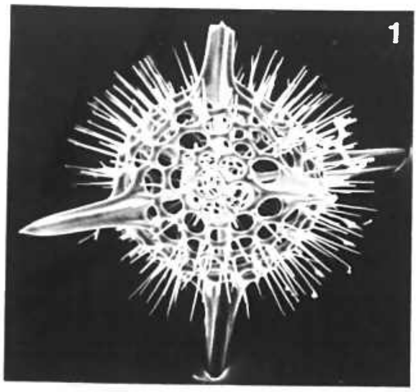
1

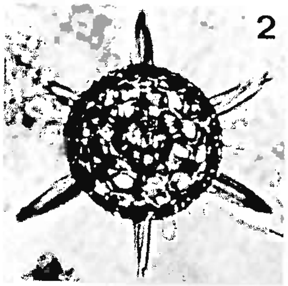
2

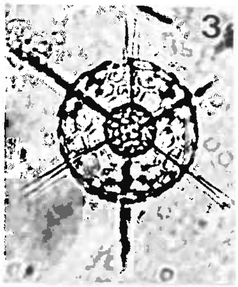
3

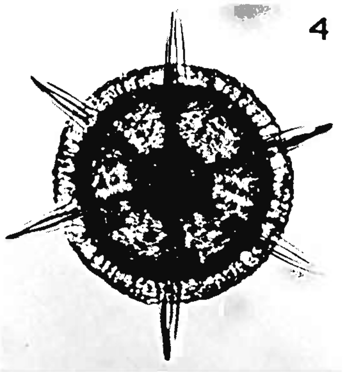
4

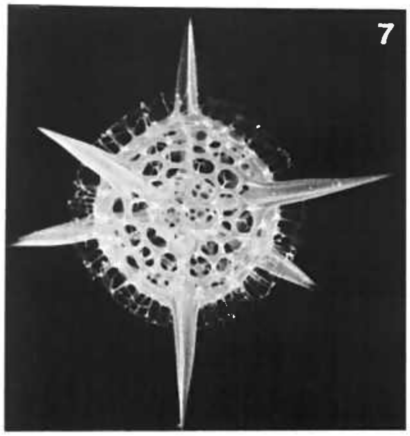
7

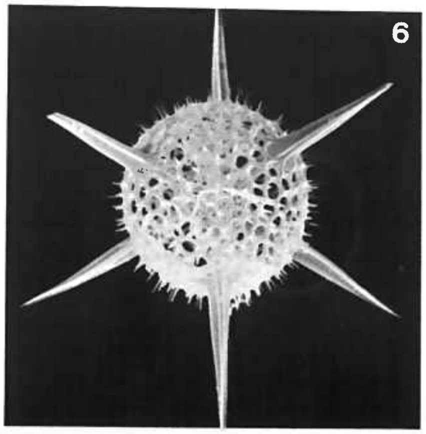
6

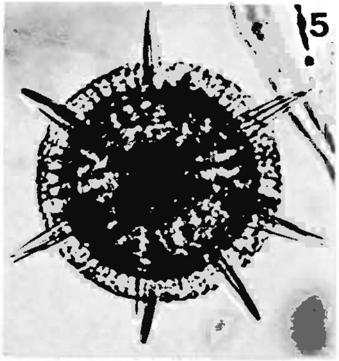
5

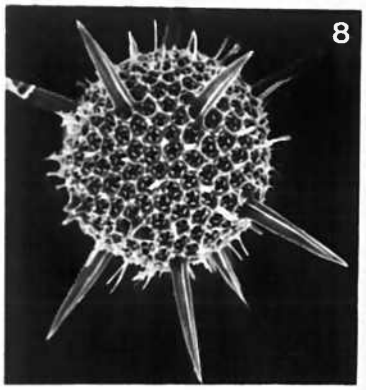
8

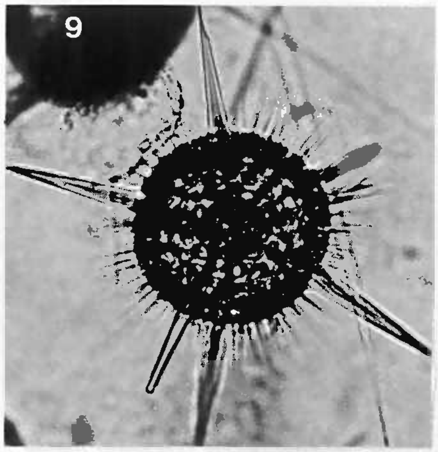
9


10

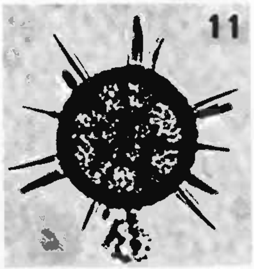
11

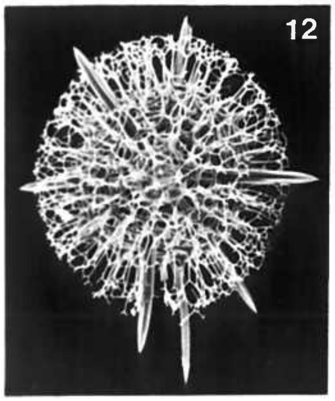
12


13

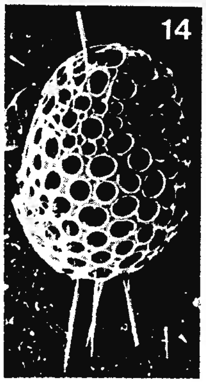
14

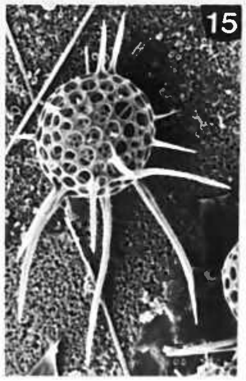
15

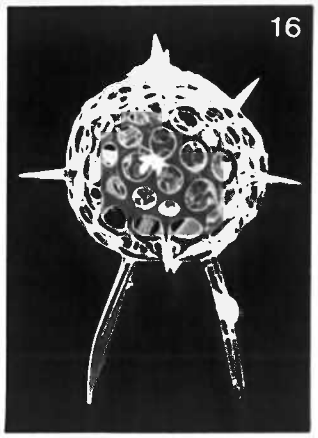
16

PLATE 14

Suborder: Spumellaria
Family: Actinommidae; Subfamily: Actinomminae

Figure		Station Depth	Type of Micrograph	Magnification
1	*Stylosphaera melpomene* Haeckel	PB2869m	LM	x210
2	*Stylosphaera melpomene* Haeckel	PB3769m	LM	x210
3	*Druppatractus ostracion* Haeckel group	PB3769m	LM	x210
4	*Druppatractus ostracion* Haeckel group	$P_1$4280m	LM	x210
5	*Stylosphaera* ? sp. B	$P_1$4280m	SEM	x250
6	*Amphisphaera* group	$P_1$5582m	SEM	x140
7	*Amphisphaera* group	$P_1$5582m	LM	x140
8	*Axoprunum stauraxonium* Haeckel	PB3769m	LM	x210
9	*Axoprunum stauraxonium* Haeckel	$P_1$5582m	LM	x210
10	*Axoprunum stauraxonium* Haeckel	$P_1$5582m	SEM	x165
11	*Ellipsoxiphium palliatum* Haecker	$P_1$5582m	SEM	x140
12	*Ellipsoxiphium palliatum* Haecker	$P_1$4280m	SEM	x165
13	*Ellipsoxiphium palliatum* Haecker	PB3791m	LM	x210
14	*Ellipsoxiphium palliatum* Haecker	$P_1$4280m	SEM	x165
15	*Ellipsoxiphium palliatum* Haecker	PB3791m	LM	x210
16	*Ellipsoxiphium palliatum* Haecker	$P_1$5582m	LM	x210
17	*Ellipsoxiphium palliatum* Haecker	E3755m	LM	x210

PLATE 14 Spumellaria

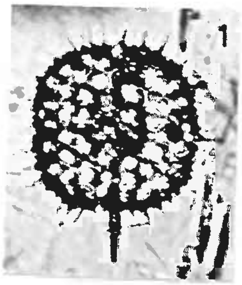
1

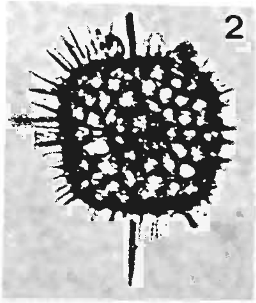
2


3

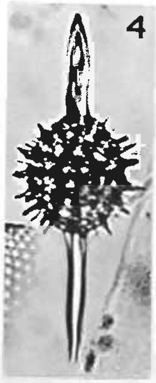
4

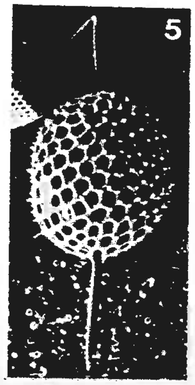
5

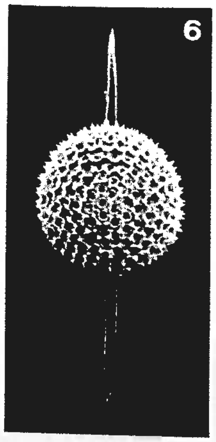
6

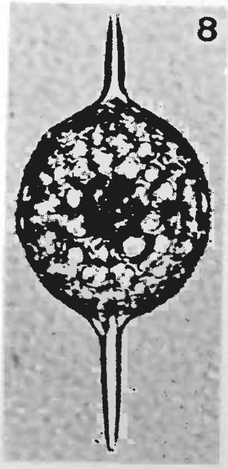
8

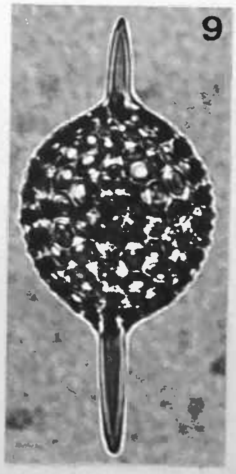
9

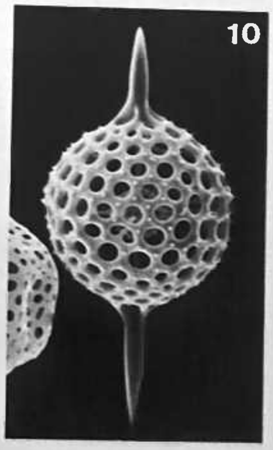
10

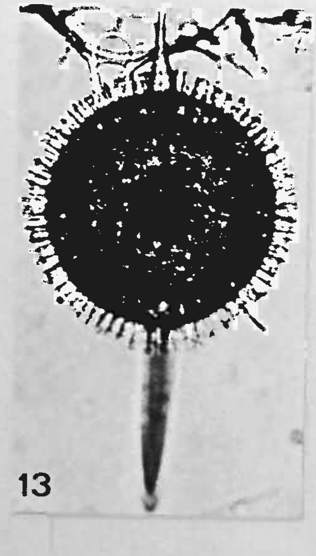
13

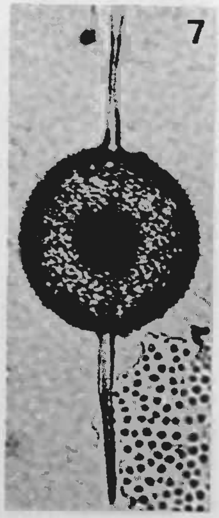
7

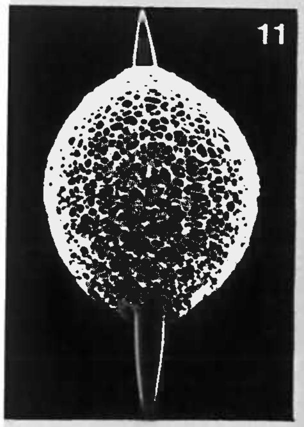
11

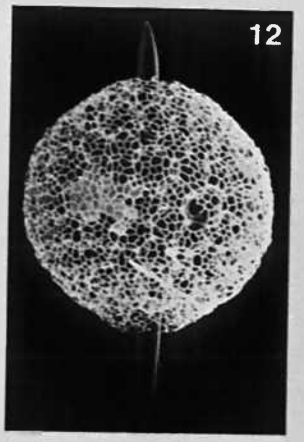
12

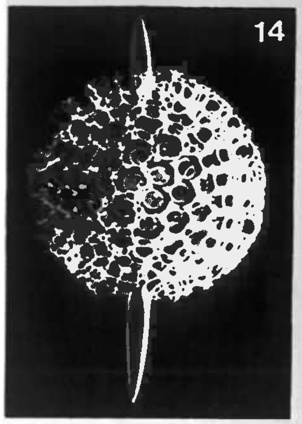
14

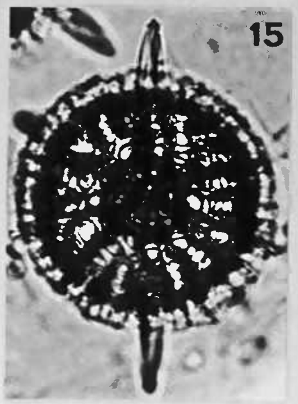
15


16

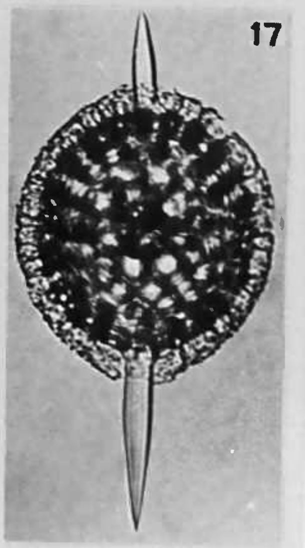
17

PLATE 15

Suborder: Spumellaria
Family: Actinommidae; Subfamilies: Actinomminae, Saturnalinae

Figure		Station Depth	Type of Micrograph	Magnification
1	Xiphatractus pluto (Haeckel)	$P_1$5582m	LM	x210
2	Xiphatractus pluto (Haeckel)	$P_1$978m	LM	x210
3	Xiphatractus pluto (Haeckel)	$P_1$5582m	LM	x210
4	Xiphatractus sp. A	E988m	LM	x210
5	Druppatractus ? sp.	$P_1$5582m	SEM	x200
6	Xiphatractus sp. B	$P_1$4280m	SEM	x250
7	Xiphatractus sp. B	$P_1$4280m	SEM	x440
8	Hexacontium heracliti (Haeckel)	PB3791m	LM	x210
9	Hexacontium heracliti (Haeckel)	PB2869m	LM	x210
10	Hexacontium hystricina (Haeckel)	PB2869m	SEM	x230
11	Dorydruppa bensoni, new name	PB2869m	LM	x210
12	Dorydruppa bensoni, new name A pear-shaped medullary shell	PB2869m	LM	x210
13	Dorydruppa bensoni, new name A specimen with thin cortical shell	$P_1$4280m	LM	x210
14	Dorydruppa bensoni, new name A pear-shaped medullary shell	PB3791m	SEM	x550
15	Saturnalis circularis Haeckel	PB3791m	LM	x210
16	Saturnalis circularis Haeckel	$P_1$4280m	SEM	x210
17	Saturnalis circularis Haeckel A close up of the cortical shell. Note presence of a fragile outer cortical meshwork.	PB2869m	SEM	x380
18	Saturnalis circularis Haeckel	PB2869m	SEM	x170

PLATE 15 Spumellaria

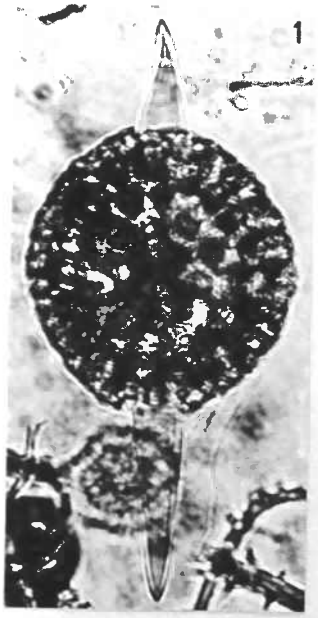
1

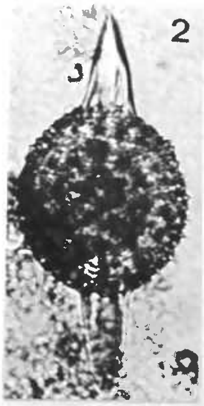
2

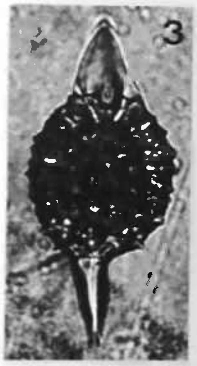
3

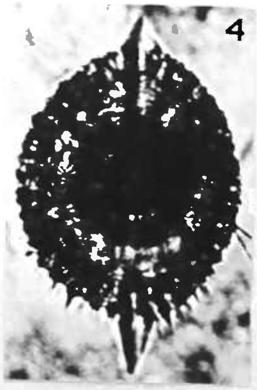
4

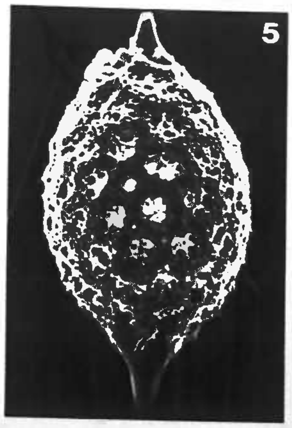
5

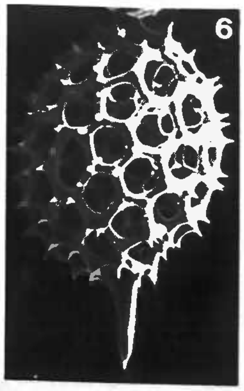
6

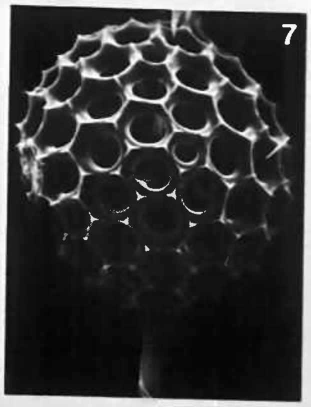
7

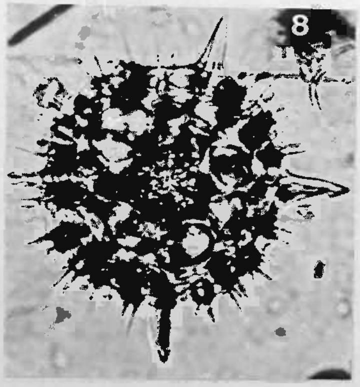
8

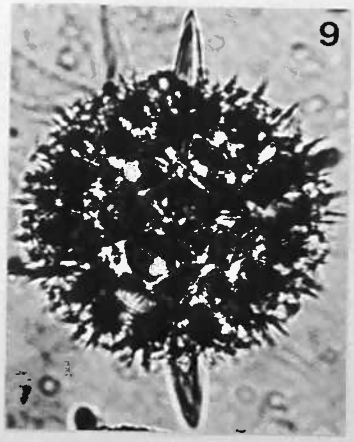
9

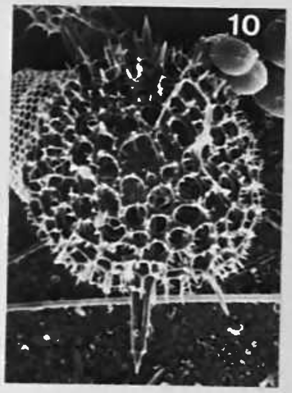
10

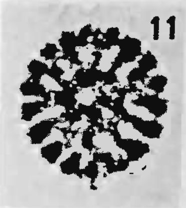
11


12

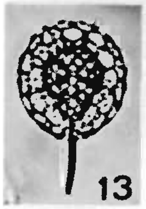
13

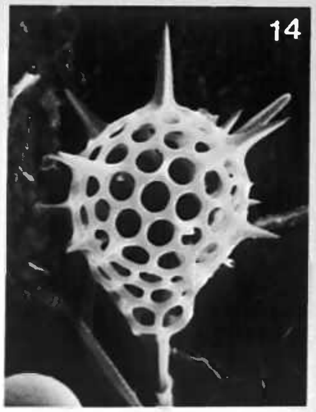
14

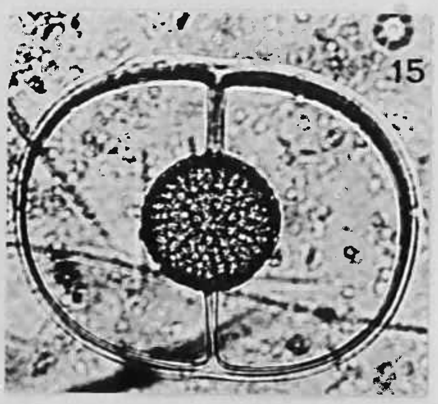
15

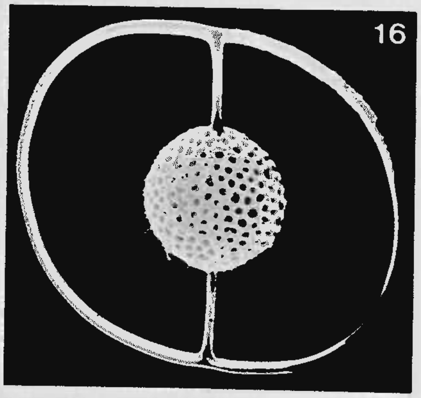
16

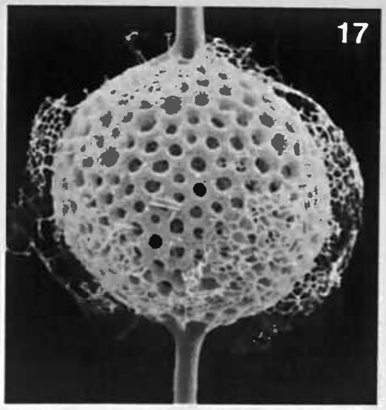
17

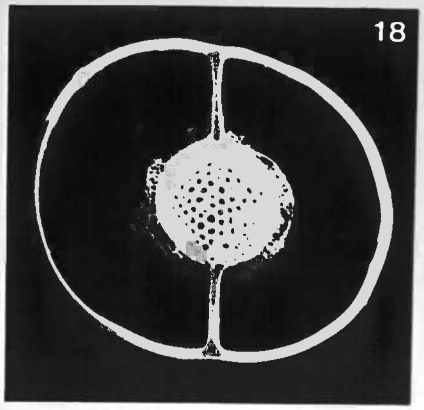
18

PLATE 16

Suborder: Spumellaria
Families: Porodiscidae, Spongodiscidae

Figure		Station Depth	Type of Micrograph	Magnification
1	Euchitonia elegans (Ehrenberg)	$P_1$978m	SEM	x120
2	Euchitonia elegans (Ehrenberg)	$P_1$5582m	SEM	x120
3	Euchitonia elegans (Ehrenberg) A specimen without a patagium	PB3791m	SEM	x80
4	Euchitonia elegans (Ehrenberg)	$P_1$2778m	LM	x100
5	Euchitonia elegans (Ehrenberg)	PB3769m	LM	x105
6	Euchitonia elegans (Ehrenberg) A specimen with a well developed patagium	PB3769m	LM	x105
7	Spongodiscus sp. A	$P_1$4280m	SEM	x430
8	Euchitonia cf. furcata Ehrenberg	$P_1$4280m	SEM	x240
9	Euchitonia sp.	PB2869m	LM	x210
10	Dictyocoryne profunda Ehrenberg	$P_1$5582m	LM	x210
11	Euchitonia sp.	$P_1$4280m	SEM	x280
12	Dictyocoryne profunda Ehrenberg A specimen with a well developed patagium	PB3791m	LM	x210
13	Dictyocoryne profunda Ehrenberg	PB1268m	SEM	x110
14	Dictyocoryne truncatum (Ehrenberg)	PB1268m	SEM	x180
15	Dictyocoryne profunda Ehrenberg	$P_1$2778m	SEM	x160

PLATE 16 Spumellaria

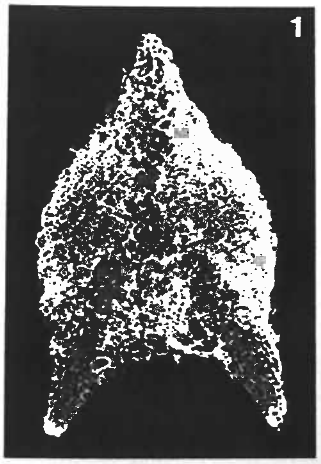
1

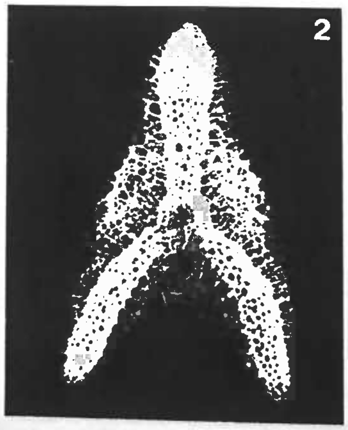
2

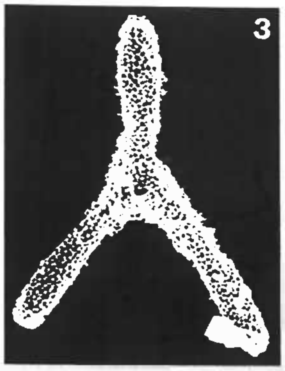
3

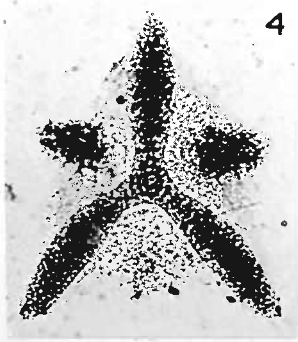
4

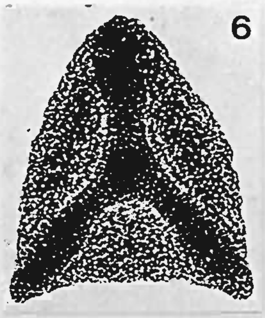
6

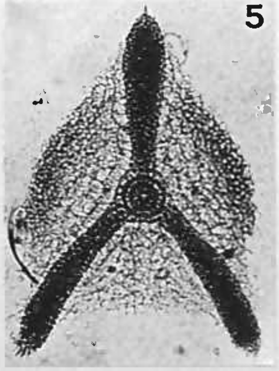
5

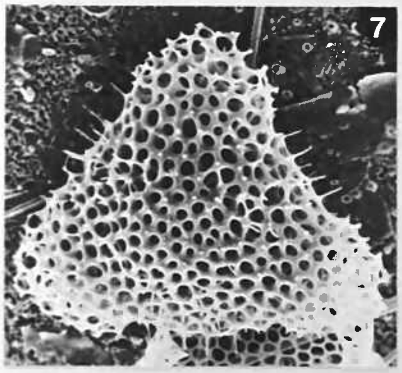
7


8

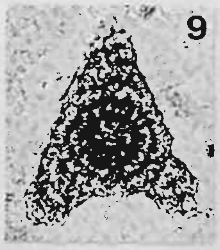
9

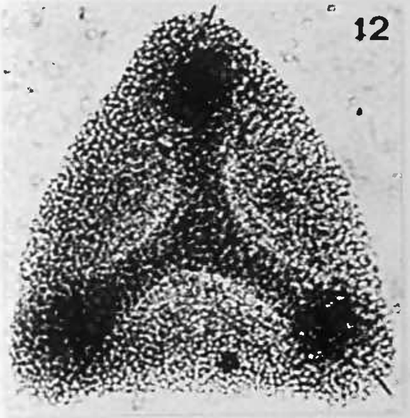
12


11

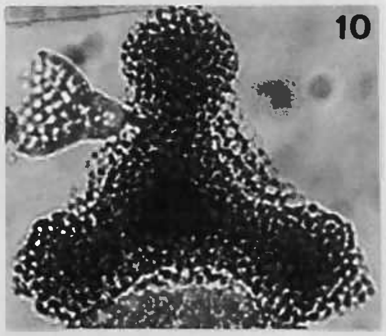
10

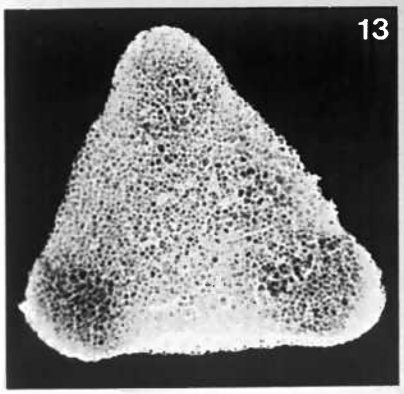
13

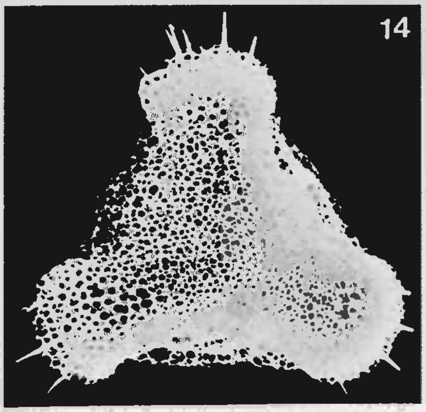
14

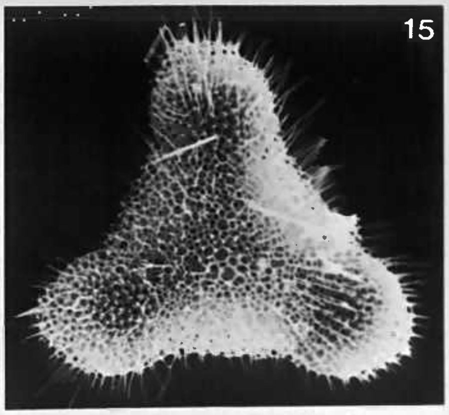
15

PLATE 17

Suborder: Spumellaria
Families: Porodiscidae, Spngodiscidae

Figure		Station Depth	Type of Micrograph	Magnification
1	*Amphirhopalum ypsilon* Haeckel	$P_1$5582m	SEM	x180
2	*Amphirhopalum ypsilon* Haeckel	PB3791m	LM	x210
3	*Amphirhopalum ypsilon* Haeckel	PB3791m	LM	x210
4	*Tessarastrum straussii* Haeckel	$P_1$5582m	LM	x210
5	*Spongocore cylindrica* (Haeckel)	$P_1$4280m	LM	x210
6	*Spongocore cylindrica* (Haeckel)	$P_1$5582m	SEM	x165
7	*Spongocore cylindrica* (Haeckel)	$P_1$5582m	LM	x210
8	*Spongocore cylindrica* (Haeckel)	$P_1$978m	SEM	x190
9	*Spongocore cylindrica* (Haeckel)	PB3791m	LM	x210
10	*Spongaster tetras tetras* Ehrenberg	PB978m	SEM	x340
11	*Spongaster tetras tetras* Ehrenberg	PB3769m	LM	x190
12	*Spongaster pentas* Riedel and Sanfilippo	PB2869m	LM	x210
13	*Spongaster pentas* Riedel and Sanfilippo Oblique ventral view	$P_1$5582m	SEM	x230
14	*Spongaster pentas* Riedel and Sanfilippo Oblique ventral view	$P_1$5582m	SEM	x230
15	*Spongaster pentas* Riedel and Sanfilippo Oblique ventral view	$P_1$5582m	SEM	x210
16	*Spongaster pentas* Riedel and Sanfilippo Oblique dorsal view	$P_1$5582m	SEM	x200

PLATE 17 Spumellaria


1

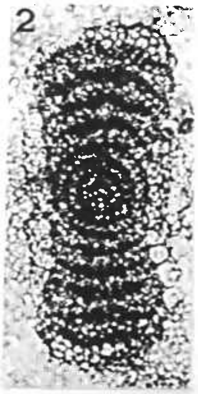
2


3

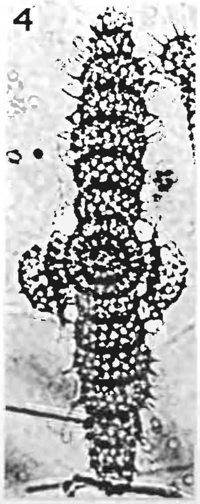
4


5

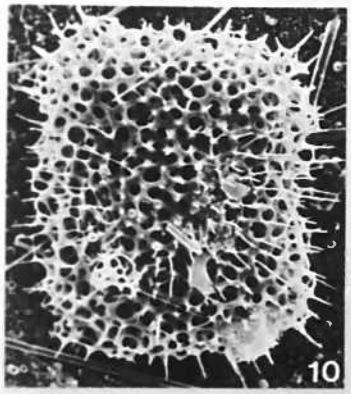
10


9

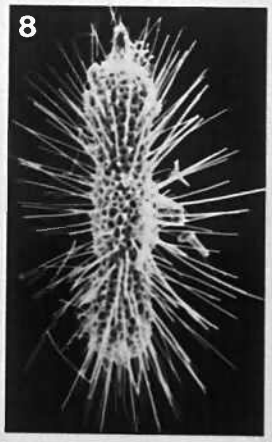
8


7

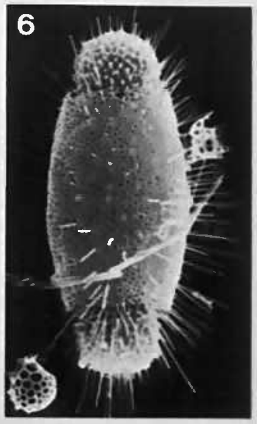
6

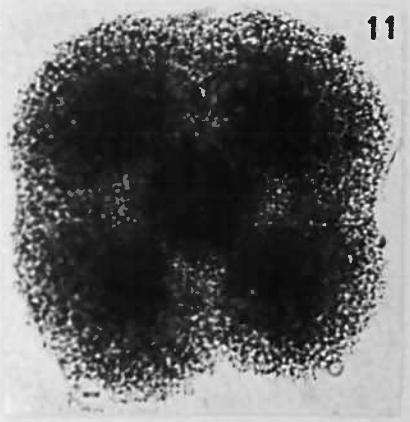
11

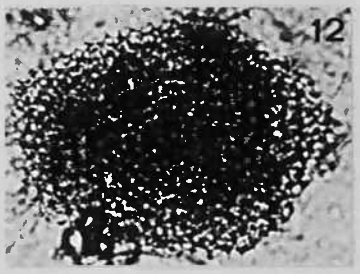
12

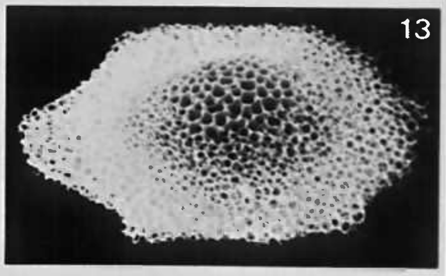
13

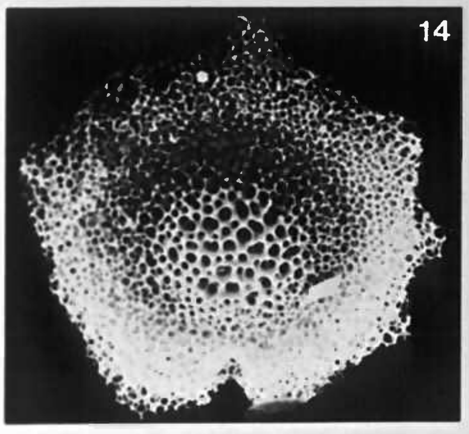
14

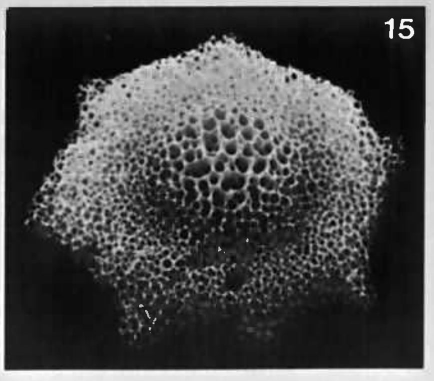
15

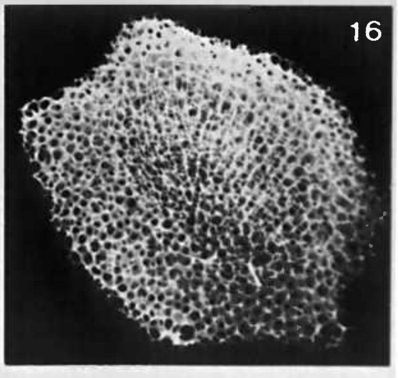
16

PLATE 18

Suborder: Spumellaria
Family: Myelastridae

Figure		Station Depth	Type of Micrograph	Magnification
1	*Myelastrum quadrifolium* n.sp.	PB3791m	SEM	x55
2	*Myelastrum quadrifolium* n.sp. Holotype	PB3791m	RLM	x64
3	*Myelastrum quadrifolium* n.sp. Paratype	PB3791m	RLM	x64
4	*Myelastrum quadrifolium* n.sp. Oblique view	PB3791m	SEM	x50
5	*Myelastrum quadrifolium* n.sp. Paratype	PB667m	SEM	x50
6	*Myelastrum quadrifolium* n.sp. Same specimen illustrating the detail of the central area	PB667m	SEM	x500
7	*Myelastrum trinibrachium* n.sp. Paratype	PB1268m	SEM	x38
8	*Myelastrum trinibrachium* n.sp.	PB3791m	RLM	x64
9	*Myelastrum trinibrachium* n.sp. Paratype	$P_1$4280m	SEM	x50
10	*Myelastrum trinibrachium* n.sp. Holotype	PB1268m	SEM	x33
11	*Myelastrum trinibrachium* n.sp.	PB3769m	TEM	x67000
12	*Myelastrum trinibrachium* n.sp. Paratype	DOMES B56m	LM	x185

PLATE 18 Spumellaria

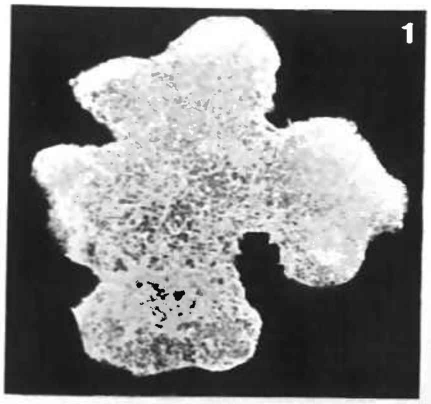

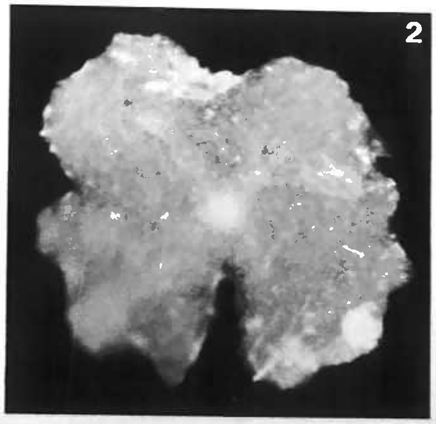

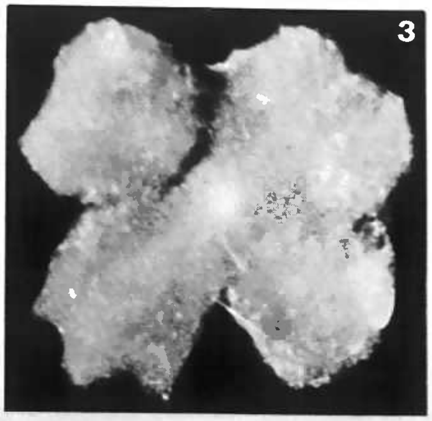

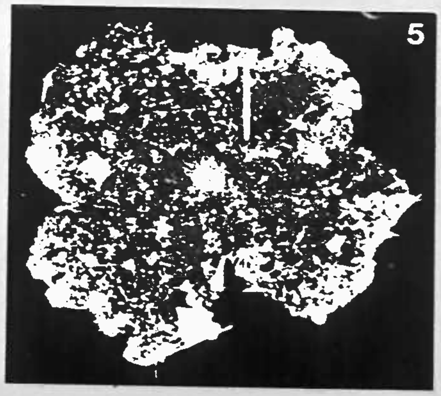

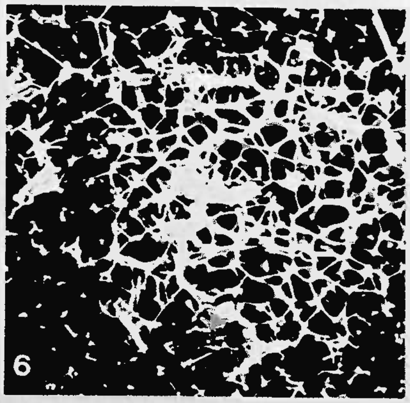

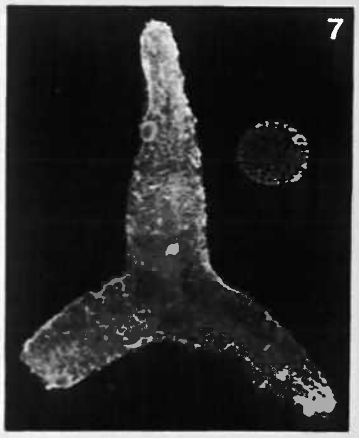

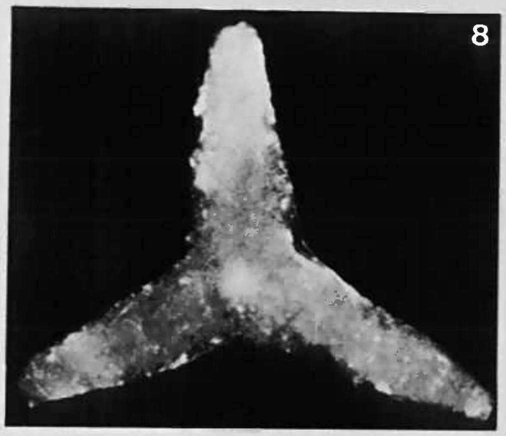

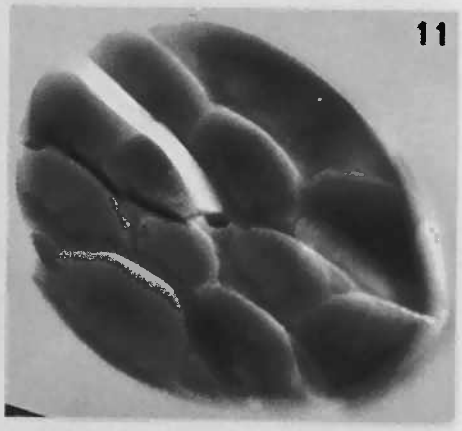

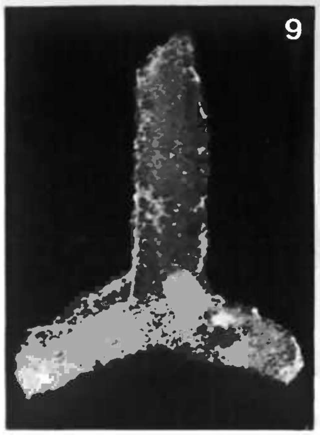

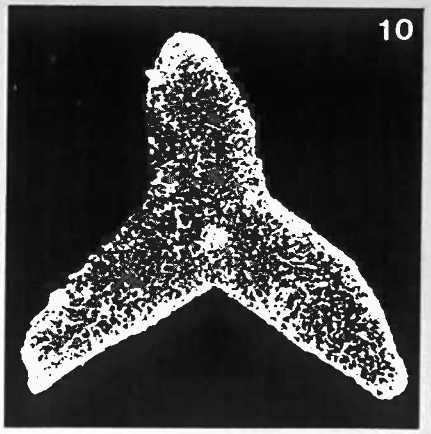

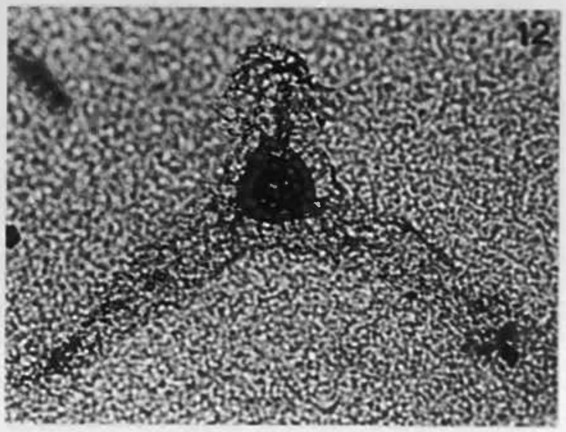

PLATE 19

Suborder: Spumellaria
Families: Spongodiscidae, Porodiscidae

Figure		Station Depth	Type of Micrograph	Magnification
1	*Spongodiscus resurgens* Ehrenberg	$P_1$978m	SEM	x270
2	*Spongodiscus* spp. B group	$P_1$5582m	SEM	x450
3	*Spongodiscus* spp. B group	$P_1$978m	SEM	x440
4	*Spongodiscus biconcavus* Haeckel	$P_1$5582m	SEM	x150
5	*Spongodiscus biconcavus* Haeckel Same specimen, oblique view	PB1268m	SEM	x150
6	*Spongodiscus biconcavus* Haeckel	PB3769m	LM	x157
7	*Spongotrochus* sp. A	$P_1$5582m	SEM	x154
8	*Stylospongia huxleyi* Haeckel	$P_1$4280m	SEM	x280
9	*Spongopyle setosa* Dreyer	$P_1$5582m	LM	x210
10	*Spongotrochus glacialis* Popofsky	PB3791m	LM	x210
11	*Stylodictya validispina* Jørgensen	$P_1$978m	LM	x210
12	*Stylodictya* ? sp.	PB3791m	LM	x210
13	*Stylodictya* ? sp.	PB3791m	LM	x210

PLATE 19 Spumellaria

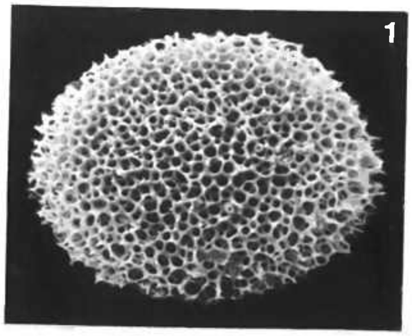

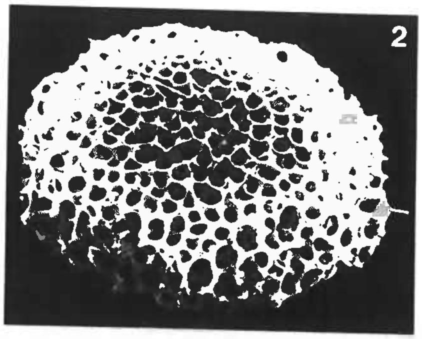

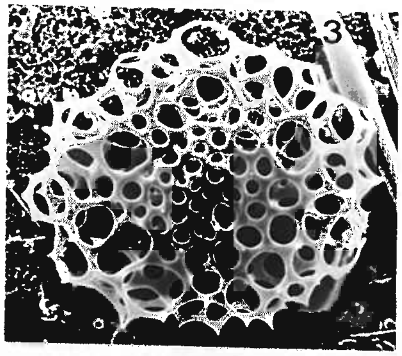

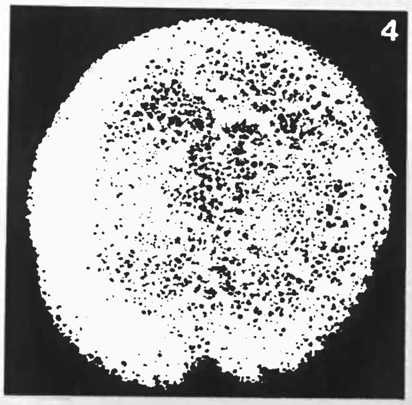

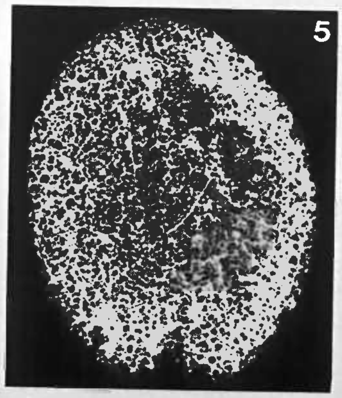

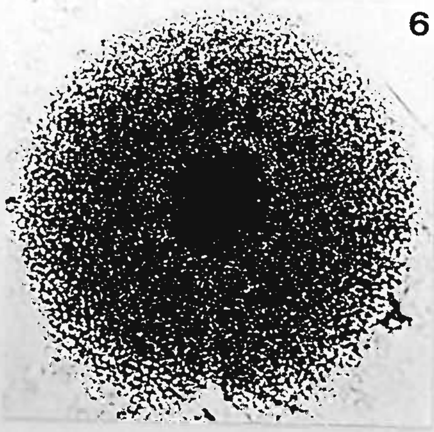

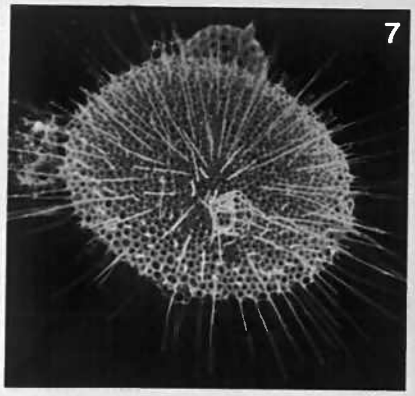

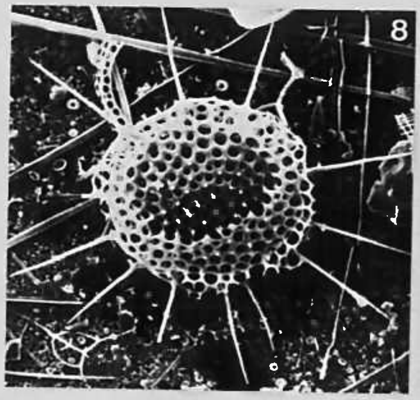

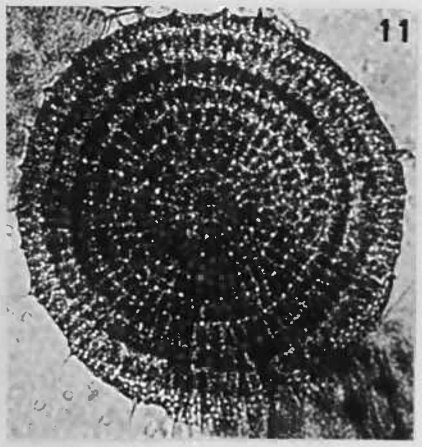

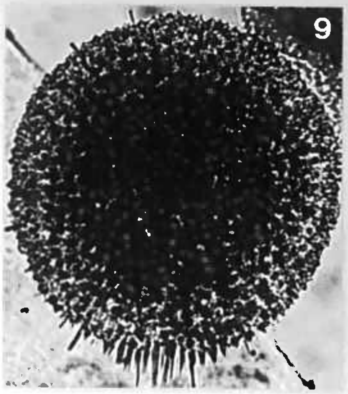

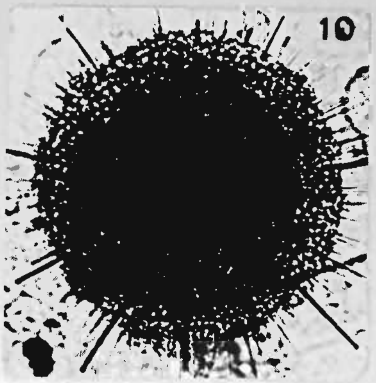

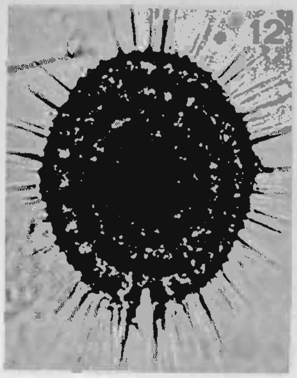

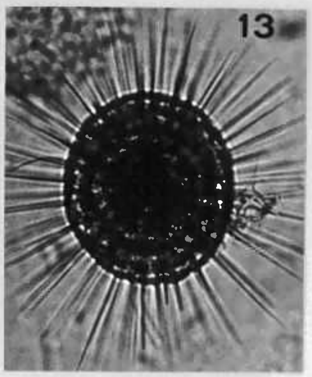

PLATE 20

Suborder: Spumellaria
Families: Spongodiscidae, Porodiscidae

Figure		Station Depth	Type of Micrograph	Magnification
1	*Spongopyle osculosa* Dreyer	$P_1$978m	SEM	x390
2	*Spongopyle osculosa* Dreyer	PB1268m	SEM	x200
3	*Spongopyle osculosa* Dreyer	PB3769m	LM	x210
4	*Spongopyle osculosa* Dreyer	PB1268m	SEM	x180
5	*Circodiscus* spp. group A specimen with broken surface membrane	$P_1$978m	SEM	x180
6	*Circodiscus* spp. group	PB667m	SEM	x165
7	*Circodiscus* spp. group Apical view	$P_1$2778m	LM	x210
8	*Circodiscus* spp. group	$P_1$2778m	LM	x210
9	*Circodiscus* spp. group	$P_1$978m	LM	x210
10	*Stylodictya multispina* Haeckel	$P_1$5582m	LM	x210
11	*Stylochlamydium venustrum* (Bailey)	$P_1$978m	LM	x210
12	*Stylodictya multispina* Haeckel	PB3769m	LM	x210
13	*Porodiscus micromma* (Harting)	$P_1$5582m	LM	x210
14	*Porodiscus micromma* (Harting)	$P_1$5582m	LM	x210

PLATE 20 Spumellaria

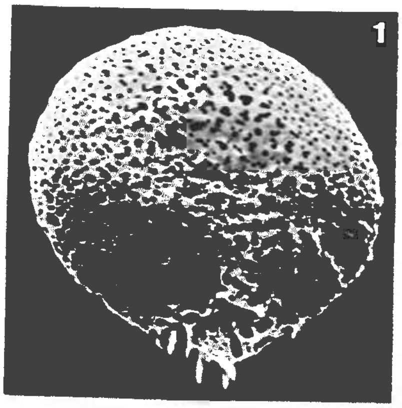

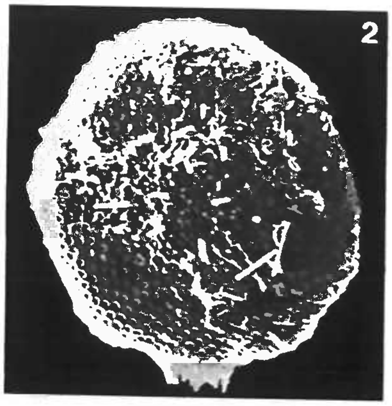

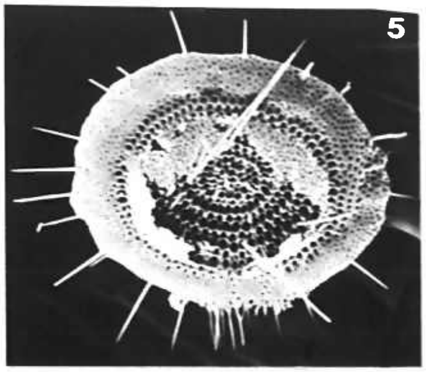

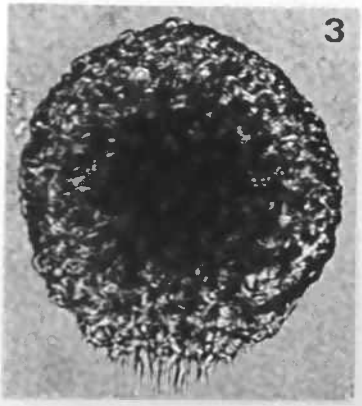

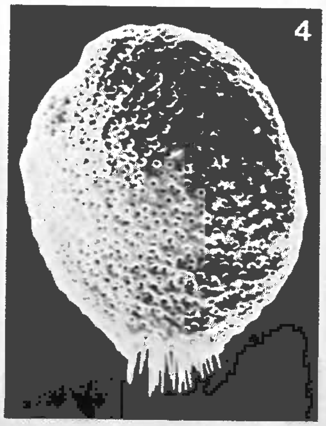

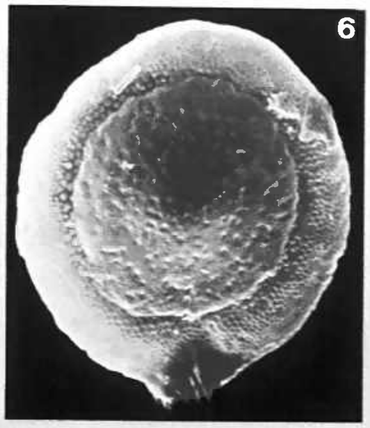

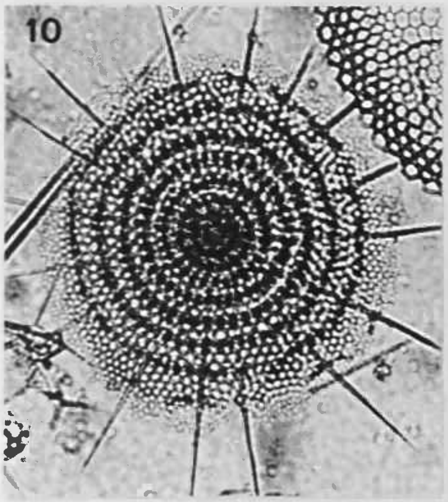

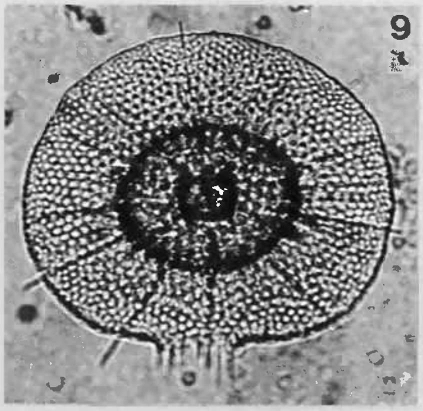

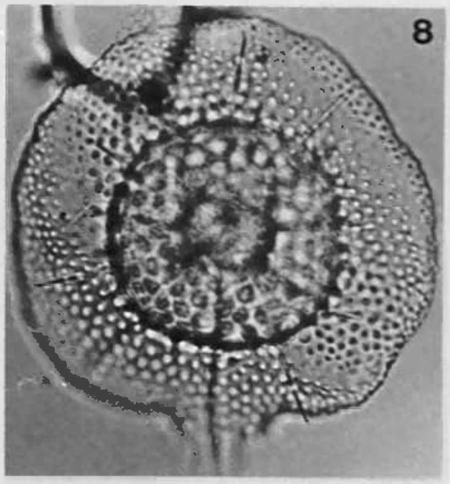

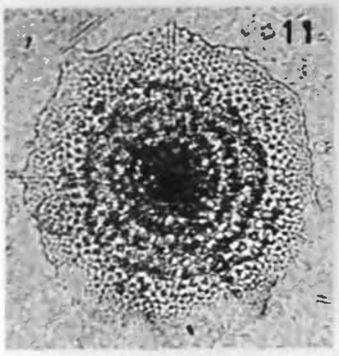

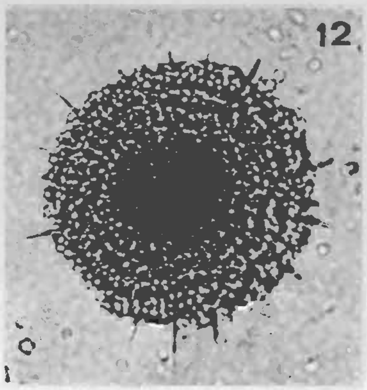

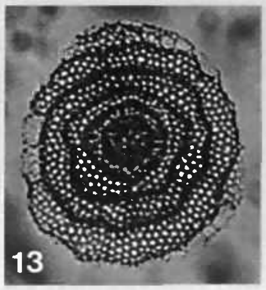

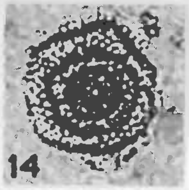

PLATE 21

Suborder: Spumellaria
Families: Coccodiscidae; Larnacillidae

Figure		Station Depth	Type of Micrograph	Magnification
1	*Didymocyrtis tetrathalamus tetrathalamus* (Haeckel) juvenile form Oblique view of a specimen having only equatorial part. Note that cortical-medullary interconnecting bars lie in the vicinity of an equatorial plane.	$P_1$4280m	SEM	x550
2	*Didymocyrtis tetrathalamus tetrathalamus* (Haeckel) Oblique lateral view	$P_1$4280m	SEM	x440
3	*Didymocyrtis tetrathalamus tetrathalamus* (Haeckel) Oblique polar view	$P_1$4280m	SEM	x440
4	*Didymocyrtis tetrathalamus tetrathalamus* (Haeckel) Lateral view	$P_1$4280m	SEM	x440
5	*Didymocyrtis tetrathalamus tetrathalamus* (Haeckel) Polar view of an incompletely developed specimen	$P_1$5582m	LM	x210
6	*Didymocyrtis tetrathalamus tetrathalamus* (Haeckel) Lateral view of an incompletely developed specimen	$P_1$5582m	LM	x210
7	*Didymocyrtis tetrathalamus tetrathalamus* (Haeckel)	PB2869m	LM	x210
8	*Didymocyrtis tetrathalamus tetrathalamus* (Haeckel) A specimen with well developed outer cortical mesh	PB667m	LM	x210
9	*Didymocyrtis tetrathalamus tetrathalamus* (Haeckel)	$P_1$4280m	SEM	x260
10	*Didymocyrtis tetrathalamus tetrathalamus* (Haeckel) Oblique polar view	$P_1$978m	SEM	x400
11	*Didymocyrtis tetrathalamus tetrathalamus* (Haeckel)	$P_1$5582m	SEM	x220
12	*Didymocyrtis tetrathalamus tetrathalamus* (Haeckel) A specimen with well developed polar caps	$P_1$5582m	SEM	x215
13	*Didymocyrtis tetrathalamus tetrathalamus* (Haeckel)	$P_1$4280m	SEM	x170
14	*Didymocyrtis tetrathalamus tetrathalamus* (Haeckel)	$P_1$4280m	SEM	x280
15	*Didymocyrtis* sp.	PB2869m	LM	x210
16	*Larnacalpis* sp. Frontal view	PB2869m	LM	x210
17	*Larnacalpis* sp. Lateral view	PB2869m	LM	x210
18	*Larnacalpis* sp. Frontal view	PB3769m	SEM	x170

PLATE 21 Spumellaria

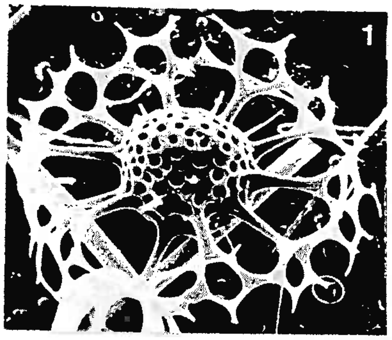

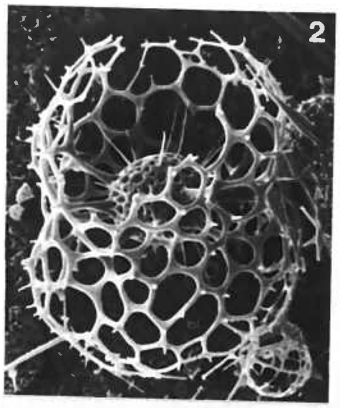

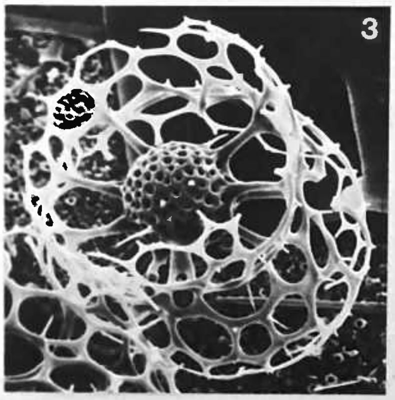

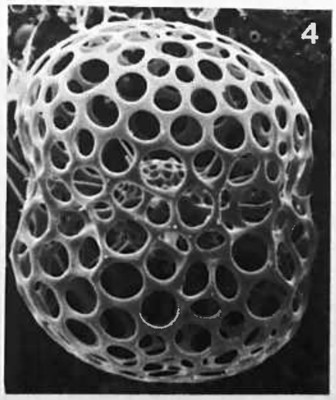

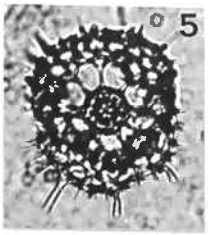

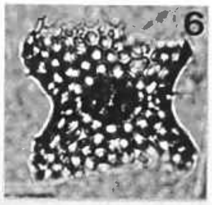

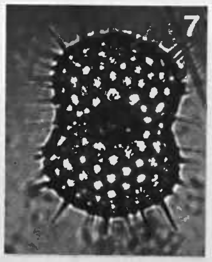

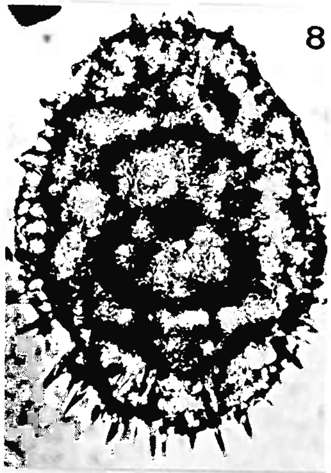

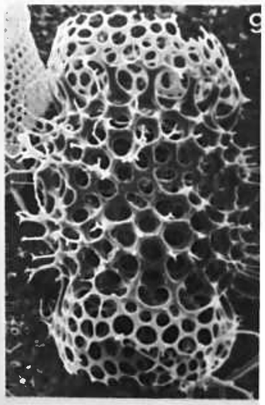

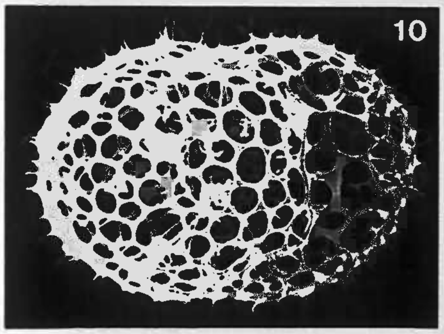

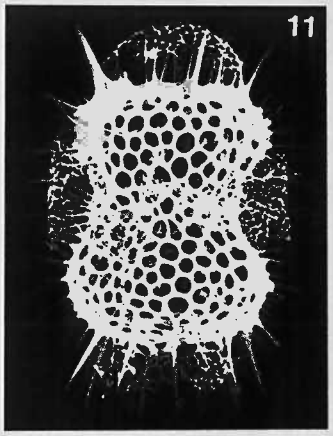

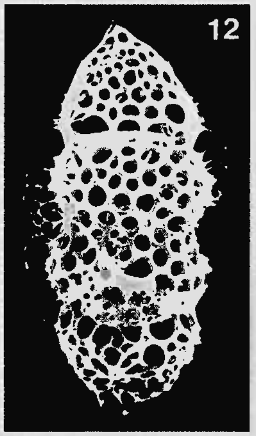

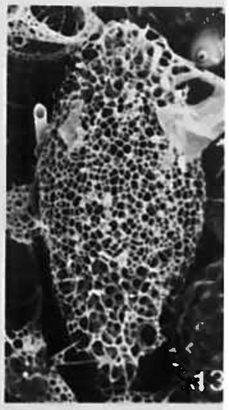

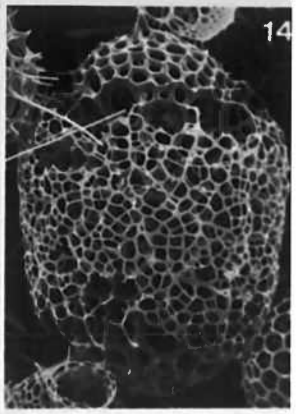

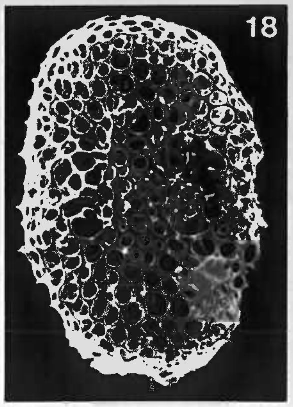

PLATE 22

Suborder: Spumellaria
Families: Litheliidae, Phacodiscidae; Actinommidae; Coccodiscidae

Figure		Station Depth	Type of Micrograph	Magnification
1	*Larcopyle butschlii* Dreyer	$P_1$4280m	SEM	x280
2	*Larcopyle butschlii* Dreyer	E389m	LM	x210
3	*Larcopyle butschlii* Dreyer	PB3791m	LM	x210
4	*Larcopyle butschlii* Dreyer	PB3791m	LM	x210
5	*Larcopyle* sp. A	$P_1$978m	SEM	x450
6	*Larcopyle* sp. A	PB3791m	SEM	x440
7	*Tholospira cervicornis* Haeckel group	PB2869m	LM	x210
8	*Tholospira cervicornis* Haeckel group	PB3791m	LM	x210
9	*Tholospira cervicornis* Haeckel group	PB2869m	LM	x210
10	*Lithelius minor* ? Jorgensen	PB667m	LM	x210
11	*Tholospira dendrophora* Haeckel	PB3791m	LM	x210
12	*Tholospira cervocornis* Haeckel group	PB2869m	LM	x210
13	Actinommidae gen. et sp. indet.	$P_1$5582	SEM	x350
14	*Heliodiscus* ? sp. Oblique view	$P_1$5582m	SEM	x165
15	*Spongoliva ellipsoides* Popofsky	PB667m	LM	x210
16	*Spongoliva ellipsoides* Popofsky	PB3769m	LM	x210

PLATE 22 Spumellaria

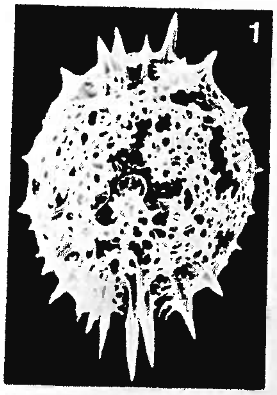

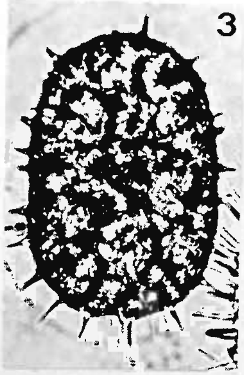

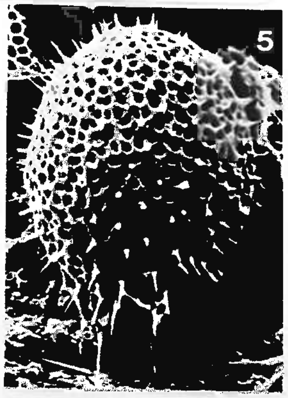

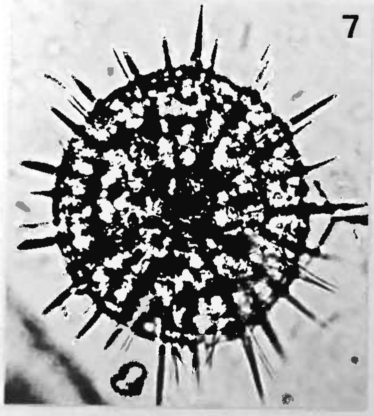

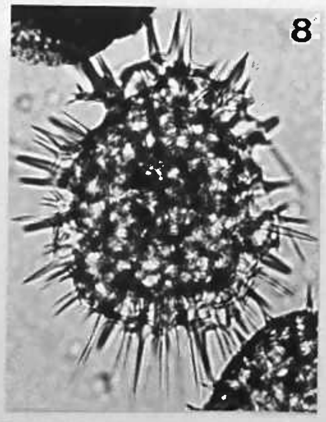

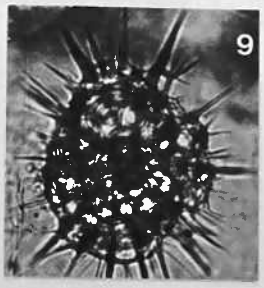

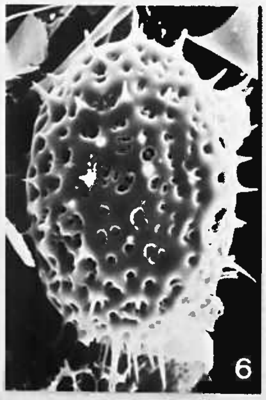

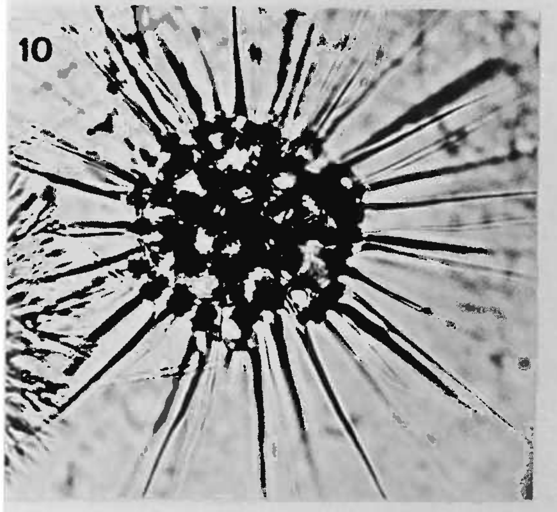

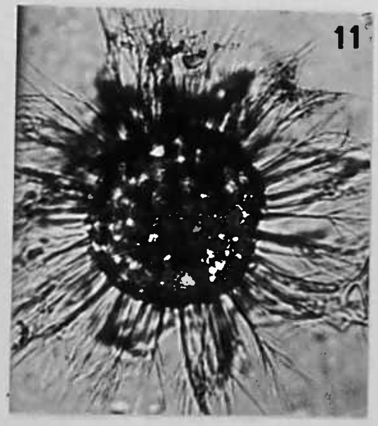

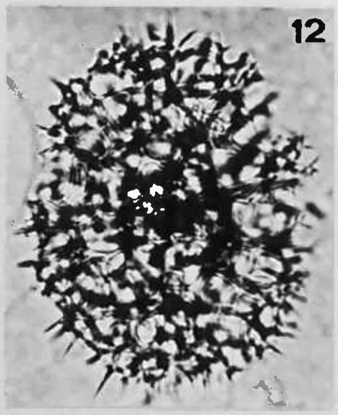

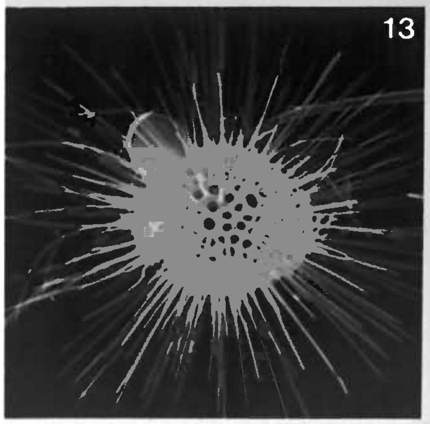

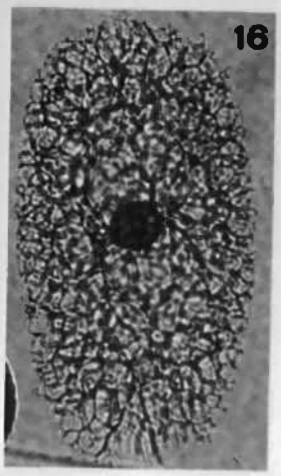

PLATE 23

Suborder: Spumellaria
Families: Phacodiscidae, Phyloniidae, Litheliidae

Figure		Station Depth	Type of Micrograph	Magnification
1	*Heliodiscus asteriscus* Haeckel Oblique view	$P_1$978m	SEM	x165
2	*Heliodiscus asteriscus* Haeckel	PB1268m	LM	x210
3	*Heliodiscus asteriscus* Haeckel	PB667m	LM	x210
4	*Heliodiscus echiniscus* Haeckel	$P_1$5582m	SEM	x215
5	*Heliodiscus echiniscus* Haeckel	$P_1$4280m	SEM	x210
6	*Heliodiscus echiniscus* Haeckel Oblique edge view	PB667m	LM	x210
7	*Hexapyle* sp.	$P_1$4280m	SEM	x960
8	*Octopyle stenozona* Haeckel Frontal view	$P_1$2778m	SEM	x330
9	*Tetrapyle octacantha* Müller Frontal view	PB3769m	LM	x210
10	*Tetrapyle octacantha* Müller Polar view	E389m	SEM	x315
11	*Larcospira quadrangula* Haeckel Orientation illustrating the apparent double spiral arrangement of girdles	$P_1$5582m	SEM	x154
12	*Larcospira quadrangula* Haeckel Orientation perpendicular to fig. 11	$P_1$978m	SEM	x180

PLATE 23 Spumellaria

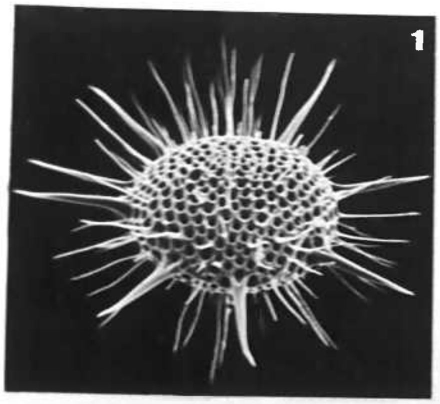
1

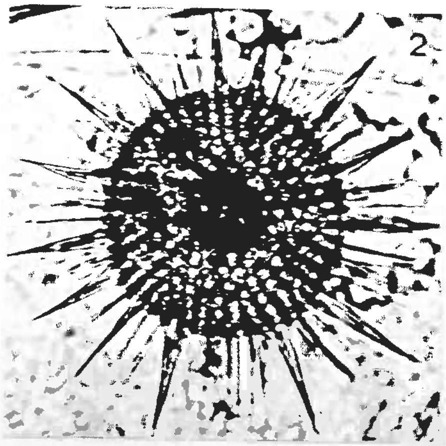
2

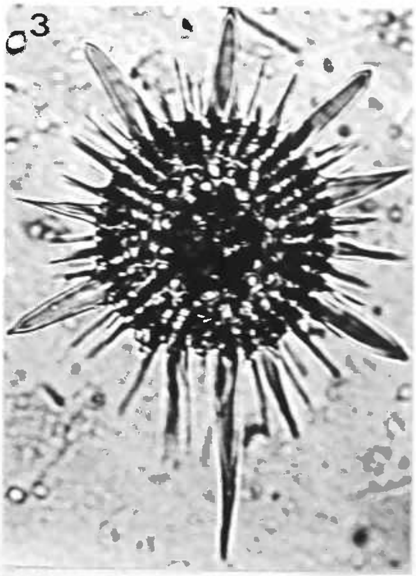
3

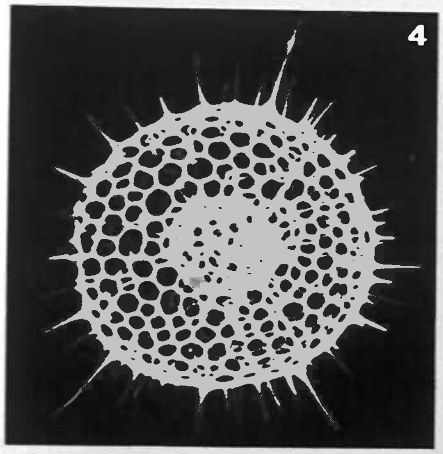
4

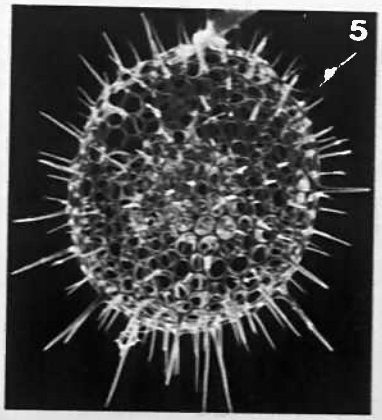
5


6

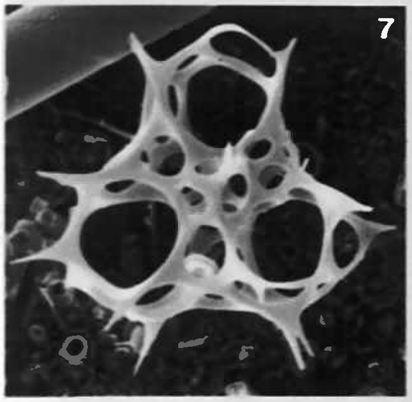
7

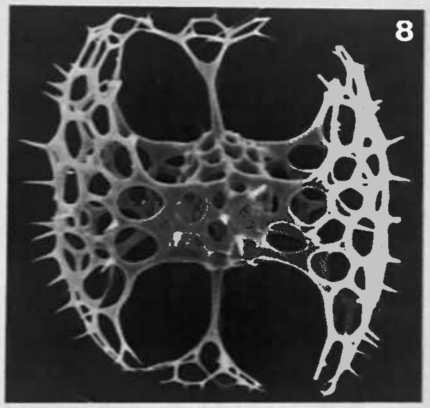
8

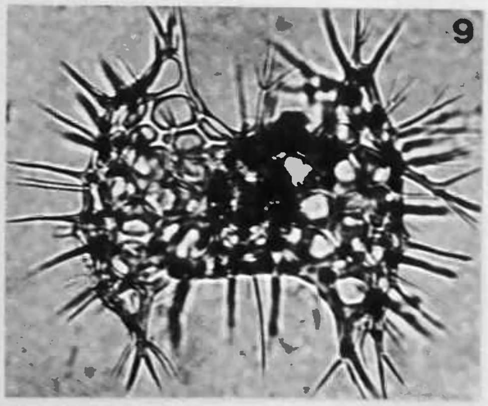
9

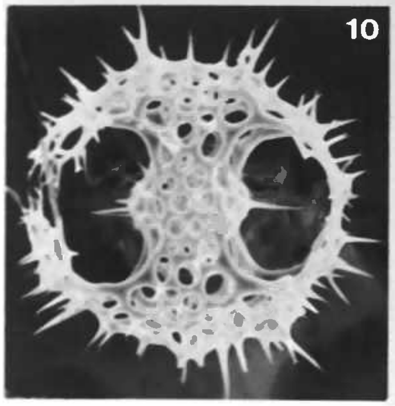
10

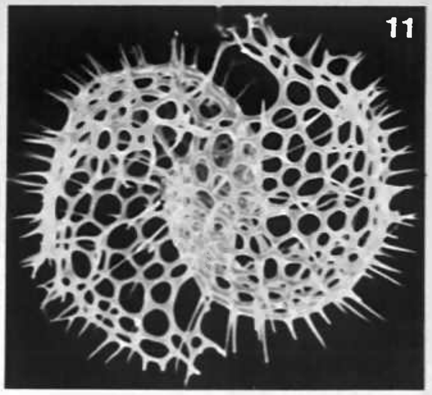
11

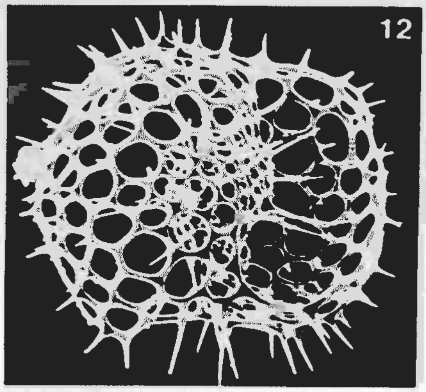
12

PLATE 24

Suborder: Nassellaria
Family: Plagiacanthidae; Subfamily: Plagiacanthinae

Figure		Station Depth	Type of Micrograph	Magnification
1	*Tetraplecta pinigera* Haeckel	PB3791m	LM	x160
2	*Tetraplecta pinigera* Haeckel	P1978m	SEM	x290
3	*Tetraplecta pinigera* Haeckel Detail of central part; note that the skeleton is cylindrical rod.	P14280m	SEM	x1100
4	*Tetraplecta pinigera* Haeckel	P14280m	SEM	x150
5	*Tetraplecta pinigera* Haeckel	P14280m	LM	x210
6	*Tetraplecta corynephorum* ? Jørgensen	PB1268m	LM	x105
7	*Tetraplecta plectaniscus* Haeckel	E5068m	LM	x210
8	*Clathromitra pterophormis* Haeckel	P15582m	SEM	x120
9	*Cladoscenium ancoratum* Haeckel	PB3791m	SEM	x440
10	*Cladoscenium ancoratum* Haeckel	P15582m	LM	x210
11	*Cladoscenium ancoratum* Haeckel	PB2869m	LM	x210
12	*Cladoscenium ancoratum* Haeckel	PB2869m	LM	x210
13	*Cladoscenium ancoratum* Haeckel	PB2869m	LM	x210
14	*Cladoscenium ancoratum* Haeckel	PB2869m	LM	x210
15	*Semantis gracilis* ? Popofsky	PB3769m	SEM	x1100
16	*Semantis gracilis* ? Popofsky	P14280m	SEM	x1000
17	*Deflandrella cladophora* Jørgensen	P15582m	SEM	x72

PLATE 24 Nassellaria

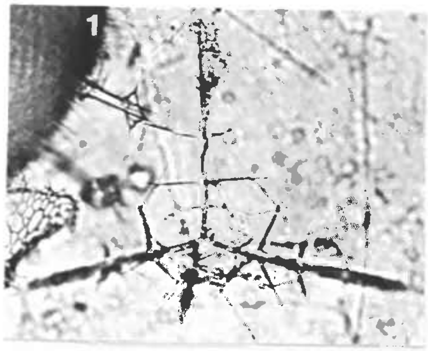

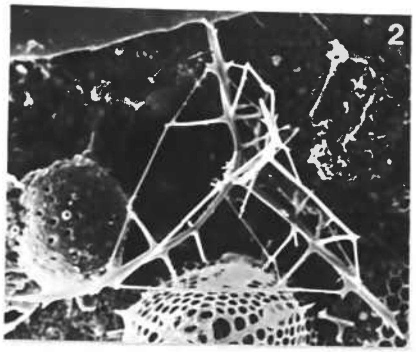

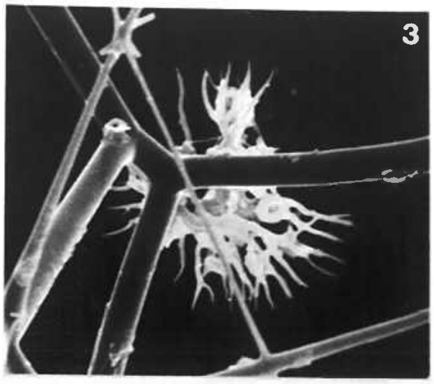

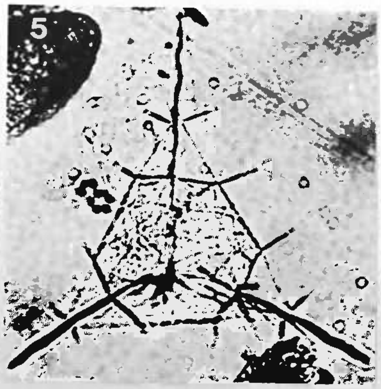

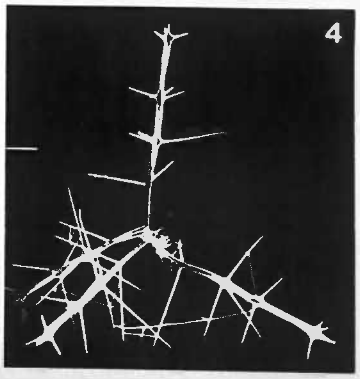

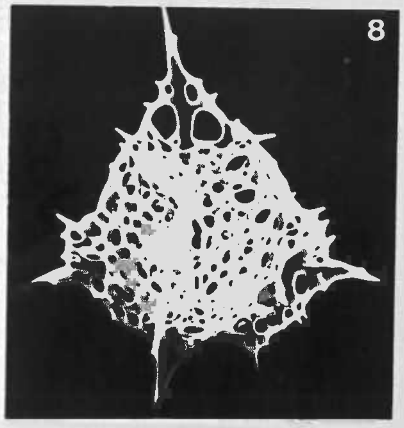

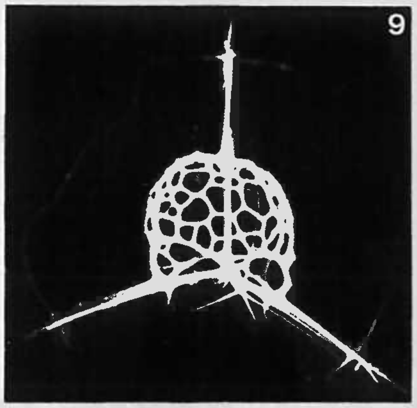

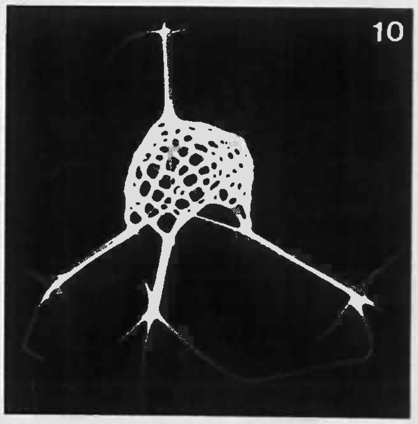

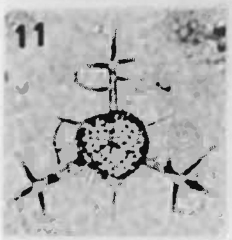

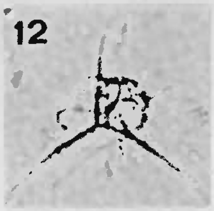

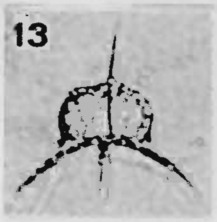

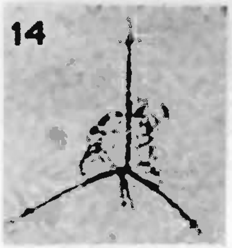

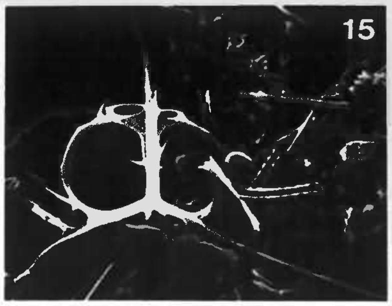

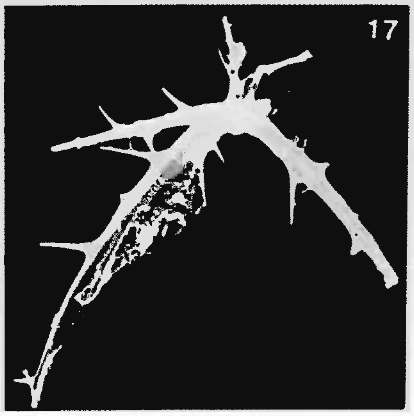

PLATE 25

Suborder: Nassellaria
Family: Plagiacanthidae; Subfamily: Lophophaeninae

Figure		Station Depth	Type of Micrograph	Magnification
1	*Acanthocorys* cf. *variabilis* Popofsky	PB2869m	LM	x210
2	*Lophophaena decacantha* (Haeckel) group	PB1268m	LM	x210
3	*Lophophaena cylindrica* (Cleve)	$P_1$4280m	SEM	x440
4	*Lophophaena cylindrica* (Cleve)	$P_1$4280m	SEM	x500
5	*Lophophaena cylindrica* (Cleve)	PB3791m	LM	x210
6	*Lophophaena* cf. *capito* Ehrenberg	PB3769m	LM	x210
7	*Lophophaena* cf. *capito* Ehrenberg	$P_1$4280m	SEM	x300
8	*Lophophaena* cf. *capito* Ehrenberg	$P_1$2778m	SEM	x300
9	*Lophophaena* cf. *capito* Ehrenberg	PB1268m	SEM	x250
10	*Lophophaena decacantha* (Haeckel) group	PB3791m	LM	x210
11	*Peromelissa phalacra* Haeckel	$P_1$4280m	SEM	x340
12	*Peromelissa phalacra* Haeckel	PB2869m	LM	x210
13	*Peromelissa phalacra* Haeckel	PB2869m	LM	x210
14	*Peromelissa phalacra* Haeckel	$P_1$978m	SEM	x500
15	*Peromelissa phalacra* Haeckel	$P_1$4280m	SEM	x520
16	*Lithomelissa setosa* Jørgensen	PB2869m	LM	x210
17	*Lithomelissa setosa* Jørgensen	PB2869m	LM	x210
18	*Lithomelissa setosa* Jørgensen	PB3769m	SEM	x1400
19	*Lithomelissa setosa* Jørgensen	PB3769m	SEM	x1100
20	*Lithomelissa setosa* Jørgensen	PB3769m	SEM	x1710
21	*Lithomelissa setosa* Jørgensen	PB2869m	LM	x210
22	*Lithomelissa setosa* Jørgensen	$P_1$2778m	LM	x210

PLATE 25 Nassellaria

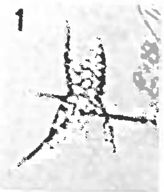
1

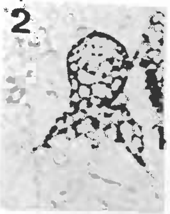
2

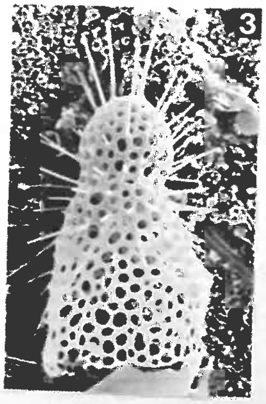
3

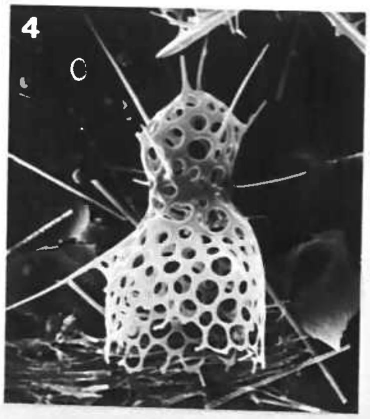
4

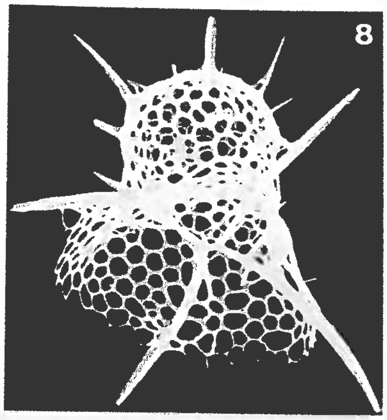
8


5

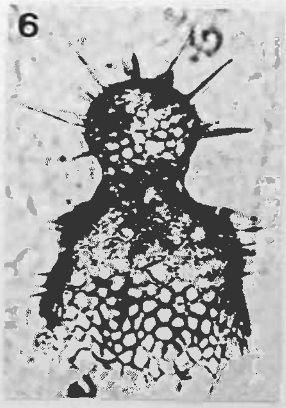
6

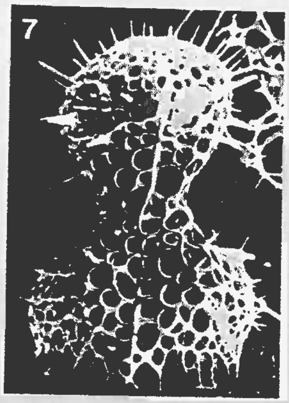
7


9

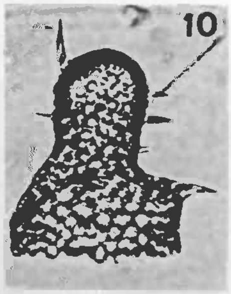
10


12

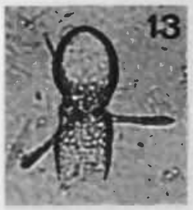
13


11


16

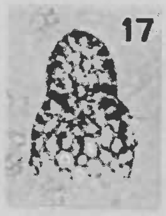
17

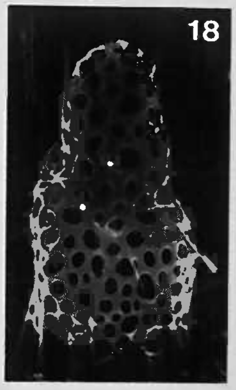
18

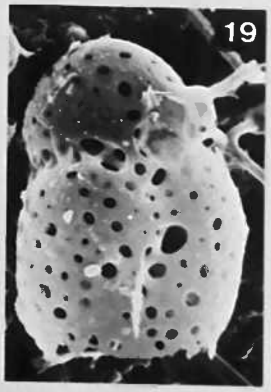
19


14


15

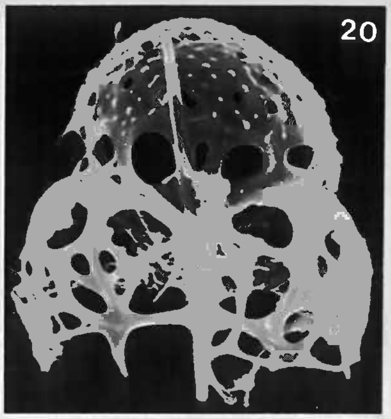
20


21


22

PLATE 26

Suborder: Nassellaria
Family: Plagiacanthidae; Subfamilies: Plagiacanthinae, Sethoperinae

Figure		Station Depth	Type of Micrograph	Magnification
1	*Talariscus pseudocuboides* (Popofsky)	$P_1$4280m	SEM	x720
2	*Gonosphaera primordialis* ? Jørgensen	PB3769m	SEM	x1100
3	*Phormacantha hystrix* Jørgensen	$P_1$5582m	SEM	x1200
4	*Peridium spinipes* Haeckel	PB3769m	SEM	x660
5	*Peridium spinipes* Haeckel	PB3769m	LM	x210
6	*Peridium spinipes* Haeckel	PB3769m	SEM	x500
7	*Clathrocanium insectum* (Haeckel)	PB2869m	LM	x210
8	*Clathrocanium insectum* (Haeckel)	$P_1$4280m	SEM	x230
9	*Clathrocanium insectum* (Haeckel)	$P_1$5582m	SEM	x290
10	*Lithopilium recticulatum* Popofsky	$P_1$5582m	SEM	x190
11	*Clathrocanium coarctatum* Ehrenberg	$P_1$4280m	SEM	x440
12	*Clathrocanium coarctatum* Ehrenberg	$P_1$4280m	SEM	x440
13	*Clathrocanium coarctatum* Ehrenberg	$P_1$4280m	SEM	x390
14	*Callimitra emmae* Haeckel	$P_1$4280m	SEM	x165
15	*Callimitra annae* Haeckel	$P_1$4280m	SEM	x160
16	*Clathrocorys giltschii* Haeckel Note presence of a cephalic tubule.	PB1268m	SEM	x190

PLATE 26 Nassellaria

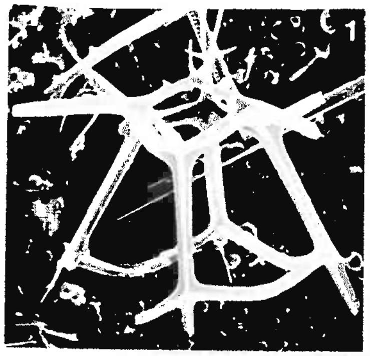
1

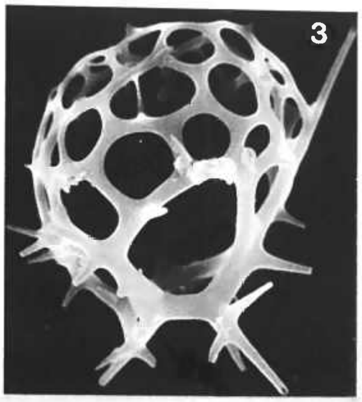
3

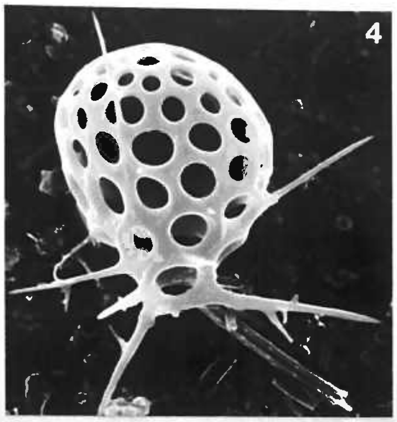
4


5

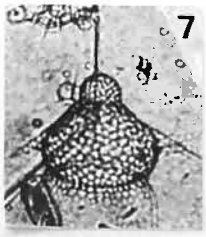
7

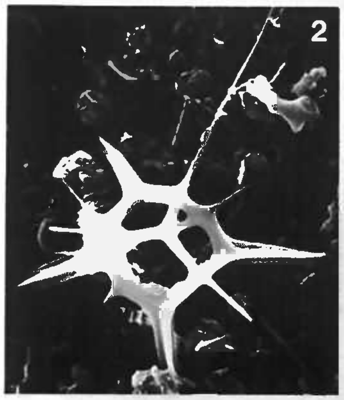
2


6

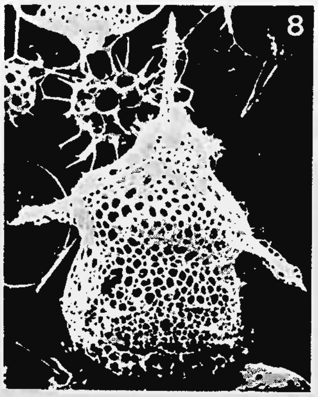
8

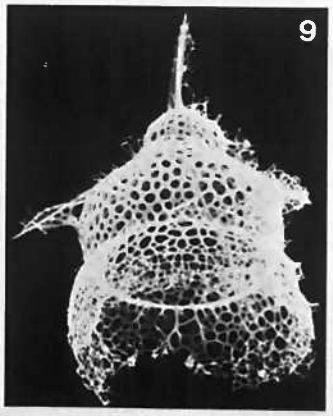
9

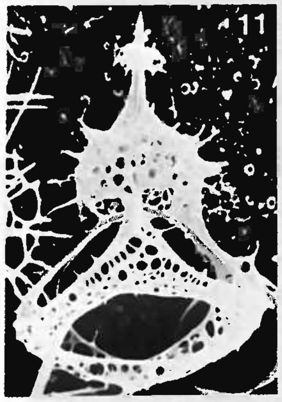
11

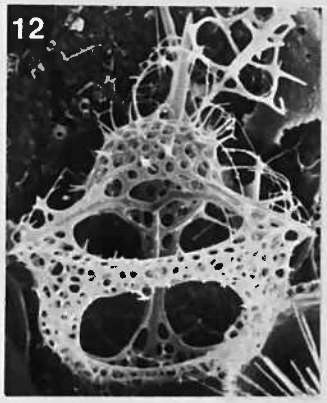
12


13

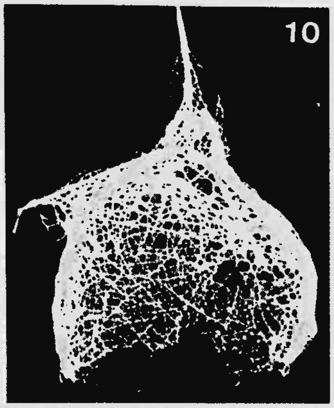
10

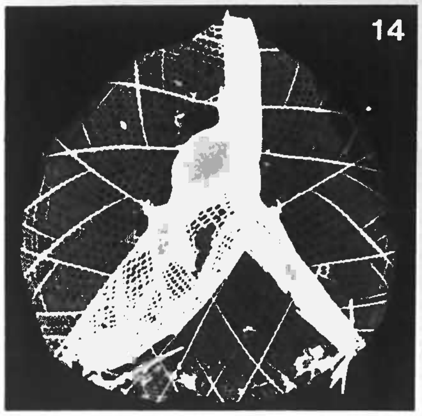
14

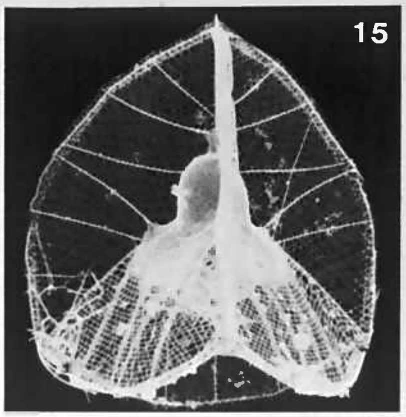
15

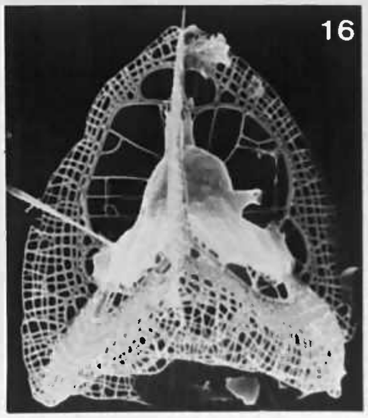
16

PLATE 27

Suborder: Nassellaria
Family: Plagiacanthidae; Subfamilies: Plagiacanthinae, Sethoperinae
Family: Acanthodesmiidae

Figure		Station Depth	Type of Micrograph	Magnification
1	*Clathrocorys giltschii* Haeckel	PB2869m	LM	x210
2	*Clathrocorys giltschii* Haeckel	PB1268m	SEM	x165
3	*Clathrocorys giltschii* Haeckel Same specimen; detail of the cephalis and cephalic tubule.	PB1268m	SEM	x390
4	*Clathrocorys murrayi* Haeckel	PB2869m	LM	x210
5	*Clathrocorys murrayi* Haeckel	PB3791m	LM	x210
6	*Clathrocorys murrayi* Haeckel	PB2869m	LM	x210
7	*Clathrocorys murrayi* Haeckel	$P_1$4280m	SEM	x250
8	*Clathrocorys murrayi* Haeckel	$P_1$2778m	SEM	x260
9	*Clathrocorys giltchii* Haeckel	PB3791m	LM	x210
10	*Callimitra solocicribrata* n.sp. Paratype	PB3791m	LM	x210
11	*Callimitra solocicribrata* n.sp. Holotype	PB3791m	LM	x210
12	*Neosematis distephanus* Popofsky	$P_1$4280m	SEM	x520
13	*Zygocircus productus* (Hertwig) group	$P_1$978m	SEM	x440
14	*Zygocircus productus* (Hertwig) group	PB2869m	LM	x210
15	*Tholospyris* sp. group	PB2869m	LM	x210
16	*Tholospyris* sp. group	PB2869m	LM	x210
17	*Tholospyris* sp. group	$P_1$978m	SEM	x440
18	*Zygocircus* sp. *piscicaudatus* Popofsky	$P_1$4280m	SEM	x560

PLATE 27 Nassellaria

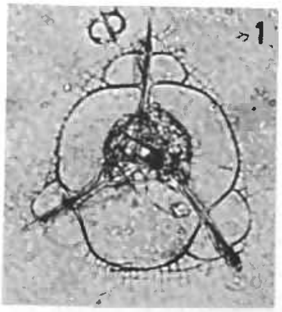
1

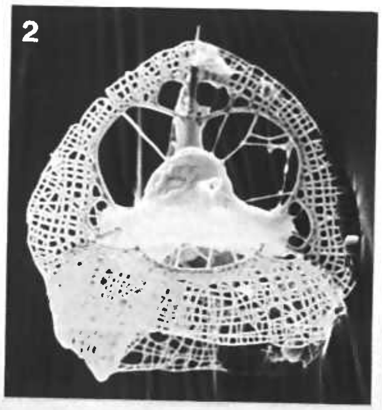
2

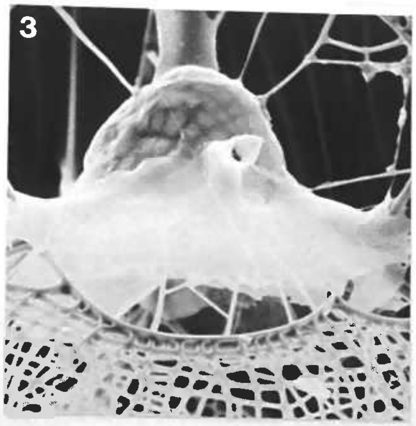
3

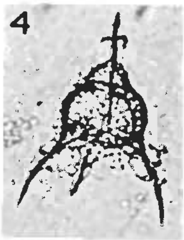
4

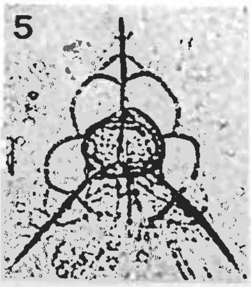
5


9

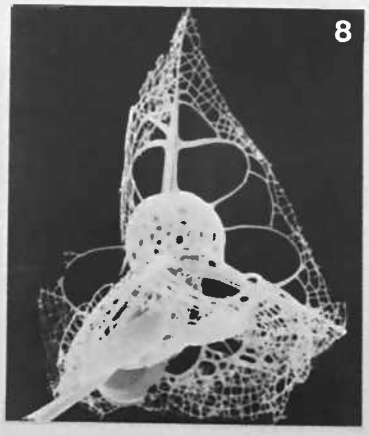
8

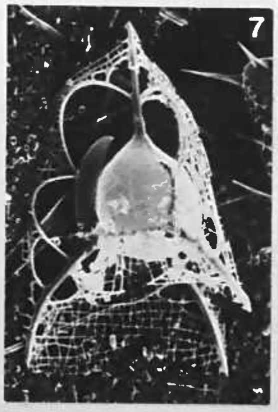
7

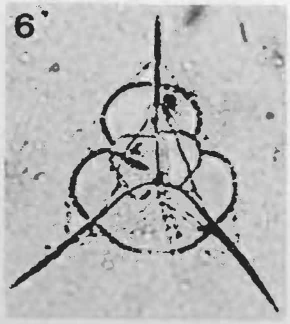
6

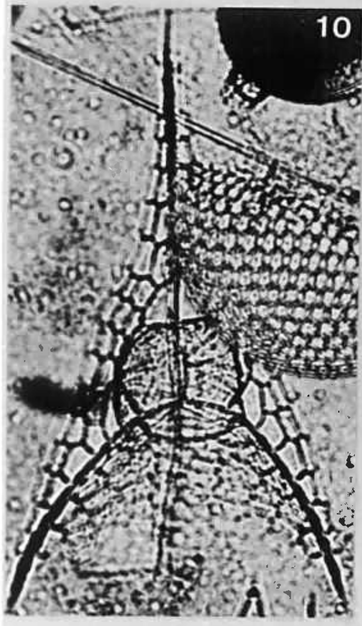
10

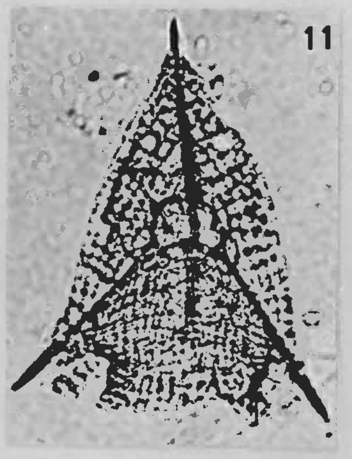
11


12


13

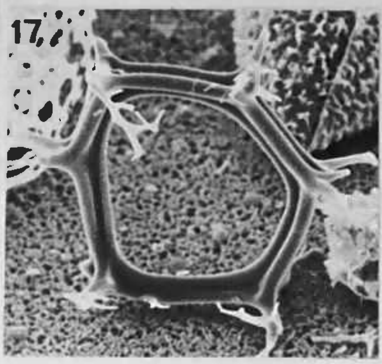
17

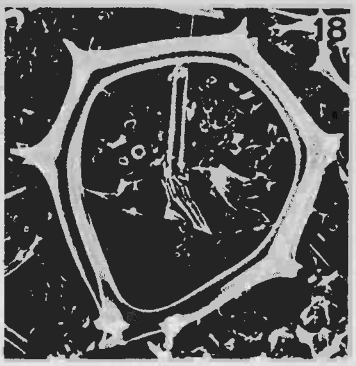
18

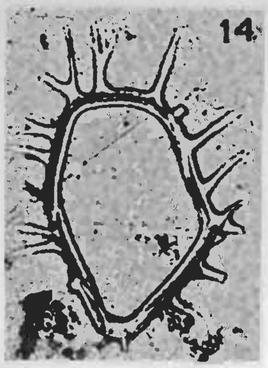
14

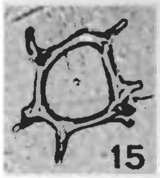
15


16

PLATE 28

Suborder: Nassellaria
Family: Acanthodesmiidae

Figure		Station Depth	Type of Micrograph	Magnification
1	*Lophospyris* juvenile form group	P$_1$4280m	SEM	x630
2	*Lophospyris* juvenile form group	P$_1$5582m	SEM	x400
3	*Lophospyris* juvenile form group	P$_1$4280m	SEM	x440
4	*Lophospyris* juvenile form group	P$_1$4280m	SEM	x330
5	*Lophospyris pentagona quadriforis* (Haeckel), emend. Goll	P$_1$4280m	SEM	x390
6	*Acanthodesmia vinculata* (Müller)	PB3791m	SEM	x180
7	*Acanthodesmia vinculata* (Müller)	P$_1$978m	SEM	x180
8	*Acanthodesmia vinculata* (Müller)	PB2869m	LM	x210
9	*Lophospyris pentagona pentagona* (Ehrenberg) emend. Goll	PB3791m	LM	x210
10	*Lophospyris pentagona pentagona* (Ehrenberg) emend. Goll	PB2869m	LM	x210
11	*Lophospyris pentagona pentagona* (Ehrenberg) emend. Goll	PB2869m	LM	x210
12	*Lophospyris pentagona pentagona* (Ehrenberg) emend. Goll	P$_1$4280m	SEM	x200
13	*Lophospyris pentagona pentagona* (Ehrenberg) emend. Goll	P$_1$2778m	SEM	x300
14	*Lophospyris pentagona pentagona* (Ehrenberg) emend. Goll	P$_1$5582m	SEM	x300

PLATE 28 Nassellaria

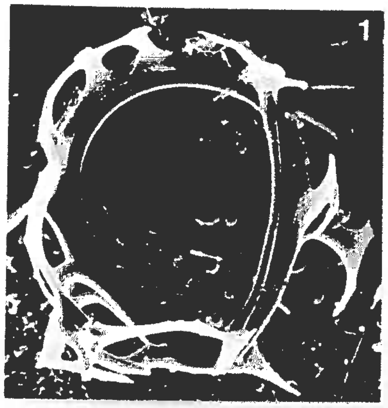
1


3


4

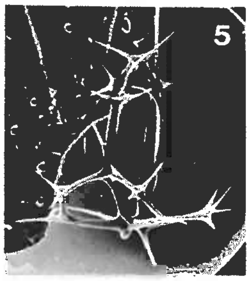
5

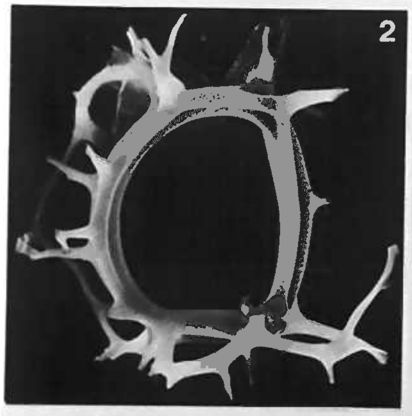
2

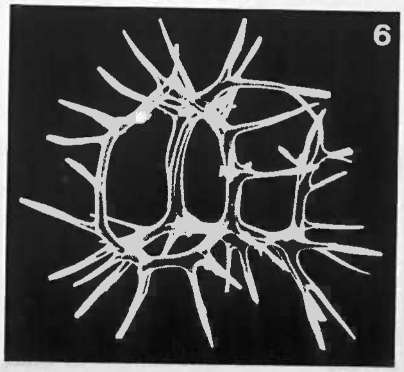
6

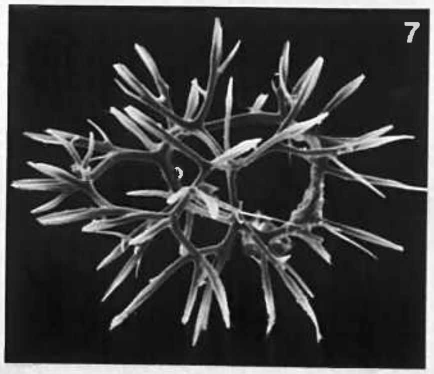
7

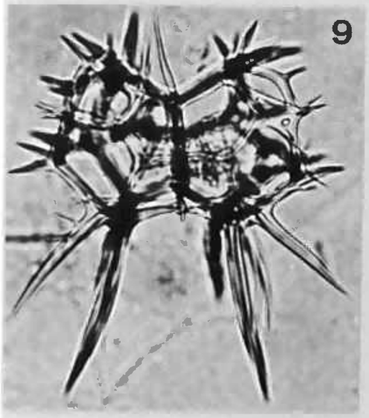
9

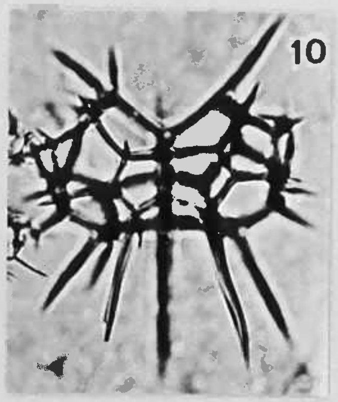
10


11

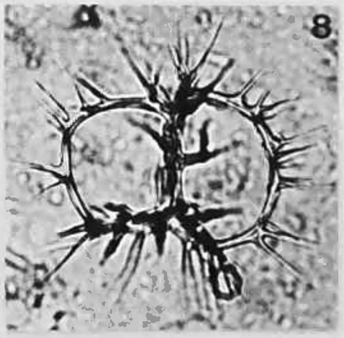
8

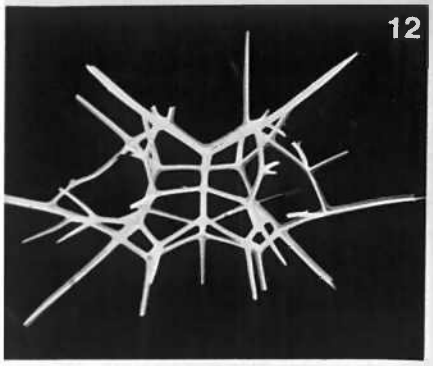
12

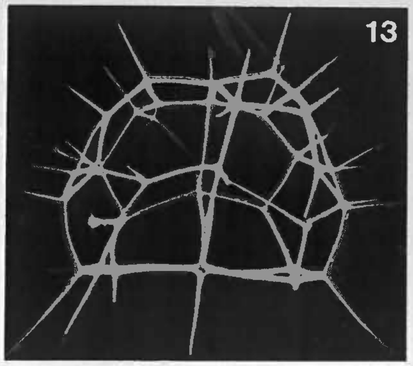
13

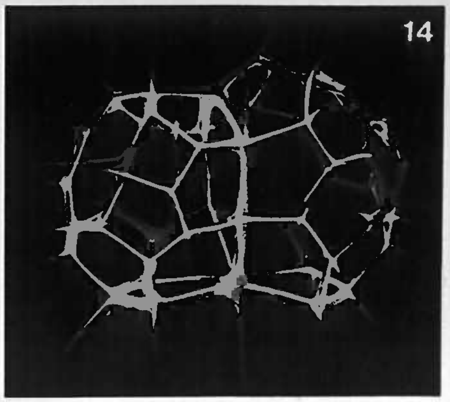
14

PLATE 29

Suborder: Nassellaria
Family: Acanthodesmiidae

Figure		Station Depth	Type of Micrograph	Magnification
1	*Lophospyris pentagona hyperborea* (Jørgensen) emend. Goll	$P_1$4280m	SEM	x360
2	*Lophospyris pentagona hyperborea* (Jørgensen) emend. Goll	$P_1$4280m	SEM	x360
3	*Lophospyris pentagona hyperborea* (Jørgensen) emend. Goll	PB2869m	LM	x210
4	*Lophospyris cheni* Goll	PB3791m	LM	x210
5	*Lophospyris pentagona hyperborea* (Jørgensen) emend. Goll	$P_1$978m	SEM	x210
6	*Lophospyris pentagona hyperborea* (Jørgensen) emend. Goll	$P_1$4280m	SEM	x470
7	*Lophospyris pentagona hyperborea* (Jørgensen) emend. Goll	PB3791m	LM	x210
8	*Lophospyris pentagona hyperborea* (Jørgensen) emend. Goll Apical view	PB2869m	LM	x210
9	*Lophospyris pentagona hyperborea* (Jørgensen) emend. Goll	$P_1$5582m	LM	x210
10	*Lophospyris pentagona hyperborea* (Jørgensen) emend. Goll	PB2869m	LM	x210
11	*Phormospyris stabilis scaphipes* (Haeckel)	$P_1$4280m	SEM	x500
12	*Phormospyris stabilis scaphipes* (Haeckel)	PB3791m	SEM	x720
13	*Phormospyris* sp. aff. *L. pentagona hyperborea*	$P_1$978m	SEM	x440
14	*Phormospyris stabilis scaphipes* (Haeckel)	$P_1$978m	SEM	x770
15	*Phormospyris stabilis capoi* Goll	PB3769m	LM	x210
16	*Phormospyris stabilis capoi* Goll	$P_1$4280m	SEM	x280
17	*Phormospyris stabilis capoi* Goll	$P_1$2778m	LM	x210
18	*Phormospyris stabilis capoi* Goll	$P_1$2778m	LM	x210

PLATE 29 Nassellaria

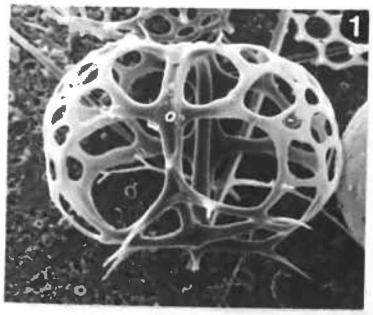
1

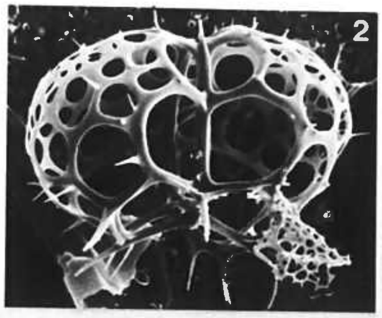
2

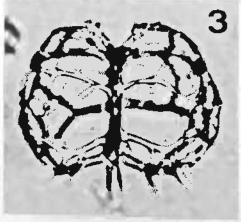
3

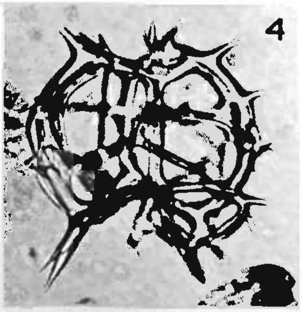
4

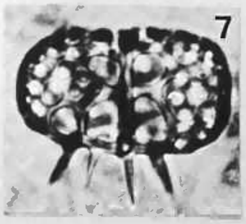
7

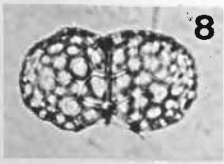
8

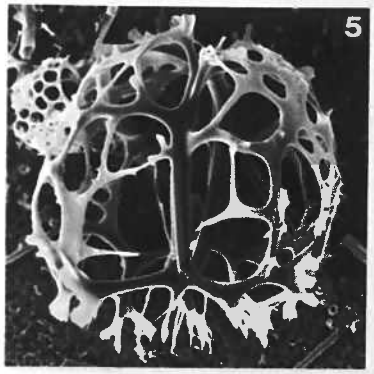
5

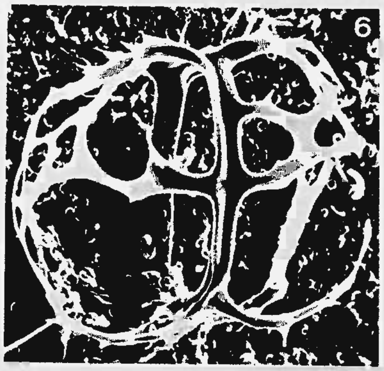
6


9

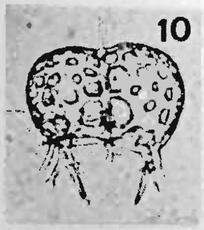
10


11

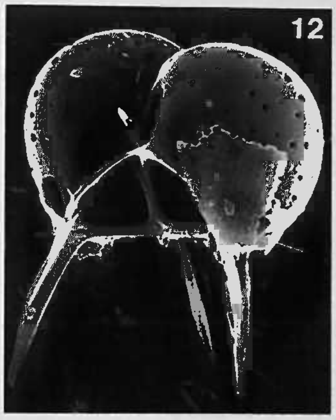
12


13

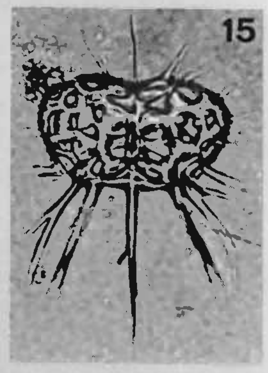
15

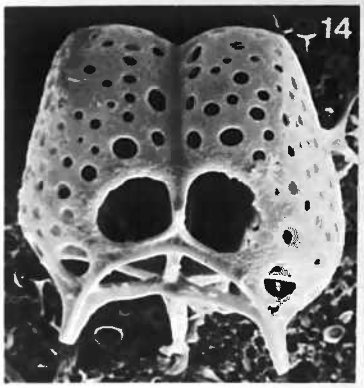
14

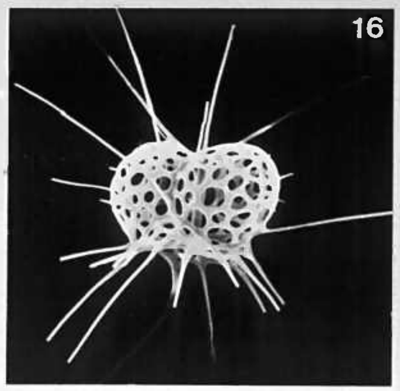
16

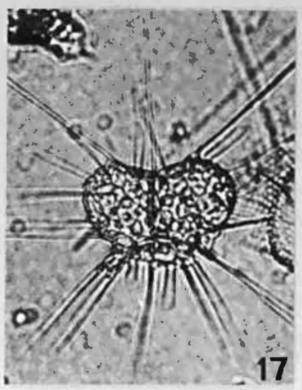
17

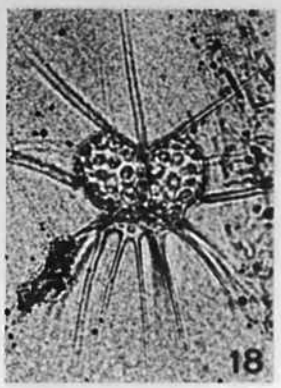
18

PLATE 30

Suborder: Nassellaria
Family: Acanthodesmiidae

Figure		Station Depth	Type of Micrograph	Magnification
1	*Dictyospyris* sp. group	PB3791m	LM	x210
2	*Phormospyris stabilis stabilis* (Goll)	$P_1$2778m	LM	x210
3	*Phormospyris stabilis stabilis* (Goll)	PB2869m	LM	x210
4	*Phormospyris stabilis stabilis* (Goll)	$P_1$2778m	LM	x210
5	*Phormospyris stabilis stabilis* (Goll)	$P_1$4280m	SEM	x390
6	*Phormospyris* ? sp.	PB3769m	LM	x210
7	*Nephrospyris renilla renilla* Haeckel	PB3769m	LM	x106
8	*Nephrospyris renilla renilla* Haeckel	PB3769m	SEM	x80
9	*Nephrospyris renilla renilla* Haeckel A specimen with only a central part.	$P_1$4280m	LM	x210
10	*Nephrospyris renilla lana* Goll	PB3791m	RLM	x80
11	*Liriospyris* sp.	PB3769m	SEM	x140
12	*Androspyris reticulidisca* n.sp. Holotype	PB3791m	LM	x160
13	*Androspyris reticulidisca* n.sp. Paratype	PB667m	SEM	x110
14	*Androspyris retidisca* n.sp.	PB3791m	RLM	x80
15	*Androspyris huxleyi* (Haeckel)	PB3791m	RLM	x80
16	*Androspyris huxleyi* (Haeckel)	PB667m	LM	x157

PLATE 30 Nassellaria

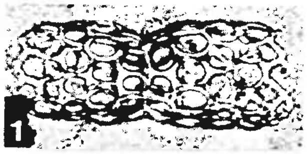
1

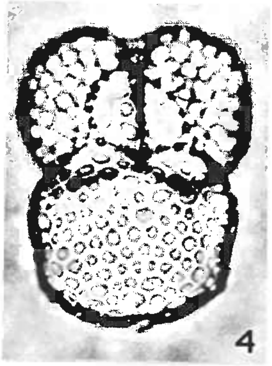
4

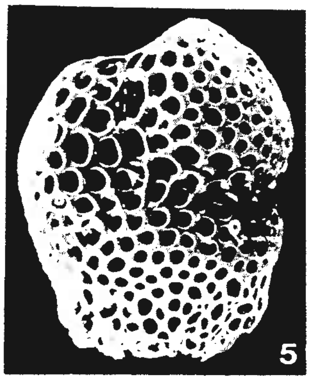
5

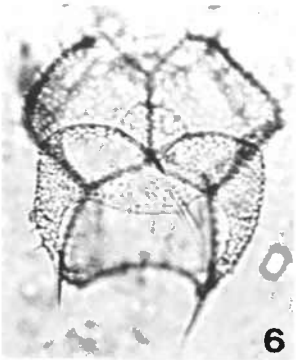
6

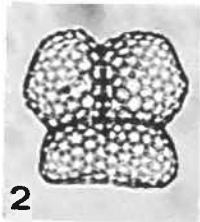
2


3

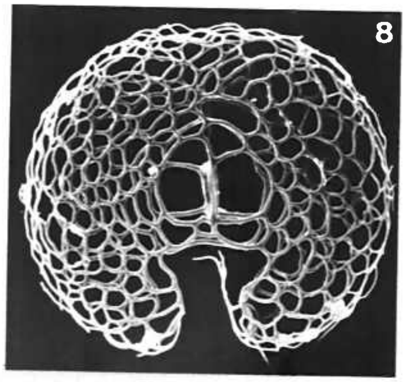
8

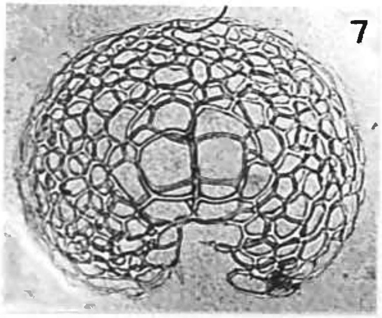
7

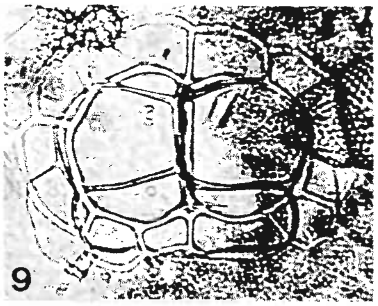
9

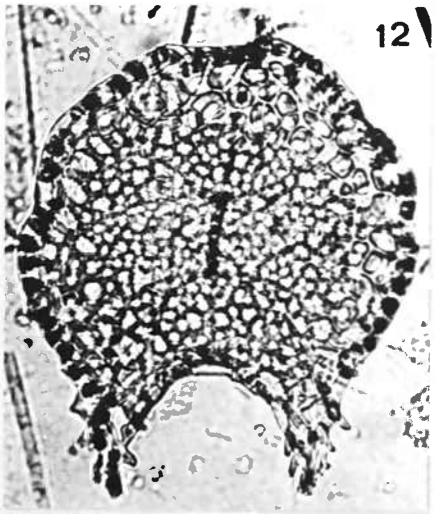
12

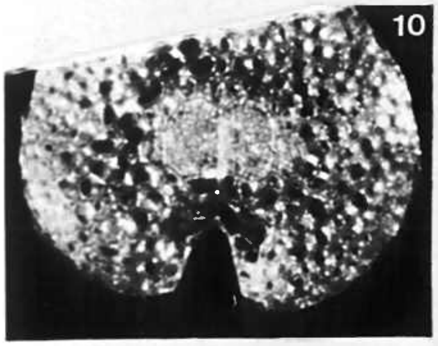
10

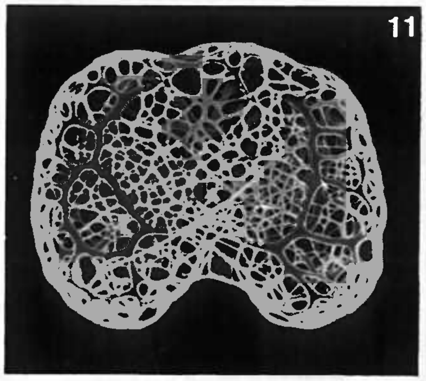
11

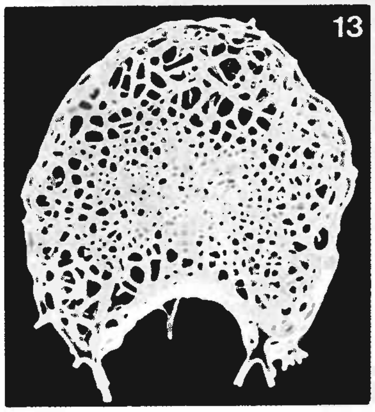
13


14


15

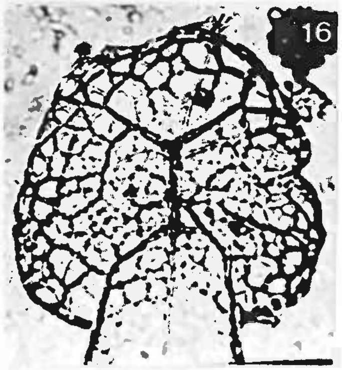
16

PLATE 31

Suborder: Nassellaria
Family: Acanthodesmiidae

Figure		Station Depth	Type of Micrograph	Magnification
1	Androspyris ramosa (Haeckel)	$P_1$4280m	SEM	x220
2	Androspyris ramosa (Haeckel)	$P_1$4280m	SEM	x250
3	Cephalospyris cancellata Haeckel	PB3791m	LM	x170
4	Cephalospyris cancellata Haeckel	PB2869m	LM	x210
5	Cantharospyris platybursa Haeckel	PB2869m	LM	x210
6	Tholospyris baconiana baconiana Goll	PB2869m	LM	x210
7	Tholospyris baconiana baconiana Goll	PB3769m	LM	x210
8	Tholospyris baconiana variabilis Goll	E389m	LM	x210
9	Tholospyris macropora (Popofsky)	E389m	LM	x210
10	Liriospyris thorax (Haeckel) laticapsa, n. subsp. Paratype	PB1268m	LM	x210
11	Liriospyris thorax (Haeckel) laticapsa, n. subsp. Holotype	PB3791m	LM	x210
12	Liriospryis thorax thorax	PB1268m	SEM	x250
13	Liriospryis thorax (Haeckel) laticapsa, n. subsp.	PB667m	SEM	x130
14	Liriospyris reticulata (Ehrenberg)	$P_1$4280m	SEM	x250
15	Liriospyris reticulata (Ehrenberg)	$P_1$4280m	SEM	x350
16	Liriospyris reticulata (Ehrenberg)	$P_1$4280m	SEM	x250

PLATE 31 Nassellaria

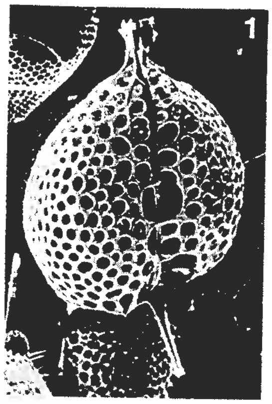

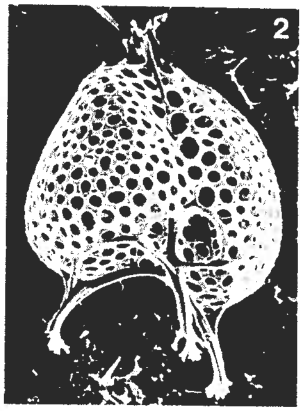

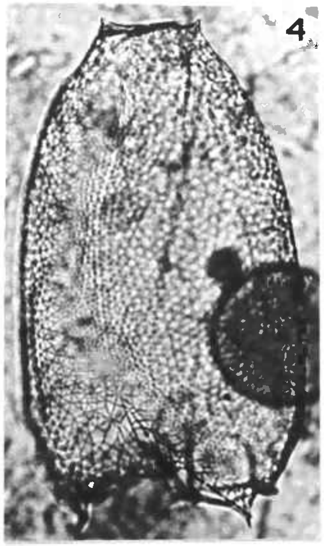

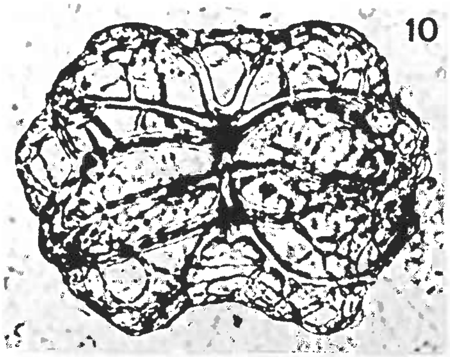

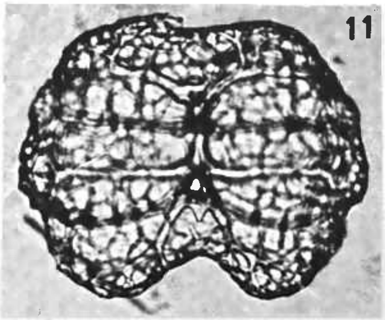

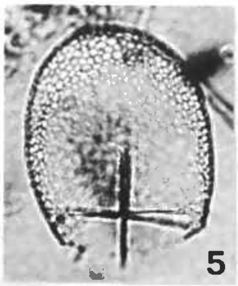

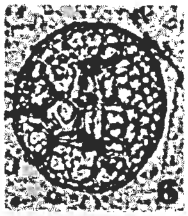

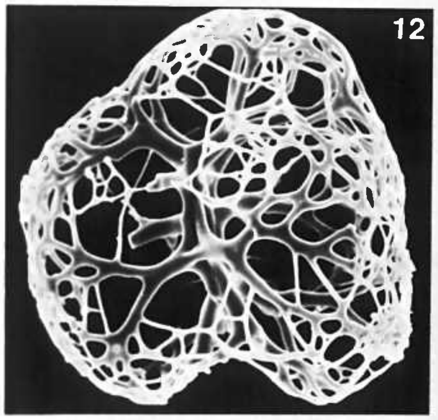

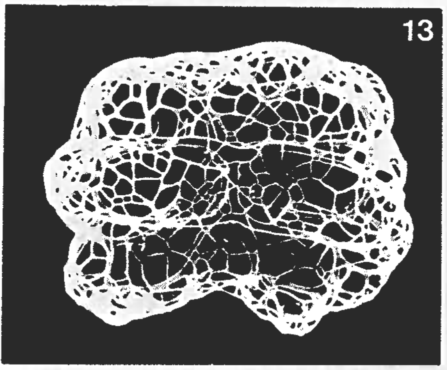

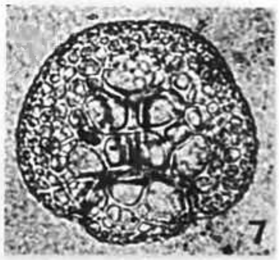

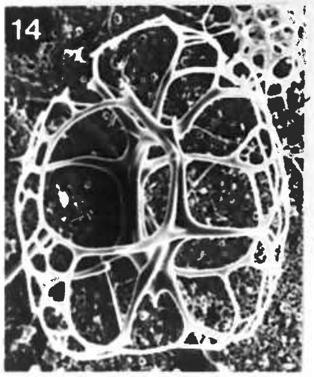

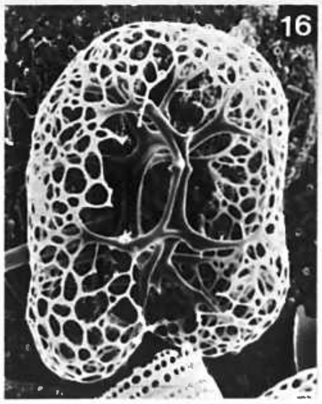

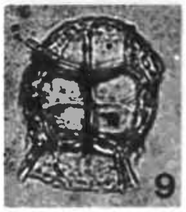

PLATE 32

Suborder: Nassellaria
Family: Sethophormididae

Figure		Station Depth	Type of Micrograph	Magnification
1	*Tetraphormis rotula* (Haeckel)	$P_1$4280m	SEM	x180
2	*Tetraphormis rotula* (Haeckel)	$P_1$5582m	LM	x210
3	*Tetraphormis rotula* (Haeckel)	$P_1$5582m	LM	x210
4	*Lampromitra schultzei* (Haeckel)	$P_1$4280m	SEM	x180
5	*Lampromitra schultzei* (Haeckel)	PB3791m	LM	x210
6	*Dictyophimus butschlii* Haeckel	$P_1$2778m	LM	x210
7	*Tetraphormis dodecaster* (Haeckel)	PB3791m	SEM	x340
8	*Lampromitra cracenta* n.sp.	PB3791m	LM	x210
9	*Theophormis callipilium* Haeckel Oblique basal view	$P_1$4280m	SEM	x100
10	*Theophormis callipilium* Haeckel Apical view	$P_1$5582m	SEM	x120
11	*Theophormis callipilium* Haeckel Basal view	PB3791m	LM	x153
12	*Theophormis callipilium* Haeckel Apical view	$P_1$5582m	LM	x210

PLATE 32 Nassellaria

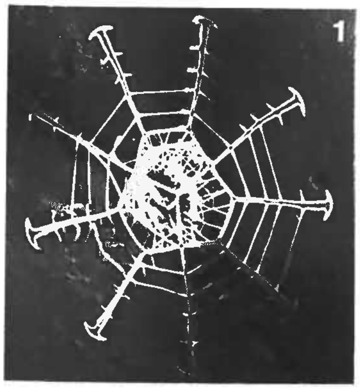
1

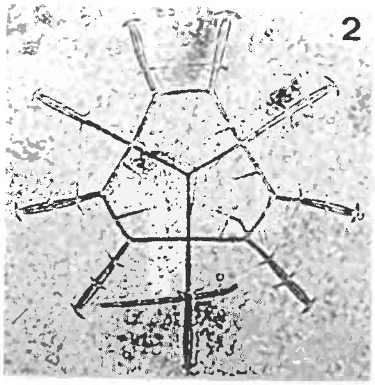
2

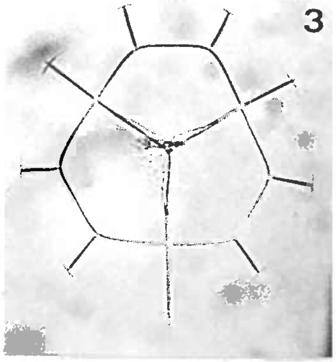
3

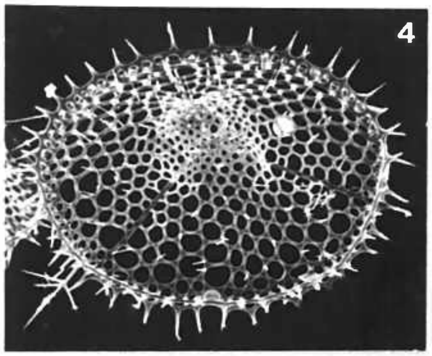
4

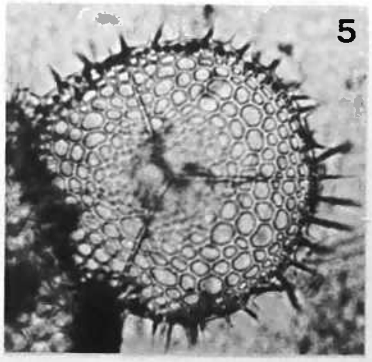
5

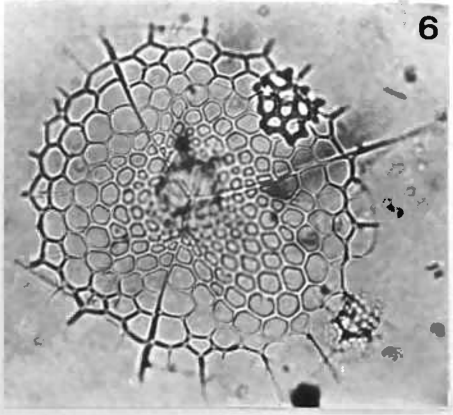
6

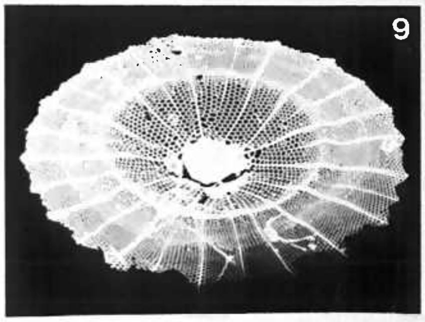
9

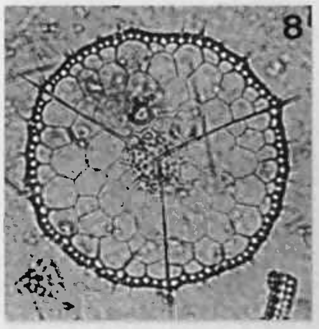
8


7

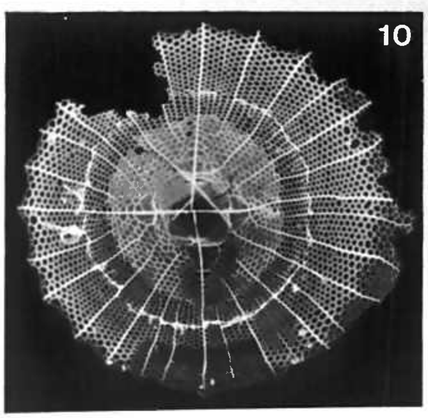
10

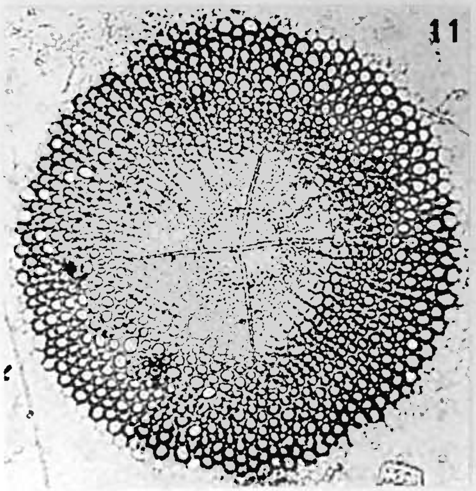
11

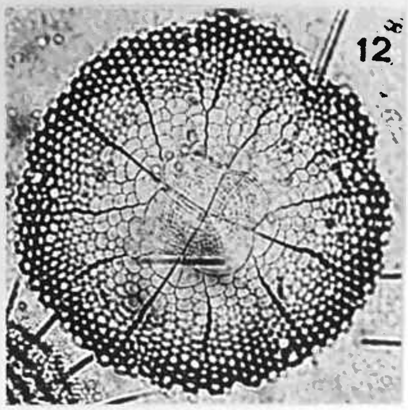
12

PLATE 33

Suborder: Nassellaria
Family: Sethophormididae

Figure		Station Depth	Type of Micrograph	Magnification
1	*Eucecryphalus* sp.	PB1268m	LM	x210
2	*Lampromitra cachoni* Petrushevskaya	PB2869m	LM	x210
3	*Lampromitra cachoni* Petrushevskaya	PB3791m	LM	x210
4	*Eucecryphalus tricostatus* Haeckel	PB2869m	LM	x210
5	*Eucecryphalus sestrodiscus* (Haeckel)	PB3791m	LM	x210
6	*Eucecryphalus tricostatus* Haeckel Oblique apical view	PB1268m	SEM	x200
7	*Eucecryphalus sestrodiscus* (Haeckel)	$P_1$2778m	SEM	x220
8	*Eucecryphalus sestrodiscus* (Haeckel)	$P_1$4280m	SEM	x340
9	*Corocalyptra cervus* (Ehrenberg)	PB3791m	LM	x210
10	*Corocalyptra cervus* (Ehrenberg)	PB2869m	SEM	x280
11	*Corocalyptra cervus* (Ehrenberg)	$P_1$4280m	SEM	x250
12	*Corocalyptra cervus* (Ehrenberg)	$P_1$2778m	SEM	x220
13	*Eucecryphalus gegenbauri* Haeckel	$P_1$978m	LM	x210
14	*Eucecryphalus gegenbauri* Haeckel	$P_1$978m	LM	x210
15	*Eucecryphalus gegenbauri* Haeckel	PB3791m	SEM	x450

PLATE 33 Nassellaria

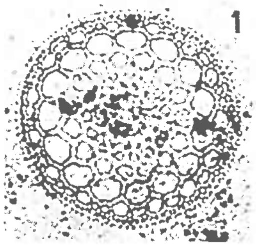

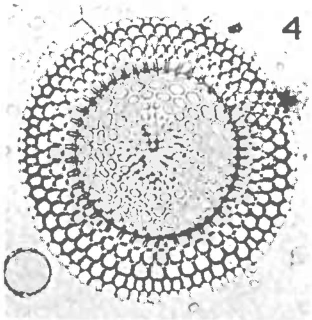

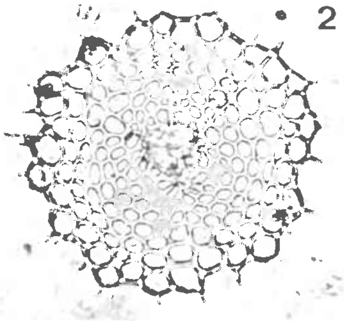

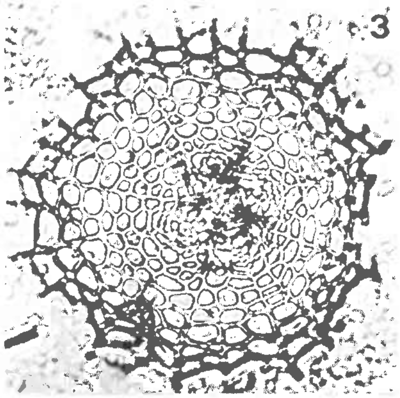

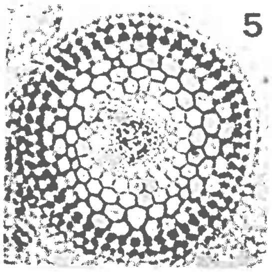

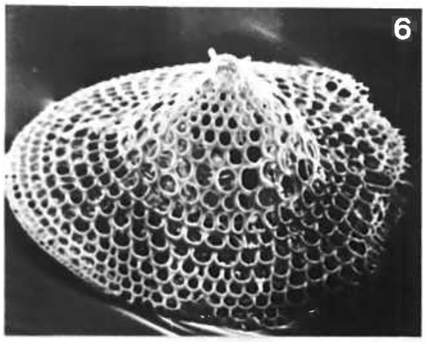

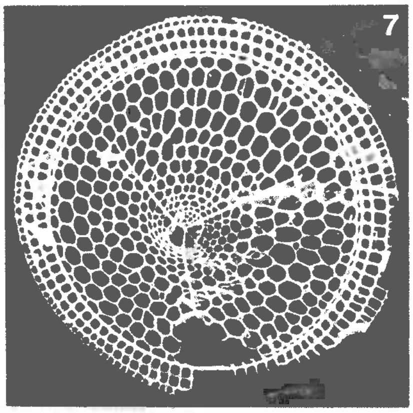

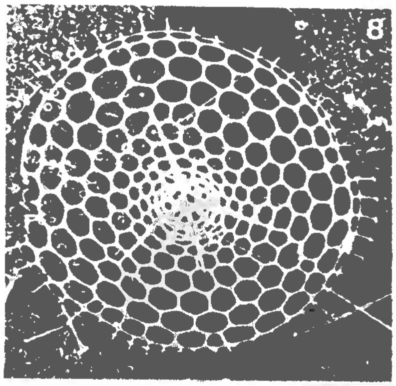

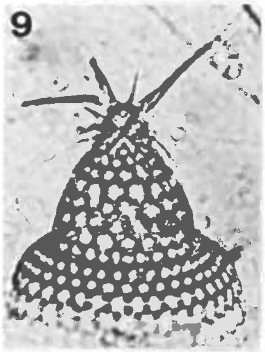

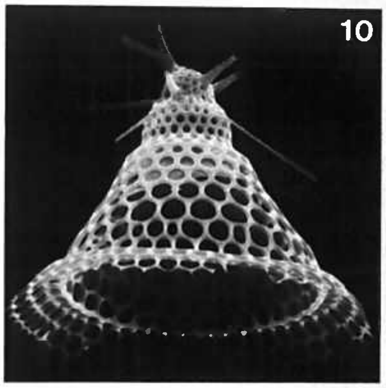

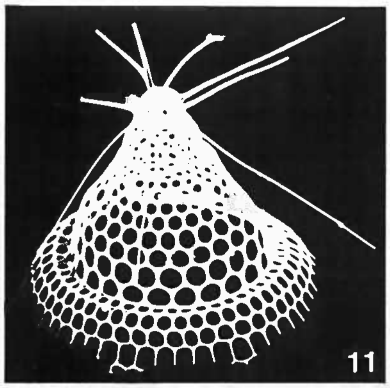

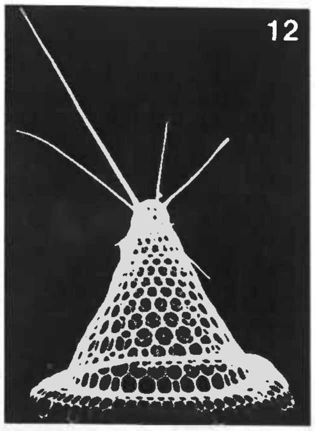

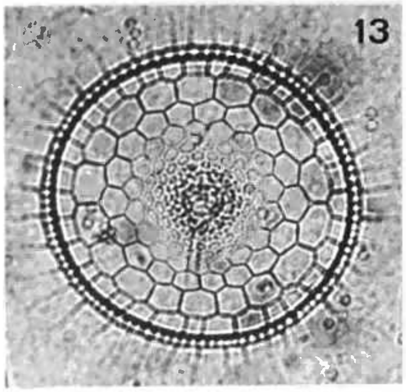

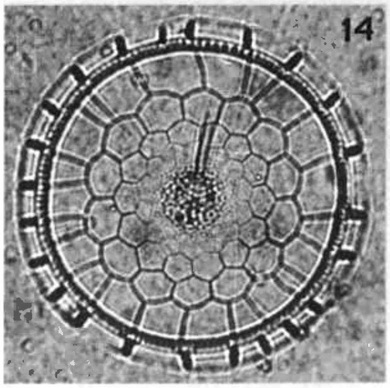

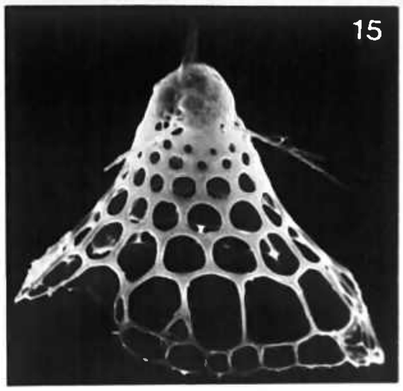

PLATE 34

Suborder: Nassellaria
Family: Sethophormididae

Figure		Station Depth	Type of Micrograph	Magnification
1	*Lampromitra spinosiretis* n.sp. Holotype	PB3791m	SEM	x165
2	*Lampromitra spinosiretis* n.sp. Paratype	PB3791m	LM	x210
3	*Phrenocodon clathrostomium* Haeckel	$P_1$4280m	LM	x210
4	*Phrenocodon clathrostomium* Haeckel	PB3769m	LM	x210
5	*Eucecryphalus europae* (Haeckel)	PB3791m	LM	x210
6	*Eucecryphalus europae* (Haeckel)	$P_1$5582m	LM	x210
7	*Lampromitra spinosiretis* n.sp.	PB2869m	LM	x210
8	*Clathrocyclas* sp.	$P_1$4280m	SEM	x280
9	*Clathrocyclas monumentum* (Haeckel)	$P_1$2778m	LM	x210
10	*Clathrocyclas monumentum* (Haeckel)	$P_1$4280m	LM	x210
11	*Clathrocyclas monumentum* (Haeckel)	$P_1$2778m	LM	x210
12	*Clathrocyclas cassiopejae* Haeckel Lateral view	$P_1$4280m	SEM	x150
13	*Clathrocyclas cassiopejae* Haeckel Apical view	$P_1$5582m	SEM	x220
14	*Clathrocyclas cassiopejae* Haeckel Oblique apical view	$P_1$5582m	SEM	x220

PLATE 34 Nassellaria

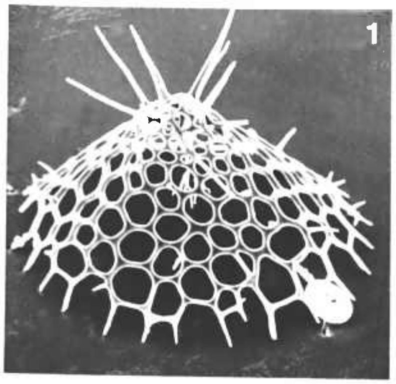
1

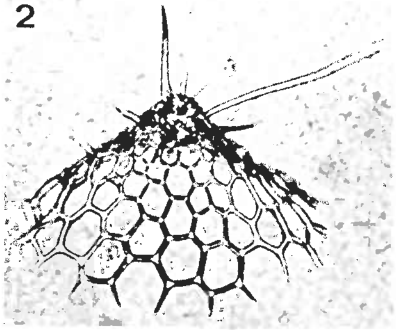
2

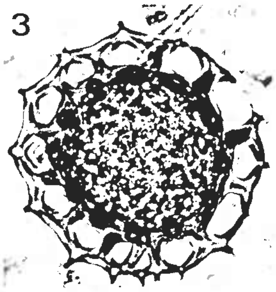
3

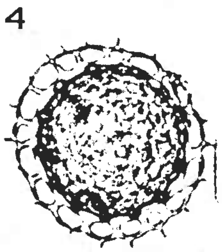
4

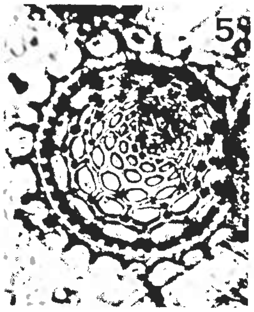
5

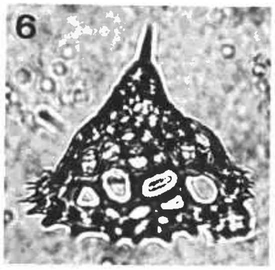
6


7

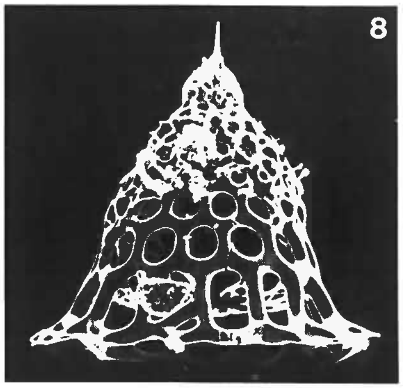
8

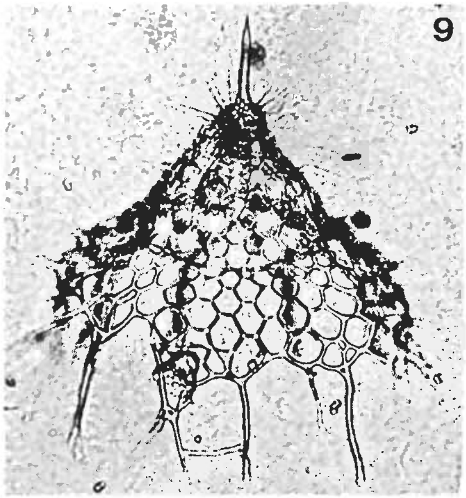
9


10

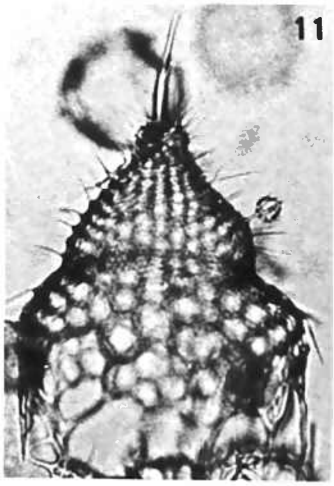
11

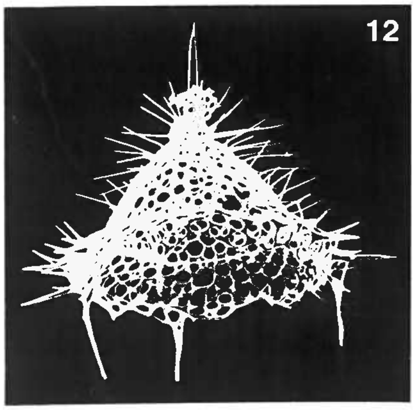
12

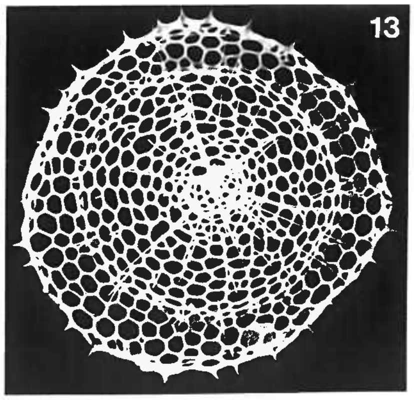
13

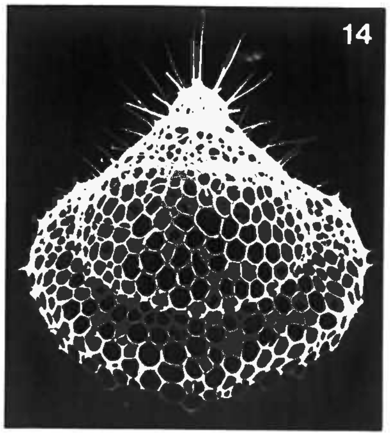
14

PLATE 35

Suborder: Nassellaria
Family: Sethophormididae
Family: Theoperidae; Subfamily: Plectopyramididae

Figure		Station Depth	Type of Micrograph	Magnification
1	*Eucecryphalus clinatus* n.sp. Holotype	PB2869m	LM	x210
2	*Eucecryphalus clinatus* n.sp. Paratype	PB2869m	LM	x210
3	*Cornutella profunda* Ehrenberg	E988m	LM	x210
4	*Cornutella profunda* Ehrenberg A specimen with a long thick apical horn	$P_1$4280m	LM	x210
5	*Cornutella profunda* Ehrenberg	PB3769m	SEM	x280
6	*Cornutella profunda* Ehrenberg Detail of shell surface	PB3769m	SEM	x2040
7	*Cornutella profunda* Ehrenberg Same specimen	PB3769m	SEM	x330
8	*Cornutella profunda* Ehrenberg	$P_1$2778m	LM	x210
9	*Cornutella profunda* Ehrenberg A specimen with thick skeleton	$P_1$978m	LM	x210
10	*Peripyramis circumtexa* Haeckel A specimen with long ribs	$P_1$2778m	SEM	x80
11	*Peripyramis circumtexa* Haeckel	E988m	LM	x210
12	*Peripyramis circumtexa* Haeckel Apical view	E5068m	LM	x210
13	*Peripyramis circumtexa* Haeckel	$P_1$5582m	SEM	x180
14	*Litharachnium tentorium* Haeckel	PB2869m	LM	x210
15	*Litharachnium tentorium* Haeckel Apical view	PB3791m	LM	x210
16	*Litharachnium tentorium* Haeckel Apical view	PB3769m	SEM	x83
17	*Litharachnium tentorium* Haeckel Oblique view	$P_1$5582m	SEM	x150
18	*Litharachnium tentorium* Haeckel Lateral view	$P_1$2778m	LM	x210

PLATE 35 Nassellaria

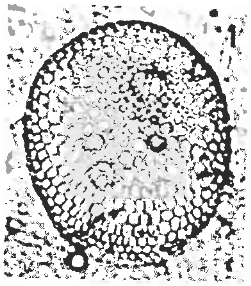
1

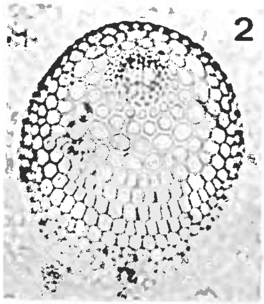
2

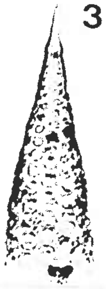
3

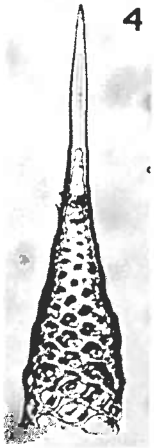
4

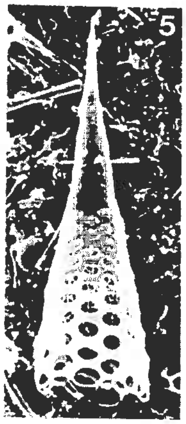
5

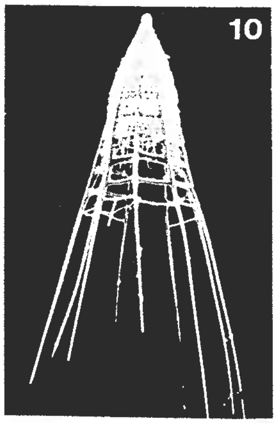
10

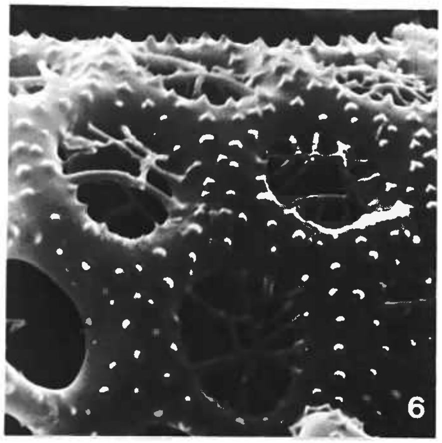
6


7


8

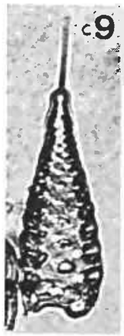
9

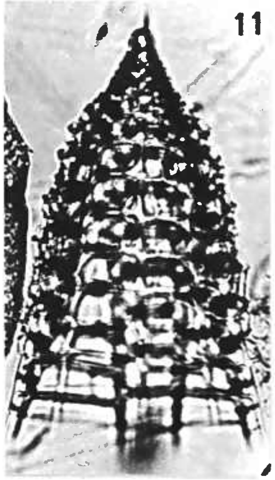
11

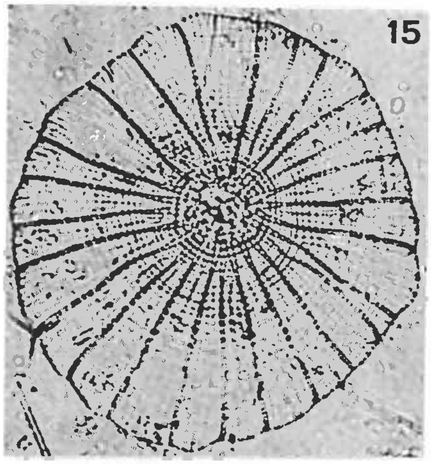
15

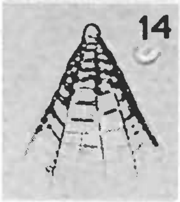
14

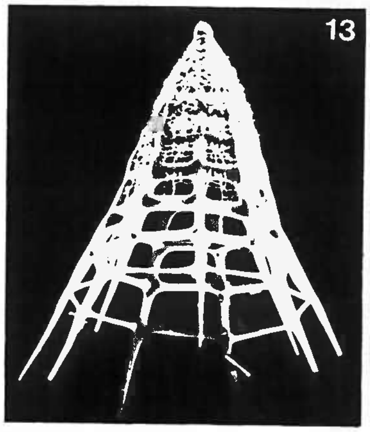
13

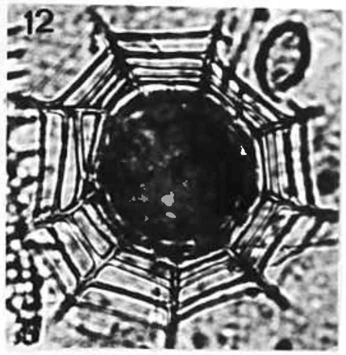
12

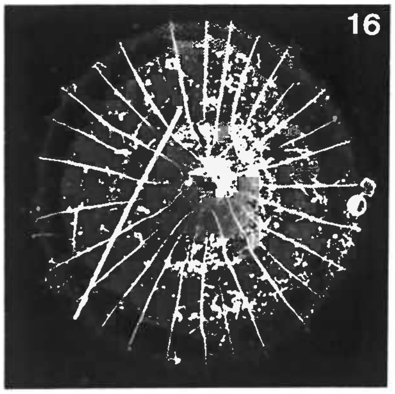
16

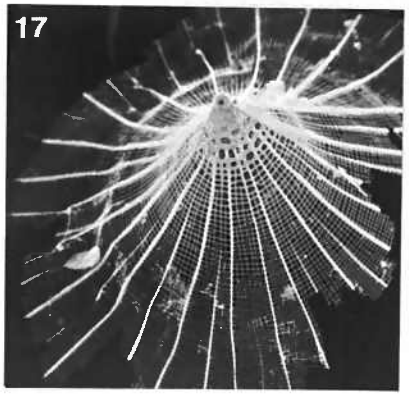
17

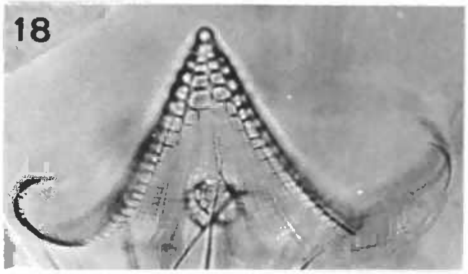
18

PLATE 36

Suborder: Nassellaria
Family: Theoperidae; Subfamilies: Plectopyramidinae, Eucyrtidiinae

Figure		Station Depth	Type of Micrograph	Magnification
1	*Litharachnium eupilium* (Haeckel) Apical view	PB3769m	LM	x210
2	*Litharachnium eupilium* (Haeckel) Apical view	PB3769m	LM	x210
3	*Litharachnium eupilium* (Haeckel) Lateral view	PB1268m	SEM	x220
4	*Litharachnium eupilium* (Haeckel) Oblique lateral view	PB3791m	LM	x210
5	*Archipilium* sp. aff. *A.* *orthopterum* Haeckel	$P_1$4280m	SEM	x370
6	*Archipilium macropus* ? (Haeckel)	PB3769m	LM	x210
7	*Archipilium* sp. aff. *A.* *orthopterum* Haeckel	$P_1$4280m	SEM	x430
8	*Pteroscenium pinnatum* Haeckel	PB667m	LM	x210
9	*Pteroscenium pinnatum* Haeckel	PB3791m	SEM	x140
10	*Pterocanium trilobum* (Haeckel)	$P_1$4280m	SEM	x230
11	*Pterocanium trilobum* (Haeckel)	$P_1$5582m	SEM	x130
12	*Pterocanium granidporus* Nigrini	PB3791m	LM	x210
13	*Pterocanium granidporus* Nigrini	PB3791m	LM	x210
14	*Pterocanium praetextum* (Ehrenberg) *eucolpum* Haeckel	PB1268m	SEM	x154
15	*Pterocanium praetextum praetextum* (Ehrenberg)	E389m	LM	x210
16	*Pterocanium praetextum praetextum* (Ehrenberg)	$P_1$5582m	LM	x210
17	*Pterocanium praetextum praetextum* (Ehrenberg)	$P_1$5582m	LM	x210
18	*Pterocanium praetextum praetextum* (Ehrenberg)	$P_1$5582m	SEM	x220

PLATE 36 Nassellaria

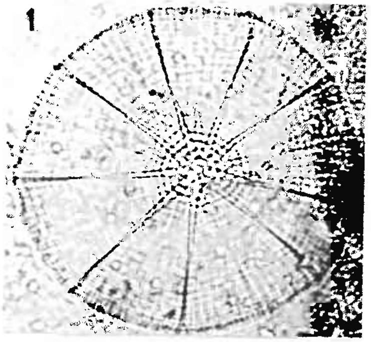
1

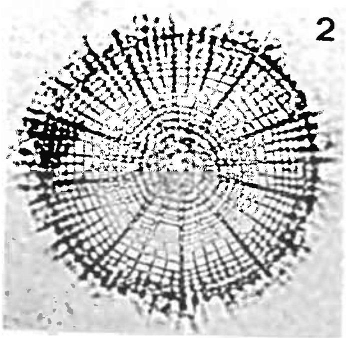
2

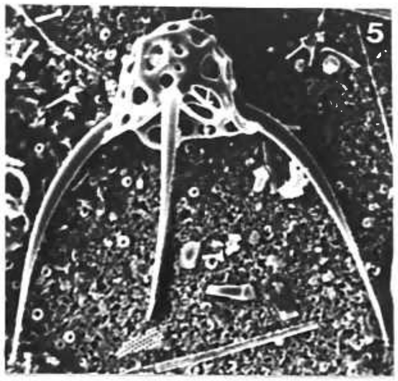
5

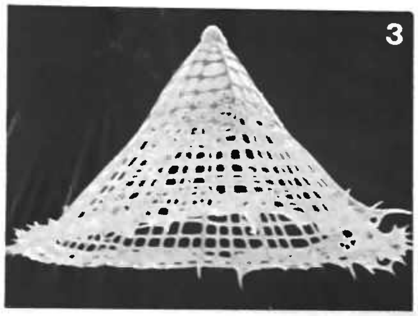
3

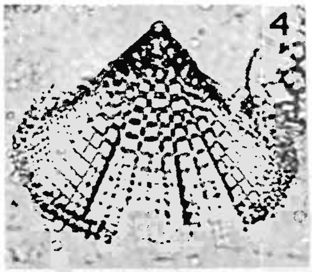
4

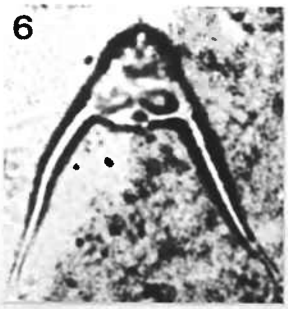
6


7

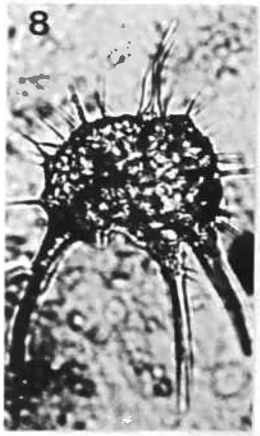
8

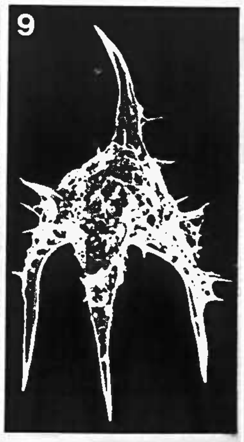
9

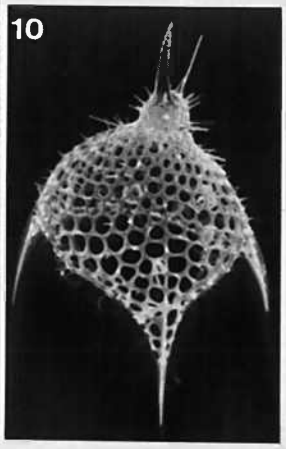
10

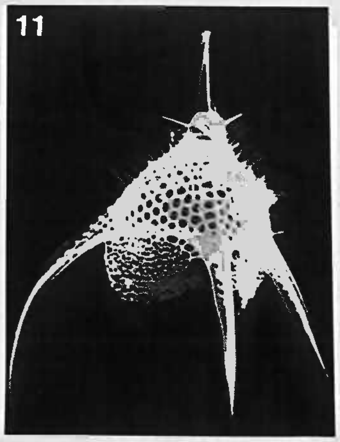
11

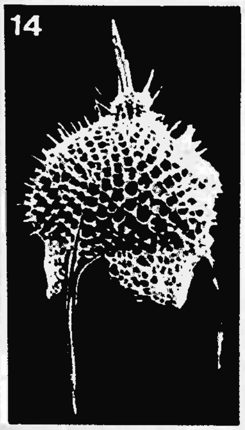
14

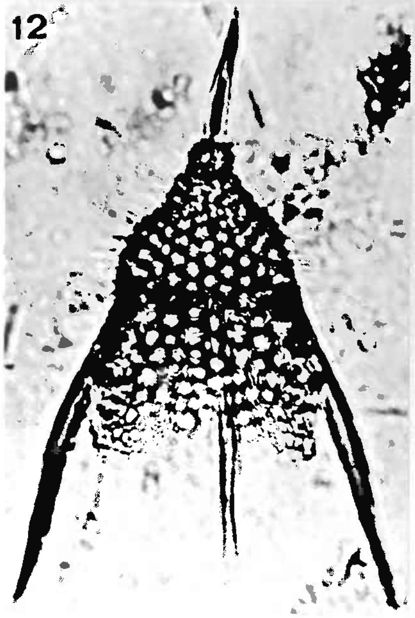
12

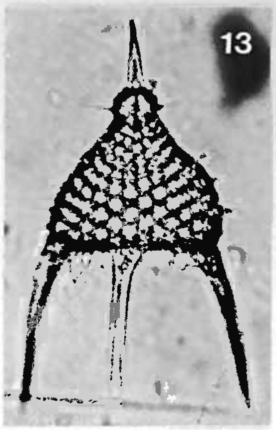
13

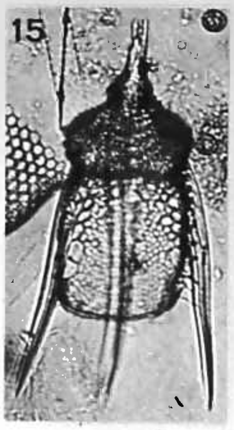
15


16


17

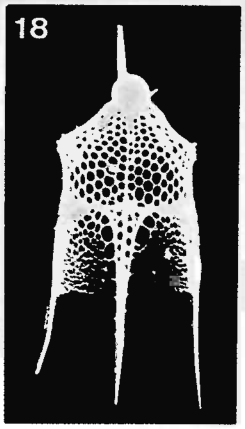
18

PLATE 37

Suborder: Nassellaria
Family: Theoperidae; Subfamily: Eucyrtidinae

Figure		Station Depth	Type of Micrograph	Magnification
1	*Dictyophimus* sp. A	PB667m	SEM	x120
2	*Dictyophimus crisiae* Ehrenberg	$P_1$4280m	SEM	x130
3	*Dictyophimus infabricatus* Nigrini	$P_1$978m	SEM	x230
4	*Dictyophimus infabricatus* Nigrini	PB3791m	LM	x210
5	*Dictyophimus infabricatus* Nigrini	PB2869m	SEM	x220
6	*Dictyocodon elegans* (Haeckel)	PB3769m	LM	x210
7	*Dictyocodon elegans* (Haeckel)	$P_1$5582m	SEM	x154
8	*Dictyocodon palladius* Haeckel One spine on the cephalis broken off	$P_1$2778m	SEM	x180
9	*Dictyocodon elegans* (Haeckel)	$P_1$5582m	SEM	x100
10	*Dictyocodon palladius* Haeckel	$P_1$4280m	SEM	x130
11	*Dictyocodon palladius* Haeckel	PB2869m	SEM	x105
12	*Pseudodictyophimus gracilipes* (Bailey)	PB3769m	SEM	x610
13	*Pseudodictyophimus gracilipes* (Bailey)	$P_1$4280m	SEM	x350
14	*Pseudodictyophimus gracilipes* (Bailey)	PB3769m	LM	x210

PLATE 37 Nassellaria

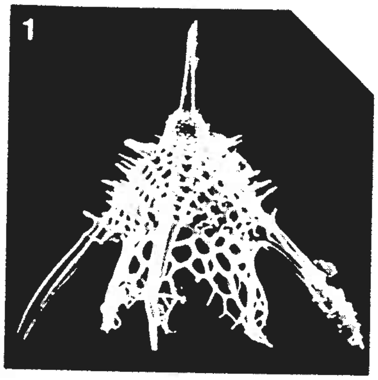
1

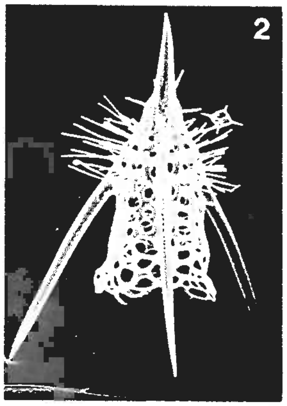
2

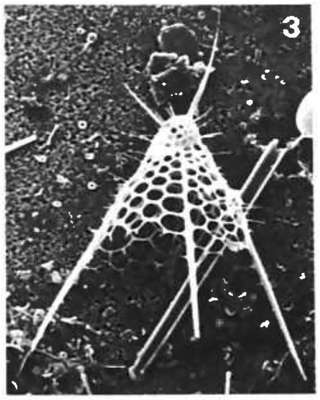
3

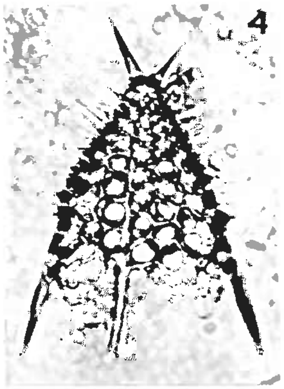
4

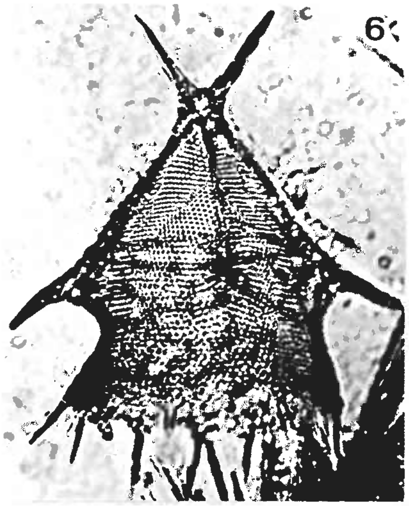
6

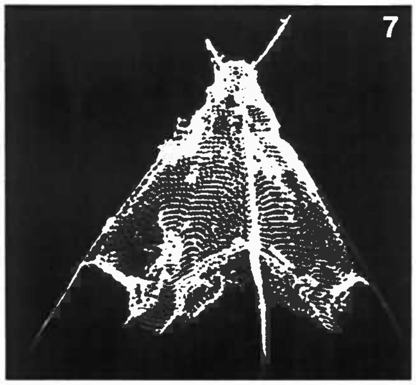
7

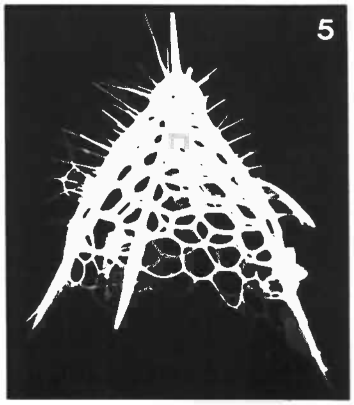
5

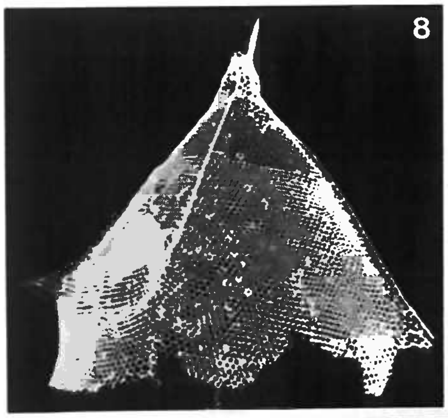
8

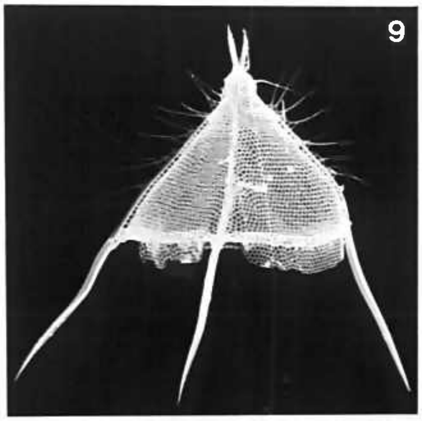
9

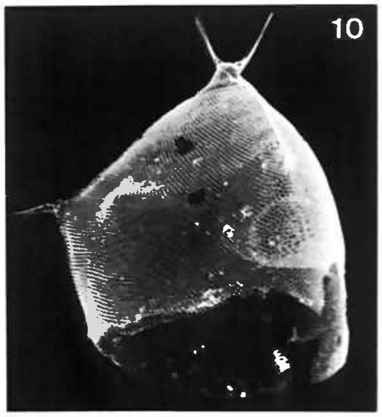
10

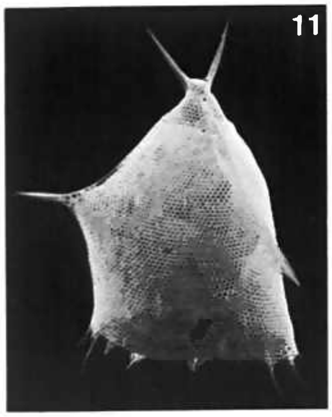
11

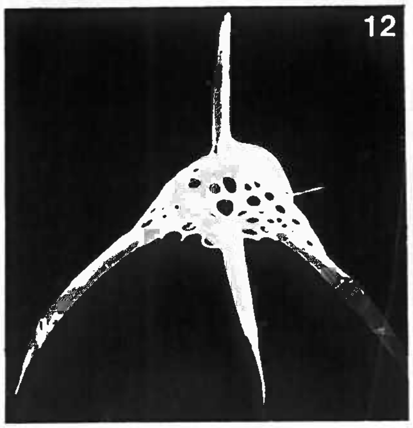
12

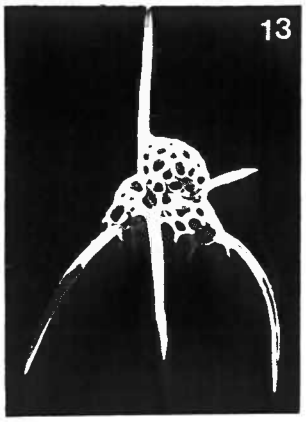
13

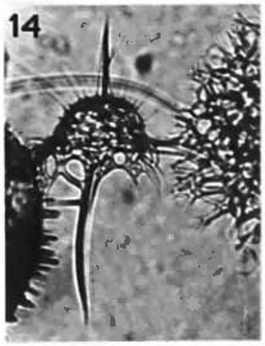
14

PLATE 38

Suborder: Nassellaria
Family: Theoperidae; Submfaily: Eucrytidinae
Families: Pterocorythidae, Artostrobiidae

Figure		Station Depth	Type of Micrograph	Magnification
1	*Conicavus tipiopsis* n.sp. Paratype	PB1268m	SEM	x66
2	*Conicavus tipiopsis* n.sp.	PB3791m	RLM	x80
3	*Conicavus tipiopsis* n.sp. a-c: specimens with 3 feet; d: a specimen with 4 feet	PB3791m	RLM	x80
4	*Conicavus tipiopsis* n.sp. Holotype	PB3791m	LM	x92
5	*Conicavus tipiopsis* n.sp. Paratype	PB3769m	LM	x66
6	*Conicavus tipiopsis* n.sp. Paratype	PB667m	SEM	x100
7	*Sethoconus myxobrachia* Strelkov and Reshetnyak	P12778m	LM	x100
8	*Sethoconus myxobrachia* Strelkov and Reshetnyak	PB3769m	LM	x60
9	*Artostrobus annulatus* (Bailey)	E988m	LM	x210
10	*Artostrobus annulatus* (Bailey)	E988m	LM	x210
11	*Eucyrtidium* spp. A group	P12778m	LM	x210
12	*Eucyrtidium* spp. A group	P15582m	LM	x210
13	*Eucyrtidium* spp. A group	PB3791m	LM	x390

PLATE 38 Nassellaria

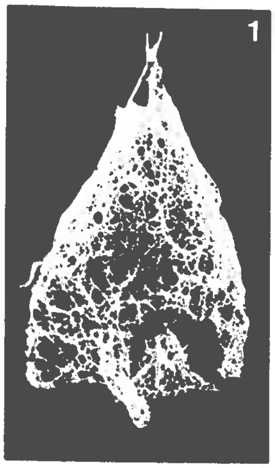
1

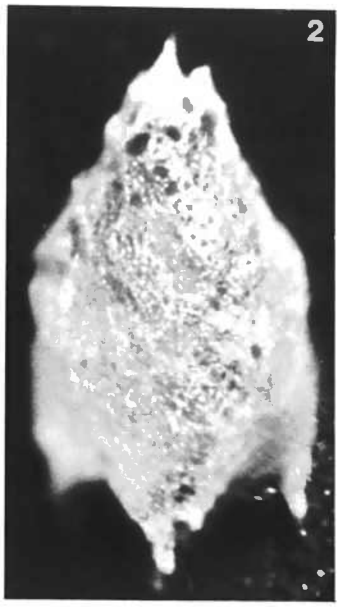
2


3

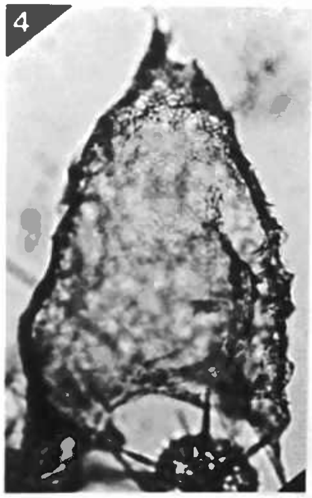
4

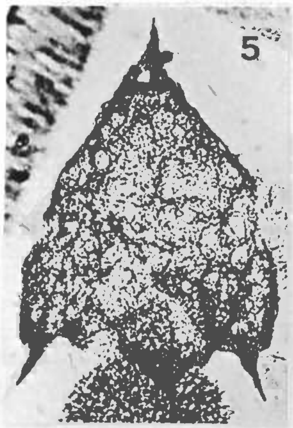
5


9


10


11


12

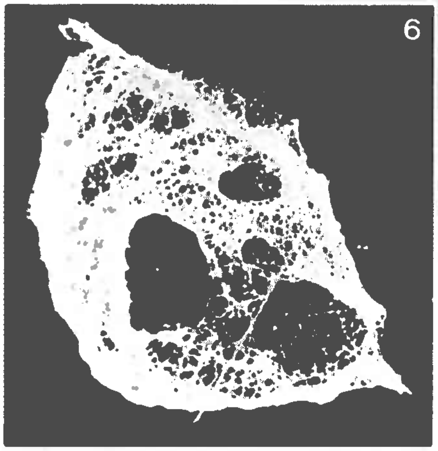
6

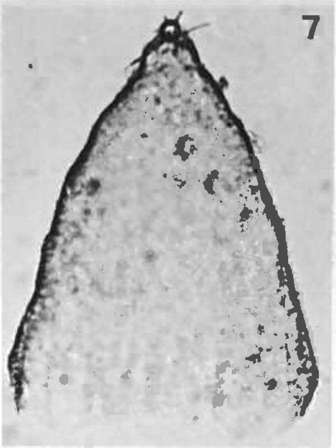
7

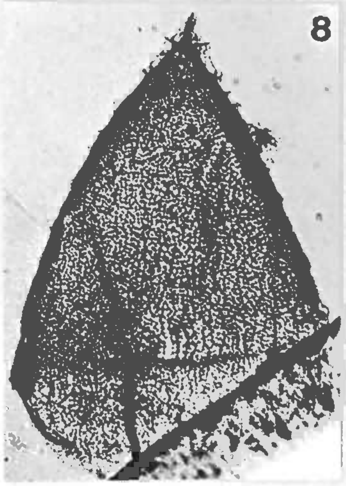
8

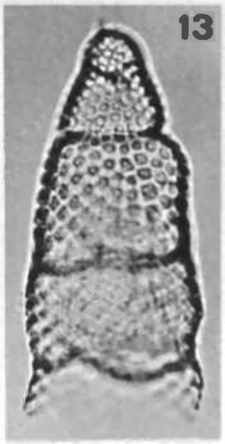
13

PLATE 39

Suborder: Nassellaria
Family: Theoperidae; Subfamily: Eucyrtidiinae

Figure		Station Depth	Type of Micrograph	Magnification
1	*Conarachnium polyacanthum* (Popofsky)	$P_1$2778m	LM	x240
2	*Conarachnium polyacanthum* (Popofsky)	$P_1$4280m	SEM	x120
3	*Conarachnium polyacanthum* (Popofsky)	PB2869m	LM	x210
4	*Conarachnium polyacanthum* (Popofsky)	PB3791m	LM	x210
5	*Conarachnium parabolicum* (Popofsky)	$P_1$5582m	SEM	x100
6	*Conarachnium parabolicum* (Popofsky)	PB3769m	LM	x156
7	*Conarachnium facetum* (Haeckel)	$P_1$5582m	SEM	x165
8	*Dictyophimus macropterus* (Ehrenberg)	$P_1$4280m	SEM	x550
9	*Dictyophimus macropterus* (Ehrenberg)	$P_1$978m	SEM	x440
10	*Dictyophimus macropterus* (Ehrenberg)	PB3769m	LM	x210
11	*Dictyophimus macropterus* (Ehrenberg)	$P_1$5582m	LM	x210
12	*Dictyophimus* sp. B	$P_1$4280m	SEM	x340
13	*Stichopilium bicorne* Haeckel	PB3769m	LM	x210
14	*Stichopilium bicorne* Haeckel	PB3791m	LM	x210
15	*Stichopilium bicorne* Haeckel	PB1268m	SEM	x220
16	*Stichopilium bicorne* Haeckel	$P_1$4280m	LM	x210
17	*Stichopilium bicorne* Haeckel	PB3769m	LM	x210
18	*Stichopilium bicorne* Haeckel	PB3791m	SEM	x230
19	*Stichopilium bicorne* Haeckel	$P_1$4280m	SEM	x250

PLATE 39 Nassellaria

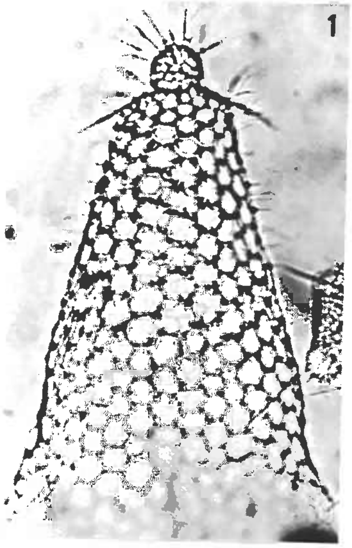
1

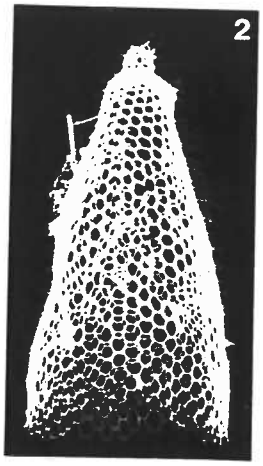
2

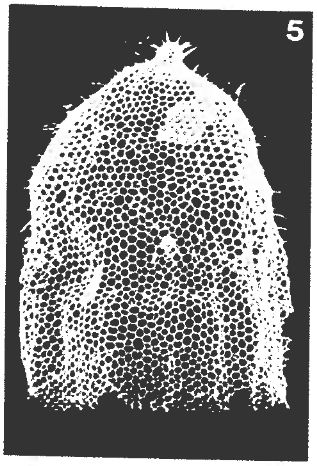
5

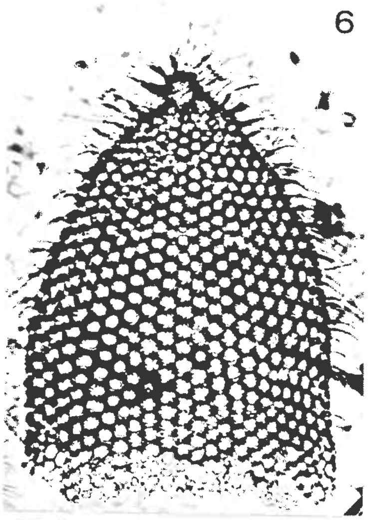
6

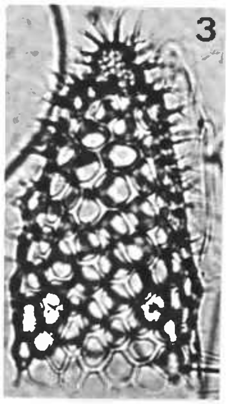
3

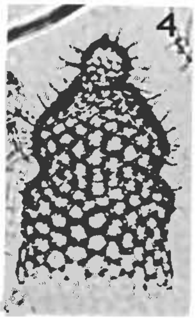
4

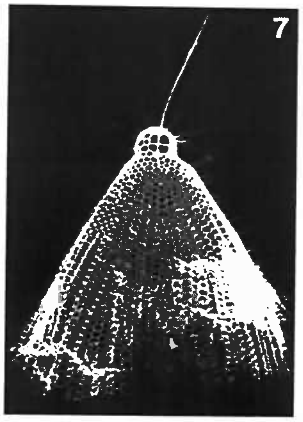
7

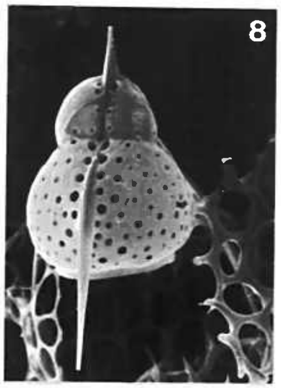
8


9

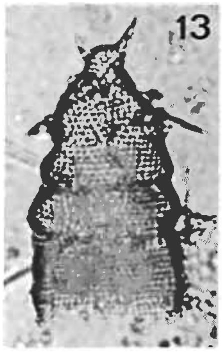
13

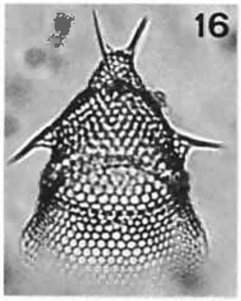
16

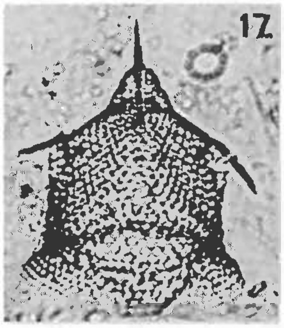
17

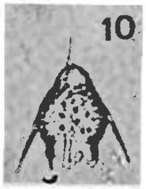
10

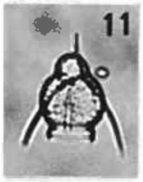
11

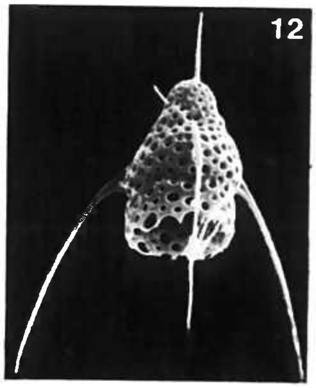
12


14

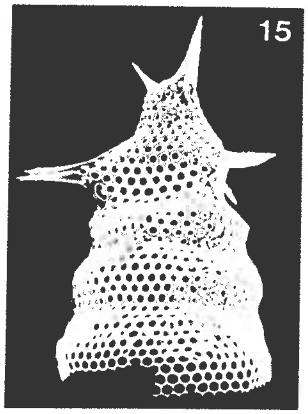
15

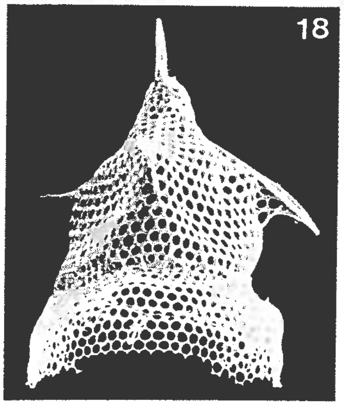
18

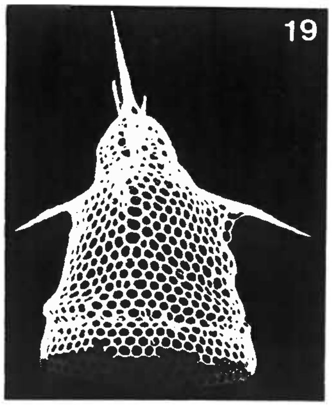
19

PLATE 40

Suborder: Nassellaria
Family: Theoperidae; Subfamily: Eucyrtidiinae

Figure		Station Depth	Type of Micrograph	Magnification
1	*Lithopera bacca* Ehrenberg	$P_1$4280m	SEM	x390
2	*Lithopera bacca* Ehrenberg	$P_1$4280m	SEM	x230
3	*Cyrtopera languncula* Haeckel	PB3769m	SEM	x190
4	*Cyrtopera languncula* Haeckel	PB3769m	SEM	x140
5	*Cyrtopera languncula* Haeckel	$P_1$4280m	SEM	x440
6	*Cyrtopera languncula* Haeckel	PB3791m	LM	x210
7	*Cyrtopera aglaolampa* n.sp. Holotype	$P_1$2778m	LM	x210
8	*Cyrtopera aglaolampa* n.sp. Paratype	PB3769m	SEM	x120
9	*Triacartus undulatum* (Popofsky)	$P_1$4280m	SEM	x280
10	*Triacartus undulatum* (Popofsky)	PB2869m	LM	x210
11	*Theocorys veneris* Haeckel	$P_1$4280m	SEM	x440
12	*Theocorys veneris* Haeckel	PB3791m	SEM	x370
13	*Theocorys veneris* Haeckel	PB2869m	LM	x210
14	*Theocorys veneris* Haeckel	PB2869m	LM	x210
15	*Theocorythium trachelium trachelium* (Ehrenberg)	$P_1$5582m	SEM	x240
16	*Theocorythium trachelium trachelium* (Ehrenberg)	$P_1$978m	LM	x210
17	*Lipmanella dictyoceras* (Haeckel)	PB2869m	LM	x210
18	*Lipmanella pyramidale* (Popofsky)	$P_1$5582m	SEM	x280
19	*Lipmanella virchowii* (Haeckel)	PB2869m	LM	x210
20	*Lipmanella virchowii* (Haeckel)	PB2869m	LM	x210
21	*Lipmanella virchowii* (Haeckel)	PB2869m	LM	x210

PLATE 40 Nassellaria

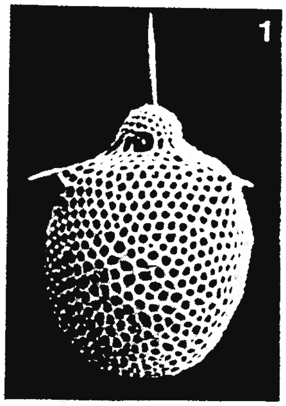

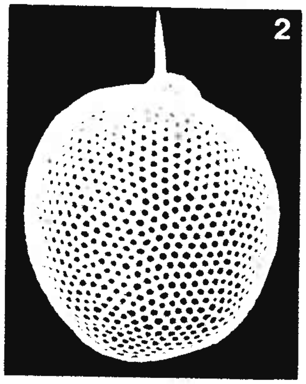

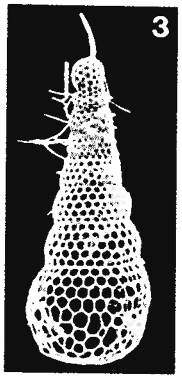

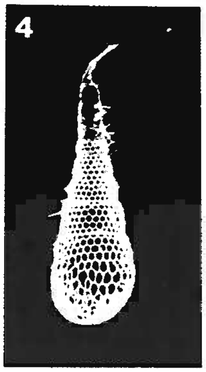

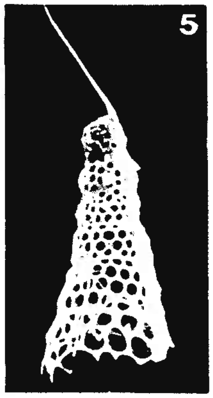

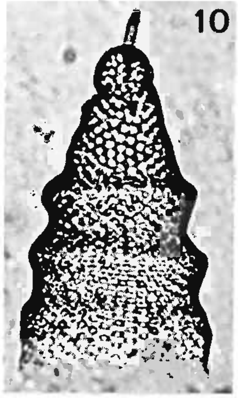

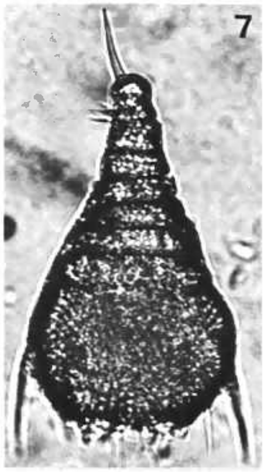

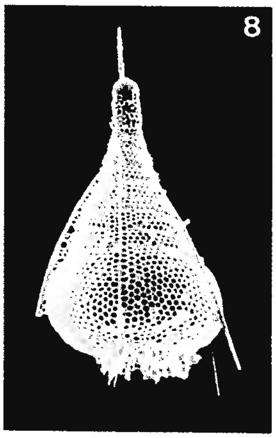

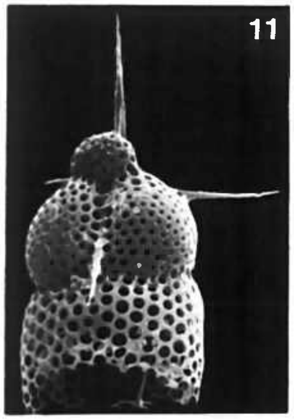

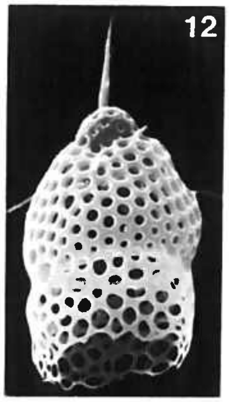

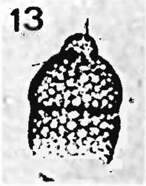

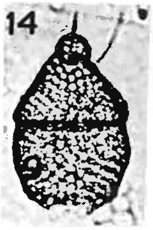

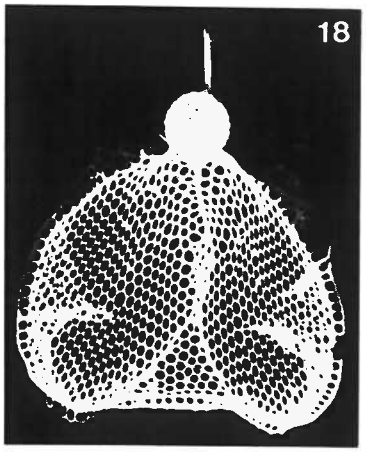

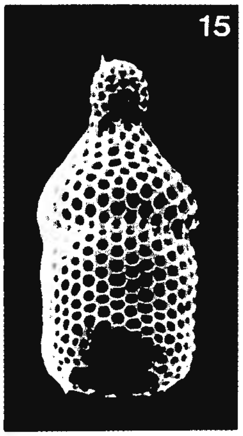

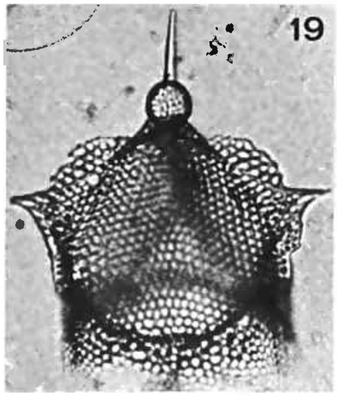

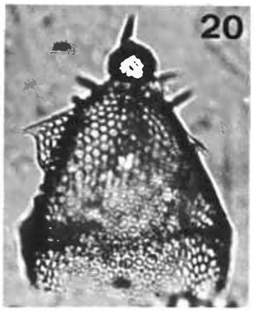

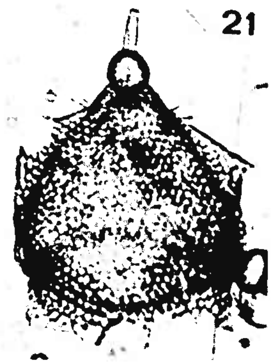

PLATE 41

Suborder: Nassellaria
Family: Theoperidae; Subfamily: Eucyrtidiinae
Family: Pterocorythidae

Figure		Station Depth	Type of Micrograph	Magnification
1	Lithostrobus hexagonalis Haeckel	PB667m	LM	x210
2	Lithostrobus hexagonalis Haeckel	$P_1$5582m	SEM	x220
3	Lithostrobus hexagonalis Haeckel	PB3791m	SEM	x165
4	Theocalyptra bicornis (Popofsky)	E988m	LM	x210
5	Theocalyptra bicornis (Popofsky)	$P_1$378m	LM	x210
6	Theocalyptra bicornis (Popofsky)	E988m	LM	x210
7	Theocalyptra davisiana davisiana (Ehrenberg)	PB3791m	LM	x210
8	Theocalyptra bicornis (Popofsky)	$P_1$5582m	LM	x210
9	Theocalyptra bicornis (Popofsky)	$P_1$4280m	SEM	x550
10	Theocalyptra bicornis (Popofsky)	$P_1$4280m	SEM	x440
11	Theocalyptra bicornis (Popofsky)	$P_1$4280m	SEM	x390
12	Theocalyptra davisiana cornutoides (Petrushevskaya)	PB3791m	LM	x210
13	Theocalyptra davisiana cornutoides (Petrushevskaya)	$P_1$5582m	LM	x210
14	Theocalyptra davisiana cornutoides (Petrushevskaya)	$P_1$4280m	SEM	x830
15	Theocalyptra davisiana cornutoides (Petrushevskaya)	$P_1$4280m	SEM	x440
16	Theocalyptra davisiana cornutoides (Petrushevskaya)	$P_1$4280m	SEM	x360
17	Tetracorethra tetracorethra (Haeckel)	PB3769m	LM	x85
18	Tetracorethra tetracorethra (Haeckel)	$P_1$5582m	SEM	x154
19	Anthocyrtidium zanguebaricum (Ehrenberg)	PB2869m	LM	x210
20	Anthocyrtidium zanguebaricum (Ehrenberg)	$P_1$4280m	SEM	x230
21	Anthocyrtidium zanguebaricum (Ehrenberg)	PB3791m	SEM	x250
22	Anthocyrtidium zanguebaricum (Ehrenberg)	$P_1$4280m	SEM	x360

PLATE 41 Nassellaria


1

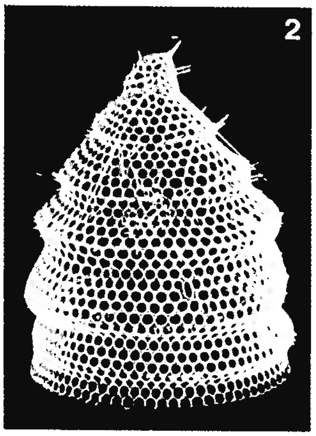
2

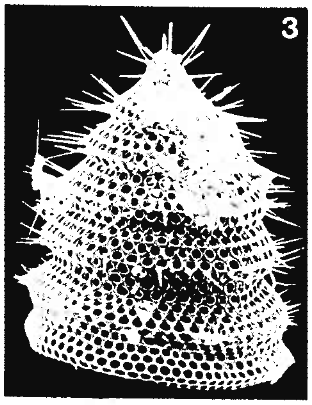
3

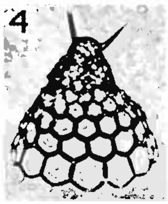
4

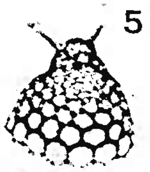
5

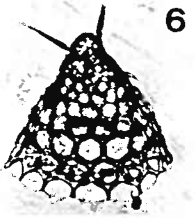
6


7

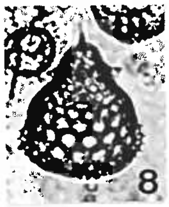
8

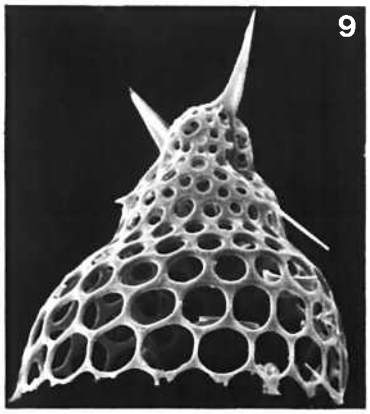
9


10

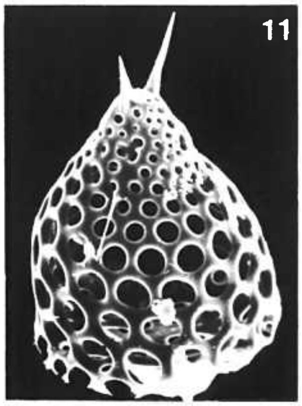
11


12

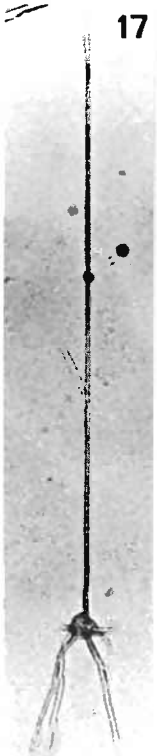
17


13

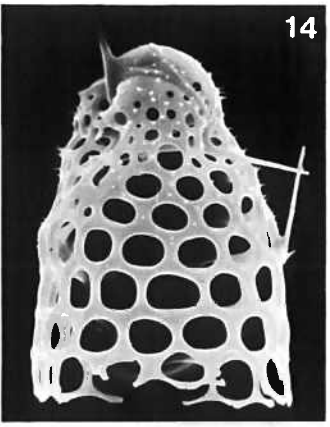
14

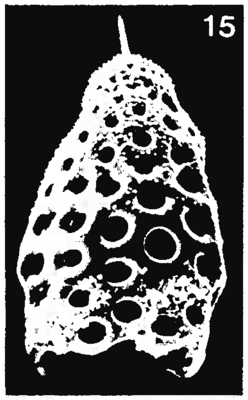
15


16

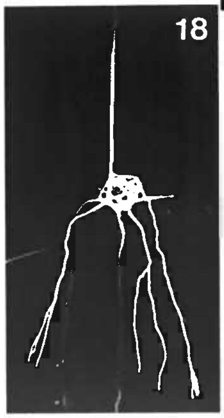
18

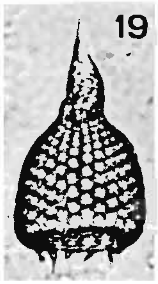
19

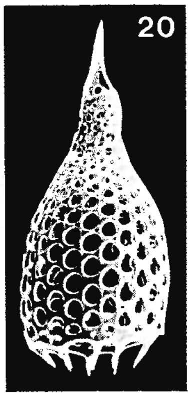
20

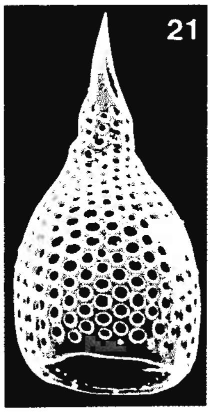
21

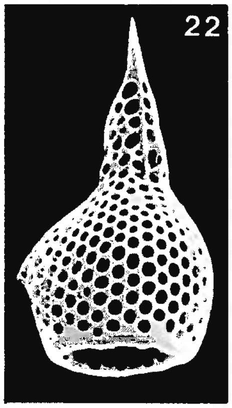
22
]

PLATE 42

Suborder: Nassellaria
Family: Pterocorythidae

Figure		Station Depth	Type of Micrograph	Magnification
1	*Pterocorys zancleus* (Müller)	$P_1$5582m	SEM	x300
2	*Pterocorys zancleus* (Müller)	$P_1$4280m	SEM	x440
3	*Pterocorys zancleus* (Müller)	$P_1$4280m	SEM	x300
4	*Pterocorys zancleus* (Müller)	$P_1$4280m	LM	x210
5	*Pterocorys campanula* Haeckel	$P_1$978m	SEM	x580
6	*Pterocorys campanula* Haeckel	PB667m	LM	x210
7	*Pterocorys campanula* Haeckel	PB3769m	LM	x210
8	*Pterocorys campanula* Haeckel	$P_1$4280m	SEM	x220
9	*Eucyrtidium acuminatum* (Ehrenberg)	PB1268m	SEM	x180
10	*Eucyrtidium acuminatum* (Ehrenberg)	PB1268m	SEM	x165
11	*Eucyrtidium anomalum* Haeckel	$P_1$5582m	SEM	x220
12	*Eucyrtidium anomalum* Haeckel	PB2869m	LM	x210
13	*Eucyrtidium anomalum* Haeckel	PB3769m	LM	x210
14	*Eucyrtidium anomalum* (Haeckel)	$P_1$4280m	LM	x210
15	*Eucyrtidium* sp. aff. *E. anomalum* (Haeckel)	$P_1$5582m	LM	x210
16	*Eucyrtidium acuminatum* (Ehrenberg)	$P_1$4280m	SEM	x250
17	*Eucyrtidium acuminatum* (Ehrenberg)	$P_1$4280m	SEM	x250
18	*Eucyrtidium hexagonatum* Haeckel	$P_1$5582m	SEM	x220
19	*Eucyrtidium hexagonatum* Haeckel	PB2869m	LM	x210
20	*Eucyrtidium acuminatum* (Ehrenberg)	PB3769m	LM	x210
21	*Eucyrtidium dictyopodium* (Haeckel)	$P_1$5582	SEM	x165
22	*Eucyrtidium hexastichum* (Haeckel)	PB3769m	LM	x210

PLATE 42 Nassellaria

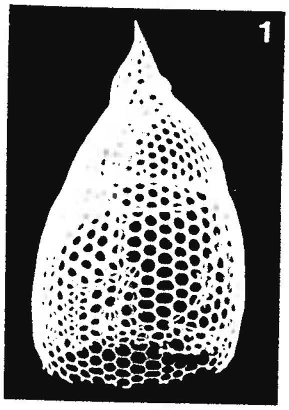
1

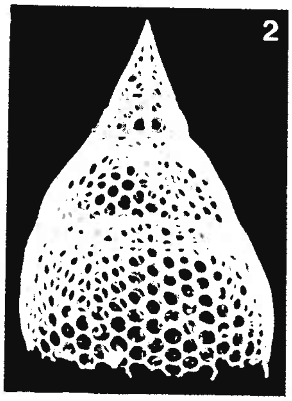
2

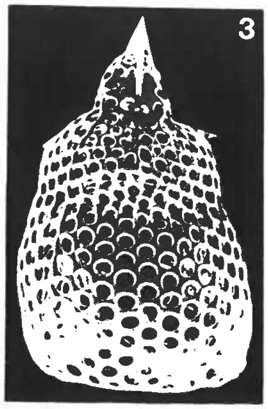
3

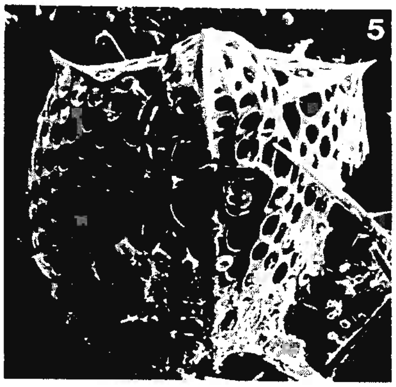
5

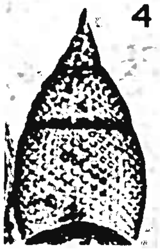
4


6

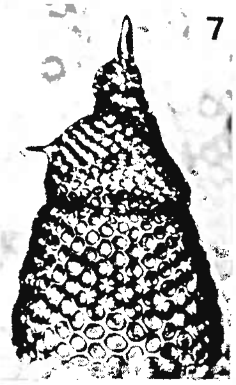
7

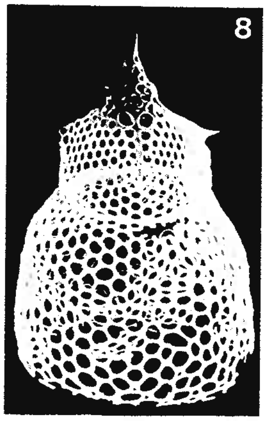
8

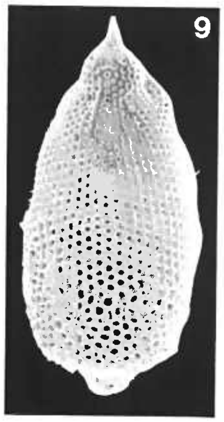
9

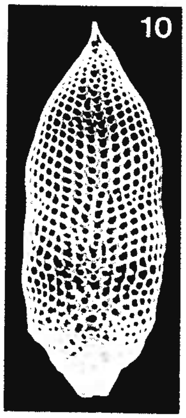
10

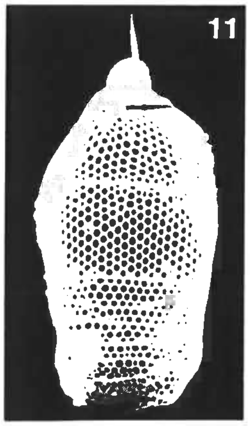
11

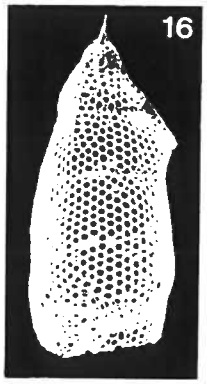
16

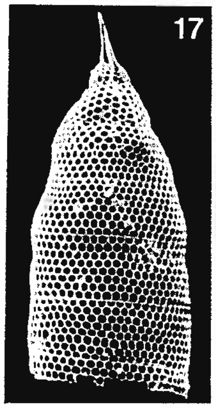
17

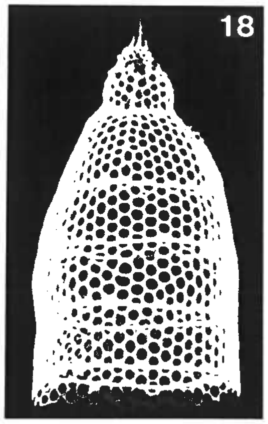
18

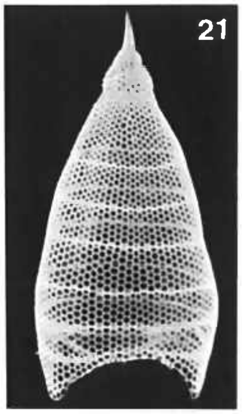
21


12


13

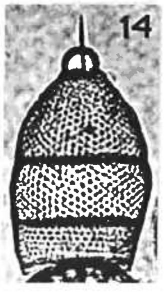
14

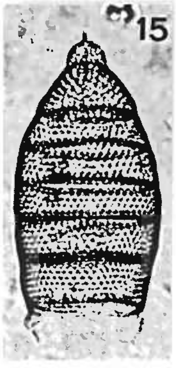
15

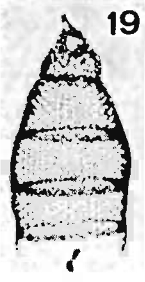
19

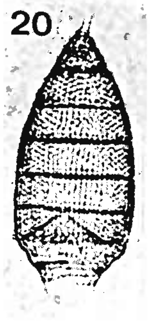
20


22

PLATE 43

Suborder: Nassellaria
Family: Pterocorythidae

Figure		Station Depth	Type of Micrograph	Magnification
1	*Anthrocyrtidium ophirense* (Ehrenberg)	PB2869m	LM	x210
2	*Anthrocyrtidium ophirense* (Ehrenberg)	$P_1$5582m	SEM	x200
3	*Anthrocyrtidium ophirense* (Ehrenberg)	$P_1$4280m	SEM	x230
4	*Anthrocyrtidium ophirense* (Ehrenberg)	PB3791m	SEM	x165
5	*Anthrocyrtidium ophirense* (Ehrenberg)	$P_1$4280m	SEM	x220
6	*Anthrocyrtidium ophirense* (Ehrenberg)	$P_1$978m	LM	x210
7	*Anthrocyrtidium ophirense* (Ehrenberg)	$P_1$4280m	SEM	x340
8	*Lamprocyclas maritalis maritalis* Haeckel	$P_1$4280m	SEM	x170
9	*Lamprocyclas maritalis maritalis* Haeckel	E3755m	LM	x210
10	*Lamprocyclas maritalis maritalis* Haeckel A skeletal cross section of an interporous bar showing uniform and solid features with little dissolution on the margin. The conchoidal fractures are due to sectioning.	$P_1$2778m	TEM	x19,200
11	*Lamprocyclas maritalis maritalis* Haeckel A more progressed stage of dissolution than the above fig. 10 showing porous marginal area.	$P_1$5582m	TEM	x52,200
12	*Lamprocyclas maritalis polypora* Nigrini	PB3791m	LM	x210
13	*Lamprocyclas maritalis maritalis* Haeckel	E5068m	LM	x210
14	*Lamprocyclas maritalis maritalis* Haeckel	PB3791m	SEM	x180
15	*Lamprocyclas maritalis polypora* Nigrini	PB3791m	LM	x210
16	*Lamprocyrtis* sp.	PB3791m	LM	x210
17	*Lamprocyrtis nigriniae* (Caulet)	PB2869m	LM	x210
18	*Lamprocyrtis nigriniae* (Caulet)	PB2869m	LM	x210
19	*Lamprocyrtis nigriniae* (Caulet)	PB3769m	LM	x210

PLATE 43 Nassellaria

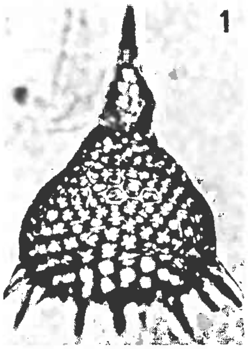
1

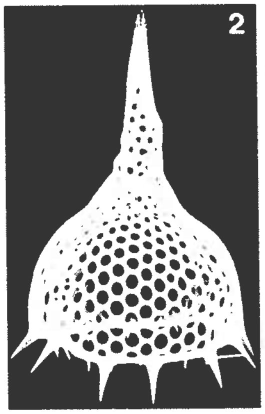
2

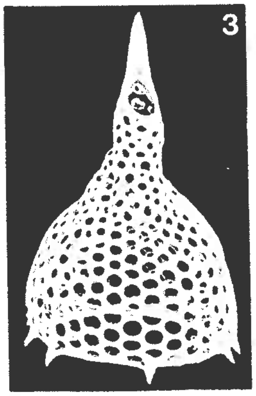
3

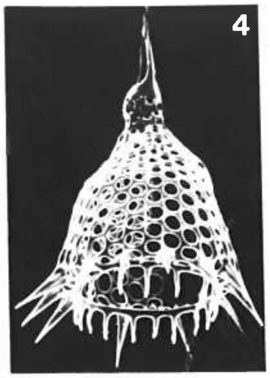
4

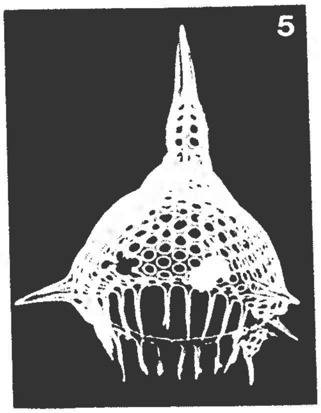
5

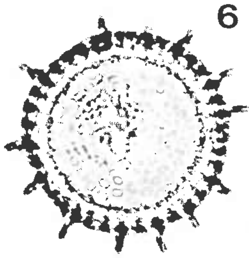
6

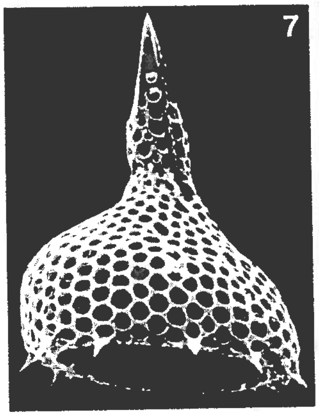
7

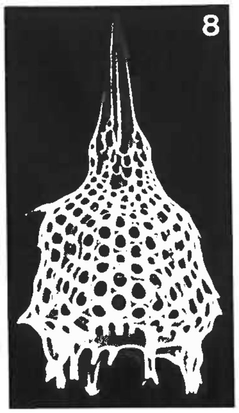
8


10

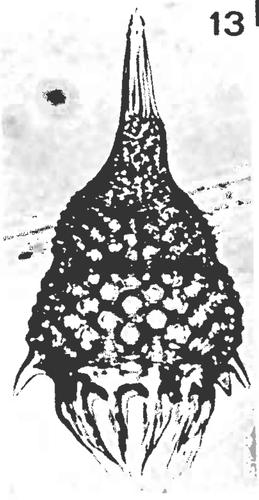
13


12

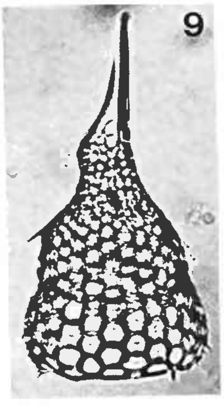
9


11

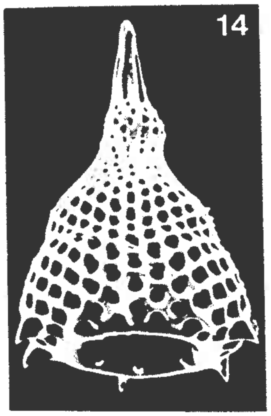
14

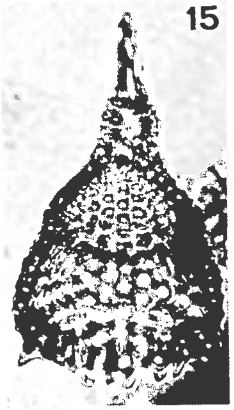
15

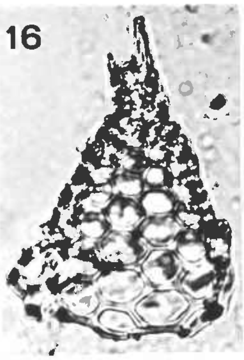
16

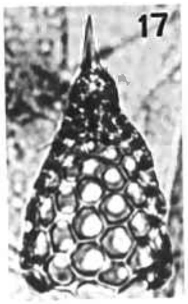
17


18

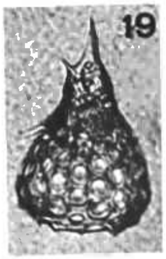
19

PLATE 44

Suborder: Nassellaria
Family: Artostrobiidae

Figure		Station Depth	Type of Micrograph	Magnification
1	*Spirocyrtis scalaris* Haeckel	E389m	LM	x210
2	*Spirocyrtis scalaris* Haeckel	PB1268m	SEM	x200
3	*Spirocyrtis subscalaris* Nigrini	PB3791m	SEM	x330
4	*Spirocyrtis subscalaris* Nigrini	PB1268m	SEM	x330
5	*Spirocyrtis subscalaris* Nigrini An inside view of purposely broken specimen.	PB3769m	SEM	x440
6	*Spirocyrtis subscalaris* Nigrini	PB3791m	LM	x210
7	*Spirocyrtis* ? *platycephala* (Ehrenberg)	PB3791m	LM	x210
8	*Spirocyrtis* ? *platycephala* (Ehrenberg)	P15582m	LM	x210
9	*Botryostrobus aquilonaris* (Bailey)	E5068m	LM	x210
10	*Botryostrobus aquilonaris* (Bailey)	PB2869m	LM	x210
11	*Botryostrobus aquilonaris* (Bailey)	P1978m	SEM	x370
12	*Botryostrobus aquilonaris* (Bailey)	PB3791m	SEM	x250
13	*Botryostrobus aquilonaris* (Bailey) A specimen with rough surface.	PB1268m	SEM	x390
14	*Phormostichoartus corbula* (Harting)	PB2869m	LM	x210
15	*Phormostichoartus corbula* (Harting)	PB2869m	LM	x210
16	*Phormostichoartus corbula* (Harting)	P14280m	SEM	x420
17	*Siphocampe lineata* (Ehrenberg)	PB1268m	SEM	x280
18	*Siphocampe lineata* (Ehrenberg)	PB3769m	SEM	x250
19	*Siphocampe lineata* (Ehrenberg)	PB2869m	LM	x210
20	*Siphocampe lineata* (Ehrenberg) Same specimen as in fig. 17; detail of surface texture.	PB1268m	SEM	x880
21	*Siphocampe arachnea* (Ehrenberg)	PB3769m	SEM	x410
22	*Siphocampe arachnea* (Ehrenberg)	PB3769m	SEM	x520
23	*Siphocampe arachnea* (Ehrenberg)	PB2869m	LM	x210
24	*Artobotrys borealis* (Cleve)	P1978m	SEM	x660

PLATE 44 Nassellaria


1

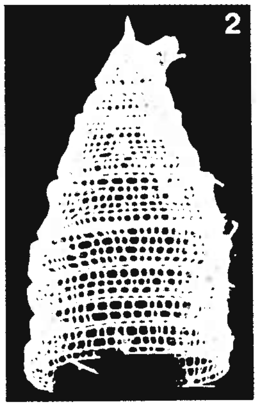
2

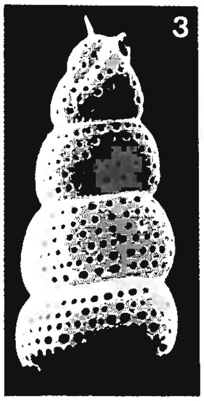
3

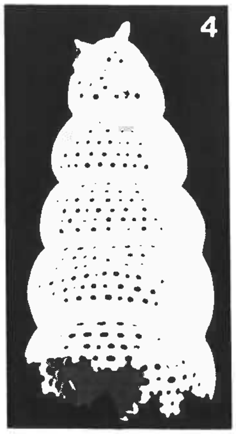
4


5

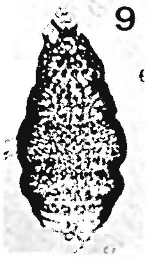
9


10

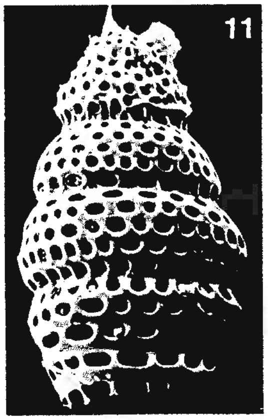
11

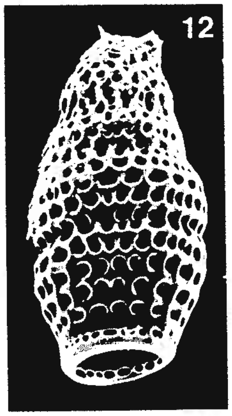
12

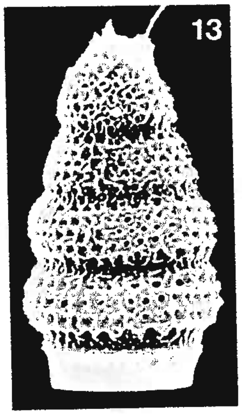
13


6


7


8


14

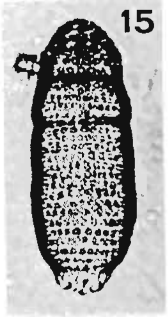
15

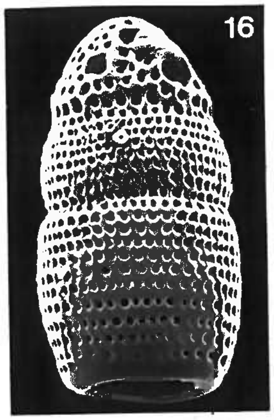
16

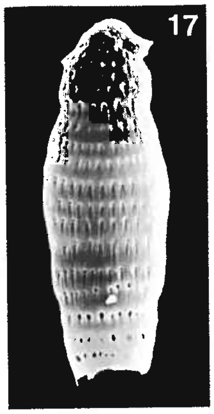
17


18

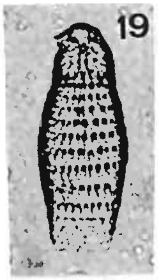
19

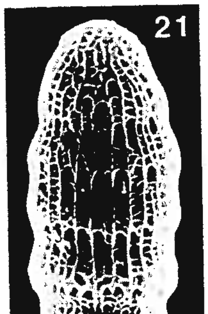
21

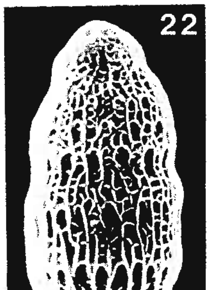
22


23

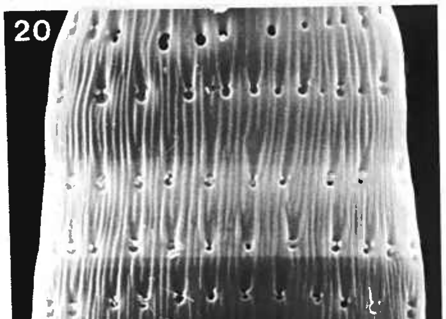
20

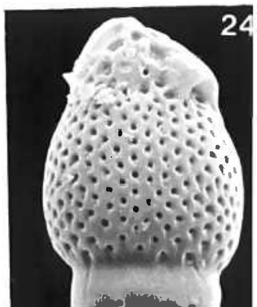
24

PLATE 45

Suborder: Nassellaria
Families: Artostrobiidae, Carpocaniidae, Cannobotryidae

Figure		Station Depth	Type of Micrograph	Magnification
1	*Artobotrys borealis* (Cleve)	PB3769m	SEM	x610
2	*Artobotrys borealis* (Cleve)	PB2869m	LM	x405
3	*Artobotrys borealis* (Cleve)	PB2869m	LM	x210
4	*Carpocanistrum flosculum* Haeckel	$P_1$4280m	SEM	x470
5	*Carpocanistrum cephalum* Haeckel	$P_1$5582m	SEM	x450
6	*Carpocanistrum flosculum* Haeckel	$P_1$4280m	SEM	x550
7	*Carpocanistrum flosculum* Haeckel	$P_1$5582m	SEM	x470
8	*Carpocanistrum favosum* (Haeckel)	$P_1$978m	SEM	x470
9	*Carpocanistrum acutidentatum* n.sp.	$P_1$4280m	SEM	x440
10	*Carpocanistrum coronatum* Haeckel	$P_1$5582m	LM	x210
11	*Carpocanistrum* sp.			
12	*Carpocanistrum cephalum* Haeckel	$P_1$5582m	LM	x210
13	*Carpocanistrum acutidentatum* n.sp. Holotype	$P_1$4280m	SEM	x340
14	*Carpocanistrum acutidentatum* Paratype	PB1268m	SEM	x300
15	*Carpocanistrum acutidentatum* Paratype	PB1268m	SEM	x330
16	*Carpocanarium papillosum* Ehrenberg	PB3791m	LM	x210
17	*Carpocanarium papillosum* Ehrenberg	PB2869m	LM	x210
18	*Acrobotrys teralans* Renz	PB2869m	LM	x210
19	*Acrobotrys teralans* Renz	PB2869m	LM	x210
20	*Acrobotrys tessarolobon* n.sp.	$P_1$978m	SEM	x450
21	*Saccospyris preantarctica* Petrushevskaya	$P_1$4280m	SEM	x630
22	*Acrobotrys chelinobotrys* n.sp. Paratype	$P_1$4280m	SEM	x550
23	*Acrobotrys chelinobotrys* n.sp. Paratype	PB3769m	LM	x210
24	*Acrobotrys chelinobotrys* n.sp. Holotype	$P_1$978m	LM	x210

PLATE 45 Nassellaria

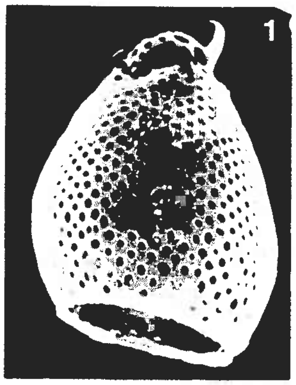
1

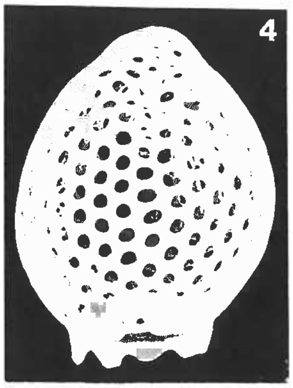
4

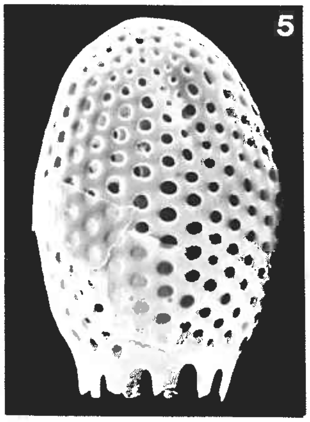
5

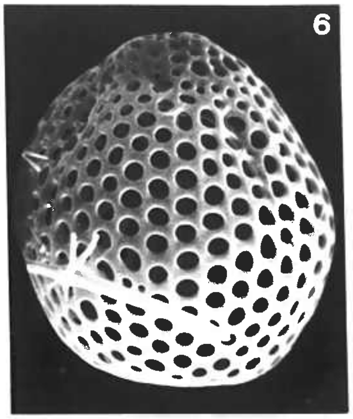
6


2


3

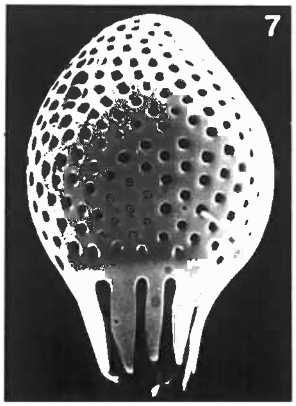
7

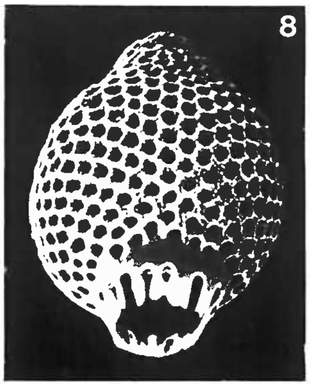
8

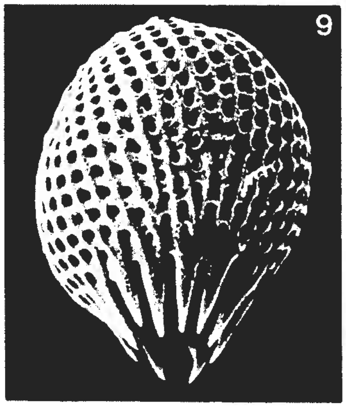
9


10


11


12

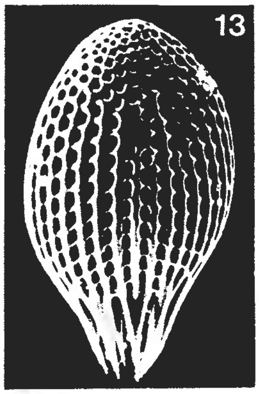
13

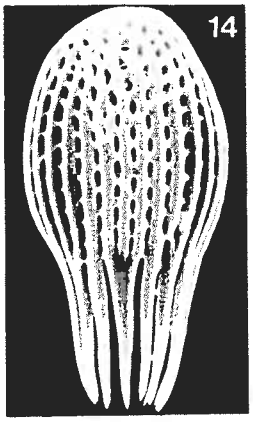
14

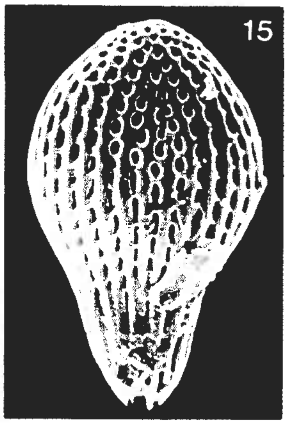
15


16


17

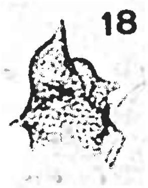
18

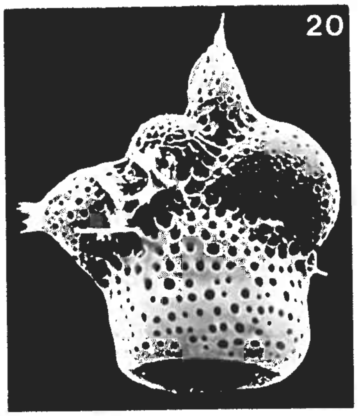
20

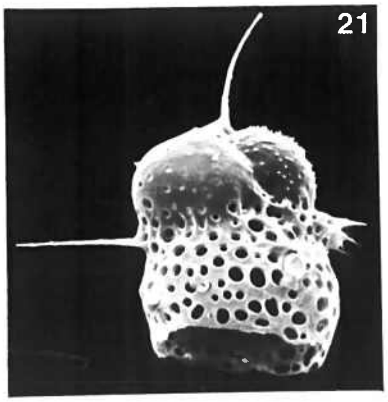
21

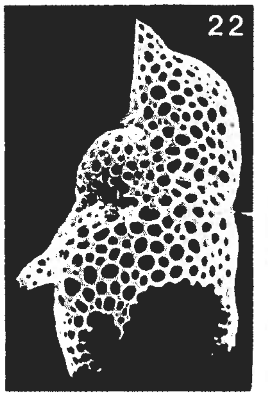
22


23


19

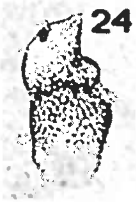
24

PLATE 46

Suborder: Nassellaria
Families: Cannobotryidae, Archiphomididae

Figure		Station Depth	Type of Micrograph	Magnification
1	*Centrobotrys thermophila* Petrushevskaya	$P_1$4280m	SEM	x350
2	*Centrobotrys thermophila* Petrushevskaya	$P_1$4280m	LM	x210
3	*Neobotrys quadrituberosa* Popofsky	PB2869m	LM	x210
4	*Botryocyrtis* sp. A	$P_1$4280m	SEM	x580
5	*Botryocyrtis* sp. A	$P_1$978m	SEM	x660
6	*Botryocyrtis scutum* (Harting)	PB2869m	LM	x210
7	*Botryocyrtis scutum* (Harting)	$P_1$5582m	LM	x210
8	*Botryocyrtis elongatum* n.sp. Holotype	PB3769m	LM	x210
9	*Botryocyrtis elongatum* n.sp. Paratype	$P_1$4280m	SEM	x230
10	*Arachnocalpis* ? sp. A	PB1268m	LM	x84
11	*Arachnocalpis* sp. B	PB3769m	LM	x210
12	*Arachnocalpis* ? *ovatiretalis* n.sp. Paratype	PB3769m	LM	x210
13	*Arachnocalpis* ? *ovatiretalis* n.sp. Paratype	PB3791m	LM	x210
14	*Arachnocalpis* ? *ovatiretalis* n.sp. Holotype	PB667m	SEM	x180
15	Probably a deformed or broken specimen of *Arachnocalpis ellipsoides* ? Haeckel	$P_1$2778m	LM	x210
16	*Arachnocalpis* ? sp. C	$P_1$2778m	LM	x210
17	*Arachnocalpis ellipsoides* Haeckel	$P_1$2778m	LM	x210
18	A typical view of a portion of untreated filtered sample (250-63 µm fraction). Note predominance of Radiolaria over diatoms and Foraminifera in this size fraction.	$P_1$4280m	SEM	x80

PLATE 46 Nassellaria

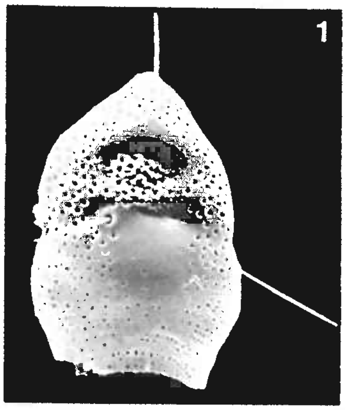
1

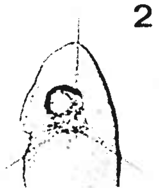
2


4

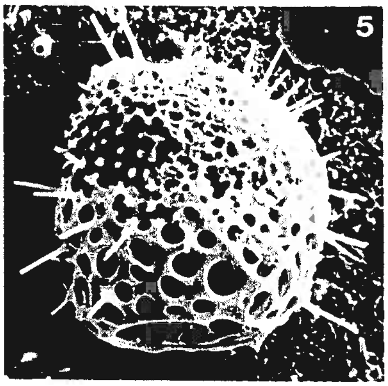
5


10

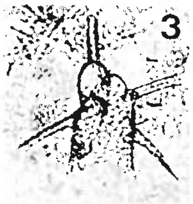
3


6


7

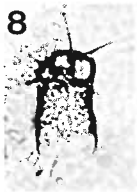
8


9

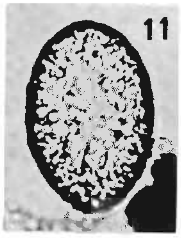
11


12

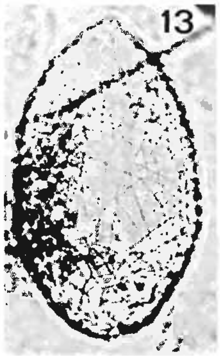
13

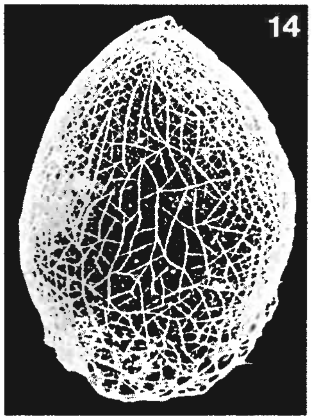
14

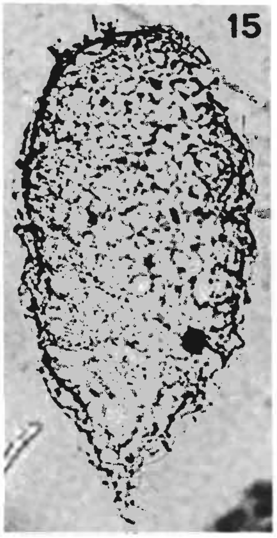
15


16

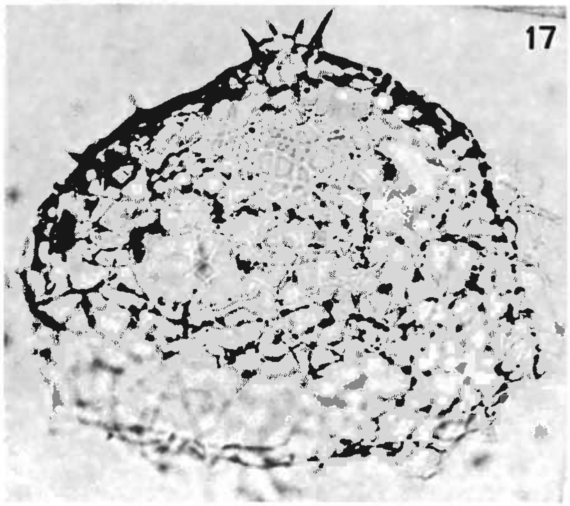
17


18

PLATE 47

Suborder: Phaeodaria
Family: Challengeriidae

Figure		Station Depth	Type of Micrograph	Magnification
1	<u>Challengeron</u> <u>willemoesii</u> Haeckel Ovate form, lateral view	PB667m	SEM	x120
2	<u>Challengeron</u> <u>willemoesii</u> Haeckel Ovate form, oblique dorsal view	PB667m	SEM	x100
3	<u>Challengeron</u> <u>willemoesii</u> Haeckel Ovate form, lateral view	E988m	LM	x210
4	<u>Challengeron</u> <u>willemoesii</u> Haeckel Ovate form, lateral view	E988m	LM	x210
5	<u>Challengeron</u> <u>willemoesii</u> Haeckel Ellipsoidal form, lateral view	PB1268m	LM	x210
6	<u>Challengeron</u> <u>willemoesii</u> Haeckel Ellipsoidal form, lateral view	$P_1$2778m	SEM	x190
7	<u>Challengeron</u> <u>willemoesii</u> Haeckel Ellipsoidal form, lateral view of a purposely broken specimen for microstructural observations	PB1268m	SEM	x215
8	<u>Challengeron</u> <u>willemoesii</u> Haeckel An extensively dissolved specimen revealing its skeletal microstructure	PB3791m	SEM	x330
9	<u>Challengeron</u> <u>willemoesii</u> Haeckel Same specimen, outside surface	PB3791m	SEM	x800
10	<u>Challengeron</u> <u>willemoesii</u> Haeckel Same specimen, both inside and outside surfaces of amphora structure are shown	PB3791m	SEM	x2600
11	<u>Challengeron</u> <u>willemoesii</u> Haeckel A typical sediment trap specimen showing a solid unit of amphorae and a porous cementing unit between the amphorae; cross section and inside surface.	PB1268m	SEM	x3400
12	<u>Challengeron</u> <u>willemoesii</u> Haeckel A corresponding section of fig. 11; note the porous area is composed of tubes.	PB667m	TEM	x11900
13	<u>Challengeron</u> <u>willemoesii</u> Haeckel A relatively undissolved specimen showing indistinguishable porocity between amphorae and cementing units; inside surface, notice that necks of the amphorae play a role in securing themselves with inside surface membrane.	$P_1$978m	SEM	x2400
14	<u>Challengeron</u> <u>willemoesii</u> Haeckel A cross section of an undissolved specimen; note that pores (ca. 50-500 angstrom in diameter) are distributed to the part which corresponds to cementing units of figs. 8-12 but not on the surfaces of amphorae and outside of the shell; conchoidal fractures are artifact due to sectioning.	PB 0-100m plankton tow	TEM	x6700

PLATE 47 Phaeodaria

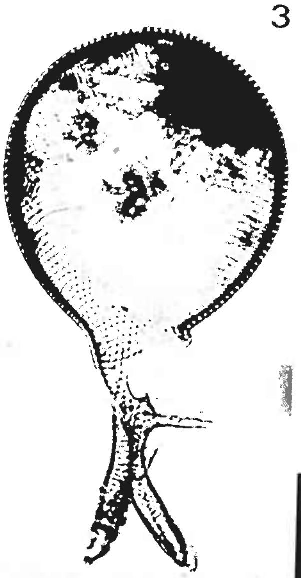

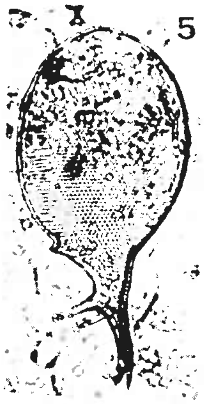

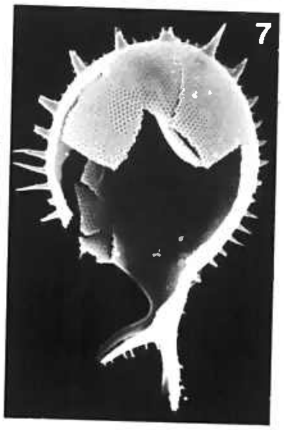

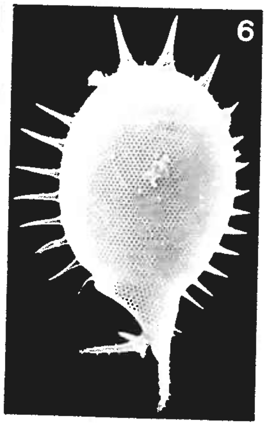

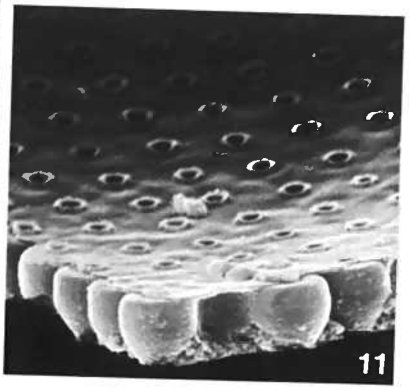

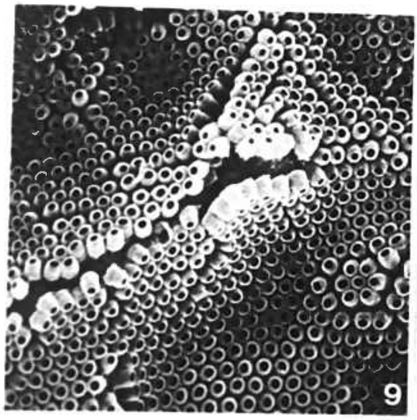

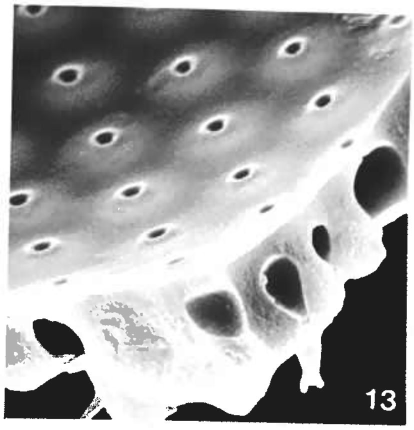

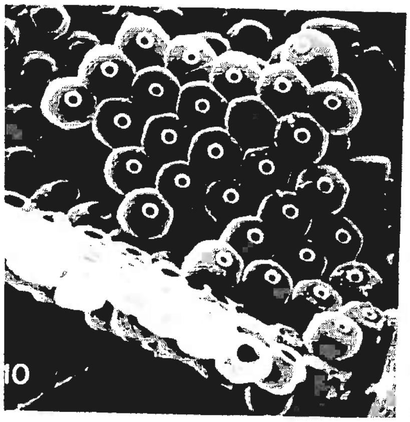

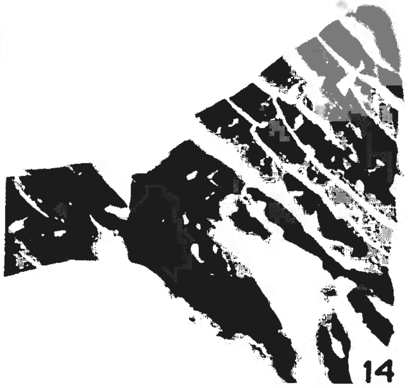

PLATE 48

Suborder: Phaeodaria
Family: Challengeriidae

Figure		Station Depth	Type of Micrograph	Magnification
1	*Challengeron lingi* n.sp. Ovate form, oral view	$P_1$378m	SEM	x385
2	*Challengeron lingi* n.sp. Ovate form, oblique oral view. Paratype.	PB2869m	SEM	x230
3	*Challengeron lingi* n.sp. Ovate form, oblique ventral view. Holotype.	$P_1$978m	SEM	x180
4	*Challengeron lingi* n.sp. Ovate form, lateral view. Paratype.	$P_1$2778m	LM	x210
5	*Challengeron lingi* n.sp. Ellipsoidal form, lateral view. Paratype.	$P_1$978m	SEM	x220
6	*Challengeron radians* Borgert	E389m	LM	x210
7	*Challengerosium balfouri* (Murray)	E389m	LM	x210
8	*Challengerosium balfouri* (Murray) Microstructure composed of amphorae, outside and inside surface layers and porous cement.	E389m	SEM	x5760
9	*Challengerosium balfouri* (Murray) Ventral view with alveolate stripe on the sagital margin.	E389m	SEM	x140
10	*Challengerosium balfouri* (Murray) Lateral view with alveolate zone on the marginal edge.	E389m	SEM	x190
11	*Challengeron tizardi* (Murray) Microstructure showing regularly arranged amphorae cemented with porous silica.	PB1268m	SEM	x2100
12	*Challengeron tizardi* (Murray) A purposely broken specimen for microstructural observations.	PB1268m	SEM	x140
13	*Challengeron tizardi* (Murray) Lateral view.	PB1268m	LM	x160
14	*Challengeron tizardi* (Murray) Lateral view.	PB1268m	SEM	x120
15	*Challengeron tizardi* (Murray) Same specimen, oblique apical view.	PB1268m	SEM	x120
16	*Challengeron tizardi* (Murray) Same specimen, ventral view.			

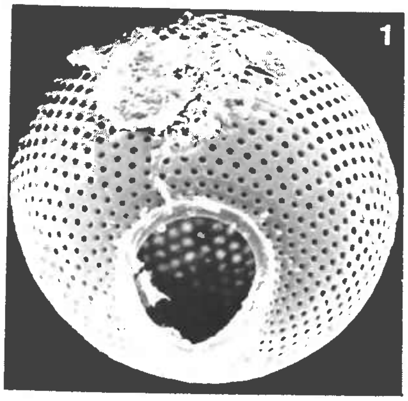
1

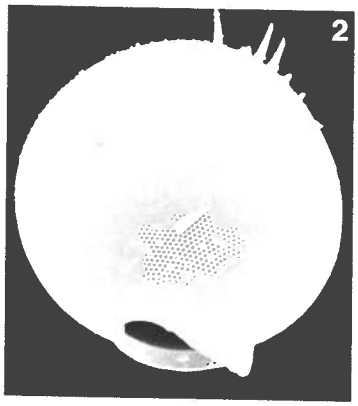
2

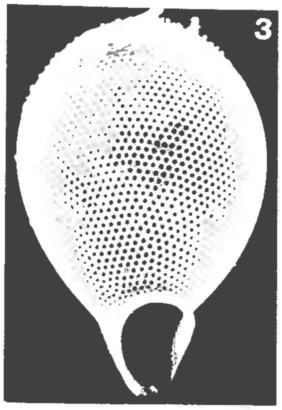
3


4


5

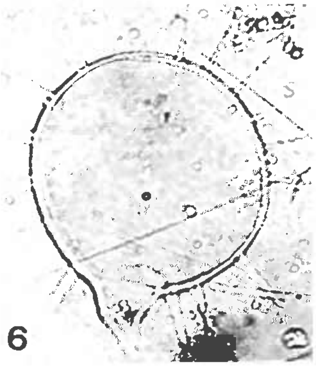
6


7


8

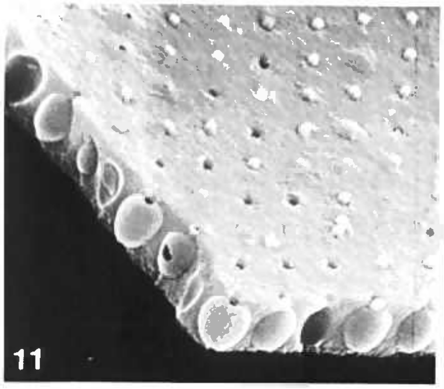
11

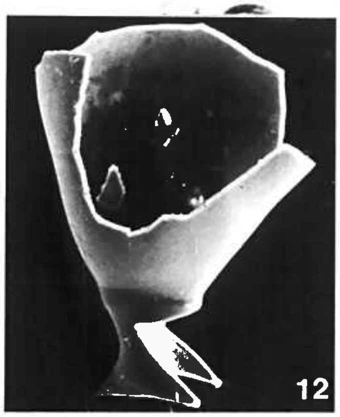
12

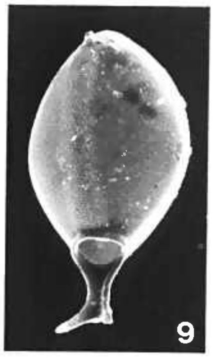
9


10

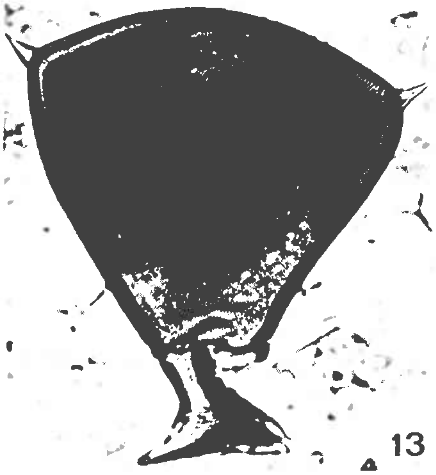
13

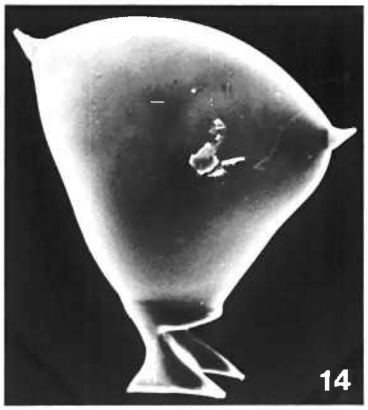
14

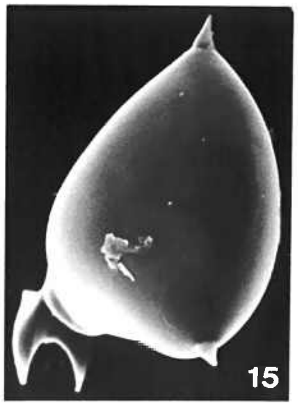
15

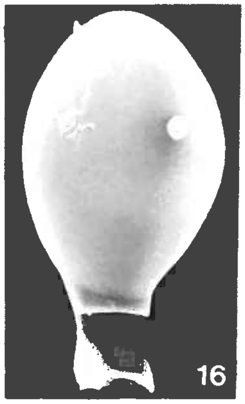
16

PLATE 49

Suborder: Phaeodaria
Family: Challengeriidae

Figure		Station Depth	Type of Micrograph	Magnification
1	*Challengerosium avicularia* Haecker Ventral view.	$P_1$2778m	SEM	x215
2	*Challengerosium avicularia* Haecker Lateral view.	$P_1$978m	SEM	x215
3	*Challengerosium avicularia* Haecker Lateral view.	$P_1$2778m	SEM	x210
4	*Challengerosium avicularia* Haecker Lateral view.	$P_1$2778m	LM	x210
5	*Challengerosium avicularia* Haecker Lateral view.	$P_1$2778m	SEM	x220
6	*Challengerosium avicularia* Haecker Same specimen, oblique lateral view.	$P_1$2778m	SEM	x200
7	*Challengerosium avicularia* Haecker Oblique lateral view.	$P_1$2778m	LM	x210
8	*Challengerosium avicularia* Haecker A specimen with two spines, lateral view.	$P_1$2778m	SEM	x240
9	*Challengerosium avicularia* Haecker A specimen with pores connected with outside surface; considered to be dissolved.	$P_1$4280m	SEM	x250
10	*Challengerosium avicularia* Haecker A specimen without spines.	$P_1$2778m	LM	x210
11	*Challengerosium avicularia* Haecker Microstructure near the oral teeth; note that amphoral structure predominant in the main body of the shell does not extend to the teeth.	$P_1$2778m	SEM	x830
12	*Challengerosium avicularia* Haecker Two different kinds of surfaces: alveolate marginal zone and smooth central zone.	$P_1$978m	SEM	x1000
13	*Challengerosium avicularia* Haecker Cross sectional microstructure showing the same morphology in the alveolate and smooth zones.	$P_1$2778m	SEM	x2150
14	*Protocystis* sp. A	$P_1$978m	SEM	x280
15	*Protocystis* sp. A	$P_1$978m	SEM	x280

PLATE 49 Phaeodaria

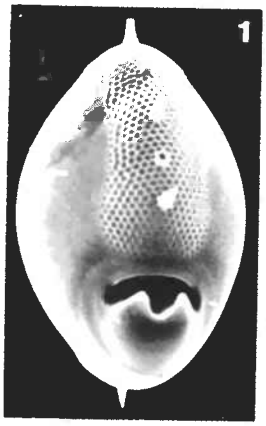

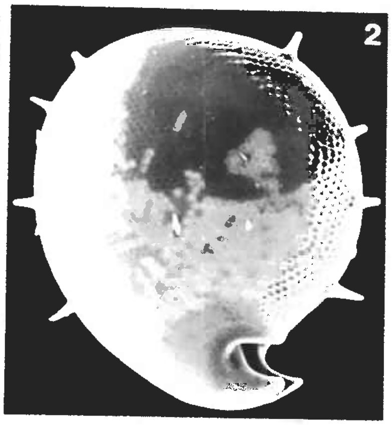

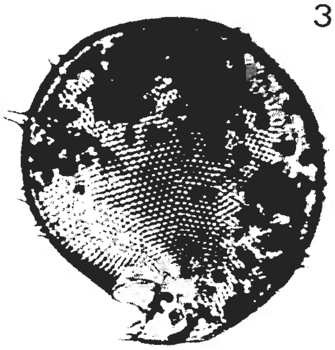

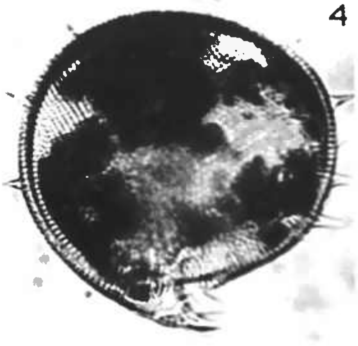

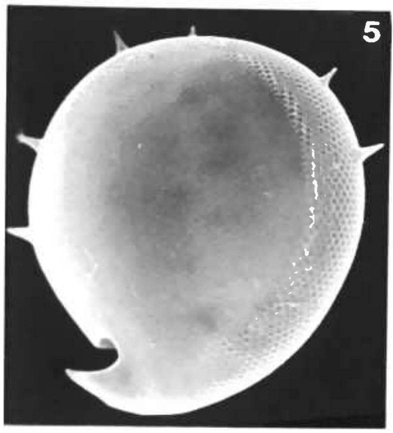

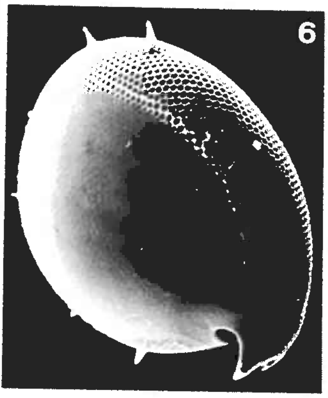

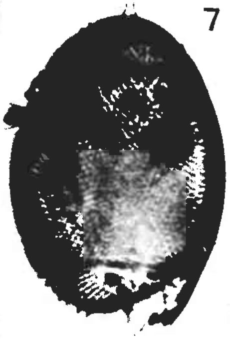

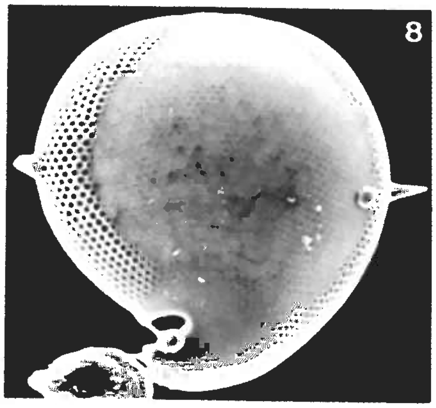

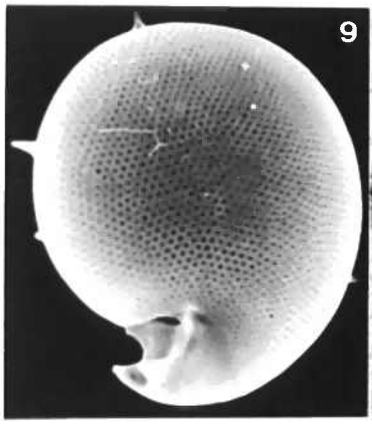

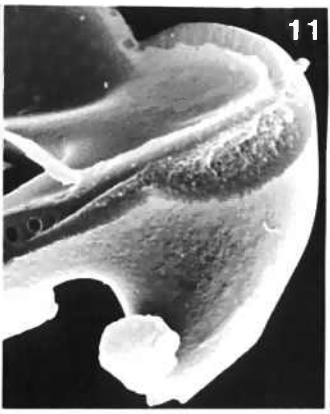

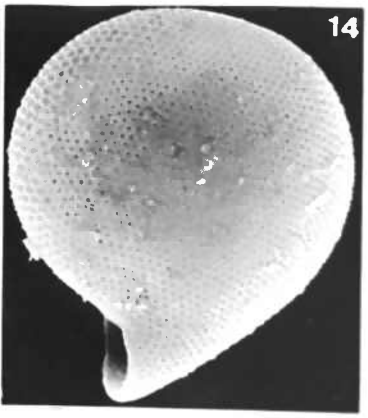

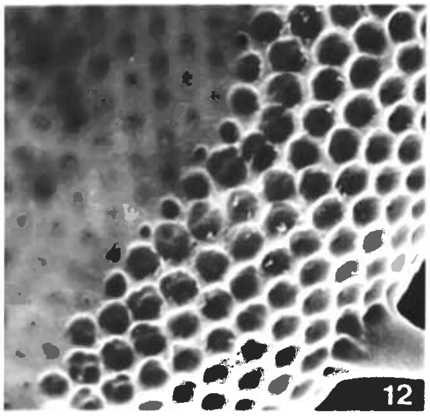

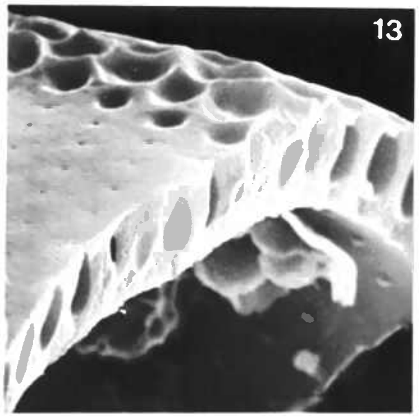

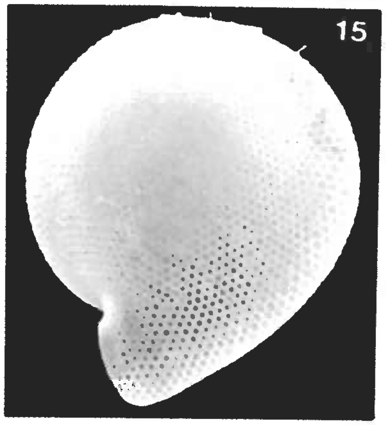

PLATE 50

Suborder: Phaeodaria
Family: Challengeriidae

Figure		Station Depth	Type of Micrograph	Magnification
1	*Protocystis honjoi* n.sp. Paratype	PB1268m	SEM	x280
2	*Protocystis honjoi* n.sp. Holotype	PB2869m	LM	x210
3	*Protocystis tridentata* Borgert A specimen with blue tint.	PB2869m	LM	x210
4	*Protocystis auriculata* n.sp. Oblique ventral view; paratype.	PB1268m	SEM	x440
5	*Protocystis auriculata* n.sp. Lateral view; paratype.	PB1268m	SEM	x440
6	*Protocystis auriculata* n.sp. Lateral view; holotype.	PB2869m	LM	x210
7	*Protocystis auriculata* n.sp. Oblique ventral view; paratype	PB2869m	LM	x210
8	*Protocystis aduncicuspis* n.sp. Paratype.	PB3791m	SEM	x220
9	*Protocystis aduncicuspis* n.sp. Holotype.	PB3791m	LM	x210
10	*Protocystis aduncicuspis* n.sp.	PB2869m	LM	x210
11	*Protocystis* sp. B	PB3791m	SEM	x165
12	*Protocystis sloggetti* (Haeckel)	PB1268m	LM	x210
13	*Protocystis sloggetti* (Haeckel)	$P_1$978m	SEM	x120
14	*Protocystis sloggetti* (Haeckel) A purposely broken specimen, note many spherical organic aggregates inside of the shell.	PB1268m	SEM	x160
15	*Protocystis sloggetti* (Haeckel) A specimen with broken teeth.	PB1268m	SEM	x250
16	*Protocystis murrayi* (Haeckel) Ventral view	$P_1$2778m	LM	x210
17	*Protocystis murrayi* (Haeckel) Microstructure showing a cross section of amphorae and outside surface.	$P_1$2778m	SEM	x2500
18	*Protocystis murrayi* (Haeckel) Same specimen, the amphorae are buried in the siliceous cement and pores are open.	$P_1$2778m	SEM	x3600

PLATE 50 Phaeodaria

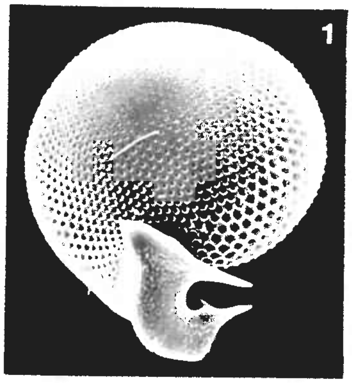
1

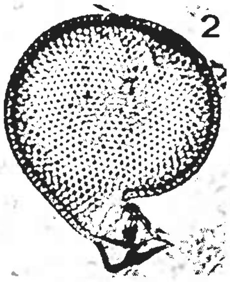
2

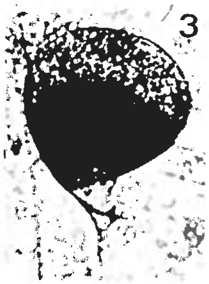
3

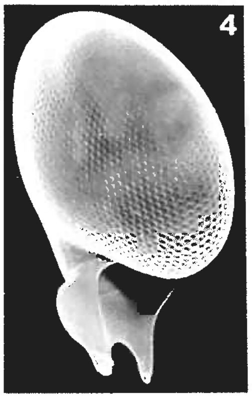
4

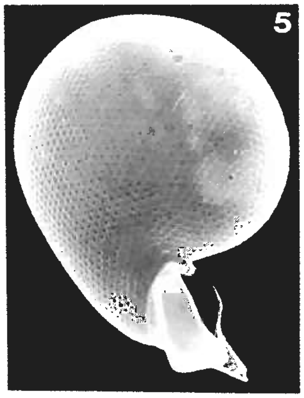
5

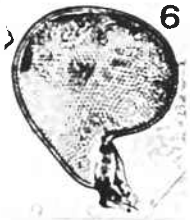
6


7

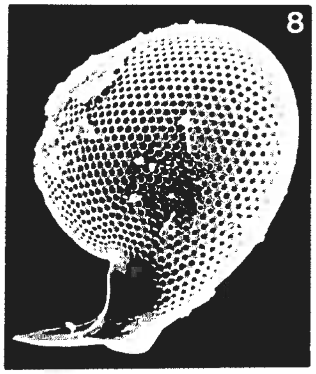
8


9

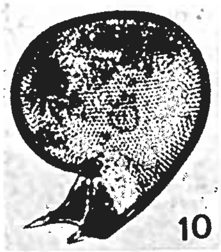
10

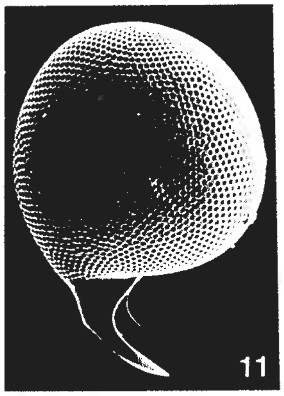
11

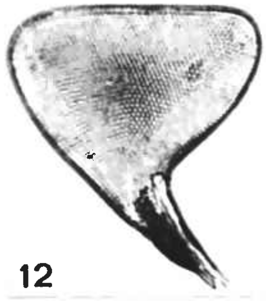
12

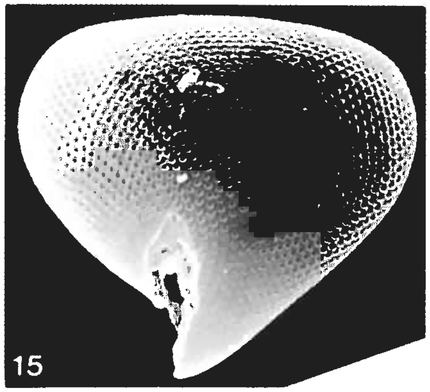
15

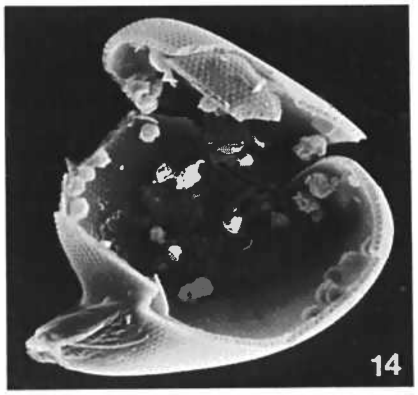
14

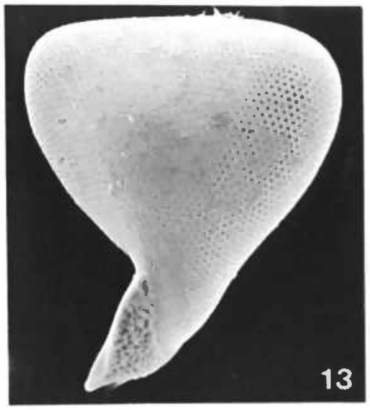
13

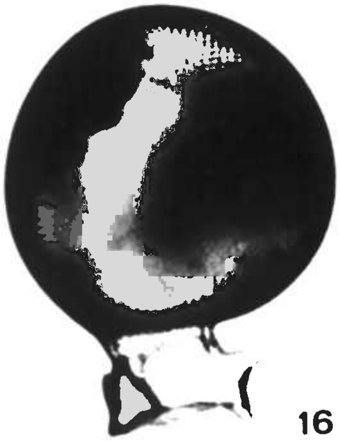
16

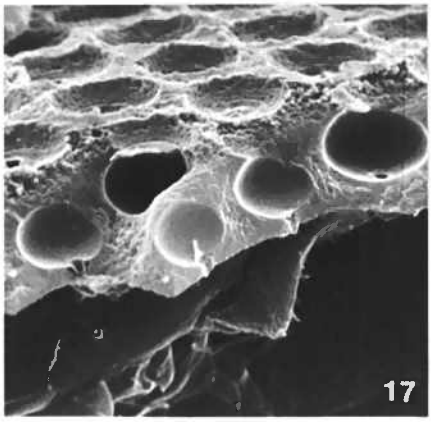
17

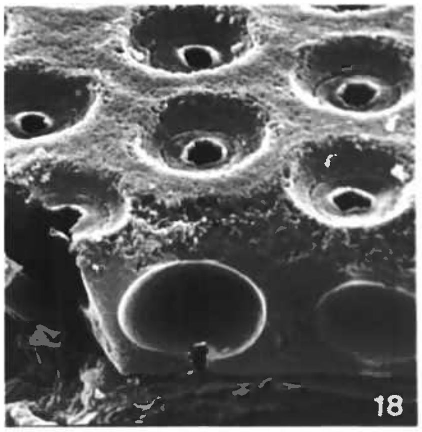
18

PLATE 51

Suborder: Phaeodaria
Family: Challengeriidae

Figure		Station Depth	Type of Micrograph	Magnification
1	*Protocystis murrayi* (Haeckel) Oral view	$P_1$2778m	SEM	x230
2	*Protocystis murrayi* (Haeckel) Ventral view	$P_1$2778m	SEM	x180
3	*Protocystis murrayi* (Haeckel) Lateral view	$P_1$2778m	SEM	x160
4	*Protocystis* sp. C Ventral view	$P_1$2778m	LM	x210
5	*Protocystis thomsoni* (Murray) Lateral view	E988m	LM	x210
6	*Pharyngella gastrula* Haeckel Dorsal view	E988m	SEM	x100
7	*Pharyngella gastrula* Haeckel Lateral view	E988m	SEM	x90
8	*Pharyngella gastrula* Haeckel Dorsal view	E988m	LM	x210
9	*Pharyngella gastrula* Haeckel Inside view showing detail of a pharynx.	E988m	SEM	x320
10	*Pharyngella gastrula* Haeckel Microstructure showing amphorae and partially peeled off inside surface membrane.	E988m	SEM	x9000
11	*Pharyngella gastrula* Haeckel Microstructure showing amphorae and outside surface.	E988m	SEM	x3200
12	*Pharyngella gastrula* Haeckel Lateral view of a pharynx.	E988m	SEM	x340
13	*Pharyngella gastrula* Haeckel Same specimen, microstructure of the peristome.	E988m	SEM	x1400
14	*Pharyngella gastrula* Haeckel Same specimen, an enlarged view of figs. 12-13. Note that this structure is a lateral cross section of amphorae which are slightly different in size and shape from those in main part of the shell.	E988m	SEM	x3000

PLATE 51 Phaeodaria

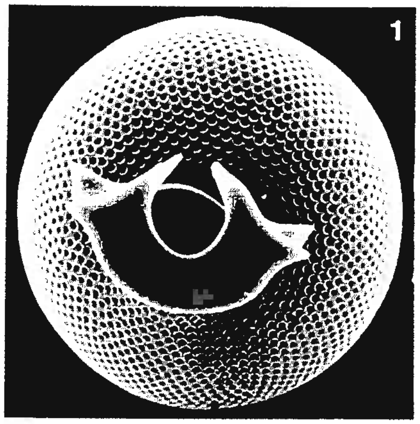

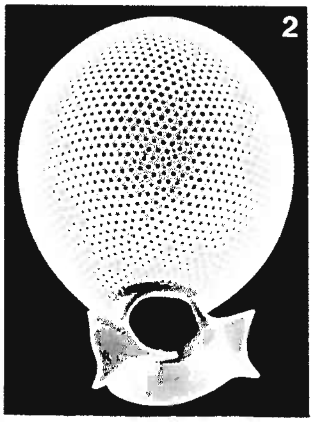

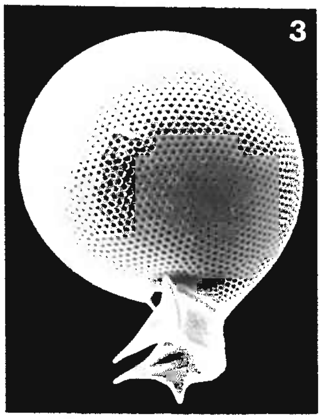

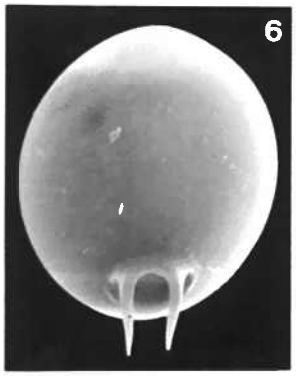

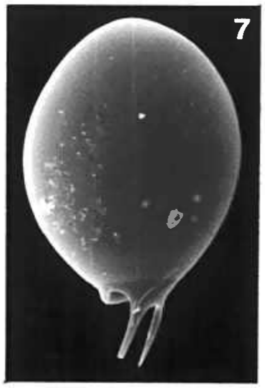

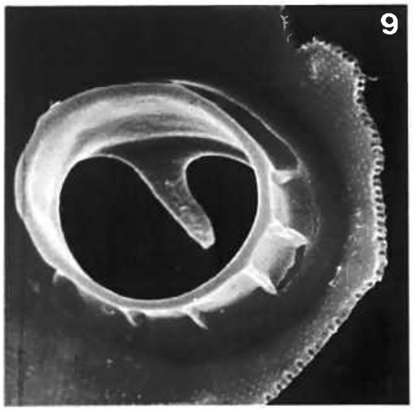

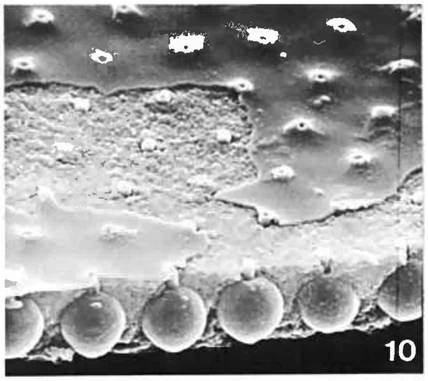

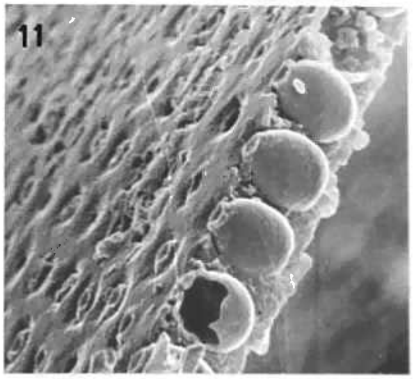

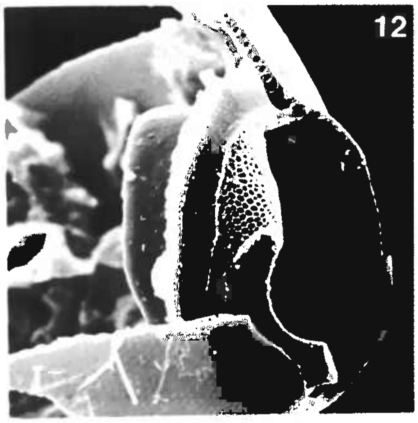

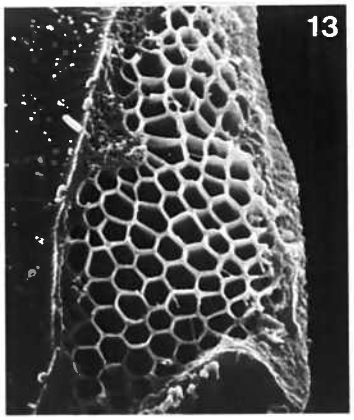

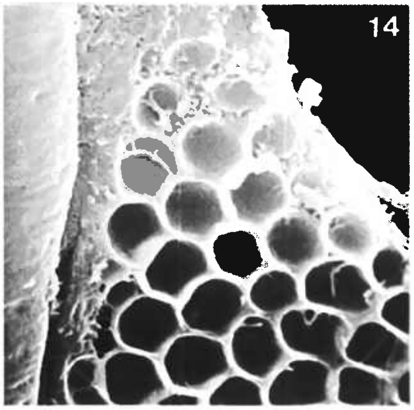

PLATE 52

Suborder: Phaeodaria
Family: Challengeriidae

Figure		Station Depth	Type of Micrograph	Magnification
1	*Protocystis xiphodon* (Haeckel)	PB1268m	SEM	x220
2	*Protocystis xiphodon* (Haeckel)	PB1268m	LM	x210
3	*Protocystis xiphodon* (Haeckel) View from inside of a broken specimen showing amphorae and their necks securing themselves to inside surface membrane.	PB1268m	SEM	x4700
4	*Protocystis tritonis* (Haeckel)	E389m	LM	x210
5	*Protocystis tritonis* (Haeckel)	E389m	LM	x210
6	*Protocystis naresi* (Murray) Lateral view	E988m	SEM	x47
7	*Protocystis naresi* (Murray) Microstructure showing amphorae which are slightly more elongated than those in other 16 species of Challengeriidae.	E988m	SEM	x3600
8	*Protocystis naresi* (Murray) Oblique oral view.	E988m	SEM	x75
9	*Entocannula infundibulum* Haeckel	PB1268m	LM	x160
10	*Entocannula infundibulum* Haeckel	PB3769m	SEM	x110
11	*Challengeranium diodon* (Haeckel) Microstructure showing delicate amphorae which have many small pores connected with inside of the shell.	PB1268m	SEM	x4000
12	*Challengeranium diodon* (Haeckel) Shell surface is alveolate and very different from all other *Challengeriidae* studied here, dorsal view.	PB1268m	SEM	x900
13	*Challengeranium diodon* (Haeckel) Lateral view	PB1268m	LM	x210
14	*Challengeranium diodon* (Haeckel) Oblique ventral view	PB389m	LM	x210
15	*Challengeranium diodon* (Haeckel) Ventral view	PB667m	LM	x210
16	*Challengeranium diodon* (Haeckel) Ventral view	E988	SEM	x385

PLATE 52 Phaeodaria

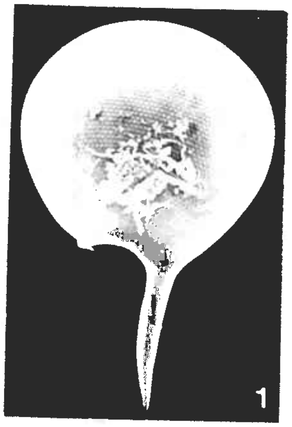
1


2


4

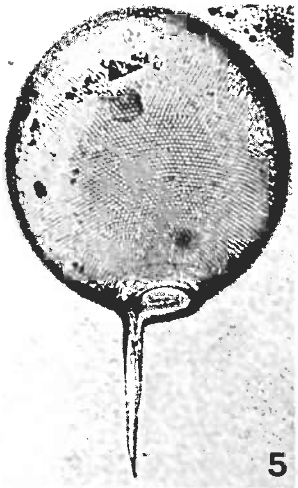
5


6

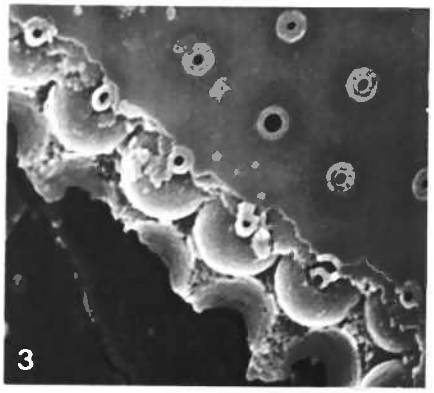
3


7

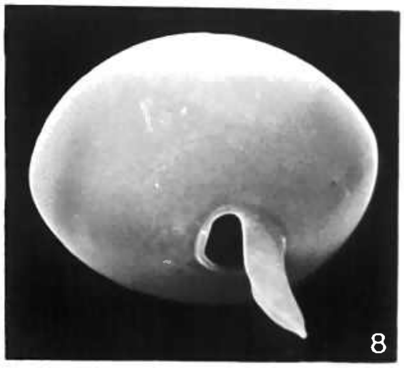
8

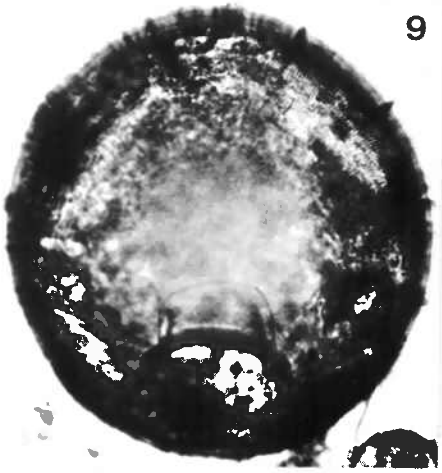
9

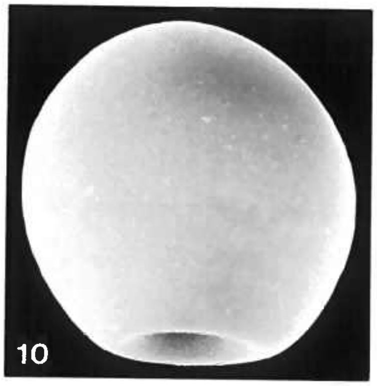
10

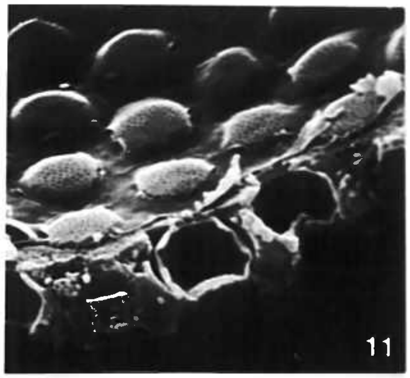
11

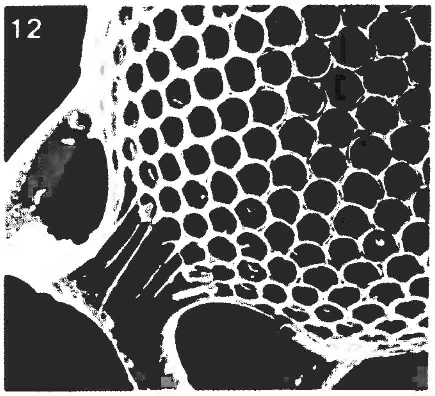
12


13


14


15

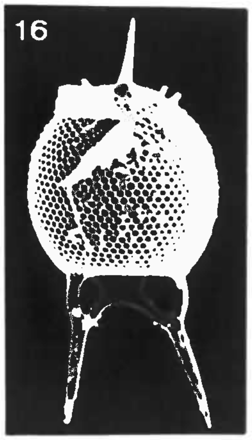
16

PLATE 53

Suborder: Phaeodaria
Family: Medusettidae

Figure		Station Depth	Type of Micrograph	Magnification
1	*Euphysetta elegans* Borgert Ventral view	$P_1$2778m	LM	x210
2	*Euphysetta elegans* Borgert Lateral view	PB2869m	LM	x210
3	*Euphysetta elegans* Borgert Oblique lateral view	$P_1$978m	SEM	x280
4	*Euphysetta elegans* Borgert Oblique ventral view	$P_1$2778m	SEM	x230
5	*Euphysetta elegans* Borgert Ventral view	$P_1$978m	SEM	x290
6	*Euphysetta elegans* Borgert Specimen with a long apical horn and a foot. Ventral view.	E3755m	SEM	x320
7	*Euphysetta elegans* Borgert Specimen with a long apical horn and a foot. Lateral view.	PB2869m	LM	x210
8	*Euphysetta elegans* Borgert Cross section across oblique transverse plane including the base of large foot. Specimen ashed at 500°C for one hour.	PB2869m	TEM	x1300
9	*Euphysetta elegans* Borgert Microstructure showing two layers of large pores, additional layers of small pores and inside shell surface.	PB1268m	SEM	x4460
10	*Euphysetta elegans* Borgert Micro- and ultrastructures showing circular pores and alveolate outside surface; note porosity varies from one part to another and wavy lines are artifact of the sectioning.	PB1268m	TEM	x6700
11	*Euphysetta staurocodon* Haeckel A small specimen with blue tint, lateral view.	PB2869m	LM	x210
12	*Euphysetta staurocodon* Haeckel A large specimen with spherical shells and blue tint, lateral view.	$P_1$2778m	LM	x210
13	*Euphysetta staurocodon* Haeckel Lateral view	PB3769m	SEM	x410
14	*Euphysetta staurocodon* Haeckel A specimen with blue tint, ventral view.	PB2869m	LM	x210
15	*Euphysetta pusilla* Cleve	E389m	LM	x850

PLATE 53 Phaeodaria

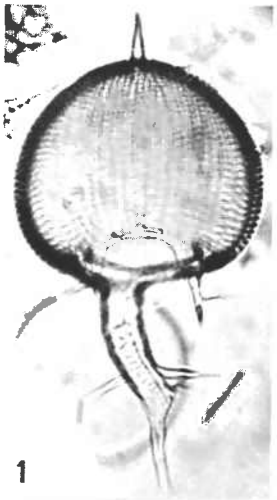
1


2

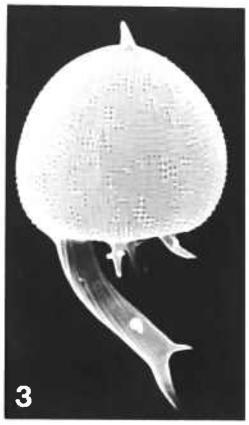
3

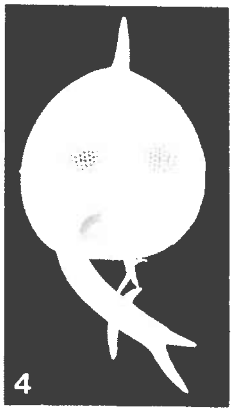
4

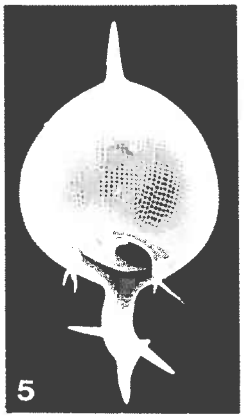
5

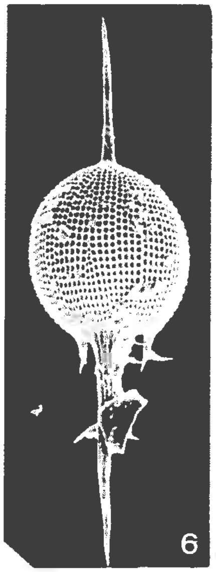
6

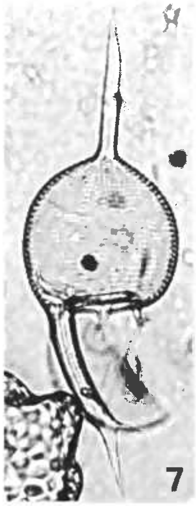
7

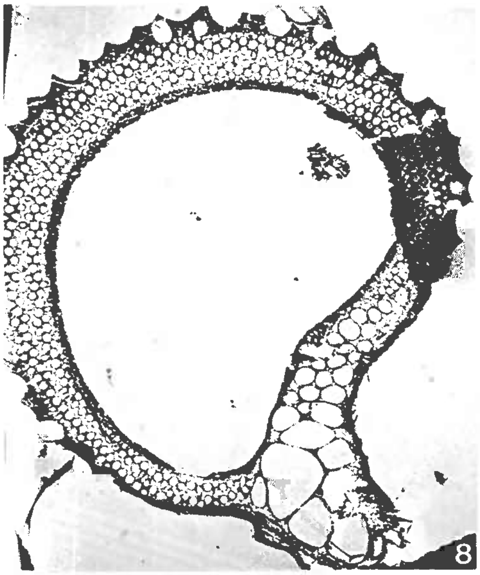
8

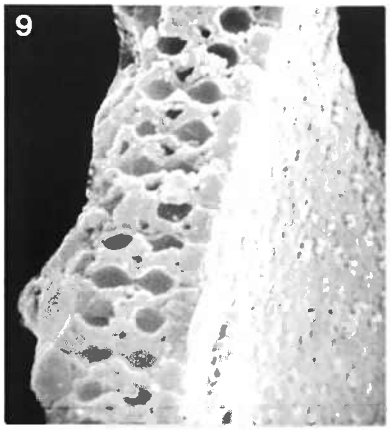
9

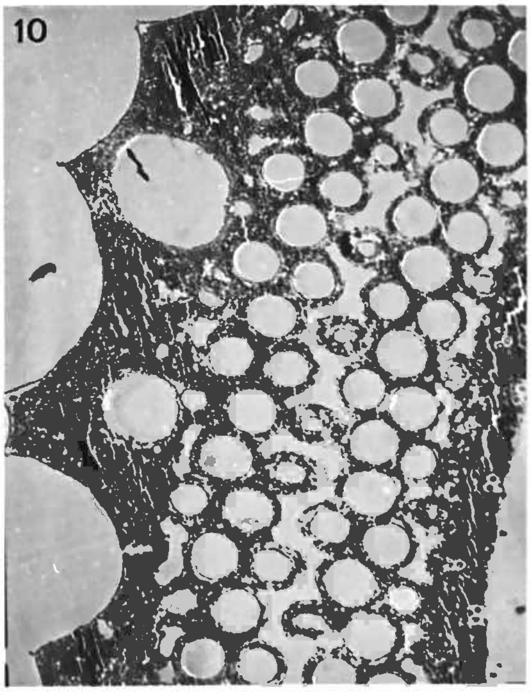
10


11

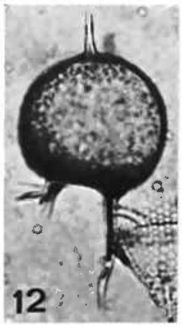
12


13

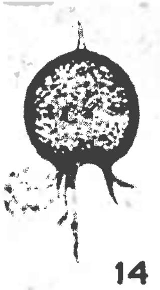
14


15

PLATE 54

Suborder: Phaeodaria
Family: Medusettidae, Lirellidae

Figure		Station Depth	Type of Micrograph	Magnification
1	*Medusetta ansata* Borgert	E389m	SEM	x450
2	*Medusetta ansata* Borgert	PB3769m	LM	x210
3	*Medusetta ansata* Borgert	E389m	LM	x210
4	*Medusetta ansata* Borgert	E389m	LM	x210
5	*Medusetta ansata* Borgert Cross section of the shell showing rectangular pores	E389m	SEM	x6400
6	*Medusetta ansata* Borgert	PB2869m	SEM	x280
7	*Medusetta ansata* Borgert	$P_1$2778m	LM	x210
8	*Medusetta* sp.	E389m	LM	x210
9	*Medusetta* sp.	E389m	LM	x210
10	*Euphysetta lucani* Borgert	$P_1$978m	SEM	x170
11	*Euphysetta lucani* Borgert View from oral side showing sub-triangular perimeter.	E3755m	SEM	x230
12	*Euphysetta lucani* Borgert	E3755m	LM	x210
13	*Borgetella candata* (Wallich)	$P_1$4280m	SEM	x4500
14	*Borgetella candata* (Wallich) Note that the hollow ring is attached to the outisde of the shell near the peristome.	PB3769m	SEM	x830
15	*Borgetella candata* (Wallich)	PB3769m	SEM	x830
16	*Borgetella candata* (Wallich)	E389m	LM	x850
17	*Borgetella candata* (Wallich)	$P_1$4280m	SEM	x470

PLATE 54 Phaeodaria

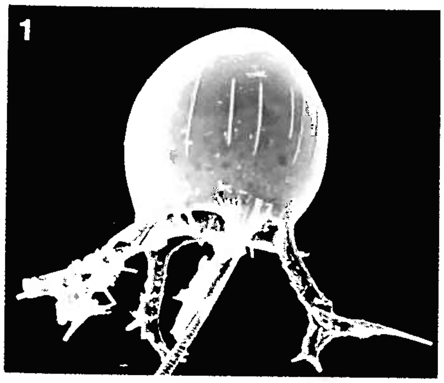

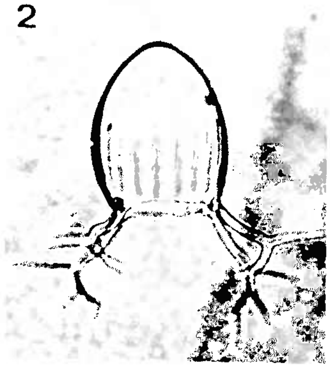

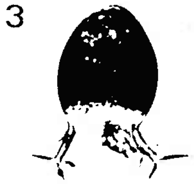

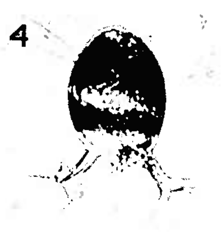

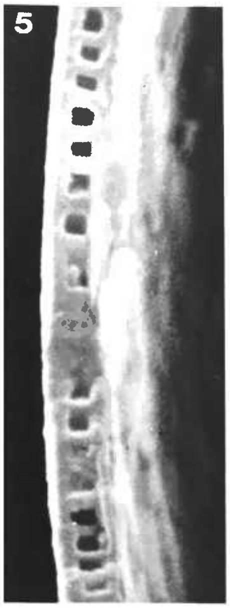

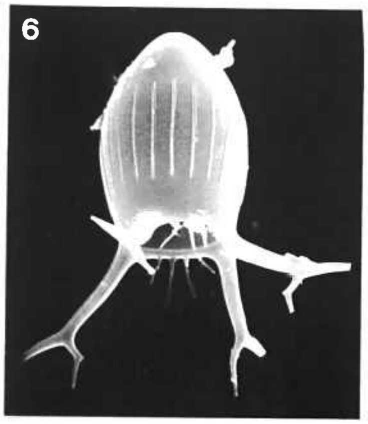

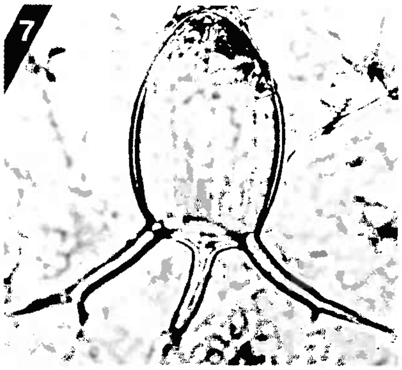

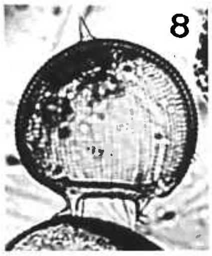

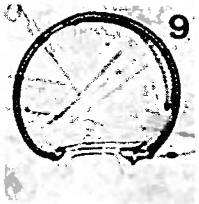

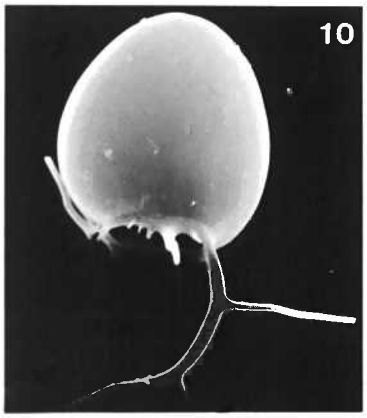

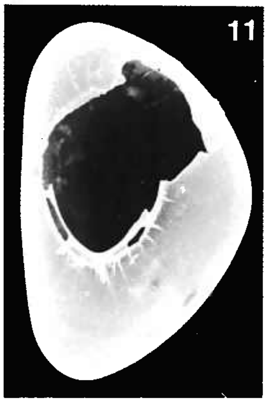

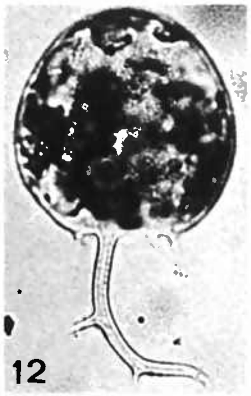

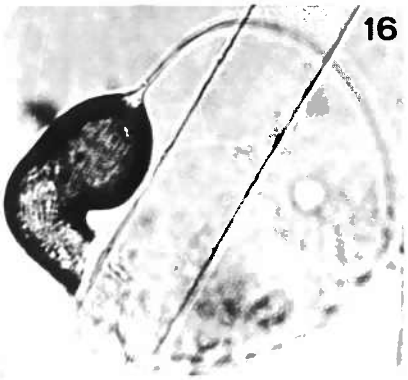

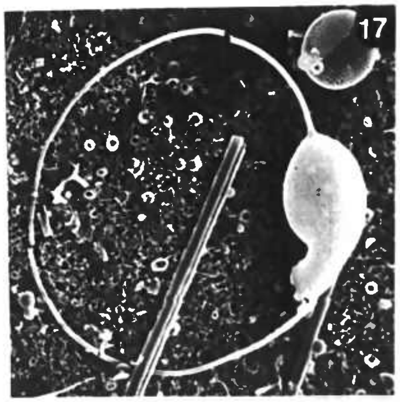

PLATE 55

Suborder: Phaeodaria
Family: Lirellidae

Figure		Station Depth	Type of Micrograph	Magnification
1	*Borgetella candata* (Wallich) The hollow ring	PB3769m	SEM	x4410
2	*Borgetella candata* (Wallich)	PB3769m	SEM	x990
3	*Borgetella candata* (Wallich) Specimen of slightly dissolved.	PB3769m	SEM	x1100
4	*Borgetella candata* (Wallich) Specimen of extensively dissolved and lost integrity of wavy crests and striae.	PB3769m	SEM	x660
5	*Borgetella candata* (Wallich) Same specimen, pores showing hexagonal meshwork.	PB3769m	SEM	x2480
6	*Borgetella candata* (Wallich) Penetration of electron beam provides viewing of skeletal internal structure made of hexagonal meshwork.	PB3769m	SEM	x2260
7	*Lirella baileyi* Ehrenberg	PB3769m	SEM	x830
8	*Lirella bullata* (Stadum and Ling) Ventral view.	PB3769m	SEM	x880
9	*Lirella bullata* (Stadum and Ling) Oblique ventral view.	PB3769m	SEM	x740
10	*Lirella bullata* (Stadum and Ling) Oblique apical view.	E3755m	SEM	x1290
11	*Lirella bullata* (Stadum and Ling) Lateral view.	PB1268m	LM	x850
12	*Lirella melo* (Cleve)	PB1268m	SEM	x470
13	*Lirella melo* (Cleve) Same specimen	PB1268m	SEM	x600
14	*Lirella melo* (Cleve)	E3755m	SEM	x370
15	*Lirella melo* (Cleve)	PB3769m	SEM	x550
16	*Lirella melo* (Cleve)	PB3769m	SEM	x410
17	*Lirella melo* (Cleve)	PB2869m	LM	x210
18	*Lirella melo* (Cleve)	PB2869m	LM	x210
19	*Lirella tortuosa* n.sp. Right coiled; paratype.	PB2869m	LM	x210
20	*Lirella tortuosa* n.sp. Left coiled; paratype.	PB1268m	LM	x210

PLATE 55 Phaeodaria


1


2

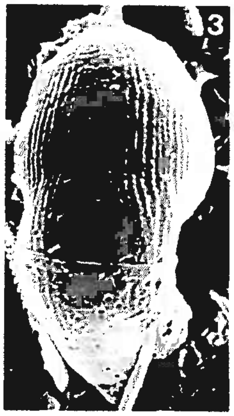
3


4

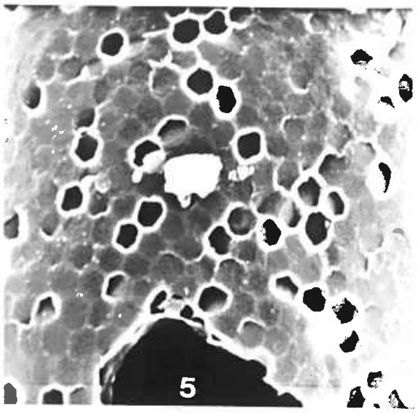
5

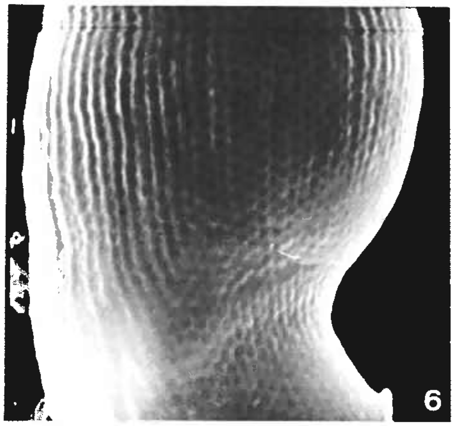
6

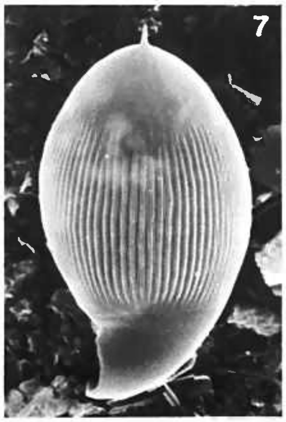
7

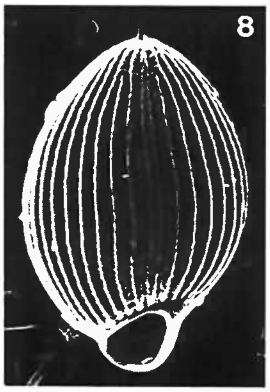
8


9

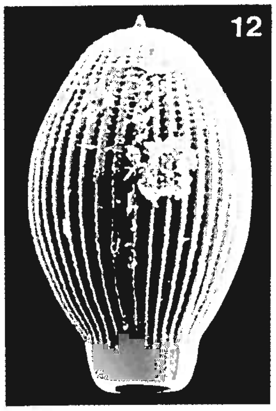
12


13

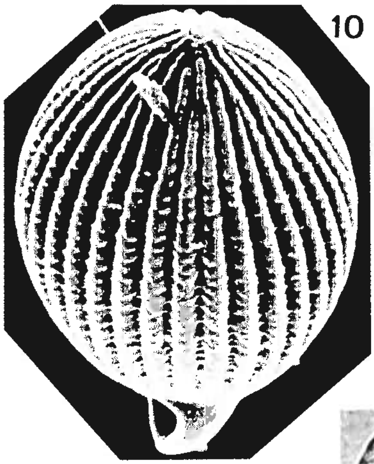
10


11

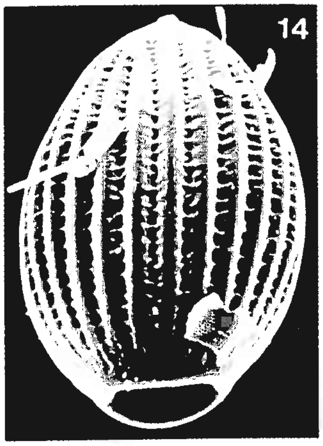
14

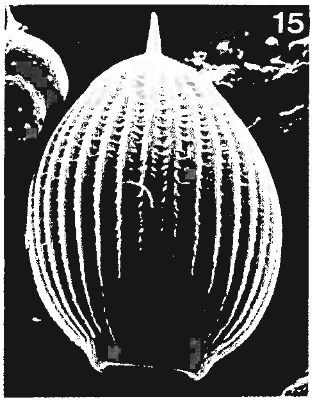
15

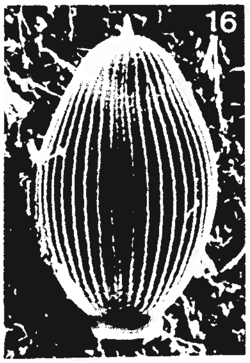
16


17


18


19


20

PLATE 56

Suborder: Phaeodaria
Family: Lirellidae

Figure		Station Depth	Type of Micrograph	Magnification
1	*Lirella bullata* (Stadum and Ling) Same specimen as Pl. 55, fig. 10. Detail of wavy crests and striae.	E3755m	SEM	x6400
2	*Lirella melo* (Cleve) Cross section of a part of peristome showing several layers of different porosity.	PB1268m	SEM	x3000
3	*Lirella melo* (Cleve) Cross section corresponding to fig. 2 showing polygonal meshwork in the central part and two other layers of different porocity, specimen ashed at 500°C for one hour.	PB2869m	TEM	x8300
4	*Lirella melo* (Cleve) Same specimen.	PB2869m	TEM	x2000
5	*Lirella melo* ? (Cleve) Extensively dissolved specimen losing its shell integrity	PB3769m	SEM	x1600
6	*Lirella melo* (Cleve) Cross section showing polygonal meshwork and the pores.	PB1268m	SEM	x5000
7	*Lirella melo* (Cleve) Same specimens as fig. 3, cross section showing polygonal meshwork and porous outer layers, note that the polygons are made of tubes.	$P_1$978m	TEM	x7600
8	*Lirella melo* (Cleve) Cross section showing irregular pores bounded by tubular structure which is different from figs. 3,7.	$P_1$4280m	TEM	x6100
9	*Lirella tortuosa* n.sp. Right coiled; paratype.	PB1268m	SEM	x500
10	*Lirella tortuosa* n.sp. Left coiled; holotype.	$P_1$4280m	SEM	x450
11	*Lirella tortuosa* n.sp. Right coiled.	$P_1$4280m	SEM	x470

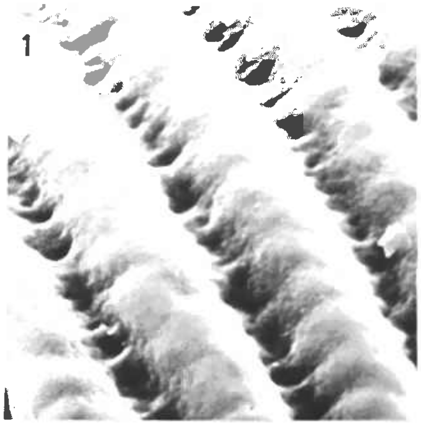
1

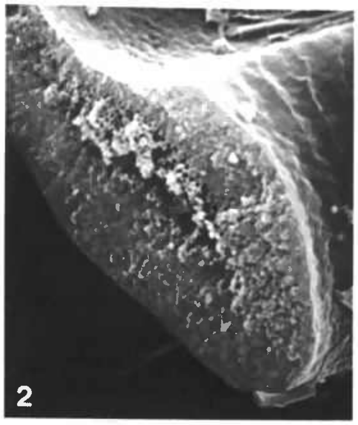
2

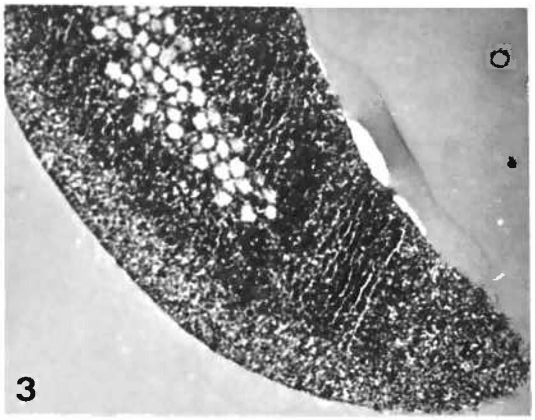
3

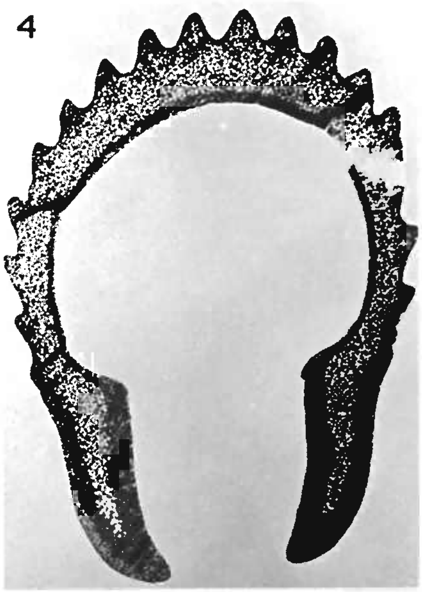
4


5


6


7


8

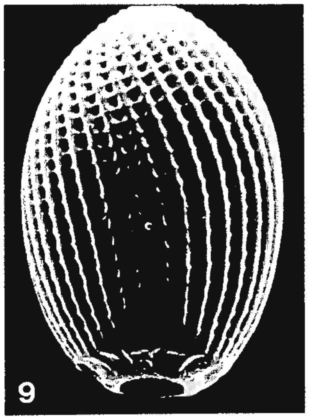
9


10


11

PLATE 57

Suborder: Phaeodaria
Family: Porospathididae, Castanellidae

Figure		Station Depth	Type of Micrograph	Magnification
1	*Porospathis holostoma* (Cleve) Oblique ventral view	$P_1$978m	SEM	x130
2	*Porospathis holostoma* (Cleve) Lateral view	$P_1$4280m	SEM	x165
3	*Porospathis holostoma* (Cleve) Lateral view	PB3791m	LM	x210
4	*Porospathis holostoma* (Cleve) Ventral view	$P_1$2778m	LM	x380
5	*Porospathis holostoma* (Cleve) Lateral view	PB3769m	SEM	x360
6	*Porospathis holostoma* (Cleve) Same specimen as fig. 1, showing detail of surface morphology near the projected tube-like mouth.	$P_1$978m	SEM	x1300
7	*Porospathis holostoma* (Cleve) Same specimen as fig. 5, surface detail morphology.	PB3769m	SEM	x5500
8	*Porospathis holostoma* (Cleve) Same specimen as fig. 2, cross section near a spine.	$P_1$4280m	SEM	x2200
9	*Castanidium longispinum* Haecker	PB667m	SEM	x70
10	*Castanidium longispinum* Haecker	PB1268m	LM	x106
11	*Castanidium longispinum* Haecker	Gulf of Oman, surface plankton tow	SEM	x55
12	*Castanidium longispinum* Haecker	P2778m	SEM	x130
13	*Castanidium longispinum* Haecker	PB3791m	LM	x65

PLATE 57 Phaeodaria

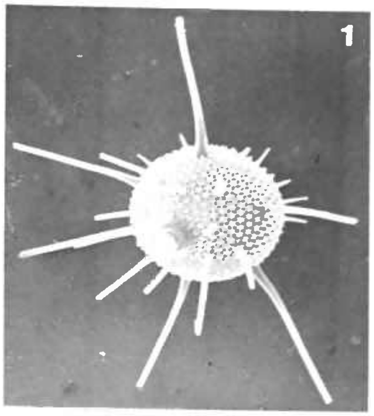
1

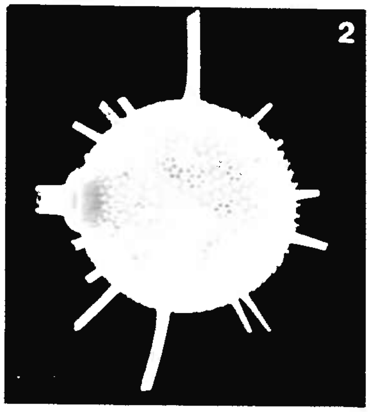
2

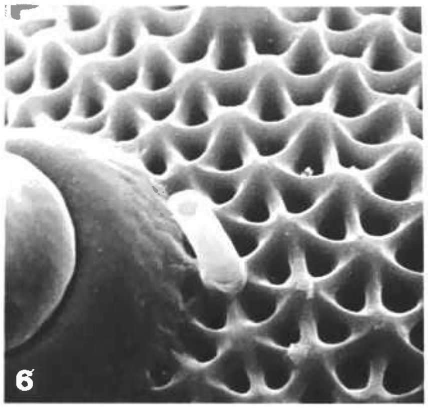
6

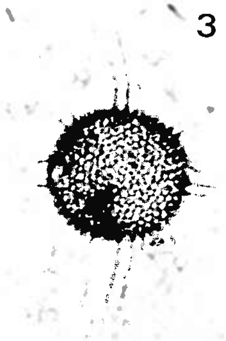
3

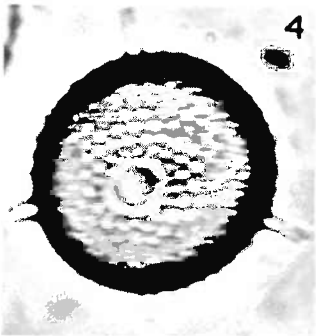
4

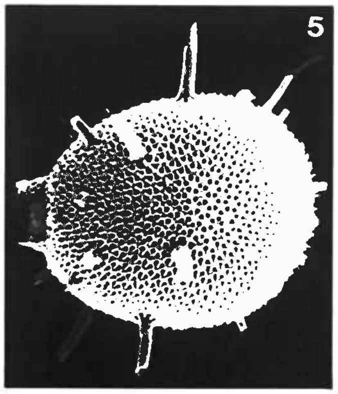
5

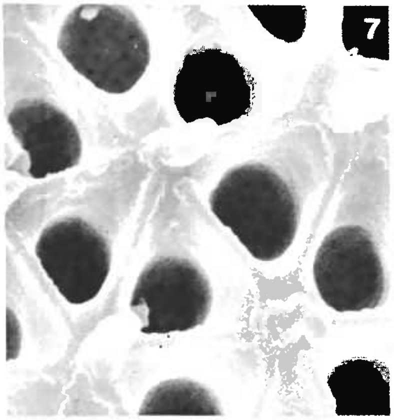
7

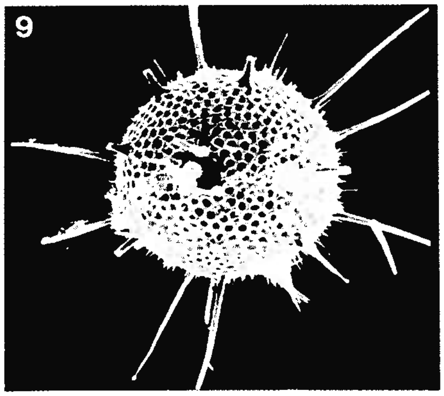
9

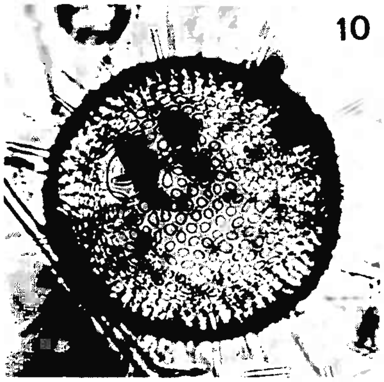
10

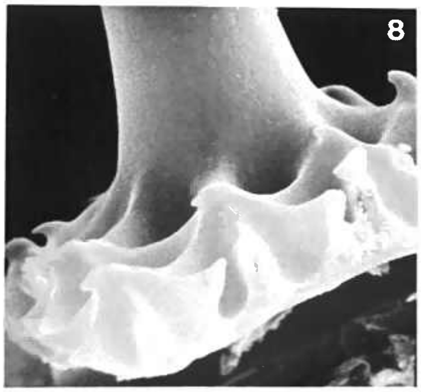
8

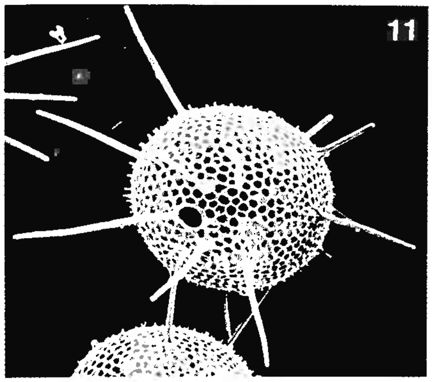
11

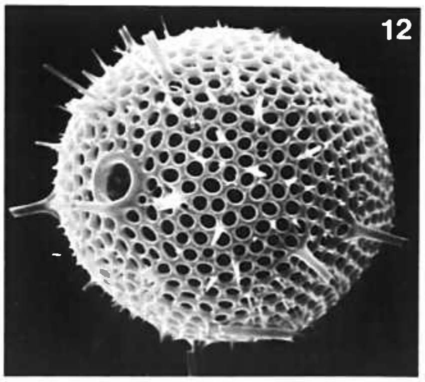
12

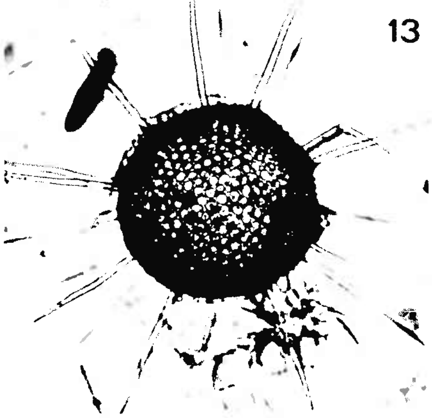
13

PLATE 58

Suborder: Phaeodaria
Family: Castanellidae

Figure		Station Depth	Type of Micrograph	Magnification
1	*Castanidium longispinum* Haecker Primary feature of relatively solid unit having ca. 150-800 angstrom pores in the central part of skeleton; the conchoidal fractures are artifact with the sectioning.	PB 0-100 plankton tow	TEM	x17,000
2	*Castanidium longispinum* Haecker Cross section of relatively undissolved specimen showing brittle texture of the broken surface.	E389m	SEM	x1920
3	*Castanidium longispinum* Haecker Secondary feature due to dissolution having pores bounded by tubular skeleton.	PB1268m	TEM	x5600
4	*Castanidium longispinum* Haecker Corresponding morphology to fig. 3; note presence of the slit-like space which occasionally observed in many specimens.	PB667	SEM	x2260
5	*Castanidium abundiplanatum* n.sp. Elongated specimen, an early stage of binary fission ?.	PB3769m	SEM	x60
6	*Castanidium abundiplanatum* n.sp. Two specimens splitting apart.	PB3769m	SEM	x55
7	*Castanidium abundiplanatum* n.sp. Holotype	PB1268m	LM	x105
8	*Castanidium abundiplanatum* n.sp. Paratype	PB3769m	SEM	x90
9	*Castanissa circumvallata* Schmidt Bi-spines broken off.	E389m	SEM	x130
10	*Castanidium* sp.	PB3769m	SEM	x66
11	*Castanella aculeata* Schmidt	$P_1$4280m	SEM	x90
12	*Castanella macropora* (Borgert)	$P_1$4280m	SEM	x200
13	*Castanella aculeata* Schmidt	$P_1$978m	SEM	x80

PLATE 53 Phaeodaria

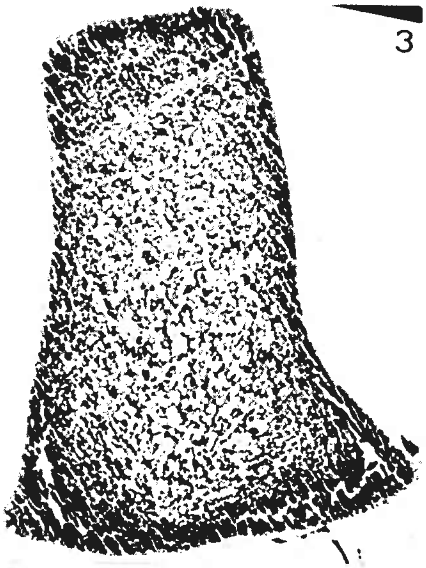

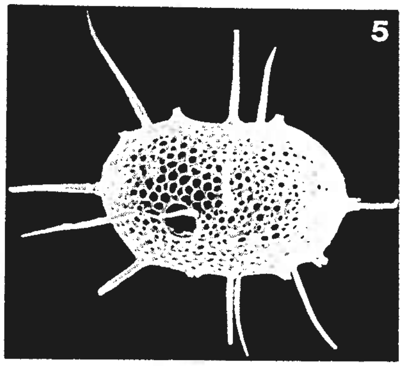

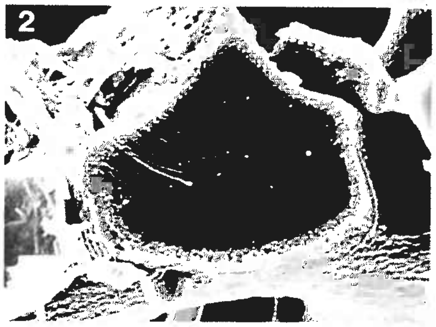

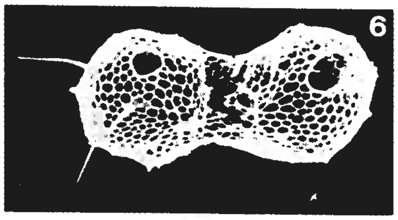

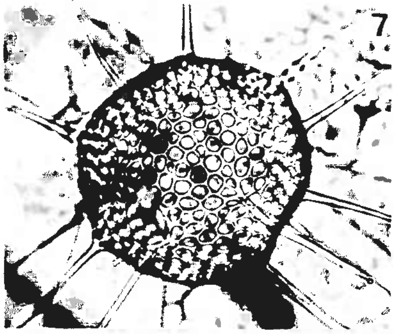

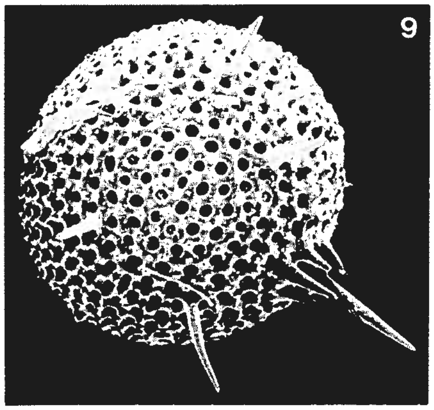

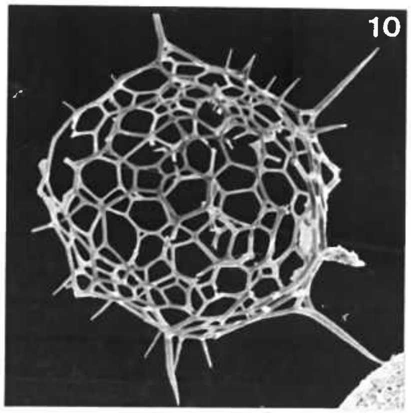

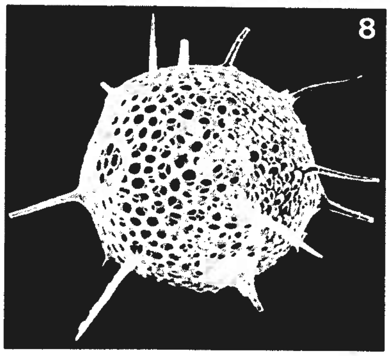

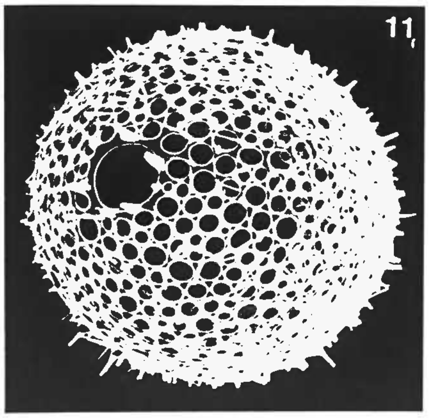

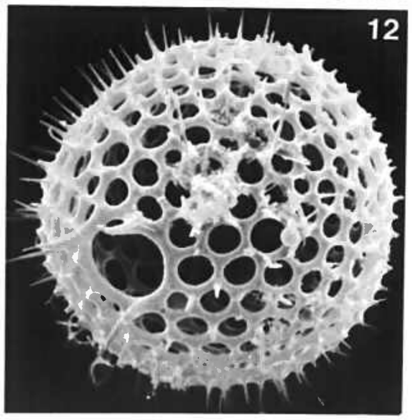

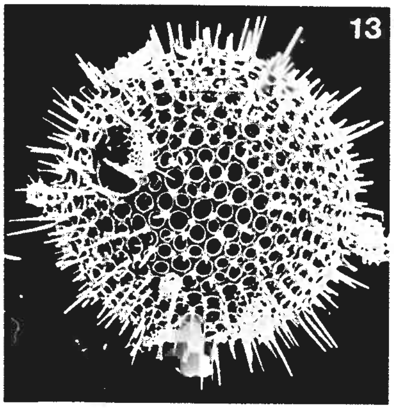

PLATE 59

Suborder: Phaeodaria
Family: Castanellidae, Circoporidae

Figure		Station Depth	Type of Micrograph	Magnification
1	<u>Castanella</u> <u>aculeata</u> Schmidt Typical specimen of having glassy texture.	E389m	RLM	x54
2	<u>Castanella</u> <u>sloggetti</u> Haeckel	$P_1$978m	LM	x106
3	<u>Castanella</u> <u>balfouri</u> Haeckel	$P_1$2778m	LM	x125
4	<u>Haeckeliana</u> <u>porcellana</u> Haeckel	$P_1$978m	LM	x100
5	<u>Haeckeliana</u> <u>porcellana</u> Haeckel	$P_1$978m	SEM	x77
6	<u>Haeckeliana</u> <u>porcellana</u> Haeckel	E988m	SEM	x64
7	<u>Haeckeliana</u> <u>porcellana</u> Haeckel A specimen without bi-spines	E988m	SEM	x130
8	<u>Haeckeliana</u> <u>porcellana</u> Haeckel A specimen without bi-spines	E988m	SEM	x190
9	<u>Haeckeliana</u> <u>porcellana</u> Haeckel An extensively dissolved specimen	$P_1$4280m	SEM	x100
10	<u>Haeckeliana</u> <u>porcellana</u> Haeckel A cross section showing porous inner layer and relatively solid outer layer.	$P_1$978m	SEM	x1490
11	<u>Haeckeliana</u> <u>porcellana</u> Haeckel A cross section showing porous and relatively solid layer	E988m	SEM	x2560
12	<u>Haeckeliana</u> <u>porcellana</u> Haeckel A cross sectional ultrastructure showing polygonal pores bounded by tubes.	$P_1$978m	TEM	x26,700
13	<u>Haeckeliana</u> <u>porcellana</u> Haeckel Same specimen, showing layers of several different morphology.	$P_1$978m	TEM	x7600

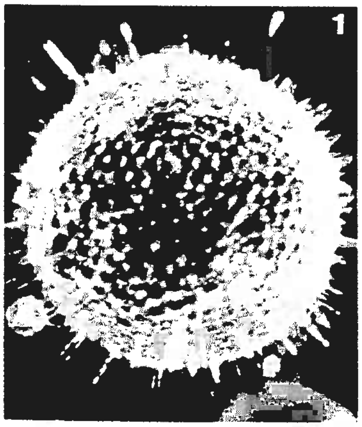
1

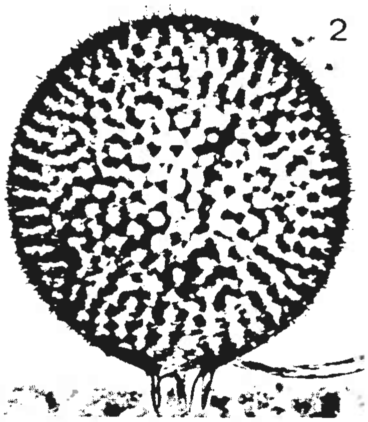
2

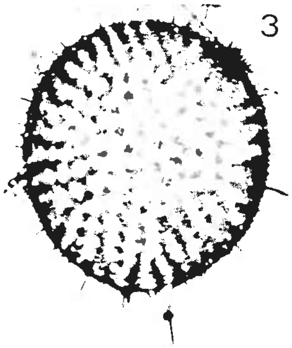
3

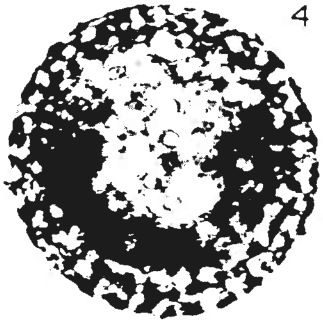
4

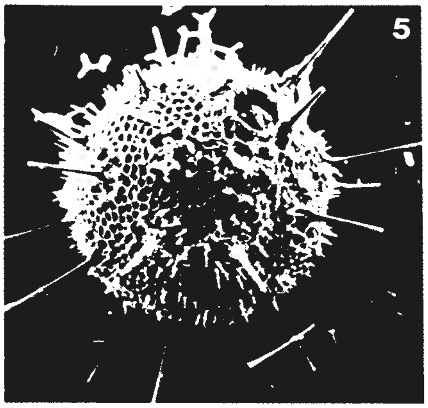
5

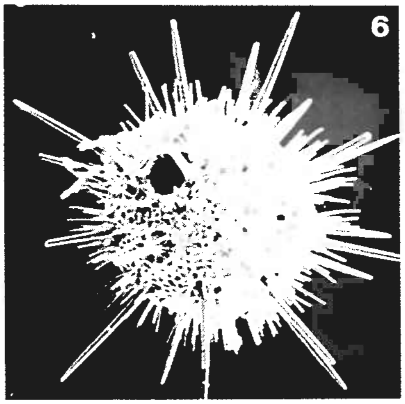
6

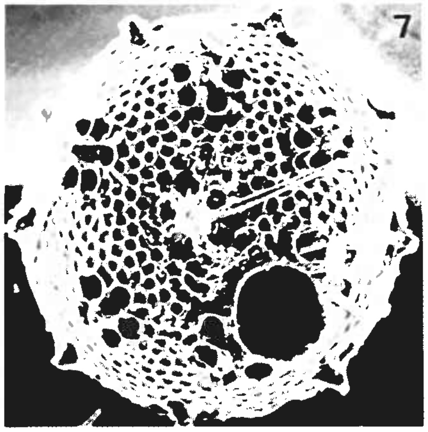
7

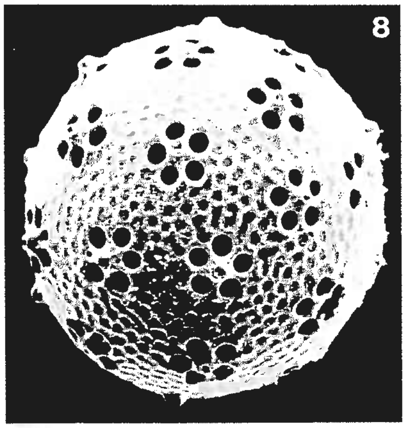
8

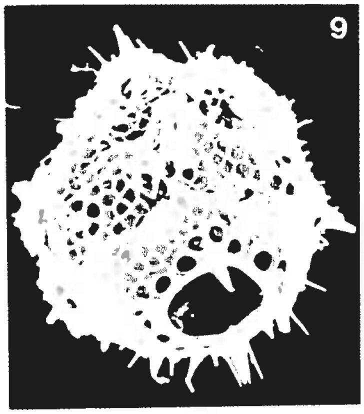
9

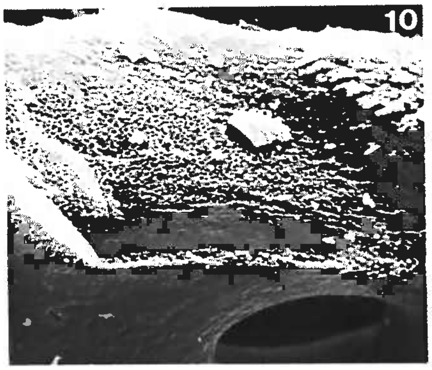
10

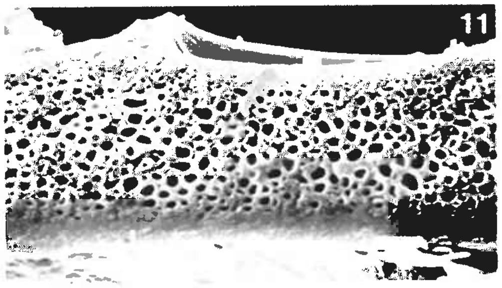
11

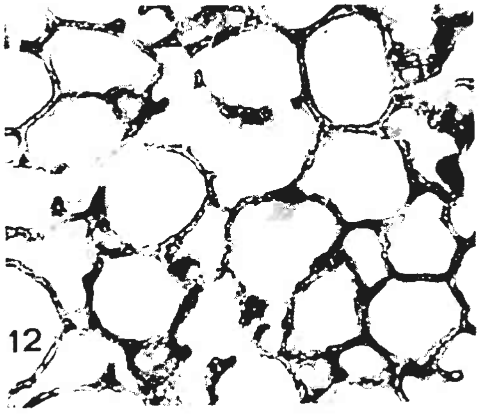
12


13

PLATE 60

Suborder: Phaeodaria
Family: Circoporidae

Figure		Station Depth	Type of Micrograph	Magnification
1	<u>Circoporous</u> <u>sexfuscinus</u> Haeckel	PB2869m	LM	x210
2	<u>Circoporous</u> <u>oxyacanthus</u> Borgert	PB3791m	LM	x210
3	<u>Circoporous</u> <u>sexfuscinus</u> Haeckel	PB667m	SEM	x165
4	<u>Circoporous</u> <u>oxycanthus</u> Borgert	E389m	SEM	x190
5	<u>Circoporous</u> <u>sexfuscinus</u> Haeckel Same specimen as fig. 3, view from oral side.	PB667m	SEM	x180
6	<u>Circoporous</u> <u>oxyacanthis</u> Borgert Detail near the base of a hollow spine which has fibers inside.	PB667m	SEM	x1500
7	<u>Circoporous</u> <u>oxyacanthus</u> Borgert Irregular size and shape of internal structure is seen through thin membrane.	PB667m	SEM	x1460
8	<u>Circoporous</u> <u>oxyacanthus</u> Borgert Circular to polygonal pores varying in size.	PB3769m	SEM	x2100
9	<u>Circogonia</u> sp.	E3755m	SEM	x90
10	<u>Circogonia</u> sp.	E389m	SEM	x100
11	<u>Circoporus</u> <u>oxyacanthus</u> Borgert Near the base of a spine.	PB667m	SEM	x1050
12	<u>Circoporus</u> <u>oxyacanthus</u> Borgert Same specimen	PB667m	SEM	x3030
13	<u>Circoporus</u> <u>oxyacanthus</u> Borgert A cross section across near the base of a spine; pores are variable in shape and size.	PB3769m	TEM	x2700

PLATE 60 Phaeodaria

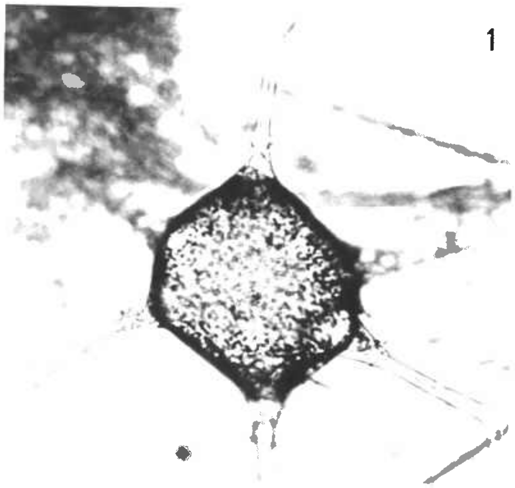
1

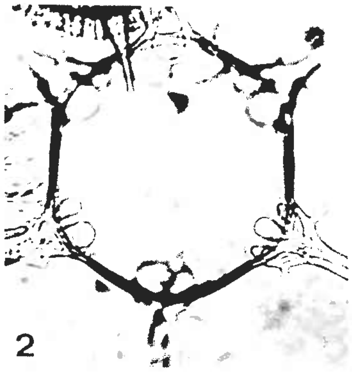
2

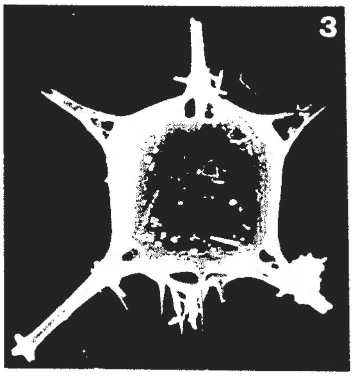
3

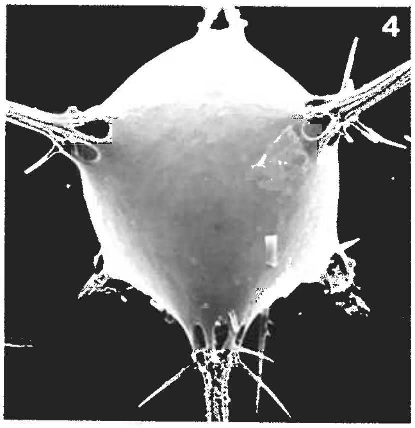
4


5

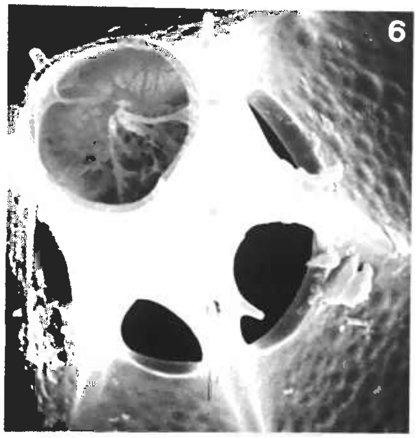
6

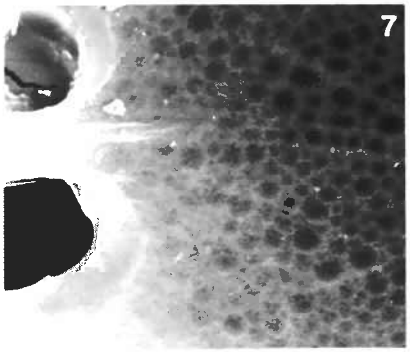
7

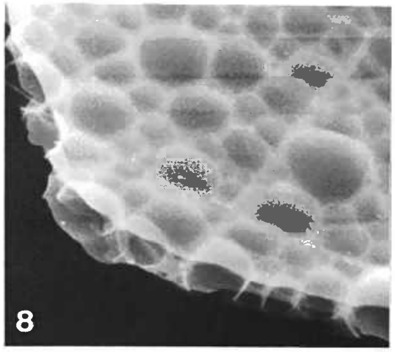
8


11


13

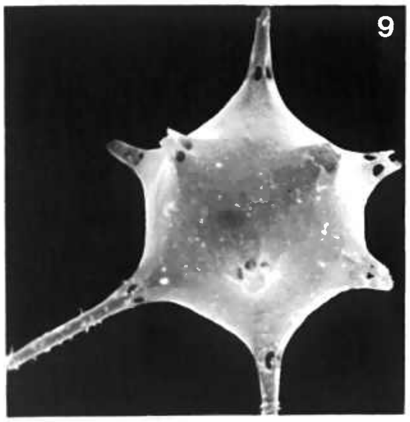
9

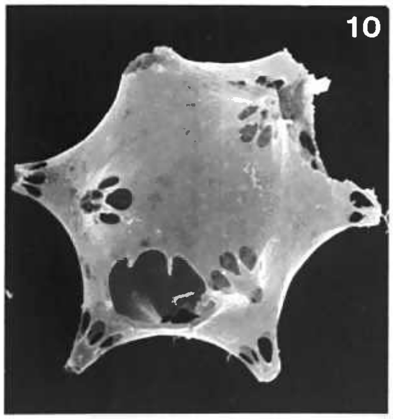
10


12

PLATE 61

Suborder: Phaeodaria
Family: Conchariidae

Figure		Station Depth	Type of Micrograph	Magnification
1	*Conchellium capsula* Borgert Lateral view	E389m	LM	x210
2	*Conchellium capsula* Borgert A cross section of having central solid parts, porous layer and less porous outer layer.	E3775m	TEM	x11,900
3	*Conchellium capsula* Borgert A relatively undissolved specimen having only outermost thin layer porous.	$P_1$2778m	TEM	x11,900
4	*Conchellium capsula* Borgert Lateral view	E389m	SEM	x150
5	*Conchellium capsula* Borgert View from inside of a valve	E389m	LM	x210
6	*Conchellium tridacna* Haeckel Oblique lateral view	E3755m	SEM	x120
7	*Conchellium capsula* Borgert Oral view	E389m	SEM	x150
8	*Conchellium capsula* Borgert Oblique view from inside of a valve	$P_1$2778m	SEM	x180
9	*Conchellium tridacna* Haeckel Surface texture of having six denticles and less marked triangular facets than those shown by Haeckel (1887).	E3755m	SEM	x610
10	*Conchellium capsula* Borgert Partially dissolved specimens thin solid outer layer covering porous inner layer.	E3755m	SEM	x3840
11	*Conchellium tridacna* Haeckel Dorsal view	$P_1$978m	LM	x150
12	*Conchophacus dioatomeum* Haeckel Dorsal view	E988m	LM	x210

PLATE 61 Phaeodaria


1

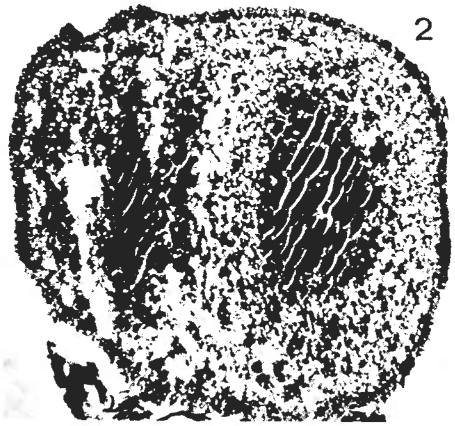
2


3

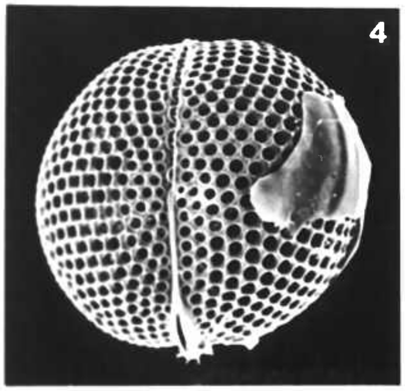
4

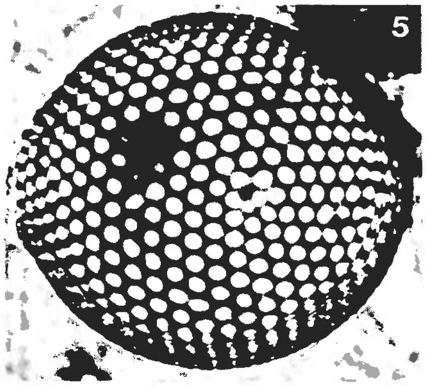
5

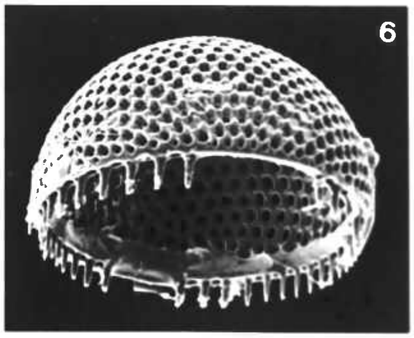
6

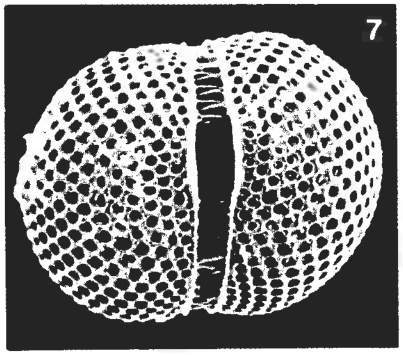
7

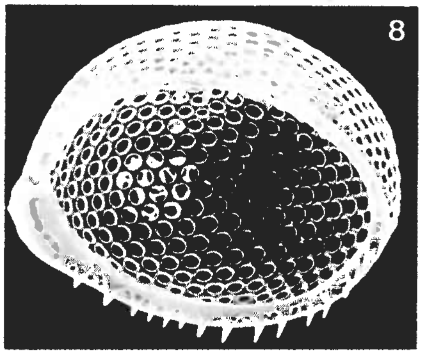
8

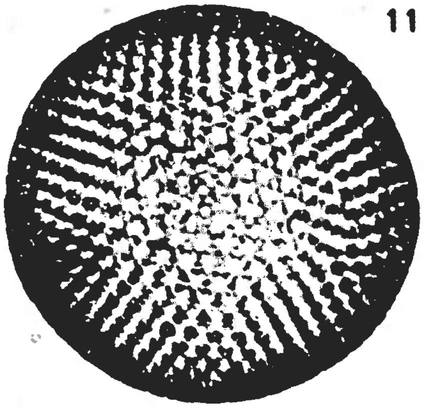
11

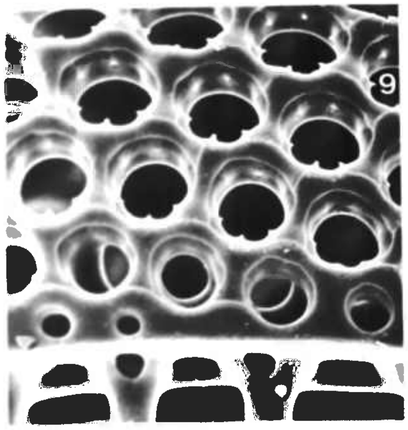
9

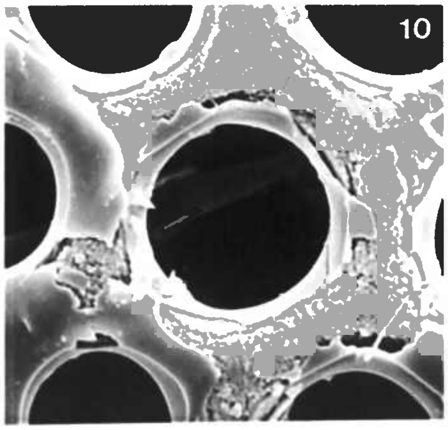
10

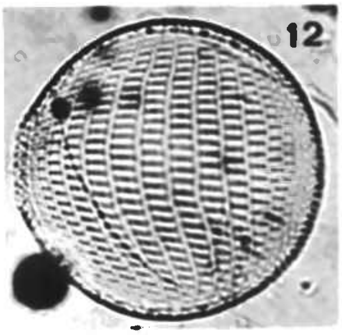
12

PLATE 62

Suborder: Phaeodaria
Family: Conchariidae

Figure		Station Depth	Type of Micrograph	Magnification
1	Conchidium argiope Haeckel Dorsal view	PB1268m	LM	x210
2	Conchidium argiope Haeckel Lateral view	$P_1$2778m	SEM	x150
3	Conchidium caudatum Haeckel Lateral view	E389m	LM	x210
4	Conchidium caudatum Haeckel Lateral view	$P_1$4280m	SEM	x150
5	Conchidium caudatum Haeckel Lateral view of bivalves	E389m	SEM	x100
6	Conchidium caudatum Haeckel Oblique apical view	E389m	SEM	x150
7	Conchidium caudatum Haeckel A cross section showing several layers of different morphology whose dissolution is underway.	$P_1$2778m	TEM	x19,200
8	Conchidium caudatum Haeckel Skeletal surface morphology showing smooth texture.	E389m	SEM	x1920
9	Conchopsis compressa Haeckel Lateral view	E988m	LM	x95
10	Conchopsis compressa Haeckel Lareral view of bivalves.	E988m	SEM	x64
11	Conchopsis compressa Haeckel Skeletal surface morphology showing rough surface.	E988m	SEM	x3200
12	Conchopsis compressa Haeckel View from inside of a valve.	$P_1$2778m	LM	x95
13	Conchopsis compressa Haeckel View from inside of a valve.	E988m	SEM	x63
14	Conchopsis compressa Haeckel Dorsal view showing a prominent keel.	E988m	SEM	x63
15	Conchopsis compressa Haeckel Lateral view showing teeth.	E988m	SEM	x66
16	Conchopsis compressa Haeckel Oblique view showing teeth and inside.	E988m	SEM	x61

PLATE 62 Phaeodaria

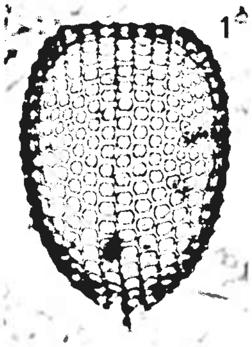
1

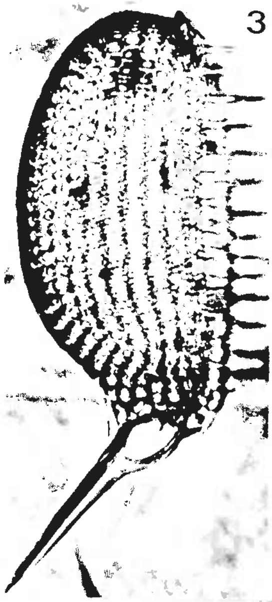
3

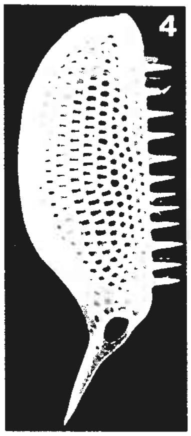
4

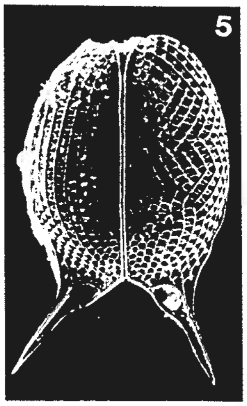
5

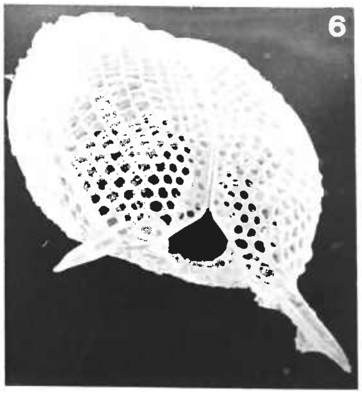
6

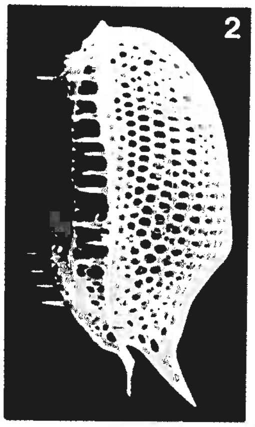
2

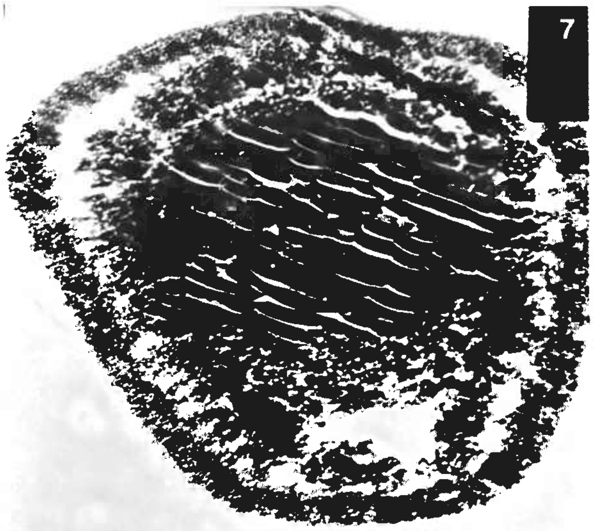
7


9

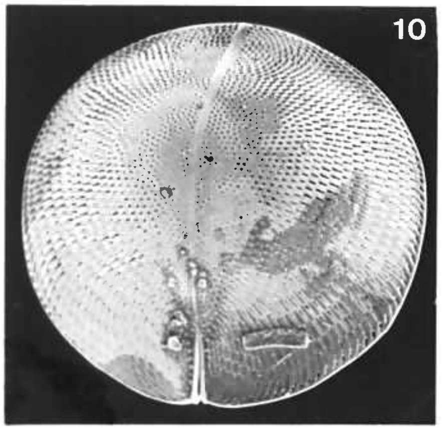
10


8

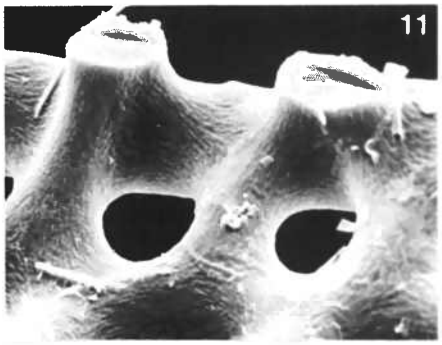
11


12

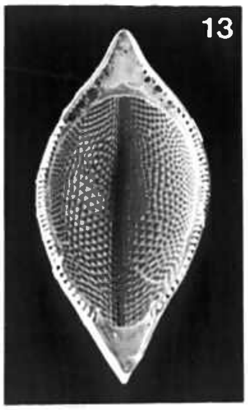
13

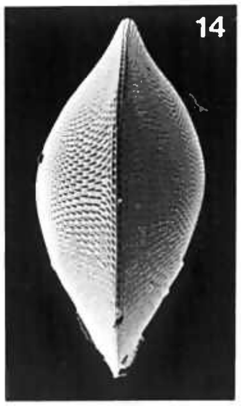
14

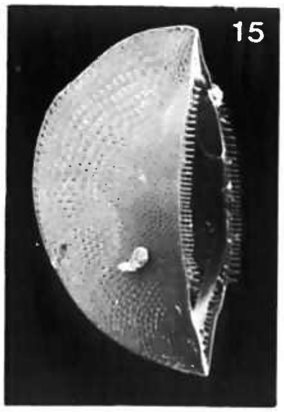
15

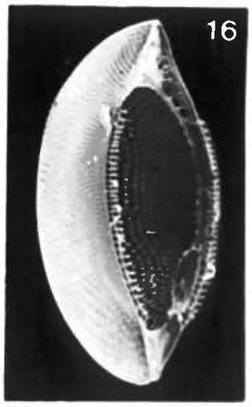
16

PLATE 63

Family: Aulosphaeridae, Medusettidae

Figure		Station Depth	Type of Micrograph	Magnification
1	*Aularia ternaria* Haeckel Portion of a shell made of triangular meshwork of tubes.	PB3791m	LM	x84
2	*Aularia ternaria* Haeckel Portion of triangular meshwork.	E3755m	SEM	x230
3	*Aulographis stellata* Haeckel	PB1268m	LM	x210
4	*Auloceras spathillaster* Haeckel	PB1268m	LM	x210
5	*Aulogarphonium bicorne* Haecker	PB3769m	LM	x210
6	*Aulographonium bicorne* Haecker	$P_1$4280m	SEM	x100
7	*Aulospathis taumorpha* ? Haeckel	$P_1$4280m	SEM	x1900
8	*Aulospathis taumorpha* ? Haeckel Same specimen.	$P_1$4280m	SEM	x94
9	*Auloceros arborescens* Haeckel *birameus* (Immerman)	$P_1$5582m	LM	x210
10	*Aulographis tetrancistra* Haeckel	$P_1$5582m	SEM	x220
11	*Aulospathis variabilis* Haeckel *bifurca* Haecker	$P_1$5582m	SEM	x47
12	*Medusetta* sp. B Skeleton made of a single layer of thin tubes.	PB 0-100m plankton tow	TEM	x20,000
13	*Medusetta* sp. B Same specimen showing variable shape of pores	PB 0-100 m plankton tow	TEM	x1700

PLATE 63 Phaeodaria

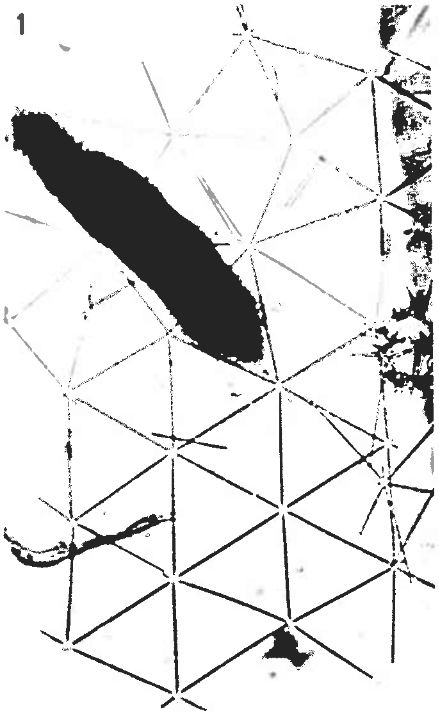
1


3

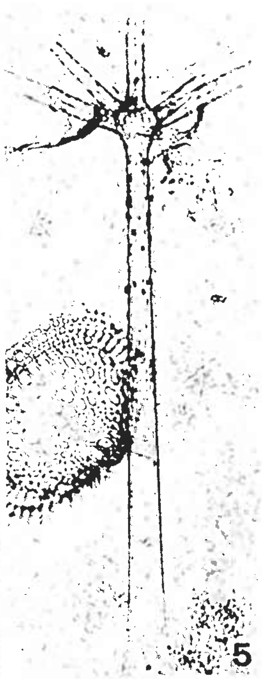
5

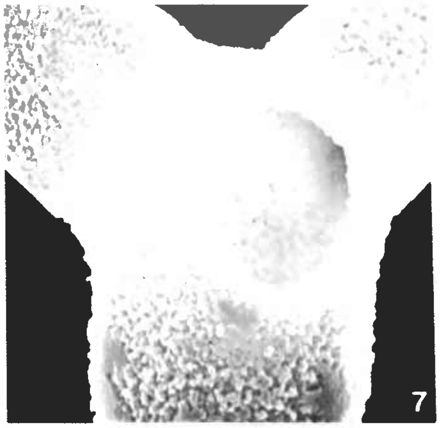
7

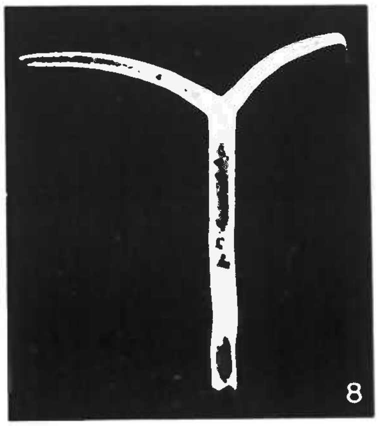
8

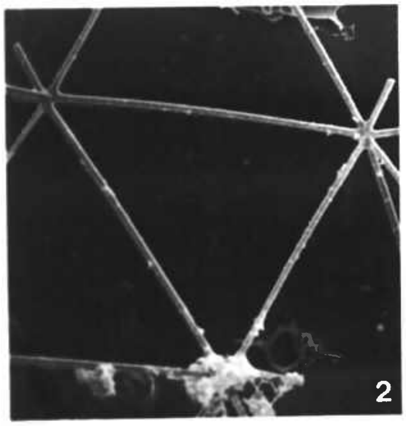
2

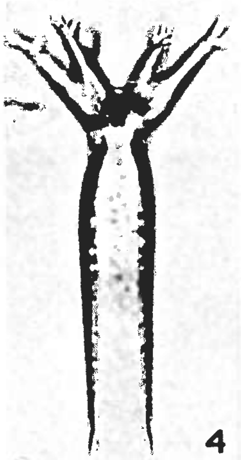
4

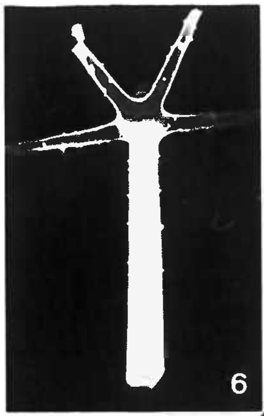
6

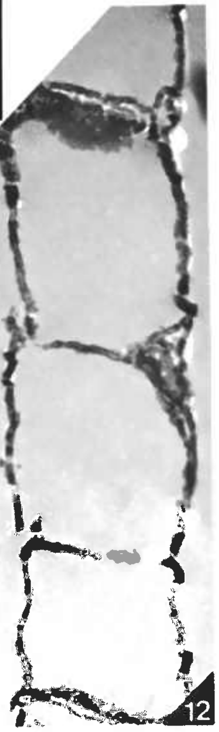
12


13

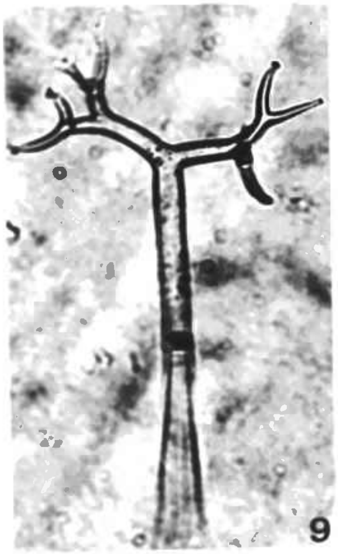
9


10

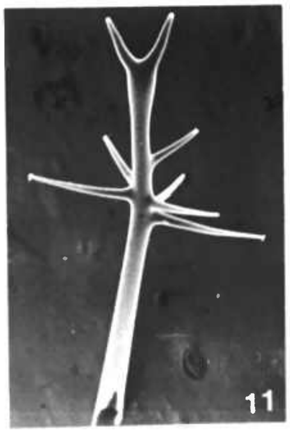
11

CURRICULUM VITAE

KOZO TAKAHASHI

Birthdate: January 17, 1948

Citizenship: Japanese

Marital Status: Married, one son and one daughter

Education:

B.A., Hokkaido University, Hakodate, Japan, 1972
B.Sc., University of Washington, Seattle, Washington, 1975
M.Sc., University of Washington, Seattle, Washington, 1977
Ph.D., Massachusetts Institute of Technology/
Woods Hole Oceanographic Institution, expected October 1981)

Professional Experience:

Research Laboratory Chemist, Mitsubishi Chemical Machinery Manufacturing, Ltd., Kawasaki, Japan, 1972-1974
Research Assistant, University of Washington, 1975-1977
Teaching Assistant, University of Washington, 1977-1978
Graduate Research Assistant, Woods Hole Oceanographic Institution, 1978-1981

Professional Societies:

Americal Geophysical Union;
North American Micropaleontology Section of Society of Economic Paleontologists and Mineralogists
Plankton Society of Japan

Present Research Interests:

Biogeochemical intertactions of biogenic silica with seawater in the water column and sediments. Ecology of Radiolaria, silicoflagellates and diatoms. Silica budget in the world oceans.

Awards:

Research grant: Pelagic opal: vertical flux and preservation of radiolarians and silicoflagellates (NSF Grant OCE 80-19386)
Postdoctoral Fellowship 1981-1982, Woods Hole Oceanographic Institution

PUBLICATIONS

Takahashi, K., and Honjo, S., 1981. Vertical flux of Radiolaria: A taxon-quantitative sediment trap study from the western Tropical Atlantic. Micropaleontology, 27(2): 140-190.

Takahashi, K., and Ling, H.Y., 1980. Distribution of Sticholonche (Radiolaria) in the upper 800 m of the waters in the equatorial Pacific. Marine Micropaleontology, 5: 311-319.

Baker, E.T., Feely, R.A., and Takahashi, K., 1979. Chemical composition, size distribution and particle morphology of suspended particulate matter at DOMES Sites A, B and C: relationships with local sediment composition. In: Bischoff, J.L., and Piper, D.Z., Eds., Marine Geology and Oceanography of the Pacific Manganese Nodule Province. Plenum Publ. Corp., p. 163-201.

Ling, H.Y., and Takahashi, K., 1977. Observation on microstructure of selected phaeodarian Radiolaria. Geol. Soc. China, Memoir, 2: 207-212.

Hurd, D.C. and Takahashi, K., in press. On the estimation of minimum mechanical loss during an in situ biogenic silica dissolution experiment. Marine Micropaleontology.

Erez, J., Takahashi, K. and Honjo, S., in press. In situ dissolution of Radiolaria in the Central North Pacific Ocean. Earth Planet. Sci. Lett.

PAPERS IN PREPARATION

Takahashi, K., in prep., Radiolaria. In: Biocoenosis in the Open Ocean, Ed., Honjo, S. To be published by Micropaleontology Press in 1981.

Takahashi, K., Hurd, D. C., Asper, V., in prep. Micro and ultrastructures of radiolarian skeletons. In: Biocoenosis in the Open Ocean, Ed., Honjo, S. To be published by Micropaleontology Press in 1981.

Takahashi, K., in prep. Silicoflagellates. In: Biocoenosis in the Open Ocean, Ed., Honjo, S. To be published by Micropaleontology Press in 1981.

Takahashi, K., and Honjo, S., in prep., Radiolarian sinking speed, residence time and sequential dissolution in the tropical oceans. To be submitted to Jour. Mar. Res.

Takahashi, K., Honjo, S., and Ling, H. Y., in prep., Morphological significance of phaeodarian radiolarian skeletons. To be submitted to Science.

Hurd, D. C., Takahashi, K., Asper, V., Houghton, S., and Honjo, S., in prep. Micro and ultrastructures of radiolarian skeletons and the relationships with dissolution time in the water column. To be submitted to Mar. Micropaleontology.

Takahashi, K., Hurd, D. C., Asper, V., and Honjo, S., in prep. TEM and SEM observations on radiolarian skeletons. To be published as a Technical Report, Woods Hole Oceanographic Institution.

ABSTRACTS

Takahashi, K., and Honjo, S., 1980. Radiolarian flux to the deep-sea and depth of production and dissolution in the tropical Atlantic and Pacific. Geol. Soc. Amer. Proc., 12(7): 533.

Takahashi, K., and Honjo, S., 1981. Sinking speed, residence time and dissolution of Radiolaria. Geol. Soc. Amer. Proc., 13(7): 564.

Takahashi, K., Hurd, D. C., Asper, V., and Honjo, S., 1981. Sequential dissolution of Radiolaria in the tropical water column and sediments. Geol. Soc. Amer. Proc., 13(7): 564.

Takahashi, K., and Honjo, S., 1981. Radiolaria: standing stock, residence time and turnover time in the equatorial Atlantic Ocean. Geol. Soc. Amer. Proc., 13(7): 564.

Takahashi, K., Hurd, D.C., and Honjo, S., 1981. Dissolution of Radiolaria during settling in the water column and preservation in the sediments. EOS, Transactions, Amer. Geophys. Union, 62(45): 938 (abstarct).

INVITED PRESENTATIONS

In: 1st International Conference (NATO Advanced Research Institute) on ECOLOGY OF MARINE PLANKTONIC PROTOZOA held at Station Zoologique, Villefranche-sur-Mer, France, 10-23 May 1981:

(1) On the methods of taxonomy of Radiolaria;
(2) Morphological significance of phaeodarian Radiolaria (poster session);
(3) Spacial distribution of Radiolaria;
(4) On the sampling of radiolarian biocoenosis; and
(5) Turnover time and sinking speed of Radiolaria.

BIOGRAPHY

I was born on January 17, 1948, in Oonohara-cho, Kagawa-prefecture, Japan. My childhood was spent in Kawasaki-shi, Kanagawa-prefecture, which was mostly surrounded by agricultural fields at the time. I received my primary and secondary school education there. As an undergraduate I attended Hokkaido University at Sapporo and Hakodate, graduating in 1972. I was married to Kayoko Murakoshi in October 1971. While I had been active in mountain climbing and skiing in the University Climbing Club there I was, on the other hand, very much interested in studying Oceanography. A decision of moving to the U.S. was inevitable for my strong desire in pursuing the best Oceanography in the world.

I came to the U.S. in February 1974 and began polishing my English at the Grays Harbor College, Aberdeen, Washington. Drs. John M. Smith and James Phipps of the College introduced me to fascinating marine sciences through engaged in a Sea Grant Project besides course work. I transferred to the University of Washington in September 1974 and continued more course work in Oceanography. I worked on biogenic suspended particles in the Deep Ocean Manganese Nodule Mining and Environmental Studies area with Dr. Edward T. Baker of Pacific Marine Environmental Laboratories, N.O.A.A. for my Master of Science. Interactions with Professors Hsin Yi Ling and Francis A. Richards at the University convinced me to further pursue blue-water particle oceanography.

I came to Woods Hole in the summer of 1978 to work with Dr. Susumu Honjo on biogenic opal particles. During the last three years here and a part of the time at M.I.T., I have been spending the most satisfactory and productive time during the past to become a full scientist mainly owing to extremely good advisors and scientists around me. Among many professional meetings that I participated in, the 1st International Conference on Ecology of Marine Planktonic Protozoa held at Villefranche-sur-Mer, France, 10-23 May 1981, was the most influential and beneficial for my career. We had a son in May 1979 and a daughter in March 1981.

I plan to continue doing research in the related field of this thesis work as a postdoctoral fellow at the Woods Hole Oceanographic Institution beginning December 1, 1981.